IMPERIAL COLLEGE LONDON
Division of Cancer, Department of Surgery and Cancer

Identifying mechanisms of resistance to CDK4/6 inhibitors in breast cancer

Hailing Fan

Thesis submission for the degree of Doctor of philosophy

Supervisors: Professor Simak Ali, Professor Laki Buluwela and Dr Georgina Sava

September 2022

Abstract

Breast cancer is the most diagnosed cancer worldwide and a leading cause of cancer-related deaths in women. Estrogen receptor positive (ER^+) breast cancer accounts for more than 70% of all cases. The development and use of endocrine therapies (ET) aimed at inhibiting the ER has demonstrated clinical benefits in ER^+ breast cancer. However, some patients are intrinsically resistant to ET and a high proportion of patients will eventually become resistant to ET. This highlights a critical gap in the current management for advanced ER^+ breast cancer and the urgent need for the development of alternative targeted therapies. Highly selective inhibitors of cyclin dependent kinases, CDK4 and CDK6 (CDK4/6), namely palbociclib, abemaciclib and ribociclib have been developed and have the potential to change the treatment landscape for advanced breast cancer patients. These CDK4/6 inhibitors (CDK4/6i) demonstrate great clinical efficacy when used in combination with ET. Thus, this therapeutic strategy has been approved by regulatory bodies in many countries as first-line therapy for advanced breast cancer. Despite their clinical success, resistance to CDK4/6i is often seen, representing a major clinical challenge to their widespread use. Investigations to understand mechanisms of resistance to CDK4/6i will contribute to the better use of current CDK4/6i through identification of biomarkers to response and for development of additional therapeutic strategies following progression on CDK4/6i.

Towards understanding CDK4/6i resistance, I have investigated potential resistance mechanisms through the generation of resistance models in ER^+ cell lines. I have adapted the Synergistic activating mediator (SAM) and inducible dihydrofolate reductase (DHFR) systems to singly over-express cyclins and CDKs to determine if upregulation of alternative cell cycle CDKs can promote evasion of CDK4/6- directed growth inhibition. Altogether, I have shown that over-expression CDK2 and CDK6 in MCF7 cells leads to rapid emergence of resistance to CDK4/6i. In addition, these resistance models with CDK2 and CDK6 over-expression retained sensitivity to CDK7/12/13 inhibitors.

Moreover, acquired resistance to palbociclib was also achieved in ER^+ cell lines by long term culturing in the presence of palbociclib. ChIP-seq and RNA-seq analysis of the acquired resistance models highlights the upregulation of a small subset of cell cycle related genes, including PLK1, AURKB, CCNA2 and MCM10. Expression of these genes is inhibited by

palbociclib treatment, but their expression is regained following resistance to palbociclib. Moreover, the S100P, GDF15 and DKK1 genes were upregulated in palbociclib resistance. These genes may form a gene signature that aids prediction of palbocicib resistance. Some of these genes also provide opportunities for new therapies. Thus, the findings reported in this thesis provide insights into resistance to clinical CDK4/6i and point to biomarker and therapeutic opportunities, including the possible use of CDK7 and CDK12/13 inhibitors.

Declaration of originality

This thesis is submitted in fulfilment of the requirements for the degree of Doctor of Philosophy. I declare that the work reported in this thesis is my own. Where results generated by a colleague are included, this is clearly stated and fully acknowledged. MCF7 RB knockout cells and DHFR-CDK/cyclin over-expressing lines were generated by Dr Georgina Sava. AcCas9-CDK/cyclin over-expressing cells were generated by Dr Chun Fui Lai and Ms Xiaobei Xiong. Palbociclib resistance cell lines were kindly provided by Dr Lesley Ann Martin's group. Nanopore RNA seq and ChIP seq were performed by Dr Mariana Leal. The initial quality check and alignment of Nanopore RNA seq data were kindly performed by Dr Eugene Schuster. The initial quality check on ChIP seq data were also performed by Dr Eugene Schuster.

Copyright declaration

The copyright of this thesis rests with the author. Unless otherwise indicated, its contents are licensed under a Creative Commons Attribution-Non Commercial 4.0 International Licence (CC BY-NC). Under this licence, you may copy and redistribute the material in any medium or format. You may also create and distribute modified versions of the work. This is on the condition that: you credit the author and do not use it, or any derivative works, for a commercial purpose. When reusing or sharing this work, ensure you make the licence terms clear to others by naming the licence and linking to the licence text. Where a work has been adapted, you should indicate that the work has been changed and describe those changes. Please seek permission from the copyright holder for uses of this work that are not included in this licence or permitted under UK Copyright Law.

Acknowledgments

Firstly, I would like to sincerely thank my supervisors, Professor Simak Ali, Professor Laki Buluwela and Dr. Georgina Sava for their patience, guidance and support throughout my PhD and for providing me with the opportunities to progress as a scientist.

I would also like to express my appreciation to all group members, Dr. Van Thuy Mai Ngyuen, Dr. Isabella Goldsbrough, Dr. Chun Fui Lai, Dr. Kirsty Balanchran, Miss Georgia Simmons, Miss Kaste Jurgaityte, Dr. Alison Harrod, Dr. Carolina Gemma, Dr. Manikandan Periyasamy and Dr. Anup Singh for their support in the lab and stimulating discussions. I would also like to thank Dr Georgina Sava for the generation of the MCF7 RB KO and DHFR over-expressing lines. Also, I would like to thank Dr. Chun Fui Lai and Miss Xiao Bei Xiong for generating MCF7- and T47D-AcCas9 cell lines. I would also thank Dr. Lesley Ann Martin (ICR) and her group members for providing PalboR cells for my project. In particular, Dr Mariana Ferreira Leal (ICR) and Dr Eugene Schuster (ICR) for performing ChIP-seq and RNA-seq experiment and the initial RNA-seq alignment, respectively. I am also so grateful for Dr. Van Thuy Mai Nguyen for teaching me the basics of ChIP- and RNA-seq analysis and her support throughout the process. I would also like to express gratitude to Breast Cancer Now for their generous funding and Imperial College London for providing their support during my studies.

I would also like to acknowledge the love and their encouragements of my dear friends, Dr. Yakinthi Chryschondou, Miss Therodora Constantin, Miss Ruxandra Constantin, Dr. Paula Saavedra-Garcia, Miss Jinrui Wen, Dr. Angela Yiu, Dr. Ning Wang, Dr. Marc Lorenzo and Martina. In particular, Miss Cici Wu, Miss Charlene Magada, Miss Wei (Megan) Wang, Miss RuiHui Li and Miss Fangyan Cheng for all your patience and support throughout the years.

I would like to thank all my friends and family for their support. Finally, I would also like to acknowledge the greatest heroes in my life, my parents, May and Hung, thank you for your understanding and patience while I tried to achieve my dreams. I would also like to use this opportunity to thank my Grandma, MeiZhen, I will always miss you. I would also like to express my appreciation and love to my dearest cousin, CiQi, you have been there through all my ups and downs, I cannot thank you enough for your unconditional love and support.

Table of Contents

Abstract **2**

Copyright declaration **5**

Acknowledgments **6**

Table of Contents **7**

List of Figures **13**

List of Tables **15**

1. Introduction **21**

1.1 Breast cancer overview **21**

1.1.1 Molecular classification of Breast cancer 21

1.2 Estrogen receptor-alpha in breast cancer 25

1.2.1 Estrogen as a steroid hormone 25

1.2.2 The estrogen receptor in mediating estrogens 27

1.2.3 Estrogen receptor-alpha in normal mammary gland development 34

1.2.4 The role of Estrogen receptor-α in breast cancer 34

1.2.5 Endocrine therapy for ER-positive breast cancer 35

1.2.6 Resistance to Endocrine Therapies – the clinical problem and possible mechanisms 38

1.2.6.1 Mutations in the ESR1 gene as a mechanism for acquired resistance to endocrine therapies 40

1.2.6.2 Upregulation of mitogenic pathways in ET resistance 42

1.3 Cell cycle Regulators in ER$^+$ Breast Cancer **44**

1.3.1. Cell cycle progression regulated by cyclins and cyclin-dependent kinases (CDKs) 46

1.3.1.1 Negative regulation of cell cycle regulation by endogenous CDK inhibitors 46

1.3.1.2 Cell cycle: CDK4 and CDK6 mediates the entry of G0/1 phase.....48

1.3.1.3 Cell cycle: CDK2 regulates the progression through S phase.....55

1.3.1.4 Cell cycle: CDK1 is essential for transition and progression during G2/mitosis phases.....59

1.3.2 Aberrant action of cell cycle CDKs and cyclins contributes to cancer development 66

1.4 CDKs and cyclins in transcription regulation.....68

1.4.1. CDKs and cyclins modulate RNA Polymerase II (Pol II) mediated transcription 69

1.4.1.1 Transcription initiates with the formation of a pre-initiation complex (PIC) 69

1.4.1.2 Proximal promotor pause and release for elongation.....71

1.4.1.3 Transcription termination.....72

1.4.2 Transcription-associated CDKs contribute to tumourigenesis.....75

1.5 Development and application of CDK inhibitors as targeted cancer therapies....76

1.5.1 New era of targeted therapy: CDK inhibitors.....76

1.5.1.1 First generation pan-CDK inhibitors.....77

1.5.1.2 Second generation: selective CDK inhibitors.....77

1.5.2 Developing selective CDK inhibitors.....78

1.5.2.1 Identification of CDK4/6 inhibitors and success in clinical trials.....79

1.5.2.1.1 Palbociclib and PALOMA trials.....83

1.5.2.1.2 Abemaciclib in MONARCH trials.....84

1.5.2.1.3 Ribociclib in MONALEESA trials.....85

1.5.2.2 Resistance to CDK4/6 inhibitors.....91

1.5.3 Development of selective inhibitors for other CDK implicated in cancer.....96

1.5.3.1 CDK1 and CDK2 inhibitors.....96

1.5.3.2 CDK7 inhibitors.....96

1.5.3.3 CDK9 inhibitors 100
1.5.3.4 CDK12/13 inhibitors 101
1.5.3.5 CDK8/19 inhibitors 101
1.6 Hypothesis and aims 104
2. Materials and Methods 106
2.1 Materials 106
2.1.1 Reagents 106
2.1.2 Sundries 106
2.1.3 General laboratory equipment 107
2.1.4 Cell culture reagents 107
2.1.5 Chemicals 108
2.1.6 General solutions 108
2.2 Methods 110
2.2.1 Tissue culture 110
2.2.2 Cell counting 111
2.2.3 Generating RB Knockout (KO) stable lines 111
2.2.4 Generation of DHFR-CDK/cyclin conditional over-expression stable lines 113
2.2.5 Generation of Ac-Cas9 stable over-expression lines 116
2.2.5.2 Generating CDK6 Small hairpin RNA (shRNA) stable lines 118
2.2.5.1 Generating CDK4/6 inhibitor resistant breast cancer cell lines 118
2.2.6 Transfection and Transduction 119
2.2.7 Genomic DNA (gDNA) extraction 120
2.2.7.1 End-point Polymerase chain reaction (PCR) 120
2.2.7.2 Agarose gel electrophoresis 121
2.2.7.3 Sanger DNA Sequencing 121
2.2.8 Total RNA extraction 121

2.2.8.1 Complementary DNA (cDNA) by reverse transcription.....122
2.2.8.2 Real time reverse transcription quantitative PCR (RT-qPCR).....122
2.2.9 Protein lysate preparation.....124
2.2.9.1 Protein extraction 124
2.2.9.2 Protein quantification 125
2.2.9.3 SDS-Polyacrylamide gel electrophoresis (Western blotting).....125
2.2.10 Sulforhodamine B (SRB) cell growth assay 127
2.2.10.1 CDK4/6 inhibitors.....127
2.2.10.2 CDK7 inhibitors.....127
2.2.10.3 Growth assays in estrogen-free medium.....128
2.2.10.4 SRB assay 128
2.2.11 siRNA-directed CDK6 knockdown 128
2.2.11.1 Growth assays 128
2.2.11.2 RNA and protein extraction 129
2.2.12 Nanopore RNA sequencing 129
2.2.13 Chromatin immunoprecipitation (ChIP) assay and sequencing.....130
3. Results 131
3.1 Retinoblastoma RB1 gene knockout MCF7 cells are resistant to CDK4/6 inhibitors 131
3.1.1 Establishing RB1 gene knockout MCF7 cells 131
3.1.2 RB KO MCF7 cells are resistant to CDK4/6 inhibitors, but remain responsive to CDK7 inhibitors.....134
3.2 Can over-expression of cell cycle CDKs promote resistance to CDK4/6 inhibitors? 137
3.2.1 Using dihydrofolate reductase fusion proteins as an approach for inducible over-expression of CDKs and Cyclins. 137
3.2.1.1 Inducible CDK over-expression in MCF7 cells provides only limited evidence for CDK over-expression in promoting resistance to CDK4/6 inhibitors. 141

3.2.2 Using activating-Cas9 to over-express endogenous CDK and cyclin genes in MCF7 cells 144

3.2.2.1 Cyclin E1 over-expression and response to CDK4/6 inhibitors 149

3.2.2.2 Investigating MCF7-AcCas9-CDK2 over-expressing cells in sensitivity to CDK4/6 inhibitors 152

3.2.2.2.3 Over-expression of CDK2 also resulted in the fast development of resistance to ribociclib 154

3.2.2.3 CDK6 over-expression in the emergence of resistance CDK4/6 inhibitors 160

3.2.2.3.1 Drug response of CDK6 over-expressing cells with short term treatment with CDK inhibitors 160

3.2.2.3.2 Development of acquired resistance in MCF-7AcCas9-CDK6 cells through prolonged exposure to CDK4/6 inhibitors 160

3.2.2.3.3 GI_{50} determination confirms that over-expression of endogenous CDK6 can promote acquired resistance to CDK4/6 inhibitors 166

3.2.2.3.4 CDK6 knockdown did not revert sensitivity of MCF7-AcCas9-CDK6 resistant cells to palbociclib 170

3.3 Epigenetic and transcriptomic profiling of estrogen receptor positive breast cancer cell lines with acquired resistance to palbociclib 173

3.3.1 Acquired resistance to palbociclib led to changes in global H3K27ac signalling in MCF7 cells 174

3.3.2 Identification of differentially expressed genes following development of palbociclib resistance in ER^+ breast cancer cell lines 186

3.3.2.1 Integration analysis of H3K27ac ChIP-seq and nanopore RNA-seq data 198

3.3.3. Initial validation of nanopore sequencing data in ER^+ breast cancer cell lines 207

4. Discussion 209

4.1 The loss of retinoblastoma protein in MCF7 cells rendered resistance to CDK4/6 inhibitors 209

4.2 The investigation of the role of over-expressing CDKs/cyclins in CDK4/6 inhibitor resistance mechanisms 210

4.2.1 Cyclin E1 over-expression model remained sensitive to CDK4/6 inhibitors ... 210

4.2.2. Increased expression of CDK2 led to rapid development of resistance to palbociclib and ribociclib 212

4.2.3 CDK6 amplification led to rapid development of acquired resistance to abemaciclib 213

4.3. Global transcriptomic and epigenetic profiling of palbociclib resistance models 215

4.3.1 Reset of cell cycle related genes in palbociclib resistant cells to overcome palbociclib inhibition 215

4.3.2 The identification of potential biomarkers of resistance to palbociclib 217

5. Summary 220

References 221

Appendix 299

Appendix I - Summary of common peaks in H3K27ac ChIP-seq comparing Vehicle vs PalboT vs PalboR MCF7 cells 299
Appendix II - Summary of common peaks in H3K27ac ChIP-seq comparing Vehicle vs PalboT vs PalboR in MCF7 LTED Y537C cells 300
Appendix III – GSEA pathway analysis in MCF7 cells 301
Appendix IV –– Heatmap cluster gene list in MCF7 cells 302
Appendix V – GSEA pathway analysis in LTED Y537C cells 307
Appendix VI –– Heatmap cluster gene list in MCF7 LTED Y537C cells 308
Appendix VII – GSEA pathway analysis in HCC1428 LTED cells 313
Appendix VIII – Heatmap cluster gene list in HCC1428 LTED cells 314
Publications 312

List of Figures

Figure 1. 1. Histopathological and molecular analysis for breast cancer subtypes. 24
Figure 1. 2. Estrogen biosynthesis pathway.....26
Figure 1. 3. Estrogen receptor alpha signalling 29
Figure 1. 4. Frequency of ESR1 mutations.....41
Figure 1. 5. CDKs, cyclins and the cell cycle.....45
Figure 1. 6. CDK4/6-cyclin D1 mediates G1 entry. 54
Figure 1. 7. CDK2 promotes progression through S phase. 58
Figure 1. 8. CDK1 and CDK2 regulate activities during G2 transition.....60
Figure 1. 9. CDK1-cyclin B1 key mediators of Mitosis. 65
Figure 1. 10. Transcriptional CDKs and RNA PolII transcription. 74
Figure 1. 11. CDK4/6 inhibitors and potential resistant pathways. 82
Figure 1. 12. CDK4/6 inhibitors and potential resistant pathways. 95
Figure 1. 13. CDK7 inhibitor as potential treatment for ER+ breast cancer. 99
Figure 2. 1. Plasmid map of the CDK6-DHFR construct. Plasmid map shows the positions of the forward and reverse primers, the CDK1, HA, YFP and DHFR open reading frames. 115
Figure 3. 1. Generation of RB KO clones in MCF7 breast cancer cells. 133
Figure 3. 2. RB1 KO cells are resistant to CDK4/6 inhibitors, but maintained sensitivity to CDK7 inhibitors. 136
Figure 3. 3. Generating CDK and cyclin over-expressing MCF7 cells using the DHFR inducible system.....139
Figure 3. 4. Generating CDK and cyclin over-expressing MCF7 cells using the DHFR inducible system.....140
Figure 3. 5. Drug response of DHFR-CDKs lines cultured in estrogen-depleted medium. ..143
Figure 3. 6. Using the gene activating Cas9 method to over-express endogenous CDK and cyclin genes.....146
Figure 3. 7. Determining the effect of over-expressing CDKs and cyclins on MCF7 cell growth. 148
Figure 3. 8. Response of MCF7-AcCas9-CCNE1 cells to CDK4/6 inhibitors. 150
Figure 3. 9. Over-expressing CCNE1 had limited effect on growth recovery after culturing with continuous treatment with CDK4/6 inhibitors. 151
Figure 3. 10. MCF7-AcCas9-CDK2 show reduced response to palbociclib in estrogen depleted medium supplemented with 10nM 17β-estradiol. 153
Figure 3. 11. MCF7-AcCas9-CDK2 promote rapid emergence of resistance to palbociclib. 157
Figure 3. 12. Over-expressing CDK2 is associated with a rapid development of resistance to ribociclib. 158
Figure 3. 13. MCF7-AcCas9-CDK2 does not promote resistance to abemaciclib. 159
Figure 3. 14. CDK6 over-expression does not reduce sensitivity to CDK4/6 inhibitors.....162
Figure 3. 15. CDK6 over-expression promotes resistance to abemaciclib in MCF7 cells. Response of MCF7-AcCas9-CDK6 cells to prolonged exposure to palbociclib. 163

Figure 3. 16. Response of MCF7-AcCas9-CDK6 cells to prolonged exposure to palbociclib. 164
Figure 3. 17. Response of MCF7-AcCas9-CDK6 cells to prolonged exposure to palbociclib. 165
Figure a3. 18. Response of MCF7-AcCas9-CDK6 cells to prolonged exposure to palbociclib.(Figure 3.18).....169
Figure 3. 19. CDK6 knockdown in palbociclib-resistant MCF7-AcCas9-CDK6 had limited effect on reversing resistance to palbociclib.. 171
Figure 3. 20. CDK6 knockdown using short hairpin RNA (shRNA) in palbociclib resistant MCF7-AcCas9-CDK6 had limited effect on reversing. 172
Figure 3. 21. H3K27ac ChIP-seq analysis in MCF7 cells following acquired resistance to palbociclib. 176
Figure 3. 22. Differential analysis of H3K27ac ChIP-seq in MCF7 cells following acquired resistance to palbociclib. 179
Figure 3. 23. Pathway analysis of differentially enriched H3K27ac signals in MCF7 cells with acquired resistance to palbociclib. 180
in PalboR vs Vehicle (q-value≤0.05). 180
Figure 3.24. H3K27ac ChIP-seq analysis of MCF7 LTED Y537C cells after acquiring resistance to palbociclib. 182
Figure 3.25. Differential enrichment analysis of H3K27ac signal after acquiring resistance to palbociclib in MCF7 LTED Y537C cells. 183
Figure 3.26. Comparison of differential H3K27ac signals in PalboR vs Vehicle in MCF7 and MCF7 LTED Y537C cells 184
Figure 3.28. Differential analysis of gene expression in MCF7 palbociclib treated and palbociclib resistant cells. 191
Figure 3.29. Cluster analysis of 577 differentially expressed genes in palbociclib treated and resistant MCF7 cells. 192
Figure 3.30. Differential gene expression analysis of MCF7 LTED Y537C palbociclib treated and resistant cells. 194
Figure 3.31. Cluster analysis in MCF7 LTED Y537C cells treated with palbociclib and palbociclib resistance. 195
Figure 3.32. Pair-wise comparison of differential gene expression between MCF7 and MCF7 LTED Y537C palbociclib resistant cells. 197
Figure 3. 33. Integration analysis of H3K27ac ChIP-seq and Nanopore data in MCF7 PalboT and PalboR cells. 200
Figure 3. 34. Integration analysis of H3K27ac ChIP and Nanopore data of MCF7 LTED Y537C cells. 201
Figure 3. 35. Differential gene expression analysis of palbociclib treated and palbociclib resistance in HCC1428 LTED cells. 204
Figure 3. 36. Cluster analysis of differentially express genes in HCC1428 LTED cells treated with palbociclib and palbociclib resistant. 205
Figure 3. 37. Differentially expressed gene enriched in palbociclib resistant cells. 206
Figure 3. 38.. Validation of differentially expressed genes enriched in palbociclib resistant cells. 208

List of Tables

Table 1. 1 Summary of alterations in cell cycle related CDKs and cyclins in breast cancer. .68
Table 1. 2 Summary of clinical trials involving CDK4/6 inhibitors.....87
Table 1. 3 Clinical development of transcriptional CDK inhibitors.....102

Table 2. 1 General stock solution composition.....108
Table 2. 2 Microbiological reagents 109
Table 2. 3 Summary of sgRNA targeting RB1 exon 1 112
Table 2. 4 List of CDKs and cyclin D1-HA constructs 113
Table 2. 5 List of custom primers and restriction enzymes to generate DHFR-CDK/cyclin-HA fusion constructs.....114
Table 2. 6 List of three independent sgRNAs for each CDK/cyclin 117
Table 2. 7 shRNA constructs used in this study 119
Table 2. 8 List of SYBR Green primers used in RT-qPCR. 123
Table 2. 9 immunoblotting buffer solution 126
Table 2. 10 SDS page acrylamide gel.....126
Table 2. 11 List of antibodies used for immunoblotting diluted in blocking buffer.....126
Table 2. 12 List of custom made small interfering RNAs targeting Cas9.....129

Abbreviations

AF1	Activation function 1
AF2	Activation function 2
AI	Aromatase inhibitor
AP1	Activator protein 1
APS	Ammonium persulfate
AR	Androgen receptor
AurA	Aurora A
AurB	Aurora B
AurC	Aurora C
BCa	Breast cancer
BETA	Binding and Expression Target Analysis
CAF	Cancer associated fibroblast
CAK	CDK-activating kinase
CARM1	Coactivator-associated arginine methyltransferase 1
Cas	CRISPR-associated proteins
CCDC170	Coiled-coil domain containing 170
CCND1	Cyclin D1
CDC6	cell cycle division 6
CDK	Cyclin-dependent kinase
CDK4/6i	Cyclin dependent kinase 4/6 inhibitor
CDKI	cyclin dependent kinase inhibitor
cDNA	Complementary DNA
CDT1	CDC10 division transcript 1
ChIP	Chromatin immunoprecipitation
ChIP-seq	Chromatin immunoprecipitation sequencing
CPC	chromosome passenger complex
CREB	cAMP-response element binding protein
CRISPR	Clustered regularly interspaced short palindromic repeats
CRS	cytomplasmic rention sequence
CTD	C-terminal domain

DBD	DNA binding domain
ddH2O	Double-distilled deionised water
DKK1	Dickkopf1
DEG	Differentially expressed gene
DHFR	dihydrofolate reductase
DMEM	Dulbecco's modified eagle's medium
DMSO	Dimethyl sulfoxide
DSS	Dextran-coated charcoal-stripped FCS
E1	Estrone
E2	17β-estradiol
E3	Estriol
EDTA	Ethylenediaminetetraacetic acid
EGF	Epidermal growth factor
EGFR	Epidermal growth factor receptor
EMT	Epithelial to mesenchymal transition
ER	estrogen receptor
ERE	Estrogen response elements
ERK	Extracellular regulated kinase
EtOH	Ethanol
ETS1	E26 transformation specific 1
FCS	Fetal calf serum
FGFR	Fibroblast growth factor receptor
FOXA1	Forkhead box protein A1
FSH	Follicle-stimulating hormone
GATA3	GATA binding protein 3
GDF15	Growth differentiation factor 15
gDNA	Genomic DNA
GR	Glucocorticoid receptor
GPER	G-protein coupled estrogen receptor
GSEA	Gene set enrichment analysis
H3K27ac	acetylation of histone 3 at lysine 27 residue
HDAC	Histone deacetylase

HER2	Human epidermal growth factor receptor 2
HMT	Histone methyltransferase
HP1	Heterochromatin protein 1
IGF-1R	Insulin-like growth factor-1 receptor
INM	inner nuclear membrane
Interferon	IFN
IP	Immunoprecipitation
JAK/STAT	Janus kinase/signal transducers and activators of transcription
KO	knockout
KIF	kinase-like motor proteins
LB	Luria-Bertani
LBD	Ligand binding domain
LHRH	Lutenising hormone-releasing hormone
lncRNA	long non-coding RNA
LOG2FC	Log2 fold change
LRH-1	Liver-receptor homolog 1
LTED	Long term estrogen deprived
MALAT1	Metastasis associated lung adenocarcinoma transcript 1
MAPK	mitogen activated protein kinase
MARGE	model analysis of regulation of gene expression
MARGE-RP	model analysis regulation of gene expression regulatory potential
MCM	mini chromosome maintenance
MKLP1	mitotic kinesin-like protein 1
NEAT	nuclear enriched abundant transcript 1
NFκB	Nuclear factor-κB
NR	Nuclear receptor
ORC	origin recognition complex
p300/CBP	P300/CREB-binding protein
padj	Adjusted p-value
PalboR	palbociclib resistant
PalboT	palbociclib treated
PAM	Protospacer adjacent motif

PBS	Phosphate buffered saline
PBST	Tween 20 in PBS
PCA	Principle component analysis
PCNA	proliferating cell nuclear antigen
PCR	Polymerase chain reaction
PDX	Patient-derived xenograft
PFS	Progression-free survival
PI3K	Phosphoinositide 3-kinase
PKA	Protein kinase A
PLK1	polo like kinase 1
PolII	RNA polymerase II
PP2A	SGO1-phosphatase type 2A
PR	Progesterone receptor
PSA	prostate specific antigen
PSG	L-glutamine/penicillin/streptomycin
qPCR	Quantitative PCR
RAN-GTP	Ran associated GTPase
RB	Retinoblastoma protein
RIPA	Radioimmune precipitation buffer
RNA-seq	RNA-sequencing
RPMI-1640	Roswell Park Memorial Institute-1640
RT-PCR	Reverse transcriptase-PCR
RT-qPCR	Reverse transcriptase-quantitative PCR
SAC	spindle assembly checkpoint
SAM	synergistic activating mediator
SDS	Sodium dodecycl sulphate
SDS-PAGE	SDS-polyacrylamide gel electrophoresis
SEM	Standard error of the mean
SERCA	Selective estrogen receptor covalent antagonist
SERD	Selective estrogen receptor downregulator
SERM	Selective estrogen receptor modulator
sgRNA	Single guide RNA

SMRT	Silencing mediator for retinoid or thyroid-hormone receptors
SP1	Specificity protein 1
SRB	Sulforhodamine B
SRC	Steroid receptor coactivator
TALEN	Transcription activator-like effector nuclease
TBE	Tris-borate-EDTA
TBP	TATA Box binding protein
TCA	Trichloroacetic acid
TE	Tris-EDTA
TFIIH	Transcription factor II H
TMP	trimethoprim
TNFα	Tumour necrosis factor α
TSS	transcription start site
WT	Wild-type
YAP1	Yes-associated protein 1
ZFN	Zinc finger nuclease

1. Introduction

1.1 Breast cancer overview

Breast cancer (BCa) is the most common form of cancer diagnosed each year, with 2.26 million new cases in 2020 worldwide, accounting for 11.7% of all newly diagnosed cancers (Sung *et al.*, 2021). Notably, BCa is the single largest cause of cancer-related deaths in women worldwide, responsible for 15.5% of all cancer deaths in women. This is despite the considerable advances in early detection, surgical removal of tumours, together with chemotherapeutic and targeted drug therapies, which have all contributed to reductions in patient mortality, at least in the Western world (Harbeck *et al.*, 2019).

BCa is a heterogeneous disease comprised of several distinct histological subtypes whose identification is of paramount prognostic value for patient survival, as it determines the most appropriate therapeutic approaches (Waks and Winer, 2019). A systematic study of the transcriptional profiles more than two decades ago has revealed different molecular subtypes within traditional histological classifications of BCa that have further refined stratification of BCa subtypes (Dai *et al.*, 2015; Perou *et al.*, 2000; Weigelt *et al.*, 2010a). Molecular and histopathological grouping is used to guide clinical decisions for treatments, leading to improvements in clinical outcomes and reduced mortalities (Figure 1.1).

1.1.1 Molecular classification of Breast cancer

Histopathological stratification considers the morphology, tumour grading and phenotypic markers (mainly hormone receptors (HR) and human epidermal growth factor receptor 2 (HER2)) to stratify a tumour into one of three main groups. Each group is characterized by the expression of a specific combination of phenotypic markers, which all have prognostic values (Curtis *et al.*, 2012; Onitilo *et al.*, 2009; Tan *et al.*, 2020; Weigelt *et al.*, 2010b). The largest subgroup is defined by the expression of HRs, namely estrogen receptor-alpha (ERα), frequently together with the progesterone receptor (PR) and mostly lacking in HER2

expression. The second immunohistochemically distinct group is the subtype characterized by the overexpression of HER2 (encoded by the ERBB2 gene), often through amplification of the ERBB2 gene. A proportion of HR^+ breast cancers are found to also be $HER2^+$. The third main group is characterised by the absence of HR and HER2, the so-called triple-negative breast cancer (TNBC).

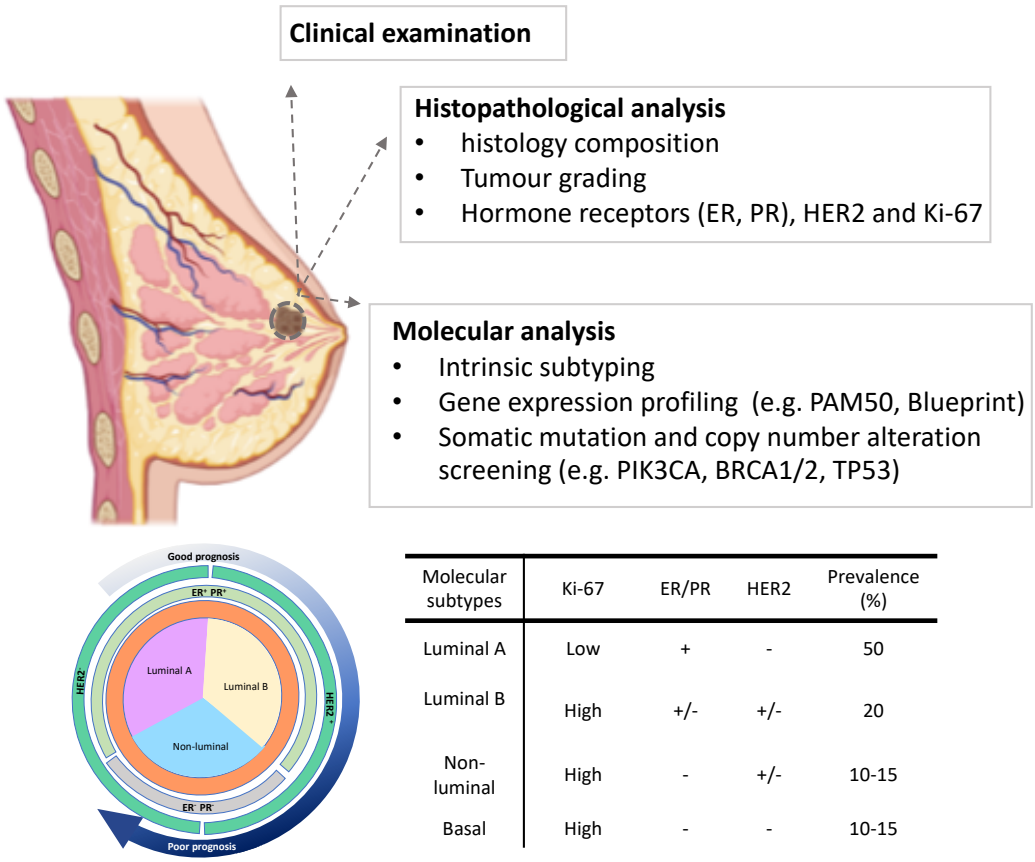
These phenotypic markers are used for patient stratification and treatment decisions. Around two thirds of HR^+ BCa cases express PR in addition to ERα (Rakha *et al.*, 2007). PR expression is routinely used as an independent indicator of response to endocrine therapy (ET), as increased expression of PR has been correlated with fewer metastatic events (Blows *et al.*, 2010; Osborne *et al.*, 1980; Pichon *et al.*, 1980). Previous studies have shown the use of high dose synthetic progesterone (referred to as progestins for commercial use) had beneficial effects in advanced BCa (Bines *et al.*, 2014; Lundgren *et al.*, 1989; Mattsson, 1983; Morgan, 1985). Furthermore, the combination of anti-estrogens and progestins improved anti-tumour effect in BCa cell line tumour xenografts, compared to anti-estrogen treatment alone (Mohammed *et al.*, 2015). On the other hand, some recent clinical data suggest that women who had menopausal hormone therapy (MHT) with estrogen plus particular progestins such as levonorgestresl, medroxyprogesterone acetate (MPA) or norethindrone acetate (NETA) have increased risk of developing BCa (Carroll *et al.*, 2017; Chlebowski *et al.*, 2009; Fournier *et al.*, 2008; Lyytinen *et al.*, 2010). Therapeutic strategies targeting PR involving anti-progestins and selective progesterone receptor modulators (SPRMs) are under investigation for use in patients who have progressed on ET targeting ER. In particular, SPRMs have been shown to possess both agonistic and antagonistic properties, to recruit coactivators or compete with agonists and recruit corepressors, respectively (Chabbert-Buffet *et al.*, 2005; Liu *et al.*, 2002). Therefore, further clinical investigations are ongoing to explore the use of PR agonist or antagonist in advanced BCa and for patients who have progressed from ET.

Amplification of the *ERBB2* gene, resulting in HER2 over-expression is found in around 20% of BCa and its presence is prognostic for poor clinical outcomes and increased risk of disease progression (Slamon *et al.*, 1987). Studies have shown the involvement of HER2 in activating the downstream Phosphoinositide 3 kinase (PI3K)/AKT/mTOR pathway, a key modulator of cancer cell proliferation, metabolism and survival (Goutsouliak *et al.*, 2020; Moasser, 2007). HER2 can also induce activation of the Ras/Raf/MEK/ERK pathway, which promotes cancer

cell growth and inhibits apoptosis (Dankort *et al.*, 2001; McCubrey *et al.*, 2007; Olayioye, 2001). Components of these signalling pathways are also often found to be mutated and/or amplified/lost (Saini *et al.*, 2013; Stemke-Hale *et al.*, 2008), with increased signalling through these pathways contributing to the aggressive nature of $HER2^+$ BCa.

The activation of the PI3K/AKT/mTOR and the Ras/Raf/MEK/ERK pathway is also common in TNBC, which accounts for around 10% of all BCa cases. Notwithstanding, TNBC is an aggressive form of BCa, with treatment options limited to chemotherapy, due to the lack of targeted therapies. This is, at least in part, likely to be because TNBC is comprised of several heterogeneous subgroups, as revealed by gene expression profiling (Curtis *et al.*, 2012; Foulkes *et al.*, 2010; Sorlie *et al.*, 2001). Many TNBCs are characterised by mesenchymal characteristics, high expression of immune system related genes and defective DNA repair pathways (Metzger-Filho *et al.*, 2012). While targeted therapies are currently limited, recent clinical studies provide evidence for the potential utility of immunotherapy drugs for treating at least some TNBC patients (Loibl *et al.*, 2019; Mittendorf *et al.*, 2020; Schmid *et al.*, 2020). The combination of immunotherapy such as pembrolizumab and durvalumab with chemotherapy showed a favourable outcome compared to the chemotherapy alone, patients demonstrated higher percentage of complete response (Loibl *et al.*, 2019; Mittendorf *et al.*, 2020; Schmid *et al.*, 2020).

Molecular classifications using expression profiles of 50 genes, the PAM50 signature, have emerged to further subdivide BCa groups into five different subgroups: luminal A, luminal B, HER2 overexpressing, basal-like and normal-like (Cancer Genome Atlas, 2012; Dowsett *et al.*, 2013; Perou *et al.*, 2000; Sorlie *et al.*, 2001). Most luminal A and luminal B groups are HR^+, but with luminal B BCa being associated with worse patient outcomes than luminal A. Luminal B BCa are often PR^- and $HER2^+$. Luminal A and B subtypes have also been differentiated on the basis of low or high expression of the proliferation marker, Ki67, respectively (Cheang *et al.*, 2009). Moreover, genetic profiling studies have also identified genomic alternations such as gene mutations and copy number alterations in oncogenes, as well as tumour suppressor genes such as TP53, PIK3CA and BRCA1/2. Distinct gene signatures and histological groups are useful for distinguishing clinical phenotypes and disease management in each BCa subgroup.



Molecular subtypes	Ki-67	ER/PR	HER2	Prevalence (%)
Luminal A	Low	+	-	50
Luminal B	High	+/-	+/-	20
Non-luminal	High	-	+/-	10-15
Basal	High	-	-	10-15

Figure 1.1. Histopathological and molecular analysis for breast cancer subtypes.
Systemic diagnostic techniques including clinical examination, histological and molecular analysis have therapeutic and prognostic implications. IHC and gene expression analyses are used to distinguish BCa subtypes: ER^+ PR^+ $HER2^-$ with luminal A and low proliferation marker, Ki-67 that is indicative of a good prognosis. $HER2^+$ with/without ER/PR expression that also features luminal B or non-luminal and high Ki-67 are indicative of a poor prognosis. ER^- PR^- HER2, basal-like and high Ki-67 also implicated to a poor clinical outcome. ER, estrogen receptor-alpha; PR, progesterone receptor; HER2, human epidermal receptor 2; IHC, immunohistochemistry. Figure was generated in BioRender

1.2 Estrogen receptor-alpha in breast cancer

1.2.1 Estrogen as a steroid hormone

Estrogen is a steroidal hormone that has a wide spectrum of regulatory and functional roles during development and in particular in reproductive processes, including mammary gland development, pregnancy and in the menstrual cycle (Couse and Korach, 1999). There are three major forms of circulating estrogen, estrone (E1), 17β-estradiol (E2) and estriol (E3), with E2 being the major form of circulating estrogen. In adult women, E2 synthesis occurs primarily in the ovaries and requires conversion from androgens by the aromatase enzyme (Figure 1.2). Additionally, small amounts of estrogen can be produced in peripheral tissues such as adrenal glands, adipose, bone and breast tissues, again requiring conversion of peripheral androgens by aromatase (Nelson and Bulun, 2001). E3 and E1 are mainly synthesised in the placenta during pregnancy and by aromatization of androstenedione by the aromatase enzyme in peripheral tissues in post-menopausal women (Nelson and Bulun, 2001). Epidemiological studies have shown that the length of the period from menarche to menopause is linked to the risk of developing breast cancer (Clemons and Goss, 2001; Key *et al.*, 2001). In particular, early onset of menarche and late age of onset of menopause have both been associated with increased risks of BCa development. The implication is that the lifetime of exposure to high, unopposed estrogen action promotes breast cancer development (Collaborative Group on Hormonal Factors in Breast, 2012). Additionally, disruption of estrogen release through menstrual cycles, as occurs during pregnancy and lactation, reduces BCa risk. Indeed, early age of first pregnancy, as well as multiparity compared with nulliparity, are both associated with reduced risk of BCa (Albrektsen *et al.*, 2005; Husby *et al.*, 2018). Together, these findings strongly support the premise that the lifetime of exposure to estrogens defines an important risk factor for BCa.

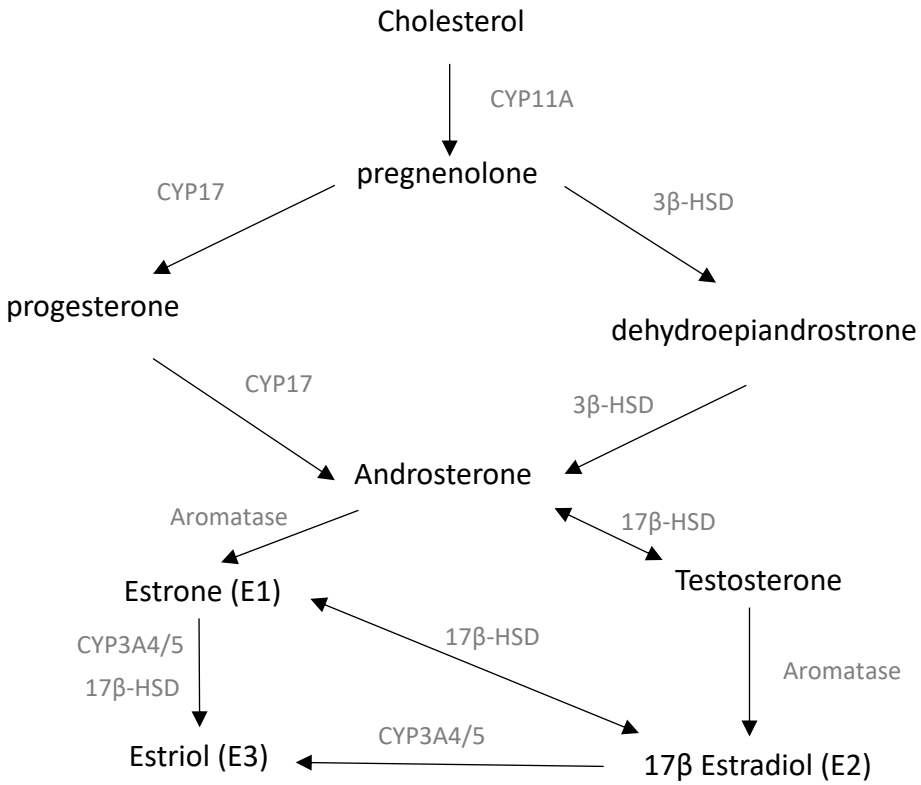


Figure 1.2. Estrogen biosynthesis pathway
Schematic showing the biosynthesis of endogenous estrogens. Enzymes involved in the biosynthesis pathway: 3β-HSD, 3β-hydroxysteroid dehydrogenase; CYP17, 17α-hydroxylase, 17β-HSB, 17β-hydroxysteroid dehydrogenase; CYP11A, cholesterol side chain cleavage enzyme; CYP3A4/5, 16α-hydroxylase. Diagram adapted from Farkas *et al* ., 2022.

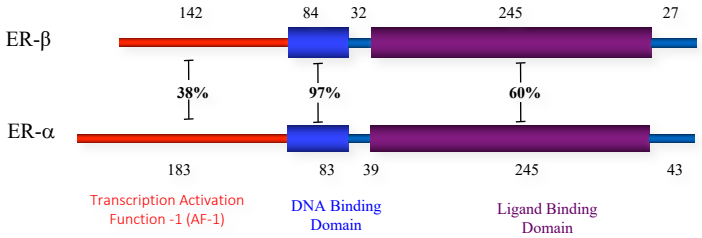
1.2.2 The estrogen receptor in mediating estrogen effects

The actions of estrogens are mainly mediated by their binding to estrogen receptors. Estrogen receptors are members of the nuclear receptor (NR) superfamily of ligand activated transcription factors, a 48-member family of related transcription factors in humans (De Bosscher *et al.*, 2020; Gronemeyer *et al.*, 2004). The NR superfamily in humans also includes steroid hormones receptors, PR, the androgen receptor (AR), glucocorticoid receptor (GR) and the mineralocorticoid receptor (MR). Additionally, retinoid receptors, vitamin D3 receptor, thyroid hormone receptors are included in this superfamily. Some NRs are important in lipid metabolism and detoxification processes, being activated upon binding to a wealth of dietary, as well as xenobiotic small molecules.

The first evidence for an estrogen receptor protein was provided in 1958 by Elwood Jensen, who demonstrated the cellular uptake of estrogen from circulation (Jensen *et al.*, 1967). The estrogen receptor-α (ERα) gene was successfully cloned by screening of a cDNA expression library using antibodies to ERα (Green *et al.*, 1986; Greene *et al.*, 1986). A homologue of ERα, named estrogen receptor-β (ERβ), was later discovered (Kuiper *et al.*, 1996; Mosselman *et al.*, 1996). Functional and structural studies have revealed that both ERs are comprised of an N-terminal domain (NTD) for gene transactivation and a highly conserved DNA binding domain (DBD) that enables the binding of ER to chromosomal DNA. Estrogen and coregulators can bind to ERs via the ligand binding domain (LBD) (Bourguet *et al.*, 1995; Schwabe *et al.*, 1993; Tanenbaum *et al.*, 1998). The LBD is one of the principal functional domains, which is located C-terminal to the DBD and shows strong homology (60% amino acid sequence identity) between the two ERs (Cowley *et al.*, 1997) (Figure 1.3A). The ERα and ERβ DBDs show an even higher degree of homology in sequence, with 98% amino acid sequence identity, whereas the NTD is much more divergent in sequence, sharing only 38% amino acid sequence identity (Cowley *et al.*, 1997). The N-terminal region is required for transcription activation and is named transcription activation function AF-1. The LBD is comprised of 12 α-helices arranged in three layers to form the hydrophobic ligand-binding cavity, with helix 12 (H12) flanking the ligand-binding pocket (Shiau *et al.*, 1998). Additionally, there is a region C-terminal to the ER-α LBD, known as the F-region. Although its exact function is unclear, some studies have provided evidence for the involvement of this region in regulating co-regulator recruitment,

receptor dimerization and receptor stability (Arao *et al.*, 2013; Koide *et al.*, 2007; Montano *et al.*, 1995).

A



B

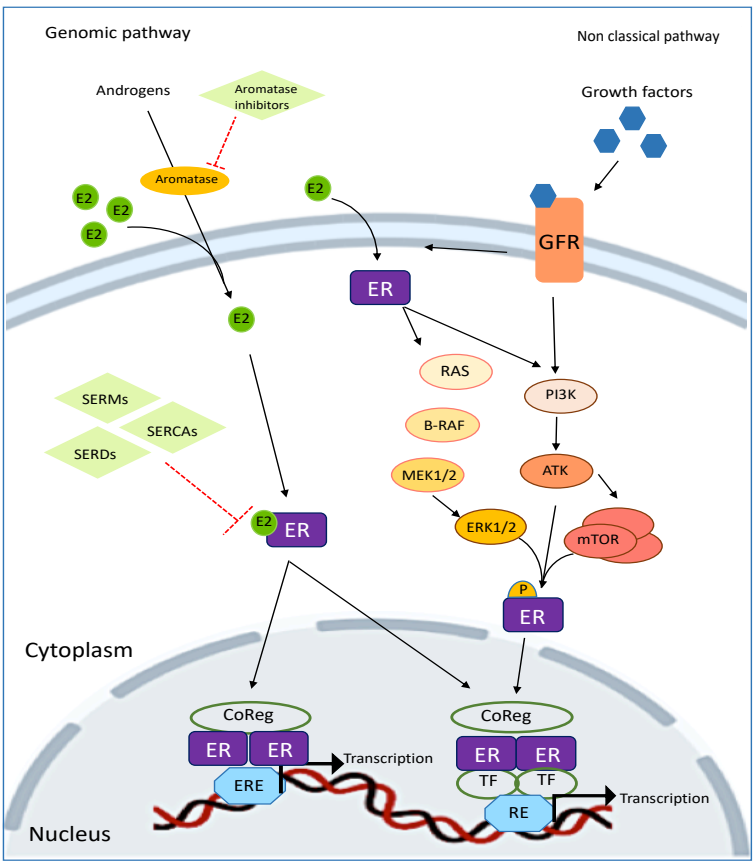


Figure 1.3. Estrogen receptor-alpha signalling.
(A) Schematic representation of the structural domains in human ER-a and ER-ß. The numbers above and below refer to the number of amino acids in each functional domain. The numbers in the centre (bold) show percentage amino acid sequence identity between ER-a and ER-ß in each structural domain. (B) ER-mediated transcription is a multistep process in which recruitment to gene regulatory regions allows the recruitment of transcriptional co-regulators that facilitate chromatin remodelling, to drive expression of ER target genes. Estrogen (E2) binding to ER promotes its dimerization and binding to estrogen response elements (EREs) in gene regulatory regions. Alternatively, ER can be recruited to gene promoters via interactions with other transcription factors. In addition to ER activation by binding E2, ER activity can be stimulated by phosphorylation at specific residues. Many kinases have been linked to ER phosphorylation, most prominently ERK1/2 MAPK, AKT and mTOR. There is evidence that estrogen binding to ER can promote PI3K and ERK1/2 MAPK activities, which may in turn promote the transcriptional activity of ER. SERMs SERDs and SERCAs inhibit ER activity by binding to ER, while AI inhibit estrogen biosynthesis, to prevent ER activation. AI, aromatase inhibitors; E2, estradiol; ER, estrogen receptor; ERE, estrogen response element; RE, response element; CoR, co-regulator; SERD, selective estrogen receptor degrader; SERM, selective estrogen receptor modulator; SERCA, selective estrogen receptor covalent antagonist. (A) Figure was kindly provided by Prof S. Ali. (B) Figure was generated using BioRender

ERα and ERβ have similar binding affinities for estrogen and bind to identical consensus DNA sequences known as estrogen response elements (EREs). However, they only share a subset of regulatory roles, such as in the development of the ovaries and in mediating the roles of estrogens in the cardiovascular system (Heldring *et al.*, 2007; Schwabe *et al.*, 1993). ERα is predominately expressed in uterine, mammary, liver and adipose tissues and is involved in development and regulation of the uterus and mammary gland. In contrast, ERβ is mainly expressed in the bladder, cells of the immune system, ovaries and prostate and has been implicated in regulatory roles in the immune system and the central nervous system (Taylor and Al-Azzawi, 2000). Notwithstanding, gene knockout (KO) studies in mice clearly demonstrate major physiological impacts in ERα KO mice, but with very mild phenotypes observed in ERβ KO mice (Couse and Korach, 1999). Certainly, ERα KO mice have only rudimentary mammary gland development, like those observed in aromatase (CYP19) KO mice (Fisher *et al.*, 1998). By contrast, mammary gland development in the pre-pubertal and adult stages, including differentiation during pregnancy and lactation are normal in ERβ KO mice (Couse and Korach, 1999). With the profound role of ERα contributing to BCa progression (discussed below) and the focus of this thesis, hereafter ERα will be referred as to ER, unless otherwise specified.

Binding of estrogen to the ER LBD stimulates ER-mediated transcription of target genes (Figure 1.3B). E2 diffuses through the cell and binds to ER in the nucleus. Upon binding of E2 to the ligand binding cavity, the LBD undergoes structural shifts, particularly in the positioning of H12, which promotes interactions with coactivator proteins (Brzozowski *et al.*, 1997; Pike *et al.*, 2000; Vajdos *et al.*, 2007). There is evidence that the unliganded ER is bound to heat shock protein complexes, upon E2 binding induces dissociation from heat shock proteins and receptor is translocated to the nucleus, a necessary step in appropriate dimerization (Stice and Knowlton, 2008). Most studies agree that both ERs are nuclear even in the absence of ligand, but that a small proportion of ER is present in the cytoplasm and may be associated with the cell membrane through interaction with cell surface receptors (Kocanova *et al.*, 2010). ER dimers are stabilised upon binding to DNA (Powell *et al.*, 2010). The DBD is composed of two zinc finger motifs, with the N-terminal zinc finger mediating specific DNA base contacts and the C-terminal zinc finger being involved in additional DNA contacts, but also for receptor dimerisation (Kumar and Thompson, 1999; Mader *et al.*, 1989). The E2-bound ER dimer binds to EREs in gene regulatory regions of ER target genes. The ERE is a palindromic sequence

conforming to the consensus sequence: 5'-AGGTCAnnnTGACCT-3' (Carroll *et al.*, 2005; Seiler-Tuyns *et al.*, 1986). Dissociation from heat shock proteins and recruitment to the chromatin upon E2 binding results in the activation of AF-1, alongside the E2-directed activation of the transcription activation function within the LBD. The transcription activation function of the LBD is named AF-2 and often represents sequences near the C-terminal end of the LBD, mainly H12 sequences.

There are no crystal structures available for AF-1 and it is believed to have a disordered structure. Phosphorylation of specific residues in AF-1 can modulate ER activity and regulate ER degradation (Dutertre and Smith, 2003; Rogatsky *et al.*, 1999; Thomas *et al.*, 2008). In some contexts, phosphorylation at these residues, particularly serine 118 (Ser118) can promote ligand-independent ER activation. Indeed, Ser118 is the most well-characterised ER phosphorylation site, which has been shown to be phosphorylated by several protein kinases including extracellular signal-regulated kinases 1 and 2 (ERK1/2) (Kato *et al.*, 1995), cyclin dependent kinase 7 (CDK7) (Chen *et al.*, 2000; Chen *et al.*, 2002b) and mammalian target of rapamycin (mTOR) (Anbalagan and Rowan, 2015). There is considerable *in vitro* evidence to demonstrate that activation of the mitogen activated protein kinase (MAPK) (ERK1/2) pathway can promote ER-mediated gene expression in the absence of E2, through the phosphorylation of Ser118 and possibly other phosphorylation sites in AF-1, particularly Ser104 and Ser106 (Likhite *et al.*, 2006; Thomas *et al.*, 2008; Vendrell *et al.*, 2005). Another key phosphorylation site in AF-1 is Ser167. Ser167 can be phosphorylated by the p90 ribosomal S6 kinase (p90RSK), which itself is activated by ERK1/2, casein kinase 2 (CK2), mTOR/p70SK6 and AKT (Murphy *et al.*, 2011). Ser167 phosphorylation can also promote the recruitment of coactivators and enhance ER activity (Arnold *et al.*, 1994; de Leeuw *et al.*, 2011; Joel *et al.*, 1998; Yamashita *et al.*, 2005). Moreover, the activation of AKT promotes ER recruitment to specific ER binding regions, indicative of estrogen-independent ER activation by AKT-mediated ER phosphorylation (Bhat-Nakshatri *et al.*, 2008). While these findings provide *in vitro* evidence for the importance of crosstalk with other signalling pathways in regulation of ER activation, *in vivo* confirmation has been best demonstrated for uterine proliferation. Uterine proliferation is estrogen- and ER-dependent. Studies from several groups demonstrated that epidermal growth factor (EGF) can promote uterine proliferation in ovariectomised mice (Ignar-Trowbridge *et al.*, 1992; Nelson *et al.*, 1991). The EGF-mediated

uterine proliferation was blocked by anti-estrogens and was abrogated in ERα KO mice (Curtis *et al.*, 1996). While these studies have not provided direct confirmation of AF-1 phosphorylation being required for this crosstalk, they do demonstrate that ER can be activated in a ligand-independent manner by growth factor signalling cascades that activate the RAS/RAF/MEK/MAPK and PI3K/AKT/mTOR pathways. Other post-translational modifications such as ubiquitination, acetylation and methylation in different domains have also been shown to be important for regulating DNA binding and dimerization, protein stabilisation and transcription activation by ER (Le Romancer *et al.*, 2011).

A key step in recruitment of ER to its binding sites in chromatin, has been revealed by defining genome-wide binding of ER using chromatin immunoprecipitation (ChIP), followed by hybridisation to tiled arrays (ChIP-chip) or next generation sequencing (ChIP-seq). These studies have revealed the importance of pre-existing transcription factors (TF), for directing and allowing ER binding. These so-called pioneer factors are believed to aid decompaction of closed chromatin, to permit ER recruitment to DNA. Key factors among these pioneer factors are the forkhead box protein A1 (FOXA1) and GATA binding protein 3 (GATA3) (Carroll *et al.*, 2005; Eeckhoute *et al.*, 2007; Laganiere *et al.*, 2005; Takaku *et al.*, 2016). ChIP-chip and ChIP-seq studies also demonstrated that most ER binding occurs at gene regulatory regions known as enhancers that are located at considerable distances from the transcription start sites of regulated genes (Kubo *et al.*, 2021; Schoenfelder and Fraser, 2019; Welboren *et al.*, 2009). ER recruitment stimulates the subsequent recruitment of transcriptional coactivator complexes such as p160 family members and p300 that promote chromatin remodelling and modification, to allow for transcription initiation by RNA polymerase II (PolII) (Farcas *et al.*, 2021; Kim *et al.*, 2006; Xu and Li, 2003). Several studies have shown that chromatin looping between ER and recruited coactivator complexes in gene enhancers facilitates interaction between the enhancers and promoters that aids transcription initiation of ER targets such as PDZK1 and that have a role in proliferation and invasion (Carroll and Brown, 2006; Fullwood *et al.*, 2009). Furthermore, studies also suggest the involvement of the ER/FOXA1/GATA3 axis in the development of ER^+ BCa. Hence, the expression of FOXA1 is considered as a good prognosis factor and a marker of response to ET (Bernardo *et al.*, 2010; Carroll and Brown, 2006; Kouros-Mehr *et al.*, 2006; Oh *et al.*, 2006; Yan *et al.*, 2010).

Besides directly binding to EREs in enhancer regions, ER can be recruited by interaction with other, DNA-bound transcription factors (TFs) (Safe and Kim, 2008). In this context, ER is able to regulate gene expression through protein-protein interactions with other TFs (Gottlicher *et al.*, 1998). For example, several estrogen responsive genes have been shown to contain GC-rich regions or half ERE sites where ER is able to bind directly to the DBD of the SP-1 protein. For example, ER-mediated stimulation of E2F1 has been reported to require ER recruitment via interaction with SP1 and NFYA (Ngwenya and Safe, 2003; Wang *et al.*, 1999). Another well-described tethering factor for ER is AP-1 (Shaulian and Karin, 2002; Teyssier *et al.*, 2001). In turn, ER signalling initiates transcription of downstream genes such as CSTD, CCND, PZDK1 and GREB1, which is involved in estrogen mediated proliferation and also contributes to BCa progression and metastasis (Bretschneider *et al.*, 2008; Ghosh *et al.*, 2000).

The mechanisms by which ER acts as a transcription factor, being recruited by direct binding to EREs, or indirectly via interactions with other TFs, are well-defined. Interestingly, there is also evidence that ER can act in a non-genomic fashion to activate several protein kinase signalling cascades (Acconcia and Kumar, 2006). There is evidence for plasma membrane localisation of a small proportion (5-10%) of ER (Pedram *et al.*, 2006) and rapid activation of cAMP activity (Aronica *et al.*, 1994), calcium mobilisation (Improta-Brears *et al.*, 1999), MAPK activation and PI3K/AKT activation. leading to activation of the MAPK cascade. E2-mediated activation of MAPK promotes phosphorylation of ELK1, C/EBPβ and cAMP response element-binding (CREB) protein (Bonni *et al.*, 1999; Buck *et al.*, 1999; Cruzalegui *et al.*, 1999; Driggers and Segars, 2002). The rapid activation of protein kinase cascades provides the means of rapid enhancement in the transcriptional response to estrogens (Hammes and Levin, 2007).

However, non-genomic actions of estrogen can also be attributed to the more recently described G-protein coupled estrogen receptor (GPER, also known as GPR30) (Prossnitz and Barton, 2011; Xu *et al.*, 2019). GPER has been shown to mediate non-genomic action of E2 that would be independent of nuclear ER. Among the activities attributed to GPER are calcium mobilisation, cAMP generation and PKA activation, as well as c-SRC activation leading to PI3K/AKT and MAPK activation. It is likely, therefore, that some rapid non-genomic actions of estrogens are due to GPER and not ER. Previous studies have shown in the combination

treatment of estrogen and GPER agonist led to the upregulation of genes such as CCNA, CCND1, CCNE, vascular endothelial growth factor (VEGF) and ERK that contributes to tumour progression (Albanito *et al.*, 2007; Filardo *et al.*, 2000; Prossnitz and Barton, 2014).

1.2.3 Estrogen receptor-alpha in normal mammary gland development

As mentioned previously, ERα plays the predominant role at all stages of estrogen-driven mammary gland development (Feng *et al.*, 2007). The mammary gland is composed of a rudimentary ductal tree that is embedded in a fatty stroma. The ductal tree undergoes elongation and branching during puberty in response to E2. The ductal epithelial layer consists of luminal epithelium responsible for milk production and the outer layer of basal myoepithelial cells with contractile properties for milk expulsion. The myoepthelial cells also play a critical role in laying down the basement membrane surrounding the epithelial layer. ERα is mainly found to have a heterogeneous expression in the lobules and ducts of breast tissue, being expressed in around 10% of luminal epithelial cells. In mice, ERα-positive cells stimulate the growth of surrounding ERα negative cells through paracrine signalling and ERα KO models showed absence of ductal maturation (Walker and Korach, 2004). During the follicular stage in menstruation, the levels of ERα in mammary epithelial cells increases and is responsible for the proliferation of epithelial cells in response to high levels of E2. As stated above, there is very little apparent role for ERβ in mammary gland development, at least in mice (Krege *et al.*, 1998).

1.2.4 The role of Estrogen receptor-α in breast cancer

The first observation linking menopause and breast atrophy in the 1860s, offered a possible connection between ovarian function and BCa progression. The subsequent demonstration by Sir George Beatson that oophorectomy causes tumour regression in premenopausal women with metastatic breast cancer (Beatson, 1896), provided clear evidence for the importance of hormonal regulation in BCa. Subsequent work identified the ovarian hormone estrogen as being necessary for breast development and in the development and progression of BCa (see Ali and Coombes (2002)). As described above, ER has a role in normal breast tissue

development and maintenance. However, in response to abnormal growth or mitogen signals which activates ER-mediated transcription, ultimately leading to tumour growth in ER^+ BCa. In particular, the increased expression of ER can also be found in normal tissue or in benign tumours that becomes more sensitive to estrogens, thus increasing the risk of developing ER^+ BCa (Khan *et al.*, 1998; Woolcott *et al.*, 2008). The elevated expression of ER drives the transcription of estrogen responsive genes, leading to the deregulated expression of proliferation- and survival-related genes (Manavathi *et al.*, 2013). In addition, the dysregulated ER and its coactivators such as p300/CBP and SRC1/2/3 are involved in epigenetic reprogramming and the recruitment of further transcription factors favouring tumour progression (Farcas *et al.*, 2021). ER can also promote tumorigenesis as a response to mitogen signalling such as EGF and tumour necrosis factor-α (TNF-α) via MAKP and IKK-β that phosphorylate ER to promote its binding to chromatin independently of E2 (Siersbaek *et al.*, 2018). Collectively, ER plays a central role in mediating the initiation and progression of ER^+ BCa and the presence of ER is often considered as a good prognosis factor due to response to ET as adjuvant therapies in ER^+ BCa (see Section 1.2.5).

1.2.5 Endocrine therapy for ER-positive breast cancer

ER is expressed in 70-80% of all BCa. Patients with ER^+ BCa are treated with drugs that prevent estrogen biosynthesis by inhibiting the aromatase enzyme, which converts androgens to estrogens (Figure 1.2). Indeed, aromatase inhibitors (AIs) are currently the first line adjuvant agents for most post-menopausal patients with ER^+ BCa. For pre-menopausal women, estrogen blockade is achieved with the use of of luteinzing hormone releasing hormones (LHRH) agonists, which block gonadotrophin release by the pituitary, to inhibit estrogen release in the ovaries.

Direct targeting of ER provides the second approach to inhibiting ER activity. Drugs in this category are anti-estrogens, which work by competing with estrogen for binding to ER and inhibit ER activity through several distinct modes of action. The first, selective ER modulators (SERMs) are typified by tamoxifen. Alternatively, drugs can act by binding of selective ER downregulators (SERDs) that promote ER degradation, as exemplified by fulvestrant.

Tamoxifen (Nolvadex™) was the first anti-estrogen to be used for treating ER^+ breast cancer and it was the first target-directed cancer drug (Bange *et al.*, 2001) to be developed clinically. Its active metabolite, 4-hydroxytamoxifen, binds to the ER in competition with estrogen. Its binding to ER promotes ER dimerization and recruitment to DNA. However, rather than promoting co-activator recruitment and consequently inducing expression of ER target genes, the tamoxifen-bound ER recruits transcriptional co-repressors, leading to inhibition of ER target gene expression. Interestingly, these anti-estrogenic actions of tamoxifen are tissue-specific. In other tissues, most prominently bone and uterus, tamoxifen is an estrogen agonist, promoting expression of ER target genes in those tissues. One possible mechanism for the mixed agonist/antagonist actions of tamoxifen are the different co-activator expression profiles in different tissues, whereby high expression of SRC1 in uterine cancer cells, compared with breast cancer cells, promotes its binding to tamoxifen-ER, to stimulate gene expression, whereas the different co-activator expression in BCa cells results in inhibition of ER target gene expression by tamoxifen-ER (Garcia-Martinez *et al.*, 2021; Shang and Brown, 2002). These mixed agonist/antagonist properties of tamoxifen and related anti-estrogens has led to the development of a series of additional SERMs, such as raloxifene. Tamoxifen initially gained success in treating metastatic BCa in postmenopausal patients in the 1970s and subsequently progressed to becoming the first-line adjuvant agent for the treatment of ER^+ breast cancer in premenopausal, as well as postmenopausal patients, either as a monotherapy in post-menopausal women or in combination with LHRH agonists in pre-menopausal women. In early stage BCa the use of tamoxifen as a five-year adjuvant therapy reduces the annual risk of recurrence by about 50% and breast cancer morality by 33% (Early Breast Cancer Trialists' Collaborative *et al.*, 2011). While there are clinical benefits to the extended use of tamoxifen for up to 10 years in prolonging progression free survival (PFS) (Davies *et al.*, 2013), clinical evidence of tamoxifen acting as an agonist in other tissue types, particularly in an increased risk of endometrial cancer development and venous thromboembolic events has meant that tamoxifen treatment has historically been limited to 5 years (Bergman *et al.*, 2000; Cuzick *et al.*, 2010). The agonistic properties of tamoxifen and the non-responsive population of BCa patients has prompted the development of other SERMs. The chief aim of alternative SERM development has been to maintain the anti-estrogenic activity of tamoxifen but agonist activities in other tissues, particularly the endometrium (Ali et al., 2011). Raloxifene, for example is an anti-estrogen in the breast, but does not have agonist activity in the endometrium

(Rey et al., 2009). Other SERMs that have been evaluated in the clinic include lasofoxifene and bazedoxifene

Fulvestrant (Faslodex^{TM}), discovered by ICI (now AstraZeneca), is a potent anti-estrogen. The chief modes of action of fulvestrant are inhibiting ER dimerization, ER export from the nucleus and accelerated ER degradation and consequent lack of clear agonistic activity in any tissue (Traboulsi *et al.*, 2017). The ER degradation promoting activity of fulvestrant has led to this class of anti-estrogen being named as selective ER downregulators (SERDs). Originally used clinically for treating patients with metastatic breast cancer following progression on tamoxifen or AI, recent successes in combination with other targeted therapies, especially CDK4/6 inhibitors (see below), fulvestrant is being moved towards first-line adjuvant use (Robertson *et al.*, 2016). However, an important limitation of fulvestrant is that it is not orally bioavailable, necessitating 4-weekly intramuscular injection. In consequence, several new SERDs have been developed (Fanning and Greene, 2019), some of which are in late-stage clinical trials.

Two newer classes of anti-estrogens include ER-binding PROTACs (proteolysis targeting chimera). These are mostly based on the structure of estrogen or an anti-estrogen, but with additional motifs that promote targeting of ER for ubiquitination and subsequent proteasomal degradation (Lin *et al.*, 2020), as exemplified by ARV-471 (Flanagan *et al.*, 2019). ARV-471 entered phase I/II clincial trials alone vs in combination with CDK4/6 inhibitor, palbociclib (clinical trial information: NCT04072952) or mTOR inhibitor, everolimus (clinical trial information: NCT05501769). Finally, a class of anti-estrogens known as selective ER covalent antagonists (SERCA) act by covalently binding ER and acts as an ER antagonist (Puyang *et al.*, 2018). Even though ER PROTACs and SERCAs appear promising, they have only recently been developed and are in early-stage clinical assessment. One of these SERCAs, H3B-6545, has progressed to phase 1/2 clinical trials in advanced ER+ breast cancer patients as a single agent or in combination with CDK4/6 inhibitors (Hamilton *et al.*, 2021)

A distinct class of ET, known as AIs, function by targeting the aromatase enzyme, which catalyses the aromatisation of androgens to various estrogens, including E2. In postmenopausal

women, the main source of circulating estrogens is through conversion of adrenal androgens in peripheral tissues such as the skin, liver and adipose tissue (Miki *et al.*, 2007; Nelson and Bulun, 2001). There are two main classes of AIs. Noncovalent nonsteroidal AI (letrozole and anastrozole) are reversible inhibitors that bind competitively to the substrate binding site in aromatase. Alternatively, the covalent steroidal AI irreversibly inactivates aromatase. This is exemplified by exemestane which is generally used as second-line adjuvant agent, following progression on the non-steroidal, reversible AI (Bertelli *et al.*, 2005).

In pre-menopausal women suppression of ovarian function and consequently estrogen release is achieved with LHRH agonists, to disrupt the pituitary-ovarian axis for estrogen release by the ovary, as described above. Pre-menopausal women are treated with ovarian suppression drugs together with tamoxifen. Due to the very high aromatase activity in the ovaries of pre-menopausal women, AI have largely not been used in pre-menopausal women. However, recent work demonstrates that using an AI with ovarian suppression reduces the risk of BCa recurrence better than achieved with tamoxifen (Early Breast Cancer Trialists' Collaborative, 2022).

1.2.6 Resistance to Endocrine Therapies – the clinical problem and possible mechanisms

ET has proven highly efficacious in ER^+ advanced BCa and countless patients have benefited from ET with a prolonged PFS. However, many patients show intrinsic resistance and many other patients eventually become resistant to ET and relapse. A recent metadata analysis demonstrated a steady year-on-year increase in the risk of reoccurrence in ER^+ BCa patients extending over 20 years following initial presentation Pan *et al.* (2017). Indeed, near 20% of patients who presented with low grade tumours and had no involvement of the lymph nodes relapsed over this period. This rises to >49% of patients who had high tumour grade and/or lymph node positivity at presentation. Furthermore, a separate study showed the increase in mortality rate is correlated to ER status (Jayasekara *et al.*, 2019). As the data suggest, ER^- BCa patients had initial poor response but the risk of cancer related deaths peaks at 3 years after

diagnosis and subsequently the chance of mortality falls rapidly. However, in ER^+ BCa, the risk is increased in proportion to time after initial diagnosis, despite treatment with ET.

Recent studies have investigated genetic changes that accompany development of endocrine resistance. One such study of 1500 metastatic, relapsed ER^+ patients for mutational analysis of a panel of genes demonstrated that mutations in the ER LBD were enriched in 18% of patients progressing after ET (Razavi *et al.*, 2018). In an equal proportion of cases, mutations in components of the MAPK and AKT pathways or EGFR mutation/amplification was enriched, while a further 9% of resistant tumours were associated with mutation/alteration in MYC. Other studies have highlighted additional genes whose mutations are enriched following progression on ET (Rinaldi *et al.*, 2020). One example is loss-of-function mutations in ARID1A, a component of the SWI/SNF complex that mediates chromatin remodelling. Mutations in ARID1A can lead to reduced binding of ER and FOXA1 to the chromatin which may promote luminal-basal transition (Xu *et al.*, 2020). In addition, missense/frameshift mutations in C-terminal forkhead domain of FOXA1 are found in metastatic BCa (around 4.88%) resulting in increased FOXA1 activities and binding to de novo enhancers, thus suggesting that FOXA1 mutations also contribute to ET resistance (Arruabarrena-Aristorena *et al.*, 2020; Fu *et al.*, 2019; Robinson and Carroll, 2012). Epigenetic reprogramming including altered DNA methylation and histone modifying activities as a force for the development of ET resistance has also been suggested by several studies. For example, histone H3 lysine 27 acetylation (H3K27ac), which is associated with transcriptionally active chromatin was found to be profoundly altered in long-term estrogen deprived (LTED) MCF7 cells. These changes led to the upregulation of cholesterol biosynthesis pathways in BCa cells that may lead to local biosynthesis of alternative ER ligands (Nguyen *et al.*, 2015; Simigdala *et al.*, 2016). Increased activities of KDM5 histone demethylases is associated with reduced H3K4me3 levels and increased transcriptomic heterogeneity leading to reduced sensitivity to anti-estrogens (Garcia-Martinez *et al.*, 2021; Hinohara *et al.*, 2019). In sum, resistance to ET frequently arises from therapy-directed genetic alterations (e.g. *ESR1* mutations, EGFR/MAPK alterations (Razavi *et al.*, 2018) and epigenetic reprograming that work by altering ER activity or through the activation of ER-independent growth and survival pathways.

1.2.6.1 Mutations in the *ESR1* gene as a mechanism for acquired resistance to endocrine therapies

Many *in vitro* studies investigating the mechanisms of ER action identified residues whose mutation results in constitutive ER activity and resistance to anti-estrogens, including leucine-536 (L536) and tyrosine-537 (Y537) in the ER LBD (Figure 1.4). However, despite intensive sequencing efforts, mutations in the ER (*ESR1*) gene were shown to be extremely rare in primary breast cancer (Fuqua and Cui, 2004). Improvements in DNA sequencing technologies have facilitated genomic analysis of metastatic breast cancer biopsies. These studies have confirmed that *ESR1* mutations are indeed rare in primary BCa. By contrast, the *ESR1* mutations are quite common in advanced, ET-resistant BCa, with some studies identifying mutations in >50% of metastatic tumours; although the consensus is that around 18-20% of advanced, ET-resistant BCa have *ESR1* mutations (Razavi 2018; Rinaldi 2020). Mutations in Y537 and aspartate-538 to glycine (D538G) are the most common mutations, with mutations at other sites within the LBD being less frequent. Functional studies using mutant over-expression or CRISPR-Cas9 mediated gene knockin mutagenesis reveal that the mutant ERs are estrogen-independent for their growth and drive expression of ER target genes in the absence of estrogen. Some, although not all, mutations also reduce sensitivity to SERMs and SERDs (Toy *et al.*, 2017). Taken together, these studies confirm the rarity of *ESR1* mutations in endocrine therapy naïve tumours and a considerable enrichment in tumours from patients who have progressed on ET. This topic has also been covered comprehensively in numerous reviews (e.g. (Herzog and Fuqua, 2021; Jeselsohn *et al.*, 2015; Katzenellenbogen *et al.*, 2018). Although *ESR1* mutations demonstrably show estrogen-independent activity and hence drive expression of ER target genes in the absence of estrogen, there is also evidence of mutant ER specific transcriptional event, which appear to promote motility and invasion of *ESR1* mutant BCa, as well as altering immune responses (Li *et al.*, 2022a; Li *et al.*, 2022b; Williams *et al.*, 2021).

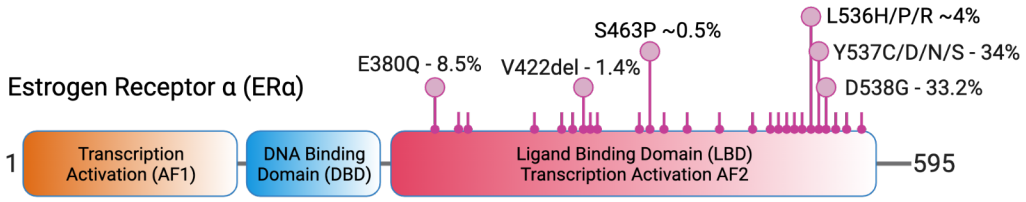


Figure 1.4. Frequency of ESR1 mutations.
Schematic showing the most common ESR1 mutation hotspots and frequencies of mutations (%) in advanced breast cancer (Rinaldi *et al.,* 2020). Figure provided by Prof. S. Ali.

ESR1 mutations are almost exclusively present in the LBD and cause estrogen-independent activation of ER. The mutant ERs are inhibited by anti-estrogens, although some mutants may be insensitive at clinical doses of anti-estrogens. Another alteration in the *ESR1* gene is fusions with diverse partner genes, in which the fusion protein lacks most of the ER LBD and would therefore be constitutively active, but are also insensitive to anti-estrogens, including PROTACs and SERCAs. This is because all anti-estrogens, including SERCas and PROTACs require binding to the LBD. The first of these *ESR1* fusions to be fully described was a fusion of intron 6 of the *ESR1* gene to sequences within intron 3 of the *YAP1* gene, in a PDX tumour developed from a patient who had progressed on prior endocrine therapies (Li *et al.*, 2013). This resulted in an ER protein containing amino acids encoded within the first 4 *ESR1* coding exons, in frame with amino acids encoded within exons 4-9 of the *YAP1* gene. Subsequent studies have reported many other fusion partner genes in advanced, endocrine therapy refractory breast cancer (Gou *et al.*, 2021; Hartmaier *et al.*, 2018; Matissek *et al.*, 2018). The ER LBD sequences are lost in all described *ESR1* fusion genes, while maintaining the AF-1 and DBD, such that the fusion proteins can be recruited to ER binding region, to promote estrogen-independent gene expression (Gou *et al.*, 2021). Since the lack of the LBD means that the fusion proteins are completely insensitive to anti-estrogens, there would be a need for alternative therapeutic approaches in these patients. While *ESR1* fusion genes appear to be relatively rare, identified in only 1-2% of ET-resistant BCa, their rarity compared with activating *ESR1* mutations may be due to the type of ET used. Thus, most *ESR1* mutations have been identified in patients treated with AI. If the use of SERDs moves towards becoming the first-line adjuvant treatment in some patients, perhaps the frequency of *ESR1* fusions detected will increase.

1.2.6.2 Upregulation of mitogenic pathways in ET resistance

There is a considerable history demonstrating elevated receptor tyrosine kinase receptor expression and/or activity in following acquisition of endocrine resistance *in vitro* (AlFakeeh and Brezden-Masley, 2018; Hanker *et al.*, 2020; Sanchez *et al.*, 2011; Servetto *et al.*, 2021). Implicated receptors include EGFR, HER2, FGFR1 and IGFR1. Their increased activities have been linked to downstream hyper-activation of RAS/RAF/MEK/ERK and PI3K/AKT/mTOR pathways and consequent growth of resistant breast cancer cell lines in the absence of estrogen (long-term estrogen-deprivation (LTED) models), or in the presence of anti-estrogens, such as

tamoxifen and fulvestrant. Genomic studies have provided confirmation of these findings in patient samples. For example, as mentioned above, Razavi *et al.* (2018) reported that approximately 20% of metastatic, endocrine-resistant breast cancer biopsies had gains in copy number alterations and/or mutations in EGFR, HER2 or in the downstream RAS/RAF/MEK/ERK genes. Interestingly, mutations in this pathway were excluded from metastatic tumours that acquired *ESR1* mutations. The reason for this exclusivity may be due to the absence of a need for upregulation of ERK activity when ER mutations can drive BCa growth. Conversely, mutations in the ERK pathway can result in increased ER activity, including estrogen-independent ER activation (see ER phosphorylation in section 1.2.2), thus obviating the need for ESR1 mutations. Other work has revealed acquired HER2 mutations (~6%) in ER^+ metastatic breast cancer (Nayar *et al.*, 2019; Razavi *et al.*, 2018), inactivating mutations in NF1 (~5%) (a negative regulator of RAS activation (Pearson *et al.*, 2020; Razavi *et al.*, 2018)) and FGFR1 (~22%) (Kingston *et al.*, 2021).

The aforementioned publications provide evidence that genetic alterations promote acquisition of endocrine resistance by causing upregulation in mitogenic and/or survival signalling pathways. It is important to note that gene alterations in these pathways are also common in primary, treatment-naïve ER^+ breast cancer, where they presumably act to promote cancer cell proliferation and aid cell survival. Indeed, activating mutations in PIK3CA are present in about 40% of primary ER^+ breast cancer, while mutations or gene rearrangements in diverse other cell signalling, as well as cell cycle related genes is also frequently observed (Nik-Zainal *et al.*, 2016). Mutations in the ESR1 gene, by contrast, are uncommon in primary, treatment-naïve breast cancer. ESR1 mutations are only observed in approximately 1% of primary breast cancer, compared with 20-40% of advanced post-endocrine therapy breast cancer (Zundelevich *et al.*, 2020)

ER^+ BCa also has a high prevalence of mutations in the PI3K/ATK/mTOR pathway often encountered at the PIK3CA, PTEN and AKT1 genes. These also result in alternative activation of ER and resistance to ET, although mutations in the PIK3CA gene have been correlated with preferential clinical outcome in early ER^+ BCa (Kalinsky *et al.*, 2009; Loi *et al.*, 2010). Dysregulation in this signalling pathway became exciting drug targets to overcome ET resistance. Alpelsib, a PIK3CA inhibitor, has shown promising results when used in

combination with fulvestrant, with an improved PFS (combination therapy of 11 months vs 5.7 months in the placebo + fulvestrant) (Andre *et al.*, 2019). Several clinical trials are ongoing to validate efficacy and safety of this treatment combination (NCT02437318 and NCT03056755). The use of AKT inhibitors is also an attractive option to overcome ET resistance. Capivasertib, an AKT inhibitor was shown to have response in combination with fulvestrant in both ET sensitive and ET resistant models (Davies *et al.*, 2012). This encouraged the phase II clinical trial using an AKT inhibitor in combination with fulvestrant in BCa patients who progressed on previous AI treatment (Jones *et al.*, 2020). A significant improvement in the PFS (10.3 vs 4.8 months) was shown in the combination group compared to the placebo group. Furthermore, mTOR in the PI3K/AKT pathway is an interesting therapeutic target and with its success in multiple clinical trials, the mTOR inhibitor, everolimus plus the AI exemestane, is clinically approved for advanced ER^+ BCa in postmenopausal patients. The use of everolimus with exemestane or tamoxifen in two independent clinical trials has shown success in prolonging PFS of 10.6 vs 4.1 months (Bachelot *et al.*, 2012) and 18.5 months vs 12.4 months (Baselga *et al.*, 2012) in patients who developed resistance to nonsteroidal AIs. However, the efficacy of everolimus is limited, as shown in the BOLERO-2 trial, where the combination therapy resulted in better PFS but did not improve overall survival (OS) (Piccart *et al.*, 2014).

1.3 Cell cycle Regulators in ER^+ Breast Cancer

Cell proliferation must be tightly controlled, to prevent inappropriate replication and survival of damaged cells. Most importantly, progression through the different phases of the cell cycle requires appropriate passage through a series of checkpoints that ensure faithful and accurate DNA replication and that DNA damage due to spontaneous, or exogenous agents is correctly repaired (Figure 1.5). Failure to suitably repair DNA damage can lead to induction of cell death or apoptosis. Cancer cells inevitably show some dysregulation of cell cycle control that leads to abnormal proliferation in response to mitogenic signalling, which is one of the hallmarks of cancer (Hanahan and Weinberg, 2011). Understanding cell cycle defects in cancer has led to the development of many drugs targeting aspects of cell cycle progression. Most pertinent for the work presented in this thesis, is development of CDK4/6 inhibitors, which prevent cell cycle progression and so cause growth arrest by blocking cells in the G1 phase.

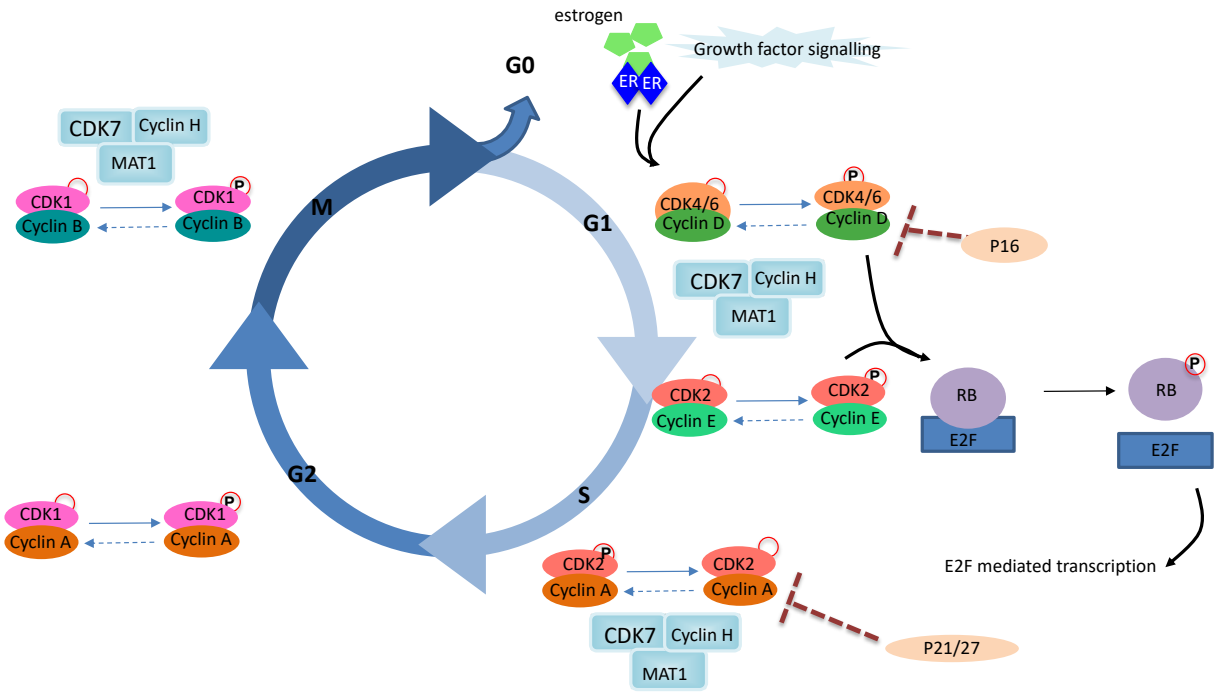


Figure 1.5. CDKs, cyclins and the cell cycle.
Cell cycle related CDKs binds to the cognate cyclins to form an active complex, sequential activation of CDKs and cyclins ensure an orderly progression through the cell cycle. Following cues from growth factors and ER signalling induces the expression of cyclin D and the binding of CDK4 and CDK6. CDK4/6-cyclin D complex is phosphorylated by CAK complex to allow cells re-entry into G1 phase from G0. During G1 phase, CDK4/6-cyclin D phosphorylates RB and releases the E2F transcription factor to allow the subsequent transcription of S phase components including CDK2, cyclin E, and cyclin A. CDK2 regulates entry into S phase by binding to cyclin E and it later adapts a new cyclin partner, cyclin A during S phase. CDK1-Cyclin A is formed and regulates progression through G2-M transition. CDK1 can also be activated by cyclin B specifically during M phase. CAK, CDK activating kinase; CDK, cyclin dependent kinase; ER, estrogen receptor; RB retinoblastoma protein.

1.3.1. Cell cycle progression regulated by cyclins and cyclin-dependent kinases (CDKs)

In normal homeostasis, the cell cycle is a tightly regulated process with an intricate network of checkpoints overseeing appropriate progression through the cell cycle. Cell cycle checkpoints are controlled by a group of proline-directed serine/threonine protein kinases known as cyclin dependent kinases (CDKs) that are activated upon binding to their cognate cyclin (Bertoli *et al.*, 2013; Matthews *et al.*, 2022; Morgan, 1997; Satyanarayana and Kaldis, 2009). Although there are around 20 CDK genes in humans (Malumbres, 2014), only CDK1, CDK2, CDK4 and CDK6 are directly involved in controlling progression through the cell cycle. There are four distinct stages in the cell cycle: G1, S, G2 and M-phase, with tightly regulated cyclin expression in each phase ensuring the sequential activation of specific CDKs and orderly progression through the cell cycle. Another key mode of regulation is provided by two CDK inhibitor (CDKI) gene families, the CIP/KIP (p21, p27, and p57) and the INK4 (p16, p15, p18, and p19) genes. Additional layers of regulation provide more subtle regulation of CDK activities, to modulate cell cycle progression. The subsections below describe some of the key events in regulation of the different phases of the cell cycle.

1.3.1.1 Negative regulation of cell cycle regulation by endogenous CDK inhibitors

The CIP/KIP genes are a three-membered gene family, which include the CDKN1A ($p21^{CIP1}$), CDKN1B (p27) and CDKN1C (p57) genes. A conserved N-terminal region in the CIP/KIP proteins is responsible for interaction with cyclin-CDK complexes. Other CIP/KIP partners have been described; most intriguingly the interaction of $p21^{CIP1}$ with proliferating cell nuclear antigen (PCNA) inhibits DNA replication by interfering with the processive movement of DNA polymerase δ during DNA chain elongation (Flores-Rozas *et al.*, 1994; Strzalka and Ziemienowicz, 2011; Waga *et al.*, 1994). The $p21^{CIP1}$ gene, CDKN1A, has long been understood to be a p53 target gene and indeed, its expression is rapidly induced upon p53 activation (Nguyen *et al.*, 2018). $p21^{CIP1}$ is found to bind to S phase and mitosis related CDK/cyclin complexes (CDK2-cyclin E and CDK4-cyclin D), resulting in their sequestration and inhibition of their activities (Xiong *et al.*, 1993).

In response to growth factor receptor activation, $p21^{CIP1}$ phosphorylation at Thr145 induces nuclear export and promotes its cytoplasmic degradation (Westbrook *et al.*, 2002; Zhou *et al.*, 2001). Likewise, c-SRC and AKT phosphorylate $p27^{KIP1}$, again inducing localisation to the cytoplasm. $p27^{KIP1}$ degradation is also fuelled by CDK2-cyclin E by phosphorylation at Thr187, which stimulates interaction with the S phase kinase-associated protein 2 (SCF^{Skp2}), E3 ubiquitin ligase, and consequently results in proteasomal degradation (Sabile *et al.*, 2006). Interestingly, the actions of $p21^{CIP1}$ and $p27^{KIP1}$ proteins extend beyond inhibition of cyclin-CDK activity. Among these, several studies have shown that CIP/KIP proteins can promote CDK4/6-cyclin D assembly and activities (Abbas and Dutta, 2009; Besson *et al.*, 2008; Cheng *et al.*, 1999; LaBaer *et al.*, 1997). The final CIK/KIP family member, $p57^{KIP2}$ inhibits CDK2, CDK4 and to a lesser extent, CDK1 and CDK6, through direct interaction with these cyclin-CDK complexes. $P57^{KIP2}$ also contains a proline and alanine rich central region for interaction with LIM-kinase (LIMK) during actin reorganisation, suggesting that $p57^{KIP2}$ has further functions outside direct regulation of cell cycle regulation (Yokoo *et al.*, 2003).

The INK4 family of CDK inhibitor proteins, $p16^{INK4a}$, $p15^{INK4b}$ and $p14^{ARF}$, mainly regulate CDK4/6 activities. While the CIP/KIP family interact with assembled cyclin-CDK complexes, INK4 proteins interact mainly with CDKs. The CDKN2A gene lies within the INK4/ARK locus on chromosome 9p21 that encodes for $p16^{INK4a}$ and acts as a tumour suppressor (Serrano, 1997). In response to oncogenic and senescence signals, transcription of $p16^{INK4a}$ is regulated by multiple TFs, for example E26 transformation specific 1 (ETS1), ETS2 and E47 that bind to the E-box motif in the promoter (Ohtani *et al.*, 2001; Zheng *et al.*, 2004). The presence of $p16^{INK4a}$ maintains the retinoblastoma protein (RB) in a hypophosphorylated state, which in turn represses E2F-regulated gene expression necessary for progression through G1. The suppressive activity of $p16^{INK4a}$ is dependent on the presence of RB (Medema *et al.*, 1995), since RB1 loss prevents its interaction E2F and consequent repression of E2F target genes. Additionally, INK4 proteins can bind to the T-loop of cyclin D that reduces the ability of cyclins to bind to CDKs (Jeffrey *et al.*, 2000; Russo *et al.*, 1998). $p15^{INK4b}$ can act as a tumour suppressor by increasing binding to CDK4 in the absence of $p16^{INK4a}$ by inhibiting the CDK4/6-cyclin D/RB axis (Krimpenfort *et al.*, 2007). In addition, $p14^{ARF}$ expression is activated by E2F1 and inhibits the E3 ubiquitin ligase activity of mouse double minute 2 (MDM2), which

in turn activates p53-dependent response, thus, subsequently inducing cell cycle arrest (Harris and Levine, 2005; Lowe and Sherr, 2003; Pomerantz *et al.*, 1998; Weber *et al.*, 1999).

1.3.1.2 Cell cycle: CDK4 and CDK6 mediates the entry of G0/1 phase

Most cells are arrested in G0 and re-entry into the cell cycle requires mitogenic signalling, such as growth factor signalling via activation of tyrosine kinase receptors (Figure 1.6). In turn, growth signals induce the expression of D-type cyclins, cyclin D1, cyclin D2 and cyclin D3 encoded by CCND1, CCND2 and CCND3 genes, respectively. Although they are encoded by three genes, their amino acid sequences have a high degree of similarity in their amino acid sequences. Interaction of CDK4 and CDK6 with cyclin D is necessary for their kinase activity and the CDK4/6-cyclin D complex formation results in phosphorylation of RB, which in turn inhibits the repressive interaction of RB with E2F (Baldin *et al.*, 1993; Kato *et al.*, 1993). The Cyclin D1 (CCND1) gene was the first D-type cyclin gene implicated in cancer through the t(11;14)(q13;q23) translocation of the CCND1 (BCL-1, PRAD1) gene on chromosome 11q13 to the immunoglobulin H (IgH) gene locus (chromosome 14q23) in B cell neoplasms (Erikson *et al.*, 1984; Tsujimoto *et al.*, 1984; Withers *et al.*, 1991). Parathyroid adenomas were also revealed to have rearrangements in the region of the BCL-1 locus (the gene was named PRAD1). The subsequent cloning of the gene demonstrated that the BCL-1/PRAD1 gene encodes, as was then a novel cyclin gene, now known as CCND1 (Arnold *et al.*, 1991; Matsushime *et al.*, 1991; Motokura *et al.*, 1991; Xiong *et al.*, 1991). The cyclin D1 protein consists of 293 amino acids, including a conserved cyclin box, RB binding motifs, a repressor binding domain, and a degradation domain containing a PEST sequence. Cyclin D1 has also been shown to bind to nuclear receptors such as ER, to promote their transcriptional activities in a CDK-independent manner (Zwijsen *et al.*, 1997). The cyclin box domain contains 11-α helices and an extended beta sheet including a region with a FLRRXSK motif that enables binding to CDK4/6 and is a substrate for the cyclic AMP (cAMP) activated protein kinase A (PKA). Cyclin D1 has two RB binding sites located at the N-terminal region, conforming to the consensus RB binding LXCXE sequence. The C-terminal region containing a polypeptide sequence rich in proline (P), glutamic acid (E), serine (S) and threonine (T) (PEST) domain that contains promotes nuclear localisation and stability but is also involved in cyclin D1 degradation. Phosphorylation of Thr286 within the PEST region by glycogen synthase kinase-

3 beta (GSK-3β) during the S phase promotes nuclear export and cyclin D1 proteolysis (Alao, 2007; Musgrove *et al.*, 2011) which acts to reduce cyclin D1 protein levels outside the G1 phase.

The cognate partners of D-type cyclins, CDK4 and CDK6 share 70% amino acid sequence homology with each other, which is considerably higher than their homology with other CDKs (Grossel and Hinds, 2006; Meyerson and Harlow, 1994). Crystallographic structure determination for the CDK4-cyclin D complex, demonstrated the interaction of cyclin D with the αC-helix of CDK4, however this assembly more closely resembles an 'inactive' CDK (Day *et al.*, 2009). Unlike other CDKs such as CDK2, the binding of its cognate partner cyclin D was not sufficient to provide the conformational changes for a fully activated CDK and how CDK4 is fully activated remains to be elucidated (Malumbres, 2014; Takaki *et al.*, 2009). Although CIP/KIP CDKIs have a role in inhibiting CDK activity, it was shown that during the G1 phase they can positively regulate cyclin D by promoting the nuclear import of cyclin D (Alt *et al.*, 2002). Upon formation of the CDK-cyclin complex, the catalytic cleft opens in preparation for T loop phosphorylation by the CDK activating kinase (CAK) (James *et al.*, 2008; Ray *et al.*, 2009). CAK phosphorylates CDK4 and CDK6 at Thr172 and Thr177, respectively (Bockstaele *et al.*, 2006; Tadesse *et al.*, 2015). T-loop phosphorylation alters the catalytic cleft of the T-loop to assist binding of cyclin to the CDK and enhances the kinase activity. CDK4/6 phosphorylate their targets at S/T-P-K/R or S/T-P-XXX-K/R motifs (Leng *et al.*, 2002; Songyang *et al.*, 1994).

In addition to the critical role of cyclin D proteins in binding to CDK4/6 for their activation, other functions for cyclin D1 have been forthcoming. A transcriptional role for cyclin D1 has been indicated by the demonstration that cyclin D1 regulates normal mouse development via direct interactions with gene regulatory regions such as the NOTCH1 gene promoter (Bienvenu *et al.*, 2010). Additionally, in a separate study of proteomic screen that revealed that CDK4/6-cyclin D can stabilise and activate the master regulator of the cell cycle, FOXM1 that leads to the entry of G1 phase (Anders *et al.*, 2011). FOXM1, is a member of the forkhead transcription factors, acting as the essential regulator of cell cycle progression, in particular G1/S and G2/M transitions (Laoukili *et al.*, 2005; Wang *et al.*, 2005). During the G1/S transition, FOMX1

activates DNA replication related genes such as MCM2, MCM10, MYB and CCNE2 (Anders *et al.*, 2011).

Previous studies have also suggested that cyclin D1 acts as prognostic factor indicative of a poor clinical outcome and high risk of relapse in ER^+ BCa and became a very attractive therapeutic target (Bieche *et al.*, 2002; Qie and Diehl, 2016). In breast adenocarcinoma tumours approximately 20% feature an amplification of the cyclin D1 gene (*CCND1*) and as much as 60% of ER^+ breast cancers have increased levels of cyclin D1 protein (Arnold and Papanikolaou, 2005; Lundberg *et al.*, 2019; Santarius *et al.*, 2010). This elevated expression of cyclin D1 may act to promote cell cycle progression. The PI3K/AKT/mTOR axis has been implicated in many cancers for contributing to tumour proliferation, survival and cell cycle progression (Zhao and Vogt, 2008).

One of the most studied pathways activated by CDK4/6-cyclin D is its phosphorylation of the tumour suppressor, RB protein and regulation of E2F-mediated transcription. The RB family consists of three members, RB1 and its paralogues, p107 and p130. The three genes share a high degree of homology in the pocket domain, responsible for many protein-protein interactions. The pocket region contains two major domains, A and B, cyclin-like folds that constitute a single subunit through covalent bonds to form a LXCXE binding cleft, which interacts with proteins such as the E2F family and proteins that have a similar LXCXE motif. (Lee *et al.*, 2002; Lee *et al.*, 1998; Xiao *et al.*, 2003). At the N-terminal part of RB proteins, there are two additional cyclin folds (RBN) that associate with the pocket region by directly binding to the transactivation domain in E2F transcription factors to inactivate E2F (Hiebert *et al.*, 1992). Additionally, the intrinsically disordered C-terminal region of RB proteins (RBC) can bind to E2F and the E2F heterodimer differentiation related polypeptide (DP) by adopting a strand-turn-helix conformation (Helin *et al.*, 1993; Rubin *et al.*, 2005). CDK4/6-cyclin D, as well as CDK2-cyclin A/E interact with the RBC (Rubin, 2013). The restriction point at G0 is regulated by the hypophosphorylated state of RB and also tethers histone deacetylases and methylases alongside DNA methylases that contribute to compacted chromatin and transcription repression at RB-E2F bound DNA (Luo *et al.*, 1998; Magnaghi-Jaulin *et al.*, 1998; Nielsen *et al.*, 2001). Activated CDK4/6-cyclin D can phosphorylate RB at Ser795, Ser780 and Ser807/811, which leads to the disassembly of RB from E2F and destabilises interactions with

transcription repressors such as histone deacetylase 1 (HDAC1). Lifting of this repression allows initiation of the transcription of E2F targets, as the cell cycle transitions from the G1 to S-phase.

The E2F family of eight TFs can be divided into two subgroups based on their action in activating or repressing gene expression through the cell cycle (Dimova and Dyson, 2005; Dyson, 1998; Johnson *et al.*, 2016; Kent and Leone, 2019). The classical E2F members E2F1, E2F2 and E2F3 are bound solely to RB1 protein and can act as activators of transcription. Conversely, E2F5 and E2F6 have a transcriptional repressor role and only bind to p107. E2F4 also acts as a repressor but has been shown to bind to all three RB proteins. Each classical E2F consists of a DNA binding domain and a DP dimerization domain to form a heterodimer with its DP protein partner. Moreover, during transcription inactivation, RB binds to the E2F transactivation domains to prevent the recruitment of transcription co-activators (Flemington *et al.*, 1993; Helin *et al.*, 1993; Helin *et al.*, 1992).

Upon CDK4/6-directed phosphorylation of RB during the G1 phase, RB dissociates from E2Fs. E2F1, E2F2 and E2F3 are able to promote transcription and facilitate entry into the S phase by stimulating the expression of cyclin E, cyclin A, as well as genes required for DNA replication (Ishida *et al.*, 2001). By contrast, the repressor E2F factors act to prevent cell cycle progression, mediated by the INK4/ARF family and p53 as their downstream targets (Carvajal *et al.*, 2012; Polager and Ginsberg, 2009). E2F4 and E2F5 form complexes with pocket proteins p107 and p130 and accumulate during the G1 phase to prevent cell cycle progression in the absence of growth factor signals (Chen *et al.*, 2002a; Iavarone and Massague, 1999; Moberg *et al.*, 1996; Vairo *et al.*, 1995). Transcription of E2F4 and E2F5 is also inhibited in response to TGF-β phosphorylation of SMADs (SMAD1, 2 and 3), which assemble into a heterotrimer that suppresses c-MYC target genes and activates $p15^{INK4b}$ and $p21^{CIP1}$ expression to further prevent cell cycle progression (Kowalik, 2002). Furthermore, E2F6, E2F7 and E2F8 are atypical E2F family members that also act as transcription repressors, but are independent of RB, p107 or p130 (Cartwright *et al.*, 1998). The atypical E2F7 and E2F8 proteins contain two DNA binding domains and lack a DP dimerization domain, as well as the RB binding domain. Rather, they can form homodimers or heterodimers. Expression of these atypical E2F repressors oscillates with cell cycle progression as their transcription is induced by E2F1 during G1 phase but

progression through G1/S phase E2F1 activities are repressed by E2F7 and E2F8 (Lammens *et al.*, 2009; Li *et al.*, 2008). Besides E2F1, p53 has also been shown to activate E2F7 and E2F8 in response to DNA damage, leading to apoptosis (Zalmas *et al.*, 2008).

Progression through the G1 phase enables the preparation for DNA replication in S phase and recruits activators and accessory factors to DNA replication origins. DNA replication origins are dynamic and plastic as some replication origins are cell type specific (Besnard *et al.*, 2012). However, the active sites have shared features such as GC-rich regions that may form G4 quadruplex structure, association with open chromatin and are often located near to active genes (Xu *et al.*, 2012a). During the G1 phase, E2F-driven transcription stimulates the expression of factors required for origin licensing, e.g. the origin recognition complex (ORC) family of genes, cell division cycle 6 (CDC6), CDC10 division transcript 1 (CDT1) and the mini chromosome maintenance (MCM) gene family (Bracken *et al.*, 2004; Dimova and Dyson, 2005; Fragkos *et al.*, 2015). Origin licensing ensures complete replication, genome stability and prevents re-replication. This multi-step and ATP-dependent process primes DNA for replication with the recruitment of replicative helicases, CDC6, CDT1 and MCM2-MCM7 by CDK2-cyclin E to the DNA bound ORC, consisting of six subunits ORC1-ORC6. CDC6 is the first to bind to ORC followed by CDT1, which recruits and aids the loading of the MCM hexamers to DNA. ATP hydrolysis leads to the release of CDC6 and CDT1 allowing further recruitment of the CDT1-MCM hexamer by CDC6 to bind at the same origin start site. The MCM hexamer bound ORC can bend the DNA leaving sufficient space on the ORC to recruit another MCM hexamer to form double MCM hexamers. N-face to N-face configuration of the double hexamers and ORC forms the pre-replication complex (pre-RC) to complete origin licensing. Regulation of origin licensing is essential for normal cell cycle progression. Pre-RC remains active and occurs solely within G1, to prevent further binding of MCM hexamers at the same origin in each cell cycle and becomes inactivated prior to S phase (Blow and Hodgson, 2002). Several factors may potentially be involved as licensing checkpoints to ensure sufficient and adequate origin licensing before DNA replication (Blow and Gillespie, 2008; Shreeram *et al.*, 2002). Rif1-PP1 is a phosphatase that stabilises ORC subunits and prevents phosphorylation and degradation during G1 (Hiraga *et al.*, 2017).

In addition, the presence of a licensing checkpoint ensures sufficient numbers of activated licensed origins, as too few licensed origins will result in DNA forks covering prolonged sections of DNA in replication and increase replication stress (Blow and Gillespie, 2008; Shreeram *et al.*, 2002). Thus, this checkpoint would delay entry to the S phase. Although this process is poorly understood, previous studies have suggested that p53 may be responsible for mediating this checkpoint response (Hills and Diffley, 2014; Nevis *et al.*, 2009). p53- and CDC6-deficient cells promote entry to S phase with CDK2 activity restoration and reduce DNA replication compared to p53-proficient cells that evade G1 arrest (Nevis *et al.*, 2009). However, the role of p53 in mediating cell cycle arrest in response to DNA damage is a well-studied pathway. As mentioned previously, $p21^{CIP1}$ as a canonical p53 target that can bind to CDK2-cyclin E, prevents hyperphosphorylation of RB and consequently suppresses the E2F-mediated transcription of E2F targets needed for DNA replication (Harper *et al.*, 1993). Alternatively, once cells enter arrest at G0 or senescence, pre-RC and ORC subunits are degraded, and licensed origins become unlicensed (Stoeber *et al.*, 2001).

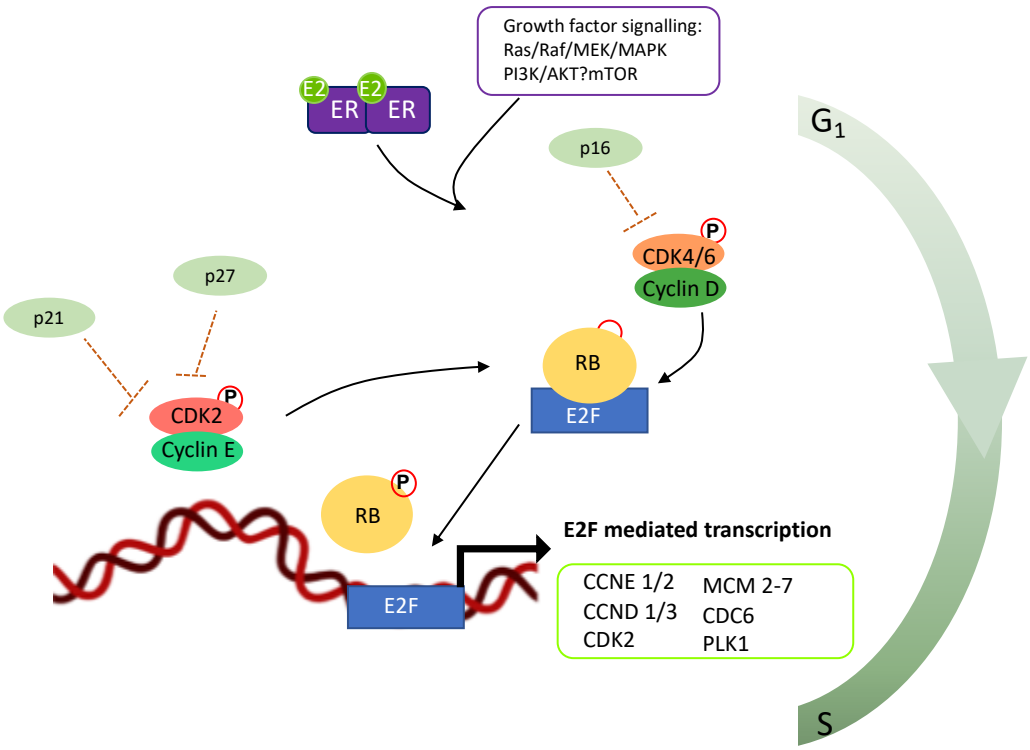


Figure 1.6. CDK4/6-cyclin D1 mediates entry into and progression through G_1 phase of the cell cycle.

Quiescent cells are stimulated through growth factor signaling or estrogen receptor queues to enter the G1 phase by inducing expression of D-types cyclins. The Cdk Activating kinase (CAK), comprised of the CDK7/cyclin H/MAT1 complex phosphorylates CDK4 and CDK6 to increase their activities. CDK4/6-cyclin D phosphorylates the retinoblastoma (RB) protein, facilitating RB release from E2F, to allow for E2F-mediated transcription. Among the E2F target genes are cyclin E, which bind to CDK2 for its activation. Again, CAK increases CDK2 activity by direct phosphorylation of CDK2. The CDK2-cyclin E complex further phosphorylates RB. For references please see text.

1.3.1.3 Cell cycle: CDK2 regulates the progression through S phase

S phase entry is induced in response to the expression of E-type cyclins via E2F mediated transcription (Figure 1.7). There are two genes encoding highly homologous E-type cyclins, with particularly high homology in their N-terminal cyclin box that provides similar activity for the two cyclins in binding to and activating CDK2. Although studies have suggested similar activities for cyclin E1 and cyclin E2 (Chu *et al.*, 2021; Hwang and Clurman, 2005), the function and characteristics of cyclin E1 are better defined and cyclin E1 will be referred to as cyclin E from hereon in, unless otherwise specified. During progress through G1/S phase, cyclin E expression is induced via E2F1-3. In G0 and mitosis phase, RB-E2F repressors inhibit cyclin E transcription via the recruitment of histone modifying enzymes such as histone deacetylase and histone methyltransferase, and nucleosome remodelling (Caldon and Musgrove, 2010).

CDK2, the cognate partner of cyclin E consists of a bilobal structure of β-sheets with a PSTAIRE helix that enables the binding of cyclins (Jeffrey *et al.*, 1995). The β-sheets are connected by a hinge region to an α-helix at the C-terminus that harbours the catalytic residues, the phosphorylation and the activation sites (Bartova *et al.*, 2008; Davies *et al.*, 2001). CDK2 is inactive as a monomer as it adapts an autoinhibition state; the αC-helix mediates the active conformation by folding itself outside of the activation site and the T-loop blocks the substrate binding site and the ATP-binding cleft (De Bondt *et al.*, 1993; Li *et al.*, 2015b). Activation of CDK2 requires a two-stage activation firstly by phosphorylation of the T-loop at Thr160 by CAK, which primes CDK2 for cyclin binding (Poon and Hunter, 1995). Binding of cyclin E in late G1 leads to conformational changes to the CDK2 activation and substrate sites, leading to inhibitory effects of the αC-helix (Jeffrey *et al.*, 1995). The CDK2-cyclin E complex can phosphorylate RB at Ser780 and Thr821; the hyperphosphorylation of RB (additional to RB phosphorylation by CDK4/6 in G1) further inhibits interaction of RB with E2F, permitting a positive feedback loop, as E2F further drives cyclin E gene expression. CDK2-cyclin E activity peaks at late G1 phase and drives cells to enter the S phase by phosphorylating CDC25A. To ensure stepwise progression through the cell cycle, SCF^{Skp}, a ubiquitin ligase is downregulated by the anaphase promoting complex/cyclosome (APC/C), an E3 ligase thereby maintaining $p21^{CIP1}$ and $p27^{KIP1}$ stability and inhibiting CDK1, CDK2 and CDC25A during the early G1

phase (Bashir *et al.*, 2004; Wei *et al.*, 2004). Subsequently, SCF^{Skp2} degrades $p21^{CIP1}$ and $p27^{KIP1}$ to promote CDK2 activities (Bornstein *et al.*, 2003)

In progression through the S phase, cyclin E is degraded and CDK2 adopts new cyclin partners, the A-type cyclins, cyclin A1 and cyclin A2. In common with the other cyclins, the cyclin box of the A-type cyclins is made up of five α-helical structure, with phosphorylation sites at the N-terminal part of the cyclin box. Additionally, at the N-terminus, there is a destruction box for programmed proteolysis at the end of mitosis (Geley *et al.*, 2001). However, cyclin A1 is expressed predominately in germ cells, while cyclin A2 is ubiquitously expressed in somatic cells. The cyclin A2 gene contains an E2F1 binding site in its promoter region and during late G1, transcription of cyclin A2 is initiated by E2F (Schulze *et al.*, 1995). Cyclin A2 expression can also be stimulated by cAMP regulated element binding protein (CREB) (Desdouets *et al.*, 1995). The degradation of cyclin E promotes the binding of cyclin A2 to CDK2 (Girard *et al.*, 1991; Walker and Maller, 1991). CDK2-cyclin A2 forms a negative feedback loop with E2F expression, with increasing cyclin A2 expression leading to the dissociation of E2F1 from DNA when cyclin A inhibits the E2F DNA binding partner (Krek *et al.*, 1995; Wong *et al.*, 2011). CDK2-cyclin A2 can recruit DNA replication components such as CDC6, pre-replication complexes (described below) and the APC/C substrate activating subunit CDC20, CDH1 and $p220^{NPAT}$ (Ma *et al.*, 2000; Ye *et al.*, 2003). Amongst these substrates, CDC25A can also be activated by CDK2-cyclin A2, a metaphase inducer protein that assists the transition from the S phase to mitosis. In late S phase, CDK2 is deactivated by its phosphorylation at Thr14 and Tyr15 by WEE1 (Watanabe *et al.*, 1995). This enables cyclin A2 to bind CDK1 for stabilisation and progression to the G2 phase (Lukas *et al.*, 1999).

Histone chaperones such as chromatin assembly factor 1 (CAF1), nucleosome assembly protein 1 (NAP1), anti-silencing function 1 (ASF1, a subunit of the replication coupling assembly factor (RCAF)) mediate the chromatin assembly of the newly synthesised DNA, where it is immediately coupled with nucleosomes (Hammond *et al.*, 2017; Haushalter and Kadonaga, 2003; Tyler *et al.*, 1999). Two copies of each histone protein are arranged into an octamer, a nucleosome, by α-helical structure to provide histone to histone interaction. Nucleosomes consist of two H2A-H2B and H3-H4 dimers (Burgess and Zhang, 2013; Jiang and Pugh, 2009; Luger *et al.*, 2012). The octamer forms a column-like structure consisting of

three complementary binding sites allowing DNA to wrap in a helical coil around each nucleosome. The tail domains of nucleosomes are exterior extensions of the cylindrical structure predominantly consisting of lysine and arginine residues. Furthermore, the presence of the H1 histone assists the stabilisation of compacted chromatins. They possess the ability to interact with enzymes for posttranslational modifications and mediation of the epigenetic landscape. Alternatively, parental H3-H4 tetramers can be recycled and deposited close to their original position. CAF1 is localised at the foci of replication via binding to canonical PCNA interacting peptides (PIPs) of PCNA to the newly replicated DNA, to recruit and deposit newly synthesised H3-H4 dimers guided by chaperone ASF1 (Mousson *et al.*, 2005). H3-H4 dimers are assembled into tetramers onto DNA and premature tetramerization is blocked by ASF1 (English *et al.*, 2006; Mousson *et al.*, 2005). *In vitro* models have suggested the regulation of CAF1 activity through phosphorylation of p60 by CDK2-cyclin E/CDK2-cyclin A2 and/or CDK1-cyclinB1 with protein phosphatase type 1 (PP1) mediates the dephosphorylation of CAF1 (Keller and Krude, 2000). Similarly, RCAF, another chaperone kinase, can also interact with and deposit H3-H4 dimers and functions synergistically with CAF1(Liu *et al.*, 2017). RPA participates in the DNA replication and coordinates histone chaperones by interacting with CAF1 and the facilitates chromatin transcription complex (FACT) (Liu *et al.*, 2017). The FACT complex, is a histone chaperone that shows nucleosome dis/assembly activity and maintains integrity of H2A-H2B and H3-H4 dimers, in both newly synthesised histones and also in the recycling of parental histones (Foltman *et al.*, 2013; Kurat *et al.*, 2017; Yang *et al.*, 2016). In contrast, the chaperone, NAP1 shows preferential binding to H2A-H2B dimers and is responsible for the nuclear transportation of H2A-H2B dimers from the cytoplasm.

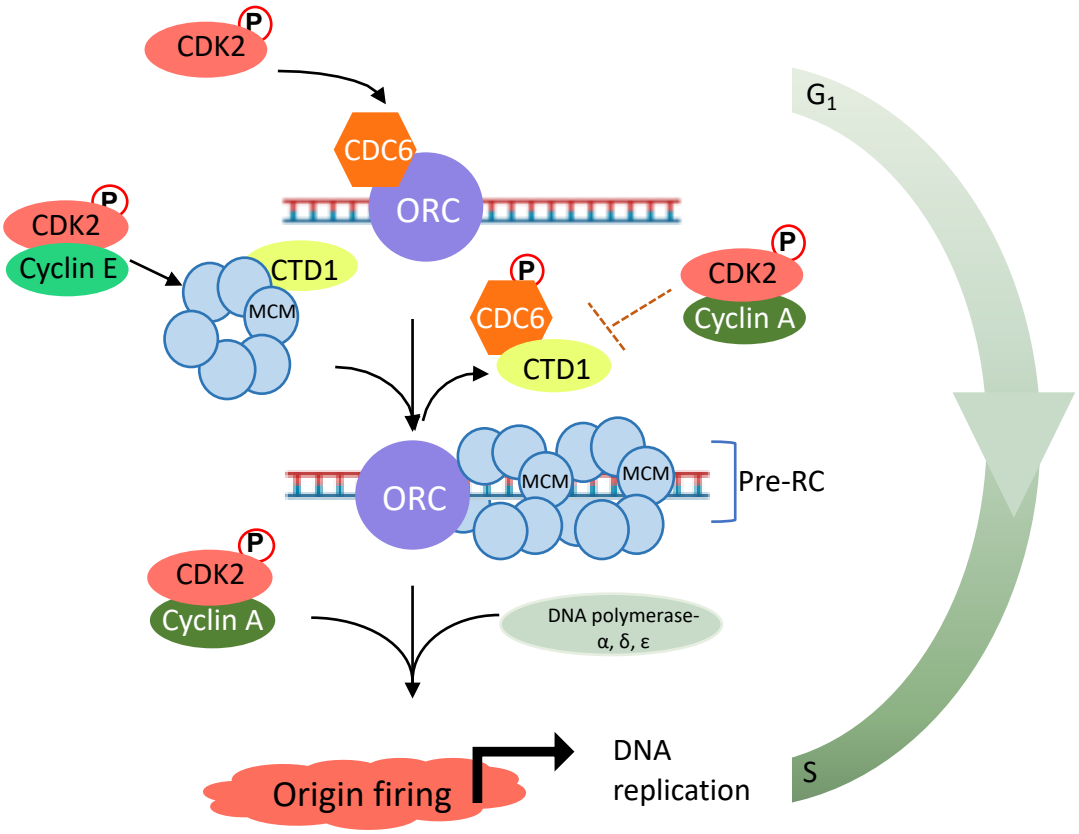


Figure 1.7. CDK2 promotes progression through S phase.

The assembly of the pre-replication complex is mediated by CDK2 in the G1 phase by stabilization of CDC6. Together, CDC6 and CDT1 help the loading of MCM hexamers to OCR. During the G1 to S transition, CDK2-cyclin E induces the further loading of CDC45 and DNA polymerase-α, δ, ε at replication forks. CDK2-cyclin E also mediates centrosome duplication and histone synthesis, followed by the activation of CDK2-cyclin A2 to phosphorylate CDC6 in the S phase to prevent re initiation at the same origin. Origin firing initiates and modulates DNA synthesis at the replication fork. MCM, minichromosome maintenance complex; OCR, origin recognition complex.

1.3.1.4 Cell cycle: CDK1 is essential for transition and progression during G2/mitosis phases

In higher eukaryotes, progression through the cell cycle requires the sequential action of CDK1, CDK2 and CDK4/6. However, a remarkable series of studies in mice has demonstrated that simultaneous knockout of CDK2, CDK4 and CDK6 does not prevent mouse embryos from developing appropriately to mid gestation (Malumbres and Barbacid, 2009). In the absence of all other cell cycle CDKs, CDK1 can bind to all cell cycle cyclins, to facilitate progression through all stages of the cell cycle. By contrast, CDK1 is required for progression through G2 and is essential for mitosis. As shown in previous work, CDK1 knockouts were unable to progress to the morula and blastocyst stages, demonstrating its essentiality (Santamaria *et al.*, 2007; Satyanarayana and Kaldis, 2009). The essential role of CDK1 and dispensable nature of the other cell cycle CDKs was also confirmed in the above studies and is in line with the fact that cell division requires just one CDK, CDK1, in unicellular organisms. This is not to say that CDK2, CDK4 and CDK6 are not needed for cell cycle progression, but their essentiality seems to show tissue-specificity (Malumbres and Barbacid, 2007, 2009). CDK1 is most closely related to CDK2, sharing 65% similarity in their amino acid sequences (Bourne *et al.*, 1996). As demonstrated for CDK2, CDK1 also adopts the active conformation by re-orientating the αC-helix away from the active cleft and phosphorylation site at the N-terminus, forming the unique compact hairpin structure for cyclin B binding. The main structural differences between CDK1 and CDK2 can be found in their activation domains, the αC-helix and the C-terminal tail. CDK1 and CDK2 both have a similar conformation of the αC-helix at the T-loop phosphorylation site, resulting in a conformational change in the mobile T-loop of CDK1 for phosphorylation by CAK at Thr161 (Larochelle *et al.*, 1998). During the G2/mitosis phase transition, CDK1-cyclin A2 and other mitotic factors are activated progressively via a feedback loop by interactions only shown with cytoplasmic cyclin A2 (Mitra and Enders, 2004; Silva Cascales *et al.*, 2021) (Figure 1.8).

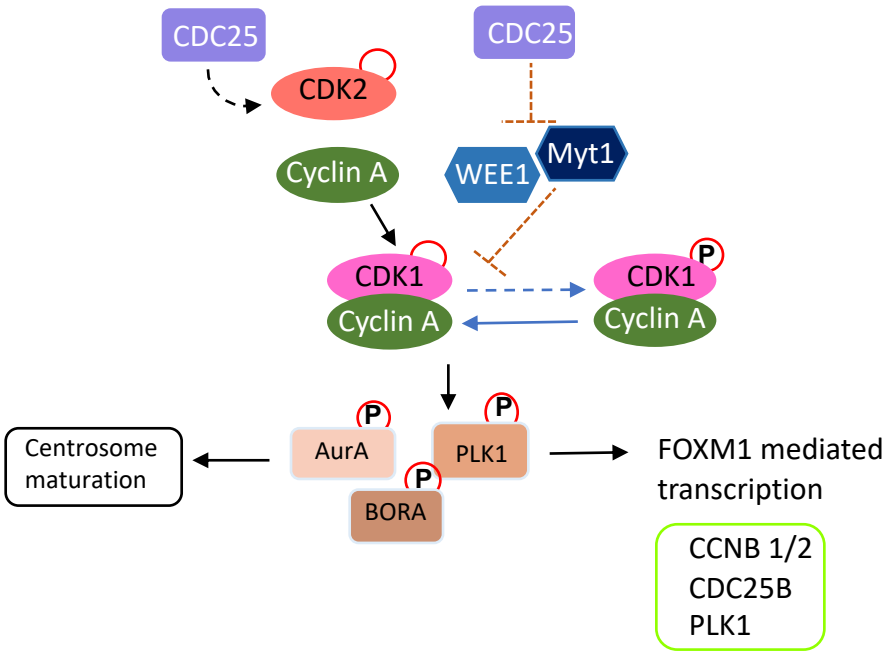


Figure 1.8. CDK1 and CDK2 regulate activities during G_2 transition.
CDK2 is degraded to allow the formation of CDK1-cyclin A, the regulator of G_2 progression. The G_2 phase involves the activation of regulators and components required for mitosis. AurA, PLK1 and BORA are recruited for centrosome maturation. PLK1 is also responsible for activating FOXM1 transcription that includes cyclin B1. AurA, Aurora A; AurB, Aurora B; PLK1, polo-like kinase 1.

Mitosis has distinct stages for cell division and segregation of newly synthesised chromosomes and is regulated by the concerted action of a group of protein kinases and phosphatases (Figure 1.9). Key mediators of mitotic entry such as CDK1, Polo-like kinase 1 (PLK1) are stimulated by Aurora A (Bachelot *et al.*) and co factor BORA (van Vugt and Medema, 2005). PLK1 activation has been suggested to be restricted by the cytoplasmic cofactor Bora, thus assembly of the cyclin A2-Aurora A-Bora activation complex occurs in the cytoplasm and this activates PLK1 (Feine *et al.*, 2014; Thomas *et al.*, 2016). AurA phosphorylates CDK1 and induces binding to B-type cyclin, and/or phosphorylates CDC25B to induce assembly and activation of CDK1-cyclin B1 (Cazales *et al.*, 2005; Timofeev *et al.*, 2010). Active PLK1 has been shown to repress WEE1 and activate CDC25C that further stimulates the binding of CDK1-cyclin B, known as the mitotic kinases. There are three B-type cyclins, cyclin B1, B2 and B3. B-type cyclins possess a destruction box and a cyclin box at the N- and C-terminal ends, respectively. They also consist of a cytoplasmic retention sequence (CRS), as studies have shown the importance of this region to enable activation of cyclin B in the cytoplasm (Li *et al.*, 1997; Yang *et al.*, 1998). Cyclin B1 and B3 have been demonstrated in previous studies to be involved in mitosis but there is limited knowledge about the role of cyclin B2 during mitosis (Jacobs *et al.*, 1998).

During interphase, CDK1-cyclin B1 is activated and accumulates in the cytoplasm and is exported from the nucleus via phosphorylation by WEE1 and PLK1 and rapidly transports into the nucleus during prophase (O'Farrell, 2001). It has been proposed that phosphorylation of cyclin B1 at Ser147 promotes nuclear import via changes in the nuclear transport machinery (Gavet and Pines, 2010; Toyoshima-Morimoto *et al.*, 2001). Furthermore, other studies have suggested that CDK2-cyclin A2 localises at the centrosome during the transition from G2 to mitosis phase and mediates the activation via cdc25 phosphatase and the nuclear import of CDK1-cyclin B1 (De Boer *et al.*, 2008; Gong *et al.*, 2007). Prometaphase entails nuclear envelope breakdown and release of the nuclear content into the cytoplasm. CDK1 modulates and phosphorylates the nuclear envelope filaments into lamin dimers by targeting Ser32 and Ser392 in lamin A and C, respectively (Heald and McKeon, 1990; Peter *et al.*, 1990; Ward and Kirschner, 1990). CDK1-cyclin B1 have also been shown to mediate the disassembly of nuclear pore complexes (NPCs) by phosphorylating nucleoporins (Blethrow *et al.*, 2008; Macaulay *et al.*, 1995). Interestingly, cyclin A has been shown to limit entry into prophase by

restricting the nuclear accumulation of cyclin B1, thus delaying nuclear envelope breakdown (Gong *et al.*, 2007).

In progression through metaphase, chromosomes are aligned at the equator with centrosomes located at opposite poles. Cyclin B1 levels are reduced during metaphase and lead to a decline in CDK1 activity, alongside which spindle assembly checkpoint (SAC) activities are also deactivated. Cohesin is a ring-shaped protein that consists of SMC1, SMC3, Scc1 and Scc3 and is activated during S phase. Acetylation of SMC3 by Esco1/2 ensures the integrity of sister chromatids by holding duplicated chromatids together throughout the S phase, through to metaphase (Zhang *et al.*, 2008). With the recruitment of sororin, which allows the attachment of cohesins to DNA and prevents binding to an antagonist of cohesion, Wapl (Gandhi *et al.*, 2006). During prophase, Wapl begins the first removal step of cohesins from the chromatid arms, except for the cohesins located in the centromere that remain to resist the tension from the bi-orientated microtubules until anaphase. Phosphorylation of cohesins by CDK1, PLK1 and AurB leads to the dissociation of sororin and cohensin allowing removal by Wapl (Nishiyama *et al.*, 2013; Sumara *et al.*, 2002). Whilst SGO1-phosphatase type 2A (PP2A) phosphatase complex protects cohesins located in the centromere from Wapl and reverses the effect of phosphorylation (Liu *et al.*, 2013).

Entry into anaphase is regulated by CDC20 activated APC/C and features the separation of chromosomes. Cohesins located at the centromere are cleaved by a caspase-related protease, Separase at the onset of anaphase (Uhlmann *et al.*, 2000). The activities of Separase are inhibited by Securin until entry into anaphase, in which Securin is degraded via proteolysis mediated by APC/C (Nasmyth, 2001; Peters, 2002). Chromosome separation is mediated by a broad range of ATP-mediated motor proteins in the dynein and kinesin families (Pfarr *et al.*, 1990; Vale *et al.*, 1985). Moreover, APC/C orchestrates the proteolysis of a range of substrates to assist chromosome segregation, such as XKid. It is involved in prometaphase that maintains a polar ejection force preventing premature separation, thus degradation of XKid enables the movement of microtubules (Funabiki and Murray, 2000). Proteolysis of cyclin B1 by APC/C starts in the metaphase-anaphase transition and continues throughout mitosis, leading to a reduction in CDK1 activity (King *et al.*, 1996; Qiao *et al.*, 2016). In contrast to cyclin B1, the delay in degradation of cyclin B3 promotes entry to anaphase and is involved in maintaining

chromosome condensation during anaphase and preventing nuclear envelope reformation. A study has demonstrated the absence of cyclin B3 after chromosome separation indicating the degradation of cyclin B3 in anaphase (Sigrist *et al.*, 1995).

Prior to anaphase, CDK1 activity prevents the interaction between PRC1 and kinase-like motor proteins (KIFs). Thus, the reduction or inactivation of CDK1 with the promotion of AurB in anaphase leads to the interaction of PRC1 and KIF with microtubules and limits the formation of microtubules to the midzone (Alsop and Zhang, 2003; Mishima *et al.*, 2002; Nunes Bastos *et al.*, 2013; Subramanian *et al.*, 2010; Zhu and Jiang, 2005). Reduction in CDK1 leads to the dephosphorylation of spindle stabilising protein PRC1, allowing the recruitment of its partner PLK1 that is also needed for cytokinesis (Jiang *et al.*, 1998; Neef *et al.*, 2007). Moreover, the decrease in CDK1 activity reduces phosphorylation of the motor domain of the mitotic kinesin-like protein 1 (MKLP1) and Fin1 that leads to the bundling of the microtubules and generates the bi-orientation and stability of spindles for chromosome segregation (Juang *et al.*, 1997; Mishima *et al.*, 2004; Woodbury and Morgan, 2007). Furthermore, MKLP1 is also phosphorylated by midzone AurB that promotes the binding of MKLP1 to centralspindlin for spindle stabilisation (Basant *et al.*, 2015; Douglas *et al.*, 2010; Hutterer *et al.*, 2009). AurB is found along the microtubule arms to the centromere, forming a phosphorylation gradient towards the midzone spindles, which is important for a robust chromosome segregation. During late anaphase, the AurB phosphorylation gradient ensures the integrity of the spindle by blocking depolymerisation by inhibiting KIF2A and activating KIF4A (Nunes Bastos *et al.*, 2013; Uehara *et al.*, 2013). The relocalisation of AurB is mediated by dephosphorylation of INCENP via a decrease in CDK1 and the binding of MKLP2 (Hummer and Mayer, 2009). Mitotic spindles stimulate the formation of the cleavage furrow and positions the actomycin contractile ring at the equator, which is essential for cytokinesis, by the tethering of the central spindlin complex to the cell membrane (Glotzer, 2004). The central spindle bundles induce regulation of GTPase RhoA that stimulates actin nucleation and activate myosin to form an actomyosin contractile ring (Wagner and Glotzer, 2016).

The anaphase-telophase transition is mediated by protein phosphatases PP1 and PP2A. which can both auto-dephosphorylate, with the declining levels of CDK1-cyclin B prior to the onset

of telophase (Grallert *et al.*, 2015; Kwon *et al.*, 1997; Wu *et al.*, 2009; Yamano *et al.*, 1994). The presence of non-degradable B-type cyclins delayed the onset of telophase, indicating that the proteolysis of B-type cyclins has a temporal control over the late mitotic events (Parry and O'Farrell, 2001; Sigrist *et al.*, 1995). Throughout progression from G1 to anaphase, CDK1 phosphorylates PP1 via its catalytic domain and represses PP1 activity to prevent a premature entry into telophase and cytokinesis (Dohadwala *et al.*, 1994). At telophase, the activation of PP1 requires the dephosphorylation of its partner, Repo-Man by PP2A, which counteracts AurB phosphorylation. PP2A repression is mediated indirectly by CDK1 via the phosphorylation of MASTL that activates the PP2A inhibitor, ENSA (Cundell *et al.*, 2013). PP1 and PP2A share a high degree of similarity in their catalytic activities and together mediate the concert of activities during the final stages of mitosis, such as nuclear envelope re-formation and chromatin decondensation in late anaphase. First, chromatin starts to decondense in preparation for the reformation of the nuclear envelope, which is dependent on the proteolysis of AurB and CDK1 by cdh1 activated APC/C (Afonso *et al.*, 2014). In the absence of/declining levels of CDK1, histone H3 is dephosphorylated at T3 and S10 by Repo-PP1 for chromatin decondensation, to reverse the effects of AurB (Qian *et al.*, 2013).

The final stages in cytokinesis involve the formation of a nuclear membrane and the separation to form two identical daughter cells through the progressive contraction of the actomyosin ring at the abscission site (Buck and Tidsale, 1962; Byers and Abramson, 1968). The midbody is compacted with microtubules that may be modulated by spastin and katanin and forms an abscission site (Connell *et al.*, 2009; Matsuo *et al.*, 2013). The timing and regulation of abscission suggests two different models of mediation via phosphorylating midbody components, CHMP4C by CPC and/or AurB, but the exact mechanism is yet to be defined (Capalbo *et al.*, 2012; Carlton *et al.*, 2012). The disposal of the midbody ring after abscission has been proposed through the inheritance of the midbody ring by one of the daughter cells and removal by autophagy (Pohl and Jentsch, 2009). These daughter cells will exit through the G0 phase or enter a new cycle of cell division through G1 checkpoint.

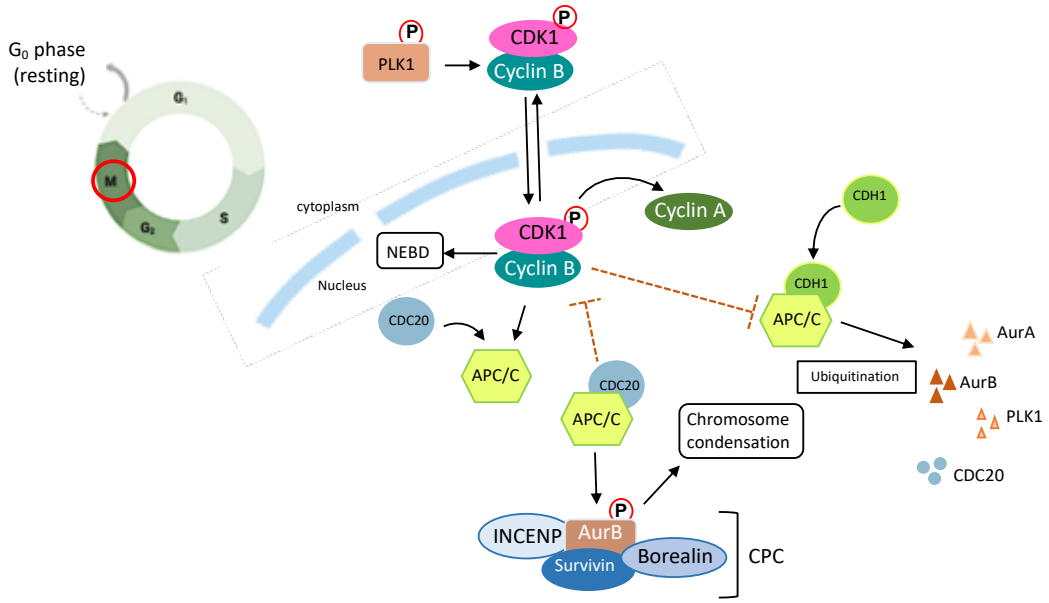


Figure 1.9. CDK1-cyclin B1 key mediators of Mitosis.
APC/C mediates progression through mitosis. CDK1-cyclin B1 activates CDC20 binding to APC/C to inhibit Securin and activates Separase that leads to separation of chromosomes in prophase. With the activation of CPC in metaphase and anaphase for spindle alignment, separation of sister chromatids and cleavage furrow formation needed for cytokinesis. The CPC consists of AurB, INCENP, survivin and Borealin as core units that stimulates the kinochores contraction of spindles to separate chromosomes. CDK1-cyclin B1 activity reduces during progression through mitosis, the phosphorylation of CDH1 reduces and maintenance of CDC20 reduces. Thus, at the end of telophase, APC/C guided by CDH1 modulates ubquitination of AurA, AurB, PLK1 and CDC20. Cytokinesis is completed, with reformation of the nuclear membrane and the cell membrane to produce two daughter cells. AurA, Aurora A; AurB, Aurora B; CPC, chromosome passenger complex; PLK1, polo-like kinase 1.

1.3.2 Aberrant action of cell cycle CDKs and cyclins contributes to cancer development

One of the hallmarks of cancer is dysregulated proliferation via promotion of entry into the cell cycle with increased mitogenic signalling (Hanahan and Weinberg, 2011). With the previous discussion of the critical roles for CDKs and cyclins in normal development and growth, dysregulated expression of these regulatory kinases is often accompanied by loss of CDKIs leading to uncontrolled proliferation (Otto and Sicinski, 2017). The inactivation of CDKIs is mediated by several signalling pathways, such as the NOTCH pathway that prevents activation of CDKI through TGF-β dependent phosphorylation of SMAD3 (Carlson *et al.*, 2008).

Interestingly, altered expression of CDKs/cyclins may be tumour-specific, such that in ER^+ BCa the overexpression of cyclin D1 may be a key driver of tumourigenesis (Gillett *et al.*, 1994; Kenny *et al.*, 1999). For example, mouse studies have demonstrated that while mammary gland development is dependent on cyclin D1, the development of other tissue types does not require cyclin D1 (Landis *et al.*, 2006; Yu *et al.*, 2001). Also, ERRB2 and/or HRAS induced mammary tumour development is dependent on the presence of CDK4 in murine models and the CDK4-cyclin D1 axis is required for neu-dependent development of BCa (Reddy *et al.*, 2005; Yu *et al.*, 2006). Cyclin D1 has additional roles in promoting invasion and metastasis when bound to $p27^{KIP1}$, blocking Rho GTPase activity and inducing expression of ROCKII and TSP1 (Li *et al.*, 2006a; Li *et al.*, 2006b). Moreover, upregulation of CDK4 and CDK6 is found in several malignancies such as sarcomas, gliomas, lymphomas and melanomas (Malumbres and Barbacid, 2001; Ortega *et al.*, 2002). CDK4 is found to have a germline mutation (denoted as Arg24Cys) in melanoma patients that prevents binding of $p16^{INK4a}$. Consequently, CDK4 acts as an oncogene contributing to melanoma pathogenesis (Puntervoll *et al.*, 2013; Zuo *et al.*, 1996). CDK6 overexpression is found in specific tumour types such as in some leukaemias, resulting from a chromosomal translocation and is used as a prognostic factor for poor clinical outcome (Placke *et al.*, 2014). Perturbated expression of CDK4/6 may be associated with other classical tumourigenesis signalling pathways such as PI3K, RAS, MYC pathways and co-expressed with a wide range of oncogenes such as MDM4, PIK3CA and MYC (Feng *et al.*, 2018; Harbeck *et al.*, 2019). The PIK3CA gene encodes for PI3K protein and genetic abnormalities of the PIK3CA gene contribute to BCa tumourigenesis (Yang *et al.*, 2019).

Somatic mutations (30%) and amplification (10%) of PIK3CA have a high prevalence in BCa as shown in previous studies (Gonzalez-Angulo *et al.*, 2013; Liu *et al.*, 2009; Wu *et al.*, 2005). ATK mutations and loss of lipid phosphatase PTEN are frequently considered as poor prognostic markers. Moreover, MAPK signalling pathway can activate ER through the phosphorylation of Ser118 to and is also involved in the hypersensitising BCa cells to E2 (Yue *et al.*, 2002). Although ample studies contributed to the understanding of the mechanisms of tumourigenesis of ER^+ BCa, current ongoing research aims to further explore potential therapeutic targets to expand treatment options and improve disease-free survival. Alternatively, BCa tumourigenesis may also be induced by other signalling pathways such as MYC and Wnt pathways, independent of CDK4/6-cyclin D1 activity (Aulmann *et al.*, 2006; Yu *et al.*, 2001). In addition, the upregulation of cyclin D1 may be a resistance mechanism to anti-estrogens both in *in vitro* models and clinical settings (Hui *et al.*, 2002; Stendahl *et al.*, 2004). CDK4/6-cyclin D is often the downstream target of these oncogenic signals, thus CDK4/6-cyclin D becomes an attractive therapeutic target (Sanchez-Vega *et al.*, 2018). The loss of the tumour suppressor, RB is also an important factor contributing to the dysregulation of cell cycle progression and tumour progression. The over-expression/amplification of cyclin D and CDK4, together with the loss of $p16^{INK4}$ are often seen in ER^+ BCa, thereby promote cell cycle progression and tumour progression (Knudsen and Knudsen, 2008; Musgrove *et al.*, 2011; Romagosa *et al.*, 2011). RB loss or mutation is found in several cancers such as TNBC, urinary bladder and ovarian cancer but common in ER^+ BCa (Herschkowitz *et al.*, 2008; Liu *et al.*, 1994; Miyamoto *et al.*, 1995).

Cyclin E amplification can be used as a primary indicator of cancer, markedly in hormone-regulated cancers such as ovarian, breast and endometrial cancer (Bedrosian *et al.*, 2004; Gray-Bablin *et al.*, 1996; Hubalek *et al.*, 2004). The overexpression of cyclin E1 has been proposed to enhance chromosome instability via the immature pre-replication licensing that promotes tumourigenesis (Loeb *et al.*, 2005; Spruck *et al.*, 1999). The overexpression of cyclin E1 can bypass the need for CDK4/6-cyclin D1 and promotes cell cycle progression via CDK2, which may lead to tumour development (Guarducci *et al.*, 2018; Min *et al.*, 2018). Moreover, in the analysis of primary breast tumours, it was found that the level of cyclin E2 was upregulated and may have prognostic value (Payton *et al.*, 2002; van 't Veer *et al.*, 2002; Wang *et al.*, 2005). Recent interrogations have found that high levels of E-types cyclins can be a predictor of poor response to tamoxifen in breast cancer (Caldon *et al.*, 2012; Guarducci *et al.*, 2018; Turner *et*

al., 2019). CDK2 has also been shown to be implicated in cancer, such that in hormone-dependent cancers, CDK2 can phosphorylate nuclear receptors, ER (Rogatsky *et al.*, 1999), PR (Pierson-Mullany and Lange, 2004) and AR (Jorda *et al.*, 2018). CDK2 was also found to be implicated in KRAS-dependent lung cancer and MYC-dependent tumours. CDK2 can phosphorylate the centrosome protein, CP110, and decreased levels of CP110 will affect centrosomal clustering leading to anaphase catastrophe, aneuploidy and tumourigenesis (Chen *et al.*, 2002c; Hu *et al.*, 2015a). Increased levels of cyclin A2 may also promote tumour development and are often found in primary tumours within different cancer types such as BCa, ovarian and leukaemias (Beck *et al.*, 1995; Blegen *et al.*, 2000; Bukholm *et al.*, 2001). As previously mentioned, CDK1 is the only essential CDK for cell cycle progression and overexpression of CDK1-cyclin B may promote tumour progression via phosphorylation of FOXO1 (Liu *et al.*, 2008). The aberrant expression of cyclin B may contribute to abnormal chromosome segregation, leading to chromosome instability and tumour development (Sarafan-Vasseur *et al.*, 2002).

Table 1. 1 Summary of alterations in cell cycle related CDKs and cyclins in ER^+ breast cancer.

CDK/cyclin	Alteration	
Cyclin D	Amplification	10-35% (Jeffreys *et al.*, 2022)
CDK4	Amplification	15.8% (An *et al.*, 1999)
$p16^{INK4}$	Loss/point mutation	12.3% (Romagosa *et al.*, 2011)
Cyclin E	Overexpression	36% (Turner *et al.*, 2019)
Cyclin A	Overexpression	34% (Gao *et al.*, 2014)
CDK7-cyclin H-MAT1 (CAK)	Overexpression	65% (Tang *et al.*, 2021)

1.4 CDKs and cyclins in transcription regulation

The focus of this introduction has been on the group of CDKs and cyclins that control cell cycle progression. There is also a group of CDKs and cognate cyclins that play critical roles in the regulation of RNA polymerase II (Pol II) mediated gene transcription (Figure 1.10). The functional roles of these CDKs is described in some detail below.

1.4.1. CDKs and cyclins modulate RNA Polymerase II (Pol II) mediated transcription

1.4.1.1 Transcription initiates with the formation of a pre-initiation complex (PIC)

CDK7 is unique among CDKs by being required in both the regulation of the cell cycle and in its critical role in Pol II-directed transcription (Fisher, 2005). The CDK activating kinase (CAK) phosphorylates the cell cycle CDKs (CDK1, CDK2, CDK4 and CDK6) in the activating T-loop, to either stimulate cyclin-CDK activity or to stabilise cyclin-CDK interaction (as described in Sections 1.3.1). In CAK, CDK7 is associated with its cyclin partner, cyclin H and the accessory protein ménage à trois (MAT1). However, CAK is also part of the 10 subunit TFIIH pre-initiation complex, in which CDK7 phosphorylates Pol II, for promoter release and transcription initiation.

CDK7 has a typical central kinase interacting domain and an N-terminal region consisting of α-helices and β-sheets, enabling the interaction between its cognate partner, cyclin H which activates CDK7 by promoting phosphorylation of the Thr170 residue (Lolli *et al.*, 2004). Additionally, the C-terminal part of CDK7 includes an α-helical region that mediates interaction with MAT1. In contrast to other CDKs, activation of CDK7 requires the binding of cyclin H at the cyclin binding region, T-loop phosphorylation at Thr170 and interaction with MAT1, for maximal kinase activity (Martinez *et al.*, 1997). Furthermore, *in vitro* studies have shown that Thr170 and another phosphorylation site, Ser164, can be phosphorylated in the T-loop by CDK1-cyclin B and CDK2-cyclin A but not by CDK4 or CDK7 itself (Garrett *et al.*, 2001; Glover-Cutter *et al.*, 2009), which provides evidence for cell cycle regulation of CDK7 activity.

Cyclin H consists of five α-helices at the N- and C-terminal regions, denoted as Repeat 1 and Repeat 2, each connected by the central domain helix 3 bound by hydrophobic bonds (Andersen *et al.*, 1997; Andersen *et al.*, 1996; Kim *et al.*, 1996). Repeat 1 encompasses the highly conversed cyclin box, a central linker peptide connects the analogous Repeat 2, sharing

topological similarity with cyclin A. Activation of CDK7 is cyclin H dependent and the activation of cyclin H is mediated by several factors such as CK2 via phosphorylation at Thr315 near the C-terminus, promoting the binding of cyclin H to CDK7 via the cyclin H helix 3 that pushes the CDK7 C-helix into the active site. p53 has been shown to bind to cyclin H directly to negatively regulate its activity as an indirect mechanism for suppressing Pol II activity (Schneider *et al.*, 1998).

CAK formation requires the additional protein, MAT1 to bind to CDK7 to stabilise CDK7-cyclin H. MAT1 is a RING finger protein, with a N-terminal ring finger structure and C-terminal hydrophobic residues, connected by a central coiled domain. Interestingly, the interaction of MAT1 and CDK7 does not require T-loop phosphorylation. Each domain of MAT1 is functionally distinct, such that MAT1 interacts with CDK7-cyclin H through its C-terminal region. Indeed, deletion of the MAT1 protein RING finger does not affect CDK7 activation (Tassan *et al.*, 1995). Although the MAT1 RING finger may not be required for assembly of functional CAK, several studies have shown that this region of MAT1 is necessary for anchoring CAK to TFIIH (Yankulov and Bentley, 1997). TFIIH consists of seven core proteins with catalytic subunits such as the ATP-dependent helicases XBP and XPD that have important activities in DNA damage repair and unwinding DNA during transcription (Drapkin *et al.*, 1994; Fishburn *et al.*, 2015; Grunberg *et al.*, 2012). Other subunits such as p8, p34, p44 and p52 have been shown to regulate XPB and XPD activities and contribute to the stabilisation of the TFIIH complex (Aguilar-Fuentes *et al.*, 2008; Jawhari *et al.*, 2002; Kainov *et al.*, 2008; Rimel and Taatjes, 2018). Collectively, these core unit proteins form parts of the pre-initiation complex (PIC) with Pol II (discussed below) (Di Lello *et al.*, 2006; Di Lello *et al.*, 2008; Fregoso *et al.*, 2007; Marinoni *et al.*, 1997).

The first step of the transcription cycle begins with the recruitment and assembly of the PIC at the gene promoter and DNA opening. This complex consists of the Pol II enzyme, the Mediator complex, TFIIA, TFIIB, TFIID, TFIIE, TFIIF and TFIIH complexes (Orphanides *et al.*, 1996; Roeder, 1996). TFIID is first recruited to the core promotor with TBP-associated factors (TAFs) that recognise and interact with the TATA box just upstream of the transcription start site (TSS) (Louder *et al.*, 2016). The binding of TFIID aids the recruitment and stabilisation of other TFII complexes in a sequential manner (Buratowski *et al.*, 1989). The XPB subunit of the TFIIH

complex can subsequently open the promoter via its ATP-dependent DNA translocase activities to reel DNA onto Pol II (Fishburn *et al.*, 2015; Grunberg *et al.*, 2012). Meanwhile, the Pol II enzyme is responsible for genomic-wide transcription of all protein coding and some non-coding RNAs. Pol II is comprised of 12 subunits and through the central regulatory domain of its CTD, consisting of tandem repeats of a heptapeptide motif, conforming to the consensus sequence, Tyr1-Ser2-Pro3-Thr3-Ser5-Pro6-Ser7. In mammals, the Pol II CTD contains 52 tandem heptad repeats (Corden *et al.*, 1985). The three serine residues in the heptad repeat are phosphorylated by transcriptional CDKs, including CDK7. In addition, the Mediator complex consists of four main components, CDK8 and its cognate partner cyclin C together with subunits MED12 and MED13 (Firestein *et al.*, 2008; Galbraith *et al.*, 2010; Kapoor *et al.*, 2010; Knuesel *et al.*, 2009). Comparably to other CDKs, CDK8 does not require phosphorylation of the T-loop for full activation, but is activated through the binding of Med12, in addition to its cyclin (Klatt *et al.*, 2020). The Mediator complex has been shown to both positively and negatively regulate the onset of Pol II mediated transcription (Allen and Taatjes, 2015; Soutourina, 2018). It has also been suggested to have a role in recruiting TFIIE and TFIIH and enhances TFIIH dependent phosphorylation (Esnault *et al.*, 2008). Alternatively, the Mediator complex can act as a repressor of transcription via phosphorylation of cyclin H to block TFIIH activities (Akoulitchev *et al.*, 2000). Once the assembly of PIC is completed, with DNA translocase activity of TFIIH via ATP-dependent formation of a transcription bubble, open complex formation (Fishburn *et al.*, 2015; Hahn, 2004), Pol II switches to an open complex that induces promotor escape and transcription initiation via the phosphorylation of Ser5 and Ser7 by CDK7-TFIIH (Compe and Egly, 2012).

1.4.1.2 Proximal promotor pause and release for elongation

Initiation of transcription by Pol II continues for about 20-50 bp past the transcription start site, at which point transcription is paused. This promoter proximal pausing and release from the pause is dependent on further Pol II CTD phosphorylation by elongation complexes (Dollinger and Gilmour, 2021; Shao and Zeitlinger, 2017). Metazoan models have demonstrated the regulation of transcription pause by two proteins, DRB sensitivity inducing factor (DSIF) and negative elongation factor (NELF) (Rahl *et al.*, 2010; Yamaguchi *et al.*, 1999; Zeitlinger *et al.*, 2007). CDK9 is activated by T-loop phosphorylation by CDK7 and with cyclin T1 to form a positive transcription elongation factor b (P-TEFb) complex. P-TEFb is then recruited to the

paused Pol II by bromodomain containing protein 4 (Brd4) via interaction with cyclin T1 (Jang *et al.*, 2005; Yang *et al.*, 2005). Activated P-TEFb phosphorylates the Spt5 unit of DSIF transforming it to a positive elongation factor, in addition to the phosphorylation of the subunit of NELF leading to its dissociation from Pol II (Jonkers and Lis, 2015). To reinitiate Pol II, P-TEFb phosphorylates Ser2 in the Pol II CTD heptad repeat, to process PolII to the elongation stage of transcription (Larochelle *et al.*, 2012; Wada *et al.*, 1998). As Pol II progresses towards the 3' end of the gene body, Ser2 is critical for elongation and the phosphorylation of Ser5 is progressively lost (Peterlin and Price, 2006).

1.4.1.3 Transcription termination

At transcription termination, Pol II elicits termination through one of two well-established pathways recognised as poly(A) signalling or in yeast the Sen1 signalling (Kuehner *et al.*, 2011). Most of the protein coding transcripts in eukaryotes have a polyadenylation signal, a sequence consisting of 5'-AAUAAA-3', coupled with the RNA maturation event at a G/U rich region on the 3' end. Therefore, the reduction of the productivity is dependent on Pol II transcription of the poly(A) tail signal leading to Pol II pause via cleavage and polyadenylation specificity factor (CPSF) binding to CTD of Pol II (Nag *et al.*, 2007; Park *et al.*, 2004). A cleavage stimulating factor (CstF) is recruited to the GU rich region and binds to CSPF to induce endoribonucleolytic cleavage of the nascent transcript and release of Pol II (Nag *et al.*, 2007). This is followed by an intricate system of 3' end processing with the involvement of multiple proteins (Mandel *et al.*, 2008; Millevoi *et al.*, 2009; Shi *et al.*, 2009). Secondly, transcription terminates in a Sen1 dependent pathway, as first identified in yeast *S. cerevisiae*. Sen1 is recruited to Ser5 of Pol II CTD and prompts recruitment of further cofactors, such as Nrd1 and Nab3 (Steinmetz and Brow, 1996; Steinmetz *et al.*, 2001; Steinmetz *et al.*, 2006). Sen1 directs termination by unwinding the DNA-RNA hybrid at the active site. The human analogue of Sen1, senataxin, may also be involved in poly(A) dependent termination through activating the 3' end by 5'-3' exonuclease Xrn2 leading cleavage at the poly(A) site (Skourti-Stathaki *et al.*, 2011). Further work is required to determine the complex mechanism of Pol II termination, as a study has shown that inhibition of CDK7 delayed transcription termination, suggesting CDK7 may also be required for appropriate termination (Glover-Cutter *et al.*, 2009).

CDK12 and CDK13 have been shown in yeast and metazoan studies to be involved in transcription elongation by phosphorylating Ser2 of the Pol II CTD (Bartkowiak *et al.*, 2010). CDK12/13 have a high degree of similarity in their sequence and functionality in which both CDKs are associated with cyclin K (Blazek *et al.*, 2011). Recent advances in global proteomic and transcriptomic data have helped to elucidate the role of CDK12/13 (Blazek *et al.*, 2011; Chen *et al.*, 2006; Chirackal Manavalan *et al.*, 2019; Lei *et al.*, 2018). CDK12/13 were shown to participate in several other important pathways, such as RNA splicing, DNA damage and repair pathways and may participate in different stages of the cell cycle.

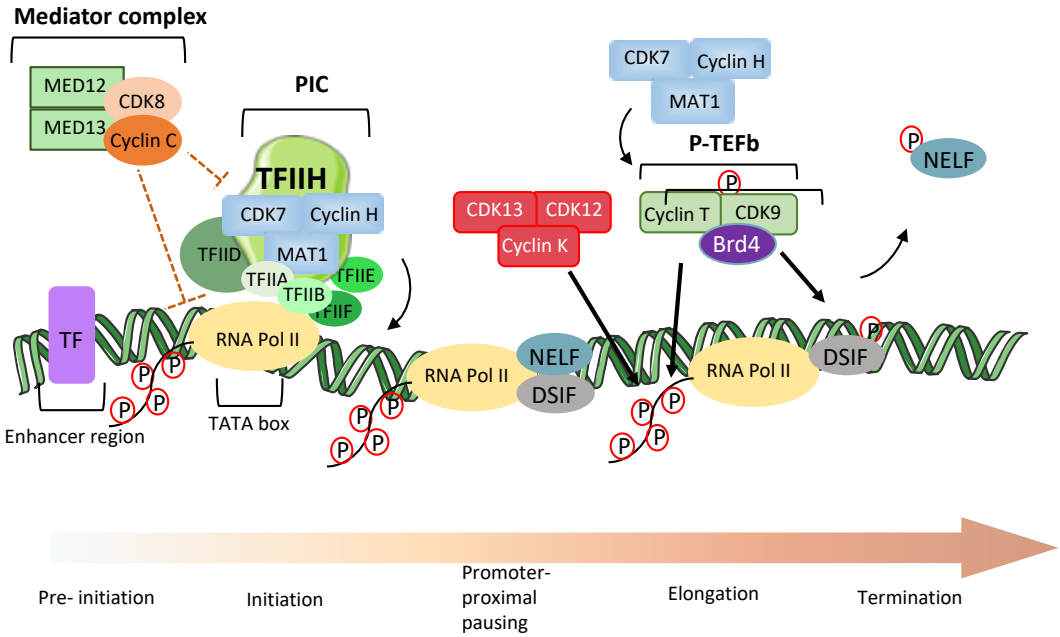


Figure 1.10. Transcriptional CDKs and RNA PolII transcription.
CDK7 acts as a master regulator of Pol II mediated transcription. At pre-initiation TFIIA, B, D, E, F and H are recruited to the gene promoter to form the PIC. CDK7-cyclin H-MAT1 is a component of TFIIH that phosphorylates Ser5 and Ser7 of Pol II to initiate transcription. CDK7 also phosphorylates CDK9 that allows the formation of the P-TEFb complex with cyclin T1 and Brd4. The P-TEFb complex releases Pol II from proximal promoter pausing by inhibiting the activities of negative elgongation factors, NELF and DISF. P-TEFb also enables elongation through the gene body by phosphorylating Ser2 of Pol II. Additional regulation is provided by the mediator complex that phosphorylates cyclin H and Pol II to prevent PIC formation and binding of Pol II to promoter. CDK12/13-cyclin K may also phosphorylate Pol II to promote elongation. DSIF, DRB sensitivity inducing factor.; NELF, negative elongation factor; PIC, Pre-initiation complex; Pol II, RNA polymerase II; P-TEFb, positive transcription elongation factor b; TFII, transcription factor II.

1.4.2 Transcription-associated CDKs contribute to tumourigenesis

Knowledge that many cancers display dependence on transcriptional-related genes for dysregulated proliferation has led to the term "transcriptional addition" in cancer (Bradner *et al.*, 2017; Weinstein and Joe, 2006). This understanding has opened up therapeutic opportunities for targeted therapies, such as BET inhibitors and transcriptional CDK inhibitors that can exploit this vulnerability, where transcriptionally addicted cancer cells would be much more sensitive to transcription inhibitors than healthy cells. Breast and prostate cancer represent very good examples of transcriptional addiction, due to their dependence on estrogen and androgen receptors, respectively. Other examples include the dependence of many cancer types on c-MYC or N-MYC (e.g. TNBC, glioblastomas) and the many transcription factor fusion genes in leukaemias (such as PML-RARα and PLZF-RARα fusions in acute promyelocyctic leukaemia (Bradner *et al.*, 2017).

One example of the possibility of targeting transcriptional kinases is presented by work from our laboratory on CDK7. Previous work from our group found that expression of CDK7, as well as cyclin H and MAT1, was higher in breast cancers than in normal breast epithelium (Patel *et al.*, 2016). Their expression was higher in ER^+ BCa than in ER-negative BCa, with high CDK7 expression significantly correlating with patient survival. Moreover, in low E2 conditions, or when ER is anti-estrogen bound, Ser118 in the AF1 region of ER is phosphorylated by TFIIH-associated CDK7, resulting in increased ER activity (Chen *et al.*, 2000). Elevated expression of CDK7 has also been described in other cancers, including TNBC, hepatocellular carcinoma and oral squamous cell carcinoma (Jiang *et al.*, 2019; Tsang *et al.*, 2019; Wang *et al.*, 2015).

Increased expression of CDK9 has been shown to stimulate expression of the TNF-α gene, with TNF-α promoting in an autocrine and paracrine manner matrix metalloproteinase 9 (MMP-9), thus aiding invasion and metastasis in lung adenocarcinoma (Shan et al., 2005). Another described role for CDK9 in cancer is via alterations in BRD4 and CDK9, which may direct ERE dependent transcription via modifications on histones, like H2B monoubiquitination, in a ligand dependent manner (Nagarajan et al., 2014; Pirngruber et al.,

2009; Prenzel et al., 2011). BRD4 also has a potential role in promoting invasion and epithelial to mesenchymal transition (EMT) in advanced TNBC (Andrieu *et al.*, 2016; Lu *et al.*, 2020; Shu *et al.*, 2016). CDK8 and Mediator complex components may also promote carcinogenesis. For example, CDK8 may act as an oncogene in colorectal cancer through the activation of the Wnt/β-catenin pathway and loss of APC (Firestein *et al.*, 2008). Amplification of CDK8, cyclin C, MED13 and mutated MED12 have been found in BCa, with a suggested correlation to MYC expression and mutatant p53 (Broude *et al.*, 2015). Due to their recognised involvement in regulating multiple tumour-associated mechanisms, such as promoting transcription and cell cycle progression, CDK12/13 also have an emerging role in cancer. Further to this, CDK12 has recently been shown to contribute to some hormone related cancers (Bell, 2011; Tien *et al.*, 2017; Wu *et al.*, 2018), with investigators contributing their involvement in the initiation of ER^+ BCa by promoting cancer stem cells via activation of PI3K/AKT and Wnt pathways (Choi *et al.*, 2019).

1.5 Development and application of CDK inhibitors as targeted cancer therapies

1.5.1 New era of targeted therapy: CDK inhibitors

There is growing evidence that dysregulation of cell cycle checkpoints in cancer cells represents a vulnerability that can be exploited therapeutically. However, development of pan-CDK inhibitors and their clinical testing proved to be disappointing, not only due to their lack of clinical activity but often broad toxicities. Nevertheless, these initial drug development efforts have paved the way for drugs targeting specific CDKs. Some of these selective CDK inhibitors are showing considerable promise in the clinical setting, with the most notable advances being made for CDK4/6 inhibitors with potent activities in ER^+ BCa. Indeed, as described below, success of CDK4/6 inhibitors in treating patients with advanced ER^+ BCa has led to their progression to first-line adjuvant agents in combination with ET. As such, these recent successes facilitate the development of even more cancer drugs targeting cell cycle CDKs, as well as inhibitors of the CDKs implicated in transcription.

1.5.1.1 First generation pan-CDK inhibitors

The first CDK inhibitors were reported in the 1990s, including flavopiridol (alvocidib) (Sedlacek *et al.*, 1996), roscovitine (seliciclib) (Alvi *et al.*, 2005) and olomoucine (Carnero, 2002; Meijer *et al.*, 1999; Vesely *et al.*, 1994). These inhibitors were trialled in numerous clinical trials involving various cancer types, but all had very limited success clinically, owing to their lack of selectivity. This first generation of CDK inhibitors was found to target multiple CDKs and so are referred to as 'pan-CDK' inhibitors. Extensive research was invested in understanding the characteristics of these pan-CDK inhibitors. Specifically, flavopiridol, a semi-synthetic compound derived from rohitukine (a naturally occurring plant flavonoid alkaloid), has been evaluated in more than 60 clinical trials (Asghar *et al.*, 2015). Another pan-CDK inhibitor, roscovitine (CYC202, Seleciclib), is a purine-based compound that has been shown to inhibit CDK1, CDK2, CDK5 and CDK7 via competitive binding to the ATP-binding site of CDKs (with IC_{50} values between 0.2-0.7 μM). Again, only limited success has been achieved for roscovitine in clinical trials due to poor tolerability and limited improvements in progression-free survival (Cicenas *et al.*, 2015). Although the first generation of pan-CDK inhibitors, typified by roscovitine and flavopiridol, have had very little clinical success, their development and clinical testing has undoubtedly contributed to the development of second and third generation of CDK inhibitors, directed to achieve selectivity for specific CDKs and thus reduce potential toxicities. Indeed, many drug discovery efforts used these compounds as the starting points for development of more selective CDK inhibitors, for example CDK7 inhibitors developed in our own lab (Ali *et al.*, 2009).

1.5.1.2 Second generation: selective CDK inhibitors

The second generation of CDK inhibitors improved upon potency and selectivity. However, very few second generation CDK inhibitors progressed beyond phase I clinical trials. Dinaciclib was one of the pan-CDK inhibitors that entered clinical trials for different cancer types (reviewed in (Cicenas *et al.*, 2014; Zhang *et al.*, 2021)). Dinaciclib targets several CDKs, including CDK1, CDK2, CDK5 and CDK9 with similar IC_{50} values of 4, 1, 1 and 4nM respectively, and has higher anti-tumour activity compared to flavopridol (Parry *et al.*, 2010). Furthermore, dinaciclib can prevent the phosphorylation of RB and demonstrated xenograft

tumour regression in mouse models. Although dinaciclib displayed good efficacy and tolerability in Phase I clinical trials, no improvement in PFS was observed in Phase II trials in BCa and non-small lung cancer (NSCLC) patients (Mita *et al.*, 2014; Stephenson *et al.*, 2014). Interestingly, both flavopiridol and dinaciclib revealed significant clinical activity in haematological malignancies (Byrd *et al.*, 2007; Flynn *et al.*, 2015; Ghia *et al.*, 2017), therefore further investigation is warranted. A panel of pan-CDK inhibitors were developed showing anti-tumour activity preclinically (Zhang *et al.*, 2021). Yet, to date these inhibitors have not progressed beyond Phase I/II clinical trials for solid tumours and further evaluation is needed to determine if they could be used in combination with other drugs. The main reason for the failure of these pan-CDK inhibitors appears to reside with the fact that they target CDKs that are essential for the proliferation and survival of normal cells, in particular CDK1. As such, intolerable adverse events detailed in pan-CDK clinical trials include diarrhoea, myelosuppression and anaemia (Le Tourneau *et al.*, 2010; Nemunaitis *et al.*, 2013). However, current studies have opened up potential opportunities for the use of CDK inhibitors within specific therapeutic windows. For example, KRAS mutant lung cancer shown have shown to be particularly sensitive to CDK1 and CDK2 inhibition (Danilov *et al.*, 2016; Galimberti *et al.*, 2010; Hu *et al.*, 2015a; Hu *et al.*, 2015b; Kawakami *et al.*, 2018). Moreover, cancers with MYC overexpression are sensitized to CDK9 inhibition (Hashiguchi *et al.*, 2019; Huang *et al.*, 2014).

1.5.2 Developing selective CDK inhibitors

The poor clinical activity and considerable toxicity of the first generation of largely pan-CDK inhibitors prompted the development of inhibitors that have high selectivity for non-essential CDKs. In particular, attempts to select against inhibition of the essential activity of CDK1 towards reducing cytotoxicity have been made. The reasoning was that cancers with dependencies for specific CDKs would be susceptible to drugs that selectively inhibit the specific CDK activity. This would have the benefit of limiting toxicity in normal tissues that are less dependent on that CDK. The possibility that selective CDK inhibitors could be developed was demonstrated by the differential CDK selectivity of flavopiridol. Flavopiridol (Alvocidib) is an inhibitor of CDK1, CDK2, CDK4, CDK6, CDK7 and CDK9, which can induce growth arrest and apoptosis in cancer cell lines (with IC_{50} values of 30, 170, 100, 60, 300 and 10nM, respectively). Although this is a first generation pan-CDK inhibitor, it was shown that its main anti-tumour activity was achieved via inhibition of CDK9 (Krystof *et al.*,

2012). With its preclinical success, flavopiridol became the first CDK inhibitor to be entered into clinical trials (Kelland, 2000). However, the severe cytotoxicity and poor efficacy of flavopiridol limited its progression. As mentioned above, the essential nature of CDK1 might preclude the utility of selective CDK1 inhibitors. Supporting this premise is the above-described (see Section 1.5.1.1) non-essentiality of CDK2 and CDK4/6 for complete cell cycle progression, but rather the finding that CDK2 and CDK4/6 demonstrate tissue-specific essentiality. For example, CDK4 and CDK6 double knockout mice, as well as cyclin D knockout mice, developed normally (Kozar *et al.*, 2004; Malumbres *et al.*, 2004). The particular importance of CDK4 and cyclin D1 in ER^+ BCa, provided by frequent gene alterations resulting in their over-expression, as well as the implication of cyclin D1 in ET resistance, (see section 1.2.5), further supported the possibility that ER^+ BCa would be susceptible to selective CDK4/6 inhibitors.

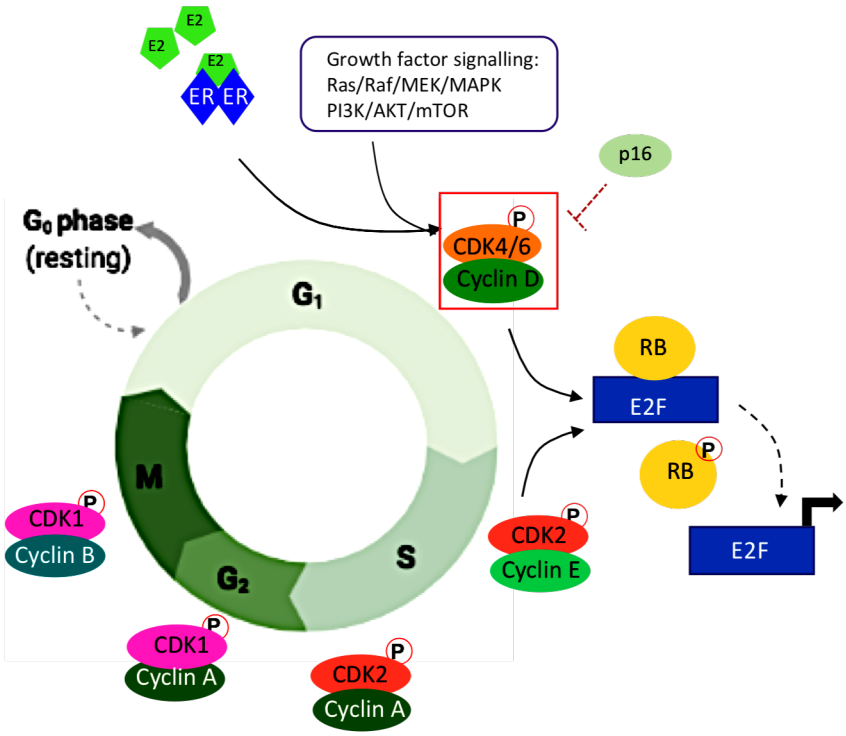
1.5.2.1 Identification of CDK4/6 inhibitors and success in clinical trials

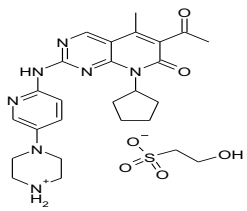
PD-0332991 (palbociclib, Ibrance, Pfizer, USA), a piperazine pyridopyrimidine derived compound inhibiting CDK4 and CDK6 *in vitro*, with IC_{50} of 11 nM and 15 nM, respectively, and with no detectable inhibitory activity for 36 other kinases (including CDK1 and CDK2), was reported in 2004 (Fry *et al.*, 2004) (Figure 1.11). Palbociclib inhibits CDK4 and CDK6 by forming hydrogen bonds with the ATP binding cleft in CDK4/6 and has anti-tumour activity in both *in vitro* and *in vivo* cancer models (Toogood *et al.*, 2005; VanderWel *et al.*, 2005). Growth inhibition was considerably stronger in ER^+ BCa cell lines than in ER-negative lines, while cell lines lacking RB were insensitive to palbociclib (Finn *et al.*, 2009). It was suggested that palbociclib exerts its inhibitory activity by preventing the phosphorylation of RB at Ser780 and Ser795, thus blocking progression through G1 phase, leading to cytostasis. Strikingly, palbociclib as a single agent can inhibit the growth of ER^+ BCa cell lines that have acquired resistance to tamoxifen. These findings paved the way for the assessment of palbociclib in phase I clinical trials to investigate its uses as a monotherapy, as well as its potential for combination therapy with ET for patients who have progressed on ET. The clinical development of palbociclib is described below.

In parallel, two other highly selective CDK4/6 inhibitors were developed. LY-293219 (abemaciclib, Verzenio, Elli Lily, USA) inhibits CDK4 and CDK6 with IC_{50} values of 2 nM and 9.9 nM, respectively (Gelbert *et al.*, 2014) (Figure 1.11). Abemaciclib is at least 50x more potent at inhibiting CDK4/6 than other CDKs. LEE-011 (ribociclib, Kisquali) developed by Novartis, has IC_{50} values of 10 nM and 39 nM for CDK4 and CDK6, respectively (Tripathy *et al.*, 2017). Abemaciclib and robiciclib have a similar mechanism of action to palbociclib, binding to the ATP cleft of CDK4/6 to block their enzymatic activity (Chen *et al.*, 2016), resulting in the inhibition of RB phosphorylation, and as such promoting cell cycle arrest. Moreover, recent work also suggested CDK4/6 inhibition can lead to the activation of anti-tumour activity by two distinct pathways (Goel *et al.*, 2017). Goel et al. (Goel *et al.*, 2017), used abemaciclib to model CDK4/6 inhibition, showing that abemaciclib treatment activated endogenous tumour retroviral elements, resulting in the induction of type III interferons (IFNs). Secondly, the suppression of T regulatory cells (Trova *et al.*, 2009) was suggested to be in correlation with reduction in E2F and DNA methyltransferase 1 activities that stimulated tumour cell clearance by cytotoxic T-cells. Other studies have also suggested the use of CDK4/6 inhibitors can enhance phosphorylation of nuclear factor for activated T cells (NFAT) family and induce anti-tumour activity (Deng *et al.*, 2018; Nebenfuehr *et al.*, 2020). Furthermore, CDK4/6 inhibition can induce quiescence, senescence and apoptosis in different cell contexts (Goel *et al.*, 2022; Wagner and Gil, 2020). CDK4/6 inhibitors show induction of a senescence-like state in an RB- and p53-dependent manner and this was well-tolerated *in vivo* (Guan *et al.*, 2017; Wang *et al.*, 2022). However, a study showed that palbociclib induces senescence in bladder cancer cells, independent of RB status but instead dependent on FOXM1 (Castellano *et al.*, 2016). This may indicate that CDK4/6 inhibitors have different modes of action depending on the cancer type.

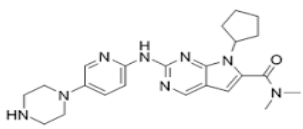
All three CDK4/6 inhibitors were entered into phase I clinical trials for advanced ER^+ BCa. Palbociclib was first tested in the phase I clinical trials with RB+ advanced solid tumours to study its efficacy as a monotherapy and interrogate drug tolerance (Flaherty *et al.*, 2012; Schwartz *et al.*, 2011). That resulted in partial responses and prolonged PFS in some patients. Palbociclib was administered in a three-week on, one-week off manner to improve tolerability. Likewise, abemaciclib was entered into a phase I clinical trial as a monotherapy for a small group of patients with metastatic BCa and showed good anti-tumour activity and disease stabilisation (Shapiro *et al.*, 2013). Ribociclib was also well-tolerated and stabilised disease

progression in patients with advanced solid tumours and lymphomas (Infante *et al.*, 2014). Through the preclinical results and data from phase I clinical trials, all CDK4/6 inhibitors demonstrated anti-tumour activity in ER^+ BCa, which provided the rationale for further investigation of the use of CDK4/6 inhibitors for ER^+ BCa patients.

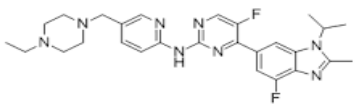




Palbociclib
PD-0332991
Ibrance



Ribociclib
LEE011
Kisqali



Abemaciclib
LY2835219
Verzenios

Figure 1.11. CDK4/6 inhibitors and potential resistant pathways.
In BCa, several signaling pathways are altered that can activate CDK4/6-cyclin D1 to promote G1 entry, such as increased ER signalling, altered PI3K and MAPK pathways. The loss of the CDK inhibitor, p16INK4 is one mechanism for elevated CDK4/6 activity. Cyclin D1 gene amplification/over-expression is observed in more than 50% of ER+ BCa and its over-expression is associated with poor clinical outcome in patients treated with endocrine therapy. In addition, CDK4 amplification is found in 19% of ER+ BCa. These findings together provide the rationale for developing treatments targeting the CDK4/6-cyclin D1 axis. CDK4/6 inhibitors, palbociclib, ribociclib and abemaciclib have been extensively evaluated in clinical trials of advanced ER+ BCa and are now approved as adjuvant therapies for advanced BCa. BCa, breast cancer; CDK, cyclin dependent kinase; CDKI, cyclin dependent kinase inhibitor; ER, estrogen receptor.

1.5.2.1.1 Palbociclib and PALOMA trials

In 2015, the PALOMA-1 phase II clinical trial (Finn *et al.*, 2015) recruited 165 treatment-naïve postmenopausal, advanced ER^+ BCa patients, who were given either letrozole or the combination of palbociclib plus letrozole. The combination treatment resulted in significantly improved PFS for palbociclib+letrozole compared to letrozole alone (20.2 versus 10.2 months). However, there was no significant difference between the treatment groups for OS (37.5 versus 34.5 months), although the median time before the requirement for chemotherapy was significantly extended to 26.7 and 17.7 months, respectively (Finn *et al.*, 2020).

PALOMA-1 encouraged the development of the phase III trials, PALOMA-2 and PALOMA-3, that further explored the use of palbociclib in combination with letrozole and fulvestrant, respectively. In PALOMA-2, 666 treatment-naïve postmenopausal advanced ER^+ BCa patients were recruited for assessment of the quality of life (QOL) after treatment with letrozole and placebo versus the combination therapy of letrozole and palbociclib (Rugo *et al.*, 2018). Data revealed that the combination therapy significantly delayed deterioration in QOL, compared to letrozole alone. With the additional follow-up study of a further 23 months, data showed a prolonged median time before requiring chemotherapy intervention of 40.4 months in the combination arm versus 29.9 months in the single agent arm (Rugo *et al.*, 2019). Collection of data for determining OS is in progress.

The PALOMA-3 trial aimed to test the efficacy of combining palbociclib and fulvestrant compared to fulvestrant alone, in 521 pre- and post-menopausal women who had relapsed on prior ET (Turner *et al.*, 2015). The median PFS of 9.2 months for the combination group, compared to the 3.8 months in the fulvestrant alone group, demonstrated the benefit of palbociclib. Furthermore, a follow-up study found augmented PFS of 11.2 months versus 4.6 months in the combination and monotherapy arms, respectively (Turner *et al.*, 2018). The extended 44 months follow-up study was recently updated and reported that the palbociclib and fulvestrant treatment group has an improved OS of 34.9 months, compared to 28 months for fulvestrant alone (Cristofanilli *et al.*, 2021). Although palbociclib is generally well-tolerated, some patients experience adverse effects, most serious of which are neutropenia and leukopenia. With the encouraging clinical data from the PALOMA trials, palbociclib was the

first CDK4/6 inhibitor to be approved as first line treatment for advanced ER^+ BCa patients in combination with AIs or fulvestrant. There are ongoing clinical trials that are assessing the use of the combination of CDK4/6 inhibitors with ET in early-stage ER^+ BCa (Pernas *et al.*, 2018). Additional clinical trials are in progress to explore the use of palbociclib with different therapeutic combinations in other cancer types (Table 1.2).

1.5.2.1.2 Abemaciclib in MONARCH trials

Abemaciclib is the most potent of the three CDK4/6 inhibitors (CDK4/6i) (Chen *et al.*, 2016). Moreover, abemaciclib may be unique among the three CDK4/6i in crossing the blood-brain barrier (Raub *et al.*, 2015), which would extend its utility to the treatment of patients with brain metastases. Clinical trials have been carried out to investigate the safety and efficacy of abemaciclib in BCa and NSCLC patients, including patients with brain metastases (Patnaik *et al.*, 2016; Tolaney *et al.*, 2020a), although the current trials are inconclusive in this respect. To explore the use of abemaciclib as a monotherapy, the phase II MONARCH-1 trial was conducted in 132 patients with advanced ER^+ BCa who had progressed from ET or chemotherapy, to assess response to abemaciclib (Dickler *et al.*, 2017). Results were promising, with median PFS of 19.7% and median OS of 17.7 months. However, some patients experienced varying degrees of gastrointestinal related adverse effects such as nausea, fatigue and diarrhoea.

MONARCH-1 supported the progression to the phase III MONARCH-2 trial (Sledge *et al.*, 2017), to interrogate the combinational use of abemaciclib and fulvestrant. 669 advanced BCa patients who had progressed on ET were recruited, although patients who had received two prior treatments of ET, or had prior treatment of chemotherapy, fulvestrant or other CDK4/6 inhibitors, were excluded. The median PFS was 16.4 months for the combination arm versus 9.3 months in the fulvestrant monotherapy group. Long term follow-up to a median of 44.7 months showed a significantly prolonged OS of 46.7 months in the abemaciclib plus fulvestrant group, compared to 37.3 months in patients receiving fulvestrant and placebo (Sledge *et al.*, 2020).

The Phase III MONARCH-3 trial was conducted to test the combination of abemaciclib with AI in 493 postmenopausal women with advanced ER^+ BCa treated who had not received any prior treatment for advanced disease (Goetz *et al.*, 2017; Johnston *et al.*, 2019). Interim analysis of the trial data showed that combination treatment versus AI monotherapy resulted in median PFS rates of 28.1 and 14.7 months, respectively. Follow-up after a median of 26.7 months for the MONARCH-3 trial was recently published with subgroup analysis. Data suggest that the combination had beneficial effects for all groups, even in groups of poor prognostic factors including liver metastasis, PR-ve status and high tumour grade (Johnston *et al.*, 2021). Based on the significantly improved PFS in MONARCH-2, abemaciclib in combination with AI was clinically approved in 2017 for treating metastatic BCa. Moreover, abemaciclib is the only CDK4/6 inhibitor that is clinically approved for use as a single agent following the success of the MONARCH-1 trial (Table 1.2).

1.5.2.1.3 Ribociclib in MONALEESA trials

Ribociclib has also shown remarkable benefits in phase I clinical trials (Table 1.2). Ribociclib was entered into the phase III MONALEESA-2 trial, to study the efficacy of combination with letrozole as first line therapy for advanced ER^+ breast cancer in 668 postmenopausal, treatment naïve and ET sensitive patients (Hortobagyi *et al.*, 2016). The trial revealed improved median PFS in the combination arm of 25.3 months compared to 16 months in the letrozole plus placebo arm. Further phase III MONALEESA-3 trials explored the use of ribociclib plus fulvestrant in ET-resistant patients (Slamon *et al.*, 2019). In 484 postmenopausal patients with metastatic ER^+ BCa, which also included patients who have progressed from first line ET treatment, significant augmentation in median PFS was shown in the combined therapy arm of 20.5 months, versus 12.8 months for the single agent group. OS was shown to be improved with ribociclib, with 53.7 months versus placebo of 41.5 months over the extended follow-up over the period of 56.3 months (Slamon *et al.*, 2021). In parallel, the MONALEESA-7 trial was conducted with 627 ER^+ BCa premenopausal patients, with anastrazole/letrozole in combination with ribociclib or placebo as the first line therapy for advanced disease (Tripathy *et al.*, 2018). Like the other trials, the combination treatment increased median PFS to 23.8 months, compared with 13.0 months for the AI alone. OS data are yet to be reported. As with the other CDK4/6i, patients treated with ribociclib experienced adverse effects such as neutropenia, nausea and leukopenia. Following the success demonstrated in the MONALEESA

trials, ribociclib in combination with AI was clinically approved in 2018 for premenopausal and perimenopausal patients with advanced ER^+ BCa. Moreover, ribociclib in combination with fulvestrant has also been approved for postmenopausal patients.

Table 1. 2 Summary of clinical trials involving CDK4/6 inhibitors.

Tumour type	Study	Phase	Description	Study endpoint	Median OS	Ref
Palbociclib						
Advanced tumours: melanoma, liposarcoma, breast, renal, ovarian and colon cancer	NCT00141297	I	Palbociclib	SD: 27%	NA	(Flaherty *et al.*, 2012)
Liposarcoma, melanoma, colon cancer		I	Palbociclib	SD: 29% PR: 3%	NA	(Schwartz *et al.*, 2011)
Relapsed mantle cell lymphoma	NCT00420056	I	Palbociclib	SD: 43% PR: 12%	NA	(Leonard *et al.*, 2012)
ER^+ $HER2^-$ metastatic BCa		I	Palbociclib	SD: 75% PR: 25%	NA	(Slamon *et al.*, 2010)
ER^+ $HER2^-$ metastatic BCa in postmenopausal women	PALOMA-1	II	Palbociclib and letrozole vs Letrozole	PFS: 20.2 months vs 10.2 months	37.5 months vs 34.5 months	(Finn *et al.*, 2015)
ER^+ $HER2^-$ metastatic BCa in postmenopausal women	PALOMA-2	III	Palbociclb and letrozole vs Placebo and letrozole	PFS: 24.5 months vs 14.5 months	36-months OS: 77% vs 60.6%	(Finn *et al.*, 2016)
ER^+ $HER2^-$ metastatic BCa in postmenopausal women	PALOMA-3	III	Palbociclib and fulvestrant vs Placebo and fulvestrant	PFS: 9.5 months vs 4.6 months	5-year OS: 23.3% vs 16.8%	(Turner *et al.*, 2018)
sarcoma with CDK4 overexpression and other advanced tumours	NCT03242382	II	Palbociclib	Pending		*ClinicalTrials.gov*; U.S. National Library of Medicine, **2022.**
ER^+ $HER2^-$ metastatic BCa progression from ET	NCT02690480 NCT02549430 NCT02491983 NCT02684032 NCT02668666 NCT02599714 NCT02297438 NCT02389842 NCT02028507 NCT01823835 NCT02536742 NCT02448771 NCT02592746 NCT02778685 NCT02384239	I/II/III	Palbociclib with ET in combination PI3K or mTOR inhibitors and immunotherapy	Pending		
ER^+ $HER2^-$ early BCa	NCT01864746 NCT02513394	III	Palbociclib with ET as adjuvant/post neoadjuvant therapy	Pending		*ClinicalTrials.gov*; U.S. National Library of Medicine, **2022.**
ER^+ $HER2^-$ early BCa	NCT02296801 NCT02624973 NCT02400567 NCT02008734 NCT02592083 NCT02764541 NCT02603679	II	Palbociclib with ET as neoadjuvant therapy	Pending		*ClinicalTrials.gov*; U.S. National Library of Medicine, **2022.**
Abemaciclib						
NSCLC		I	Abemaciclib	PFS: 2.1 months		

Tumour type	Study	Phase	Description	Study endpoint	Median OS	Ref
Advanced HR^+ BCa		I	Abemaciclib vs Abemaciclib and fulvestrant	PR: 17% vs 6%		
ER^+ $HER2^-$ metastatic BCa in postmenopausal women	MONARCH-1	II	Abemaciclib	PFS: 6 months	22.3 months	(Dickler *et al.*, 2017)
ER^+ $HER2^-$ metastatic BCa	MONARCH-2	III	Abemaciclib and fulvestrant vs Placebo and fulvestrant	PFS: 16.4 months vs 9.3 months		(Sledge *et al.*, 2017)
ER^+ $HER2^-$ metastatic BCa in postmenopausal women	MONARCH-3	III	Abemaciclib and letrozole/exemestane vs Placebo and letrozole/exemestane	PFS: 28.2 months vs 14.8 months		(Goetz *et al.*, 2017)
ER^+ $HER2^-$ metastatic BCa in postmenopausal women	MONARCH PLUS	III	Abemaciclib and letrozole/Anastrozole/fulvestrant vs Placebo and letrozole/Anastrozole/ fulvestrant	PFS: 11.5 months vs 5.6 months	Pending	
ER^+ $HER2^-$ metastatic BCa	Next MONARCH-1	II	Abemaciclib Vs Abemaciclib and tamoxifen Vs Abemaciclib and propholatic loperaminde	PFS: 9.1 months vs 6.5 months vs 7.4 months	20.8months vs 24.2 months vs 17 months	
ER^+ $HER2^-$ metastatic BCa	Abema-Pembo	I	Abemacilcib, anatrazole and Pembrolizumab	DCR: 77%	Pending	
ER^+ $HER2^+$ metastatic BCa in postmenopausal women	monarchHER	II	Abemaciclib, fulvestrant and trastuzumab vs Abemaciclib and trastuzumab Vs Trastuzumab and single chemotherapy	PFS: 8.3 months vs 5.7 months vs 5.7 months	Pending	(Tolaney *et al.*, 2020b)
ER^+ $HER2^-$ RB^+ metastatic BCa in postmenopausal women	NCT031030439	II	Abemaciclib	Pending	Pending	*ClinicalTrials.gov*; U.S. National Library of Medicine, **2022.**
ER^+ $HER2^-$ early BCa	neoMONARCH	II	Abemacilcib and anatrazole vs Abemaciclib vs anatrazeole	Ki-67 decrease: 93% vs 91% vs 63%	Pending	(Hurvitz *et al.*, 2020)
ER^+ $HER2^-$ early high risk, node positive BCa	monarchE	III	Abemaciclib and Standard of care ET vs standard of care ET	IDSF: 92.2 % vs 88.7%	Pending	(Johnston *et al.*, 2020)
Ribociclib						
Advanced solid tumours and lymphoma	NCT01237236	I	Ribociclib	PR: 2.9% SD: 26%		*ClinicalTrials.gov*; U.S. National Library of Medicine, **2022.**
ER^+ $HER2^-$ metastatic BCa in postmenopausal women	NCT01857193	I	Ribociclib and exemestane	SD: 28.6%		*ClinicalTrials.gov*; U.S. National Library of Medicine, **2022.**

ER^+ $HER2^-$ metastatic BCa in postmenopausal women	NCT01872260	I	Ribociclib and letrozole for treatment naïve and pretreated patients	PFS: 25.3 months Vs 5.5 months		*ClinicalTrials.gov*; U.S. National Library of Medicine, **2022.**
ER^+ $HER2^-$ metastatic BCa in postmenopausal women	NCT02088684	I	Ribociclib and fulvestrant with continuous vs sequential treatment	SD: 32.1% vs 25.1%		*ClinicalTrials.gov*; U.S. National Library of Medicine, **2022.**
Tumour type	**Study**	**Phase**	**Description**	**Study endpoint**	**Median OS**	**Ref**
ER^+ $HER2^-$ early BCa in postmenopausal women	NCT01919229	I	Ribociclib and letrozole vs Letrozole	Ki67 decrease: 96% vs 69%		*ClinicalTrials.gov*; U.S. National Library of Medicine, **2022.**
ER^+ $HER2^-$ metastatic BCa in postmenopausal women	NCT01872260	I	Ribociclib, Alpelisib and letrozole	DCR: 70%		*ClinicalTrials.gov*; U.S. National Library of Medicine, **2022.**
ER^+ $HER2^-$ metastatic BCa in postmenopausal women	MONALEESA-2	III	Ribociclib and letrozole vs Placebo and letrozole	PFS: 25.3 months vs 16.0 months		(O'Shaughnessy *et al.*, 2018)
ER^+ $HER2^-$ metastatic BCa in postmenopausal women	MONALEESA-7	III	Ribociclib and goserelin/AI/tamoxifen vs Placebo and goserelin/AI/tamoxifen	PFS: 23.8 months Vs 13.0 months		(Tripathy *et al.*, 2018)

Data as of September 2022. AI aromatase inhibitor, BCa breast cancer, DCR disease control rate, ER estrogen receptor, ET endocrine therapy, PFS progression free survival, PR partical response, SD stable disease

As described earlier, CDK4/6 is highly expressed in some cancers other than BCa and so studies have suggested expanding the utility of CDK4/6i in these other cancer types, as well as investigating the potential for CDK4/6i in combination with other targeted therapies. Indeed, CDK4/6i have been tested in clinical trials involving other cancers, with some good responses. In a phase II trial of palbociclib for lymphoma patients, 57% of patients had 12-week PFS and the median PFS was 17.7 months in well-differentiated and dedifferentiated lymphoma (Dickson *et al.*, 2016). In a phase I study investigating the use of abemaciclib as a single agent in BCa, NSCLC and other advanced solid tumours, it was reported that 46% of patients reach stable disease and 49% show disease control rate (Patnaik *et al.*, 2016). In addition, in a phase II trial for BRAF mutant melanoma, ribociclib showed a 44% disease control rate (Taylor *et al.*, 2014). Current studies are limited to pre-clinical investigations and data collected from phase I/II trials, hence further work is needed for to determine the potential efficacy of CDK4/6i in cancers other than ER^+ BCa, either as monotherapy or in combination with other treatments.

Tumourigenesis and metastasis involve the dysregulation of multiple signalling pathways, which provides opportunities for combining drugs with various therapeutic targets. Identifying appropriate combination therapies could increase the range of cancers that could be treated with CDK4/6i, as exemplified by the clinical trials combining CDK4/6i with ET in ER^+ BCa (Yuan *et al.*, 2021). CDK4/6 inhibition has been shown to trigger anti-tumour activity and upregulation of major histocompatibility complex class I (MHC I) in BCa cell lines (Goel *et al.*, 2017). These results suggest an alternative therapeutic strategy of combining CDK4/6i with immunotherapy, as CDK4/6i may ameliorate the immune checkpoint blockade. Additionally, a separate study has suggested an alternative role of CDK4/6i, in which CDK4-cyclin D1 phosphorylates the speckle-type POZ protein (SPOP) and in turn leads to the destabilisation of PD-L1 (Zhang *et al.*, 2018). In the same study, the use of anti-PD-1 together with palbociclib was shown to have greater anti-tumour effects *in vivo* than single treatments, providing the rationale for a possible combination therapy. Other studies have proposed targeting the PI3K/ATK/mTOR axis in combination with CDK4/6i, as this pathway is upstream of the CDK4/6-cyclin D axis and may sensitise cells for CDK4/6 inhibition (Cortes *et al.*, 2017; Michaloglou *et al.*, 2018). Indeed, the combination of PI3K and CDK4/6 inhibitors has demonstrated combinatorial anti-proliferative effects in TNBC cell lines and caused tumour regression in mouse xenograft tumour models (Teo *et al.*, 2017). CDK4/6i were shown to re-

sensitise EGFR/HER2 resistant lung cancer and oesophageal squamous cell carcinomas to EGFR/HER2 inhibitors (Liu *et al.*, 2016; Zhou *et al.*, 2017). The combination of EGFR inhibitor, cetuximab and palbociclib has also been tested in a Phase II trial for human papillomavirus unrelated head and neck cancer patients with resistance to platinum and cetuximab (Adkins *et al.*, 2019). The data demonstrated improved objective response rates of 39% in the combination arm versus 19% for cetuximab and placebo. BRAF or MEK inhibitors have also been proposed for use with CDK4/6i in BRAF mutant cancers such as colorectal cancer and melanoma, with preclinical data showing anti-proliferative effects (Pek *et al.*, 2017). Moreover, additional publications have highlighted the importance of the appropriate therapeutic window (Martin *et al.*, 2018; O'Leary *et al.*, 2016; Shi *et al.*, 2022). Particularly, in melanoma cancer models, the synergism between CDK4/6 and BRAF/MEK inhibitors was only seen in treatment-naïve models, with resistance models showing limited benefit using this combination.

1.5.2.2 Resistance to CDK4/6 inhibitors

Despite the clinical success of CDK4/6i, emergence of resistance was observed in many patients and might result from intrinsic or acquired resistance mechanisms (Knudsen and Witkiewicz, 2017; O'Leary *et al.*, 2016) (Figure 1.12). Investigations into the mechanisms of response and resistance are important, firstly to identify biomarkers that would predict patient response, important to avoid unnecessary treatment. Secondly, understanding mechanisms of resistance would aid in the development of combination treatments that avoid resistance development, and/or treatments that can be used following emergence of resistance. One mechanism for resistance to CDK4/6i that is already well-established is loss of RB function. This was clearly demonstrated in the growth inhibition determined from 44 BCa cell lines in which RB mutant cell lines did not respond to palbociclib (Finn *et al.*, 2009). Whether RB loss is a mechanism for acquired resistance to CDK4/6i, at least in ER^+ BCa, remains unclear. Certainly, long term culturing of BCa cell lines in the presence of palbociclib, resulted in RB loss in the emergent palbociclib-resistant cells, although RB loss was not observed in all models (Pancholi *et al.*, 2020). The amplification of $p16^{INK4a}$ has been shown to avert response to CDK4/6 inhibition, and so $p16^{INK4a}$ levels can be used as a marker of response for treatment stratification (Dean *et al.*, 2012; Witkiewicz *et al.*, 2011). The exact resistance mechanism is

unclear, but tumours with intrinsically high $p16^{INK4a}$ levels may lose their dependence on CDK4/6 and so reduce the effectiveness of clinical CDK4/6i (Witkiewicz *et al.*, 2011).

The overexpression of CDK4 or CDK6 may also provide a potential mechanism of resistance to CDK4/6i. CDK4 overexpression can act as an intrinsic mechanism of resistance, as rhabdomyosarcoma with increased CDK4 levels had reduced sensitivity to ribociclib (Olanich *et al.*, 2015). A recent study has also suggested that the phosphorylation state of Thr172-CDK4 in BCa may be predictive of palbociclib sensitivity (Raspe *et al.*, 2017). The absence of Thr172 phosphorylation indicates that an inactive CDK4 was found in palbociclib resistant BCa cell lines and some cancer types, which may suggest that a bypass in cell cycle progression decreases dependence on CDK4. Thus, the phosphorylation state of CDK4 may be a possible biomarker. CDK6 gene amplification was observed in abemaciclib-resistant BCa cells, here linking alterations in CDK6 as a mechanism of acquired resistance to abemaciclib (Yang *et al.*, 2017). Indeed, CDK6 knockdown in MCF7 cells with acquired abemaciclib-resistance was sufficient to resensitise cells to abemaciclib, while ectopic over-expression of CDK6 in MCF7 and T47D cells was sufficient to establish resistance to abemaciclib.

There is also evidence implicating cyclin E in response to CDK4/6i. It is possible that aberrant expression of cyclin E could lead to activation of CDK2, such that inhibition of progression through G1 by CDK4/6i is bypassed. In this model, CDK2 activation would lead to RB phosphorylation, promoting the E2F-directed gene expression needed for G1 progression. Cyclin E over-expression may also overcome CDK2 suppression of $p21^{CIP1}$ and $p27^{KIP1}$, however, the definitive role of cyclin E is an ongoing investigation. The role of cyclin E1 has shown conflicting results in clinical trials such as PALOMA-3, in which CCNE1 expression level can be used as a biomarker of response to palbociclib in ER^+ BCa (Turner *et al.*, 2019). However, other clinical studies have found no predictive value for cyclin E1 protein levels in sensitivity to palbociclib plus fulvestrant (Pascual *et al.*, 2021).

The investigation also extended to studying the role of overexpression of cyclin E2 on responsiveness to CDK4/6 inhibition (Caldon *et al.*, 2012; Wander *et al.*, 2020). This possibility is supported, at least in part by a recent publication by genomic, transcriptomic and

proteomic analysis of isogenic ER^+ BCa cell lines, long-term estrogen-deprived (LTED) counterparts and palbociclib-resistant LTED cells (Pancholi *et al.*, 2020). The authors reported increased expression of cyclin E1 and E2 in some of the palbociclib-resistance models. However, CDK2, CDK4 and CDK7 expression was also elevated in these models, as were EGFR and MAPK levels. Other studies have shown that G2/mitosis checkpoint proteins, including PLK1, were upregulated in patient derived xenograft (PDX) models from ER^+ BCa bone metastases in which palbociclib resistance was generated by treatment of the PDX tumours in mice (Montaudon *et al.*, 2020). In these PDX models, the PLK1 inhibitor, volasertib caused significant tumour regression, prompting the suggestion that PLK1 inhibitors might be used after progression on CDK4/6i.

ER status may also be a contributing factor to the sensitivity of ER^+ BCa to CDK4/6i due to its role in driving cyclin D1 expression. Irrespective of the role of ER in regulating cyclin D1 expression, TNBC patients do not respond to CDK4/6i, at least in the current clinical settings. Interestingly, the PALOMA-1 trial enrolled two patient cohorts (Finn *et al.*, 2015). Cohort one (N=50 patients) were randomized to letrozole or letrozole+palbociclib. The second cohort (N=150) comprised of patients with CCND1 amplification and/or $p16^{INK4a}$ loss. Response to palbociclib in both cohorts was the same, so CCND1 amplification and/or p16 loss made no difference to response. This indicates that over-expression of CCND1 is not in itself a factor in the response to CDK4/6i. Given that CCND1 expression is increased by ER, as well as through PI3K/AKT/mTOR signalling and the fact that CCND1 protein or mRNA levels were not assessed in the PALOMA trials, CCND1 levels may still be important in response to CDK4/6i. Indeed, one study using BCa cell lines with early adaptation to palbociclib, identified an increase in CCND1 expression via copy number alteration and increased CCND1 transcript and the authors proposed that CDK2-cyclin D1 complexes may act to drive G1 (Arnold and Papanikolaou, 2005; Chytil *et al.*, 2004; Herrera-Abreu *et al.*, 2016). Reduced expression of ER or PR was observed in ER^+ BCa cell lines with acquired resistance to abemaciclib and ribociclib, which suggested reduced dependence on ER signalling (Iida *et al.*, 2020; Yang *et al.*, 2017).

Upregulation of PI3K/AKT/mTOR pathway may also provide a resistance mechanism to CDK4/6i, as previous investigations have shown that activation of this pathway leads to the

stabilisation of the CDK4/6-cyclin D complex, hence reducing CDK4/6 inhibition (Miller *et al.*, 2011). Another study suggested that resistance to CDK4/6 inhibition could result from the loss of PTEN and increased activation of ATK leading to inhibition of $p27^{KIP1}$ and increasing CDK4 and CDK2 activities (Costa *et al.*, 2020). Furthermore, metabolic reprogramming in pancreatic cancer led to increased activity of mTORC1 that mediates increased metabolic rate, leading to the proposal that increased mTOR activity enhances the ability of cancer cells to enter the cell cycle after termination of CDK4/6i treatment (Franco *et al.*, 2016). These reports highlight the need for additional work to investigate the efficacy of PI3K/ATK/mTOR inhibitors in combination with CDK4/6i. Moreover, fibroblast growth factor receptor (FGFR)-1 and FGFR2 can activate PI3K/ATK/mTOR and Ras/MEK/ERK pathways that may contribute to CDK4/6i resistance (Turner *et al.*, 2010). Preclinical data have shown the amplification of FGFR2 in a metastatic ER^+ BCa patient who achieved a significant clinical benefit from the mTOR inhibitor, everolimus, together with the AI exemestane (Wein *et al.*, 2017), further supporting the possibility of targeting the PI3K/AKT/mTOR pathway alongside CDK4/6i.

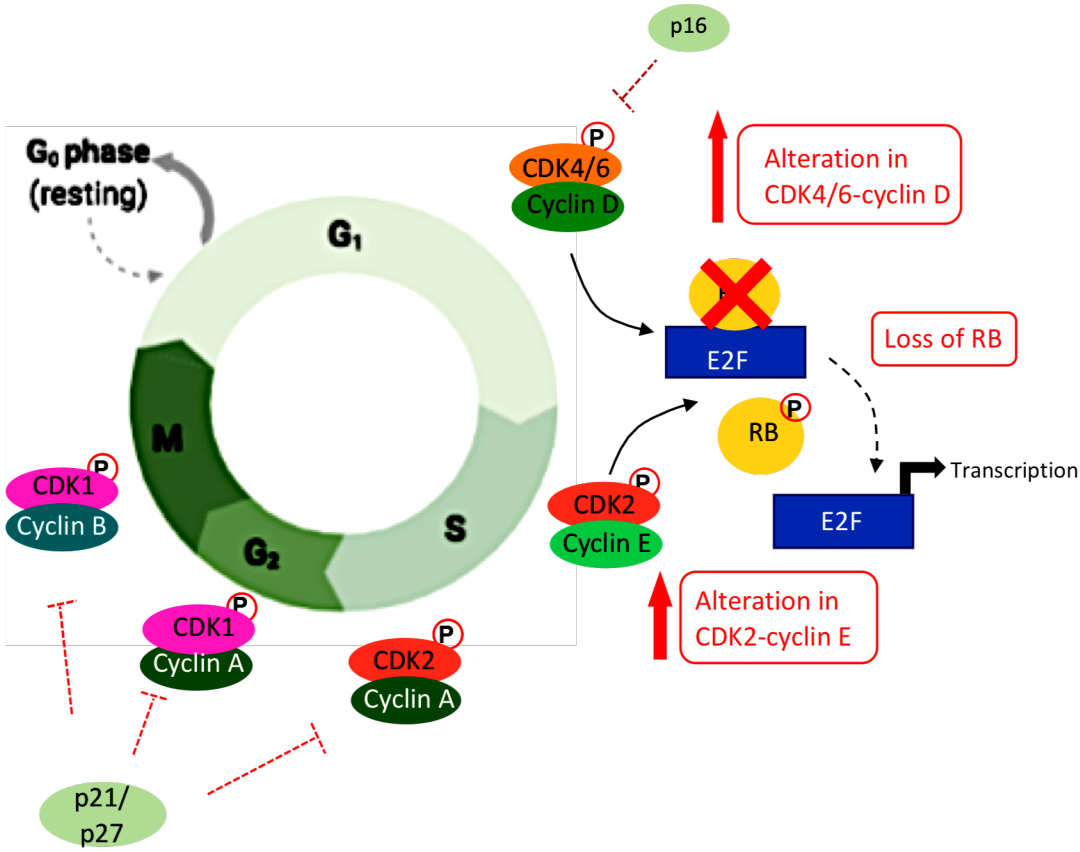


Figure 1.12. CDK4/6 inhibitors and potential resistant pathways.
Palbociclib, abemaciclib and ribociclib targets CDK4/6-cyclin D-RB axis leading to cell cycle arrest. However, with raising concern of resistance development to CDK4/6 inhibitors, recent literature proposed several potential resistance pathways such as through loss of RB, alterations of CDK4/6-cyclin D and CDK2-cyclin E axes.

1.5.3 Development of selective inhibitors for other CDK implicated in cancer

1.5.3.1 CDK1 and CDK2 inhibitors

Like CDK4 and CDK6, CDK2 is a non-essential CDK, which opens up its potential for novel targeted therapies with fewer toxicities. However, the development of highly selective CDK2 inhibitors has presented many challenges due to the similarities between the amino acid sequence CDK2 and CDK1, thus attaining highly selective CDK2 inhibitors remains difficult. Notwithstanding, there are now several CDK2 inhibitors that have shown promising preclinical data and that have been enrolled in clinical trials. One of the best clinically studied CDK2 inhibitors is AT7519 (IC_{50} value of 47nM). However, AT7519 does also inhibit other CDKs, including CDK1, CDK4, CDK6 and CDK9, with IC_{50} values of 210, 100, 170 and <10nM, respectively (Santo *et al.*, 2010; Squires *et al.*, 2009; Wyatt *et al.*, 2008). Though AT7519 is therefore a pan-CDK inhibitor, it has been entered into several clinical trials for various advanced cancer types, and it was also studied in combination with heat shock protein 90 (hsp90) inhibitor, onalespib and the proteaosome inhibitor, bortezomib for metastatic solid tumours and multiple myeloma, respectively (Table 1.3). A further CDK2 inhibitor, PF-06873600, targets CDK2/4/6 with IC_{50} values between 0.48-1.6nM and with 47- and 83-fold increased selectivity to CDK1 and CDK9, respectively (Freeman-Cook *et al.*, 2021a; Freeman-Cook *et al.*, 2021b). With promising anti-tumour activities in preclinical data, this compound has advanced to ongoing phase II clinical trials for breast, ovarian and fallopian tube cancers in combination with ET (Table 1.3).

1.5.3.2 CDK7 inhibitors

As related above, the critical role of CDK7 in both cell cycle regulation and transcription led to the interrogation of CDK7 as a potential druggable target for cancer therapy (Sava *et al.*, 2020). Supplemented with previous work from our group that identified a role for CDK7 in stimulating ER activity, as well as the demonstration that CDK7 expression is increased in BCa directed research towards the development of CDK7 inhibitors (Chen *et al.*, 2000; Patel *et al.*, 2016). To this end, our group described the first selective CDK7 inhibitor, BS-181 (Ali *et al.*, 2009). BS-181 is a pyrazole-pyrimidine derived compound that showed high specificity for CDK7 with an IC_{50} value of 21 nM and considerably higher IC_{50} values for other CDKs, 386-,

42- and 200-fold higher for CDK1, CDK2 and CDK9, respectively. BS-181 inhibited phosphorylation of Pol II at Ser2 and Ser5 in the CTD, as well as ER at Ser118. Consequently, BS-181 reduced the growth of cancer cell lines *in vitro* and *in vivo*. However, BS-181 had little potential for progression clinically due to its poor cell permeability and lack of oral bioavailability. Nevertheless, BS-181 provided good proof-of-concept for further CDK7 inhibitor development. Subsequent efforts allowed our group to develop an orally bioavailable, non-covalent, ATP competitive CDK7 inhibitor, ICEC0942 (Patel *et al.*, 2018) (Figure 1.13). ICEC0942 inhibits CDK7 with an IC_{50} of 40 nM. IC_{50} values for CDK2, CDK9 and CDK1 were 15-, 30- and 230-fold higher than that for CDK7, while CDK4/6 were not inhibited even at a concentration of 10 μM. Screening of a panel of 117 kinases confirmed CDK7 selectivity. ICEC0942 inhibited phosphorylation of Pol II, CDK1, CDK2 and ER. Crucially, ICEC0942 inhibited a wide range of cancer cell lines, including MCF7 and the colorectal cancer HCT116 in tumour xenografts (Patel *et al.*, 2018). *In vitro*, growth inhibition involved growth arrest in multiple phases of the cell cycle. Moreover, ICEC0942 worked combinatorially with tamoxifen and fulvestrant, to inhibit MCF7 cell growth. These findings led to the progression to phase I clinical trials for advanced solid malignancies (clinicaltrials.gov: NCT03363893), with results demonstrating an acceptable safety profile and disease stabilisation in some patients. Subsequent combination of ICEC0942 (clinical name CT7001 or samuraciclib) with fulvestrant demonstrated the potential efficacy of this combination therapy, resulting in FDA Fast Track designation for samuraciclib with SERDs in ER^+ BCa patients for CDK4/6i-resistant ER^+ BCa patients. FDA fast track designation has also been granted for samuraciclib with chemotherapy drugs for advanced TNBC (see https://www.esmo.org/oncology-news/safety-and-antitumour-activity-of-a-first-in-class-oral-selective-cdk7-inhibitor; https://www.pharmatimes.com/news/fda_fast_tracks_breast_cancer_candidate_samuraciclib_1375147 – websites accessed 4th Dec. 2021) (Table 1.3).

Several other selective CDK7 inhibitors are also being progressed to the clinic, with the most prominent ones emerging from THZ1 (Kwiatkowski *et al.*, 2014). THZ1 is a covalent, irreversible CDK7 inhibitor, which links to Cys312 of CDK7. Potent activity for THZ1 was demonstrated for T-cell acute lymphoblastic leukaemia (T-ALL), neuroblastoma and small cell lung cancer (Chipumuro *et al.*, 2014; Christensen *et al.*, 2014; Kwiatkowski *et al.*, 2014), purportedly by targeting transcriptional dependencies in these cancers. However, it has subsequently emerged that the strong transcriptional action of THZ1 is likely to result from the

inhibition of CDK12/13, in addition to CDK7 (Olson *et al.*, 2019; Zhang *et al.*, 2016). These promising results for THZ1 have nevertheless led to the development of YKL-5-124, a derivative of THZ1 and a PAK4 inhibitor, PF3758309 (Murray *et al.*, 2010), with high specificity for CDK7 and no interaction with CDK12/13 (Olson *et al.*, 2019). Interestingly, YKL-5-124, also a covalent CDK7 inhibitor appears to lack activity against transcriptional targets of CDK7 and mainly acts by inhibiting cell cycle progression. Another THZ1 analogue, the covalent CDK7 inhibitor SY-1365 had good efficacy in preclinical data and progressed to Phase I clinical trial for patients with advanced solid tumours (Hu *et al.*, 2019b). However, progression of this drug was halted due to the shift in focus to an alternative non-covalent selective CDK7 inhibitor, SY-5609 (Marineau *et al.*, 2021). Preclinical results demonstrated that SY-5609 stunted tumour growth in PDX models of ovarian, colorectal, lung and BCa (Hu *et al.*, 2019a; Johannessen *et al.*, 2019; Papadopoulos *et al.*, 2020). SY-5609 has recently started in a phase I clinical trial for BCa, NSCLC and other solid tumours (*ClinicalTrials.gov*; U.S. National Library of Medicine, **2021**. https://ClinicalTrials.gov/show/NCT04247126) (Table 1.3).

One other CDK7 inhibitor has been started in a phase I clinical trial. XL102, created by Exelisis Inc. (Study of XL102 as single-agent and combination therapy in subjects with solid tumors (ClinicalTrials.gov: NCT04726332). However, there is no publicly available data on XL102, either on the mechanism by which XL102 inhibit CDK7, level of CDK7 selectivity, or pre-clinical data on target engagement and consequence for cancer cell growth.

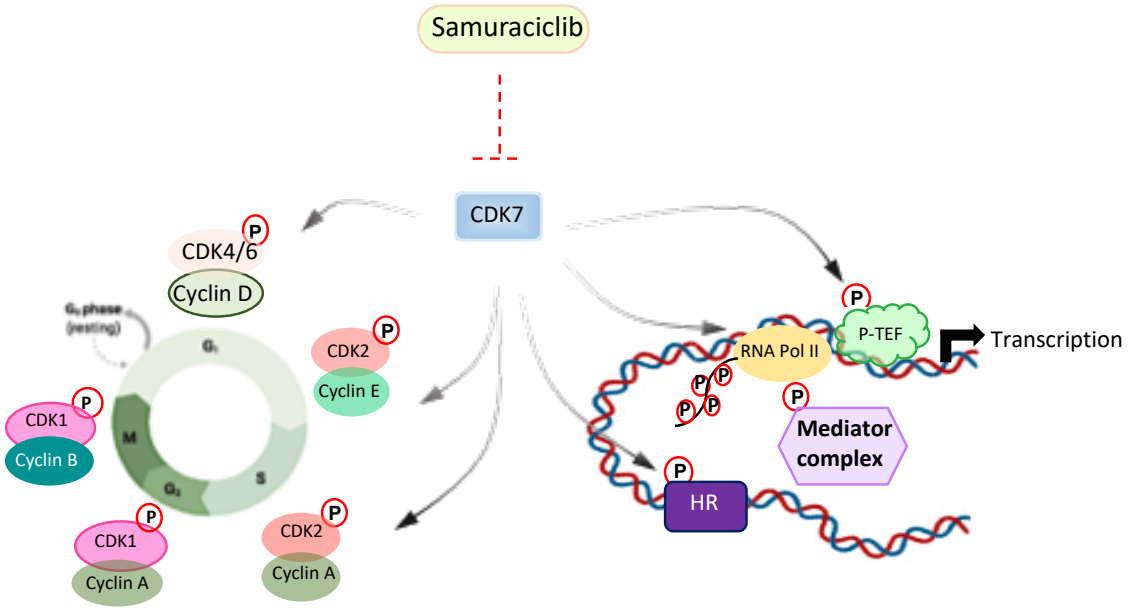


Figure 1.13. CDK7 inhibitor as potential treatment for ER$^+$ breast cancer.
CDK7 as the master regulator of cell cycle and mediates PolII transcription of oncogenes and anti-apoptotic genes is an attractive therapeutic target in BCa, in particular its role in activating CDK4/6-cyclin D1 and ER. Samuraciclib (also known as CT7001 and ICEC0942) has shown to inhibit tumour growth in in vitro and in vivo models. BCa, breast cancer; CDK, cyclin dependent kinase; ER, estrogen receptor; PolII, RNA polymerase II.

1.5.3.3 CDK9 inhibitors

Most of the first generation CDK inhibitors inhibited CDK9, as well as other CDKs. Subsequent efforts have been aimed at developing selective CDK9 inhibitors. BAY-1143572 (Atuveciclib) was the first clinical CDK9 inhibitor to be described (Lucking *et al.*, 2017). Preclinical data revealed the mode of action through inhibition of PolII-Ser2 phosphorylation, resulting in inhibition of transcription. The mechanism of growth inhibition was linked to the fact that transcription inhibition resulted in rapid loss of short-lived mRNAs, in particular MYC and MCL1 and consequently protein. BAY-1143572 showed high efficacy and good tolerability in both cancer cell lines and in PDX models. This prompted the entry of BAY-1143572 into a phase I trial with TNBC, gastric and other advanced tumours (NCT01938638), the findings of which are yet to be published. Separately, a derivative of BAY-1143572 was developed, BAY-1251152, which had improved upon the biochemistry, cell permeability and selectivity against other CDKs (Luecking *et al.*, 2017). BAY-1251152 was enrolled into two different phase I clinical trials for advanced haematological malignancies, which are ongoing.

AZD4573 is also a potent, highly selective CDK9 inhibitor, with strong activities in *in vitro* and *in vivo* models of haematological cancers (Barlaam *et al.*, 2020; Cidado *et al.*, 2020). These findings have allowed progression of AZD4573 to an ongoing phase I clinical trial to evaluate efficacy in advanced haematological cancers (NCT03262637) (Table 1.2). Two other CDK9 inhibitors, NVP-2 and THAL-SNS-032 have also been described recently (Olson *et al.*, 2018). NVP-2, an ATP-competitive CDK9 inhibitor has high specificity for CDK9 and has been shown to block transcription elongation. THAL-SNS-032 can recruit the E3 ligase Cereblon, to promote proteasomal degradation of CDK9. The anti-tumour activity of THAL-SNS-032 is mediated by induction of apoptosis. Interestingly, the apoptotic effects persist even after drug washout. NVP-2 and THAL-SNS-032 have not yet been progressed to phase I clinical trials. Two additional highly selective CDK9 inhibitors, GFH009 and KB-0742 (Richters *et al.*, 2021) have also progressed to ongoing phase I clinical trials for haematological cancers and advanced solid tumours, respectively (Table 1.2).

1.5.3.4 CDK12/13 inhibitors

Unlike the selective CDK inhibitors described above, CDK12/13 inhibitors remain to be more fully developed. Initial studies have begun into the utility of CDK12/13 inhibitors in preclinical cancer models. As mentioned above, THZ1 was recently recognised as a CDK7/CDK12/13 inhibitor, while small molecule compounds that have high selectivity for CDK12/13 have also been described (Ito *et al.*, 2018; Johannes *et al.*, 2018; Zhang *et al.*, 2016). THZ531, derived from THZ1, shows high selectivity for CDK12 and 13, with IC_{50} values of 158nM and 69nM, respectively, which is more than 50-fold lower than the IC_{50} values for CDK7 or CDK9 (Zhang *et al.*, 2016). Initial characterisation showed that THZ531 inhibits transcription elongation and strongly induces apoptosis in Jurkat cells. An unrelated series of non-covalent CDK12 inhibitors that inhibit Pol II-Ser2 phosphorylation and exhibit cytotoxicity in OV90 and THP1 cells, have also been developed (Johannes *et al.*, 2018). A recent publication reported the development of a novel CDK12 degrader, BSJ-4-116, which reduced expression of DNA damage response genes and has anti-proliferative activity in cancer cells (Jiang *et al.*, 2021). Current studies of CDK12/13 inhibitors remain at early preclinical stage and further investigation will contribute to the ongoing quest to widen therapeutic strategies in cancer with CDK12/13 inhibitors.

1.5.3.5 CDK8/19 inhibitors

The use of CDK8/19 inhibitors, to target the mediator complex a transcriptional regulator, is a developing area of research and several selective CDK8 inhibitors are in development. However, despite the success using *in vitro* models, only a limited number of compounds progressed to Phase I/II clinical trials, including BCD-115 (ClinicalTrials.gov: NCT03065010) and RUV120 (ClinicalTrials.gov: NCT05052255) for ER^+ BCa and advanced solid tumours, respectively (Dziadziunszko *et al.*, 2022; Rzymski *et al.*, 2015). The stunted development of CDK8/19 inhibitors was reported to be due to the dual inhibitory effects of both CDK8 and CDK19 having been not well tolerated.

Table 1. 3 Clinical development of transcriptional CDK inhibitors

Tumour type	Study	Phase	Description	Study endpoint	Median OS	Reference
CDK2 inhibitors						
Advanced solid neoplasm	NCT02503709		Onalespib and AT7519	Pending	NA	(Santo *et al.*, 2010) *ClinicalTrials.gov*; U.S. National Library of Medicine, **2022**. https://clinicaltrials.gov/ct2/show/NCT02503709
HR Breast cancer, ovarian cancer, fallopian tube cancer and perinoeal cancer	NCT03519178		PF-06873600 vs PF-06873600 with ET	Pending	NA	*(Freeman-Cook et al., 2021b)* *ClinicalTrials.gov*; U.S. National Library of Medicine, **2022.** https://clinicaltrials.gov/ct2/show/NCT03519178
CDK7 inhibitors						
ER^+ BCa, AML and advanced solid tumours	NCT03363893	II	ICEC0942 and fulvestrant Vs ICEC0942	Pending	NA	(Patel *et al.*, 2018) *ClinicalTrials.gov*; U.S. National Library of Medicine, **2022**. https://ClinicalTrials.gov/show/NCT04247126
Advance cancers	NCT03770494	I	LY3405105	Pending	NA	*ClinicalTrials.gov*; U.S. National Library of Medicine, **2022** https://clinicaltrials.gov/ct2/show/NCT03770494
BCa, NSCLC and other solid tumours	NCT04247126	I	SY 5609 with fulvestrant vs SY 5609	Pending	NA	(Marineau *et al.*, 2022) *ClinicalTrials.gov*; U.S. National Library of Medicine, **2022**. https://ClinicalTrials.gov/show/NCT04247126
BCa, ovarian cancer and other advance solid tumours	NCT03134638	I	SY-1365 with venetoclax	Terminated	NA	(Hu *et al.*, 2019b) *ClinicalTrials.gov*; U.S. National Library of Medicine, **2022. https://clinicaltrials.gov/ct2/show/NCT03134638**
Solid tumours	NCT04726332	I	XL102 as single agent or combination treatment	Pending	NA	*ClinicalTrials.gov*; U.S. National Library of Medicine, **2022.** https://clinicaltrials.gov/ct2/show/NCT04726332
CDK9 inhibitors						
Advanced cancers and acute leukaemia	NCT01938638 NCT02345382	I	BAY-1143572	Data not published	NA	(Lucking *et al.*, 2017) *ClinicalTrials.gov*; U.S. National Library of Medicine, **2022.** https://clinicaltrials.gov/ct2/show/NCT01938638, https://clinicaltrials.gov/ct2/show/NCT02345382
Haematological malignancies and advanced solid tumours	NCT02745743 NCT02635672	I	BAY-1251152	Pending	NA	*ClinicalTrials.gov*; U.S. National Library of Medicine, **2022.** https://clinicaltrials.gov/ct2/show/NCT02745743, https://clinicaltrials.gov/ct2/show/NCT02635672
CML, multiple myeloma and B-lymphoid maglinancies	NCT00446342 NCT00292864	I	SNS-032	Data not published	NA	(Chen *et al.*, 2009) *ClinicalTrials.gov*; U.S. National Library of Medicine, **2022.** https://clinicaltrials.gov/ct2/show/NCT00446342, https://clinicaltrials.gov/ct2/show/NCT00292864
Advacned haematological malignancies	NCT04630756 NCT03263637	I	AZD4573 with acalabrutinib	Pending	NA	(Barlaam *et al.*, 2020) *ClinicalTrials.gov*; U.S. National Library of Medicine, **2022.** https://clinicaltrials.gov/ct2/show/NCT04630756, https://clinicaltrials.gov/ct2/show/NCT03263637

Advance solid tumours and sarcomas	NCT03604783	I	TP-1287	Pending	NA	(Kim *et al.*, 2017) *ClinicalTrials.gov*; U.S. National Library of Medicine, **2022.** https://clinicaltrials.gov/ct2/show/NCT03604783
Haematological malignancies	NCT04588922	I	GFH009	Pending	NA	*ClinicalTrials.gov*; U.S. National Library of Medicine, **2022. https://clinicaltrials.gov/ct2/show/NCT04588922**
Advanced solid tumours	NCT04718675	I	KB-0742	Pending	NA	(Richters *et al.*, 2021) *ClinicalTrials.gov*; U.S. National Library of Medicine, **2022.** https://clinicaltrials.gov/ct2/show/NCT0471867
CDK8/19 inhibitors						
ER^+ $HER2^-$ advanced or metastatic tumours	*NCT03065010*	I	BCD-115	Pending	NA	*ClinicalTrials.gov; U.S. National Library of Medicine, **2022.** https://clinicaltrials.gov/ct2/show/NCT03065010*
Advanced solid tumour	NCT05052255	I/II	RUV120	Pending	NA	*ClinicalTrials.gov; U.S. National Library of Medicine, **2022. https://clinicaltrials.gov/ct2/show/NCT05052255***

Data collected as of September 2022. AML acute myeloid leukaemia, BCa breast cancer, CML chronic myeloid leukaemia, ER estrogen receptor, NSCLC, non-small cell lung cancer

1.6 Hypothesis and aims

With the clinical success of CDK4/6 inhibitors in combination with ET, it progressed to the use of this combinational therapy as the first line adjuvant therapy for advanced ER^+ BCa and is progressing to first line adjuvant therapy for early stage, primary BCa. A key drawback is the rapid development of acquired resistance in BCa cell lines, which is also evident in advanced BCa patients. Several mechanisms of resistance to CDK4/6 inhibitors have been highlighted, some of which involve altered expression of other cell cycle and transcriptional CDKs. These findings led to my hypothesis that CDK4/6 inhibitor resistance can be mediated by their overexpression and/or their substitution by other CDKs. I propose to assess this possibility by developing genetic models of resistance to palbociclib in BCa cell lines by over-expressing key CDKs or cyclins. Secondly, therapeutic options for patients with disease progression after CDK4/6 inhibitors remain underexplored, emphasising the need for the ongoing development of therapeutics strategies following resistance to CDK4/6 inhibitors. Thus, I aim to exploit the recently developed CDK7 inhibitor from our lab, ICEC0942, as well as the CDK7/CDK12/13 inhibitor, THZ1, to determine if inhibiting CDK7 and other transcriptional CDKs could be used to overcome resistance to CDK4/6 inhibitors in BCa cell lines. Finally, our collaborators have developed models of resistance to palbociclib in ER^+ breast cancer cell line, either in estrogen-dependent or long-term estrogen deprived (LTED) cells for investigating the potential epigenetic and transcriptomic changes after development of resistance to palbociclib (Pancholi *et al.*, 2020). I will interrogate ChIP-seq data generated using an antibody to histone H3 acetylation on lysine 27 (H3K27ac), a histone mark associated with actively transcribed genes, for identifying altered genes and signalling pathways in association to palbociclib resistance. In addition, towards developing new insights into mechanisms of resistance to palbociclib, RNA-seq data also will be analysed in conjunction with ChIP-seq for identifying potential mechanisms of resistance.

For development of genetic models for resistance to palbociclib, I will:

- use CRISPR-Cas9 genome editing to generate RB KO model in MCF7 cells. This model will allow confirmation of the importance of RB for response to CDK4/6 inhibitors and provide models for determining the RB dependency of CDK7 inhibitors.
- In MCF7 cells, over-express CDKs and cyclins implicated in resistance to CDK4/6 inhibitors. For this purpose, I propose to develop:

    - inducible protein expression by generating fusion proteins with dihydrofolate reductase (DHFR), in which the fusion protein is rapidly degraded. Addition of trimethoprim (TMP) stabilises DHFR, for functional fusion protein expression (Iwamoto *et al.*, 2010).
    - Use the activating Cas9 system, in which a modified, enzymatically dead Cas9 is targeted to gene promoter specific sgRNAs (Konermann *et al.*, 2015), to increase expression of the endogenous gene.
- The cell lines generated by the above methods will be used to determine response to CDK4/6 inhibitors and the consequence of gene over-expression on resistance to CDK4/6 inhibitors.
- Use the CDK4/6 inhibitor resistant models to determine sensitivity to the CDK7 and CDK7/CDK12/13 inhibitors, ICEC0942 and THZ1.

2. Materials and Methods

2.1 Materials

2.1.1 Reagents

Molecular biology reagents, such as cDNA synthesis kits, Polymerase Chain Reaction (PCR) kits and DNA ladders were supplied by Thermo Fisher Scientific (Life Technologies, UK). Kits for genomic DNA preparation were obtained from Invitrogen (Life Technologies, UK) and kits for RNA and plasmid DNA preparation were purchased from QIAGEN Ltd, UK. PCR purification kits, CleanSweep and ExoSAP were obtained from Thermo Fisher Technology, UK. The site-directed mutagenesis kit was obtained from Stratagene (Agilent Technologies UK Limited, UK). Restriction enzymes were purchased from New England Biolabs, UK (NEB). Transfection reagents were purchased from Thermo Fisher Scientific, UK and Promega, UK. Oligonucleotides were synthesised by Invitrogen. siRNAs and shRNA plasmids were purchased from Horizon Discovery, UK. SYBR™ Green real-time PCR reagents were purchased from Applied Biosystems (Life Technologies, UK). Protease and phosphatase inhibitor cocktail tablets were obtained from Roche Diagnostics Ltd, UK and/or Sigma-Aldrich, UK. BCA quantification kit, as well as the SuperSignal West Pico and Femto Western blotting reagents were obtained from Thermo Scientific, UK. Protein gel size markers and 10% Tween-20 solution was obtained from Bio-Rad Laboratories Ltd, UK (Bio-Rad).

2.1.2 Sundries

1.5mL and 2mL microcentrifuge tubes and pipette tips were purchased from STARLAB Ltd, UK. 0.2ml Thermo-PCR tubes were obtained from Thermo Fisher Scientific (Life Technologies, UK). Serological stripette pipettes, tissue culture and microbiology grade plastics were purchased from Corning®, UK. 30ml round bottom centrifuge tubes and 250ml centrifuge bottles were purchased from SARSTEDT Ltd, UK and VWR International Ltd, UK, respectively. Nitrocellulose Membrane, 0.45µm, 30cm x 3.5m was obtained from Bio-Rad UK. MicroAmp® Fast 96-well reaction plate and MicroAmp® Optical 384-well Reaction Plate with barcodes was purchased from Applied Biosystems (Life Technologies, UK).

2.1.3 General laboratory equipment

BIOMAT 2 Microbiological Safety Cabinets (Contained Air Solutions Ltd, UK) were used for tissue culture work. Cells were maintained at 37°C in a humidified air atmosphere supplied with 5% CO_2 in RS Biotech Galaxy R+ CO_2 incubators. Sorvall RC6 Plus centrifuges with Fiberlite™ F21-8 x50y and Fiberlite™ F14-6 x 250y Fixed-Angle Rotors (Thermo Fisher Scientific) were used for high speed centrifugation of large volumes. Benchtop microcentrifuges, Sorvall Pico™ (Sorvall, UK) or Heraeus™ Biofuge Pico™ (Thermo Fisher Scientific) were used for centrifuging with microcentrifuge tubes. Incubations were carried out in an incubator oven (LEEC, UK), shaking incubator (New Brunswick Scientific Company Incorporated, USA) or block heater (Grant-bio, Wolf Laboratories, UK). Applied Biosystems Veriti™ 96 well thermal cyclers (Life Technologies) were used for PCR reactions. StepOne™ Plus Real Time PCR system (Applied Biosystems, Life Technology, UK) or the QuantStudio™ 7 Flex Real Time PCR system (Applied Biosystems, Life Technology, UK) were used to perform RT-qPCR. Horizontal agarose gel electrophoresis tanks were obtained from Thistle Scientific, UK. Power packs and apparatuses used in western blotting vertical gel electrophoresis and transfer tanks were supplied by Bio-Rad, UK. DNA and RNA quantification were carried out by performing spectrophotometric measurements using a Nanodrop™ND-1000 (Labtech International, UK). Samples were mixed using a Vortex-Genie 2 (Scientific Industries, UK). A Tecan Sunrise™ absorbance microplate reader (Tecan UK Ltd, UK) was used to obtained absorbance readings. Chemiluminescence imaging was performed using iBright™ CL 1500 imaging system (Thermo Fisher Scientific, UK) and Fusion Solo system (Vilber Lourmat, France). Long term cell growth was monitored and cell images obtained using an Incucyte Zoom live cell imaging system (Essence Bioscience, UK).

2.1.4 Cell culture reagents

L-Glutamine (200mM L-glutamine in 0.9% sodium chloride), L-Glutamine-Penicillin-Streptomycin (200mM L-glutamine, 10,000 units/ml penicillin and 10mg/ml streptomycin in 0.9% sodium chloride) (PSG), L-Glutamine (200mM L-glutamine in 0.9% sodium chloride), 0.02% ethylenediaminetetraacetic acid (EDTA) solution and 10X trypsin-EDTA solution were supplied by Sigma-Aldrich, UK. Dulbecco's Modified Eagle's Medium (DMEM) was supplied by Sigma-Aldrich, UK and Lonza, UK. Phenol red-free DMEM, Roswell Park Memorial Institute-1640 (RPMI-1640) lacking phenol-red and Opti-MEM reduced serum medium were

supplied by Gibco™, Life Technologies, UK. Accutase® Cell Detachment Solution (Accutase® enzymes in Dulbecco's PBS containing 0.5mM EDTA and phenol red) was supplied by BioLegend UK Ltd, UK. Fetal calf serum (FCS) and dextran-coated, charcoal-treated FCS (DSS) were purchased from First Link Ltd, UK.

2.1.5 Chemicals

Dimethylsulfide (DMSO) was purchased from Sigma-Aldrich, UK. Palbociclib Hydrochloride (Sigma-Aldrich, UK), Abemaciclib (Selleck, UK) and Ribociclib (Selleck, UK), were re-constituted with DMSO to a stock concentration of 10mM. THZ1 was purchased from Apexbio, UK. ICEC0942 was kindly provided by Carrick Therapeutics Ltd. THZ1 and ICEC0942 were re-constituted in DMSO to a stock concentration of 20mM. 17-β-estradiol (E2) (Sigma Aldrich, UK) was prepared in ethanol at a stock concentration of 10mM. Trimethoprim (TMP, Sigma-Aldrich, UK), 1mg/mL Blasticidin S HCl (Corning, UK), 1mM Puromycin (Sigma-Aldrich, UK) and 1g/mL Doxocycline (TakaRa, Japan) were prepared with sterile double distilled water (ddH_2O, Invitrogen, UK). Geneticin® solution (G418, Gibco, UK), 50mg/mL Hygromycin b solution (Invitrogen, UK and Thermo Fisher Scientific, UK) were used to supplement DHFR and AcCas9 cells. All stock solutions were stored at -20°C.

2.1.6 General solutions

Solutions were prepared in double distilled water (ddH_2O), autoclaved and stored at room temperature, unless stated otherwise.

Table 2. 1 General stock solution composition

Phosphate buffered saline (PBS) 10x	**137mM NaCl, 3mM KCl, 8mM Na_2HPO_4, 1.5mM KH_2PO_4, pH 7.4**
Tris-borate-EDTA (TBE) buffer (10x)	89mM Tris-base pH 8.0, 89mM boric acid, 2mM Na-ethylenediaminetetraacetic acid (EDTA)
Tris-EDTA (TE) buffer	10mM Tris-HCl pH 8.0, 1mM Na-EDTA pH8.0
1% Ammonium Persulfate (APS)	1g in 10ml of ddH_2O, aliquoted and stored at -20°C

2.1.7 Microbiological reagents and stock composition

Luria-Bertani (LB)-broth and LB-broth agar capsules (obtained from MP Biomedical, France) were prepared with ddH_2O, autoclaved and stored at room temperature. Ampicillin was used as the antibiotic selection, which was added just before use, as summarised in Table 2.2.

Table 2. 2 Microbiological reagents

LB agar plates	**10g tryptone-B, 5g yeast extract-B, 10g NaCl, 15g agar-B in 1 litre ddH_2O and autoclaved before use. Antibiotic was added when cooled to 50°C, the solution was poured into 10 cm^2 Sterilin Petri dishes (Thermo Fisher Scientific, UK) and left to set at room temperature and stored at 4°C for short term storage.**
LB broth	10g tryptone-B, 5g yeast extract-B, 10g NaCl in 1 litre ddH_2O.
Ampicillin	Ampicillin sodium salt (Sigma-Aldrich, UK), dissolved in ethanol to 100mg/ml. Ampicillin solution was added to bacterial media at time of use, to a final concentration of 100µg/ml.
S.O.C media	2% Tryptone, 0.5% yeast extract, 10mM NaCl, 2.5mM KCl, 10mM $MgCl_2$, 10mM $MgSO_4$, 20mM glucose. Purchased from Invitrogen.

2.2 Methods

2.2.1 Tissue culture

The MCF7 cell line was obtained from ATCC. These MCF7 and derived cell lines were maintained at 37°C with 5% CO_2, in DMEM supplemented with 10% FCS and 1% PGS. Stable MCF7 cell lines expressing DHFR fusion constructs were additionally supplemented with 600µg/mL G418. Ac-Cas9 expressing cells were routinely maintained in the presence of 200µg/mL Hygromycin, 10µg/mL Blasticidin and 1µg/mL Puromycin. Ac-Cas9 palbociclib-resistant (PalboR), abemaciclib-resistant (AbemaR) and ribociclib-resistant (RiboR) lines were cultured in the presence of 250nM palbociclib, 50nM abemaciclib or 500nM ribociclib, respectively.

MCF7, T47D and HCC1428 and the matched PalboR cell lines obtained from Dr Lesley-Ann Martin (Institute of Cancer Research (ICR)) have been described (Pancholi *et al.*, 2020). These cells were maintained in phenol-red free RPMI-1640 with 10% FCS and 1% PSG, supplemented with 1nM E2. Long term estrogen-deprived (LTED) cell lines derived from the ICR cell lines were maintained in phenol red-free RPMI-1640 with 10% DSS and 1% PSG. The PalboR lines from the ICR were maintained in media additionally containing 1µM Palbociclib.

Cell lines were cultured in 25cm^2 or 75cm^2 cell culturing flasks (Corning®, UK) and incubated at 37°C and 5% CO_2 with humidified conditions. Cells were routinely passaged when they reached 70-80% confluency. For each passage, culture medium was removed and the cells washed twice with 0.02% EDTA solution (Sigma-Aldrich, UK). 0.5-1mL of 1% trypsin (Sigma-Aldrich, UK) was added for detachment of the adherent cells. Cell suspensions were obtained after 3-5 minutes of incubation at 37°C and 5mL of fresh medium was added to inactivate the trypsin. Cell suspensions were serially passaged in new culture flasks. All cell lines were routinely tested for Mycoplasma using Mycoplasma Detection kit, every 3-4 months (MycoAlert™ Mycoplasma detection kit, Lonza, UK).

For long-term storage, cell suspensions were obtained as above, followed by centrifugation at 1200rpm for 5 minutes to obtain a cell pellet in a 15mL falcon tube. Cell pellets were re-suspended at a concentration of 1-2x10^6 cells per mL of freezing mix (FCS filtered with a

0.45µM syringe filter (Sartorius, UK), containing 10% DMSO). 1mL of cells in the freezing mix was transferred to each cryovial and stored at -80°C for 24 hours before long-term storage in liquid nitrogen.

2.2.2 Cell counting

To determine the number of cells for seeding in specific experiments, homogenized cell suspensions were obtained (See 2.1.1). Equal volumes of cell suspension and 0.04% Trypan blue solution (Thermo Fisher Scientific, UK) were mixed well in 1.5mL Eppendorf tubes before loading 10µL of the cell/Trypan blue mixture to each chamber of a Countess™ cell counting chamber slide (Thermo Fisher Scientific Fisher, UK) or Countess™ II resusable slides (Thermo Fisher Scientific, UK). The slides were loaded into the Countess™ II FL Automated Cell Counter (Thermo Fisher Scientific, UK) for determining cell viability and total cell number per mL. Total number of live cells was calculated and trypsinised cells diluted accordingly for desired seeding concentrations.

2.2.3 Generating RB Knockout (KO) stable lines

Four CRISPR RNAs (crRNA) targeting exon 1 of the RB1 gene (Table 2.3), were identified using the online CRISPR design tools hosted by Horizon Discovery and obtained as Edit-R Modified Synthetic RNAs (https://horizondiscovery.com/). These were used in combination, together with Edit-R tracrRNAi (Horizon Discovery U-002005-05), to programme nuclear localisable Cas9 protein (EnGen Cas9 NLS S pyogenes, New England Biolabs). Nucleofection was used for transduction of the resulting Cas9 RNP complexes with $2x10^6$ MCF7 cells and the Lonza SE cell line 4D-Nucleofector™ kit with an Amaxa™ 4D-NucleofectorTMX Unit (Amaxa, Germany), according to manufacturer's instructions. Electroporated cells were re-suspended in 30mL fresh media and plated in 15cm^2 dishes (Corning®, UK). Once single clones were visible to the naked eye, medium was removed and plates were washed twice with sterilized phosphate buffer saline (PBS), at which point clones were detached using sterile paper discs soaked with Accutase® (BioLegend Ltd, UK) with incubation for 10-15 minutes at 37°C. Each clone was transferred to individual wells in a 12-well plate (Corning, UK) with fresh medium for clonal expansion. Clones with deletions within exon 1 of the RB1 gene were subsequently identified by using a genomic DNA based PCR assay (for method see Section 2.2.7) (primers SA4813RBf1 5'-TTTTCTCAGGGGACGTTGAAA-3'; SA4814RBr1 5'-

GTCAAGTTGAAGCCGAGACC-3') for amplification of RB1 sequences around exon 1 (product size: 484bp). Clones were selected based on the presence of smaller PCR products, consistent with Cas9-driven deletions. The RB KO stable lines were generated by Dr Georgina Sava (Division of Cancer, Imperial College London).

Table 2. 3 Summary of sgRNA targeting RB1 exon 1

sgRNA	Sequence
CRIPSR 27487504	GGTGGCGGCCGTTTTTCGGG
CRIPSR 27487517	AGGACGACGCGCGCGCACGT
CRIPSR 27487476	CTGACGAGAGGCAGGTCCTC
CRIPSR 27487475	AGAGCAGGACAGCGGCCCGG

Further sub-cloning was carried out on candidate clones from the initial screen to obtain three independent clones with complete RB loss. Clones were seeded at 2,000 cells in a 15cm^2 dish and allowed to grow to visible colonies, when they were detached and expanded using Accutase, as described above. End-point PCR was performed for genomic DNA, on selected candidates to identify deletions in the RB1 exon 1 region with agarose gel electrophoresis (for method see Section 2.2.7) and RB1 gene knockout was confirmed by Western blotting (for method see Section 2.8).

To determine the precise sequences deleted in the RB1 KO, gDNA PCR products were cloned into the CloneJet PCR cloning vector (Thermo Fisher Scientific, UK). Taq DNA polymerase was used in end-point PCR to amplify RB1 exon 1 which led to production of a 3' adenine tail in the PCR product; thus, the sticky end protocol was followed according to manufacturer's instructions. In brief, reactions were set up on ice, in which the PCR product was incubated with a blunting enzyme to remove 3' overhangs prior to ligation of DNA in a 3:1 ratio of blunt end DNA fragment to linearized cloning vector. Ligated products were then transformed into 5-alpha Competent *E. coli* cells (NEB, UK), according to manufacturer's instructions. 100µL of diluted bacterial cells in S.O.C media was plated on LB agar plates supplemented with 100µg/mL Ampicillin and plates were incubated overnight at 37°C. Single bacterial colonies were collected and grown in 3mL LB broth containing 100µg/mL Ampicillin overnight at 37°C in a shaker at 250rpm. Plasmid DNA was extracted and purified using Plasmid miniprep kit: QIAprep Spin miniprep kit (Qiagen, UK) and CleanSweep (Thermo Fisher Scientific, UK), following manufacturer's instructions (Section 2.6.3). DNA was eluted in 35µL TE buffer and DNA concentrations were determined by NanoDrop™ ND-1000 Spectrometer at 260nm and 280nm. Samples were sent for Sanger Sequencing (GENEWIZ, UK) using universal PJet1-2F

primers and aligned to WT RB1 exon1 using an online alignment tool, CLUSTAL (http://ebi.ac.uk/Tools/msa/clustalo).

2.2.4 Generation of DHFR-CDK/cyclin conditional over-expression stable lines

Fusion of the protein of interest to engineered *E. coli* dihydrofolate reductase (ecDHFR), promotes degradation of the protein of interest (Iwamoto *et al.*, 2010). Addition of the membrane penetrant small molecule DHFR ligand trimethoprim (TMP) provides a rapid and reversible stabilisation of the protein of interest. The DHFR expression plasmid (pcDNA3-HA-YFP-DHFR, #29325) was a kind gift of Prof Thomas Wandless, Stanford University. The CDK and cyclin D1 constructs, all expressing C-terminal HA-tags were obtained from Addgene (Table 2.4). DH5α bacterial stabs obtained from Addgene were plated on LB agar plates with ampicillin, to obtain single colonies. Plasmid DNAs were obtained by culturing in 100mL of fresh LB broth with ampicillin overnight at 37°C, and plasmid DNA was extracted using the Qiagen plasmid Maxiprep kit (Qiagen, UK). All plasmids were verified by Sanger sequencing (Genewiz, UK).

Table 2. 4 List of CDKs and cyclin D1-HA constructs

Plasmids	Addgene plasmid no.		Reference
Cdc2 (CDK1)-HA	1888	Cdc2-HA was a gift from Sander van den Heuvel	(van den Heuvel and Harlow, 1993)
CDK2-HA	1884	CDK2-HA was a gift from Sander van den Heuvel	(van den Heuvel and Harlow, 1993)
CDK4-HA	1876	CDK4-HA was a gift from Sander van den Heuvel	(van den Heuvel and Harlow, 1993)
CDK6-D224Y-HA	1868	CDK6-HA was a gift from Sander van den Heuvel	(van den Heuvel and Harlow, 1993)
CDK7-HA	14647	CDK7-HA was a gift from Matija Peterlin	(Kanazawa *et al.*, 2003)
CDK9-HA	14640	CDK9-HA was a gift from Matija Peterlin	(Kanazawa *et al.*, 2003)
Rc/CMV-Cyclin D1-HA	8948	Rc/CMV-cyclin D1-HA was a gift from Philip Hinds	(Baker *et al.*, 2005)

PCR reactions using primers designed to amplify CDK1 (Cdc2), from the Cdc2 plasmid (Table 2.4), to include incorporation of 5' HindIII and 3' BsiWI restriction enzymes sites (Table 2.5), were carried out using Phusion High-fidelity PCR master mix (Thermo Fisher Scientific, UK). QIAquick PCR purification kit (QIAGEN, UK) was used before and after enzyme restriction digestion to remove primers. Purified PCR reaction products were digested using the restriction enzyme combination in Table 2.5 and pcDNA3-HA-YFP-DHFR were digested using the same restriction enzyme combination for each reaction. Digested PCR and pcDNA3-HA-YFP-DHFR vector were ligated in a 2:1 ratio using T4 DNA ligase (NEB, UK) and the ligated

products were transformed using 5-alpha Competent *E.coli* cells (NEB, UK). Bacterial colonies were grown and plasmid DNA was purified using the Qiagen Plasmid Maxiprep kit, as described above. Sanger Sequencing (Genewiz, UK) was used to confirm the appropriate construct sequences. The pcDNA3-CDK6-HA-YFP-DHFR construct is shown in Figure 2.1. DHFR fusion constructs for CDK4, CDK7, CDK9 and cyclin D1 were obtained exactly as above, except for the use of alternative restriction enzymes due to the absence of appropriate HindIII sites.

Table 2. 5 List of custom primers and restriction enzymes to generate DHFR-CDK/cyclin-HA fusion constructs.

Plasmids	Primer sequence	Restriction enzyme 1	Restriction enzyme 2
Cdc2 (CDK1)-HA	Forward: 5'-CCCAAGCTTGGTACCGAGCTCGGATCCATGGAAGATTATACCAAAATAG-3' Reverse: 5'-CGTCGTACGGATAGAATTGCATCTTCTTAATCTGATTGTC-3'	HindIII	BsiWI
CDK2-HA	Forward: 5'-CCCAAGCTTGGTACCGAGCTCGGATCCATGGAGAACTTCCAAAAGG-3' Reverse: 5'-CGTCGTACGGATAGAATTGGAGTCGAAGATGGGGTAC-3'	HindIII	BsiWI
CDK4-HA	Forward: 5'-CCCAAGCTTGGTACCGAGCTCGGATCCATGGCTACCTCTCGATATGAG-3' Reverse: 5'-CGTCGTACGGATAGAATTGCTCCGGATTACCTTCATC-3'	HindIII	BsiWI
CDK6-D224Y-HA	Forward: 5'-CTTGGTACCGAGCTCGGATCCGCCACCATGGAGAAGGACGGCCTGTG-3' Reverse: 5'-CGTCGTACGGATAGAATTGGGCTGTATTCAGCTCCGAGGTG-3'	Kpn1	BsiWI
CDK7-HA	Forward: 5'-CTTGGTACCGAGCTCGGATCCGCCACCATGGCTCTGGACGTGAAGTCTC-3' Reverse: 5'-CGTCGTACGGATAGAATTGAAAAATTAGTTTCTTGGGCAATC-3'	Kpn1	BsiWI
CDK9-HA	Forward: 5'-CTTGGTACCGAGCTCGGATCCGCCACCATGGCAAAGCAGTACGACTC-3' Reverse: 5'-CGTCGTACGGATAGAATTGGAAGACGCGCTCAAACTC-3'	BamHI	BsiWI
Rc/CMV-Cyclin D1-HA	Forward: 5'-CTTGGTACCGAGCTCGGATCCGCCACCATGGAACACCAGCTCCTGTG-3' Reverse: 5'-CGTCGTACGGATAGAATTGGATGTCCACGTCCCGCAC-3'	Kpn1	BsiWI



Figure 2. 1. Plasmid map of the CDK6-DHFR construct. Plasmid map shows the positions of the forward and reverse primers, the CDK1, HA, YFP and DHFR open reading frames.

The CDK2 open reading from contains a BsiWI restriction site. As BsiWI offers the only 3' restriction site for cloning, site-directed mutagenesis (QuickChange site-directed mutagenesis kit (Ailgent Technology, UK)) was used to introduce a single base, silent change in the CDK2 ORF (bp G39C) using primers having the following sequences 5'-GATCGGAGAGGGCACCTACGGAGTTGTGTAC-3' and 5'-GTACACAACTCCGTAGGTGCCCTCTCCGATC-3'. The only CDK6-HA construct available from Addgene carries a D224Y mutation. Prior to cloning in the DHFR construct, therefore, site-directed mutagenesis (primers 5'-GCCTCTTTTTCGTGGAAGTTCAGATGTTGATCAACTAGGAAAAAT-3' and 5'-ATTTTTCCTAGTTGATCAACATCTGAACTTCCACGAAAAAGAGGC-3') was used to generate CDK6-D224. All constructs were verified by Sanger sequencing prior to use.

$1x10^6$ MCF7 cells (Cells purchased from ATCC) were seeded in 6 well plates (Corning, UK) and transfected with 2.5µg of CDK/cyclin-HA-DHFR DNA constructs using Lipofectamine 3000 (Invitrogen, UK), according to manufacturer's protocol. In brief, MCF7 cells were seeded in 6-well plates 24 hours prior to transfection using a master mix containing the DHFR fusion

construct and Lipofectamine 3000 reagent diluted in Opti-MEM medium and incubated at 37°C with 5% CO_2. Cells were supplemented with fresh media after 24 hours of transfection. 600µg/mL of Geneticin (Gibco, UK) was added after 48 hours for continual selection. The DHFR stable lines were generated by Dr Georgina Sava.

To determine the optimal induction by trimethoprim (TMP) (Sigma-Aldrich, UK), $1x10^6$ CDK/cyclin-HA-DHFR cells were seeded in 6 well plates and treated with increasing doses of TMP (10, 20, 50, 70, 100µM) for 24 hours. Protein lysates were collected, and Western blotting was used to determine induction of the DHFR fusion proteins (Section 2.8).

2.2.5 Generation of Ac-Cas9 stable over-expression lines

The synergistic activation mediator (SAM) comprises a three-component lentiviral vector system for targeting gene promoter regions with single guide RNAs (sgRNAs) for activation of the expression of a specific gene (Konermann *et al.*, 2015). This includes lenti-dCas9-VP64-Blast (#61425), lenti-MS2-P65-Hygro (#61426) and lenti-sgRNA (MS2)-puro backbone (#73795) for sgRNA cloning. These lentiviral vectors were gifts from Feng Zhang and acquired from Addgene (USA). MCF7 cells (Provided by Professor Phillipa Darbre, University of Reading) were transduced with viral concentrates of dCas9-VP64-Blast (#61425), lenti MS2-P65-Hygro (as described in Section 2.2.6) and subjected to selection with 10µg/ml Blasticidin and 200µg/ml Hygromycin over a 2-week period, to establish stable pools expressing dCas9-VP64 and MS2-p65 proteins.

We used the database from Joung *et al.* (2017); Konermann *et al.* (2015) of computationally designed sgRNAs mapping within a region approximately 200bp upstream of the transcription start sites for all human genes, to identify the three sgRNA sequences for each gene of interest (Table 2.6). Candidate trascrRNA sequences were synthesised as part of a 100nt oligonucleotide framework incorporating homology arms to allow Gibson assembly into the lenti sgRNA (MS2)-puro backbone. The sequences of these were organised as follows: 5'-TGTGGAAAGGACGAAACACCG<sgRNA>GTTTTAGAGCTAGGCCAACATGAGGATCACCCATGTCTGCAGGGCCTAGCAAGTTAAAA-3'. PCR was performed using oligonucleotide templates, Q5 High-Fidelity enzyme (NEB, UK) and amplification primers (5'-TGTGGAAAGGACGAAACACC-3' and 5'-TTTTAACTTGCTAGGCCCTGC-3'). The

resulting PCR products were purified by spin column chromatography (Qiagen, UK) before being used in Gibson assembly (Gibson Assembly Kit, E2611S, NEB, UK) for cloning into the Lenti-MS2-puro plasmid DNA linearised with the restriction enzyme Esp3I (NEB, UK).

5-Alpha Competent *E. coli* cells were transformed with the assembled DNAs, as described in Section 2.2. HEK293T cells were transfected with lentivirus to package individual sgRNA constructs and viral medium was collected (see Section 2.2.6). To generate a pooled Ac-Cas9 line consisting of three independent sgRNAs for each gene, equal volumes of the three sgRNA viral media were used to transduce MCF7-dCas9-VP64/MS2-P65 cells. Culture medium was replaced 24 hours after transduction with fresh medium supplemented with Hygromycin, Blasticidin and Puromycin to select for the Lenti-MS2-puro sgRNAs. Cells were allowed to recover in culture after the addition of antibiotics for at least 10 days before proceeding to further experiments. RNA and protein were prepared as outlined in Sections 2.7 and 2.8.1, for determination of increases in gene expression at the mRNA and protein levels. The AcCas9 lines were generated by Dr Chun Fui Lai and Ms Xiaobei Xiong.

Table 2. 6 List of three independent sgRNAs for each CDK/cyclin

Target	Genebank ID	sgRNA sequences
CDK1	NM_033379	AGGGCGGCTAGAGAAAAAGC
		CGCTTGCGCTCGCACTCAGT
		GACGACACTCTCCCGACTGG
CDK2	NM_052827	AGAGACATAGGTAGGAAACT
		GGGCGGGATCATTTGCGGGG
		TAGACAAGTTTCTTCCCCGG
CDK4	NM_000075	AGCGGTGAGGGGGACAAGAG
		GCTGCCACAACCCCCGCTGC
		GGAGCAGAGGTGTGGCTACG
CDK5	NM_004935	CTCTGCAGCACTCGACTCCA
		GTTTGCCTCCGCGGTAGAAA
		TTCCTGGGACTTGAAGTCCA
CDK6	NM_001259	AGCCGTGACATTGACGTGCC
		CCTCCCCGCCTCCTGAGGCC
		CGGCGCAACACAATGATATA
CDK7	NM_001799	CTAATTTGGTGTTCCATGTT
		GTCTGTGAATGTAGAAAGTT
		TTTTCTACATTACCAGGAAC
CDK8	NM_001260	GGGACATCCAGGGGGACGGC
		TCTTGCCGCATCAGTCGGGC
		TGCGGCCGGCGGGCGTAGAG
CDK9	NM_001261	CCCGAGAGGCCAGGGGGAGC
		CGGAGGCGCCTCTGCAGCTC
		GCGGCCCCGATCGGGGGCGC

CDK12	NM_015083	GTGAAACGCGTTTCTAGTTT
		GTTTGATAAGCAGGGGAATG
		TGAGTCTCGCGATGAGCTCC
CCND1	NM_053056	ACTCCGCCGCAGGGCAGGCG
		CTATGAAAACCGGACTACAG
		GCGCCTCAGGGATGGCTTTT
CCNE1	NM_001238	CCGTGGAGGGGCGGGTCCGG
		CGGCCCGCGAGGCGCAGGGA
		GACGGGCTCTGGGTCCCGCG
CCNT1	NM_001240	GCGGCCGCCCACGCGCCGCT
		GGCAGTGGTGATGTAAAATG
		TACGAGAACTTTGTTTGTGA
NMAT1	NM_002431	AAGTTCCCCTGTCAAATTCA
		CAACTGGGTGCGTGGAGATA
		GTATTAAGTTGCTTTATGGA

2.2.5.1 Generating CDK4/6 inhibitor resistant breast cancer cell lines

$5x10^4$ MCF7-AcCas9-CDK/cyclin cells were seeded per 24 well (Corning, UK). Cells were incubated for 48 hours before treatment with a CDK4/6i at different concentrations (10nM, 50nM, 250nM, 500nM, and 1000nM). DMSO was added to the vehicle controls. Medium was replenished every three days. Percentage confluency was calculated as a measure of cell numbers using the Incucyte Zoom live cell imaging system (Essence Bioscience, UK), with live cell images taken every 12 hours at 4x magnification. Once cells reached 80-100% confluency, they were trypsinized as described in Section 2.1.1, and re-plated at 1:5 dilution. Resistant lines treated with 250nM palbociclib, 50nM abemaciclib and 500nM ribociclib were transferred into $25cm^2$ flask once they reached 80% confluency in 24 well plates and subsequently expanded in the presence of the appropriate concentration of the relevant drug.

2.2.5.2 Generating CDK6 Small hairpin RNA (shRNA) stable lines

Three independent lentiviral TRIPZ inducible CDK6 shRNA constructs were obtained from Horizon Discovery, UK (Table 2.7). Plasmid DNAs were prepared as described in Section 2.4. Each of the three shRNA constructs was transfected individually into Ac-Cas9-EV and Ac-Cas9-CDK6 control (DMSO treated) and PalboR lines.

Table 2. 7 shRNA constructs used in this study

TRIPZ shRNA	Sequence	Location
RHS4696-200685040	5'-TCCTTTATGGTTTCAGTGG-3'	ORF
RHS4696-200765976	5'- TAACTTGCTATGAGCTGCT-3'	3'UTR
RHS4696-200768244	5'- TACTGACCACCTTGAGTCT-3'	3'UTR

Transfected cells were first allowed to recover in culture for at least 72 hours in fresh growth media. For selecting cells with successful integration of the TRIPZ constructs, transfected cells were incubated with 50ng/mL of doxycycline (DOX; TakaRa, Japan) for 72 hours to induce expression of red fluorescent protein (RFP) encoded in the TRIPZ vector. Cells were washed twice and trypsinized as described above (Section 2.1.1), $5x10^6$ cells were then re-suspended in 1% EDTA supplemented with 1% filtered FCS. The cell-EDTA suspension was transferred through the strainer cap to 5mL FALCON™ Round Bottom polystyrene test tubes with cell strainer snap caps (Fisher Scientific, UK). Samples were sent to LMS/NIHR Imperial Biomedical Research Centre Flow Cytometry Facility for fluorescence activated cell sorting (FACS). RFP-positive cells were isolated by double exclusion, collected in FCS and subsequently transferred to $25cm^2$ flask with fresh DMEM growth medium to allow cells to recover.

Growth assays were performed as described in Section 2.9, except that 50ng/mL DOX was added for 48 hours prior to the addition of CDK4/6i. Additionally, RNA and protein lysates were prepared as in Sections 2.7 and 2.8.1.

2.2.6 Transfection and Transduction

$1.5x10^6$ HEK293T cells were seeded in $10cm^2$ dishes 24 hours prior to transfection and incubated at 37°C with 5% CO_2 in DMEM supplemented with 10% FCS and 1% PSG. A mixture of 0.6pmol of lentiviral construct, 0.47pmol of lentiviral packaging plasmid, psPAX2, and 0.26pmol of lentiviral envelope plasmid (pMD2.G), were added into a 1.5mL Eppendorf tube. The DNA mix was diluted with OptiMEM medium to make up to a total of volume of 400µL (Sigma, UK). pS2PAX2 and pMD2.G were gifts from Didier Trono (Addgene plasmid #12260; https://www.addgene.org/12260/; Addgene plasmid #12259; https://www.addgene.org/12259/). The FuGENE HD® (Promega, UK) transfection agent was

used following manufacturer's instructions. Briefly, the transfection mix was obtained by the combination of 2.5µL of FuGENE HD reagent per µg of DNA constructs. The transfection mixture was added to HEK293T cells and incubated for 24 hours at 37°C with 5% CO_2. Culture medium containing shed virus was collected in a 10mL Syringe and filtered through a 0.45µM syringe filter (Sartorius, UK). The cell line of interest was seeded at $0.15x10^6$ cells per well of a 6 well plate for 24 hours prior to transduction. 3mL of viral medium was added to each well and incubated at 37°C with 5% CO_2 for 24 hours. The culture medium was removed after 24 hours and cells were allowed to recover in fresh growth medium. Appropriate antibiotic was added when cells reached 60-70% confluency. Selection was carried out over a 2-3 week period to obtain antibiotic resistant pools of transfected cells prior to continue to further experiments.

2.2.7 Genomic DNA (gDNA) extraction

Around $5x10^6$ cells were harvested and pelleted in a 1.5mL Eppendorf tube by centrifuging at 1300 rpm and washed twice with ice-cold PBS, before resuspending in 200µL of PBS. Genomic DNA was extracted using the PureLink Genomic DNA kit (Invitrogen, UK), gDNA was eluted with 100µL of Elution buffer (100mM Tris-HCI, pH 9.0, 0.1mM EDTA). DNA concentrations and purity were determined using a NanoDrop™ ND-1000 Spectrometer (Thermo Fisher, UK) to measure absorbance at 260nm and 280nm.

2.2.7.1 End-point Polymerase chain reaction (PCR)

PCR was carried out using 2x RedTaq ReadyMix PCR reaction mix (Sigma-Aldrich, UK). Reaction mixes were set up in thin wall PCR tubes (Thermo Fisher, UK). Each reaction consisted of:

- 10µL RedTaq ReadyMix
- 1µL 10µM Forward primer
- 1µL 10µM Reverse primer
- 100-200ng DNA made up to 8µL ddH_2O

PCR reactions were run in an Applied Biosystems Veriti™ 96 well thermal cycler (Life Technologies), at:

Temperature (°C)	Time (mins)	
95	5	1 cycle
95	1	30-40 cycles
72	2	
72	5	1 cycle

2.2.7.2 Agarose gel electrophoresis

1-2% (w/v) gels were prepared by dissolving agarose (Fisher Scientific, Life Technology, UK) in 100mL of 1X Tris-borate buffer (TBE) (Thermo Fisher Scientific, UK). 10µL of Gel Red™ Nucleic Acid Stain (Biotium, USA) was added to the agarose-TBE before the gel set. Gels were electrophoresed in 1x TBE buffer in a horizontal gel electrophoresis unit at 100V. GeneRuler 1kb DNA ladder (Thermo Fisher, UK), MassRuler™ Low Range DNA ruler (Thermo Fisher, UK) and MassRuler™ High Range Ruler (Thermo Fisher, UK) were used as markers to estimate size of the DNA fragments and PCR products. Gels were visualised using an UVIpro Platinum GelDoc System ultraviolet transilluminator (UVItec, Cambridge, UK).

2.2.7.3 Sanger DNA Sequencing

PCR products were first purified using CleanSweep™ (Thermo Fisher, UK) or ExoSAP-IT™ (Applied Biosystems, UK) for enzymatic removal of excess primers and dNTPs. 2µL of the reagent was added per 5µL of PCR product in thin wall PCR tubes. A thermocycler was used at 37°C for 15 minutes, then at 80°C for 15 minutes to inactivate the enzymes. 200ng/µL of each DNA sample was submitted for Sanger sequencing following the guidelines of the sequencing company, GENEWIZ (UK). DNA sequences and chromatograms were analysed using SnapGene Viewer (GSL Biotech LLC, Chicago, USA).

2.2.8 Total RNA extraction

For cultures with fewer than $5x10^6$ cells the growth medium was removed from cell cultures and cells were washed twice with ice-cold PBS before addition of 350µL RLT buffer (QIAGEN, UK) supplemented with 1% β-mercaptoethanol (Sigma-Aldrich, UK) and cells

were harvested using a cell scraper. RNA was extracted using the RNeasy Plus Kit (QIAGEN, UK), following manufacturer's instructions. RNA was eluted with 30-50µL of RNase-free water. RNA concentration and purity were measured determined a NanoDrop™ ND-1000 Spectrometer at 260nm and 280nm absorbance.

2.2.8.1 Complementary DNA (cDNA) by reverse transcription

Reactions were prepared in thin-wall PCR tubers with reagents (RevertAid cDNA synthesis kit purchased from Thermo Fisher, UK), as follows:

- 4µl of 5x Reaction buffer for RT
- 2µl of dNTP mix (10mM each)
- 1µl of random hexamer primer (0.2µg/µl)
- 2µg of RNA made up to 12µl with RNase free water
- 1µl of RevertAid Reverse Transcriptase

The reaction mixes were incubated in an Applied Biosystems Veriti™ 96 well thermal cycler at 42°C for an hour followed by heating at 95°C for 5 minutes to inactivate the reverse transcriptase enzyme. cDNAs were diluted 1:20 with RNase-free water and 2µL of diluted cDNA was used for each Real-time reverse transcription quantitative PCR (RT-qPCR).

2.2.8.2 Real time reverse transcription quantitative PCR (RT-qPCR)

RT-qPCR was carried out for gene expression analysis following guidelines and thermocycling conditions for SYBR™ Green reporter assays in Real Time PCR machines. Reactions were set up using MicroAmp® Optical 96-well Reaction plates (Applied Biosystems, UK) in a StepOne™ Plus Real Time PCR system (Applied Biosystems, Life Technology, UK) or in MicroAmp® Optical 384-well Reaction Plates with barcode (Applied Biosystems, Life Technology, UK) for the QuantStudio™ 7 Flex Real Time PCR system (Applied Biosystems, Life Technology, UK). Plates were sealed by using MicroAmp® Optical adhesive films (Applied Biosystems, Life Technology, UK). SYBR™ primers used are summarised in Table 2.8.

Each reaction was set up as follows:

- 5µl of PowerUp™ SYBR™ Green Master Mix
- 0.5µl of 10µM forward primer
- 0.5µl of 10µM reverse primer

- 2µl of nuclease-free water
- 2µl of 1:20 diluted cDNA

Thermocycling conditions were set up:

Stage 1: 1 cycle

- 50°C for 2 minutes
- 95°C for 2 minutes

Stage 2: 30-40 cycles

- 95°C for 3 seconds
- 60°C for 30 seconds

Gene expression was normalised to TBP, and relative gene expression was analysed using the $2^{-\Delta\Delta Ct}$ method.

Table 2. 8 List of SYBR Green primers used in RT-qPCR.

TBP	Forward: 5'-GTTTGCCAAGAAGAAAGTGAAC-3' Reverse: 5'-GGGTCAGTCCAGTGCCAT-3'
BIRC5	Forward: 5'-AGGACCACCGCATCTCTACAT-3' Reverse: 5'-AAGTCTGGCTCGTTCTCAGTG-3'
CCNA1	Forward: 5'-GAGGTCCCGATGCTTGTCAG-3' Reverse: 5'-GTTAGCAGCCCTAGCACTGTC-3'
CCND1	Forward: 5'-GCTGCGAAGTGGAAACCATC-3' Reverse: 5'-CCTCCTTCTGCACACATTTGAA-3'
CCNE1	Forward: 5'-GCCAGCCTTGGGACAATAATG-3' Reverse: 5'-CTTGCACGTTGAGTTTGGGT-3'
CCNT1	Forward: 5'-ACAACAAACGGTGGTATTTCACT-3' Reverse: 5'-CCTGCTGGCGATAAGAAAGTT-3'
CDK1	Forward: 5'-AAACTACAGGTCAAGTGGTAGCC-3' Reverse: 5'-TCCTGCATAAGCACATCCTGA-3'
CDK2	Forward: 5'-CCAGGAGTTACTTCTATGCCTGA-3' Reverse: 5'-TTCATCCAGGGGAGGTACAAC-3'
CDK4	Forward: 5'-ATGGCTACCTCTCGATATGAGC-3' Reverse: 5'-CATTGGGGACTCTCACACTCT-3'
CDK5	Forward: 5'-GGAAGGCACCTACGGAACTG-3' Reverse: 5'-GGCACACCCTCATCATCGT-3'
CDK6	Forward: 5'-TCTTCATTCACACCGAGTAGTGC-3' Reverse: 5'-TGAGGTTAGAGCCATCTGGAAA-3'
CDK7	Forward: 5'-GGAGCCCCAATAGAGCTTATACA-3' Reverse: 5'-TCCACACCTACACCATACATCC-3'
CDK8	Forward: 5'-ACCTGTTTGAATACGAGGGCT-3' Reverse: 5'-TGCCGACATAGAGATCCCAGT-3'
CDK9	Forward: 5'-TTGCGGGAGATCAAGATCCTT-3' Reverse: 5'-TACCCTTGCAGCGGTTATAGG-3'

CDK12	Forward: 5'-CTAACAGCAGAGAGCGTCACC-3' Reverse: 5'-AAAGGTTTGATAACTGTGCCCA-3'
CDK13	Forward: 5'-CCCCTAGTCCCTACAGCAG-3' Reverse: 5'-GCCTAGATGAATACGGGCTTCTG-3'
DKK1	Forward: 5'-CCTTGAACTCGGTTCTCAATTCC-3' Reverse: 5'-CAATGGTCTGGTACTTATTCCCG-3'
DOK7	Forward: 5'-GACAAGTCGGAGCGTATCAAG-3' Reverse: 5'-ATGTCCTCTAGCGTCAGGCT-3'
ESR1	Forward: 5'-AAGAAAGAACAACATCAGCAGTAAA-3' Reverse: 5'-TCTTTGGATGACCTAGCCTCTC-3'
GDF15	Forward: 5'-GACCCTCAGAGTTGCACTCC-3' Reverse: 5'-GCCTGGTTAGCAGGTCCTC-3'
HSPB8	Forward: 5'-CTCCTGCCACTACCCAAGC-3' Reverse: 5'-GGCCAAGAGGCTGTCAAGT-3'
IFI6	Forward: 5'-GGTCTGCGATCCTGAATGGG-3' Reverse: 5'-TCACTATCGAGATACTTGTGGGT-3'
IFIT2	Forward: 5'-AAGCACCTCAAAGGGCAAAAC-3' Reverse: 5'-TCGGCCCATGTGATAGTAGAC-3'
MALAT1	Forward: 5'-TCCAAGTTGGCAAGTAACTCC-3' Reverse: 5'-GTACACCCAGTGGCTCATATTT -3'
MXD4	Forward: 5'-AACAGGTCTTCACACAACGAG-3' Reverse: 5'-CTGCTCCTTGATGCTCAGTG-3'
NPY1R	Forward: 5'-GAGGCGATGTGTAAGTTGAATCC-3' Reverse: 5'-TGGAACGGCTCATCATCAGTCATT-3'
PGR	Forward: 5'-GAGTCACCTTGCCCCTTCA-3' Reverse: 5'-GCCTTTTATGCTTGCCTGTAAA-3'
RHOBTB3	Forward: 5'-GGGGCTTATCCGCACTTACC-3' Reverse: 5'-TGGCCTGATACTCGGTGAACA-3'
S100P	Forward: 5'-AAGGATGCCGTGGATAAATTGC-3' Reverse: 5'-ACACGATGAACTCACTGAAGTC-3'
SMC3	Forward: 5'-AACATAATGTGATTGTGGGCAGA-3' Reverse: 5'-TCCTTTTTGGCACCAATAACTCT-3'

2.2.9 Protein lysate preparation

2.2.9.1 Protein extraction

Radioimmunoprecipitation Buffer (RIPA; 50mM Tris-HCl pH8.0, 150mM NaCl, 1% Igepal CA-630 (NP-40), 0.5% sodium deoxycholate, 0.1% SDS (Sigma-Aldrich, UK)) was prepared with Pierce™ Protease inhibitor cocktail mini tablets and Pierce™ phosphatase inhibitors cocktail tablets (Thermo Fisher, UK). Medium was removed from seeded cells and cells were washed twice with ice-cold PBS before adding 500µL of ice-cold RIPA buffer per 10cm^2 plate. Lysates were collected by scraping and transferred to a 1.5mL microcentrifuge tube for

incubation on ice for 30 minutes and vortexed every 5 minutes to facilitate cell lysis. To pellet and remove cell debris, lysates were centrifuged at 13,000 rpm for 10 minutes at 4°C and supernatants were transferred to fresh 1.5mL microcentrifuge tubes.

2.2.9.2 Protein quantification

Concentrations of protein lysates were determined by using Pierce™ BCA protein assay kit (Thermo Fisher, UK), according to manufacturer's instructions. A serial dilution series of bovine serum albumin (BSA) was set up as 9 standards (from 0-16 µg/µl) and 10µl of each BSA concentration was placed in triplicates in a 96-well flat bottom plate (Corning, UK). 2µl of protein samples were diluted with 8µl ddH_2O and loaded in triplicates. 200µl of BCA solution (50:1 ratio of reagent A to reagent B) was added to each well, before incubating the plate at 37°C for 30 minutes. Absorbance was measured with a Tecan Sunrise™ Microplate Reader at 562nm. Protein concentrations were calculated with extrapolation of a standard curve generated for BSA.

.

2.2.9.3 SDS-Polyacrylamide gel electrophoresis (Western blotting)

Protein lysates were diluted to 1-2µg/µL and 4x Laemmli sample buffer (Bio-Rad, UK, supplemented with 10% β-mercaptoethanol) (Table 2.9) was added, to achieve a final dilution of 1x Laemmli buffer. Samples were denatured by heating at 100°C for 5 minutes and cooled to room temperature prior to loading on polyacrylamide gels. 10-30µg of protein sample was loaded into each well of the SDS-polyacrylamide gel (5% stacking gel and 8-10% resolving gel) (Table 2.10). Precision Plus Protein Dual colour standards (Bio-Rad, UK) were loaded alongside samples to use as a ladder to estimate size of the protein of interest. Electrophoresis was set up in Mini-Protean Tetra Vertical Electrophoresis system (Bio-Rad, UK) and run at 60V for 40 minutes followed by 100V for 1-2 hours in 1x running buffer, until the bromophenol blue dye reaches the bottom of the gel. Gels were electroblotted to nitrocellulose membranes (Bio-Rad, UK) in a Bio-rad transfer system at 90V for 90 minutes in 1x transfer buffer. The membrane was incubated with blocking buffer at room temperature for 1-3 hours to block unspecific binding. The membrane was incubated with primary antibodies diluted in blocking buffer overnight at 4°C. Primary antibodies are detailed in Table 2.11. The membrane was

washed three times with PBST (see Table 2.9), with 5 minutes for each wash, followed by an hour incubation at room temperature with HRP-conjugated secondary antibody (Dako, Aligent, UK) diluted in blocking buffer. The membrane was washed three times with PBST. The proteins were visualised after adding SuperSignal West Pico Chemiluminescent Substrate or SuperSignal West Femto Maximum Sensitivity Substrate (Thermo Fisher Scientific) in a Fusion Solo Chemiluminescence imager (Vilber Lourmat) or iBright™ CL 1500 imaging system (Thermo Fisher).

Table 2. 9 immunoblotting buffer solution

4x Laemmli sample buffer	**62.5 mM Tris-HCl, pH 6.8 10% glycerol, 1% SDS, 0.005% Bromophenol Blue**
Upper Buffer 10x	1.25M Tris-HCl pH 6.8, 1% w/v SDS
Lower buffer 4x	1.5M Tris-HCl pH 8.8, 0.4% w/v SDS
SDS Running buffer 10x	0.25M Tris, 1.9M glycine, 1% w/v SDS, pH 8.3
Transfer buffer 50x	0.25M Tris, 1.9M glycine, 20% v/v methanol
Tween 20	10% v/v Tween 20 in PBS
PBST	0.1% v/v Tween 20 in PBS
Blocking buffer	5% w/v dry skimmed milk powder in PBST solution

Table 2. 10 SDS page acrylamide gel

8% acrylamide SDS page gel	**8mL lower buffer, 8.5mL Acrylamide solution (Acrylamide/Bis-acrylamide, 30% solution), 62.5µL TEMED, 250µL 10% APS, 15.3mL ddH_2O**
10% acrylamide SDS page gel	8mL lower buffer, 10.6mL Acrylamide solution, 50µL TEMED, 200µL 10% APS, 13.4mL ddH_2O
12% acrylamide SDS page gel	8mL lower buffer, 12.7mL Acrylamide solution, 41.7µL TEMED, 166.7µL 10% APS, 11.4mL ddH_2O

Table 2. 11 List of antibodies used for immunoblotting diluted in blocking buffer

Antibody	Company	Catalogue	Dilution	Size (kDa)
β-actin	Abcam	Ab2380	1:100000	46
CDK1	CST	POH1	1:500	34
CDK2	CST	78B2	1:500	33

CDK4	CST	D9GE3	1:500	30
CDK5	CST	1H5	1:1000	30
CDK6	CST	DCS83	1:500	36
CDK7	Santa Cruz	C4	1:500	40
CDK8	CST	P455	1:1000	53
CDK9	CST	C12F7	1:1000	42, 55
Cyclin A	Santa Cruz	H143	1:100	52
Cyclin D1	Santa Cruz	H295	1:200	36
Cyclin E1	Santa Cruz	C19	1:100	48
Cyclin T1	Santa Cruz	T18	1:50	81
ERα	Santa Cruz	HC20	1:100	66
Total RB	CST	4H1	1:500	110
RB (Ser795)	Abcam	131347	1:500	110
RB (Ser807/811)	CST	9308	1:500	110
RB (Ser780)	CST	9307	1:500	110
RB (Thr821)	Abcam	Ab4787	1:500	110
MAT1 (MNAT1)	Santa Cruz	FL309	1:100	34

2.2.10 Sulforhodamine B (SRB) cell growth assay

2.2.10.1 CDK4/6 inhibitors

$2x10^3$ cells were seeded in 96-well culture plates (Corning, UK) and treated with four-fold serial dilutions of CDK4/6 inhibitors from the highest concentration of 10μM, over nine concentrations 48 hours (D0) after seeding. An equal volume of DMSO was added to the vehicle controls. Culture media, including drugs, were changed every three days over the course of treatment.

2.2.10.2 CDK7 inhibitors

$4x10^3$ cells were seeded for 48 hours (D0) prior to the addition of CDK7 inhibitors, THZ1 and ICEC0942, in a four-fold dilution series from a maximum concentration of 20μM for 48 hours. DMSO was used as a vehicle control.

2.2.10.3 Growth assays in estrogen-free medium

Normal growth medium was removed, cells were detached as described in Section 2.1.1. Cells were resuspended and washed twice with "stripped" medium (phenol red-free DMEM with 10% DSS and 1% PSG). Cells were cultured in stripped growth medium for at least 48 hours prior to assessing growth following the addition of E2 to a final concentration of 10 nM. An equal volume of DMSO was added to the no E2 controls. CDK4/6i or CDK7i were added as described above.

2.2.10.4 SRB assay

All plates were fixed with 100µL of 40% w/v Trichloroacetic acid (TCA) (Sigma-Aldrich, UK) and incubated for 1 hour at 4°C. Plates were washed five times with ddH_2O and 0.4% w/v SRB dye was added to the wells. 0.04% SRB dye (w/v) was prepared by dissolving SRB salt (Sigma-Aldrich, UK and Alfa Aesar, UK) in 1% acetic acid for 1 hour at room temperature. Plates were subsequently washed five times with 1% v/v acetic acid and were left to dry at room temperature. SRB dye was solubilised by addition of 100µL of 10mM Tris base (pH 6.5) and plates were left on a shaker for gentle shaking for 10 minutes at room temperature. Absorbance was measured using a Tecan Sunrise™ Microplate Reader at 492nm. 50% maximal inhibition of cell proliferation (GI_{50}) was estimated and standard error of the mean (SEM) was calculated from 3 independent experiments, each set up with six technical replicates.

2.2.11 siRNA-directed CDK6 knockdown

2.2.11.1 Growth assays

A transfection master mix was prepared, consisting of equal volumes of small interfering RNA (siRNA) (25nM). The siRNA SMARTpool for knockdown of CDK6 (L-003240-0), non-targeting negative control pool (D-001810-02) and three custom-made siRNAs targeting Cas9 were purchased from Dharmacon, UK (Table 2.12). 5µL of Lipofectamine RNAi-MAX (Life technologies, UK) and 25nM of the individual siRNA were diluted in 100µL of Opti-MEM media to produce a master mix followed by 20 minutes of incubation at room temperature. 11µL of the master mix was added per 96 well. $3x10^3$ cells were resuspended in 200µL antibiotics-free medium (DMEM with 10% FCS and 1% L-Glutamine) before being added to

the master mix in each well. Cells were incubated with the transfection master mix for 24 hours at 37°C with 5% CO_2, at which point the medium was replaced with fresh normal growth medium supplemented with CDK4/6 inhibitors. Cells were treated for 6 days with fresh medium change on after 3 days.

Table 2. 12 List of custom made small interfering RNAs targeting Cas9

siRNA	Sequence
siCas9 #1	5'-CCGAAGAGGUCGUGAAGAAUU-3'
siCas9 #2	5'-GGGAAAAGAUCGAGAAGAUUU-3'
siCas9 #3	5'-GCGAACUGCACAAGGGAAAUU-3'

2.2.11.2 RNA and protein extraction

$4x10^5$ cells were seeded in 2mL of antibiotic-free growth medium with 110µL of transfection master mix per 6-well. Cells were incubated for 24 hours before the culture medium was replaced with fresh growth medium and further culturing for 48 hours at 37°C with 5% CO_2. Total RNA and protein were extracted using above-described methods (Section 2.7 and 2.8.1).

2.2.12 Nanopore RNA sequencing

Total RNA was collected using RNeasy Extraction Kit (QIAGEN, UK) with DNase incubation to remove gDNA. Concentrations and purities of RNA samples were measured by using Qubit™ and Nanodrop™. Quality control of RNA was assessed using a bioanalyzer to ensure RNA integrity number (RIN) was around 10. Polyadenylated transcripts were isolated from total RNA using Dynabeads® mRNA purification kit (Thermo Fisher, UK), following manufacturer's instructions. The direct cDNA sequencing kit (SQK-D109, Oxford Nanopore Technology, UK) was used for library preparation with native barcoding (EXP-NBD104), following manufacturer's protocol. Samples were prepared and the sequencing was performed by Dr Mariana Ferriera Leal (ICR), using the Oxford Nanopore MinION device. Quality control checks (such as FASTQC) were performed before alignment. Minimap2 (Li, 2018) was used to overlap reads to reference genome, GRCh38.94 and read counts was determined using featureCounts (Liao *et al.*, 2014). The above initial alignments and analyses were performed by Dr Eugene Schuster (ICR).

The R package 'DeSeq2' (Love *et al.*, 2014) was used for downstream analysis to normalize read counts using a regularized log transformation (rlog). To identify differentially expressed genes (DEGs) shrunken log_2 fold change (log_2 FC) was calculated between cell lines and conditions. Heatmaps were generated with 'gplots' and 'ComplexHeatmap' using rlog normalized read counts of DEGs. Venn diagram was redrawn from the web-application Bio-Venn (Hulsen *et al.*, 2008). Gene Set Enrichment Analysis (GSEA) analysis was performed with default settings and online 'compute overlaps' tool, to overlaps between DEGs within the Molecular Signature Databases (MSigDB), 'Hallmark' gene set collection (http://www.gsea-msigdb.com).

2.2.13 Chromatin immunoprecipitation (ChIP) assay and sequencing

Sample preparation and quality check was performed by Dr Mariana Ferriera Leal (ICR), as previous described (Pancholi *et al.*, 2020; Ribas *et al.*, 2015; Schmidt *et al.*, 2009). Samples were treated with DMSO or 1μM palbociclib for 24 hours before cells were cross-linked with 1% formaldehyde and quenched with glycine. Samples were collected by scraping and were lysed and sonicated for 14 cycles with 10 seconds on/off. Cell pellets were obtained after washing with cold PBS. Chromatin was immunoprecipitated with an anti-H3K27ac antibody (#ab4729, Abcam, UK) overnight at 4°C with dynabeads (Invitrogen). DNA was collected by reverse cross-linking followed by elution with elution buffer. DNA was subsequently incubated with RNase and Protease K and purified with phenol-chloroform. Samples were sent to Novogene (Cambridge, UK) for sequencing using the HiSeq 3000/4000 SBS kit.

FASTQ files were first ran through quality checks before aligning to GChr.37 with Bowtie2 (Langmead and Salzberg, 2012). SAMtools (version: 10.1) was used to convert SAM files to bam files for downstream differentially analysis and data visualisation. Peak calling was performed using MACS2 (vesion 2.2.6) to determine enrichment at binding sites with default settings. Differential enrichment analysis was performed using R package 'DiffBind' (Stark, 2011) with ChIPSeeker (Yu *et al.*, 2015) to annotate peaks. Differentially enriched peaks were defined by FDR ≤ 0.05 and log2 FC $\geq \pm 1.5$ and used in the online GSEA 'compute overlap' tool for pathway analysis.

3. Results

3.1 Retinoblastoma RB1 gene knockout MCF7 cells are resistant to CDK4/6 inhibitors

3.1.1 Establishing RB1 gene knockout MCF7 cells

As described in the Introduction, the RB protein is a direct downstream target of the CDK4/6-cyclin D axis. Mutations and/or loss of RB is a potential resistance mechanism to CDK4/6 inhibitors, as indicated in published literature, such that breast cancer cell lines that lack RB were shown to be intrinsically resistant to palbociclib (Finn *et al.*, 2009). Additionally, acquired RB mutations have been described in three patients after treatment with palbociclib or ribociclib (Condorelli *et al.*, 2018). Thus, modelling RB KO in MCF7 would be useful to confirm the correlation between the role of RB and drug responses to CDK4/6 inhibitors.

CRISPR-Cas9, now a well-established method for generating gene mutagenesis in cell line models, was used to introduce deletions to disrupt the production of endogenous RB protein in the ER^+ breast cancer cell line, MCF7. To generate the RB KO cells, four independent sgRNAs were used in pairs to introduce specific deletions within exon 1 of the RB1 gene (Figure 3.1A). MCF7 cells were nucleofected with sgRNA pairs and recombinant Cas9 protein (as described in section 2.2). Six pools of MCF7 cells generated with different combinations of the sgRNA pairs were screened for deletions within the RB1 exon 1 sequences (data not shown). Genomic DNA prepared from each pool was assessed using end-point PCR and PCR products with evidence of RB1 deletion were plated at low cell density for establishing KO clones (data not shown). All sgRNA combinations produced a mutant product except combinations that included CRISPR27487475 (data not shown).

Candidate clones were screened using Western blotting and Sanger DNA sequencing for the absence of RB protein and the presence of deletion in the RB1 exon 1 sequence, respectively. A previous study has indicated that MCF7 cells contain three copies of the RB1 gene (Rondon-Lagos *et al.*, 2014), therefore, to evaluate the RB mutation in each allele, genomic DNA,

amplified at the region of expected deletion, was cloned into the pJet plasmid, for Sanger DNA sequencing. Sequence analysis of >10 bacterial colonies from each MCF7 RB KO clone, allowed the identification of three independent RB KO clones, A3, 1B2 and 2C3, in which no WT RB1 sequences were identified.

Clone A3 was obtained from the combination of CRISPR27487517 and CRISPR27487476. Three distinct RB1 deletions were evident in this clone (Figure 3.1B), while no sequences consistent with WT RB1 exon 1 were obtained, implying that all three alleles have been mutated. The deletions extended from the sgRNA CRISPR27487476 and caused loss of 10bp, 13bp and 37bp within exon 1. This suggests that these deletions resulted from targeting of CRISPR27487476, but no contribution of CRISPR27487517. Nevertheless, all deletions are expected to cause frameshifts and consequently lack of RB1 protein. Clone 1B2 carried deletions involving CRISPR27487504 and CRISPR27487476 (Figure 3.1C). Three different sequences, with deletions of 5bp, 101bp and 109bp within the region between the two sgRNAs, were present. Clone 2C3, also generated from the combination of CRISPR27487504 and CRISPR27487476, yielded two sequences, one of which generated a sequence with a 5bp deletion. The second sequence resulted in a more complex RB1 mutation. The mutant sequence included an inversion of sequences 66bp and 117bp 5'- and 3'- of the ATG start site, which is expected to disrupt RB protein synthesis. Of 11 bacterial colonies that were sequenced, no other mutant sequence was found, with 5/11 clones containing the 5bp deletion mutant sequence and the other 6 clones with the inverted sequence. This suggests that the third mutational event may extend beyond the region amplified by PCR primers, such that no PCR product could be obtained. In agreement with the DNA sequence analysis, none of these clones showed evidence for RB protein (Figure 3.1D).

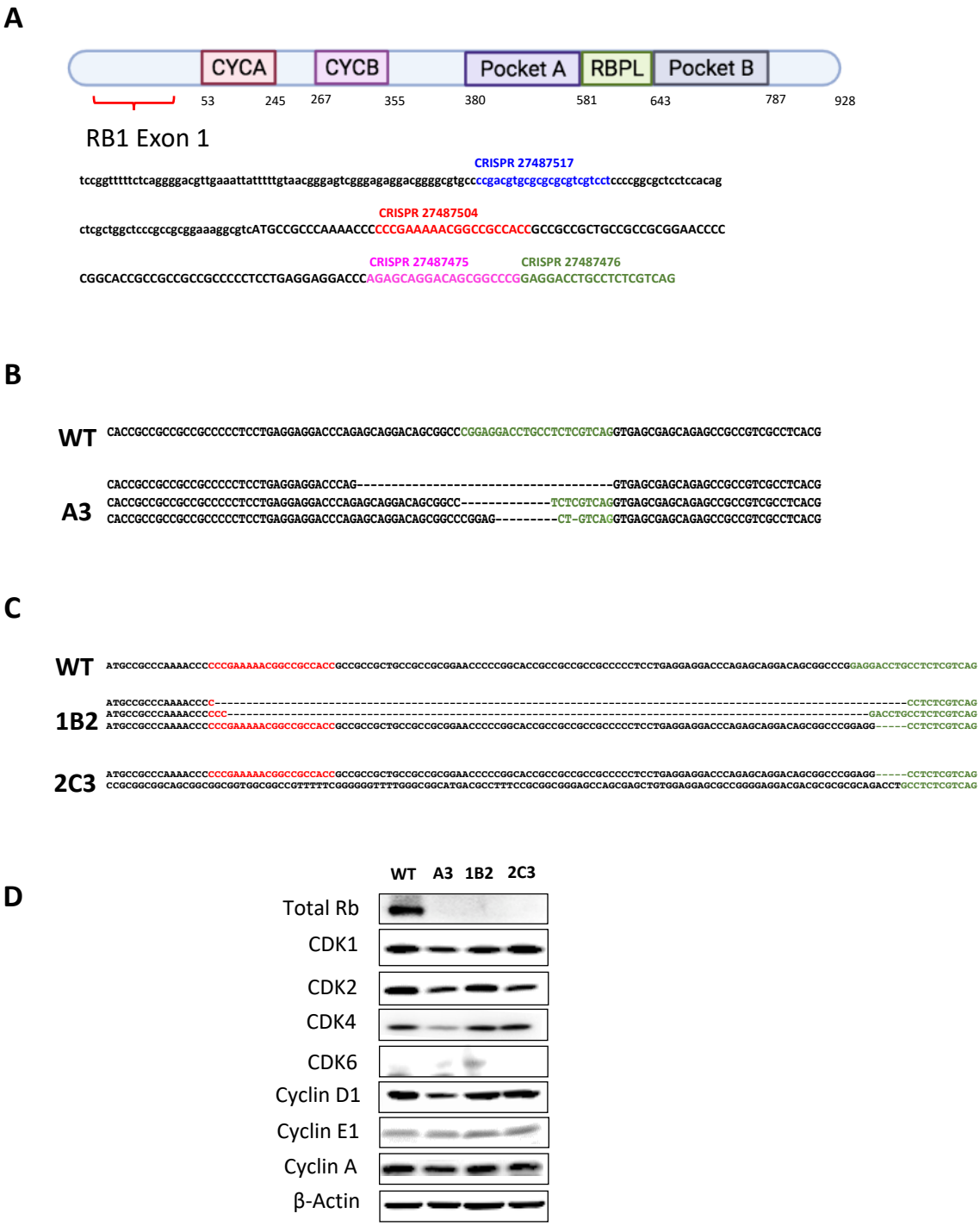


Figure 3.1. Generation of RB KO clones in MCF7 breast cancer cells.
(A) A schematic of RB1 protein highlighting functional domains including cyclin A (CYCA) and B (CYCB) domain, pocket A (Pocket A) and B (Pocket B) domain connected by the RB pocket linker region (RBPL) (redrawn from Burke, et al., 2012). The RB1 exon 1 region is highlighted. Shown below the cartoon is the exon 1 sequence, with lowercase letters representing the 5' untranslated region and uppercase denoting coding region. Sequences of four sgRNAs designed to target exon 1 of the RB1 gene, are highlighted. (B-C) Clones generated following nucleofection with different combination of the four shRNAs were confirmed by indel detection using agarose gel electrophoresis. (B) Clone A3 was generated using CRISPR27487517 and CRISPR27487476. Sanger sequencing of A3 showed three distinct RB1 mutant sequences (C) Clones 1B2 and 2C3 were obtained by using the combination of CRISPR27487504 and CRISPR27487475. Sanger sequence confirms that these are two independent clones. (D) Whole cell protein lysates were prepared from MCF7 WT and RB KO clones for Western blotting. β-Actin was used as a loading control.

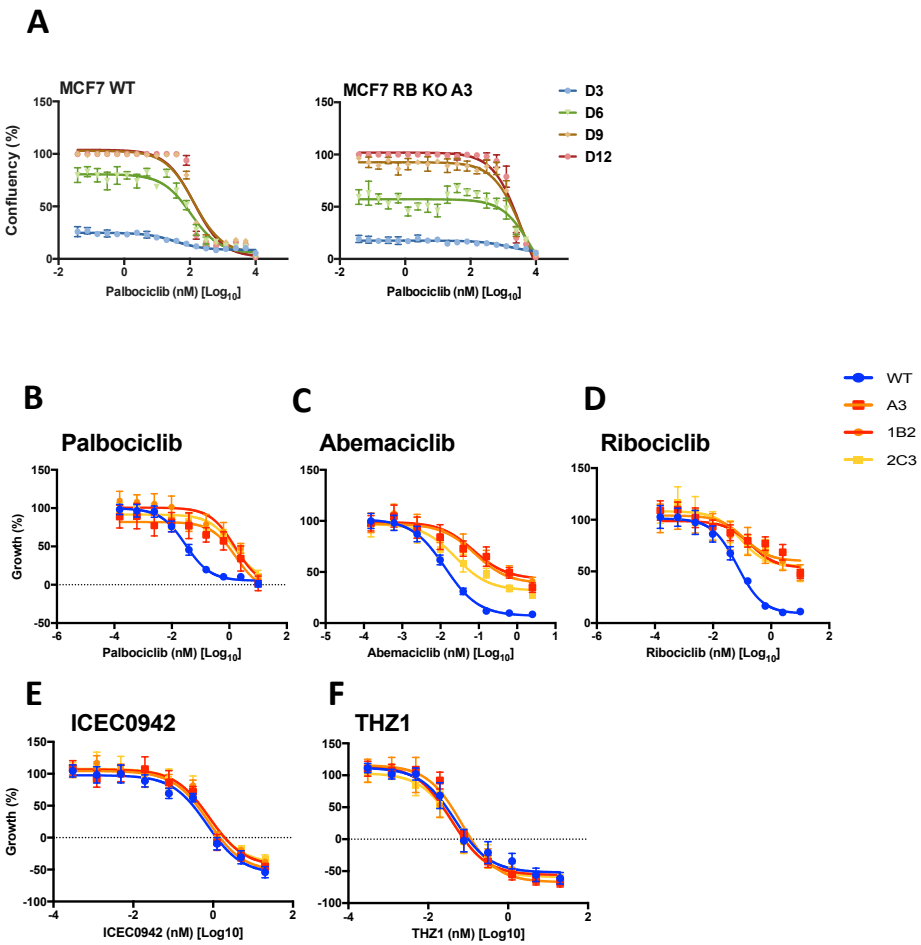
3.1.2 RB KO MCF7 cells are resistant to CDK4/6 inhibitors, but remain responsive to CDK7 inhibitors

Sanger DNA sequencing demonstrates that the A3, 1B2 and 2C3 clones are independent MCF7 RB1 KO clones, while lack of RB protein detection by western blotting confirms mutation of all RB1 alleles in these clones. The three independent RB1 KO clones were evaluated for their sensitivity to CDK4/6 inhibitors. To identify the most appropriate length of treatment, a time course study was conducted, whereby MCF7 cells and the A3 clone were assessed for response to increasing concentrations of palbociclib following treatment for 3, 6, 9 or 12 days (Figure 3.2A). Percentage confluency was tracked using the Incucyte Zoom live cell imaging system. This demonstrated that a treatment period of 6 days was sufficient to obtain robust growth inhibition and GI_{50} (concentration at which 50% growth inhibition is obtained) comparable to reported GI_{50} values for MCF7 cells treated with palbociclib. A dose-response curve was generated for parental MCF7 (WT-RB1) and the three RB KO clones, in which the cells were treated with the three main clinical CDK4/6 inhibitors, palbociclib, abemaciclib and ribociclib. Cells were treated with 2-fold dilutions of the drugs, starting from the highest concentration of 10 μM. The three RB KO clones demonstrated reduced sensitivity to all three CDK4/6 inhibitors (Figure 3.2B-D). GI_{50} values, determined from three independent experiments (Figure 3.2G) confirm the strong reductions in sensitivity of the RB KO clones to the CDK4/6 inhibitors, compared with MCF7 cells. For example, clone A3 was 28-, 59- and >116-fold less sensitive to palbociclib, abemaciclib and ribociclib, respectively, compared with MCF7 cells. Interestingly, Western blotting did not show any apparent alteration in levels of the cell cycle CDKs or cyclins in the RB KO clones, so the reduced sensitivity to CDK4/6 inhibitors is unlikely to be due to changes in levels of these key mediators of cell cycle progression and likely represents the absence of RB protein and consequent absence of E2F inhibition in the RB1 KO clones. Note that CDK6 expression is apparently low in MCF7 cells (please see below).

I next determined if RB KO causes insensitivity to CDK7 inhibitors, as CDK7 enhances the activities of the cell cycle CDKs by phosphorylating them at their gatekeeper threonine residues. Growth assays were undertaken following treatment with the CDK7 inhibitors ICEC0942 and THZ1. Following a previously established protocol in our group for CDK7 inhibitor treatment in MCF7 cells (Patel *et al.*, 2018), the cells were treated for 2 days with the CDK7 inhibitors, ICEC0942 or THZ1. All RB KO clones were sensitive to ICEC0942 and THZ1, although the sensitivity to ICEC0942 was slightly reduced in RB KO clones, with an

average of 1.5-fold decrease in sensitivity compared to MCF7 WT cells (Figure 3.2E-G). This small reduction in sensitivity to ICEC0942 is presumably a consequence of the absence of the CDK4/6-RB axis and a reflection of the role of CDK7 in stimulating CDK4/6 activity. Lack of a similar reduction in sensitivity to the covalent CDK7 inhibitor THZ1 (Figure 3.3F, G), may be because THZ1 inhibits the transcriptional CDKs, CDK12/13, in addition to CDK7 (Kwiatkowski *et al.*, 2014; Olson *et al.*, 2019).

To summarise, RB KO cells have demonstrated loss of sensitivity to CDK4/6 inhibition, which is in line with data in previous other publications (Finn *et al.*, 2009; McCartney *et al.*, 2019). The current data also showed that the use of CDK7/12/13 inhibitors represent an alternative therapeutic option as MCF7 RB KO cells remained sensitive to these inhibitors. Determination of GI50 values showed differences between RB KO clones, which may be due to clonal differences. Nevertheless, all three clones demonstrated a lack of response to CDK4/6 inhibitors but maintained sensitivity to the CDK7/12/13 inhibitor THZ1. There was evidence for a lowered response to the selective CDK7i ICEC0942. This is likely to be reflective of the fact that CDK7 inhibition would reduce CDK4/6 activity, but as RB loss prevents response to CDK4/6 inhibition, there is consequently a reduced response to ICEC0942. However, as CDK7 promotes the activities of the other cell cycle CDKs, as well as being required for PolII-directed transcription, the RB KO cells are growth inhibited.



G

Drug (nM) / Cell line	Palbociclib	Abemaciclib	Ribociclib	ICEC0942	THZ1
MCF-7 WT	34 ± 3.8	21 ± 1	86 ± 4.4	332 ± 4.4	31 ± 8.1
Clone A3	**947 ± 276.7**	**1251 ± 83.3**	**> 10000**	**499 ± 64.1**	34 ± 2.6
Clone 1B2	**1552 ± 426.8**	**1488 ± 40.1**	**> 10000**	**490 ± 24.2**	25 ± 7.0
Clone 2C3	**1382 ± 262.4**	**666 ± 7.2**	**>10000**	**472 ± 80.9**	27 ± 10.8

Figure 3.2. RB1 KO cells are resistant to CDK4/6 inhibitors, but maintained sensitivity to CDK7 inhibitors.

(A) Time course experiment was conducted to determine the optimal time to obtain GI50 values in MCF7 cells with CDK4/6 inhibitors. Increasing concentrations of palbociclib were used for 3-, 6-, 9- and 12-days treatment. Growth was measured as percentage confluency using Incucyte live cell imaging system. Graphs show the means of three independent experiments, each with six technical replicates. Error bars show standard deviation (SD). Growth inhibition was assessed using the SRB assay in RB KO clones and MCF7 WT after treatment with increasing concentrations of CDK4/6 inhibitors (B-D), a CDK7 inhibitor (ICEC0942) (E), or the CDK7/12/13 inhibitor (THZ1) (F). CDK4/6 inhibitors were added for 6 days, whereas cells were treated with ICEC0942 and THZ1 for 2 days. An equal volume of DMSO (0.1%) was added as the vehicle control. Graphs show the means of three independent experiments, each with six technical replicates. Error bars depict SD. (G) Table shows GI50 (nM) ± SEM obtained from growth inhibition curves for each CDK inhibitor from three independent experiments.

3.2 Can over-expression of cell cycle CDKs promote resistance to CDK4/6 inhibitors?

The dysregulated expression of CDKs and cyclins has been suggested as a possible resistance mechanism for CDK4/6 inhibitors (Pandey *et al.*, 2018; Teh and Aplin, 2019). It is possible that CDK2 and/or CDK1 compensate for CDK4/6 to overcome growth inhibition engendered by CDK4/6 inhibitors (Alvarez-Fernandez and Malumbres, 2020). Alternatively, over-expression of CDK4 or CDK6 might result in insufficient CDK4/6 inhibition, thus providing escape from CDK4/6 inhibitor directed growth inhibition. Finally, elevated expression of some cyclins, leading to increased activities of their cognate CDKs may provide yet another opportunity for CDK4/6 inhibitor resistance. These possibilities are described in detail in the Introduction (Section 1.5.2.2). I used two approaches for over-expressing cell cycle CDKs and cyclins, to investigate these possibilities, as detailed below.

3.2.1 Using dihydrofolate reductase fusion proteins as an approach for inducible over-expression of CDKs and Cyclins.

To singly over-express CDKs and cyclins in MCF7 cells the DHFR fusion protein system was adapted (Iwamoto *et al.*, 2010). This approach involves the protein destabilising domain region of the *E. coli* DHFR gene fused in frame to the gene of interest, to generate a fusion protein that includes the protein of interest. The vector system I used includes an HA epitope tag for ease of detection by WB, as well as YFP for protein imaging. The DHFR protein, or the DHFR fusion protein is unstable and quickly degraded. Stabilisation of the fusion protein is made possible by the addition of a high affinity ligand for DHFR called trimethoprim (TMP) (Figure 3.3A). MCF7 cells were transfected, and stable lines selected by the addition of G418 (see Section 2.3). Protein lysates were prepared from MCF7 cells expressing HA-YFP-DHFR, or the HA-YFP-DHFR-CDK/cyclin fusion constructs, after incubation with different concentrations of TMP. For ease of description, the fusion protein names have been shortened. Thus HA-YFP-DHFR-CDK1 is named DHFR-CDK1. DHFR, DHFR-CDK1 and DHFR-CDK2 levels were low in the absence of TMP but were greatly increased in the presence of 10 μM TMP for 48 hours (Figure 3.3B). Increasing TMP concentration further did not lead to further increases in fusion protein levels. DHFR-CDK4, DHFR-CDK6, DHFR-CDK7 and DHFR-CDK9 expression was similarly low in the absence of TMP, increasing with TMP

addition. The exception was DHFR-Cyclin D1, which was expressed in the absence of TMP. TMP addition did not further increase DHFR-CylinD1 levels.

Immunoblotting using the appropriate anti-CDK or anti-cyclin antibodies was also used to determine if the DHFR fusion protein is over-expressed, relative to levels of the endogenous protein. In most cases, expression levels of the fusion protein were similar, or somewhat lower than those of the endogenous protein, which may prevent clear assessment of its influence on growth and response to CDK4/6 inhibitors (Figure 3.4). Indeed, the DHFR-CDK1 and DHFR-Cyclin D1 fusion proteins were not detected, whereas the endogenous proteins were clearly present. The one exception was CDK6, where only the DHFR fusion protein was detected. As observed for the HA antibody, expression levels of the fusion proteins were not greatly increased at concentrations higher than with 10 μM TMP, so this concentration was used for subsequent studies.

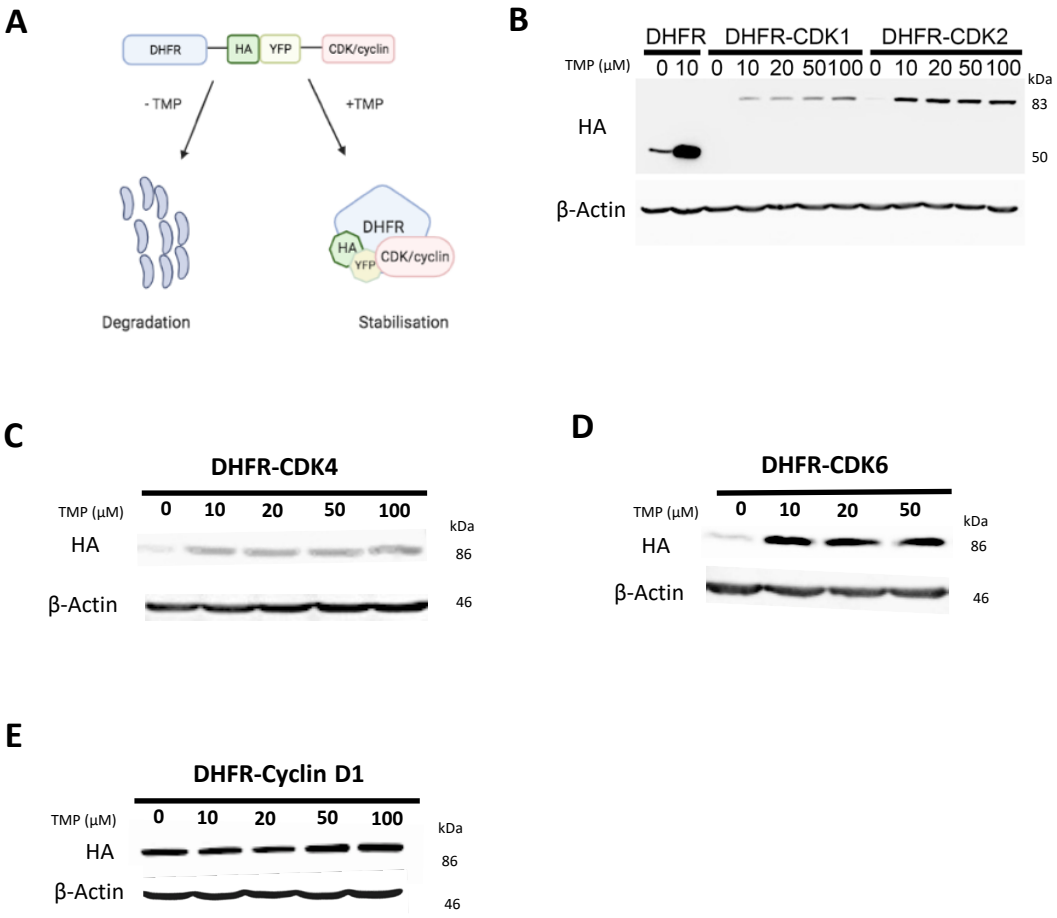


Figure 3.3. Generating CDK and cyclin over-expressing MCF7 cells using the DHFR inducible system.

(A) A simplified schematic of the DHFR inducible system showing DHFR destabilising domain fused to the protein of interest. In the presence of the DHFR high affinity ligand, TMP, the DHFR fusion protein is stablised, while in its absence the fusion protein is degraded. (B-E) Whole cell protein lysates were collected from MCF7-DHFR cell lines for immunoblotting for the HA-tag to demonstrate TMP induced the presence of DHFR-Vector in one independent experiment. β-Actin was used for loading control.

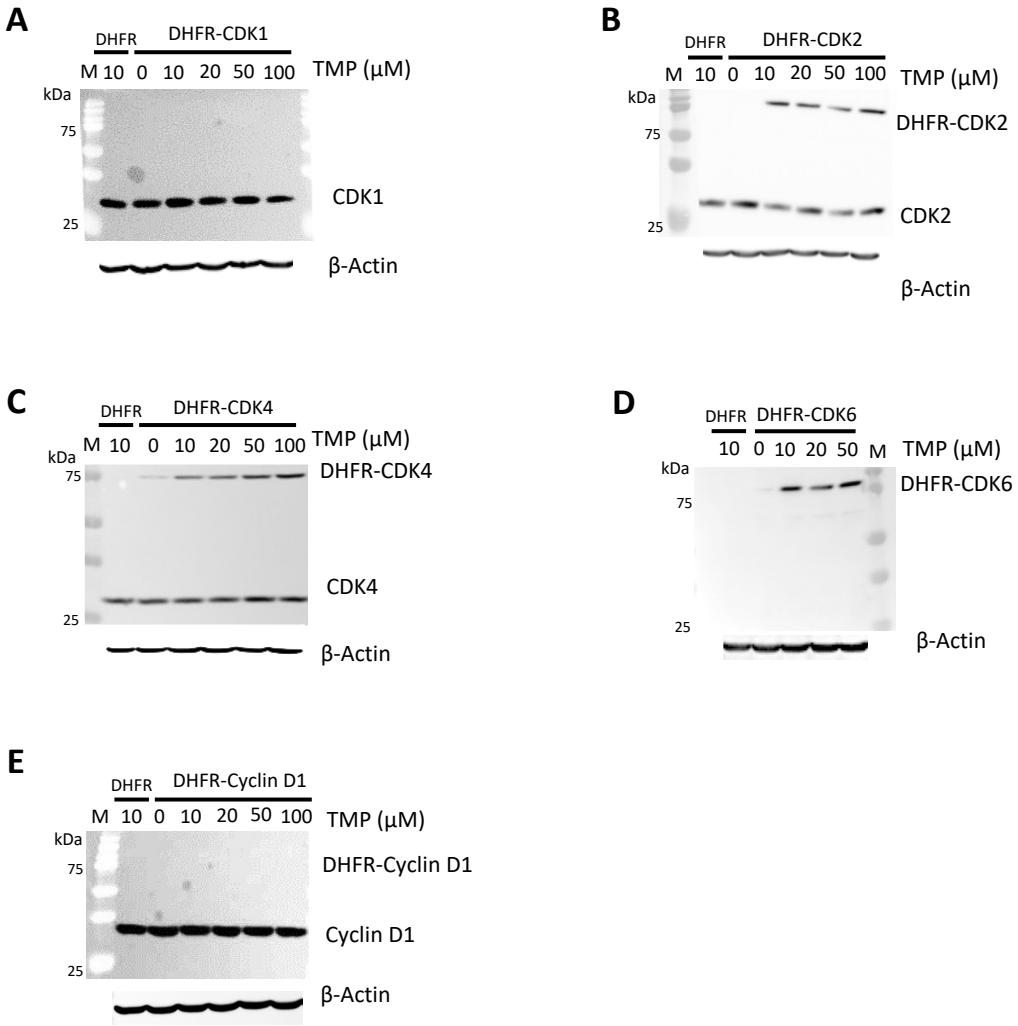


Figure 3.4. Generating CDK and cyclin over-expressing MCF7 cells using the DHFR inducible system. (A-E) Whole cell protein lysates were collected from MCF7-DHFR cell lines for immunoblotting for the indicated endogenous CDK/cyclin antibodies, to show presence of endogenous CDKs/cyclin and DHFR-CDK/cyclin fusion protein. β-Actin was used for loading control.

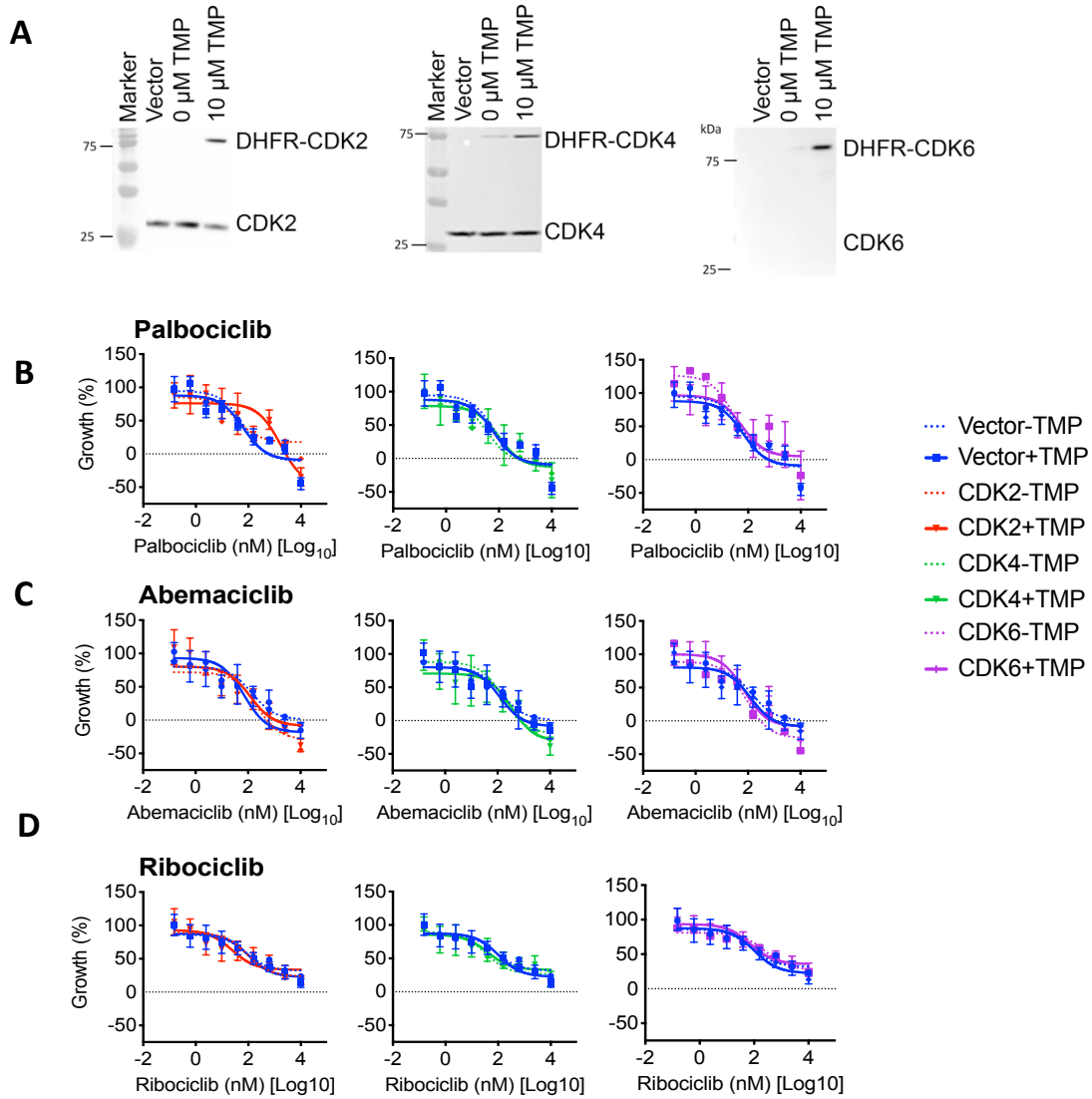
3.2.1.1 Inducible CDK over-expression in MCF7 cells provides only limited evidence for CDK over-expression in promoting resistance to CDK4/6 inhibitors.

CDK2 was previously suggested to be involved in early adaptation to palbociclib to sustain E2F transcription through activation by cyclin D1 (Herrera-Abreu *et al.*, 2016). This may allow cells to bypass dependence on CDK4/6 for progression through G1 to the S phase. Hence, mechanisms that allow CDK2 over-expression may contribute to the development of resistance to palbociclib. CDK2 over-expression may similarly promote resistance to other CDK4/6 inhibitors, including abemaciclib and ribociclib. To test this, growth assays were performed as in Section 3.1.2, except that TMP was added 48 hours prior to the addition of the CDK4/6 inhibitors. There was no difference in response to any of the CDK4/6 inhibitors in full media (Figure 3.5A, B). As MCF7 cells are estrogen-dependent for their growth, I also determined the impact of DHFR-CDK2 on growth in estrogen-depleted conditions (phenol-red free DMEM and 5% dextran-coated charcoal stripped FCS), with the addition of 10nM 17β-estradiol (E2). Interestingly, DHFR-CDK2 stabilisation with TMP resulted in an 8.2-fold reduction ($p < 0.0001$) in sensitivity to palbociclib, whereas there was no difference in sensitivity to palbociclib in the absence of TMP (Figure 3.5C-D). This indicates that CDK2 over-expression can indeed promote resistance to palbociclib. By contrast, DHFR-CDK2 induction did not result in a reduction in sensitivity to abemaciclib or ribociclib.

CDK6 over-expression has been observed in a breast cancer cell line model of acquired resistance to abemaciclib, where resistance was accompanied by amplification of the CDK6 gene (Yang *et al.*, 2017). As above for MCF7-DHFR-CDK2 cells, I determined if CDK6 over-expression promotes resistance to CDK4/6 inhibitors. There was no evident difference in sensitivity of MCF7-DHFR-CDK6 cells to palbociclib, or abemaciclib (Figure 3.5B-C). Interestingly, there was a small, near 2.0-fold reduction ($p = 0.0009$) in sensitivity to ribociclib in the presence of TMP (Figure 3.5C). However, the cells were similarly less sensitive to ribociclib in the absence of TMP. While this suggest that the ribociclib effect is non-specific, it should be noted that some DHFR-CDK6 expression was evident in the absence of TMP (Fig. 3.4B, Fig. 3.5A). Notwithstanding, these results do not confirm the previous report of resistance to abemaciclib resulting simply from CDK6 over-expression in MCF7 cells (Yang *et al.*, 2017).

The MCF7-DHFR-CDK4 cells express the fusion protein, with TMP addition increasing levels of DHFR-CDK4. However, DHFR-CDK4 levels remain considerably lower than those of endogenous CDK4 (Figure 3.5A). There was little evidence for effect of DHFR-CDK4 on sensitivity to CDK4/6 inhibitors, except for an approximately 3-fold higher GI_{50} for palbociclib (p = 0.067). Due to lack of strong evidence for expression of CDK1 and cyclin D1 fusion proteins, these cells were not assessed further.

The DHFR fusion protein method provides the possibility for inducible expression of a protein of interest. However, the stable lines generated here present several problems, such as lack of high-level expression of some proteins, particularly the DHFR-CDK1 fusion protein and detectable expression in the absence of TMP, which makes interpretation of the results more difficult, as in the case of DHFR-CDK6. Perhaps equally important is the possibility that the fusion protein may not fold for appropriate functionality. Despite the demonstration of resistance to palbociclib upon expression of the CDK2 fusion and potential link between CDK6 over-expression and resistance to ribociclib, I considered an alternative strategy for increasing expression of cell cycle CDK and cyclin genes, described in the next section.



E

Cell line \ Drug (nM)	Palbociclib	Abemaciclib	Ribociclib
DHFR + 0μM TMP	51.2 ± 4.3	48.8 ± 17.3	167.8 ± 2.2
DHFR + 10μM TMP	39.5 ± 10.7	29.1 ± 11.5	173.8 ± 72.2
DHFR-CDK2 + 0μM TMP	48.3 ± 25.7	45.3 ± 8.9	126.5 ± 17.5
DHFR-CDK2 + 10μM TMP	**418.9 ± 27.9**	68.8 ± 6.9	120.8 ± 23.2
DHFR-CDK4 + 0μM TMP	78.5 ± 67.1	53.2 ± 16.8	57.6 ± 10.1
DHFR-CDK4 + 10μM TMP	**148.1 ± 16.4**	80.1 ± 15.4	87.6 ± 14.5
DHFR-CDK6 + 0μM TMP	28.5 ± 3.0	48.0 ± 11.2	**358.0 ± 11.9**
DHFR-CDK6 + 10μM TMP	51.1 ± 6.2	60.7 ± 1.3	**224.4 ± 23.6**

Figure 3.5. Drug response of DHFR-CDKs lines cultured in estrogen-depleted medium.
(A) Immunoblotting of lysates prepared from MCF7 cells stably expressing vector (DHFR), or DHFR-CDK fusions, following 48 hours treatment with TMP. Data was shown in Figure 3.4B-D. Cells cultured in estrogen-depleted medium, supplemented with 10 nM E2, were treated with increasing concentrations of (B) Palbociclib, (C) Abemaciclib or (D) Ribociclib. 10μM TMP (solid lines) 10μM TMP (dotted lines) was added for inducing CDK activity. Cell growth was assessed by SRB assays. Graphs show the means of 2 independent experiments, each performed with 6 replicates. Error bars represent SD. (E) GI50 values (nM) obtained from growth inhibition graphs in B-D. GI50 values show means of 2 independent experiments ± SEM.

3.2.2 Using activating-Cas9 to over-express endogenous CDK and cyclin genes in MCF7 cells

The activating Cas9 method uses a nuclease deficient Cas9 mutant (dCas9), fused to a transcription activation domain, targeted to a gene of interest using sgRNAs specific for its gene promoter. I employed the well-used synthetic activating mediator (SAM) system, developed by Konermann *et al.* (2015). Here, dCas9 is fused to a transcriptional activation domain, named VP64 (dCas9-VP64), which is comprised of repeats of the transcription activation region of the Herpes simplex virus VP16 transcriptional activator protein. A second plasmid, encoding the MS2-p65-HSF1 fusion protein, includes transcriptional activation domains from the NF-κB p65 subunit and the heat shock factor 1 transcription activation domain, fused to the MS2 bacteriophage coat protein. The latter binds as a dimer to RNA stem loop structures incorporated in the sgRNA design (Figure 3.6A). This refinement effectively provides a strong transcriptional complex at sequences to which the sgRNA is recruited. MCF7 cells stably expressing dCas9-VP64 and MS2-p65-HSF1 constructs were developed with co-transduction of three sgRNAs designed to target specific gene promoters. SgRNA sequences were obtained from the resource reported by the Zhang lab (Konermann *et al.* (2015)), in which three independent sgRNAs have been designed for the region approximately -200 to the transcription start site, for all protein coding genes.

Following selection for the stable SAM lines, the initial analysis was designed to confirm over-expression both at the mRNA and protein level, compared to the control cell line expressing the SAM components, together with a non-targeting sgRNA vector (AcCas9-Vector). RT-qPCR data revealed increased expression of the endogenous CDK and cyclin genes in most of the AcCas9 lines (Figure 3.6B). AcCas9-CDK5, -CDK6 and -CCNE1 lines showed the highest increase in gene expression, 12-, 30- and 8-fold higher gene expression, respectively. In agreement, there was an increase in levels of CDK5, CDK6 and CCNE1 proteins, confirming the over-expression (Figure 3.6C). Much more modest increases in mRNA levels were evident for CDK2, CDK8, CDK12 and CCNT1, with the remaining genes showing little or no increase in mRNA levels. CDK2 and CDK8 protein levels were also elevated, while increased protein levels, despite little or no increase in mRNA levels, was evident for CDK7. None of the other lines showed increased mRNA or protein levels, including CDK1, CDK4, CCND1, CDK9 and CCND1. At least in some cases the lack of increased expression may be explained by the already high levels of expression in the parental cells. Nevertheless, the developed models

provide a good opportunity for investigating the possibility of several CDKs and cyclins in response and resistance to CDK4/6 inhibitors.

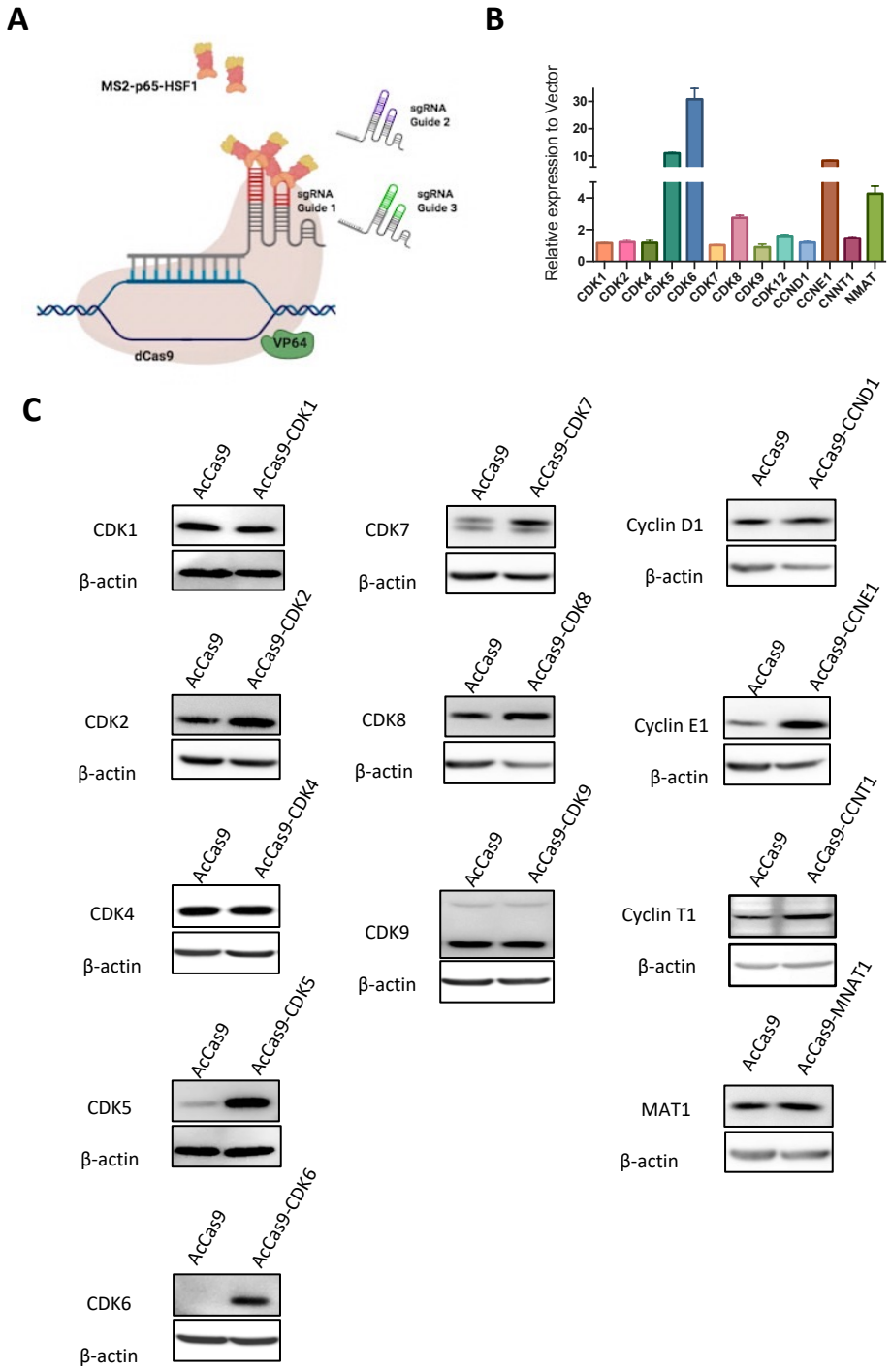


Figure 3.6. Using the gene activating Cas9 method to over-express endogenous CDK and cyclin genes. (A) A schematic of the synergistic activation mediator (SAM) system. SAM (denoted as activating Cas9 (AcCas9) involves co-expression of a nuclease-dead Cas9 fused to the transcription activation protein VP64 (dCas9-VP64), together with MS2-P65-HSP1 and sgRNAs designed for targeting the promoter region of the gene of interest (Konermann *et al.*, 2015). MCF7 cells stably transduced with dCas9-VP64 and MS2-P65-HSP were transduced with three independent sgRNAs targeting the promoter region of the gene of interest to generate pools of stable over-expression cells. (B) RT-qPCR assessed gene expression level using RNA prepared from MCF7-AcCas9 lines. Endogenous gene expression was calculated relative to TBP. Error bars represent ±SEM (n=3). Data were kindly provided by Ms X B Xiong. (C) Whole cell protein lysate was prepared from MCF7-AcCas9 lines were immunoblotted with the indicated antibodies in one independent experiment. β-Actin was used as a loading control.

Despite elevated protein levels, the AcCas9-CDK2 and AcCas9-CDK4 cells did not show any difference in growth in DMEM containing 10% FCS, over a 12-day period, compared with the AcCas9-vector control cells (Figure 3.7A). There was a very small increase in growth for the AcCas9-CDK6 and AcCas9-CDK7 cells, although independent experiments would be required to determine if the growth differences are statistically meaningful. A similar lack of growth difference was observed for AcCas9-CCND1, AcCas9-CCNE1 or the AcCas9-CCNT1 cells.

As previously mentioned, the growth of MCF7 cells is estrogen-dependent. Therefore, the growth assays were repeated in estrogen-depleted conditions with the addition of 10nM E2 or an equal volume of DMSO (vehicle control). As expected, MCF7 AcCas9-vector cells did not grow in the absence of E2. Over-expression of any of the CDKs or cyclin genes did not significantly stimulate cell growth (Figure 3.7B), indicating that over-expression of these genes is insufficient to promote estrogen-independent growth.

As expected, estrogen stimulated the growth of AcCas9-vector cells. The AcCas9-CCND1 cells showed a similar growth profile to AcCas9-vector cells. However, growth of AcCas9-CDK2, AcCas9-CDK4, AcCas9-CDK6, as well as AcCas9-CCNE1 and AcCas9-CCNT1 cells was significantly higher than that of the AcCas9-vector control cells (Figure 3.7B-C). Interestingly, growth of all lines was similar until day-6, when AcCas9-vector cells plateaued, whereas AcCas9-CDK2, AcCas9-CDK4, AcCas9-CDK6, AcCas9-CCNE1 and AcCas9-CCNT1 cell numbers continued to increase to day-12. This suggests that the CDK and cyclin over-expressing cells may continue to grow after the cultures have reached confluence, and may be piling, although this was not further investigated.

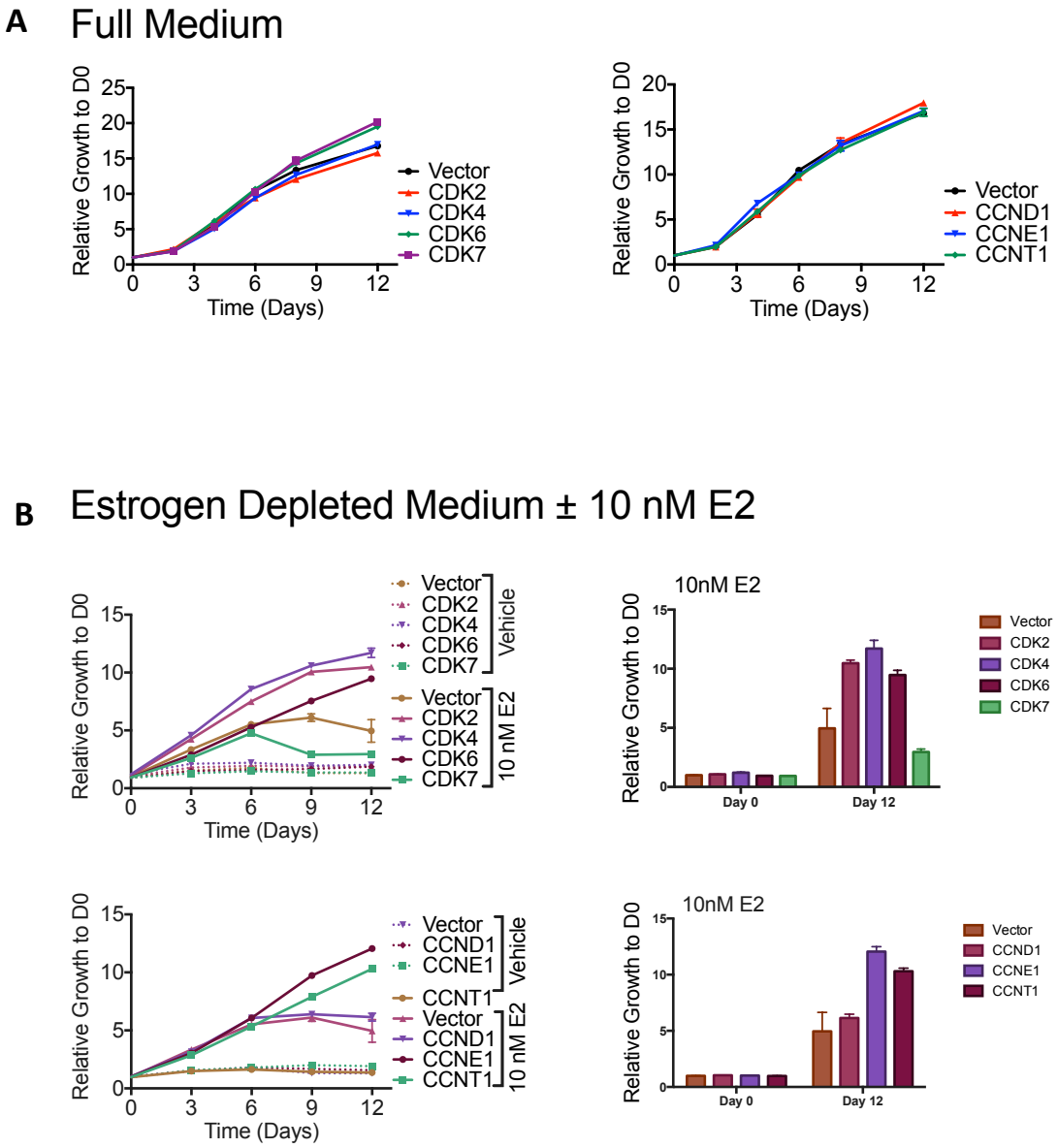


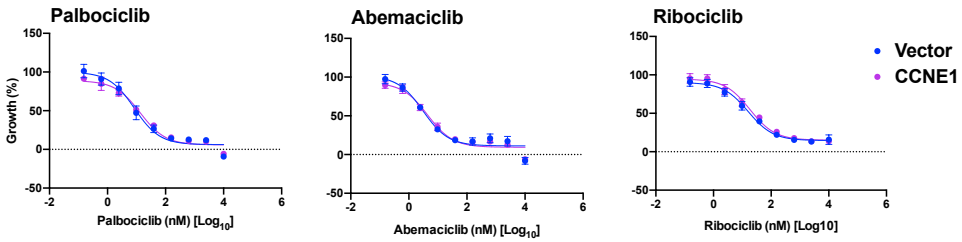
Figure 3.7. Determining the effect of over-expressing CDKs and cyclins on MCF7 cell growth.
(A-B) MCF7 cells stably expressing the two AcCas9-Vectors or cells over-expressing the indicated CDKs and cyclins were plated in 96-well plates and growth was assessed for 12-days using the SRB assay in estrogen containing medium (DMEM with 10% FCS) (A) or in estrogen depleted medium (phenol-red free DMEM with 5% dextran-coated charcoal stripped FCS), ±10nM 17β-estradiol (E2) (B). An equal volume of DMSO was added to the vehicle controls. Error bars represent SEM of means of six technical replicates (A) and three technical replicates (B). Data were kindly provided by Dr. C F Lai.

3.2.2.1 Cyclin E1 over-expression and response to CDK4/6 inhibitors

AcCas9-CCNE1 MCF7 cells show a 10-fold increase in CCNE1 expression, while Western blotting indicates at least a doubling in CCNE1 protein levels. However, CCNE1 over-expression did not promote estrogen-independent growth; nor was growth stimulated in the presence of E2. Moreover, growth assays with 6-days treatment with CDK4/6 inhibitors in either full growth medium or estrogen-depleted medium to which 10nM E2 was added, showed no difference in response to CDK4/6 inhibitors (Figure 3.8).

As no difference was observed in the sensitivity to CDK4/6 inhibitors in MCF7-AcCas9-CCNE1 cells in short-term treatments with CDK4/6 inhibitors, long term treatment with a series of concentrations of CDK4/6 inhibitors was used to determine if CCNE1 over-expression promotes acquisition of resistance to CDK4/6 inhibitors. Indeed, a previous study has shown that long-term treatment of MCF7 cells with palbociclib results in up-regulation of CCNE1 expression in the emergent palbociclib-resistant MCF7 cells (Herrera-Abreu *et al.*, 2016). Cells were treated with 10nM, 50nM, 250nM, 500nM and 1000nM concentrations of the CDK4/6 inhibitor or an equal volume of DMSO (vehicle control). Cell growth was tracked by measuring confluency using the Incucyte live cell imaging system over a period of 40 days (Figure 3.9). Although there was some indication of more rapid growth of MCF7-AcCas9-CCNE1 cells at low concentrations of all three CDK4/6 inhibitors, the increased proliferation rate was not maintained upon further culturing. At higher concentration of all three CDK4/6 inhibitors, cell growth was completed prevented. The proliferation rate was comparable to the MCF7-AcCas9-Vector cells, which suggests that cyclin E1 over-expression does not result in a growth advantage in long term exposure to CDK4/6 inhibitors. However, upon further characterisation in cells treated with 250nM palbociclib, 50nM abemaciclib and 500nM ribociclib (discussed in detail in Section 3.2.2.2 and Section 3.2.2.3), mRNA levels of cyclin E1 showed absence of over-expression after long-term culturing. Thus, investigation of the role of cyclin E1 in evading CDK4/6 inhibition was limited in the current model.

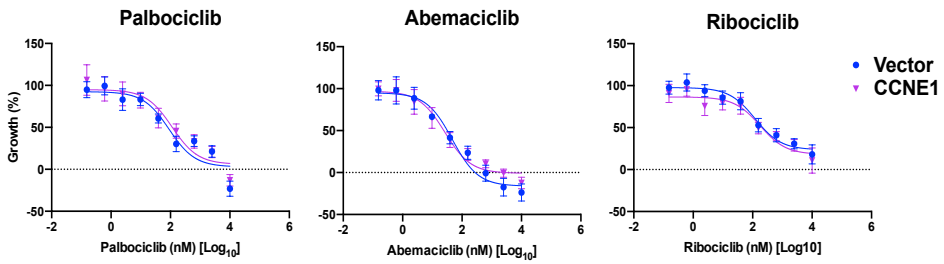
A Full medium



B

Drug (nM) / Cell line	Palbociclib	Abemaciclib	Ribociclib
AcCas9-Vector	9.7 ± 0.33	4.03 ± 0.67	18.3 ± 2.33
AcCas9-CCNE1	11.7 ± 0.33	5.0 ± 0.58	23.7 ± 0.67

C Estrogen depleted medium



D

Drug (nM) / Cell line	Palbociclib	Abemaciclib	Ribociclib
AcCas9-Vector	83.0 ± 11.5	33.9 ± 1.3	235.5 ± 52.6
AcCas9-CCNE1	116.2 ± 19.8	24.6 ± 10.5	235.6 ± 72.8

Figure 3.8. Response of MCF7-AcCas9-CCNE1 cells to CDK4/6 inhbitors.
MCF7-AcCas9-Vector and -CCNE1 lines were treated with CDK4/6 inhibitors in full growth medium (DMEM and 10% FCS) (A-B) or estrogen depleted medium phenol-red free DMEM with 5% dextran-coated charcoal stripped FCS), ±10nM 17β-estradiol (E2) (C-D). (A,C) Growth was measured using SRB assays after 6-days of treatment. Error bars represent SD of mean values (n=6) from three independent experiments. (B,D) GI50 values (nM) ± SEM were obtained from growth inhibition curves for each CDK inhibitor from the three independent experiments in A,C.

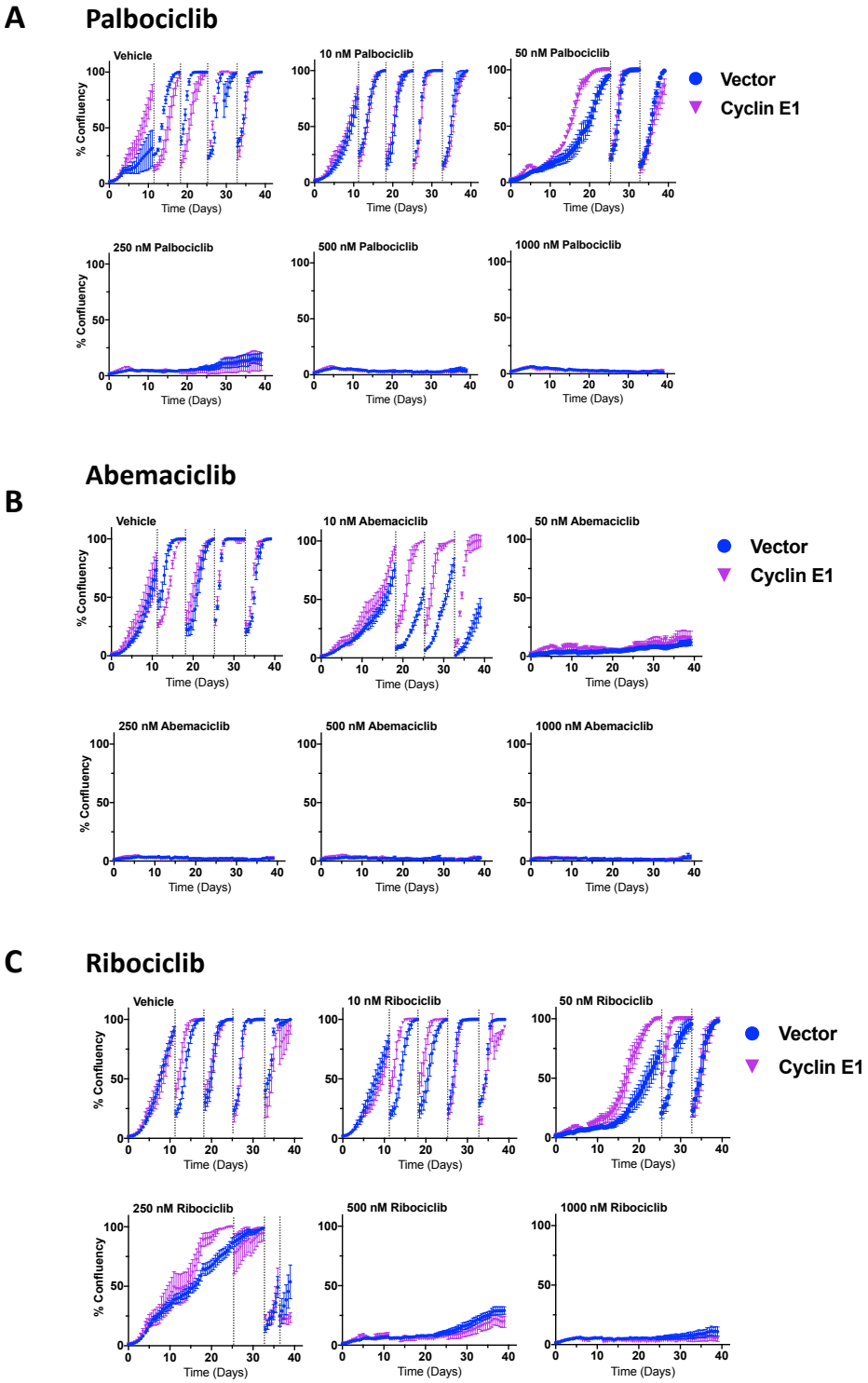


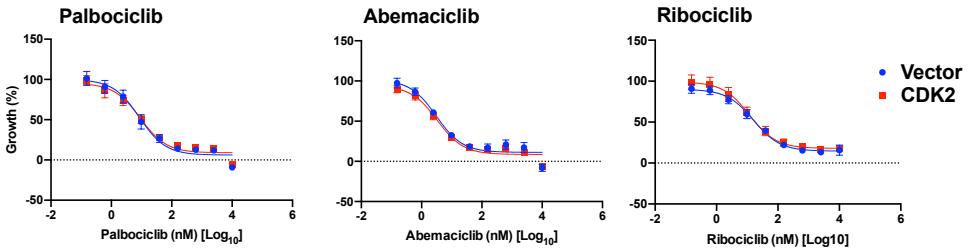
Figure 3.9. Over-expressing CCNE1 had limited effect on growth recovery after culturing with continous treatment with CDK4/6 inhibtors.

Long-term culturing of MCF7 cells was undertaken in the presence of CDK4/6 inhibitors, Palbociclib (A), Abemaciclib (B) or Ribociclib (C). Cells were cultured in the presence of each drug at concentrations of 10, 50, 250, 500 or 1000 nM. Culture media were changed every 3 days, for medium containing the appropriate CDK4/6 inhibitor, or with an equal volume of DMSO (vehicle control). Cell numbers were estimated as percentage confluency relative to day-0 using the Incucyte Zoom live cell system, error bars represent SEM (n=4). Where one of the cultures for a particular drug concentration reached confluence, all cultures in that condition were trypsinised and re-plated at 1:5 dilution.

3.2.2.2 Investigating MCF7-AcCas9-CDK2 over-expressing cells in sensitivity to CDK4/6 inhibitors

Turning to the CDK2 over-expressing MCF7-AcCas9-CDK2 cells, while CDK2 mRNA levels were not increased, protein levels were evidently elevated in these cells. Following the methodology used with the MCF7-AcCas9-CCNE1 cells, growth assays in which the CDK4/6 inhibitors were added for 6 days showed no effect on sensitivity to any of the CDK4/6 inhibitors in full medium conditions (Figure 3.10A-B). By contrast, when grown in estrogen-depleted medium, MCF7-AcCas9-CDK2 cells showed increased growth (Figure 3.7) and a 10-fold decrease ($p = 0.1$) in sensitivity to palbociclib compared to MCF7-AcCas9-Vector (Figure 3.10C-D), reflecting the decreased sensitivity to palbociclib observed with DHFR-CDK2 cells. Although a difference in response to Palbociclib appears evident, the difference was not statistically significant, the difference in response is evident, but further validation and repeats are required . However, a significant 3-fold decrease ($p = 0.0201$) in sensitivity to ribociclib was observed in MCF7-AcCas9-CDK2 cells. There was no difference in sensitivity of the MCF7-AcCas9-CDK2 cells compared with the MCF7-AcCas9-vector cells. There was no statistically significant difference in response to ICEC0942 or the CDK7/12/13 inhibitor THZ1, although there was a trend towards reduced sensitivity of the CDK2 over-expressing cells to ICEC0942 (1.6-fold, $p=0.218$).

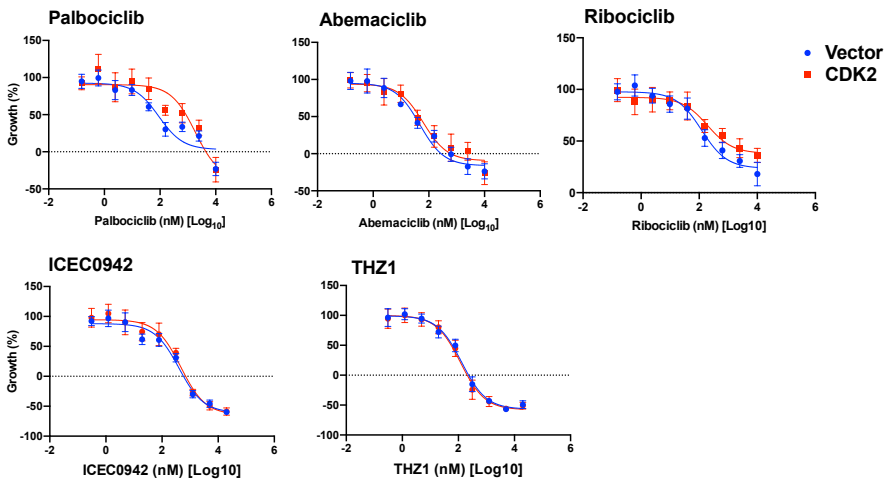
A Full medium



B

Cell line \ Drug (nM)	Palbociclib	Abemaciclib	Ribociclib
AcCas9-Vector	9.7 ± 0.33	4.03 ± 0.67	18.3 ± 2.33
AcCas9-CDK2	10 ± 1.00	3.33 ± 0.33	19.0 ± 4.51

C Estrogen depleted medium



D

Cell line \ Drug (nM)	Palbociclib	Abemaciclib	Ribociclib	ICEC0942	THZ1
AcCas9-Vector	83.0 ± 11.5	33.9 ± 1.3	235.5 ± 52.6	120.0 ± 14.0	67.23 ± 11.7
AcCas9-CDK2	**825.1 ± 347.4**	51.4 ± 19.6	**694.2 ± 111.0**	191.17 ± 13.6	69.1 ± 10.3

Figure 3.10. MCF7-AcCas9-CDK2 show reduced response to palbociclib in estrogen depleted medium supplemented with 10nM 17β-estradiol.

MCF7-AcCas9-Vector and -CDK2 lines were cultured in full growth medium (A-B) or in estrogen depleted medium (phenol-red free DMEM with 5% dextran-coated charcoal stripped FCS), ±10nM 17β-estradiol (E2). Growth was measured using SRB assays after 6-days of treatment with CDK4/6 inhibitors, 2-days treatment with CDK7 inhibitor (ICEC0942) or the CDK7/12/13 inhibitor (THZ1). Error bars represent SD of mean values (n=6) from three independent experiments. (B,D) GI50 values (nM) ± SEM were obtained from growth curves in A,C.

Long-term culturing of MCF7-AcCas9-CDK2 cells was undertaken in the presence of different concentrations of palbociclib, exactly as described above for MCF7-AcCas9-CCNE1 cells. Growth was similar for MCF7-AcCas9-Vector and MCF7-AcCas9-CDK2 cells at low concentrations of palbociclib (Figure 3.11A). However, MCF7-AcCas9-CDK2 cultured with 250nM of palbociclib showed an increase in cell growth at around 20 days of treatment compared to MCF7-AcCas9-Vector cells, suggesting a potential role of CDK2 over-expression in promoting resistance to palbociclib. In the presence of 500 nM palbociclib, growth recovery was slower, but again MCF7-AcCas9-CDK2 cell growth was evident from 35 days. No cell growth was observed in cells treated with 1000nM even after 40 days.

Both RNA and protein lysates were prepared from MCF7-AcCas9-Vector and MCF7-AcCas9-CDK2 cells recovered from long term culturing in 250nM palbociclib for investigating the expression of cell cycle CDKs and cyclins. As expected, CDK2 mRNA and protein levels were higher in the MCF7-AcCas9-CDK2 cells compared with the MCF7-AcCas9-vector cells (Figure 3.11B-D). CDK2 levels were also elevated in MCF7-AcCas9-CDK2 cells cultured with 250 nM palbociclib. Expression of CDK4 ($p = 0.0003$), as well as the CDK2 cyclin genes, CCNA1 ($p = 0.005$) and CCNE1 ($p = 0.056$) was reduced in the long-term palbociclib treated cells, while CCND1 ($p = 0.062$) expression was increased. CDK6 expression was low and remained low. So, expression of G1 and S-phase CDKs and cyclin genes did not show differential expression in the CDK2 overexpressing cells prior to or upon development of resistance to palbociclib. Other than an increase in levels of CDK6 protein ($p = 0.05$), not observed in RT-qPCR, there was little to distinguish the vector and CDK2 over-expressing cells before or after palbociclib resistance.

3.2.2.2.3 Over-expression of CDK2 also resulted in the fast development of resistance to ribociclib

Likewise, CDK2 over-expression in the MCF7-AcCas9-CDK2 cells also promoted resistance to ribociclib. With 10nM ribociclib, there was no difference in cell growth compared to MCF7-AcCas9-Vector (Figure3.12A). Although at 50nM and 250nM of ribociclib, MCF7-AcCas9-CDK2 demonstrated a fast recovery in growth, MCF7-AcCas9-Vector also reached around 90% confluency at day 25 and day 30, respectively. The advantage of CDK2 over-expression to promote resistance was most evident in cells cultured with 500nM and 1000nM ribociclib after

15- and 20-days continuous treatment, respectively. Cells treated with 500nM ribociclib were selected for further analysis.

As expected, CDK2 expression was higher in the MCF7-AcCas9-CDK2 cells, compared with MCF7-AcCas9-Vector cells growing in 500 nM ribociclib (Figure 3.12B). Interestingly, where CDK4 levels fell in the ribociclib-resistant MCF7-AcCas9-Vector cells, CDK4 levels were maintained in the ribociclib-resistant MCF7-AcCas9-CDK2 cells (p = 0.16, Figure 3.12B). Note that CDK4 levels were reduced in the palbociclib-resistant MCF7-AcCas9-Vector and MCF7-AcCas9-CDK2 cells (p= *0.0282,* Figure 3.11B). Similar reductions in CCNE1 expression in MCF7-AcCas9-Vector cells (p = *0.51)*, but maintenance of CCNE1 expression in MCF7-AcCas9-CDK2 cells, was evident (p = 0.044, Figure 3.12B). However, cyclin E1 protein levels were in fact reduced in the ribociclib-resistant MCF7-AcCas9-CDK2 cells (Figure 3.12C-D). Also, in contrast to observations in the palbociclib-resistant cells, CDK6 expression was increased in the ribociclib-resistant MCF7-AcCas9-CDK2 cells (p = 0.0307, Figure 3.12B). CDK6 protein levels were higher in the ribociclib-resistant MCF7-AcCas9-CDK2 cells, than in MCF7-AcCas9-vector cells. CCND1 gene expression was increased in the ribociclib-resistant cells (p = 0.47, Figure 3.12B) but not in the palbociclib-resistant cells (p = 0.99, Figure 3.11B). CCND1 (p = 0.0319) protein levels were similarly increased in the ribociclib-resistant cells (Figure 3.12C-D).

On the other hand, the promotion of resistance by CDK2 over-expression was not seen in long term treatment to abemaciclib, even at the high concentration of 1000 nM (Figure 3.13A). As both lines grew in 50 nM abemaciclib, a concentration similar to the GI50 for abemaciclib in short-term growth assays (Figure 3.9), these cells were used to assess gene expression and protein levels for G1 and S phase CDKs and cyclins. CDK2 gene expression was higher in MCF7-AcCas9-CDK2 cell grown in the presence of 50 nM abemaciclib than in MCF7-AcCas9-vector cells, as expected (Figure 3.13B), although CDK2 protein levels were not elevated, which may indicate a post-transcriptional alteration that reduces CDK2 levels in the presence of abemaciclib. As in the case of ribociclib, CDK6 levels were increased at the mRNA and protein level in the abemaciclib treatment conditions (Figure 3.13B-D). Interestingly, there was a lowered level of RB protein in the presence of abemaciclib, but RB phosphorylation was higher in the MCF7-AcCas9-vector cells treated with abemaciclib than in the MCF7-AcCas9-CDK2 cells.

To summarise the above findings, CDK2 was successfully over-expressed in both DHFR and AcCas9 system. Sensitivity to CDK4/6 inhibitors was reduced in estrogen depleted conditions, not in full growth medium. MCF7-AcCas9-CDK2 cells led to rapid recovery of growth after long term treatment of palbociclib and ribociclib, but limited effect in abemaciclib.

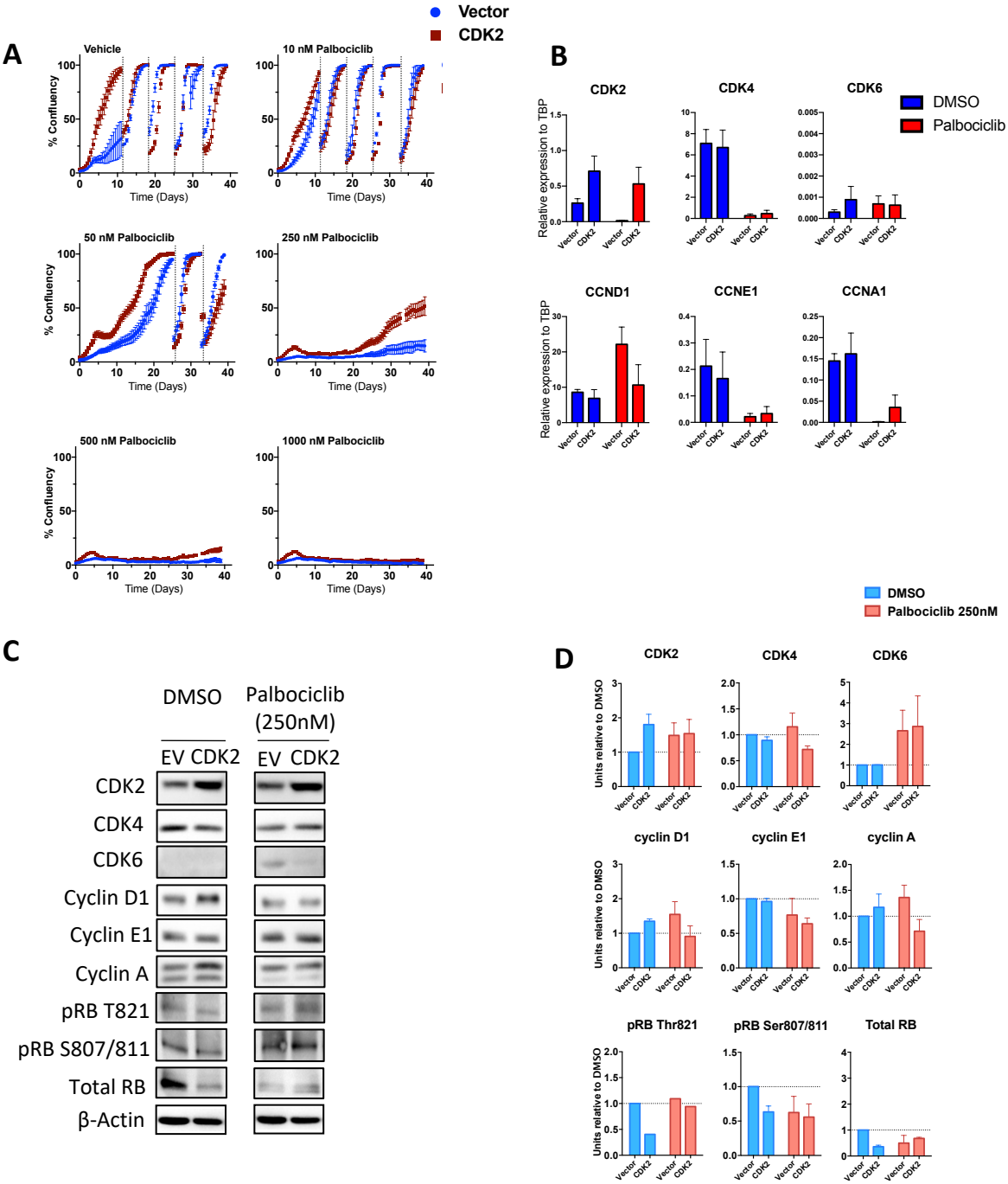


Figure 3.11. MCF7-AcCas9-CDK2 promote rapid emergence of resistance to palbociclib.
(A) MCF7-AcCas9-Vector and -CDK2 cells were treated with 10, 50, 250, 500 and 1000nM palbociclib. Cell numbers were estimated as percentage confluency relative to day 0 using the Incucyte Zoom live cell system. Error bars represent SEM from four incucyte images (n=4). Growth assays were performed in the same experiment and data of AcCas9-Vector is the same as shown in Figure 3.9. (B) RT-qPCR of RNA extracted from cells following over 5-week treatment with 250nM palbociclib. An equal amounts of DMSO was added as vehicle controls. Gene expression levels are shown relative to TBP. Error bars represent SEM (n=3). (C) Whole cell lysates were collected from cells after long term exposure to 250nM palbociclib. Representative western blots are shown from three independent experiments. β-Actin was used as a control for equal loading. (D) Western blots were quantified using ImageJ. Error bars represent SD (n=3), however, with the exception of pRB T821 (n=1).

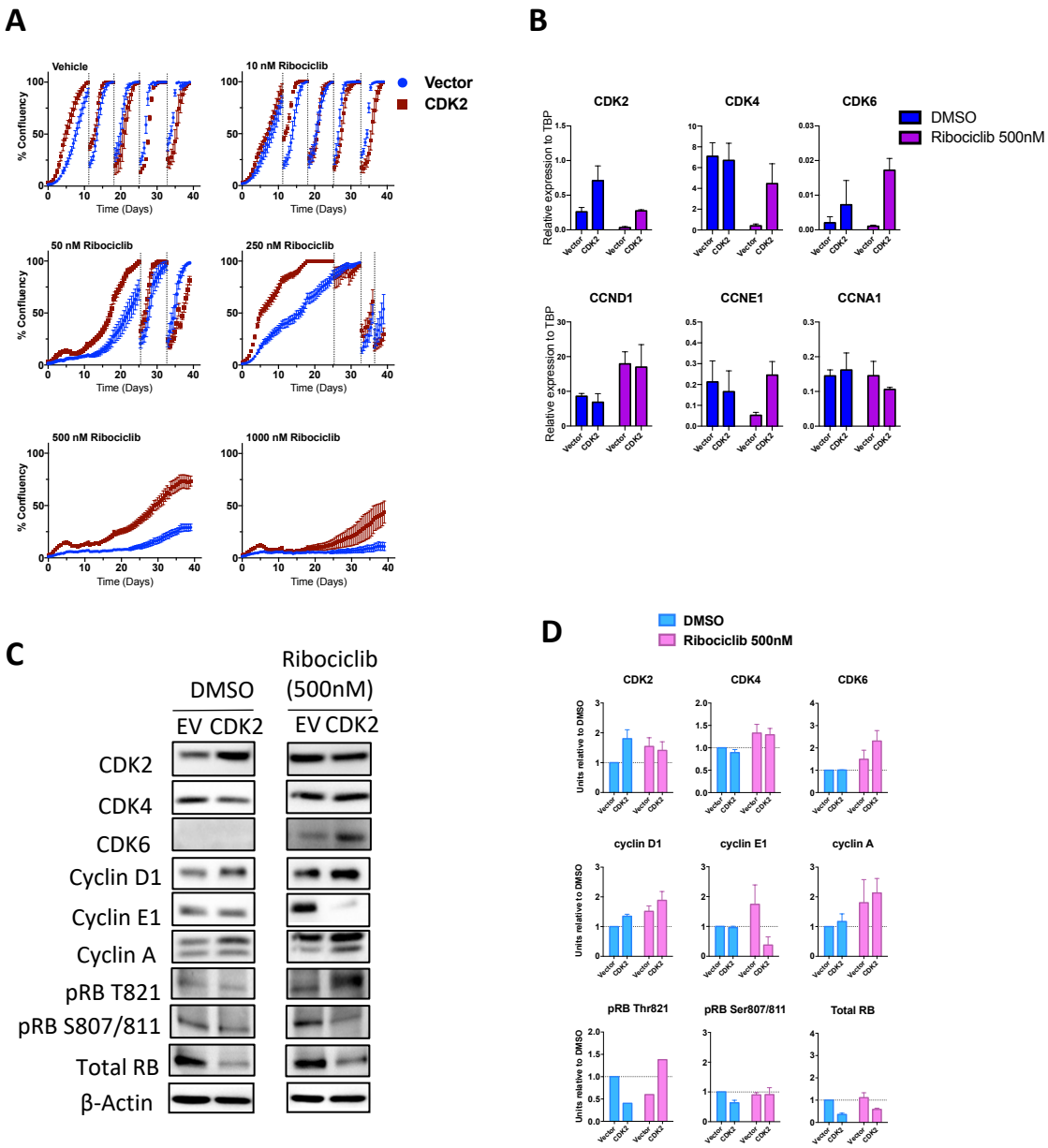


Figure 3.12. Over-expressing CDK2 is associated with a rapid development of resistance to ribociclib. (A) MCF7-AcCas9-Vector and -CDK2 cells were treated with 10, 50, 250, 500 and 1000nM abemaciclib. Cell numbers were estimated as percentage confluency relative to day 0 using the Incucyte Zoom live cell system. Error bars represent SEM (n=4). Growth assays were performed in the same experiment and data of AcCas9-Vector is the same as shown in Figure 3.9A. (B) RT-qPCR of RNA extracted from cells following over 5-week treatment with 500nM ribociclib and equal amounts of DMSO was added as vehicle controls. Gene expression levels are shown relative to TBP. Error bars represent SEM (n=3). RT-qPCR was conducted in the same experiment and data DMSO control of AcCas9-Vector and –CDK2 were the same as shown in Figure 3.12B. (C) Whole cell lysates were collected from cells after long exposure 500nM ribociclib. (D) Western blots were quantified using ImageJ. Error bars represent SD (n=3), however, with the exception of pRB T821 (n=1). Immunoblots were conducted in the same experiment and data DMSO control of AcCas9-Vector and –CDK2 were the same as shown in Figure 3.12C-D.

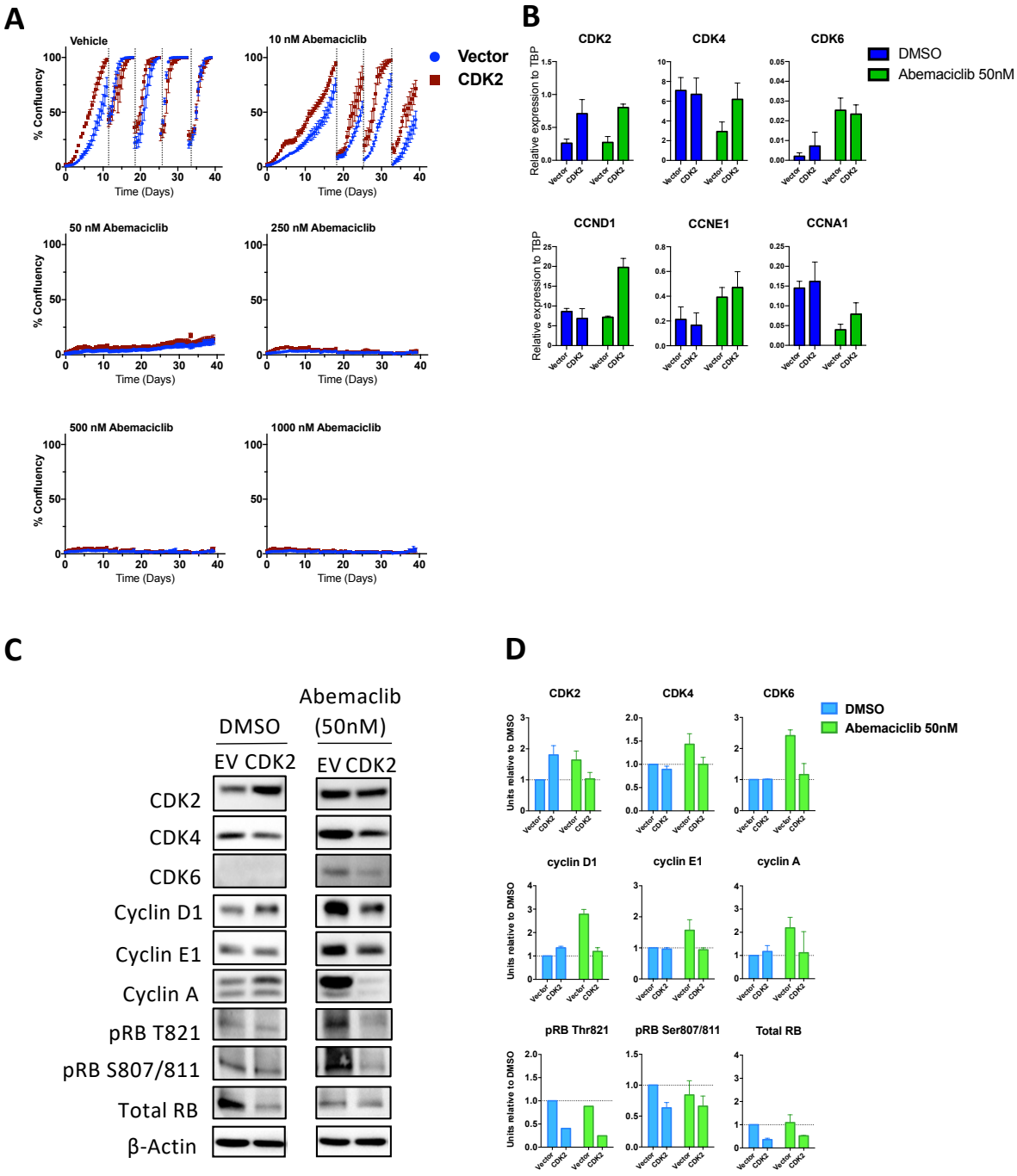


Figure 3.13. MCF7-AcCas9-CDK2 does not promote resistance to abemaciclib.
(A) MCF7-AcCas9-Vector and -CDK2 cells were treated with 10, 50, 250, 500 and 1000nM riociclib. Cell numbers were estimated as percentage confluency relative to day 0 using the Incucyte Zoom live cell system. Error bars represent SEM from four incucyte images (n=4). Growth assays were performed in the same experiment and data of AcCas9-Vector is the same as shown in Figure 3.9A. (B) RT-qPCR was performed using RNA extracted from cells following treatment with 50nM abemaciclib or an equal volume of vehicle (DMSO) over a period of 5 weeks. Gene expression levels are shown relative to expression of TBP. Error bars represent SEM (n=3). Note that the DMSO treated control RNAs were the same ones used in Figure 3.12B. (C) Whole cell lysates were collected from cells after long exposure 50nM abemaciclib. Representative Immunoblots are shown from three independent experiments. β-Actin was used as a control for equal loading. (D) Immunoblots were quantified using ImageJ. Error bars represent SD (n=3), however, with the exception of pRB T821 (n=1). Immunoblots were conducted in the same experiment and RT-qPCR data for DMSO control of AcCas9-Vector and –CDK2 are the same as those shown in Figure 3.12C-D.

3.2.2.3 CDK6 over-expression in the emergence of resistance CDK4/6 inhibitors

3.2.2.3.1 Drug response of CDK6 over-expressing cells with short term treatment with CDK inhibitors

Short term treatment with CDK4/6 inhibitors was used as the initial study of drug response in MCF7-AcCas9-CDK6 over-expressing lines in full medium and estrogen-depleted medium containing 10nM E2. MCF7-AcCas9-CDK6 demonstrated no change in sensitivity to any of the three CDK4/6 inhibitors in full growth medium (Figure 3.14A-B). Likewise, when growth assays were conducted in estrogen-free medium supplemented with 10nM of E2, no difference in growth inhibition was observed (Figure 3.14C-D). These findings concur with the findings for the MCF7-DHFR-CDK6 over-expressing cells. Intriguingly, there was a small, 1.5-fold reduction in sensitivity to ICEC0942 but no difference in sensitivity to THZ1.

3.2.2.3.2 Development of acquired resistance in MCF-7AcCas9-CDK6 cells through prolonged exposure to CDK4/6 inhibitors

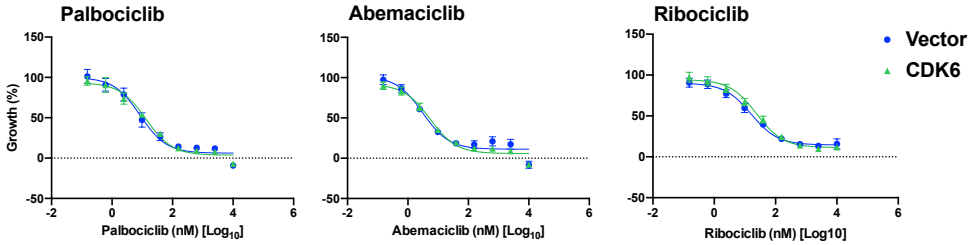
I followed the same methodology as for the MCF7-AcCas9-CDK2 cells with the MCF7-AcCas9-CDK6 cells, to determine if prolonged culturing in the presence of CDK4/6 inhibitors promotes development of resistance. Over the 40-day growth experiment, greater growth of MCF7-AcCas9-CDK6 cells was evident in 250nM and 500nM palbociclib conditions, 50nM abemaciclib and 500nM ribociclib (Figures 3.15-17). Cells from these treatments (only 250 nM palbociclib was used) were expanded and RT-qPCR and WB were undertaken.

As expected, CDK6 expression was elevated in the MCF7-AcCas9-CDK6 cells, compared with MCF7-AcCas9-vector cells (Figure 3.15C, 3.16C and 3.17C). A further increase in CDK6 expression was evident in all MCF7-AcCas9-CDK6 cell cultures following long-term culturing in palbociclib, abemaciclib or ribociclib, both at the mRNA and protein levels. Expression of other CDKs was largely the same in MCF7-AcCas9-CDK6 and MCF7-AcCas9-vector cells, whereas levels of CCNA1 (in abemaciclib-treated cells ($p = 0.006$, Figure 3.15B); palbociclib-treated cells ($p = 0.021$, Figure 3.16B); in ribociclib-treated cells ($p = 0.36$, Figure 3.17B)), CCND1 (in abemaciclib-treated cells ($p = 0.002$, Figure 3.15B); palbociclib-treated cells ($p = 0.015$, Figure 3.16B); in ribociclib-treated cells ($p = 0.08$, Figure 3.17B)), and CCNE1 (in abemaciclib-treated cells ($p = 0.024$, Figure 3.15B); palbociclib-treated cells ($p = 0.15$, Figure

3.16B); in ribociclib-treated cells (p = 0.032, Figure 3.17B)) were either the same, higher or lower for the different CDK4/6 inhibitor treatments. Thus, cyclin A levels were lower in abemaciclib-treated (p = 0.96, Figure 3.15C-D) and ribociclib-treated (p = 0.56, Figure 17C-D) MCF7-AcCas9-vector, but not in the MCF7-AcCas9-CDK6 cells, compared to the untreated cells. By contrast, cyclin A levels were reduced in palbociclib-treated cells, most prominently in the MCF7-AcCas9-CDK6 cells (p = 0.16, Figure 3.16C-D). CCND1 and CCNE1 levels did not change much. Finally, RB1 levels were unchanged, in contrast to what was seen for the MCF7-AcCas9-CDK2 cells, but RB1 phosphorylation, particularly at Ser807/811 was increased with ribociclib treatment (p = 0.30, Figure 3.17C-D).

The over-expression of CDK6 had very limited effect on sensitivity after a 6-day treatment of CDK4/6 inhibitors. Unlike MCF7-AcCas9-CDK2, the over-expression of CDK6 shown limited effect on growth after long term treatment of palbocilib. However, MCF7-AcCas9-CDK6 shown a rapid recovery after a long term treatment of abemaciclib.

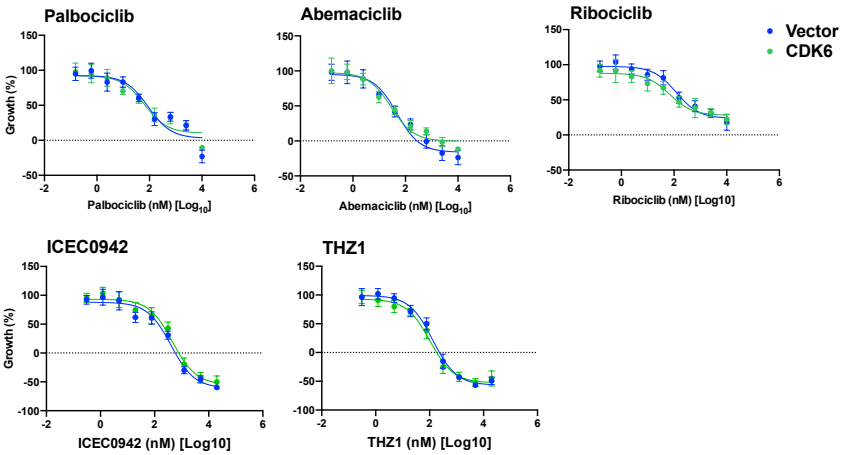
A Full medium



B

Cell line \ Drug (nM)	Palbociclib	Abemaciclib	Ribociclib
AcCas9-Vector	9.7 ± 0.33	4.03 ± 0.67	18.3 ± 2.33
AcCas9-CDK6	12.33 ± 20.88	5.0 ± 0.58	27.3 ± 1.86

C Estrogen depleted medium



D

Cell line \ Drug (nM)	Palbociclib	Abemaciclib	Ribociclib	ICEC0942	THZ1
AcCas9-Vector	83.0 ± 11.5	33.9 ± 1.3	235.5 ± 52.6	120.0 ± 14.0	67.23 ± 11.7
AcCas9-CDK6	77.6 ± 21.8	28.0 ± 0.7	126.8 ± 33.5	184.20 ± 47.2	51.53 ± 7.9

Figure 3.14. CDK6 over-expression does not reduce sensitivity to CDK4/6 inhibtiors.
MCF7-AcCas9-Vector and –CDK6 lines were cultures in full growth medium (A-B) or in estrogen depleted medium (phenol-red free DMEM with 5% dextran-coated charcoal stripped FCS), ±10nM 17β-estradiol (E2) (C-D). (A, C) Growth was measured using the SRB assays after 6-days of treatment with CDK4/6 inhibitors, 2-days treatment with a CDK7 inhibitor (ICEC0942) or with the CDK7/12/13 inhibitor (THZ1). Error bars represent SD of mean values (n=6) from three independent experiments. (B,D) GI50 values (nM) ± SEM were obtained from growth curves in A and C.

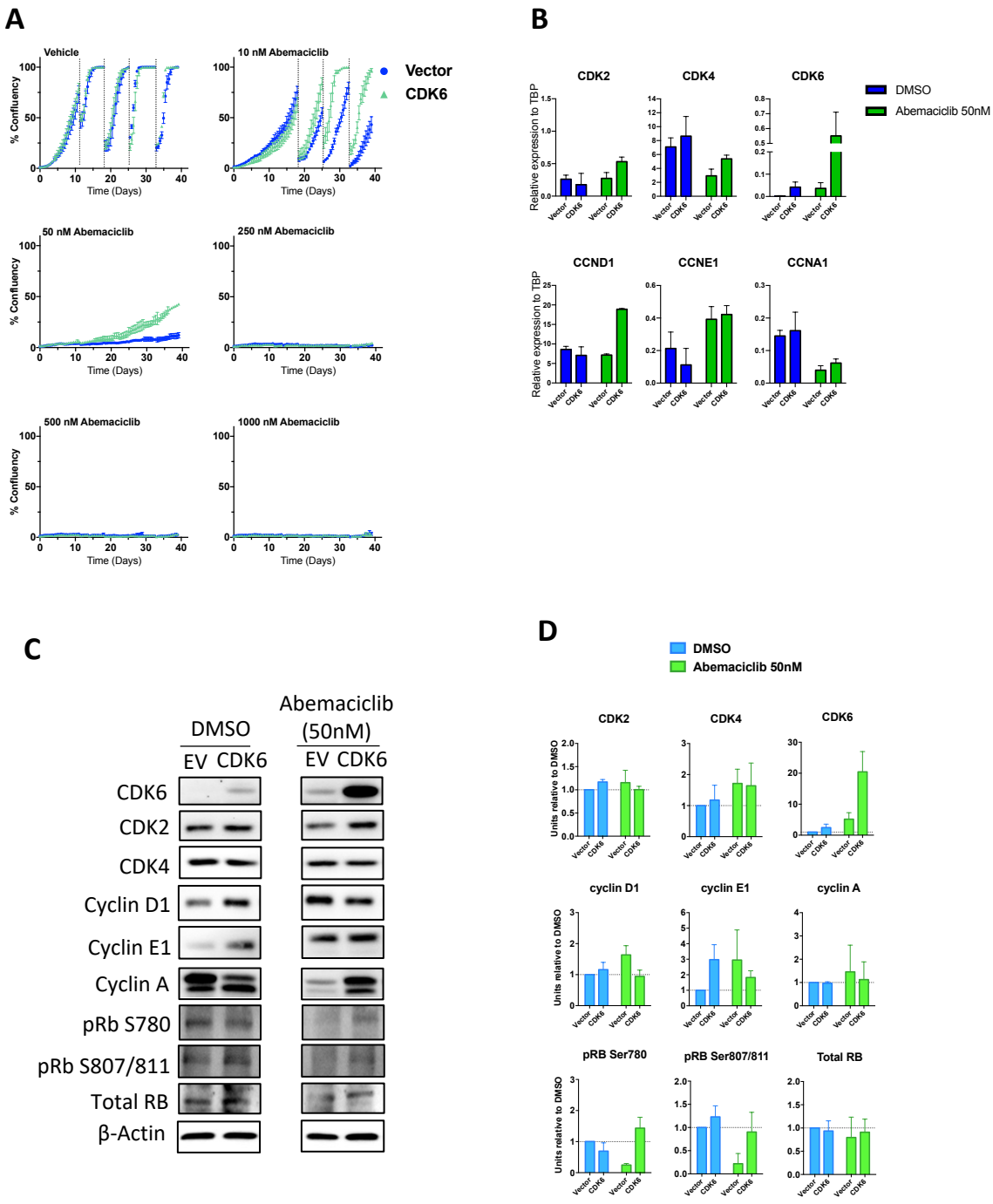


Figure 3.15. CDK6 over-expression promotes resistance to abemaciclib in MCF7 cells.
(A) MCF7-AcCas9-Vector and –CDK6 cells were treated with 10, 50, 250, 500 and 1000nM abemaciclib. Cell numbers were estimated as percentage confluency relative to day 0 using the Incucyte Zoom live cell system. Error bars represent SEM (n=4) from four Incucyte images. Growth assays were performed in the same experiment and data of AcCas9-Vector is the same as shown in Figure 3.9A. (B) RT-qPCR of RNA extracted from cells following over 5-week treatment with 50nM abemaciclib and equal amounts of DMSO was added as vehicle controls. Gene expression levels are shown relative to TBP. Error bars represent SEM (n=3). RT-qPCR was conducted in the same experiment and data DMSO control of AcCas9-Vector and –CDK6 were the same as shown in Figure 3.12B and 3.15B, respectively. (C) Whole cell lysates were collected from cells after long exposure 50nM abemaciclib. (D) Immunoblots were quantified using ImageJ. Error bars represent SD (n=3). Immunoblots were conducted in the same experiment and DMSO control of AcCas9-Vector and –CDK2 were the same as shown in Figure 3.16C-D.

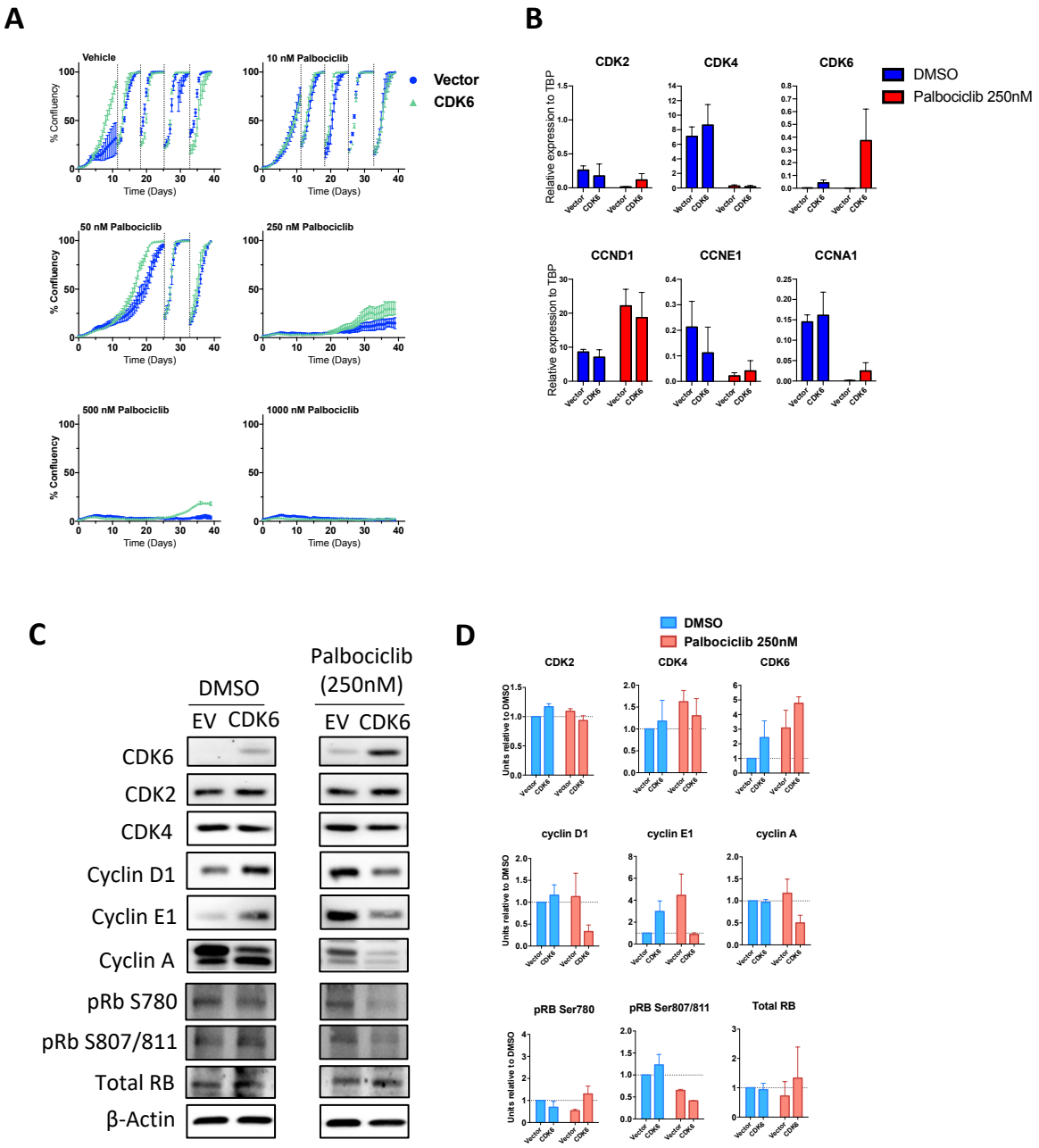


Figure 3.16. Response of MCF7-AcCas9-CDK6 cells to prolonged exposure to palbociclib.
(A) MCF7-AcCas9-Vector and –CDK6 cells were treated with 10, 50, 250, 500 and 1000nM palbociclib. Cell numbers were estimated as percentage confluency relative to day 0 using the Incucyte Zoom live cell system. Error bars represent SEM (n=4) from four Incucyte images. Growth assays were performed in the same experiment and data of AcCas9-Vector is the same as shown in Figure 3.9A. (B) RT-qPCR of RNA extracted from cells following over 5-week treatment with 250nM palbociclib and equal amounts of DMSO was added as vehicle controls. Gene expression levels are shown relative to TBP. Error bars represent SEM (n=3). RT-qPCR was conducted in the same experiment and data DMSO control of AcCas9-Vector were the same as shown in Figure 3.12B. (C) Whole cell lysates were collected from cells after long exposure to 250nM palbociclib. (D) Western blots were quantified using ImageJ. Error bars represent SD (n=3).

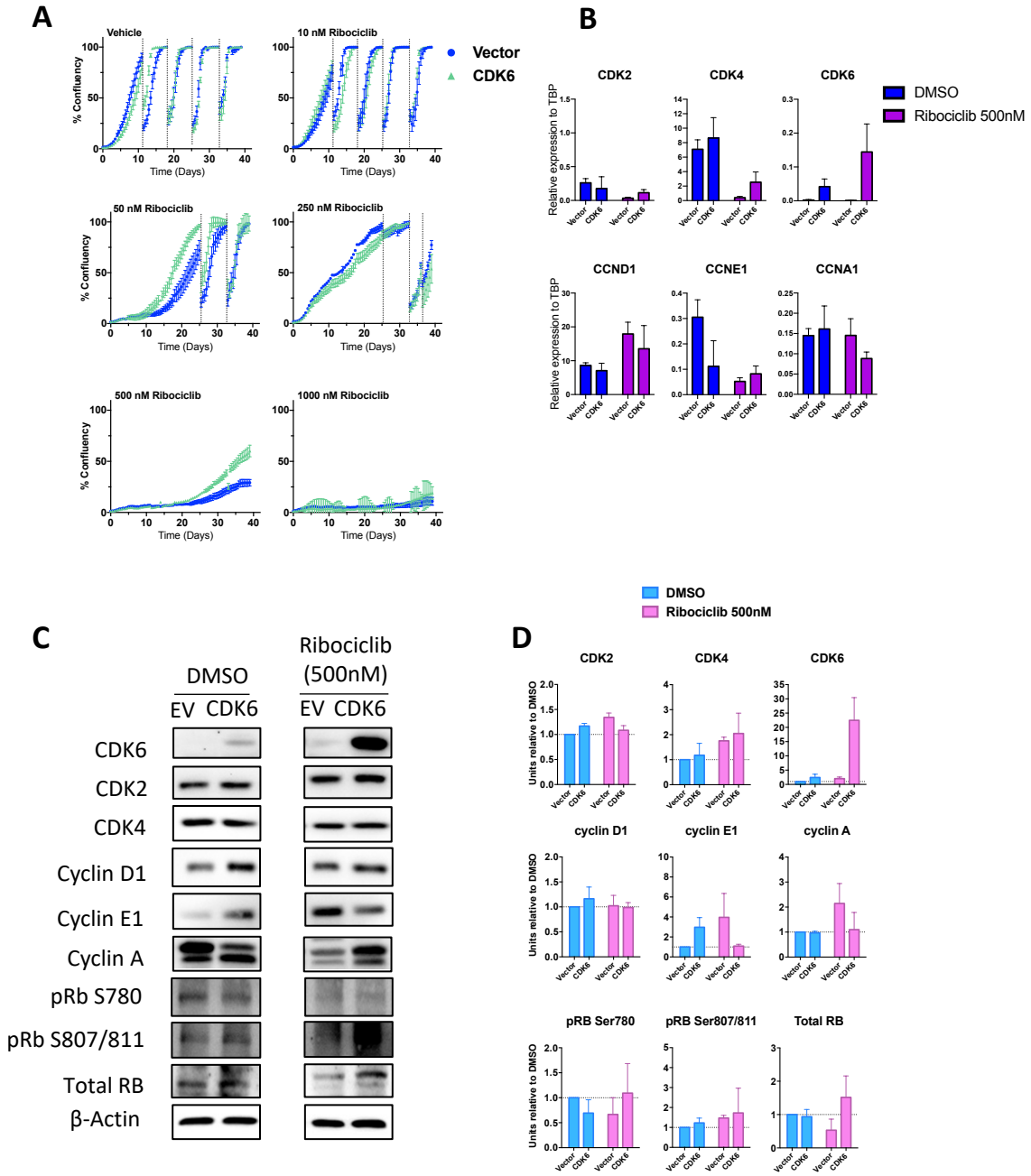


Figure 3.17. Long-term treatment with ribociclib using MCF7-AcCas9-CDK6 cells in full medium.
(A) MCF7-AcCas9-Vector and –CDK6 cells were treated with 10, 50, 250, 500 and 1000nM ribociclib. Cell numbers were estimated as percentage confluency relative to day 0 using the Incucyte Zoom live cell system. Error bars represent SEM (n=4) from four Incucyte images. Growth assays were performed in the same experiment and data of AcCas9-Vector is the same as shown in Figure 3.9A. (B) RT-qPCR of RNA extracted from cells following over 5-week treatment with 500nM ribociclib and equal amounts of DMSO was added as vehicle controls. Gene expression levels are shown relative to TBP. Error bars represent SEM (n=3). RT-qPCR was conducted in the same experiment and data DMSO control of AcCas9-Vector and –CDK6 were the same as shown in Figure 3.12B and 3.15B, respectively. (C) Whole cell lysates were collected from cells after long exposure 500nM ribociclib. (D) Western blots were quantified using ImageJ. Error bars represent SD (n=3). Immunoblots were conducted in the same experiment and DMSO control of AcCas9-Vector and –CDK2 were the same as shown in Figure 3.16C-D.

3.2.2.3.3 GI_{50} determination confirms that over-expression of endogenous CDK6 can promote acquired resistance to CDK4/6 inhibitors

The above studies show that continued over-expression of endogenous CDK6 achieved with the AcCas9 approach results in more rapid progression to CDK4/6 inhibitor independent growth than is observed for control cells. Interestingly, CDK6 expression was also elevated in vector control cells that became resistant to CDK4/6 inhibitors, although CDK6 expression in these cells never reached levels obtained in the MCF7-AcCas9-CDK6 cells. Importantly, CDK6 levels in CDK4/6 inhibitor resistant cells were much higher than those in the unselected MCF7-AcCas9-CDK6 cells. Growth assays with increasing concentrations of CDK4/6 inhibitors were used to confirm resistance and determine the GI_{50} values. Moreover, since CDK6 over-expression was associated with acquired resistance for each CDK4/6 inhibitor, cross-resistance was also determined.

As shown above for cells not previously cultured with CDK4/6 inhibitors (Figure 3.14), CDK6 over-expression alone in MCF7-AcCas9-CDK6 cells, did not reduce sensitivity to any of the three CDK4/6 inhibitors. Thus, MCF7-AcCas9-CDK6 cells that had been cultured in the vehicle (DMSO) were only marginally less sensitive to palbociclib than MCF7-AcCas9-vector cells (GI_{50}: 46.4±21.7nM v 38.4±25.5nM). To further study the role of CDK6 over-expression in the established CDK4/6 inhibitor resistant cells, firstly, growth assays with a 6-day treatment with increasing concentrations of CDK4/6 inhibitors were conducted to validate resistance and to study cross-resistance between these inhibitors. MCF7-AcCas9-Vector and -CDK6 cells that had emerged from the long-term (40 day) culturing in 250nM palbociclib (termed palbociclib-R), both showed reduced sensitivity to palbociclib, with 7.5-fold ($p = 0.037$) and 47.1-fold ($p = 0.032$) reduction in sensitivity, respectively (Figure 3.18A). MCF7-AcCas9-CDK6 palbociclib resistant cells were also 206-fold ($p < 0.001$) and 7.4-fold ($p = 0.016$) less sensitive to abemaciclib and ribociclib, respectively (Figure 3.18B, C). In addition, the MCF7-AcCas9-Vector palbociclib-R cells were 15-fold ($p = 0.016$) and 5-fold ($p = 0.035$) less sensitive to abemaciclib and ribociclib respectively.

The vector and CDK6 over-expressing abemaciclib-resistant cells (abemaciclib-R) were 2.5-fold ($p = 0.020$) and 26.7-fold ($p < 0.001$) less sensitive to abemaciclib, respectively (Figure 3.18C-D). Interestingly, abemaciclib-R MCF7-AcCas9-CDK6 cells, as well as MCF7-

AcCas9-Vector cell were only marginally less sensitive to palbociclib, 2.7-fold (p = 0.020) and 3.8-fold (p = 0.1) respectively, compared with the DMSO controls. Sensitivity of the abemaciclib-R MCF7-AcCas9-CDK6 cells to ribociclib was reduced 11.1-fold (p = 0.042).

In the case of the ribociclib-R cells, it appears that both the vector and CDK6 cells are only a little less sensitive to either palbociclib or to abemaciclib (Figure 3.18C). Thus, ribociclib-R vector and CDK6 cells are just 5.0-fold (p = 0.035) and 7.4-fold (p = 0.015) less sensitive to palbociclib than the vehicle treated cells. Sensitivity to abemaciclib is 3.3 (p = 0.069) and 11.1 (p < 0.001*)* reduced compared to the control cells.

To summarise these findings, CDK6 over-expression slightly (~2x) reduces sensitivity of MCF7 cells to the three CDK4/6 inhibitors, which is unlikely to represent a clinically relevant difference. However, following prolonged culturing with CDK4/6 inhibitors, emergent cultures from CDK6 over-expressing cells are considerably less sensitive to the appropriate CDK4/6 inhibitor than the vector cells (Figure 3.18A-C, summarised in the heat map in Figure 3.18D). The other feature of the vector cells is the fact that the GI_{50} values are about 50% lower than the concentration of the drug used in long-term culturing, which may imply that resistance in the vector cells is reversible. In the CDK6 over-expressing cells by contrast, the GI_{50} values were substantially higher than the concentrations under which they were selected. Thus, MCF7-AcCas9-CDK6 cells cultured in 250 nM palbociclib had GI_{50} values of 5-fold higher. Abemaciclib-R MCF7-AcCas9-CDK6 cells that adapted to 50 nM abemaciclib had GI_{50} values 2x higher and cells adapted to 500 nM ribociclib had GI_{50} values 3x high than those in the adaptive culture conditions. With respect to cross-resistance, the palbociclib-R cells were also less sensitive to abemaciclib and ribociclib. The ribociclib-R cells were also less sensitive to the other two CDK4/6 inhibitors. By contrast, abemaciclib-resistant cells were only maginally resistant to palbociclib or to ribociclib (Figure 3.18D). These results hint at a model in which resistance to palbociclib or ribociclib results in broad CDK4/6 inhibitor resistance, but that resistance to abemaciclib may involve a CDK4/6-independent mechanism.

In all cases of CDK4/6 inhibitor resistance, the cells were sensitive to both ICEC0942 and to THZ1 (Figure 3.18E, F), suggesting that CDK7 inhibitors would have utility following development of CDK4/6 inhibitor resistance. Interestingly, there was a suggestion that in

palbociclib-R cells when CDK6 is over-expressed, there is a small reduction in sensitivity to CDK7 inhibitors.

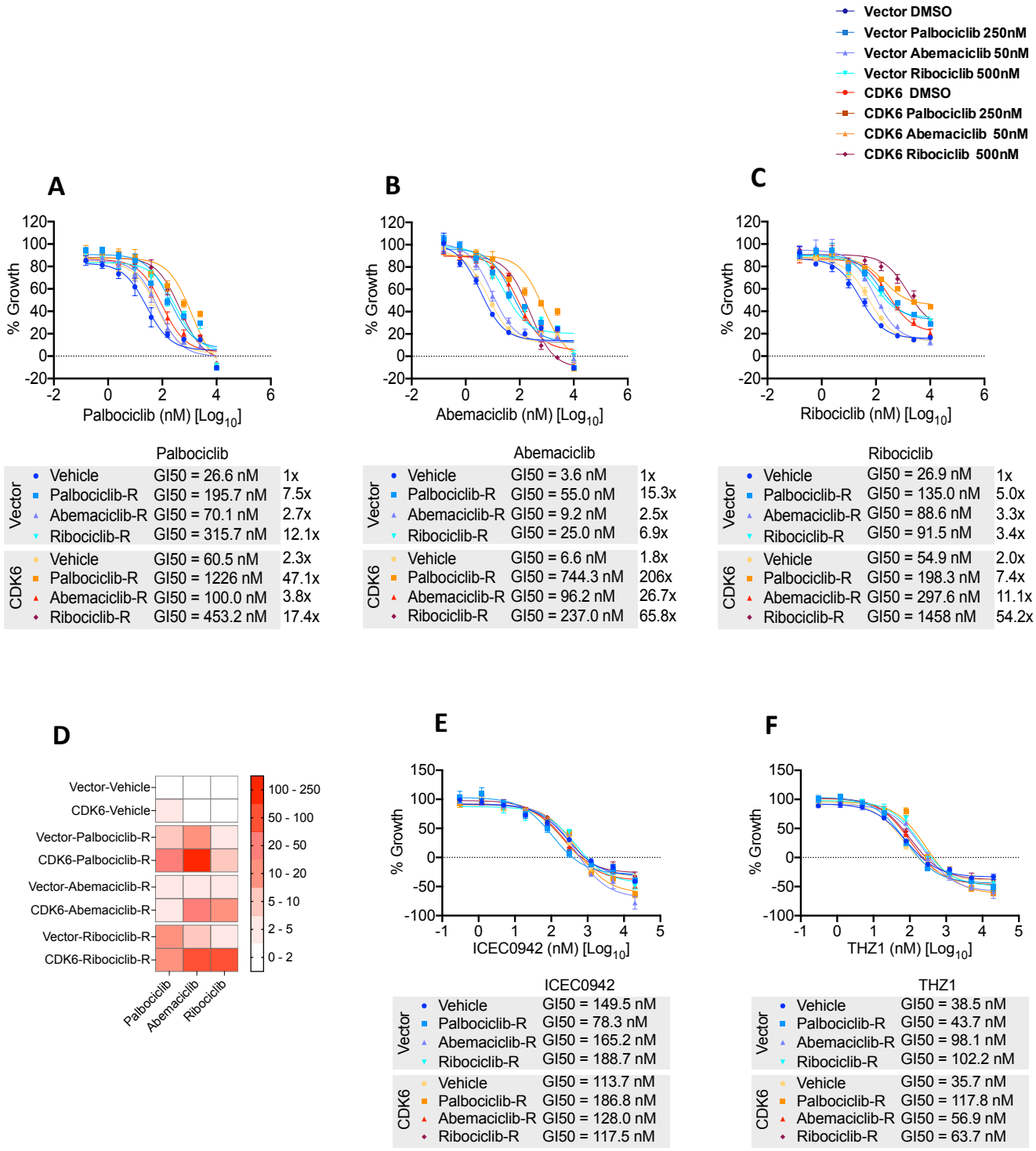


Figure 3.18. Investigating cross-resistance between MCF7-AcCas9-CDK6 over-expressing cells.
SRB assays were used to assess growth response of MCF7-AcCas9-Vector and -CDK6 lines after development of resistance to 250nM palbociclib, 50nM abemciclib and 500nM ribociclib and treated with increasing concentrations of palbociclib (A), abemaciclib (B), and ribociclib (C) and cell number estimated after 6 days. (D) A heatmap summarizing fold changes obtained from growth experiments of (A-C). The experiment in (A-C) was performed with increasing concentrations of ICEC0942 (E) or THZ1 (F) for 2 days. The results of three independent experiments, each with 6 replicates, are plotted. Error bars show standard deviation (SD). GI50 values (nM) obtained from the growth curves (A-C and E-F) are summarised for the three replicate experiments.

3.2.2.3.4 CDK6 knockdown did not revert sensitivity of MCF7-AcCas9-CDK6 resistant cells to palbociclib

To ascertain the importance of CDK6 over-expression in palbociclib resistance in my model, I kncked down CDK6 using a pool of small interfering RNAs (siRNAs) targeting either dCas9 (siCas9) or CDK6 (siCDK6) to suppress CDK6 expression. MCF7-AcCas9-Vector and MCF7-AcCas9-CDK6 adapted to grow with 250nM palbociclib were used and compared to cells treated long term with DMSO. The cells were transfected with these siRNAs, as well as a non-targeting siRNA control (NC). Subsequently, RNA and protein were collected to confirm successful knockdown of CDK6. The decreased levels of CDK6 after siRNA transfection were demonstrated at RNA and protein level, the effect of CDK6 knockdown was more evident in siCDK6 (Figure 3.19A-B). Growth assays were conducted, in which transfected cells were treated with 150nM or 500nM palbociclib for 6 days (Figure 3.19C). Growth was measured relative to the NC, which revealed cell lines with long term DMSO treatment remained sensitive to 150nM and 500nM of palbociclib treatment. The continued reduction in sensitivity to palbociclib despite CDK6 knockdown, is indicative of CDK6-independent palbociclib resistance in these cells. So, while CDK6 over-expression appears to promote resistance to palbociclib, its continued expression does not appear to be necessary to maintain resistance. As such these results may be indicative of multiple mechanisms by which CDK4/6i resistance can develop.

To confirm these findings, the cells were stably transfected with tetracycline-inducible CDK6 shRNA constructs. Addition of 100ng/mL doxycycline (DOX) for 48 hours for inducing RFP (and shRNA) expression was followed by fluorescent activated cell sorting (FACS) to enrich for RFP positive cells. RNA and protein were collected from cells after incubation with DOX for 48 hours to validate the knockdown of CDK6. All shRNAs reduced CDK6 expression in MCF7-acCas9-CDK6 cells, with shRNAs 2 and 3 yielding the most pronounced knockdowns (Figure 3.20A-B). As was observed for the siRNA experiments, sensitivity to palbociclib was not altered by CDK6 knockdown (Figure 3.20C).

Current models indicate the CDK6 over-expression is required for rapid development to CDK4/6 inhibitors but it may not be needed in maintaining resistance as the knockdown of CDK6 did not revert sensitivity to CDK4/6 inhibition.

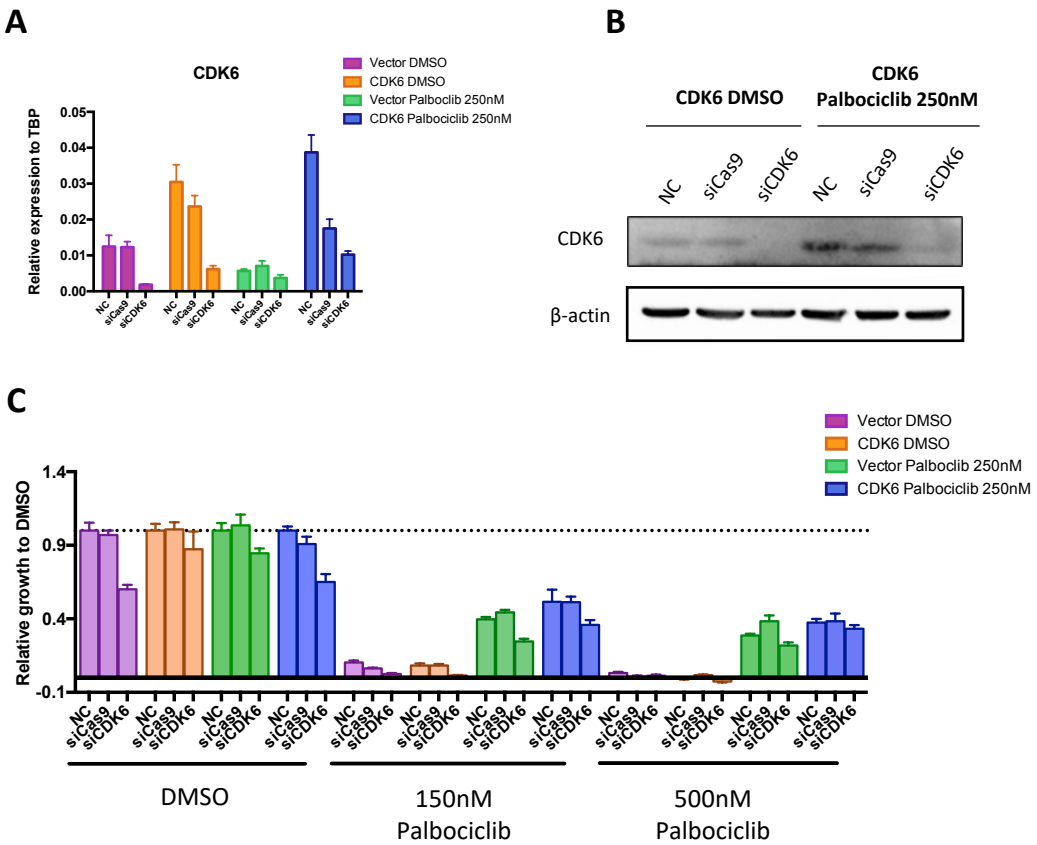


Figure 3.19. CDK6 knockdown in palbociclib-resistant MCF7-AcCas9-CDK6 had limited effect on reversing resistance to palbociclib.

MCF7-AcCas9-Vector (DMSO) and -CDK6 palbociclib resistant (250nM palbociclib) cell were used to determine the requirement for CDK6 in the resistance mechanism to palbociclib. (A) RNA was extracted after 24 hours siRNA transfections to knockdown dCas9 and CDK6 to perform RT-qPCR to validate knockdown of CDK6. Gene expression levels of CDK6 are shown relative to TBP, error bars represent SEM (n=3). (B) Whole cell lysates were collected for Western blotting for CDK6 following 24 hours siRNA transfection, β-Actin was used as a loading control. (C) SRB assays were performed after 24 hours siRNA transfection and treatment for 6 days with 150nM and 500nM of palbociclib. DMSO was used as the vehicle control. Growth was measured relative transfection with a non-targeting vector (NC). Error bars represent SD of mean values (n=6) from one independent experiments.

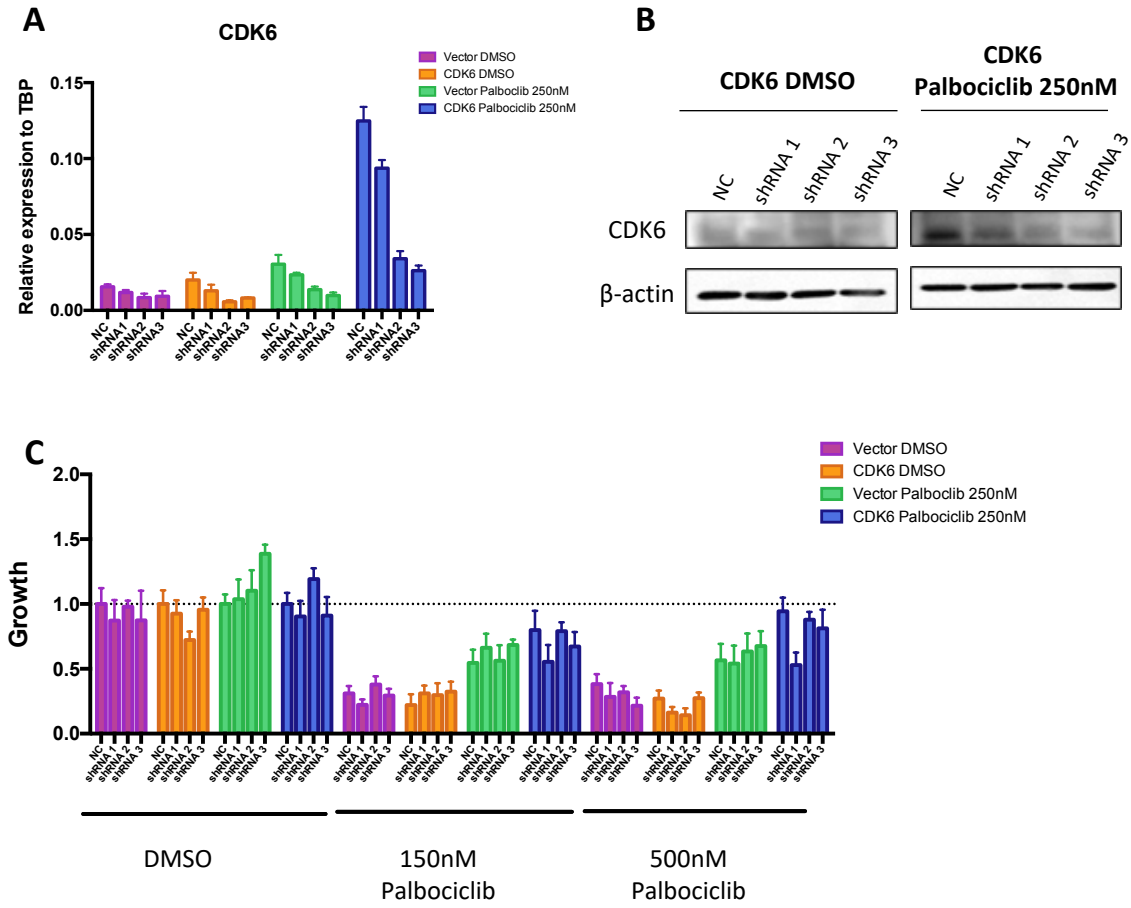


Figure 3.20. CDK6 knockdown using short hairpin RNA (shRNA) in palbociclib resistant MCF7-
AcCas9-CDK6 had limited effect on reversing resistance to palbociclib.
Three independent shRNAs were used for CDK6 knockdown (KD) in MCF7-AcCas9-Vector and MCF7-AcCas9-CDK6 cells and their PalboR derivatives to further validate the requirement for CDK6 overexpression
in palbociclib resistance. (A) RNA was extracted from cells after 48 hours incubation with 100ng/mL of DOX to induce expression of shRNAs for RT-qPCR to validate knockdown of CDK6. Gene expression levels of CDK6 are shown relative to expression of TBP, error bars represent SEM (n=3). (B) Whole cell lysates were collected for western blotting for CDK6 following 48 hours incubation with 100ng DOX, β-Actin was used as a loading control. (C) SRB assays were performed and cells treated for 6 days with 150nM and 500nM of palbociclib, DMSO was used as the vehicle control in full growth medium following a 48 hour incubation with 100ng/mL of DOX. Growth was measure relative to nontargeting vector as the negative control (NC) treated with DMSO. Error bars represent SD of mean values (n=6) in two independent experiments.

3.3 Epigenetic and transcriptomic profiling of estrogen receptor positive breast cancer cell lines with acquired resistance to palbociclib

The experimental work described above takes the approach of using published literature that provides evidence for possible altered expression of specific CDK and/or cyclin genes in intrinsic or acquired resistance to CDK4/6 inhibitors. I have used this evidence for identifying CDKs and cyclin genes which are described as being over-expressed in cell line models of resistance to CDK4/6 inhibitors and/or patient studies in which altered CDK and cyclin expression has been linked to CDK4/6 inhibitor resistance. My studies demonstrate that over-expression of CDK2 and CDK6 is sufficient to promote resistance to CDK4/6 inhibitors. Characterisation of gene expression changes was limited to immunoblotting and RT-qPCR for cell cycle CDK and cyclin genes. Further determination of the mechanisms by which CDK2 and CDK6 over-expression drives CDK4/6 inhibitor resistance would be aided by epigenomic, transcriptomic and proteomic (including phosphoproteomic) approaches. Towards these aims, I have undertaken ChIP-seq analysis using antibodies for histone H3K27 acetylation, as well as RNA-seq analysis using ER^+ BCa cell lines, in which resistance to palbociclib was achieved by growth in the continued presence of palbociclib. These palbociclib-resistant (PalboR) cells were kindly provided by our collaborator, Lesley-Ann Martin at the ICR and have already been described (Herrera-Abreu *et al.*, 2016; Martin *et al.*, 2017; Pancholi *et al.*, 2020). Dr Martin's group cultured ER^+ breast cancer cell lines in estrogen-depleted medium until cell growth was re-established. These cells are termed long-term estrogen deprived (LTED) cells. In the case of MCF7-LTED, the group reported that these cells have acquired a mutation in the *ESR1* gene that expresses ER with a tyrosine 537 to cysteine mutation (MCF7-LTED-Y537C) (Martin *et al.*, 2017). The Martin group have additionally generated developed long-term estrogen deptivation models of the ER+ HCC1428 cells (Pancholi *et al.*, 2020). The HCC1428 cell line was generated from the pleural effusion from a breast cancer patient with high grade invasive breast cancer and is $ER^+/PR^+/HER2^-$ (Gazdar *et al.*, 1998) Note that HCC1428-LTED cells encode WT ER (Pancholi *et al.*, 2020). MCF7, MCF7-LTED-Y537C and HCC1428-LTED cells were treated continuously with 1000nM palbociclib for 3-4 months to model acquired resistance to palbociclib. H3K27ac ChIP-seq was performed for MCF7-LTED-Y537C-PalboR, as well as the palbociclib-naïve MCF7-LTED-Y537C cells treated for 24 hours with 1000nM palbociclib (PalboT). In addition, H3K27ac ChIP-seq was carried out for MCF7, palbociclib-

treated MCF7 and MCF7-PalboR cells. To compare the H3K27ac profiling with gene expression patterns, RNA-seq was carried out using MCF7-LTED-Y537C and MCF7-LTED-Y537C-PalboR cells. Additionally, RNA-seq was performed for MCF7 and MCF7-PalboR cells and similar models in HCC1428 and HCC1428-LTED cells.

Post translational modifications such as phosphorylation, acetylation and methylation of H3 are implicated in chromatin regulation that control transcription activation and repression (reviewed in (Allis and Jenuwein, 2016; Bannister and Kouzarides, 2011; Calo and Wysocka, 2013; Portela and Esteller, 2010)). The H3 DNA package protein can be found throughout the genome. Accumulating evidence demonstrates enriched modifications of H3 protein at regulatory elements. In particular, acetylation of the H3 protein at the lysine residue at position 27 (H3K27ac) is commonly present at transcription start site (TSS) and enhancer regions and the presence of the H3K27ac mark denotes actively transcribing genes (Creyghton *et al.*, 2010). Chromatin immunoprecipitation sequencing (ChIP-seq) is a well-established and powerful tool in which antibodies are used to immunopurify the protein of interest and associated DNA. High-throughput DNA sequencing can then be used to identify the regions of the genome associated with the protein of interest. Similarly, antibodies for specific histone modification can be used to identify genomic regions at which the histone modification is enriched. ChIP-seq using antibodies for H3K27ac was used to profile the PalboT and PalboR cells, towards identifying epigenetic alterations in PalboR cells. Gene expression profiling was undertaken using the Oxford Nanopore long RNA fragment sequencing (https://nanoporetech.com/applications/rna-sequencing). Together, these approaches provide the means of determining epigenetic and gene expression changes accompanying development of acquired resistance to the CDK4/6 inhibitor palbociclib.

3.3.1 Acquired resistance to palbociclib led to changes in global H3K27ac signalling in MCF7 cells

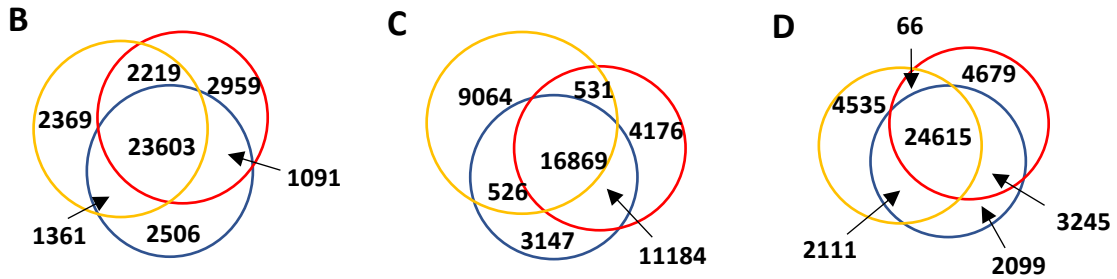
H3K27ac ChIP-sequencing was performed using HiSeq3000/4000 as previsouly described (Pancholi *et al.*, 2020; Ribas *et al.*, 2015; Schmidt *et al.*, 2009) and initial quality checks (FASTQC) were kindly performed by Dr Mariana Leal and Dr Eugene Schuster (ICR), respectively as described previously . Reads were first aligned to the reference genome and

common peaks between replicates were obtained (Figure 3.21A). I undertook all subsequent bioinformatics analysis. Peak calling was performed using MACS2 to identify peaks with enriched reads. Overlapping called peaks show that the majority of peaks were common to all three replicates, indicative of good reproducibility (Figure 3.21B-D). ChIP-seq signals are shown as heatmaps and signal around the transcription start site (TSS), showing increase in signal in PalboR (Figure 3.21E-F).

A

Input					
Cell line	**Total aligned reads**			**Aligned rate (%)**	
MCF7	9011588			96.64	
MCF7 PalboT	8833078			94.27	
MCF7 PalboR	8480938			95.67	

H3K27ac ChIP-seq						
Cell line	**Total aligned reads**			**Aligned rate (%)**		
	Replicate 1	**Replicate 2**	**Replicate 3**	**Replicate 1**	**Replicate 2**	**Replicate 3**
MCF7	9180643	8020737	6836311	97.88	97.92	95.66
MCF7 PalboT	8126536	9052197	8390310	97.73	97.97	96.7
MCF7 PalboR	8946116	8314967	9107685	98.19	96.41	96.7



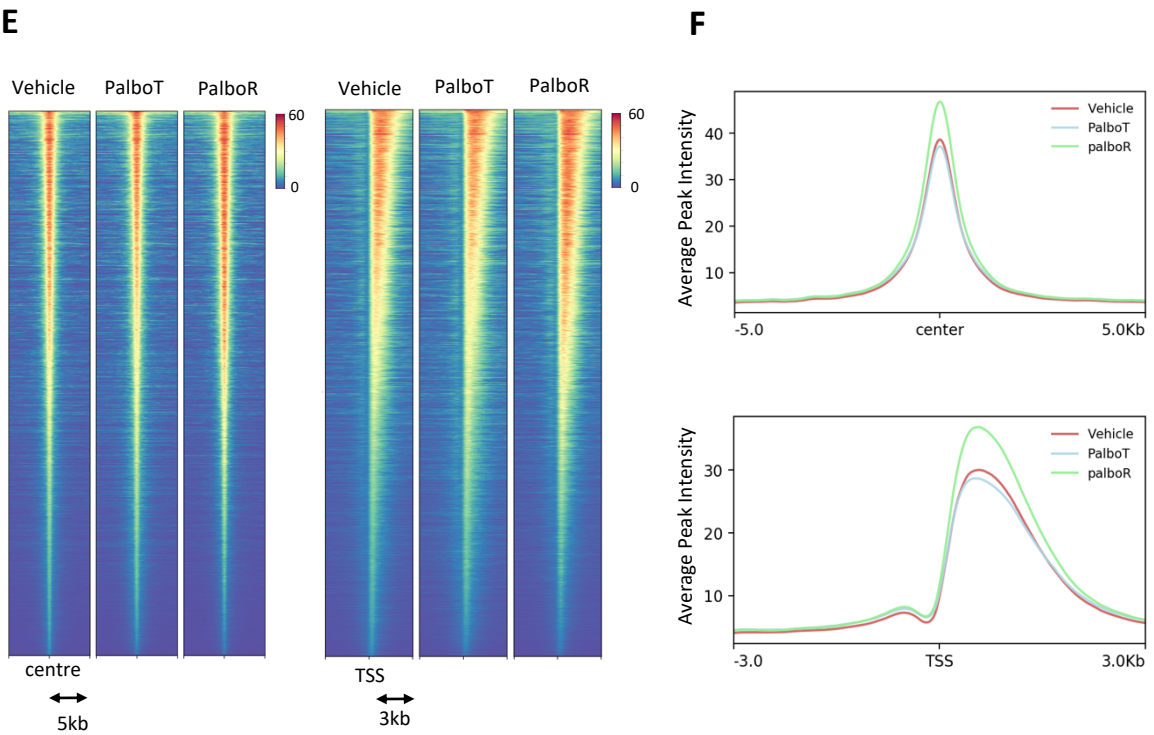


Figure 3.21. H3K27ac ChIP-seq analysis in MCF7 cells following acquired resistance to palbociclib.
H3K27ac ChIP-seq was carried out using MCF7 cells treated with palbociclib (1000 nM; PalboT) or vehicle (DMSO). ChIP-seq was also performed with palbociclib-resistant (PalboR) MCF7 cells. (A) total numbers of sequencing reads and percentage alignment rate of each replicate are shown. Total peaks of three replicates in (B) Vehicle, (C) PalboT and (D) PalboR to find common peaks which were used for downstream analysis. (E) Heatmap demonstrating peak enrichment of global H3K27ac signals around the peak centre (+/- 5kb) and peak enrichment at the transcriptional start site (TSS) (+/- 3kb). (F) Average peak intensity of peak enrichment heatmaps in (E).

Differential binding analysis was subsequently conducted using the R package DiffBind, to first re-centre peaks with peak summits extending +/- 250bp, to limit background noise and address variability between replicates but sufficient to identify enriched signals for differential analysis. Differentially enriched H3K27ac signals were annotated using the R package, ChIPSeeker to identify and calculate proximity to known genes +/-3kb from the TSS and overlap peaks with genomic features. Differential enrichment analysis of the H3K27ac signal was carried out in MCF7 Vehicle, palbociclib-treated MCF7 (PalboT) and MCF7-PalboR cells in pair-wise comparisons to identify differential signal of H3K27 acetylation in palbociclib treatment and/or palbociclib resistance. The differential analysis of each comparison is illustrated in volcano plots in which peaks with normalised $\log_2$(Fold Change) $\leq$-1 and $\geq$1 and FDR$\leq$0.05 were considered as statistically significant (Figure 3.22A-C) (Appendix I). Comparing MCF7 PalboT vs Vehicle identified upregulation of H3K27ac signal in 1410 genes and downregulation of the histone mark in 394 genes out of the total number of genes 1890 with H3K27ac signal with +/- 3k from the TSS (Figure 3.22A). Interestingly, a decrease in H3K27ac signal was found at several cell cycle-related genes, including CDK1, CCNA2, AURKB, MCM10 and PLK1 after treatment with palbociclib. In the comparison between PalboR and Vehicle samples, the differential analysis found increased signal in genes such as GPC6, SOX9 and PUF60 that may be linked to promoting BCa progression in palbociclib-resistant cells. GPC6, a cell surface glycoprotein has been shown to promote BCa invasion via activation of MAPK and JNK signalling (Yiu et al., 2011). Oncogenes, SOX9 and PUF60 have also been shown contribute to BCa initiation, migration and invasion (Jana et al., 2020; Sun et al., 2019). Finally, in the direct comparison between PalboT and PalboR cells, elevated signals were found in some cell cycle-related genes such as CCNA2, AURKB, MCM10 and PLK1 that were shown to have reduced H3K27ac signal during palbociclib treatment. Peaks were overlapped with genomic features distribution and plotted as percentages for each comparison (Figure 3.22D), showing increased H3K27ac signals in PalboR cells at gene promoters as a proportion of the total H3K27ac signal. IGV snapshots of CCNA2 and AURKB demonstrated decreased H3K27ac signal after palbociclib treatment, but signal was reversed to levels similar to those in Vehicle treated cells (Figure 3.22D).

To further elucidate differential binding of H3K27ac in relation to palbociclib resistance, 339 common genes were found by overlapping binding sites in MCF7 Vehicle vs PalboT cells, PalboR vs Vehicle and PalboR vs PalboT (Figure3.23A) (Appendix I). Gene set enrichment analysis (GSEA) pathway was performed to compute overlap of these shared genes with the

"Hallmark" signalling pathways with the q-value ≤ 0.05. The GSEA revealed enrichment in the estrogen response early and late pathways were enriched, which and may indicate the re-wiring of the estrogen response signalling after palbociclib treatment and after acquiring resistance (Figure 3.23B). Additionally, 1151 annotated genes found uniquely in PalboR vs Vehicle were also used for GSEA and revealed upregulation of pathways including epithelial to mesenchymal transition (EMT) and interferon-γ and interferon-α signalling pathways that may contribute to resistance to palbociclib and cancer progression (Figure 3.23C). Conversely, annotated genes with reduced H3K27ac signal were associated with pathways such as the UV response down and hypoxia.

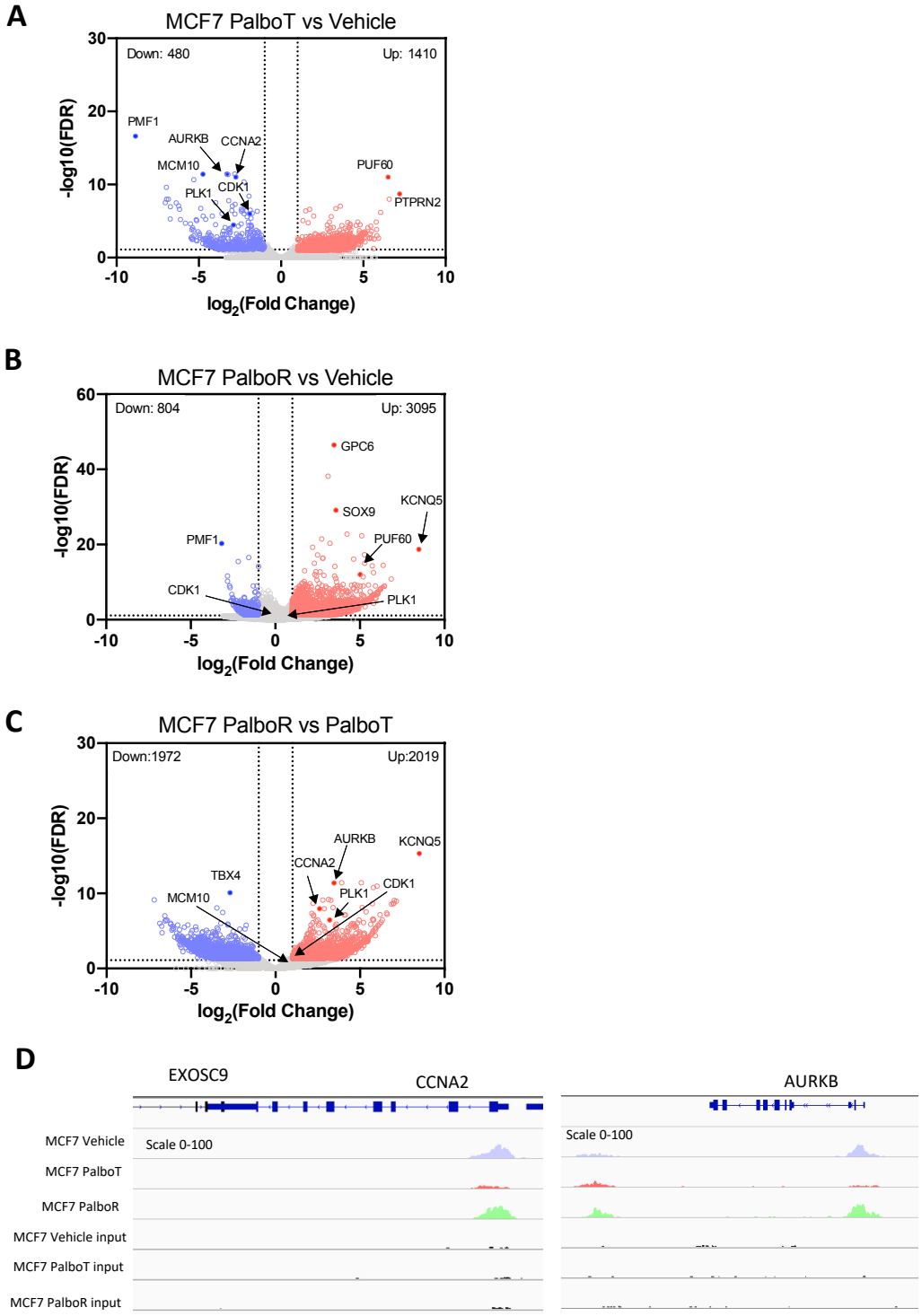


Figure 3.22. Differential analysis of H3K27ac ChIP-seq in MCF7 cells following acquired resistance to palbociclib.

(A-C) Volcano plots showing sites with differential enrichment of H3K27ac signal with log2(Fold Change) of ≤-1 and ≥1, and FDR value ≤0.05. Analysis based on annotated genes of hyperacetylated sites extended from +/- 3kb around transcription start site (TSS). (D) IGV snapshots of H3K27ac at two genomic regions.

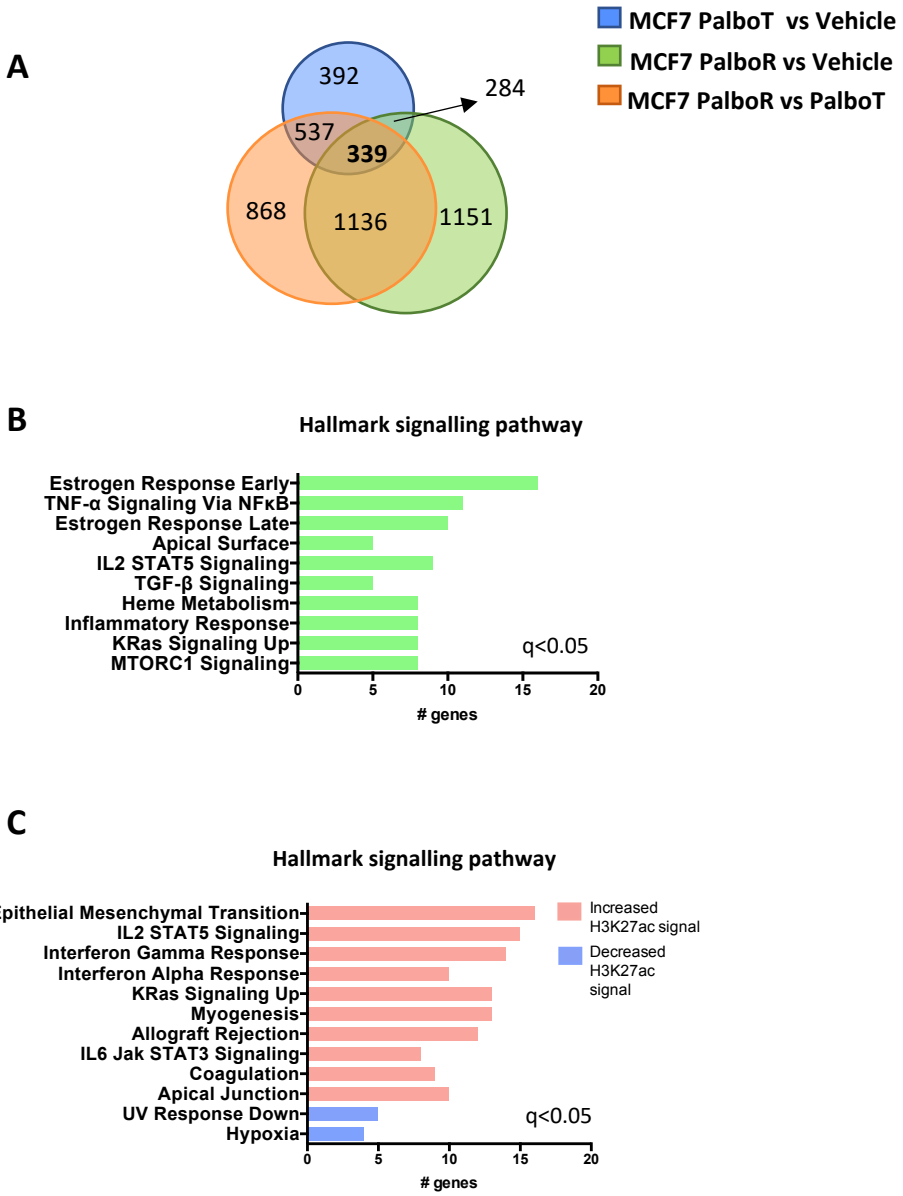


Figure 3.23. Pathway analysis of differentially enriched H3K27ac signals in MCF7 cells with acquired resistance to palbociclib.

(A) Venn diagram illustrates 339 genes associated with differential H3K27ac occupancy levels were found in PalboT vs Vehicle, PalboR vs Vehicle and PalboR vs PalboT. (B) Gene set enrichment analysis (GSEA) to identify enriched pathways using MigSigDB 'Hallmark signaling pathway' based on 326 genes overlapped in all comparisons. (C) GSEA pathway analysis was performed as (B), 1151 genes with differential H3K27ac signals uniquely found in PalboR vs Vehicle (q-value≤0.05) was overlapped with using MigSigDB 'Hallmark signaling pathway'.

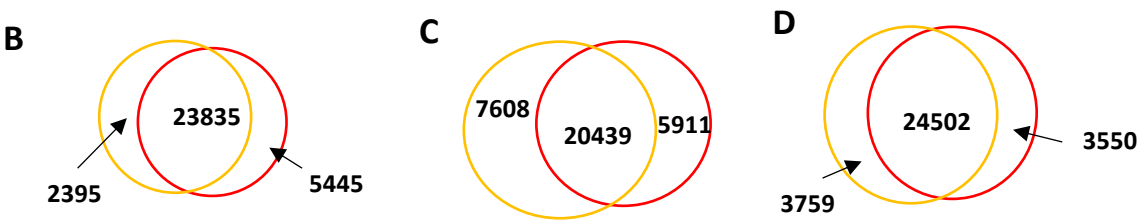
H3K27ac ChIP-seq and differential binding analysis were also performed using MCF7-LTED-Y537C cells to model resistance to palbociclib and aromatase inhibitors (Figure 3.24A). Common peaks identified from overlapping the two independent bioreplicates (Figure 3.24B-D) were used to plot global ChIP-seq signals as heatmaps, revealing little obvious change in signal intensities between the different conditions (Figure 3.24E-F). Pairwise differential comparisons were obtained and displayed as volcano plots by comparing Vehicle, PalboT and PalboR samples (Figure 3.25A-C). Interestingly, a much smaller set of genes was altered in expression in the MCF7-LTED-Y537C cells than was the case in MCF7 cells treated with palbociclib. So, whereas palbociclib treatment of MCF7 cells resulted in 1410 up and 576 downregulated genes, only 40 genes were up- and 150 genes were down-regulated in MCF7-LTED-Y537C cells (compare Figure 3.22A with Figure 3.25A). However, as seen in MCF7 cells, H3K27ac signalling of genes associated with the cell cycle was reduced in PalboT, including genes such as BIRC5 and MCM10 but many of these genes were upregulated in PalboR cells, indicative of resetting of their expression following development of resistance to palbociclib. IGV snapshots exemplifying this scenario are shown for BIRC5 and MCM10 (Figure 3.25E). One interesting observation is the increased H3K27ac signal at the *CCND1* gene in PalboR cells (Figure 3.25B), suggesting that palbociclib resistance may feature increased expression of cyclin D1. Note that this change was not identified in the MCF7-PalboR cells, so may be specific for the estrogen withdrawal setting of palbociclib resistance.

Just 22 common genes were found when overlappping with differential H3K27ac signals in PalboT vs Vehicle and binding sites with increased signal in PalboR vs Vehicle and PalboR vs PalboT ((Figure 3.26A) (Appendix II). However, 74 common peaks were found when comparing PalboT vs Vehicle and PalboR vs Vehicle that may be correlated with the progression from palbociclib (Figure 3.26A). Several cell cycle-related genes were identified such as BIRC5, MCM10, AURKB, E2F1 and E2F2 (highlighted in bold). This may be a resistance mechanism associated with cell cycle progression to evade CDK4/6 inhibition in MCF7 LTED Y537C cells. However, there were too few genes found in the overlap analysis to proceed with GSEA. When overlapping unique genes found in PalboR vs Vehicle with "Hallmark" signalling pathway found estrogen early and late response pathways, and KRas signalling pathway to be the top upregulated and downregulated pathways, respectively (Figure 3.26B).

A

Input		
Cell line	**Total aligned reads**	**Aligned rate (%)**
MCF7 LTED Y537C	8426123	96.35
MCF7 LTED Y537C PalboT	8427667	94.8
MCF7 LTED Y537C PalboR	8636413	94.96

H3K27ac ChIP-seq				
Cell line	**Total aligned reads**		**Aligned rate (%)**	
	Replicate 1	**Replicate 2**	**Replicate 1**	**Replicate 2**
MCF7 LTED Y537C	7919119	7938193	97.61	98.04
MCF7 LTED Y537C PalboT	6468759	10193408	97.79	97.57
MCF7 LTED Y537C PalboR	8667783	8123694	98.35	98.28



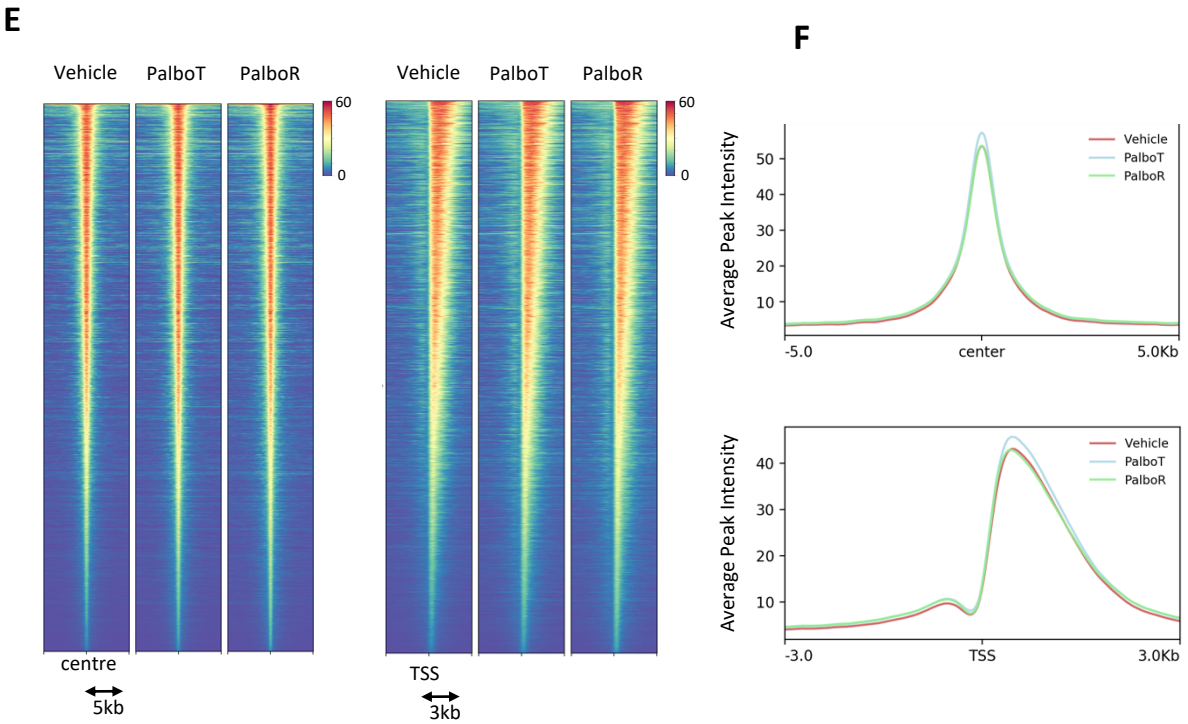


Figure 3.24. H3K27ac ChIP-seq analysis of MCF7 LTED Y537C cells after acquiring resistance to palbociclib. H3K27ac ChIP-seq was carried out using MCF7 LTED cells with a naturally occurring Y537C mutation in the ESR1 gene (MCF7 LTED Y537C), were treated with palbociclib (1000 nM; PalboT) or vehicle (DMSO). ChIP-seq was also performed with palbociclib-resistant (PalboR) MCF7 LTED Y537 cells. (A) total numbers of sequencing reads and percentage alignment rate of each replicate are shown. (B-D) Total common peaks overlapped between two replicates in each condition are represented as Venn diagram. (E) Heatmap showing global enrichment of H3K27ac signals 5kb around the peak centre and 3kb around the transcription start site (TSS). (F) Average peak intensity of heatmaps form (E).

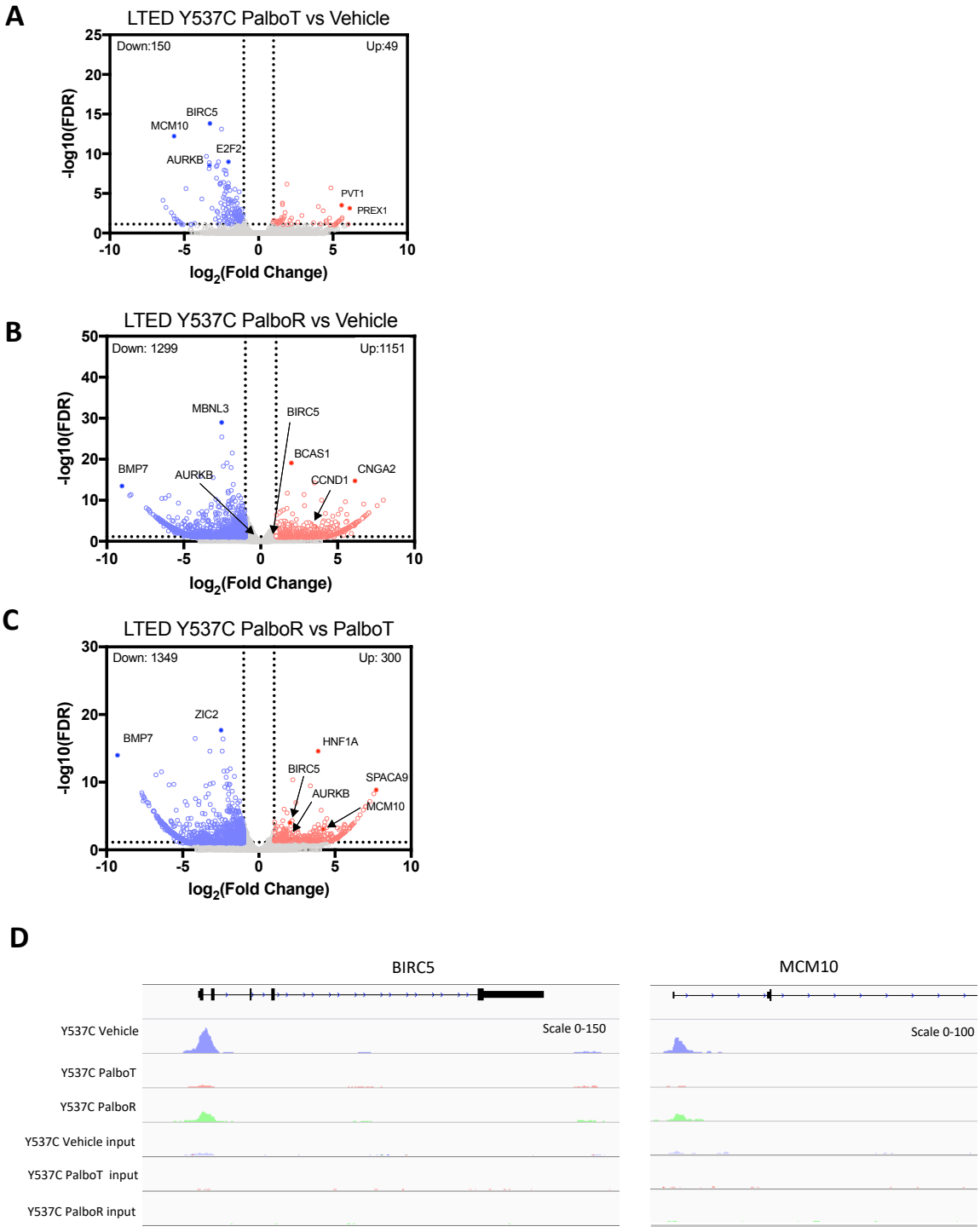


Figure 3.25. Differential enrichment analysis of H3K27ac signal after acquiring resistance to palbociclib in MCF7 LTED Y537C cells.

(A-C) Volcano plots showing sites with differential enrichment of H3K27ac signal with log2(Fold Change) of ≤-1 and ≥1, and FDR value ≤0.05. Analysis based on annotated genes of hyperacetylated sites extended from +/- 3kb around transcription start site (TSS). (D) IGV snapshots of H3K27ac at two genomic regions.

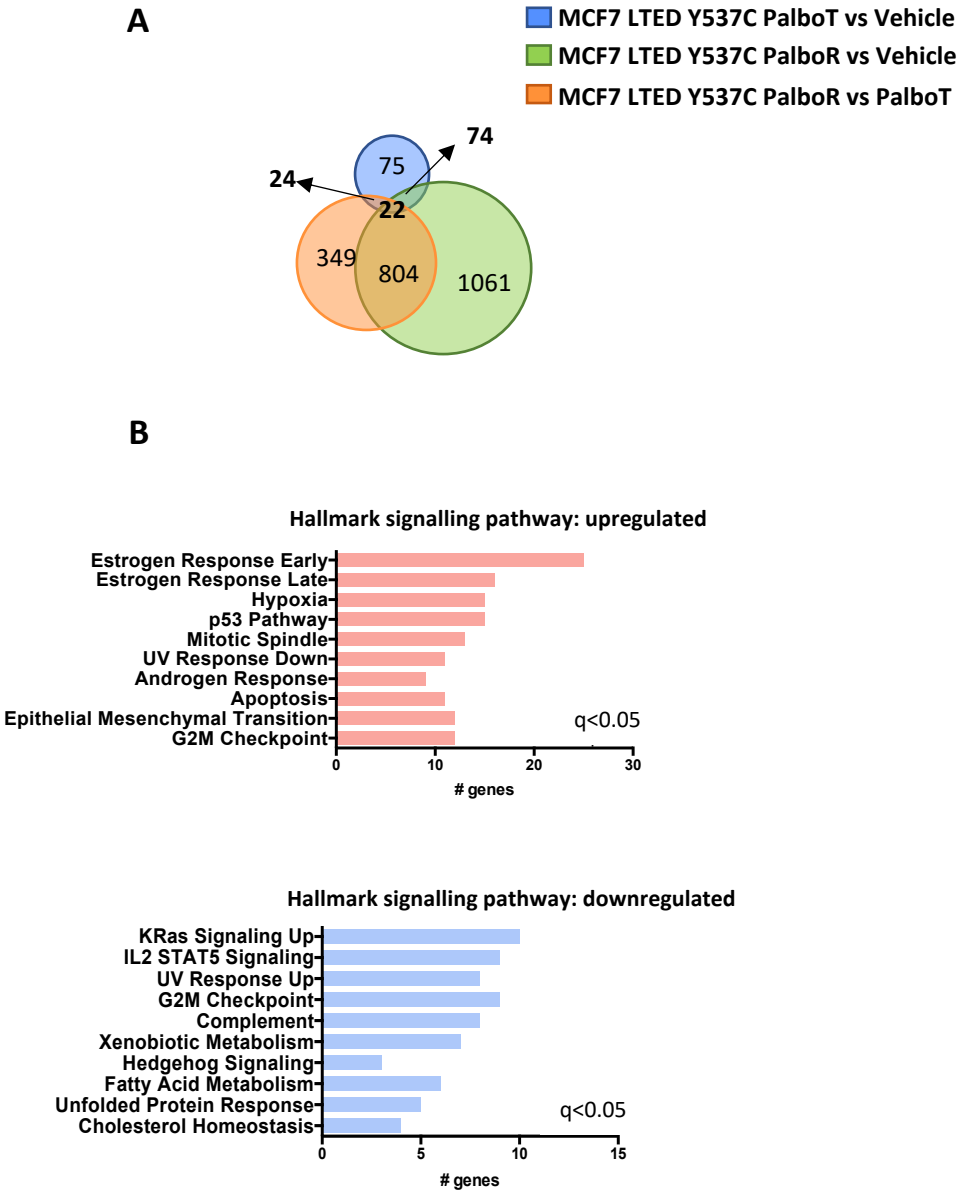


Figure 3.26. Differential enrichment analysis of H3K27ac signal after acquiring resistance to palbociclib in MCF7 LTED Y537C cells.

(A) Venn diagram illustrates overlaps of common annotated genes associated with differential H3K27ac occupancy levels in all three comparisons. (B) Gene set enrichment analysis (GSEA) to identify enriched pathways based on 1061 genes with differential H3K27ac signals uniquely found in LTED Y537C PalboR vs Vehicle (q-value≤0.05).

To summarise, the comparison of alterations in H3K27ac between MCF7 and MCF7-LTED-Y537C cells that may indicate common and different mechanisms associated with development of palbociclib resistance, genes with differential H3K27ac signal with $\log_2$ fold change > 1 or < -1 and FDR ≤ 0.05 in PalboR vs Vehicle were overlapped to obtain common genes with differential H3K27ac signals in both cell lines (Figure 3.27A-B). There were generally many more genes with gains in H3K27ac in MCF7-PalboR than in MCF7-LTED-Y537C-PalboR cells. The converse was true for the downregulated genes, where more than twice as many genes showed reduction in H3K27ac in MCF7-LTED-Y537C-PalboR cells than in MCF7-PalboR cells. Of these, 244 genes showed enhanced H3K27ac signals in both cell types. GSEA analysis of these genes using the 'Hallmark signalling pathway' gene set identified signficiant enrichment in early and late estrogen response pathways (Figure 3.27C). However, these pathways were also enriched in the genes uniquely upregulated in MCF7-LTED-Y537C-PalboR or those in MCF7-PalboR cells. Thus, increased estrogen signalling appears to be a common feature of palbociclib resistance in MCF7 cells. Also, commonly enriched was EMT. By contrast, the genes upregulated in MCF7-PalboR but not in MCF7-LTED-Y537C-PalboR cells were enriched in immune and inflammation related pathways such as the IL2/STAT3 signalling pathway. Also, uniquely enriched in MCF7-PalboR cells was androgen signalling. Interestingly, the downregulation of the E2F and G2M checkpoint pathways was solely present in genes with reduced H3K27ac signal in MCF7-LTED-Y537C-PalboR cells.

3.3.2 Identification of differentially expressed genes following development of palbociclib resistance in ER^+ breast cancer cell lines

As described above, the H3K27 acetylation mark is associated with transcriptionally active chromatin and consequently provides indirect evidence of gene expression in the form of the active epigenetic status of gene promoters, gene bodies, as well as enhancers. RNA-sequencing provides an approach for directly assessing global gene expression. RNA was prepared from MCF7, MCF7-LTED-Y537C and HCC1428-LTED cells treated with vehicle or palbociclib using the nanopore platform. Nanopore sequencing was also undertaken for the PalboR cells. Cell treatments (24-hour treatment with 1μM of palbociclib), RNA preparations and nanopore RNA sequencing using Nanopore was conducted by Dr Mariana Leal and the initial quality check and alignment was performed by Dr Eugene Schuster at ICR. I undertook all subsequent bioinformatics analysis. The R package Deseq2 was used to conduct independent differential analysis for each ER^+ BCa line to obtain normalised read counts and log_2 transformation to identify differentially expressed genes (DEGs).

Differential expression analysis was first conducted for vehicle and palbociclib-treated MCF7 and MCF7-PalboR cells in pairwise comparisons and a p-adjusted (p-adj) value of ≤0.05 was used. However, with this cut-off fewer than 436 DEGs were revealed. With a less stringent cut-off (p-adj ≤0.1), a total 577 common DEGs were identified from pair-wise comparisons from Vehicle, PalboT and PalboR (Figure 3.28A) (Appendix III). These DEGs were overlapped with the "Hallmark" signalling pathway gene set in GSEA for MCF7 Vehicle vs PalboT and MCF7-PalboR cells (Figure 3.28B). Cell cycle-associated pathways (E2F target, G2M checkpoint) showed a negative normalised enrichment score (NES). Conversely, interferon (IFN)-γ and IFN-α pathways were the most upregulated pathways following treatment and developing resistance to palbociclib. Also, strongly enriched were p53 and estrogen signalling.

Volcano plots were used to exhibit DEGs in each pair-wise comparison (Figure 3.28C-E). Treatment with palbociclib resulted in reduction in expression of a substantial number of 216 genes, with increased expression of just 60 genes. Downregulation of many genes involved in the cell cycle is highlighted and includes CCNA2 and AURKB. As was observed for the H3K27ac analysis, cell cycle related genes that were downregulated with palbociclib treatment recovered expression in the PalboR cells, further confirming that expression of these genes is reset in PalboR cells, as might be expected given their importance in progression through the

cell cycle. The elevated expression of other growth related genes when comparing vehicle-treated MCF7 cells with MCF7-PalboR cells was also noted, exemplified by S100P and GDF15 (Figure 3.28D).

Hierarchical cluster analysis of DEGs was carried out to further identify a gene set associated with palbociclib resistance (Figure 3.29A) (Appendix IV). Four main gene clusters could be identified. Expression of genes in Clusters 1 was enhanced in PalboR, compared with MCF7-vehicle or MCF7-PalboT cells. GSEA shows that these genes are especially strongly enriched for interferon response pathways (Figure 3.29B). By contrast, genes in cluster 2 were more strongly repressed in PalboT cells than in PalboR cells. These genes are enriched for cell cycle pathways (G2M checkpoint and E2F targets), so confirming the earlier observation that cell cycle associated genes regain expression following development of palbocicilb resistance. Cluster 3 appears to be genes whose expression is elevated in PalboR cells. These genes are yet more highly expressed in PalboT cells. The genes in cluster 3 are most enriched in estrogen signalling pathways. Cluster 4 contains genes that are repressed in PalboR cells, despite their expressed being greater following short treatment with palbociclib and includes genes in the p53 and apoptosis pathways, consistent with the difference in response to palbociclib in MCF7 and MCF7-PalboR cells.

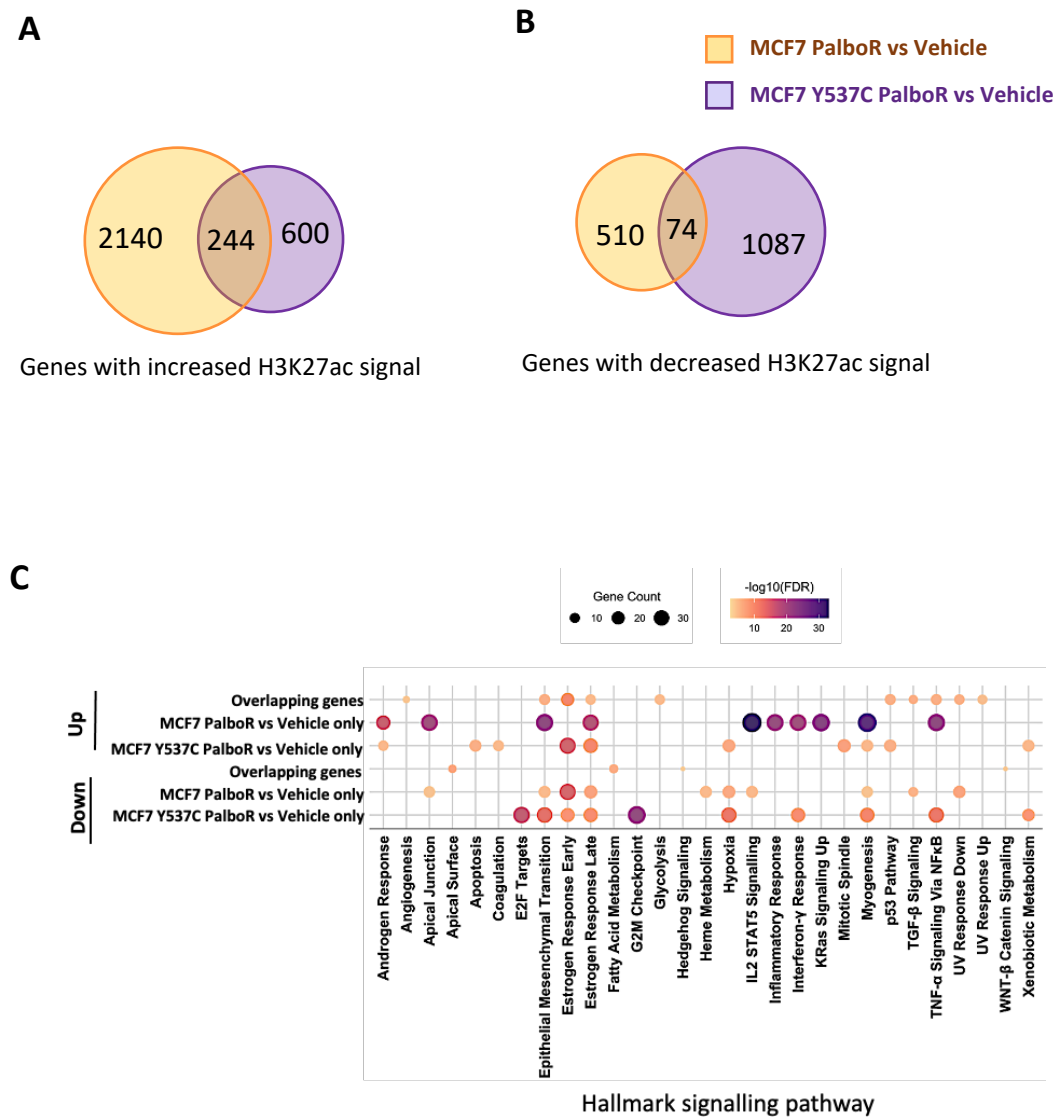


Figure 3.27. Comparison of differential H3K27ac signals in PalboR vs Vehicle in MCF7 and MCF7 LTED Y537C cells

Differential analysis was used to compare palbociclib resistant (PalboR) and DMSO treated (Vehicle) for obtaining a list of genes with differential H3K27ac signal. Genes with (A) increased (log2 fold change ≥ 1 and FDR ≤ 0.05) and (B) decreased (log2 fold change ≤ -1 and FDR ≤ 0.05) H3K27ac signals were overlapped to obtain common genes between MCF7 and MCF7 Y537C cells represented as a Venn diagram. (C) GSEA pathway analysis were carried out by overlapping with the MigSigDB 'Hallmark signalling' gene set.

A similar analysis of MCF7-LTED-Y537C (vehicle- and palbociclib-treated) and MCF7-LTED-Y537C-PalboR lines was undertaken following nanopore RNA-seq using two biological replicates (Figure 3.30A). Differential expression analysis found 628 common DEGs (p-adj≤0.1) when comparing the three treatment conditions. The most downregulated signalling pathways were E2F targets and G2M checkpoint, while estrogen response and p53 pathways were upregulated in the palbociclib treated cells (Figure 3.30B) (Appendix V). The DEGs in each pairwise comparison is shown in volcano plots (Figure 3.30C-E). As observed in MCF7 cells, expression of cell cycle associated genes, such as MCM10 and CCNA2 was reduced in MCF7-LTED-Y537C-PalboT cells and the expression of these genes recovered in MCF7-LTED-Y537C-PalboR cells. As previously seen in MCF7 cells, the MCF7-LTED-Y537C-PalboR vs MCF7-LTED-Y537C-Vehicle comparison revealed increased expression in two p53-regulated genes, S100P, a calcium binding protein and GDF15, an inflammatory marker (Figure 3.30D). The consistent increase in these genes in both of the MCF7 PalboR models is intriguing and may benefit from further investigation.

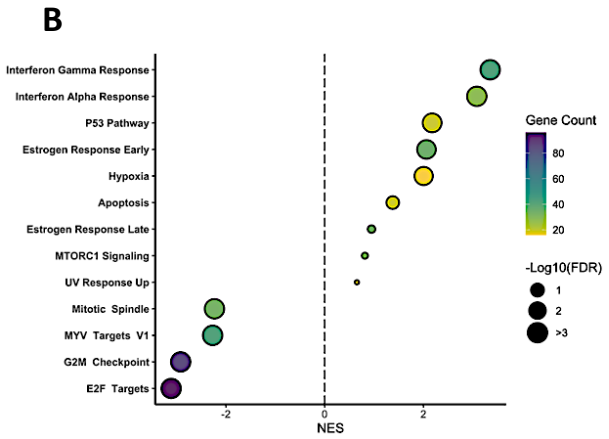
Hierarchical cluster analysis revealed 4 distinct gene clusters (Figure 3.31A) (Appendix VI). The largest cluster, cluster 1 was enriched in cell cycle pathways (Figure 3.31B), wherein these genes were reduced in expression in MCF7-LTED-Y537C-PalboT cells, but expression was higher in MCF7-LTED-Y537C-PalboR cells, albeit lower than in MCF7-LTED-Y537C-vehicle cells. The 138 genes in cluster 2 were downregulated in PalboR only and pathway analysis showed enrichment in the early and late estrogen response pathways. Cluster 3 was also enriched in estrogen response genes that were most highly expressed in PalboT. Cluster 4 contains genes most upregulated in PalboR cells and includes cholesterol homeostasis, androgen and p53 pathways.

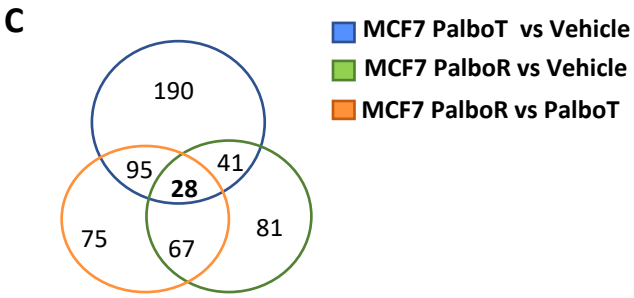
Altogether, these gene clusters reveal similar alterations in gene expression in MCF7 and MCF7-LTED-Y537C PalboT and PalboR cells, which might reflect the fact that in each case ER continues to be an important driver of proliferation and survival. This may indicate that ER activity is not particularly important for response to CDK4/6i. In MCF7 cells grown in complete medium, estrogen activation of ER occurs, whereas in MCF7-LTED-Y537C cells grown in estrogen-free conditions, the constitutive ER mutant continues to regulate ER target gene expression. This LTED model is likely to behave differently from other models of estrogen deprivation, where upregulation of other signalling pathways, such as EGFR and

IGF1R signalling cascades become important (Jones *et al.*, 2006; Nicholson *et al.*, 2004; Ribas *et al.*, 2018). The exclusive presence of either ESR1 mutations or EGFR/MAPK signalling alteration described previously in metastatic, ET-resistant breast cancer provide further evidence for these differences (Razavi *et al.*, 2018).

A

Cell line	Total aligned reads	
	Replicate 1	Replicate 2
MCF7	1156573	1259630
MCF7 PalboT	1259940	980916
MCF7 PalboR	836716	965931





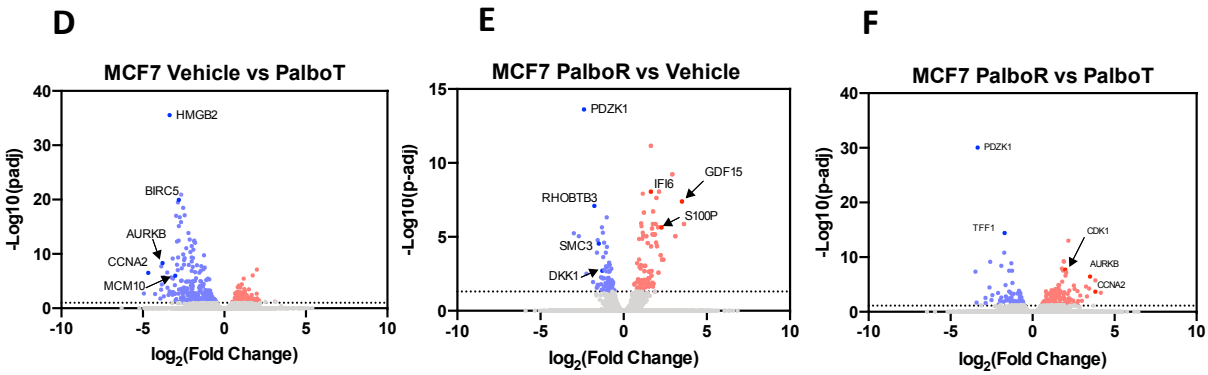


Figure 3.28. Differential analysis of gene expression in MCF7 palbociclib treated and palbociclib resistant cells.

(A) Nanopore sequencing and pairwise analysis to obtain differentially expressed genes comparing MCF7 cells treated with 1000nM palbociclib (PalboT) and equal amounts of DMSO (Vehicle) with palbociclib resistant cells (PalboR). Gene set enrichment analysis (GSEA) to identify "Hallmark" signalling pathways in the differentially expressed genes (p-adj value ≤0.1). (C) the total of 577 differentially expressed genes (DEGs) depicted as a Venn diagram. (D-F) Volcano plots showing DEGs in pairwise comparisons (p-adj ≤0.1).

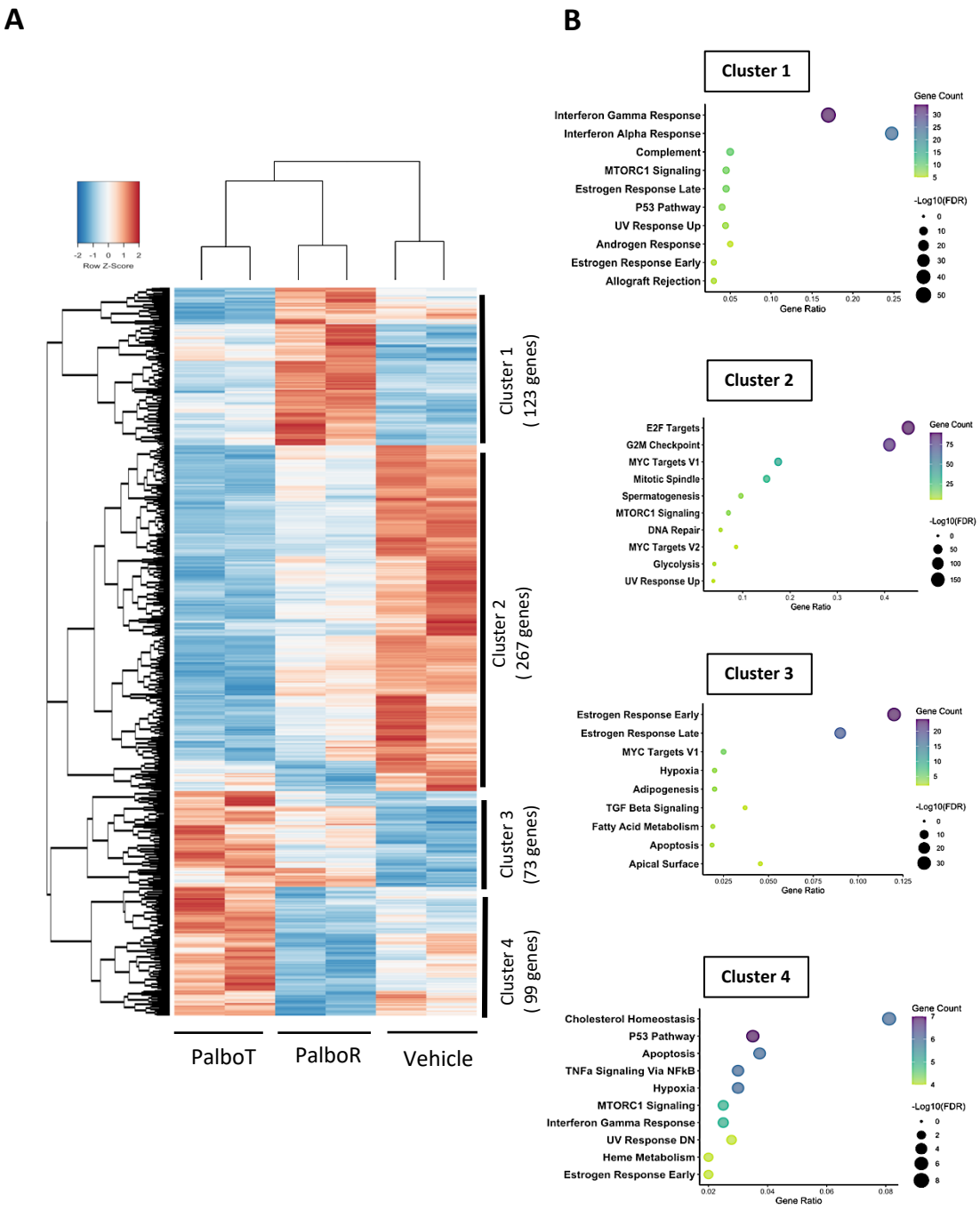


Figure 3.29. Cluster analysis of 577 differentially expressed genes in palbociclib treated and resistant MCF7 cells.

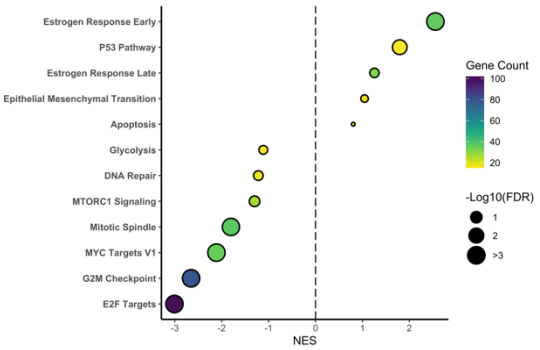
(A) Hierarchical cluster analysis of differentially expressed genes (DEGs) (p-adj value ≤0.1) represented as a heatmap. (B) Each gene cluster was overlapped with "Hallmark" for gene set enrichment analysis (GSEA).

Likewise, MCF7 LTED Y537C and PalboR lines were also sequenced (Figure 3.31A). Differential analysis found 628 commonly DEGs (p-adj≤0.1) compared to palbociclib treated and resistant cells, similarly, GSEA demonstrated most downregulated signalling pathways as E2F and G2M checkpoint (Figure 3.31B). In contrast, the early estrogen response pathway and p53 pathway were upregulated in LTED Y537 PalboT and PalboR. This may indicate the involvement of different set of DEGs in MCF7 LTED Y537C in correlation to acquired palbociclib resistance. DEGs identified in each comparison are exhibited in volcano plots (Figure 3.31C-E). As observed in MCF7 cells, the expression of MCM10 and CCNA2 was also reversed in MCF7 LTED Y537C PalboT vs PalboR (Figure 3.30E). As previously seen in MCF7 cells, the PalboR vs Vehicle comparison revealed the increased expression in cell growth related genes such as S100P, GDF15 and CCND1 (Figure 3.30D). This supports the need to further investigate the potential use of S100P and GDF15 as a marker of response to palbociclib and to study the potential role in palbociclib resistance. In addition, cluster analysis revealed DEGs in Cluster 1 were downregulated in PalboT and PalboR and GSEA showed the involvement in E2F target and G2M checkpoint pathways (Figure 3.32A-B). DEGs in Cluster 2 were downregulated in PalboR only and pathway analysis showed the downregulation of early and late estrogen response pathways. Both Cluster 3 and 4 exhibited the specific increase expression associated with palbociclib resistance, GSEA illustrating enrichment in pathways such as cholesterol homeostasis and tumour necrosis factor (TNF)-α signalling via NFκB, which indicate a different resistance mechanism in MCF7 LTED Y537C cells.

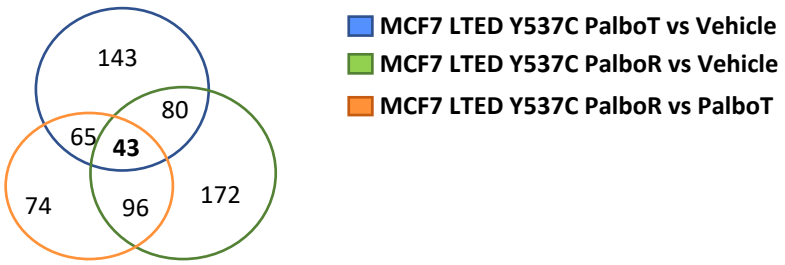
A

Cell line	Total aligned reads	
	Replicate 1	Replicate 2
MCF7 LTED Y537C	815740	947763
MCF7 LTED Y537C PalboT	1125053	1186524
MCF7 LTED Y537C PalboR	1439977	1260331

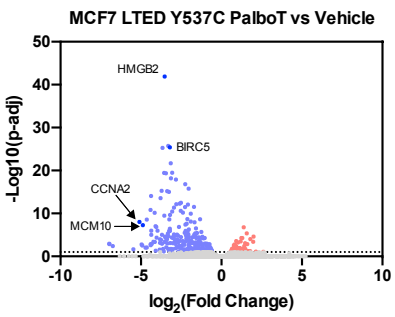
B



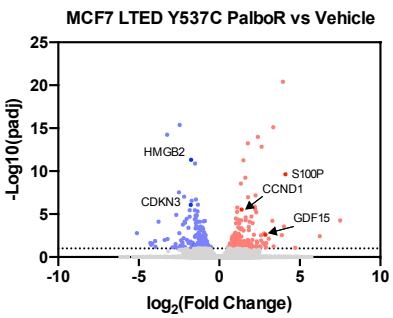
C



D



E



F

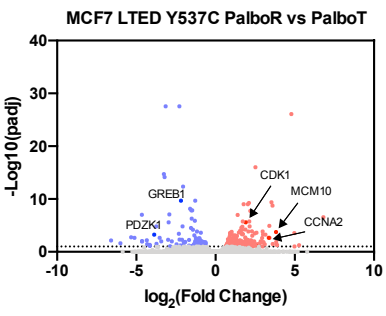


Figure 3.30. Differential gene expression analysis of MCF7 LTED Y537C palbociclib treated and resistant cells.

Nanopore sequencing was performed on MCF7 LTED cells with a Y537C mutation were treated with 1000nM palbociclib (PalboT) and equal amounts of DMSO (Vehicle), and palbociclib resistant cells (PalboR). (A) Table summarising total reads of each replicate. (B) For the global study of differentially expressed genes "Hallmark" gene set enrichment analysis was used to perform pathway analysis on the differentially expressed genes (p-adj value ≤0.1). (C) the total of 628 differentially expressed genes (DEGs) are represented in a Venn diagram. Volcano plots showing differentially regulated genes in pairwise comparisons, PalbpT vs Vehicle (D), PalboR vs Vehicle (E) and PalboR vs PalboT (F) (p-adj ≤0.05).

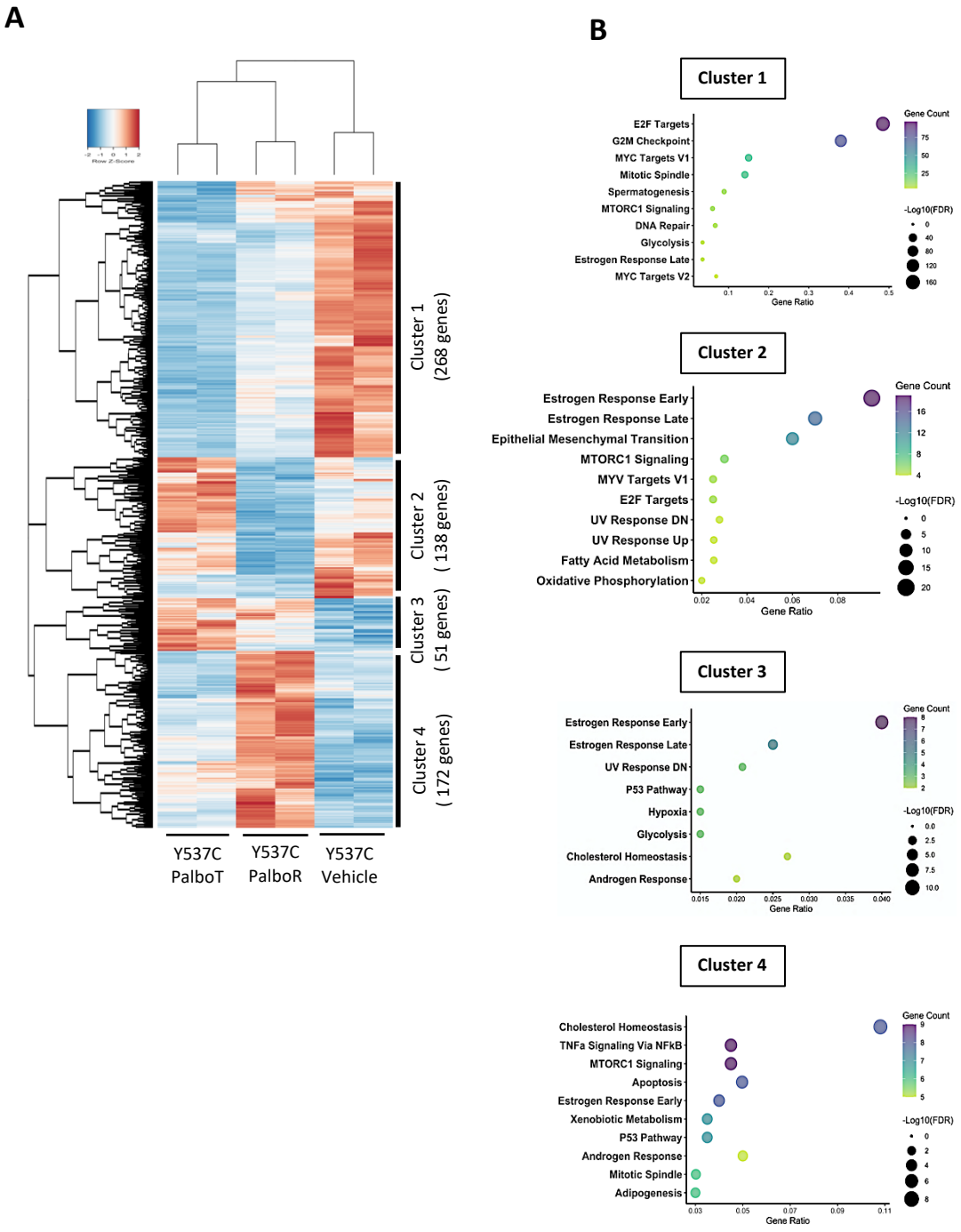


Figure 3.31. Cluster analysis in MCF7 LTED Y537C cells treated with palbociclib and palbociclib resistance.

(A) The heatmap shows two-way unsupervised hierarchical cluster analysis of differentially expressed genes (p-adj value ≤0.1) in MCF7 LTED Y537C cells after palbociclib treatment and in cells that are resistant to Palbociclib (PalboR). (B) The genes clustered in three main groups. GSEA analysis was carried out for each gene cluster using the "Hallmark" gene sets. Shown are the top 10 enriched groups for each gene cluster.

To further determine similarities and difference between the MCF7 and MCF7-LTED-Y537C cells and response and resistance to palbociclib, I performed direct comparisons. For this, the 157 genes different between vehicle treated MCF7 and MCF7-PalboR cells (padj≤0.1) and 254 differential genes between vehicle treated MCF7-LTED-Y537C and MCF7 and MCF7-LTED-Y537C-PalboR cells were compared. Just 43 genes were commonly altered in palbociclib resistant cells (Figure 3.33A). Hierarchical cluster analysis of the 43 genes segregated the cells based on palbociclib treatment and not according to estrogen dependence. As mentioned above, genes commonly upregulated in PalboR cells included GDF15 and S100P, but also the non-coding RNA genes NEAT1 and MALAT (Figure 3.32B). Also upregulated in PalboR cells was the Lemur Tyrosine kinase 3 gene (LMTK3), which has previously been associated with endocrine resistance and resistance to chemotherapy drugs in breast cancer (Stebbing *et al.*, 2013; Stebbing *et al.*, 2018; Xu *et al.*, 2014). There were too few genes to conduct pathway analysis for overlapping genes. However, GSEA was conducted on the unique genes in MCF7 and MCF7-LTED-Y537C that showed the IFN-γ and estrogen signalling pathways were the top enriched pathway, respectively (Figure 3.28B and 3.30B). In addition to the commonly altered genes in MCF7 and MCF7-LTED-Y537C PalboR cells, those genes that are altered in MCF7-LTED-Y537C PalboR cells are additionally important since current patient treatment regimens use palbociclib in combination with ET.

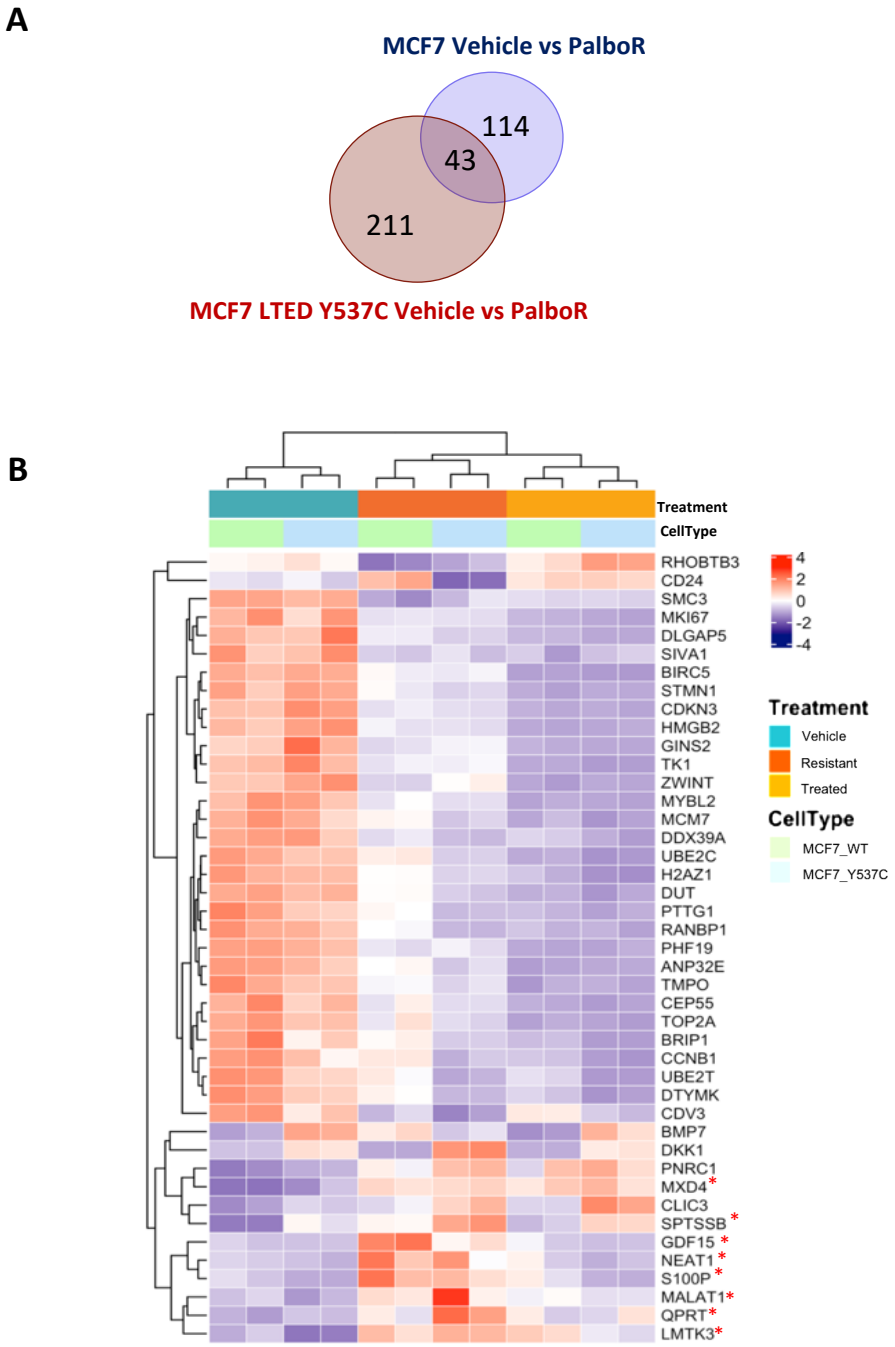


Figure 3.32. Pair-wise comparison of differential gene expression between MCF7 and MCF7 LTED Y537C palbociclib resistant cells

(A) Comparison between palbociclib resistant and vehicle-treated cells in MCF7 and MCF7 LTED Y537C lines to find common differentially expressed genes (p-adj ≤0.1) represented in a Venn diagram. (B) Cluster analysis of common genes found in palbociclib resistant cells in MCF7 (green) and MCF7 LTED Y537C (blue) lines. Mutual genes with increased expression correlated with palbociclib resistance in both MCF7 and MCF7 LTED Y537C cells (red asterisk).

3.3.2.1 Integration analysis of H3K27ac ChIP-seq and nanopore RNA-seq data

The integration of H3K27ac ChIP-seq data and Nanopore sequencing data would allow the investigation of differentially enriched H3K27ac signals and the differentially regulated genes associated with palbociclib resistance. Consistent changes in both epigenetic and transcriptomic changes may indicate essential genes that are correlated to palbociclib treatment and resistance. The integration analysis was performed using model analysis of regulation of gene expression (MARGE) developed by Wang *et al.* (2016). The package calculates the regulatory potential (MARGE-RP) of a given list of genes of interest to predict gene expression. The algorithm considers the weight of H3K27ac reads and the distance to transcription start site (TSS) of a particular gene, Thus, for the integration analysis, peaks were called using MACS2 (+/- 1kb) from the TSS as there is a higher functional impact the closer the H3K27ac signal is to the TSS. MARGE-RP was used to estimate the correlation of H3K27ac at the promoter and gene regulation. Increased MARGE-RP scores is correlated to the upregulation in gene expression.

The MARGE-RP of each ChIP-seq replicate of MCF7 cells were plotted in a heatmap based on two-way unsupervised hierarchical clustering from Figure 3.29A, to allow comparison between MARGE-RP and differential gene expression (Figure 3.33A). The average MARGE-RP of each cluster was plotted as a bar chart and compared to the average normalised read count of the same cluster (shown as line graph). MARGE-RP and normalised read count of Cluster 1, 2 and 4 had similar trends, where an increase in MARGE-RP was accompanied by an increase in gene expression. However, with the exception of Cluster 3, MARGE-RP was unable to predict the gene expression with the cluster. The clustering analysis showed upregulation of gene expression in both PalboT and PalboR but MARGE-RP had modest changes in these conditions compared to Vehicle. IGV snapshots of two representative genes from cluster 4, AURKB, demonstrate the reduction in H3K27ac Palbociclib-treated cells, which is regained in the palboR cells (Figure 3.3B). Expression of AURKB was similarly absent in Palbociclib-treated cells, but AURKB expression was similar to that in vehicle treated cells. GDF15, by contrast cluster 1 was not expressed in Palbociclib-sensitive cells, but its expression was induced in PalboR cells, with an accompanying gain in H3K27ac (Figure 3.33B). MARGE-RP was similarly calculated for H3K27ac in each of replicates in MCF7-LTED-Y537C cells and the MARGE-RP for all DEGs was plotted in a heatmap according to the two-way hierarchical clustering in Figure 3.31A. Similarly, bar charts for individual

clusters demonstrated correlation between MARGE-RP and normalised read counts of RNA-seq (Figure 3.34A). IGV snapshots of two genomic regions of DEGs indentified from both ChIP-seq and RNA-seq are showing similar trends and in concordance to MARGE-RP (Figure 3.34B). Further analysis is needed to more fully explore the potential regulatory networks associated with palbociclib resistance.

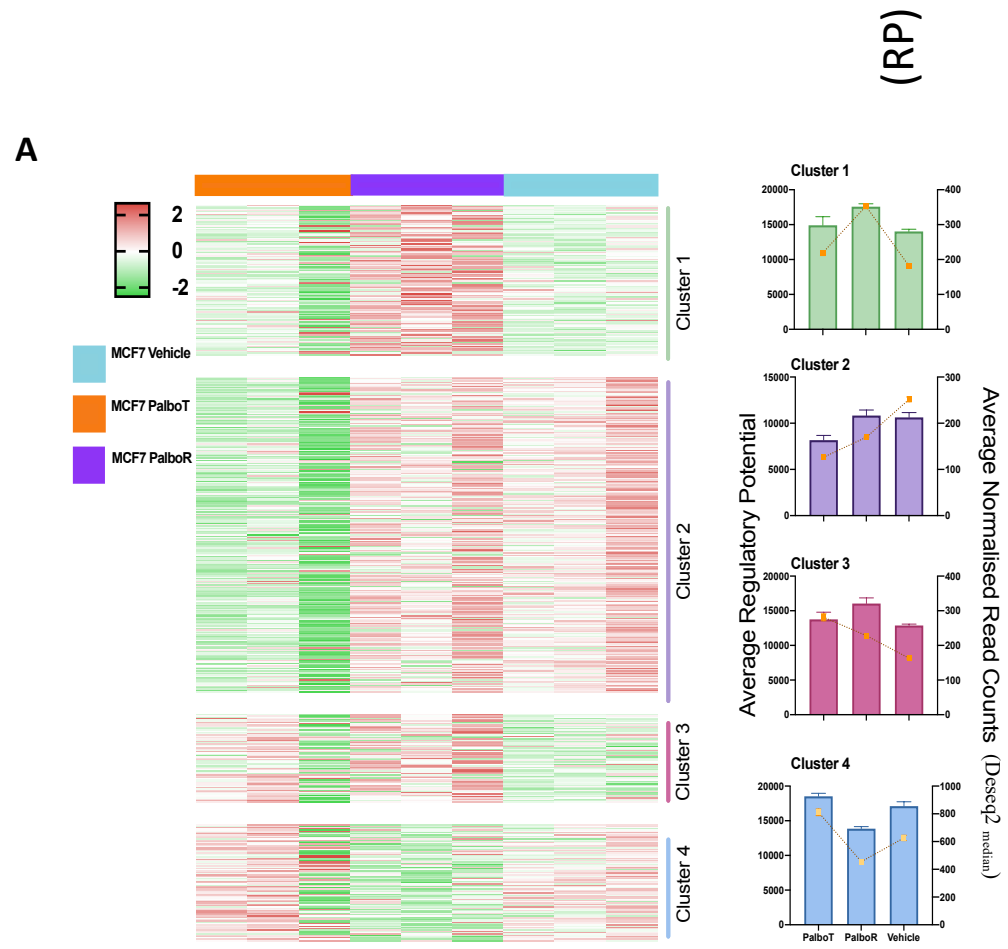


Figure 3.33. Integration analysis of H3K27ac ChIP-seq and Nanopore data in MCF7 PalboT and PalboR cells.

H3K27ac ChIP-seq and Nanopore was performed on MCF7 cells were treated with palbociclib (1000nM; PalboT) or same amounts of DMSO (Vehicle) and palbocilcib resistant cells (PalboR). (A) Integration analysis was performed using MARGE package to determine the regulatory potential (RP) of H3K27ac signal at gene promoters (+/- 1kb from transcription start site (TSS)) to predict gene regulation in the differentially expressed genes identified in nanopore RNA sequencing (p-adj value ≤0.1) represented as a heatmap. RP clustering was conducted according to two-way unsupervised hierarchical analysis from Figure 3.25. (B) The average RP in each cluster was plotted (bar chart) and compared to the average normalised read count of each cluster from Figure 3.25 (line graph). (B) IGV snapshots of ChIP-seq and RNA-seq at two genomic regions.

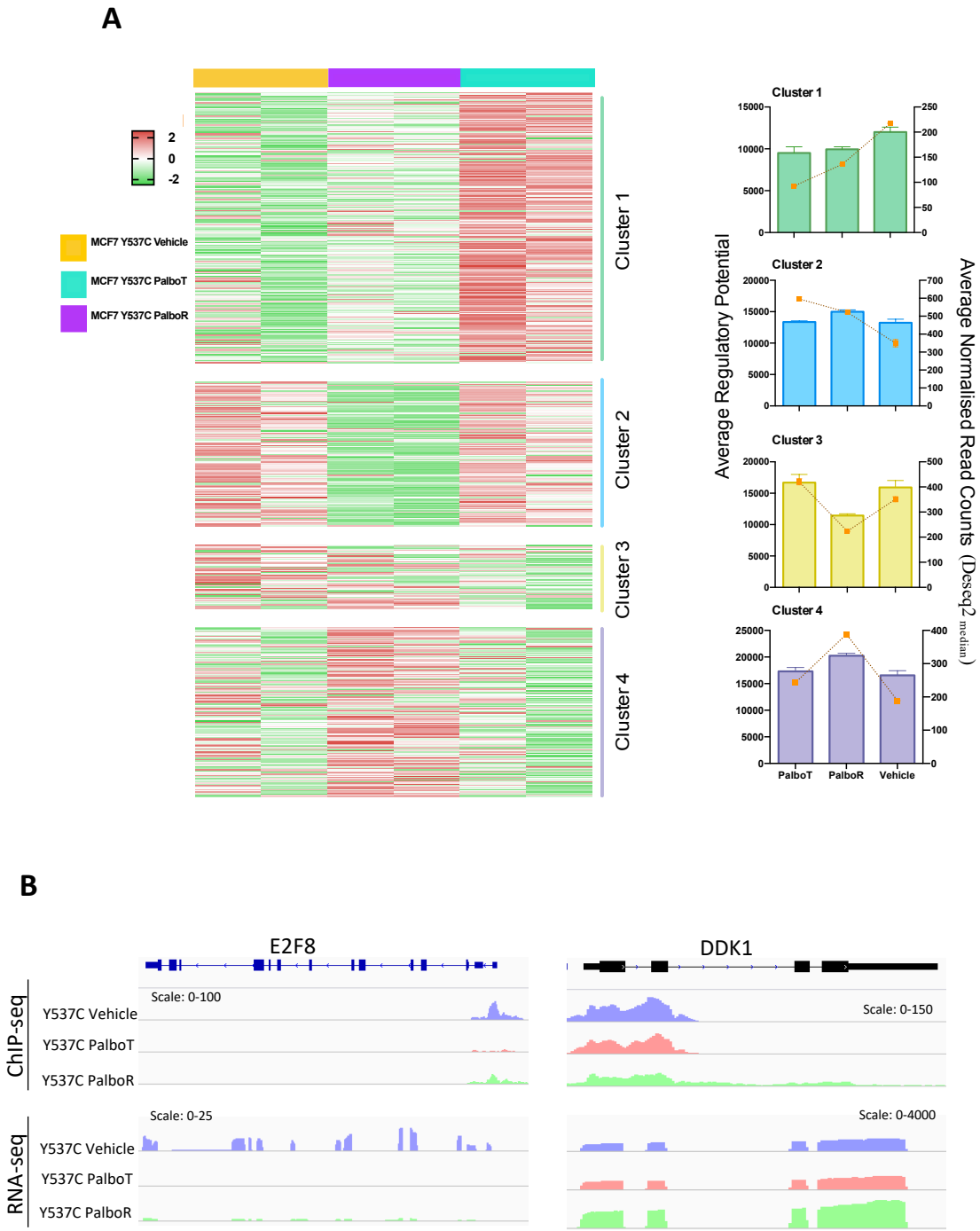


Figure 3.34. Integration analysis of H3K27ac ChIP and Nanopore data of MCF7 LTED Y537C cells.
H3K27ac ChIP-seq and Nanopore was performed on MCF7 cells were treated with palbociclib (1000nM; PalboT) or the same volume of DMSO (Vehicle), and palbociclib resistant cells (PalboR). (A) Integration analysis was performed using the MARGE package to determine the regulatory potential (RP) of the H3K27ac signal at gene promoters (+/- 1kb from transcription start site (TSS)) to predict gene regulation in the differentially expressed genes identified in nanopore RNA sequencing (p-adj value ≤0.1) represented as a heatmap. RP clustering was conducted according to two-way unsupervised hierarchical analysis from Figure 3.26. The average RP in each cluster was plotted (bar chart) and compared to the average normalised read count of each cluster from Figure 3.26 (line graph). (B) IGV snapshots of ChIP-seq and RNA-seq at two genomic regions.

To further explore the transcriptional changes resulting from the development of palbociclib resistance, nanopore RNA-seq was also conducted in HCC1428-LTED cells treated with Vehicle or palbociclib for 24 hours (Figure 3.35A). Also analysed were the HCC1428-LTED-PalboR cells. Finally, the RNA-seq also included HCC1428 parental (estrogen-dependent) cells. Differential gene expression analysis was performed on the HCC1428, HCC1428 LTED, HCC1428 LTED PalboT and HCC1428 LTED PalboR. Two thousand and three genes were differentially regulated (p-adj $\leq$0.05) across the three treatments (Appendix VII). GSEA was performed showing the comparison for LTED Vehicle and PalboT and PalboR cells (Appendix VIII). In contrast to both MCF7 lines, the E2F target and G2M signalling pathways were upregulated in HCC1428 LTED PalboT and PalboR cells (Figure 3.35B). In addition, the DEGs presented in volcano plots (Figure 3.35C-E), demonstrated the downregulation of estrogen target genes such as PDZK1 in PalboT cells, but their expression was elevated in PalboR cells. Genes such as DKK1, BIRC5 and CDK1 were also upregulated in palbociclib resistance. In contrast to MCF7 cells, S100P was found to be downregulated in PalboR vs PalboT.

Hierarchical cluster analysis revealed a high degree of similarity in DEGs between vehicle-treated HCC1428 and HCC1428-LTED (Figure 3.36A) (Appendix VIII). Cluster 1 identified 584 DEGs with increased expression in palbociclib-treated HCC1428-LTED, which were revealed to be strongly enriched in in estrogen and androgen response pathways (Figure 3.36B). Clusters 2 and 3 contained gene sets with reduced gene expression in PalboT and PalboR cells and these clsuters contained genes in estrogen response (cluster 2) and E2F and G2M pathways (cluster 3). The expression profiles in these clusters are similar to what was observed for the MCF7 models for G2/M checkpoint and E2F targets, where these genes are strongly downregulated in PalboT cells, but recovered in PalboR cells. Most divergent from the MCF7 analyses are the genes in cluster 4, which show strong upregulated in PalboR cells and appear in cell cycle (E2F targets, G2/M checkpoint) and estrogen response pathways.

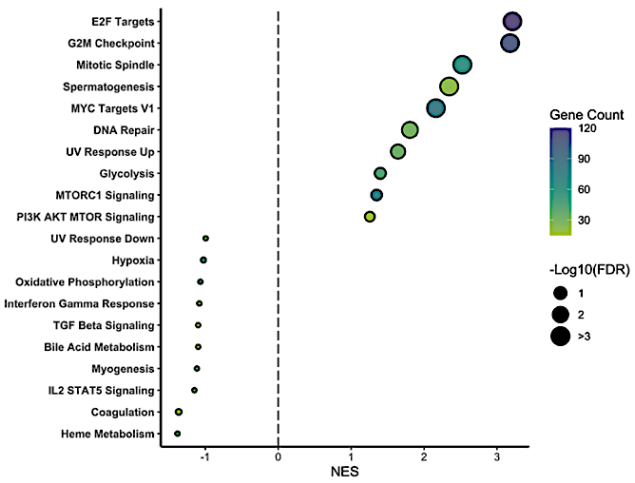
Overall, many more expression of many more genes was altered in palbocicilb resistance in HCC1428 cells than in the MCF7 models. Where 950 genes were identified in HCC1428-LTED-PalboR, 157 and 264 genes were differential in MCF7-PalboR and MCF7-LTED-Y537C-PalboR cells. Just 32 genes were common to all three models (Figure 3.37A). By and large, the genes that were upregulated in HCC1428-LTED-PalboR cells were downregulated

in the MCF7 PalboR models, possibly due to the differences in gene expression in the different cell lines (Figure 3.37B). Thus, GDF15 and SP100, which are upregulated in the MCF7-derived PalboR cells, were not expressed in HCC1428 cells (Figure 3.37C). BIRC5 followed the opposite trend, being upregulated in HCC1428-LTED PalboR cells and downregulated in the MCF7 PalboR cells. However, expression of DDK1, HSPB1 and NPY1R was increased in the MCF7 and HCC1428 LTED derived PalboR cells.

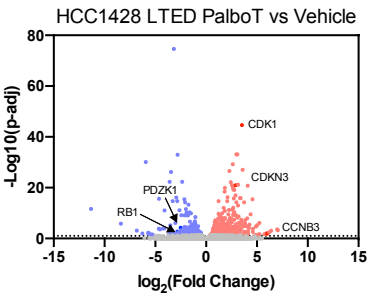
A

Cell line	Total aligned reads	
	Replicate 1	Replicate 2
HCC1428	1290219	1047414
HCC1428 LTED	1138639	1226315
HCC1428 LTED PalboT	1086520	1280511
HCC1428 LTED PalboR	943801	1135706

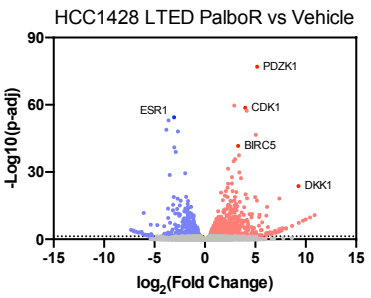
B



C



D



E

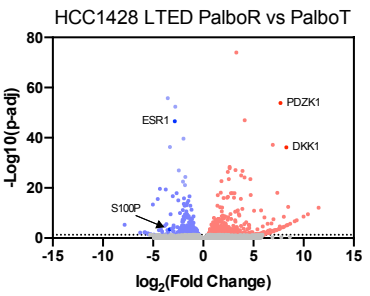


Figure 3.35. Differential gene expression analysis of palbociclib treated and palbociclib resistance in HCC1428 LTED cells.

Nanopore sequencing was performed on HCC1428 and HCC1428 LTED cells treated with 1000nM palbociclib (PalboT) and equal amounts of DMSO (Vehicle), and HCC1428 LTED palbociclib resistant cells (PalboR) to analyse differentially expressed genes. (A) Table summarising total read counts of each replicate. (B) Gene set enrichment analysis (GSEA) to identify "Hallmark" signalling pathways in the differentially expressed genes (p-adj value <0.05). Volcano plots showing differentially regulated genes in pairwise comparisons, (C) PalboT vs Vehicle, (D) PalboR vs Vehicle and (E) PalboR vs PalboT (p-adj ≤0.05).

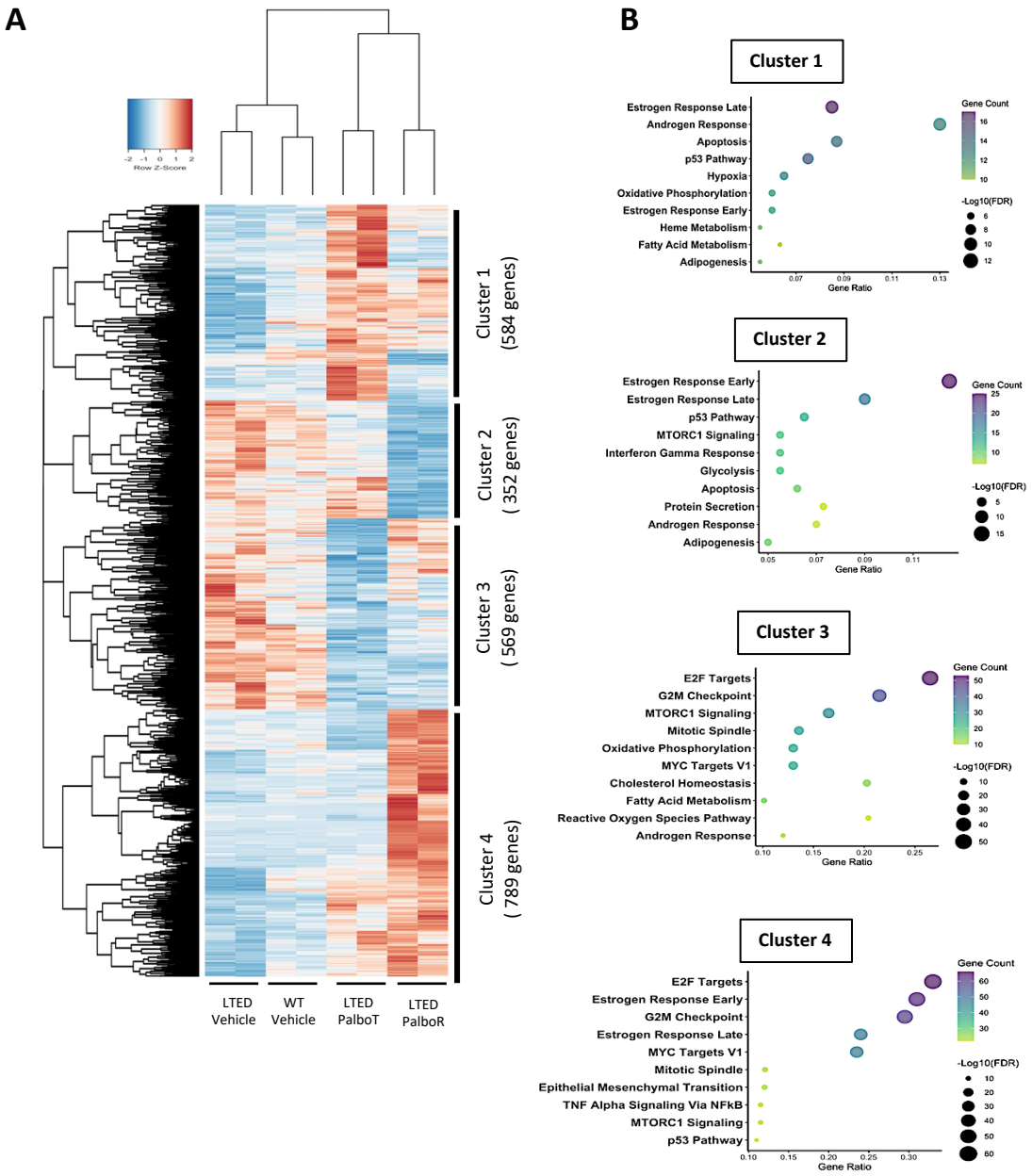


Figure 3.36. Cluster analysis of differentially express genes in HCC1428 LTED cells treated with palbociclib and palbociclib resistant.

(A) Two-way unsupervised hierarchical cluster analysis of differentially expressed genes (p-adj value ≤0.05) represented as a heatmap. (B) Each gene cluster was overlapped with "Hallmark" for gene set enrichment analysis (GSEA).

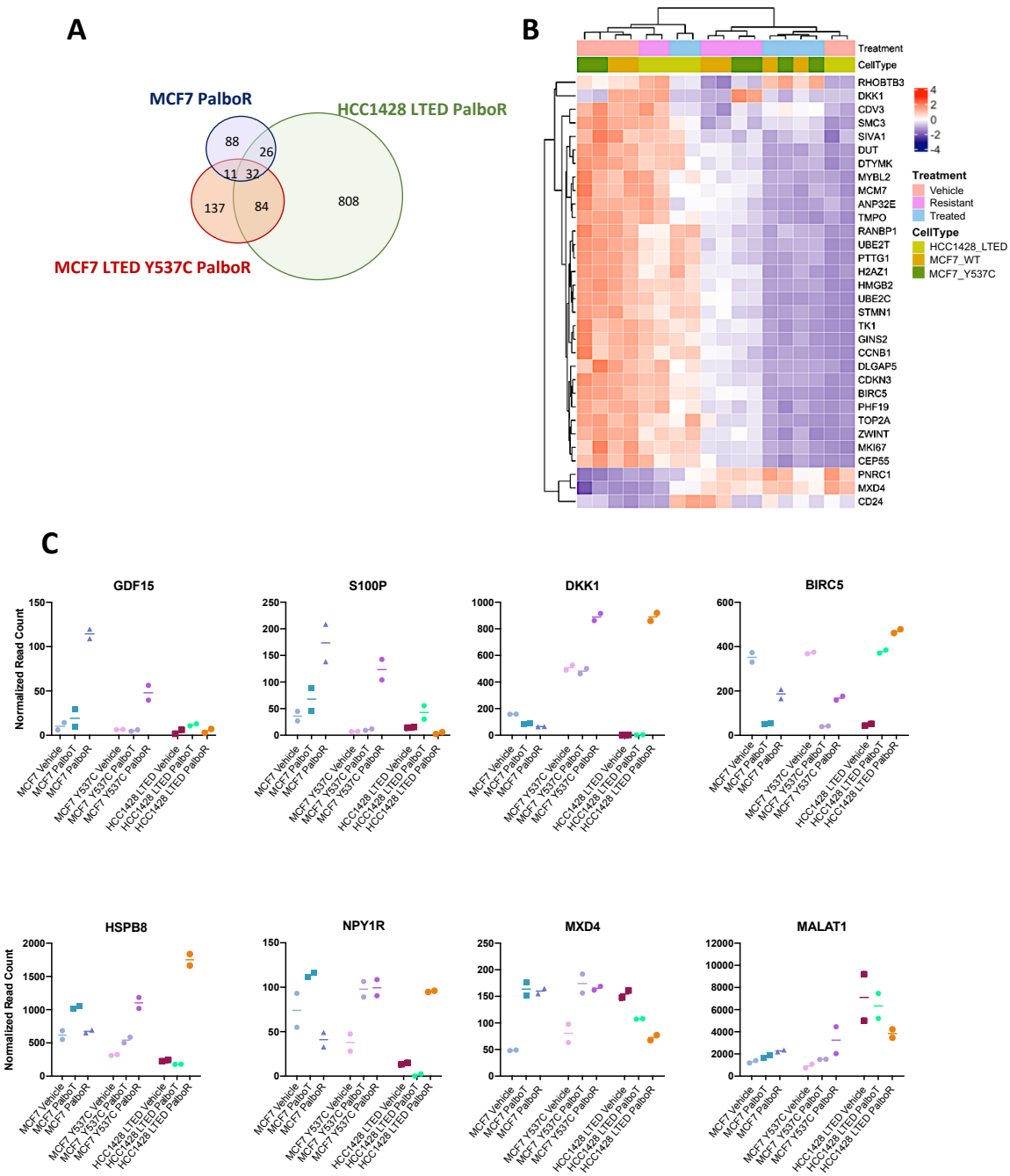


Figure 3.37. Differentially expressed gene enriched in palbociclib resistant cells.

(A) The differentially regulated genes (p-adj value ≤0.1) in the different PalboR cells compared with their Palbociclib-sensitive counterparts, were compared. As shown in the Venn diagram, just 32 genes were differentially regulated in all three PalboR models. (B) The common DEGs from A were compared using cluster analysis of the overlapping differentially expressed genes. (C) Normalised reads counts for a set of the common DEGs in MCF7 and HCC1428 PalboR models are shown. The horizontal lines represent the mean read count. The actual normalised read counts for each of the two replicate samples also are shown.

3.3.3. Initial validation of nanopore sequencing data in ER$^+$ breast cancer cell lines

Following analysis of the nanopore RNA-seq data of ER$^+$ BCa cell lines with resistance to palbociclib, a preliminary RT-qPCR analysis was conducted using a panel of genes selected from the 32 common DEGs and genes selected from analysis of the MCF7 models. Cells were processed exactly as undertaken for the RNA-seq analysis. Specifically, the cells were treated with 1μM palbociclib or an equal volume of DMSO (vehicle) for 24 hours. In addition to the MCF7 and HCC1428, I also used WT and LTED T47D cells and T47D-PalboR and T47D-LTED-PalboR (also provided by Dr Lesley-Ann Martin, ICR). For cell lines treated with palbociclib, 1μM palbociclib was added for 24 hours. Heatmap and bar charts were plotted to summarise gene expression relative to the housekeeping gene, TBP in each cell line (Figure 3.38). The expression of GDF15 and S100P was increased in MCF7 PalboR ($p = 0.001$) and MCF7 LTED Y537C PalboR ($p < 0.0001$) cells. Interestingly, GDF15 expression was also increased in MCF7 LTED PalboT ($p = 0.05$). These results indicate that further investigations are warranted to establish the importance of GDF15 and S100P in palbociclib resistance. However, enthusiasm is dampened by the fact that GDF15 was not expressed in HCC1428 or T47D cells. It should be noted, however, that GDF15 is a p53 target gene and that HCC1428 and T47D cells are mutated for p53 (Liang *et al.*, 2011)(REFs), which likely explains the lack of GDF15 expression in these cell lines. Note that p53 mutations are oonly observed in 20% of ER+ breast cancer; this is in comparison with TNBC where almost 80% of cases have TP53 mutations (Nik-Zainal *et al.*, 2016). SP100 expression was variable across the three cell lines, so again a robust case for its involvement is difficult to make on the basis of current data. Expression of DKK1 ($p = 0.002$) and NPY1R ($p = 0.03$) was elevated in MCF7 LTED Y537C PalboR cells, but not in HCC1428 LTED PalboR. Nor was DKK1 expression observed in T47D cells. NPY1R expression was also not elevated in PalboR HCC1428 or T47D cells. Similar lack of consistency in expression of the other genes in the three cell line models of Palbociclib resistance means that none of these genes is likely to be a reliable marker of Palbociclib response or resistance in ER+ breast cancer.

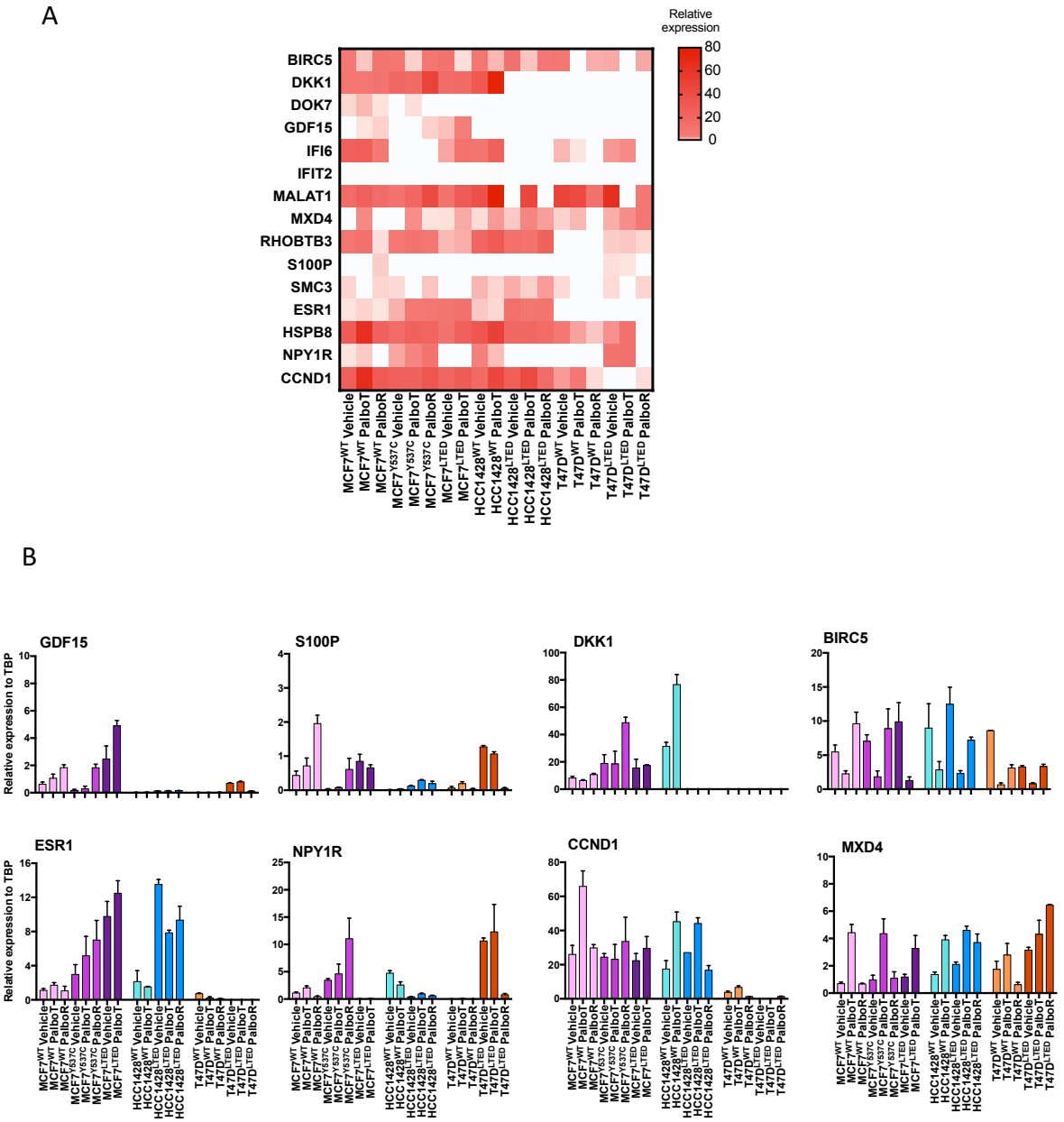


Figure 3.38. Validation of differentially expressed genes enriched in palbociclib resistant cells.

RNA was extracted from each cell line after 24 hours the addition of 1μM of palbociclib or an equal volume of DMSO as Vehicle. RT-qPCR was conducted to analyse a panel of differentially regulated genes found in the pair-wise comparison between palbociclib resistant (PalboR) cells vs DMSO treated (Vehicle) in MCF7, MCF7 LTED Y537C and HCC1428 LTED lines. Gene expression is summarised in the heatmap (A) and the results are shown in the bar charts (B). Gene expression is shown relative to expression of TBB. Error bars represent SD (n=3).

4. Discussion

Despite the relative success of selective CDK4/6 inhibitors in combination with ET in patients with advanced BCa, progression on these treatments occurred in these advanced BCa patients, which is likely to involve intrinsic resistance mechanisms in some patients and development of acquired resistance in other patients (Alvarez-Fernandez and Malumbres, 2020; Dean *et al.*, 2010; Herrera-Abreu *et al.*, 2016; McCartney *et al.*, 2019). Since these drugs are moving to first line adjuvant treatment, it is therefore important to understand mechanisms of resistance to CDK4/6 inhibitors. Indeed, despite the large numbers of patients who have already been treated with these drugs, there are no appropriate biomarkers of response beyond ER^+ status and the need for functional RB. In this thesis I have focused on investigating potential drivers of CDK4/6 resistance on the one hand by over-expressing CDKs and cyclins genes that have been linked to CDK4/6 inhibitor response and by performing analysis of epigenetic and transcriptomic profiling of ER^+ BCa cell lines following short treatment to palbociclib and cells which have been adapted to grow in palbociclib and hence represent models of palbociclib resistance. The models will assist the identification of possible markers of response and novel therapeutic targets for CDK4/6 inhibitor resistant BCa. In addition, upon the establishment of resistant models, I use these models towards the study to explore the potential to use alternative targeted therapies such as the highly selective CDK7 inhibitor ICEC0942, developed in our group, and a CDK7/12/13 inhibitor THZ1.

4.1 The loss of retinoblastoma protein in MCF7 cells rendered resistance to CDK4/6 inhibitors

The RB protein is a direct downstream target of the CDK4/6-cyclin D axis, with a suppressive role in E2F transcription and consequently controls progression through the G1 phase to the S (DNA synthesis) phase of the cell cycle. The loss of and/or mutations in RB are well-established resistance mechanisms for evading control of E2F target genes by CDK4/6 and allows cell cycle progression via uncontrolled E2F-regulated gene expression, as demonstrated in TNBC, in which RB1 loss/mutation is common (Finn *et al.*, 2009). To confirm the requirement for RB1 for the action of CDK4/6i, we knocked out the RB1 gene in MCF7 cells,

to obtain isogenic cells containing WT and deleted RB1. As expected, the RB1 knockout cells were insensitive to all three of the current clinical CDK4/6 inhibitors. Interestingly, knocking out the RB gene did not lead to observable changes in the panel of cell cycle-related proteins, raising the interesting possibility of using transcriptomic and/or proteomic studies to determine changes in gene regulation due to RB1 knockout in an isogenic model. While loss and/or mutations in RB is relatively rare in ER^+ breast cancer it is possible that the selection pressure due to CDK4/6 inhibitor treatment could result in RB1 loss, a possibility that is supported by the fact that several ER^+ cell lines with acquired resistance to CDK4/6 inhibitors show RB1 loss as determined by copy number loss and reduced/lost RB1 mRNA and protein (Pancholi *et al.*, 2020). Importantly, RB1 knockout cells remained sensitive to CDK7 inhibitors, providing at least one treatment possibility for ER^+ and RB-null breast cancer patients.

4.2 The investigation of the role of over-expressing CDKs/cyclins in CDK4/6 inhibitor resistance mechanisms

Cyclins/CDKs have regulatory roles in cell cycle progression. Several published data have suggested a role of the dysregulation in cell cycle associated cyclins and CDKs may have an active role to bypass CDK4/6 inhibition. I used two methods, the CRISPR/Cas9 Synergistic activation mediator (SAM) and DHFR inducible protein expression, to over-express individual cyclins and CDKs in MCF7 cells and proceeded to establish acquired resistance models to CDK4/6 inhibitors. The findings for the different genes are discussed in the subsections below.

4.2.1 Cyclin E1 over-expression model remained sensitive to CDK4/6 inhibitors

Cyclin E1 has a predominantly regulatory role in G1/S phase transition and progression through the S phase by interaction with its cognate partner CDK2. Cyclin E1 has been shown to act as an oncogene in various cancers that promote proliferation and can drive cancer progression (Alvarez-Fernandez and Malumbres, 2020; Chu *et al.*, 2021). The increased expression of cyclin E1 was thought to have a role in developing resistance to CDK4/6 inhibitors, following data from PALOMA3 suggesting that CCNE1 expression is correlated to response to palbociclib (Turner *et al.*, 2019). It has been suggested, together with CDK2, cyclin E1 can promote progression of the cell cycle and evade the requirement for CDK4/6 (Alvarez-

Fernandez and Malumbres, 2020). To investigate if cyclin E1 over-expression is sufficient to promote resistance to CDK4/6 inhibitors, I employed the activating Cas9 SAM system. Using the SAM system provides the advantage of increasing expression of the endogenous gene rather than using heterologous promoter driven ectopic expression that can result in massive over-expression and amplify non-specific effects of over-expression. SAM-directed cyclin E1 over-expression with 10-fold increase in mRNA levels was successfully achieved in MCF7 cells.

CCNE1 over-expression promoted estrogen-dependent growth of MCF7 cells but did not reduce sensitivity to CDK4/6 inhibitors. To determine if CCNE1 over-expression might enhance adaptation to growth in the presence of CDK4/6 inhibitors, MCF7-AcCas9-CCNE1 cells were cultured over a 40-day period. There was no obvious alteration in response to long-term culturing with any of the three CDK4/6 inhibitors used. However, over time the over-expression of cyclin E1 was lost (data not shown). Consequently, the current AcCas9-CCNE1 model cannot be used to conclude whether cyclin E1 over-expression is implicated in the resistance to CDK4/6 inhibitors. Further characterisation of AcCas9-CCNE1 cells showed that the levels of cyclin E1 expression were reduced with passaging and normal cell maintenance. Hence, further refinement has been undertaken in the group at attempts to ameliorate the loss of over-expression. This has included generating clones of MCF7-AcCas9-CCNE1 cells with highest cyclin E1 expression. As described earlier, we took the approach of co-expressing 3 different sgRNAs targeting the CCNE1 gene promoter, so for a second approach, we have generated MCF7-AcCas9 cells expressing just one of the three sgRNAs and then selecting for cells with the highest cyclin E1 expression. The latter approach has identified one sgRNA that provides a good level of CCNE1 expression and these will be assessed in future studies. Utilising inducible systems for limiting CCNE1 over-expression offer an alternative approach. Among these is the use of doxycycline-inducible lentiviral constructs, which in other projects in the lab have provided very tight regulation of the gene of interest. Yet another alternative is the DHFR fusion approach for rapid protein degradation in the absence of the stabilising DHFR ligand (although see below for some provisos). In previous studies, the role of cyclin E1 was mainly focused on the response to palbociclib (Guarducci *et al.*, 2018; Pascual *et al.*, 2021; Turner *et al.*, 2019). Further investigations may also focus of the role of cyclin E1 in response to abemaciclib and ribociclib. The second member of the cyclin E family (cyclin E2) also participates in cell cycle regulation and can activate CDK2 upon binding. Additional

characterisation may be needed to expand and include the investigation of cyclin E2 and its possible role in bypassing CDK4/6 inhibition.

4.2.2. Increased expression of CDK2 led to rapid development of resistance to palbociclib and ribociclib

The over-expression of CCNE1 was inconclusive in our over-expression models. However, the over-expression of its cognate partner CDK2 demonstrated that it may participate in resistance to palbociclib. With the established role of CDK2-cyclinE in cell cycle regulation, CDK2 over-expressing cells were developed using the DHFR fusion and the AcCas9 methods. DHFR-CDK2 over-expression did not alter the sensitivity to CDK4/6 inhibitors in full growth medium, but in estrogen-free medium supplemented E2, sensitivity to palbociclib was reduced by around 10-fold. This reduction in sensitivity was not extended to abemaciclib or ribociclib. In agreement with the results for DHFR-CDK2, CDK2 over-expression using the SAM method, also resulted in reduced sensitivity to palbociclib, again in estrogen-free medium supplemented with E2. Again, response to abemaciclib and ribociclib was unchanged. Thus, elevated expression of CDK2 can reduce sensitivity to palbociclib.

Why there should be a difference in response to palbociclib in estrogen-free media is uncertain, but dextran-coated charcoal-stripping of FCS (DSS) not only removes estrogens but also other steroid hormones including androgens and progestins. Moreover, the full medium experiments are routinely undertaken in our lab using 10%FCS, whereas 5% DSS is used for the E2 experiments. Whether the different response to palbociclib in the two growth conditions is due to lack of steroid hormones or because of reduced serum percentage is clearly required and easy to undertake. AR and PR have both been implicated in growth and survival of ER^+ breast cancer cells (Carroll *et al.*, 2017; Hickey *et al.*, 2021), so addition of agonists and antagonists for these receptors can be used.

The adaptive growth response in MCF7-AcCas9-CDK2 cells with long term culturing in the presence of CDK4/6 inhibitors readily showed development of resistance to palbociclib and to ribociclib. However, CDK2 over-expression did not reduce sensitivity to abemaciclib at all concentrations tested. A multi-omics study has differentiated abemaciclib from palbociclib and ribociclib by demonstrating an additional inhibitory effect of abemaciclib. Specifically, abemaciclib was shown to inhibit CDK2 in vitro and in vivo (Hafner *et al.*, 2019). This correlates with my findings that over-expression of CDK2 may provide a mechanism for

acquired resistance to palbociclib and ribociclib, but not to abemaciclib, potentially due to inhibition by abemaciclib, of CDK2. The study by Haffner et al (2019) and my own results also emphasise the possibility of using abemaciclib following development of resistance to Palbociclib or ribociclib, at least in cases where the resistance is accompanied by increase in CDK2 expression and/or activity. It will be useful to use the CDK2 over-expression models for testing cross-sensitivity between CDK4/6 inhibitors, as I did for the MCF7-AcCas9-CDK6 cells. The initial characterisation of the CDK4/6 inhibitor adapted MCF7-AcCas9-CDK2 cells at the mRNA and protein level in a panel of cell cycle related targets did not identify any consistent differences and global transcriptomic and proteomic analyses are warranted. Moreover, if CDK2 over-expression is indeed sufficient for development of resistance to palbociclib and/or ribociclib, then the models developed in my thesis represent useful resources not only for identifying the mechanisms by which CDK2 over-expression leads to resistance, but also for testing alternative therapies. Abemaciclib is a possibility, as stated above. The models will also allow testing of CDK2 inhibitors. A recent study has suggested that a combination of CDK4 and CDK2 inhibition can produce a durable inhibitory effect in BCa cells, which further supports the potential use of CDK2 with CDK4/6 inhibitors (Pandey *et al.*, 2020), or following progression on CDK4/6 inhibitors. Finally, I have demonstrated that CDK2 over-expressing MCF7 cells are as sensitive as parental cells to ICEC0942 and THZ1, so CDK7 inhibition is a possible avenue for CDK2-directed resistance to CDK4/6 inhibitors.

4.2.3 CDK6 amplification led to rapid development of acquired resistance to abemaciclib

CDK6 over-expression was achieved for both the SAM and the DHFR-inducible methods in MCF7 cells. CDK6 over-expression did not impact sensitivity to any of the three CDK4/6 inhibitors. These results are in disagreement with a paper showing that increased CDK6 expression promotes resistance to abemaciclib (Yang *et al.*, 2017). To address this disparity, I treated MCF7-AcCas9-CDK6 cells with palbociclib, abemaciclib or ribociclib over a 40-day period, as done for MCF7-AcCas9-CDK6 cells. CDK6 over-expression overcame growth inhibition with 50 nM abemaciclib, although not for higher concentrations of abemaciclib. Interestingly, CDK6 over-expression was much less effective in promoting growth in the presence of palbociclib or ribociclib. Notwithstanding, GI_{50} determination using cells that eventually grew out for each CDK4/6 inhibitor all showed resistance to all three drugs, although similar resistance was observed for cells that grew out in MCF7-AcCas9-vector cells. In all cases, the resistant MCF7-AcCas9-CDK6 cells were much less sensitive to the three drugs than the MCF7-AcCas9-vector cells. The main point of difference was that the

abemaciclib- and ribociclib-resistant MCF7-AcCas9-CDK6 cells were only a little less sensitive to palbociclib. Indeed, the level of resistance to palbociclib in these settings was similar to the level of resistance obtained for MCF7-AcCas9-vector cells. This implies that CDK6 over-expression does permit development of resistance to CDK4/6 inhibitors and that palbociclib-resistant MCF7-AcCas9-CDK6 cells are cross-resistant to abemaciclib and ribociclib, but that abemaciclib- and ribociclib-resistant MCF7-AcCas9-CDK6 cells are not cross-resistant to palbociclib. For reasons that are unclear and were not pursued here, resistance to Palbociclib that emerges following long term treatment of CDK6 over-expressing cells involves mechanisms that are different for palbociclib compared with abemaciclib or ribociclib.

RNAi-mediated knockdown of CDK6 in palbociclb-resistant MCF7-AcCas9-CDK6 did not abrogate resistance to palbociclib, which suggests that the palbociclib resistance in these cells does not require CDK6 over-expression. This could mean that while CDK6 over-expression accelerated progression to palbociclib resistance, it is not necessary for maintenance of the resistance. Whether abemaciclib and ribociclib resistance in these cells is dependent on CDK6 remains to be established, but previous results indicate that resistance (at least to abemaciclib) might be dependent on continued expression of CDK6 (Yang *et al.*, 2017).

As was the case for the CDK2 over-expression models, the CDK6 over-expressing and CDK4/6 inhibitor resistant cells remained sensitive to CDK7 inhibitors and support the further investigation of using other selective CDK inhibitors, CDK7 inhibitors in particular, to overcome resistance to CDK4/6 inhibitors.

To ameliorate the limitations of our current attempt to understand the pathways involved in these CDK over-expression models, multi-omic studies such as RNA-seq and total/phospho-proteomics should be performed to study the global changes after acquiring resistance. Moreover, a recent paper highlighted the importance of identifying the differences amongst the three CDK4/6 inhibitors (Hafner *et al.*, 2019). The profiling of these resistant models would contribute to the differentiation of adaptive mechanisms of cells after developing resistance to different CDK4/6 inhibitors. Furthermore, there are major limitations of utilising one cell line in the current study. Future studies should therefore extend the applications of these established over-expressing methods to other ER^+ BCa cells lines. Towards this, T47D-AcCas9 cells were generated as additional *in vitro* model to validating roles of CDKs and cyclins in drug response

to CDK4/6 inhibitors. As mentioned, other over-expression systems such as the DOX regulated TET-ON methods should also be considered to further provide confirmation of increased expression or amplifications CDKs/cyclins in CDK4/6 inhibitors.

4.3. Global transcriptomic and epigenetic profiling of palbociclib resistance models

With the aim of investigating palbociclib resistance mechanisms, global transcriptomic and epigenetic (H3K27ac ChIP-seq) studies were conducted in ER^+ breast cancer cell lines that were treated with palbociclib, comparing to cells that had been made resistant following long-term adaptive culturing in palbociclib-containing media. The primary aim was to identify gene expression changes that could point to possible biomarkers of response to palbociclib and/or identify potential therapeutic targets for palbociclib-resistant ER^+ breast cancer patients. The results of the analysis are discussed in the sections below.

4.3.1 Reset of cell cycle related genes in palbociclib resistant cells to overcome palbociclib inhibition

The H3K27ac ChIP-seq analysis identifies transcriptionally active chromatin. Using the ChIP-seq data allowed the identification of active genes and comparison of the profiles in MCF7 cells following short-term (24 hours) treatment with vehicle or 1 μM palbociclib and cells that had been treated continuously with 1μM palbociclib for development of resistance. A similar analysis was done in MCF7 cells and in long-term estrogen-deprived MCF7 (MCF7-LTED) cells. The MCF7-LTED cells used here turned out to have an ER mutation that makes the ER constitutively active, As expected, key features of the analysis, both of the H3K27ac ChIP-seq and RNA-seq was the reduction in cell cycle related pathways, including E2F targets and G2M checkpoint in cells treated with palbociclib for 24 hours, consistent with likely growth arrest. These pathways recovered in the MCF7-PalboR cells, again consistent with re-establishment of growth in the presence of palbociclib.

In addition, future experiments should expand to abemaciclib and ribociclib, alongside models of resistance to CDK4/6 inhibitors in other ER^+ cell lines. MCM10 initiates pre-RC complex

and participates in the maintaining DNA integrity and origin firing (as discussed in Section 1.3.1.3). Similar to CCNA2, the expression level of MCM10 was downregulated by palbociclib treatment in MCF7 cells, but expression was rescued following the development of resistance expression level was comparable to vehicle treated cells. MCM10 expression may participate in promoting cell cycle progression with failure to suppress MCM10 expression in palbociclib resistant cells.

The 'reset' mechanism may be one of the possible machineries adopted by resistant cells to overcome growth arrest by palbociclib. Genes such as MCM10, CCNA2, PLK1, and AURKB were highlighted and expression of these genes exhibited downregulation after palbociclib treatment, but expression was rescued in MCF7 resistant cells. This raises the potential for using this small subset of genes as biomarkers of acquired resistance to palbociclib. Should these be confirmed in further studies, including Western blotting, the possibility of targeting some of these genes becomes feasible. CCNA2 is a cyclin for CDK2 and CDK1, kinases that can be targeted with selective inhibitors such as, RO-3306 and PF-06873600 (Freeman-Cook *et al.*, 2021b; Kojima *et al.*, 2009; Vassilev *et al.*, 2006).

Aurora kinases are also implicated in the regulation of events before and during mitosis, assisting the maturation of mitotic machinery components (Carmena and Earnshaw, 2003; Fu et al., 2007). AURKB encodes for the mitotic kinase, Aurora B (AurB) and aberrant expression of AURKB has been correlated with cell cycle progression, genomic instability, aneuploidy, and tumourigenesis (Borah and Reddy, 2021; Chieffi, 2018; Goldenson and Crispino, 2015). The amplification and over-expression of AURKB is observed in several cancer types, raising the potential of targeting AurB as a cancer treatment. With high homology between AurA and AurB, several AurB inhibitors such as Hesperadin, ZM447439, and VX-680 (MK-0457, MERCK) are also potent AurA inhibitors (Georgieva et al., 2010; Harrington et al., 2004; Hauf et al., 2003). Nevertheless, these dual AurA and AurB inhibitors all demonstrate anti-tumour effects, pre-clinically. VX-680 was enrolled in phase I clinical trials and showed promising data in blood malignancies (Giles et al., 2007; Martinelli et al., 2009), but only limited anti-tumour activities were observed in solid tumours (Traynor et al., 2011). The AurB specific inhibitor, AZD1152 (Barasertib, AstraZeneca) was derived from ZM44739 (Yang et al., 2007). Although it showed good tolerability, it has not progressed beyond phase I/II trials due to the complexity of administration (Borah and Reddy, 2021). The ongoing efforts in developing

selective AurB inhibitors may bring new opportunities to use AurB inhibitors as an alternative treatment in the event of palbociclib resistance.

PLK1 also has an established role in the S phase to maintain genomic stability, mitosis entry and DNA damage response (Section 1.3.1.4). The expression of PLK1 in MCF7 palbociclib resistant cells was comparable to levels in vehicle treated cells, whereas palbociclib treatment for 24 hours had reduced PLK1 levels. This suggests that the recovery of PLK1 expression may be a contributing factor in the mechanism of resistance to palbociclib. This is in agreement with a previous study that found PDXs harbouring an upregulation of G2M pathway in bone metastases and also in PDXs that have developed resistance to palbociclib (Montaudon *et al.*, 2020). In this study, PLK1 was amongst the top-upregulated genes and the use of the PLK1 inhibitor volasertib that showed anti-tumour effect in PDXs with acquired resistance to palbociclib. This raises an opportunity in targeting PLK1 as a potential therapeutic option in palbociclib-resistant breast cancer.

4.3.2 The identification of potential biomarkers of resistance to palbociclib

Growth Differentiation factor 15 (GDF15), also known as macrophage inhibitory cytokine-1 (MIC-1) or nonsteroidal anti-inflammatory drug-activated gene-1 (NAG-1), was one of the genes that was commonly upregulated in MCF7 and MCF7-LTED PalboR cells. The baseline expression of GDF15 in MCF7 was low and expression was increased in the palbociclib resistant cells. GDF15 is a member of TGF-β family and participates in various pathways such as inflammatory response and the activation of natural killer cells (Wischhusen *et al.*, 2020). GDF15 has also been shown to have a role in multiple diseases, specifically in several cancer types, where the literature has suggested that increased expression of GDF15 is associated with cancer progression, EMT and drug resistance (Muniyan *et al.*, 2022). In cervical cancer, GDF15 can activate the PI3K/AKT/ERK pathway and it has a role as a downstream target of p53. Interestingly, it was proposed that GDF15 expression is correlated with invasion and EMT via the mediation of mesenchymal factors through insulin-like growth factor receptor (IGF-R1) and FOXM1 in cancer types such as ER^- $HER2^+$ BCa (Peake *et al.*, 2017). However, the role of GDF15 in ER^+ BCa is not well defined. In particular, the function of GDF15 in palbociclib resistance has yet to be elucidated. The current transcriptomic data suggest that the increase of GDF15 expression was associated with palbociclib resistance. T47D-PalboR also showed

increased expression of GDF15, although its expression was not increased in HCC1428-PalboR cells. It would be interesting to investigate GDF15 expression in biopsies from patients with palbociclib-resistant BCa patients. The other question to be addressed in whether GDF15 expression is also elevated in abemaciclib and ribociclib resistance, or if it is a marker relevant for palbocicilib only. Interestingly, GDF15 is a p53 target gene (Osada *et al.*, 2007) and p53 dependent cell cycle arrest and senescence has been shown to be important the action of palbociclib in breast cancer cells (Wang *et al.*, 2022). Indeed, palbociclib treated MCF7 cells had upregulation of the p53 pathway, although genes in the p53 enriched cluster were downregulated in PalboR cells. It would also be surprising if PalboR cells had activated p53 since p53 activation would result in cell cycle arrest, apoptosis or senescence. So, the elevated expression of GDF15 in PalboR cells is unexpected. Using RT-qPCR I confirmed that GDF15 expression in low in MCF7 and MCF7-LTED-Y537C cells. Its expression increased when cells were treated with palbocicilib and were further elevated in PalboR cells. However, GDF15 levels were also elevated in the MCF7-LTED cells in which ER is not mutated. GDF15 was not expressed in HCC1428 or T47D LTED or PalboR cells. However, T47D cells are mutant for p53, while p53 has been reported to be absent in HCC1428 cells (Liang *et al.*, 2005) , which provides a potential explanation for lack of GDF15 expression in T47D-PalboR and HCC1428-PalboR cells. It should be noted that p53 mutations are relatively uncommon in ER^+ BCa, being seen in approximately 20% of ER^+ BCa, compared with almost 80% of TNBC (Nik-Zainal *et al.*, 2016). Thus, measurement of GDF15 expression may represent a biomarker of resistance to palbociclib. A number of studies have suggested that serum GDF15 can be used alongside prostate specific antigen (PSA) as prognostic factor in prostate cancer (Bansal *et al.*, 2017; Li *et al.*, 2015a). Monitoring serum GDF15 levels may therefore provide a non-invasive approach to monitoring emergence of palbociclib resistance, although the upregulation in LTED cells suggests a more widespread utility for GDF15 and may argue against possible development for monitoring palbociclib resistance. Obviously, such studies should be extended to the other CDK4/6 inhibitors.

S100P was also upregulated in cells with acquired resistance to palbociclib, which may be another the potential biomarker. S100P is a member of the S100 family of calcium binding proteins and is involved in the calcium dependent transduction pathways. S100P is also expressed in several tumour types and the overexpression is correlated to disease progression and drug resistance. Studies have suggested the involvement of S100P in promoting metastasis in breast cancer and that it may be associated with chemotherapy resistance in $HER2^+$ BCa.

Although S100P emerged as a possible biomarker in the MCF7 models, as in the cases of GDF15, its expression was elevated in ER-WT MCF7-LTED cells, so its utility again needs further assessment. Also as seen for GDF15, S100P expression was not elevated in HCC1428 or T47D cells. Whether this is also a reflection of the p53 status of these cell lines is suggested by the fact that S100P has been shown to interact with p53 to repress it activity (Gibadulinova *et al.*, 2016), although if it is a p53 target gene is not clear.

Dickkopf1 (DKK1) is an antagonist of the Wnt pathway, which may have various role in tumours in different cellular contexts. Specifically, the expression of DKK1 has been reported to be associated with bone metastasis in ER^-/PR^- BCa (Xu *et al.*, 2012b). Comparing common upregulated genes of palbociclib resistant cells showed that DKK1 was highly upregulated in MCF7 LTED Y537C cells and HCC1428 LTED. The role of DKK1 to palbocilcib may be limited, as RNA-seq revealed that the increased expression of DKK1 was resulted from cells in estrogen depleted conditions. Several publications have suggested that DKK1 is regulated by estrogen and be a marker of response to ET (Forget *et al.*, 2007). Our current palbociclib resistant models showed conflicting results and current data is inadequate to support the use of DKK1 as predictive marker of response to the combination of AI and palbociclib.

A major limitation of the current study is the focus on resistance models in one ER^+ BCa cell line. Additional resistance cell lines need to be assessed in a similar way, in order to improve on the generality of the effects. Towards this end, I have characterised T47D and HCC1428 PalboR models, although the fact that these two lines are either mutated or lack p53 expression may be problematic, given the importance of p53 in CDK4/6 inhibitor action, as summarised above. Cell lines nevertheless represent an important resource for modelling breast cancer, due to the ease of their manipulation using methods such as CRISPR-Cas9 knockout, knockins, gene activation and repression. However, near-patient material provides the tumour heterogeneity that is necessarily lacking in established cell lines. Thus, further studies focussing on patient derived explants and patient-derived organoids and patient-derived xenografts offer powerful approaches for investigating resistance mechanisms, especially where developed from patients who respond or progress on relevant drugs (Byrne *et al.*, 2017; Wensink *et al.*, 2021).

5. Summary

The current major clinical problem for patients with advanced BCa is the prevalence of resistance to CDK4/6 inhibitors and the lack of therapeutic options in the event of progression on these drugs. The further rollout of CDK4/6 inhibitors, combined with ET, in early-stage BCa patients further highlights the need for identifying resistance mechanisms, towards patient stratification and further therapeutic options. Thus, my thesis focused on developing in vitro palbociclib resistant models towards identifying possible mechanisms of CDK4/6 inhibitor resistance in ER^+ breast cancer cells. Highlights of the work undertaken are the development of *in vitro* models in which the potential contribution of other CDKs and cyclins can be assessed in growth and gene/protein expression analysis. I was able to demonstrate that CDK2 over-expression is sufficient to reduced sensitivity to palbociclib, but not to ribociclib or abemaciclib.

Secondly, continuous culturing of CDK2 and CDK6 over-expressing cells led to remarkably rapid, within 20-40 days, development of CDK4/6 inhibitor resistance. In this context, it is interesting to note that development of resistance to the SERD fulvestrant requires a minimum of 3-6 months in MCF7 cells (Shaw *et al.*, 2006). Using these models, in the main the MCF7-AcCas9-CDK6 cells, also showed that there are likely to be considerable differences in mechanisms of resistance to the three clinical CDK4/6 inhibitors. The potential for using the models developed here for testing other therapies, is also demonstrated with the use of the pre-clinical CDK7 inhibitors THZ1 and ICEC0942, which are in phase II clinical trials.

Finally, gene expression profiling (H3K27ac ChIP-seq, RNA-seq) identifies signalling pathways that are altered in palbociclib-resistant breast cancer cells and reveals potential genes for future development as biomarkers or for drug development.

References

Abe, S., Nagasaka, K., Hirayama, Y., Kozuka-Hata, H., Oyama, M., Aoyagi, Y., Obuse, C., and Hirota, T. (2011). The initial phase of chromosome condensation requires Cdk1-mediated phosphorylation of the CAP-D3 subunit of condensin II. Genes Dev 25, 863-874.

Adriaens, C., Standaert, L., Barra, J., Latil, M., Verfaillie, A., Kalev, P., Boeckx, B., Wijnhoven, P.W., Radaelli, E., Vermi, W., et al. (2016). p53 induces formation of NEAT1 lncRNA-containing paraspeckles that modulate replication stress response and chemosensitivity. Nat Med 22, 861-868.

Asghar, U.S., Barr, A.R., Cutts, R., Beaney, M., Babina, I., Sampath, D., Giltnane, J., Lacap, J.A., Crocker, L., Young, A., et al. (2017). Single-Cell Dynamics Determines Response to CDK4/6 Inhibition in Triple-Negative Breast Cancer. Clin Cancer Res 23, 5561-5572.

Bansal, N., Kumar, D., Gupta, A., Chandra, D., Sankhwar, S.N., and Mandhani, A. (2017). Relevance of MIC-1 in the Era of PSA as a Serum Based Predictor of Prostate Cancer: A Critical Evaluation. Sci Rep 7, 16824.

Barr, A.R., Heldt, F.S., Zhang, T., Bakal, C., and Novak, B. (2016). A Dynamical Framework for the All-or-None G1/S Transition. Cell Syst 2, 27-37.

Borah, N.A., and Reddy, M.M. (2021). Aurora Kinase B Inhibition: A Potential Therapeutic Strategy for Cancer. Molecules 26.

Chen, R., Liu, Y., Zhuang, H., Yang, B., Hei, K., Xiao, M., Hou, C., Gao, H., Zhang, X., Jia, C., et al. (2017). Quantitative proteomics reveals that long non-coding RNA MALAT1 interacts with DBC1 to regulate p53 acetylation. Nucleic Acids Res 45, 9947-9959.

Cowley, D.O., Rivera-Perez, J.A., Schliekelman, M., He, Y.J., Oliver, T.G., Lu, L., O'Quinn, R., Salmon, E.D., Magnuson, T., and Van Dyke, T. (2009). Aurora-A kinase is essential for bipolar spindle formation and early development. Mol Cell Biol 29, 1059-1071.

Crosio, C., Fimia, G.M., Loury, R., Kimura, M., Okano, Y., Zhou, H., Sen, S., Allis, C.D., and Sassone-Corsi, P. (2002). Mitotic phosphorylation of histone H3: spatio-temporal regulation by mammalian Aurora kinases. Mol Cell Biol 22, 874-885.

Finn, R.S., Dering, J., Conklin, D., Kalous, O., Cohen, D.J., Desai, A.J., Ginther, C., Atefi, M., Chen, I., Fowst, C., et al. (2009). PD 0332991, a selective cyclin D kinase 4/6 inhibitor, preferentially inhibits proliferation of luminal estrogen receptor-positive human breast cancer cell lines in vitro. Breast Cancer Res 11, R77.

Giet, R., Uzbekov, R., Cubizolles, F., Le Guellec, K., and Prigent, C. (1999). The Xenopus laevis aurora-related protein kinase pEg2 associates with and phosphorylates the kinesin-related protein XlEg5. J Biol Chem 274, 15005-15013.

Hafner, M., Mills, C.E., Subramanian, K., Chen, C., Chung, M., Boswell, S.A., Everley, R.A., Liu, C., Walmsley, C.S., Juric, D., et al. (2019). Multiomics Profiling Establishes the Polypharmacology of FDA-Approved CDK4/6 Inhibitors and the Potential for Differential Clinical Activity. Cell Chem Biol 26, 1067-1080 e1068.

Hirota, T., Kunitoku, N., Sasayama, T., Marumoto, T., Zhang, D., Nitta, M., Hatakeyama, K., and Saya, H. (2003). Aurora-A and an interacting activator, the LIM protein Ajuba, are required for mitotic commitment in human cells. Cell 114, 585-598.

Hirota, T., Lipp, J.J., Toh, B.H., and Peters, J.M. (2005). Histone H3 serine 10 phosphorylation by Aurora B causes HP1 dissociation from heterochromatin. Nature 438, 1176-1180.

Ji, D.G., Guan, L.Y., Luo, X., Ma, F., Yang, B., and Liu, H.Y. (2018). Inhibition of MALAT1 sensitizes liver cancer cells to 5-flurouracil by regulating apoptosis through IKKalpha/NF-kappaB pathway. Biochem Biophys Res Commun 501, 33-40.

Jiang, M.C., Ni, J.J., Cui, W.Y., Wang, B.Y., and Zhuo, W. (2019). Emerging roles of lncRNA in cancer and therapeutic opportunities. Am J Cancer Res 9, 1354-1366.

Kapalczynska, M., Kolenda, T., Przybyla, W., Zajaczkowska, M., Teresiak, A., Filas, V., Ibbs, M., Blizniak, R., Luczewski, L., and Lamperska, K. (2018). 2D and 3D cell cultures - a comparison of different types of cancer cell cultures. Arch Med Sci 14, 910-919.

Kelly, A.E., and Funabiki, H. (2009). Correcting aberrant kinetochore microtubule attachments: an Aurora B-centric view. Curr Opin Cell Biol 21, 51-58.

Kufer, T.A., Sillje, H.H., Korner, R., Gruss, O.J., Meraldi, P., and Nigg, E.A. (2002). Human TPX2 is required for targeting Aurora-A kinase to the spindle. J Cell Biol 158, 617-623.

Lacey, K.R., Jackson, P.K., and Stearns, T. (1999). Cyclin-dependent kinase control of centrosome duplication. Proc Natl Acad Sci U S A 96, 2817-2822.

Li, J., Veltri, R.W., Yuan, Z., Christudass, C.S., and Mandecki, W. (2015). Macrophage inhibitory cytokine 1 biomarker serum immunoassay in combination with PSA is a more specific diagnostic tool for detection of prostate cancer. PLoS One 10, e0122249.

Li, Z., Razavi, P., Li, Q., Toy, W., Liu, B., Ping, C., Hsieh, W., Sanchez-Vega, F., Brown, D.N., Da Cruz Paula, A.F., et al. (2018). Loss of the FAT1 Tumor Suppressor Promotes Resistance to CDK4/6 Inhibitors via the Hippo Pathway. Cancer Cell 34, 893-905 e898.

Liu, S.J., Dang, H.X., Lim, D.A., Feng, F.Y., and Maher, C.A. (2021). Long noncoding RNAs in cancer metastasis. Nat Rev Cancer 21, 446-460.

Meraldi, P., Lukas, J., Fry, A.M., Bartek, J., and Nigg, E.A. (1999). Centrosome duplication in mammalian somatic cells requires E2F and Cdk2-cyclin A. Nat Cell Biol 1, 88-93.

Miao, Y., Fan, R., Chen, L., and Qian, H. (2016). Clinical Significance of Long Non-coding RNA MALAT1 Expression in Tissue and Serum of Breast Cancer. Ann Clin Lab Sci 46, 418-424.

Montaudon, E., Nikitorowicz-Buniak, J., Sourd, L., Morisset, L., El Botty, R., Huguet, L., Dahmani, A., Painsec, P., Nemati, F., Vacher, S., et al. (2020). PLK1 inhibition exhibits strong anti-tumoral activity in CCND1-driven breast cancer metastases with acquired palbociclib resistance. Nat Commun 11, 4053.

Muniyan, S., Pothuraju, R., Seshacharyulu, P., and Batra, S.K. (2022). Macrophage inhibitory cytokine-1 in cancer: Beyond the cellular phenotype. Cancer Lett 536, 215664.

Nakazawa, N., Mehrotra, R., Ebe, M., and Yanagida, M. (2011). Condensin phosphorylated by the Aurora-B-like kinase Ark1 is continuously required until telophase in a mode distinct from Top2. J Cell Sci 124, 1795-1807.

Nie, L., Wei, Y., Zhang, F., Hsu, Y.H., Chan, L.C., Xia, W., Ke, B., Zhu, C., Deng, R., Tang, J., et al. (2019). CDK2-mediated site-specific phosphorylation of EZH2 drives and maintains triple-negative breast cancer. Nat Commun 10, 5114.

Nilsson, J., Yekezare, M., Minshull, J., and Pines, J. (2008). The APC/C maintains the spindle assembly checkpoint by targeting Cdc20 for destruction. Nat Cell Biol 10, 1411-1420.

Pandey, K., Katuwal, N.B., Park, N., Hur, J., Cho, Y.B., Kim, S.K., Lee, S.A., Kim, I., Lee, S.R., and Moon, Y.W. (2022). Combination of Abemaciclib following Eribulin Overcomes Palbociclib-Resistant Breast Cancer by Inhibiting the G2/M Cell Cycle Phase. Cancers (Basel) 14.

Pandey, K., Park, N., Park, K.S., Hur, J., Cho, Y.B., Kang, M., An, H.J., Kim, S., Hwang, S., and Moon, Y.W. (2020). Combined CDK2 and CDK4/6 Inhibition Overcomes Palbociclib Resistance in Breast Cancer by Enhancing Senescence. Cancers (Basel) 12.

Pardini, B., Sabo, A.A., Birolo, G., and Calin, G.A. (2019). Noncoding RNAs in Extracellular Fluids as Cancer Biomarkers: The New Frontier of Liquid Biopsies. Cancers (Basel) 11.

Peake, B.F., Eze, S.M., Yang, L., Castellino, R.C., and Nahta, R. (2017). Growth differentiation factor 15 mediates epithelial mesenchymal transition and invasion of breast cancers through IGF-1R-FoxM1 signaling. Oncotarget 8, 94393-94406.

Ruchaud, S., Carmena, M., and Earnshaw, W.C. (2007). The chromosomal passenger complex: one for all and all for one. Cell 131, 230-231.

Spencer, S.L., Cappell, S.D., Tsai, F.C., Overton, K.W., Wang, C.L., and Meyer, T. (2013). The proliferation-quiescence decision is controlled by a bifurcation in CDK2 activity at mitotic exit. Cell 155, 369-383.

Tada, K., Susumu, H., Sakuno, T., and Watanabe, Y. (2011). Condensin association with histone H2A shapes mitotic chromosomes. Nature 474, 477-483.

Tadesse, S., Anshabo, A.T., Portman, N., Lim, E., Tilley, W., Caldon, C.E., and Wang, S. (2020). Targeting CDK2 in cancer: challenges and opportunities for therapy. Drug Discov Today 25, 406-413.

Tano, K., Onoguchi-Mizutani, R., Yeasmin, F., Uchiumi, F., Suzuki, Y., Yada, T., and Akimitsu, N. (2017). Identification of Minimal p53 Promoter Region Regulated by MALAT1 in Human Lung Adenocarcinoma Cells. Front Genet 8, 208.

Tripathi, V., Shen, Z., Chakraborty, A., Giri, S., Freier, S.M., Wu, X., Zhang, Y., Gorospe, M., Prasanth, S.G., Lal, A., et al. (2013). Long noncoding RNA MALAT1 controls cell cycle progression by regulating the expression of oncogenic transcription factor B-MYB. PLoS Genet 9, e1003368.

Turner, N.C., Liu, Y., Zhu, Z., Loi, S., Colleoni, M., Loibl, S., DeMichele, A., Harbeck, N., Andre, F., Bayar, M.A., et al. (2019). Cyclin E1 Expression and Palbociclib Efficacy in Previously Treated Hormone Receptor-Positive Metastatic Breast Cancer. J Clin Oncol 37, 1169-1178.

West, J.A., Davis, C.P., Sunwoo, H., Simon, M.D., Sadreyev, R.I., Wang, P.I., Tolstorukov, M.Y., and Kingston, R.E. (2014). The long noncoding RNAs NEAT1 and MALAT1 bind active chromatin sites. Mol Cell 55, 791-802.

Wischhusen, J., Melero, I., and Fridman, W.H. (2020). Growth/Differentiation Factor-15 (GDF-15): From Biomarker to Novel Targetable Immune Checkpoint. Front Immunol 11, 951.

Wittmann, T., Wilm, M., Karsenti, E., and Vernos, I. (2000). TPX2, A novel xenopus MAP involved in spindle pole organization. J Cell Biol 149, 1405-1418.

Yang, C., Li, Z., Bhatt, T., Dickler, M., Giri, D., Scaltriti, M., Baselga, J., Rosen, N., and Chandarlapaty, S. (2017). Acquired CDK6 amplification promotes breast cancer resistance to CDK4/6 inhibitors and loss of ER signaling and dependence. Oncogene 36, 2255-2264.

Yang, L., Lin, C., Liu, W., Zhang, J., Ohgi, K.A., Grinstein, J.D., Dorrestein, P.C., and Rosenfeld, M.G. (2011). ncRNA- and Pc2 methylation-dependent gene relocation between nuclear structures mediates gene activation programs. Cell 147, 773-788.

Allis, C.D., and Jenuwein, T. (2016). The molecular hallmarks of epigenetic control. Nat Rev Genet 17, 487-500.

Alvarez-Fernandez, M., and Malumbres, M. (2020). Mechanisms of Sensitivity and Resistance to CDK4/6 Inhibition. Cancer Cell 37, 514-529.

Bannister, A.J., and Kouzarides, T. (2011). Regulation of chromatin by histone modifications. Cell Res 21, 381-395.

Burke, J.R., Hura, G.L., and Rubin, S.M. (2012). Structures of inactive retinoblastoma protein reveal multiple mechanisms for cell cycle control. Genes Dev 26, 1156-1166.

Calo, E., and Wysocka, J. (2013). Modification of enhancer chromatin: what, how, and why? Mol Cell 49, 825-837.

Condorelli, R., Spring, L., O'Shaughnessy, J., Lacroix, L., Bailleux, C., Scott, V., Dubois, J., Nagy, R.J., Lanman, R.B., Iafrate, A.J., et al. (2018). Polyclonal RB1 mutations and acquired resistance to CDK 4/6 inhibitors in patients with metastatic breast cancer. Ann Oncol 29, 640-645.

Creyghton, M.P., Cheng, A.W., Welstead, G.G., Kooistra, T., Carey, B.W., Steine, E.J., Hanna, J., Lodato, M.A., Frampton, G.M., Sharp, P.A., et al. (2010). Histone H3K27ac separates active from poised enhancers and predicts developmental state. Proc Natl Acad Sci U S A 107, 21931-21936.

Finn, R.S., Dering, J., Conklin, D., Kalous, O., Cohen, D.J., Desai, A.J., Ginther, C., Atefi, M., Chen, I., Fowst, C., et al. (2009). PD 0332991, a selective cyclin D kinase 4/6 inhibitor, preferentially inhibits proliferation of luminal estrogen receptor-positive human breast cancer cell lines in vitro. Breast Cancer Res 11, R77.

Herrera-Abreu, M.T., Palafox, M., Asghar, U., Rivas, M.A., Cutts, R.J., Garcia-Murillas, I., Pearson, A., Guzman, M., Rodriguez, O., Grueso, J., et al. (2016). Early Adaptation and Acquired Resistance to CDK4/6 Inhibition in Estrogen Receptor-Positive Breast Cancer. Cancer Res 76, 2301-2313.

Konermann, S., Brigham, M.D., Trevino, A.E., Joung, J., Abudayyeh, O.O., Barcena, C., Hsu, P.D., Habib, N., Gootenberg, J.S., Nishimasu, H., et al. (2015). Genome-scale transcriptional activation by an engineered CRISPR-Cas9 complex. Nature 517, 583-588.

Kwiatkowski, N., Zhang, T., Rahl, P.B., Abraham, B.J., Reddy, J., Ficarro, S.B., Dastur, A., Amzallag, A., Ramaswamy, S., Tesar, B., et al. (2014). Targeting transcription regulation in cancer with a covalent CDK7 inhibitor. Nature 511, 616-620.

Martin, L.-A., Pancholi, S., Ribas, R., Gao, Q., Simigdala, N., Nikitorowicz-Buniak, J., Johnston, S., and Dowsett, M. (2017a). Abstract P3-03-09: Resistance to palbociclib depends on multiple targetable mechanisms highlighting the potential of drug holidays and drug switching to improve therapeutic outcome. Cancer Research 77, P3-03-09-P03-03-09.

Martin, L.A., Ribas, R., Simigdala, N., Schuster, E., Pancholi, S., Tenev, T., Gellert, P., Buluwela, L., Harrod, A., Thornhill, A., et al. (2017b). Discovery of naturally occurring ESR1 mutations in breast cancer cell lines modelling endocrine resistance. Nat Commun 8, 1865.

Olson, C.M., Liang, Y., Leggett, A., Park, W.D., Li, L., Mills, C.E., Elsarrag, S.Z., Ficarro, S.B., Zhang, T., Duster, R., et al. (2019). Development of a Selective CDK7 Covalent Inhibitor Reveals Predominant Cell-Cycle Phenotype. Cell Chem Biol.

Pancholi, S., Ribas, R., Simigdala, N., Schuster, E., Nikitorowicz-Buniak, J., Ressa, A., Gao, Q., Leal, M.F., Bhamra, A., Thornhill, A., et al. (2020). Tumour kinome re-wiring governs resistance to palbociclib in oestrogen receptor positive breast cancers, highlighting new therapeutic modalities. Oncogene 39, 4781-4797.

Pandey, K., An, H.J., Kim, S.K., Lee, S.A., Kim, S., Lim, S.M., Kim, G.M., Sohn, J., and Moon, Y.W. (2018). Molecular mechanisms of resistance to CDK4/6 inhibitors in breast cancer: A review. Int J Cancer.

Patel, H., Periyasamy, M., Sava, G.P., Bondke, A., Slafer, B.W., Kroll, S.H.B., Barbazanges, M., Starkey, R., Ottaviani, S., Harrod, A., et al. (2018). ICEC0942, an Orally Bioavailable Selective Inhibitor of CDK7 for Cancer Treatment. Mol Cancer Ther 17, 1156-1166.

Portela, A., and Esteller, M. (2010). Epigenetic modifications and human disease. Nat Biotechnol 28, 1057-1068.

Rondon-Lagos, M., Verdun Di Cantogno, L., Marchio, C., Rangel, N., Payan-Gomez, C., Gugliotta, P., Botta, C., Bussolati, G., Ramirez-Clavijo, S.R., Pasini, B., et al. (2014). Differences and homologies of chromosomal alterations within and between breast cancer cell lines: a clustering analysis. Mol Cytogenet 7, 8.

Teh, J.L.F., and Aplin, A.E. (2019). Arrested Developments: CDK4/6 Inhibitor Resistance and Alterations in the Tumor Immune Microenvironment. Clin Cancer Res 25, 921-927.

Wang, S., Zang, C., Xiao, T., Fan, J., Mei, S., Qin, Q., Wu, Q., Li, X., Xu, K., He, H.H., et al. (2016). Modeling cis-regulation with a compendium of genome-wide histone H3K27ac profiles. Genome Res 26, 1417-1429.

Yang, C., Li, Z., Bhatt, T., Dickler, M., Giri, D., Scaltriti, M., Baselga, J., Rosen, N., and Chandarlapaty, S. (2017). Acquired CDK6 amplification promotes breast cancer resistance to CDK4/6 inhibitors and loss of ER signaling and dependence. Oncogene 36, 2255-2264.

Abbas, T., and Dutta, A. (2009). p21 in cancer: intricate networks and multiple activities. Nat Rev Cancer *9*, 400-414.

Acconcia, F., and Kumar, R. (2006). Signaling regulation of genomic and nongenomic functions of estrogen receptors. Cancer Lett *238*, 1-14.

Adkins, D., Ley, J., Neupane, P., Worden, F., Sacco, A.G., Palka, K., Grilley-Olson, J.E., Maggiore, R., Salama, N.N., Trinkaus, K., Van Tine, B.A., Steuer, C.E., Saba, N.F., and Oppelt, P. (2019). Palbociclib and cetuximab in platinum-resistant and in cetuximab-resistant human papillomavirus-unrelated head and neck cancer: a multicentre, multigroup, phase 2 trial. Lancet Oncol *20*, 1295-1305.

Afonso, O., Matos, I., Pereira, A.J., Aguiar, P., Lampson, M.A., and Maiato, H. (2014). Feedback control of chromosome separation by a midzone Aurora B gradient. Science *345*, 332-336.

Aguilar-Fuentes, J., Fregoso, M., Herrera, M., Reynaud, E., Braun, C., Egly, J.M., and Zurita, M. (2008). p8/TTDA overexpression enhances UV-irradiation resistance and suppresses TFIIH mutations in a Drosophila trichothiodystrophy model. PLoS Genet *4*, e1000253.

Akoulitchev, S., Chuikov, S., and Reinberg, D. (2000). TFIIH is negatively regulated by cdk8-containing mediator complexes. Nature *407*, 102-106.

Alao, J.P. (2007). The regulation of cyclin D1 degradation: roles in cancer development and the potential for therapeutic invention. Mol Cancer *6*, 24.

Albanito, L., Madeo, A., Lappano, R., Vivacqua, A., Rago, V., Carpino, A., Oprea, T.I., Prossnitz, E.R., Musti, A.M., Ando, S., and Maggiolini, M. (2007). G protein-coupled receptor 30 (GPR30) mediates gene expression changes and growth response to 17beta-estradiol and selective GPR30 ligand G-1 in ovarian cancer cells. Cancer Res *67*, 1859-1866.

Albrektsen, G., Heuch, I., Hansen, S., and Kvale, G. (2005). Breast cancer risk by age at birth, time since birth and time intervals between births: exploring interaction effects. Br J Cancer *92*, 167-175.

AlFakeeh, A., and Brezden-Masley, C. (2018). Overcoming endocrine resistance in hormone receptor-positive breast cancer. Curr Oncol *25*, S18-S27.

Ali, S., and Coombes, R.C. (2002). Endocrine-responsive breast cancer and strategies for combating resistance. Nat Rev Cancer *2*, 101-112.

Ali, S., Heathcote, D.A., Kroll, S.H., Jogalekar, A.S., Scheiper, B., Patel, H., Brackow, J., Siwicka, A., Fuchter, M.J., Periyasamy, M., Tolhurst, R.S., Kanneganti, S.K., Snyder, J.P., Liotta, D.C., Aboagye, E.O., Barrett, A.G., and Coombes, R.C. (2009). The development of a selective cyclin-dependent kinase inhibitor that shows antitumor activity. Cancer Res *69*, 6208-6215.

Allen, B.L., and Taatjes, D.J. (2015). The Mediator complex: a central integrator of transcription. Nat Rev Mol Cell Biol *16*, 155-166.

Allis, C.D., and Jenuwein, T. (2016). The molecular hallmarks of epigenetic control. Nat Rev Genet *17*, 487-500.

Alsop, G.B., and Zhang, D. (2003). Microtubules are the only structural constituent of the spindle apparatus required for induction of cell cleavage. J Cell Biol *162*, 383-390.
Alt, J.R., Gladden, A.B., and Diehl, J.A. (2002). p21(Cip1) Promotes cyclin D1 nuclear accumulation via direct inhibition of nuclear export. J Biol Chem *277*, 8517-8523.
Alvarez-Fernandez, M., and Malumbres, M. (2020). Mechanisms of Sensitivity and Resistance to CDK4/6 Inhibition. Cancer Cell *37*, 514-529.
Alvi, A.J., Austen, B., Weston, V.J., Fegan, C., MacCallum, D., Gianella-Borradori, A., Lane, D.P., Hubank, M., Powell, J.E., Wei, W., Taylor, A.M., Moss, P.A., and Stankovic, T. (2005). A novel CDK inhibitor, CYC202 (R-roscovitine), overcomes the defect in p53-dependent apoptosis in B-CLL by down-regulation of genes involved in transcription regulation and survival. Blood *105*, 4484-4491.
An, H.X., Beckmann, M.W., Reifenberger, G., Bender, H.G., and Niederacher, D. (1999). Gene amplification and overexpression of CDK4 in sporadic breast carcinomas is associated with high tumor cell proliferation. Am J Pathol *154*, 113-118.
Anbalagan, M., and Rowan, B.G. (2015). Estrogen receptor alpha phosphorylation and its functional impact in human breast cancer. Mol Cell Endocrinol *418 Pt 3*, 264-272.
Anders, L., Ke, N., Hydbring, P., Choi, Y.J., Widlund, H.R., Chick, J.M., Zhai, H., Vidal, M., Gygi, S.P., Braun, P., and Sicinski, P. (2011). A systematic screen for CDK4/6 substrates links FOXM1 phosphorylation to senescence suppression in cancer cells. Cancer Cell *20*, 620-634.
Andersen, G., Busso, D., Poterszman, A., Hwang, J.R., Wurtz, J.M., Ripp, R., Thierry, J.C., Egly, J.M., and Moras, D. (1997). The structure of cyclin H: common mode of kinase activation and specific features. EMBO J *16*, 958-967.
Andersen, G., Poterszman, A., Egly, J.M., Moras, D., and Thierry, J.C. (1996). The crystal structure of human cyclin H. FEBS Lett *397*, 65-69.
Andre, F., Ciruelos, E., Rubovszky, G., Campone, M., Loibl, S., Rugo, H.S., Iwata, H., Conte, P., Mayer, I.A., Kaufman, B., Yamashita, T., Lu, Y.S., Inoue, K., Takahashi, M., Papai, Z., Longin, A.S., Mills, D., Wilke, C., Hirawat, S., Juric, D., and Group, S.-S. (2019). Alpelisib for PIK3CA-Mutated, Hormone Receptor-Positive Advanced Breast Cancer. N Engl J Med *380*, 1929-1940.
Andrieu, G., Tran, A.H., Strissel, K.J., and Denis, G.V. (2016). BRD4 Regulates Breast Cancer Dissemination through Jagged1/Notch1 Signaling. Cancer Res *76*, 6555-6567.
Arao, Y., Hamilton, K.J., Coons, L.A., and Korach, K.S. (2013). Estrogen receptor alpha L543A,L544A mutation changes antagonists to agonists, correlating with the ligand binding domain dimerization associated with DNA binding activity. J Biol Chem *288*, 21105-21116.

Arnold, A., Motokura, T., Bloom, T., Kronenberg, H., Ruderman, J., Juppner, H., and Kim, H.G. (1991). The putative oncogene PRAD1 encodes a novel cyclin. Cold Spring Harb Symp Quant Biol *56*, 93-97.

Arnold, A., and Papanikolaou, A. (2005). Cyclin D1 in breast cancer pathogenesis. J Clin Oncol *23*, 4215-4224.

Arnold, S.F., Obourn, J.D., Jaffe, H., and Notides, A.C. (1994). Serine 167 is the major estradiol-induced phosphorylation site on the human estrogen receptor. Mol Endocrinol *8*, 1208-1214.

Aronica, S.M., Kraus, W.L., and Katzenellenbogen, B.S. (1994). Estrogen action via the cAMP signaling pathway: stimulation of adenylate cyclase and cAMP-regulated gene transcription. Proc Natl Acad Sci U S A *91*, 8517-8521.

Arruabarrena-Aristorena, A., Maag, J.L.V., Kittane, S., Cai, Y., Karthaus, W.R., Ladewig, E., Park, J., Kannan, S., Ferrando, L., Cocco, E., Ho, S.Y., Tan, D.S., Sallaku, M., Wu, F., Acevedo, B., Selenica, P., Ross, D.S., Witkin, M., Sawyers, C.L., Reis-Filho, J.S., Verma, C.S., Jauch, R., Koche, R., Baselga, J., Razavi, P., Toska, E., and Scaltriti, M. (2020). FOXA1 Mutations Reveal Distinct Chromatin Profiles and Influence Therapeutic Response in Breast Cancer. Cancer Cell *38*, 534-550 e539.

Asghar, U., Witkiewicz, A.K., Turner, N.C., and Knudsen, E.S. (2015). The history and future of targeting cyclin-dependent kinases in cancer therapy. Nat Rev Drug Discov *14*, 130-146.

Aulmann, S., Adler, N., Rom, J., Helmchen, B., Schirmacher, P., and Sinn, H.P. (2006). c-myc amplifications in primary breast carcinomas and their local recurrences. J Clin Pathol *59*, 424-428.

Bachelot, T., Bourgier, C., Cropet, C., Ray-Coquard, I., Ferrero, J.M., Freyer, G., Abadie-Lacourtoisie, S., Eymard, J.C., Debled, M., Spaeth, D., Legouffe, E., Allouache, D., El Kouri, C., and Pujade-Lauraine, E. (2012). Randomized phase II trial of everolimus in combination with tamoxifen in patients with hormone receptor-positive, human epidermal growth factor receptor 2-negative metastatic breast cancer with prior exposure to aromatase inhibitors: a GINECO study. J Clin Oncol *30*, 2718-2724.

Baker, G.L., Landis, M.W., and Hinds, P.W. (2005). Multiple functions of D-type cyclins can antagonize pRb-mediated suppression of proliferation. Cell Cycle *4*, 330-338.

Baldin, V., Lukas, J., Marcote, M.J., Pagano, M., and Draetta, G. (1993). Cyclin D1 is a nuclear protein required for cell cycle progression in G1. Genes Dev *7*, 812-821.

Bange, J., Zwick, E., and Ullrich, A. (2001). Molecular targets for breast cancer therapy and prevention. Nat Med *7*, 548-552.

Bannister, A.J., and Kouzarides, T. (2011). Regulation of chromatin by histone modifications. Cell Res *21*, 381-395.

Bansal, N., Kumar, D., Gupta, A., Chandra, D., Sankhwar, S.N., and Mandhani, A. (2017). Relevance of MIC-1 in the Era of PSA as a Serum Based Predictor of Prostate Cancer: A Critical Evaluation. Sci Rep *7*, 16824.

Barlaam, B., Casella, R., Cidado, J., Cook, C., De Savi, C., Dishington, A., Donald, C.S., Drew, L., Ferguson, A.D., Ferguson, D., Glossop, S., Grebe, T., Gu, C., Hande, S., Hawkins, J., Hird, A.W., Holmes, J., Horstick, J., Jiang, Y., Lamb, M.L., McGuire, T.M., Moore, J.E., O'Connell, N., Pike, A., Pike, K.G., Proia, T., Roberts, B., San Martin, M., Sarkar, U., Shao, W., Stead, D., Sumner, N., Thakur, K., Vasbinder, M.M., Varnes, J.G., Wang, J., Wang, L., Wu, D., Wu, L., Yang, B., and Yao, T. (2020). Discovery of AZD4573, a Potent and Selective Inhibitor of CDK9 That Enables Short Duration of Target Engagement for the Treatment of Hematological Malignancies. J Med Chem *63*, 15564-15590.

Bartkowiak, B., Liu, P., Phatnani, H.P., Fuda, N.J., Cooper, J.J., Price, D.H., Adelman, K., Lis, J.T., and Greenleaf, A.L. (2010). CDK12 is a transcription elongation-associated CTD kinase, the metazoan ortholog of yeast Ctk1. Genes Dev *24*, 2303-2316.

Bartova, I., Koca, J., and Otyepka, M. (2008). Functional flexibility of human cyclin-dependent kinase-2 and its evolutionary conservation. Protein Sci *17*, 22-33.

Basant, A., Lekomtsev, S., Tse, Y.C., Zhang, D., Longhini, K.M., Petronczki, M., and Glotzer, M. (2015). Aurora B kinase promotes cytokinesis by inducing centralspindlin oligomers that associate with the plasma membrane. Dev Cell *33*, 204-215.

Baselga, J., Campone, M., Piccart, M., Burris, H.A., 3rd, Rugo, H.S., Sahmoud, T., Noguchi, S., Gnant, M., Pritchard, K.I., Lebrun, F., Beck, J.T., Ito, Y., Yardley, D., Deleu, I., Perez, A., Bachelot, T., Vittori, L., Xu, Z., Mukhopadhyay, P., Lebwohl, D., and Hortobagyi, G.N. (2012). Everolimus in postmenopausal hormone-receptor-positive advanced breast cancer. N Engl J Med *366*, 520-529.

Bashir, T., Dorrello, N.V., Amador, V., Guardavaccaro, D., and Pagano, M. (2004). Control of the SCF(Skp2-Cks1) ubiquitin ligase by the APC/C(Cdh1) ubiquitin ligase. Nature *428*, 190-193.

Beatson, G.T. (1896). On the Treatment of Inoperable Cases of Carcinoma of the Mamma: Suggestions for a New Method of Treatment, with Illustrative Cases. Trans Med Chir Soc Edinb *15*, 153-179.

Beck, J., Handgretinger, R., Dopfer, R., Klingebiel, T., Niethammer, D., and Gekeler, V. (1995). Expression of mdr1, mrp, topoisomerase II alpha/beta, and cyclin A in primary or relapsed states of acute lymphoblastic leukaemias. Br J Haematol *89*, 356-363.

Bedrosian, I., Lu, K.H., Verschraegen, C., and Keyomarsi, K. (2004). Cyclin E deregulation alters the biologic properties of ovarian cancer cells. Oncogene *23*, 2648-2657.
Bell, C.G. (2011). Integration of genomic and epigenomic DNA methylation data in common complex diseases by haplotype-specific methylation analysis. Per Med *8*, 243-251.
Bergman, L., Beelen, M.L., Gallee, M.P., Hollema, H., Benraadt, J., and van Leeuwen, F.E. (2000). Risk and prognosis of endometrial cancer after tamoxifen for breast cancer. Comprehensive Cancer Centres' ALERT Group. Assessment of Liver and Endometrial cancer Risk following Tamoxifen. Lancet *356*, 881-887.
Bernardo, G.M., Lozada, K.L., Miedler, J.D., Harburg, G., Hewitt, S.C., Mosley, J.D., Godwin, A.K., Korach, K.S., Visvader, J.E., Kaestner, K.H., Abdul-Karim, F.W., Montano, M.M., and Keri, R.A. (2010). FOXA1 is an essential determinant of ERalpha expression and mammary ductal morphogenesis. Development *137*, 2045-2054.
Bertelli, G., Garrone, O., Merlano, M., Occelli, M., Bertolotti, L., Castiglione, F., Pepi, F., Fusco, O., Del Mastro, L., and Leonard, R.C. (2005). Sequential treatment with exemestane and non-steroidal aromatase inhibitors in advanced breast cancer. Oncology *69*, 471-477.
Bertoli, C., Skotheim, J.M., and de Bruin, R.A. (2013). Control of cell cycle transcription during G1 and S phases. Nat Rev Mol Cell Biol *14*, 518-528.
Besnard, E., Babled, A., Lapasset, L., Milhavet, O., Parrinello, H., Dantec, C., Marin, J.M., and Lemaitre, J.M. (2012). Unraveling cell type-specific and reprogrammable human replication origin signatures associated with G-quadruplex consensus motifs. Nat Struct Mol Biol *19*, 837-844.
Besson, A., Dowdy, S.F., and Roberts, J.M. (2008). CDK inhibitors: cell cycle regulators and beyond. Dev Cell *14*, 159-169.
Bhat-Nakshatri, P., Wang, G., Appaiah, H., Luktuke, N., Carroll, J.S., Geistlinger, T.R., Brown, M., Badve, S., Liu, Y., and Nakshatri, H. (2008). AKT alters genome-wide estrogen receptor alpha binding and impacts estrogen signaling in breast cancer. Mol Cell Biol *28*, 7487-7503.
Bieche, I., Olivi, M., Nogues, C., Vidaud, M., and Lidereau, R. (2002). Prognostic value of CCND1 gene status in sporadic breast tumours, as determined by real-time quantitative PCR assays. Br J Cancer *86*, 580-586.
Bienvenu, F., Jirawatnotai, S., Elias, J.E., Meyer, C.A., Mizeracka, K., Marson, A., Frampton, G.M., Cole, M.F., Odom, D.T., Odajima, J., Geng, Y., Zagozdzon, A., Jecrois, M., Young, R.A., Liu, X.S., Cepko, C.L., Gygi, S.P., and Sicinski, P. (2010). Transcriptional role of cyclin D1 in development revealed by a genetic-proteomic screen. Nature *463*, 374-378.

Bines, J., Dienstmann, R., Obadia, R.M., Branco, L.G.P., Quintella, D.C., Castro, T.M., Camacho, P.G., Soares, F.A., and Costa, M.E.F. (2014). Activity of megestrol acetate in postmenopausal women with advanced breast cancer after nonsteroidal aromatase inhibitor failure: a phase II trial. Ann Oncol *25*, 831-836.

Blazek, D., Kohoutek, J., Bartholomeeusen, K., Johansen, E., Hulinkova, P., Luo, Z., Cimermancic, P., Ule, J., and Peterlin, B.M. (2011). The Cyclin K/Cdk12 complex maintains genomic stability via regulation of expression of DNA damage response genes. Genes Dev *25*, 2158-2172.

Blegen, H., Einhorn, N., Sjovall, K., Roschke, A., Ghadimi, B.M., McShane, L.M., Nilsson, B., Shah, K., Ried, T., and Auer, G. (2000). Prognostic significance of cell cycle proteins and genomic instability in borderline, early and advanced stage ovarian carcinomas. Int J Gynecol Cancer *10*, 477-487.

Blethrow, J.D., Glavy, J.S., Morgan, D.O., and Shokat, K.M. (2008). Covalent capture of kinase-specific phosphopeptides reveals Cdk1-cyclin B substrates. Proc Natl Acad Sci U S A *105*, 1442-1447.

Blow, J.J., and Gillespie, P.J. (2008). Replication licensing and cancer--a fatal entanglement? Nat Rev Cancer *8*, 799-806.

Blow, J.J., and Hodgson, B. (2002). Replication licensing--defining the proliferative state? Trends Cell Biol *12*, 72-78.

Blows, F.M., Driver, K.E., Schmidt, M.K., Broeks, A., van Leeuwen, F.E., Wesseling, J., Cheang, M.C., Gelmon, K., Nielsen, T.O., Blomqvist, C., Heikkila, P., Heikkinen, T., Nevanlinna, H., Akslen, L.A., Begin, L.R., Foulkes, W.D., Couch, F.J., Wang, X., Cafourek, V., Olson, J.E., Baglietto, L., Giles, G.G., Severi, G., McLean, C.A., Southey, M.C., Rakha, E., Green, A.R., Ellis, I.O., Sherman, M.E., Lissowska, J., Anderson, W.F., Cox, A., Cross, S.S., Reed, M.W., Provenzano, E., Dawson, S.J., Dunning, A.M., Humphreys, M., Easton, D.F., Garcia-Closas, M., Caldas, C., Pharoah, P.D., and Huntsman, D. (2010). Subtyping of breast cancer by immunohistochemistry to investigate a relationship between subtype and short and long term survival: a collaborative analysis of data for 10,159 cases from 12 studies. PLoS Med *7*, e1000279.

Bockstaele, L., Kooken, H., Libert, F., Paternot, S., Dumont, J.E., de Launoit, Y., Roger, P.P., and Coulonval, K. (2006). Regulated activating Thr172 phosphorylation of cyclin-dependent kinase 4(CDK4): its relationship with cyclins and CDK "inhibitors". Mol Cell Biol *26*, 5070-5085.

Bonni, A., Brunet, A., West, A.E., Datta, S.R., Takasu, M.A., and Greenberg, M.E. (1999). Cell survival promoted by the Ras-MAPK signaling pathway by transcription-dependent and -independent mechanisms. Science *286*, 1358-1362.

Bornstein, G., Bloom, J., Sitry-Shevah, D., Nakayama, K., Pagano, M., and Hershko, A. (2003). Role of the SCFSkp2 ubiquitin ligase in the degradation of p21Cip1 in S phase. J Biol Chem *278*, 25752-25757.

Bourguet, W., Ruff, M., Chambon, P., Gronemeyer, H., and Moras, D. (1995). Crystal structure of the ligand-binding domain of the human nuclear receptor RXR-alpha. Nature *375*, 377-382.

Bourne, Y., Watson, M.H., Hickey, M.J., Holmes, W., Rocque, W., Reed, S.I., and Tainer, J.A. (1996). Crystal structure and mutational analysis of the human CDK2 kinase complex with cell cycle-regulatory protein CksHs1. Cell *84*, 863-874.

Bracken, A.P., Ciro, M., Cocito, A., and Helin, K. (2004). E2F target genes: unraveling the biology. Trends Biochem Sci *29*, 409-417.

Bradner, J.E., Hnisz, D., and Young, R.A. (2017). Transcriptional Addiction in Cancer. Cell *168*, 629-643.

Bretschneider, N., Kangaspeska, S., Seifert, M., Reid, G., Gannon, F., and Denger, S. (2008). E2-mediated cathepsin D (CTSD) activation involves looping of distal enhancer elements. Mol Oncol *2*, 182-190.

Broude, E.V., Gyorffy, B., Chumanevich, A.A., Chen, M., McDermott, M.S., Shtutman, M., Catroppo, J.F., and Roninson, I.B. (2015). Expression of CDK8 and CDK8-interacting Genes as Potential Biomarkers in Breast Cancer. Curr Cancer Drug Targets *15*, 739-749.

Brzozowski, A.M., Pike, A.C., Dauter, Z., Hubbard, R.E., Bonn, T., Engstrom, O., Ohman, L., Greene, G.L., Gustafsson, J.A., and Carlquist, M. (1997). Molecular basis of agonism and antagonism in the oestrogen receptor. Nature *389*, 753-758.

Buck, M., Poli, V., van der Geer, P., Chojkier, M., and Hunter, T. (1999). Phosphorylation of rat serine 105 or mouse threonine 217 in C/EBP beta is required for hepatocyte proliferation induced by TGF alpha. Mol Cell *4*, 1087-1092.

Buck, R.C., and Tidsale, J.M. (1962). An electron microscopic study of the cleavage furrow in mammalian cells. J Cell Biol *13*, 117-125.

Bukholm, I.R., Bukholm, G., and Nesland, J.M. (2001). Over-expression of cyclin A is highly associated with early relapse and reduced survival in patients with primary breast carcinomas. Int J Cancer *93*, 283-287.

Buratowski, S., Hahn, S., Guarente, L., and Sharp, P.A. (1989). Five intermediate complexes in transcription initiation by RNA polymerase II. Cell *56*, 549-561.

Burgess, R.J., and Zhang, Z. (2013). Histone chaperones in nucleosome assembly and human disease. Nat Struct Mol Biol *20*, 14-22.
Burke, J.R., Hura, G.L., and Rubin, S.M. (2012). Structures of inactive retinoblastoma protein reveal multiple mechanisms for cell cycle control. Genes Dev *26*, 1156-1166.
Byers, B., and Abramson, D.H. (1968). Cytokinesis in HeLa: post-telophase delay and microtubule-associated motility. Protoplasma *66*, 413-435.
Byrd, J.C., Lin, T.S., Dalton, J.T., Wu, D., Phelps, M.A., Fischer, B., Moran, M., Blum, K.A., Rovin, B., Brooker-McEldowney, M., Broering, S., Schaaf, L.J., Johnson, A.J., Lucas, D.M., Heerema, N.A., Lozanski, G., Young, D.C., Suarez, J.R., Colevas, A.D., and Grever, M.R. (2007). Flavopiridol administered using a pharmacologically derived schedule is associated with marked clinical efficacy in refractory, genetically high-risk chronic lymphocytic leukemia. Blood *109*, 399-404.
Byrne, A.T., Alferez, D.G., Amant, F., Annibali, D., Arribas, J., Biankin, A.V., Bruna, A., Budinska, E., Caldas, C., Chang, D.K., Clarke, R.B., Clevers, H., Coukos, G., Dangles-Marie, V., Eckhardt, S.G., Gonzalez-Suarez, E., Hermans, E., Hidalgo, M., Jarzabek, M.A., de Jong, S., Jonkers, J., Kemper, K., Lanfrancone, L., Maelandsmo, G.M., Marangoni, E., Marine, J.C., Medico, E., Norum, J.H., Palmer, H.G., Peeper, D.S., Pelicci, P.G., Piris-Gimenez, A., Roman-Roman, S., Rueda, O.M., Seoane, J., Serra, V., Soucek, L., Vanhecke, D., Villanueva, A., Vinolo, E., Bertotti, A., and Trusolino, L. (2017). Interrogating open issues in cancer precision medicine with patient-derived xenografts. Nat Rev Cancer *17*, 254-268.
Caldon, C.E., and Musgrove, E.A. (2010). Distinct and redundant functions of cyclin E1 and cyclin E2 in development and cancer. Cell Div *5*, 2.
Caldon, C.E., Sergio, C.M., Kang, J., Muthukaruppan, A., Boersma, M.N., Stone, A., Barraclough, J., Lee, C.S., Black, M.A., Miller, L.D., Gee, J.M., Nicholson, R.I., Sutherland, R.L., Print, C.G., and Musgrove, E.A. (2012). Cyclin E2 overexpression is associated with endocrine resistance but not insensitivity to CDK2 inhibition in human breast cancer cells. Mol Cancer Ther *11*, 1488-1499.
Calo, E., and Wysocka, J. (2013). Modification of enhancer chromatin: what, how, and why? Mol Cell *49*, 825-837.
Cancer Genome Atlas, N. (2012). Comprehensive molecular portraits of human breast tumours. Nature *490*, 61-70.
Capalbo, L., Montembault, E., Takeda, T., Bassi, Z.I., Glover, D.M., and D'Avino, P.P. (2012). The chromosomal passenger complex controls the function of endosomal sorting complex required for transport-III Snf7 proteins during cytokinesis. Open Biol *2*, 120070.

Carlson, M.E., Hsu, M., and Conboy, I.M. (2008). Imbalance between pSmad3 and Notch induces CDK inhibitors in old muscle stem cells. Nature *454*, 528-532.
Carlton, J.G., Caballe, A., Agromayor, M., Kloc, M., and Martin-Serrano, J. (2012). ESCRT-III governs the Aurora B-mediated abscission checkpoint through CHMP4C. Science *336*, 220-225.
Carnero, A. (2002). Targeting the cell cycle for cancer therapy. Br J Cancer *87*, 129-133.
Carroll, J.S., and Brown, M. (2006). Estrogen receptor target gene: an evolving concept. Mol Endocrinol *20*, 1707-1714.
Carroll, J.S., Hickey, T.E., Tarulli, G.A., Williams, M., and Tilley, W.D. (2017). Deciphering the divergent roles of progestogens in breast cancer. Nat Rev Cancer *17*, 54-64.
Carroll, J.S., Liu, X.S., Brodsky, A.S., Li, W., Meyer, C.A., Szary, A.J., Eeckhoute, J., Shao, W., Hestermann, E.V., Geistlinger, T.R., Fox, E.A., Silver, P.A., and Brown, M. (2005). Chromosome-wide mapping of estrogen receptor binding reveals long-range regulation requiring the forkhead protein FoxA1. Cell *122*, 33-43.
Cartwright, P., Muller, H., Wagener, C., Holm, K., and Helin, K. (1998). E2F-6: a novel member of the E2F family is an inhibitor of E2F-dependent transcription. Oncogene *17*, 611-623.
Carvajal, L.A., Hamard, P.J., Tonnessen, C., and Manfredi, J.J. (2012). E2F7, a novel target, is up-regulated by p53 and mediates DNA damage-dependent transcriptional repression. Genes Dev *26*, 1533-1545.
Castellano, D.E., Rubio, C., López-Calderón, F., Segovia, C., Porto, M.D., Martinez-Fernandez, M., Otero, I., Manneh, R., Sepúlveda, J.M., Villacampa, F., and Paramio, J. (2016). RB-independent activity of Cdk4/6 in bladder cancer. Journal of Clinical Oncology *34*, e16011-e16011.
Cazales, M., Schmitt, E., Montembault, E., Dozier, C., Prigent, C., and Ducommun, B. (2005). CDC25B phosphorylation by Aurora-A occurs at the G2/M transition and is inhibited by DNA damage. Cell Cycle *4*, 1233-1238.
Chabbert-Buffet, N., Meduri, G., Bouchard, P., and Spitz, I.M. (2005). Selective progesterone receptor modulators and progesterone antagonists: mechanisms of action and clinical applications. Hum Reprod Update *11*, 293-307.
Cheang, M.C., Chia, S.K., Voduc, D., Gao, D., Leung, S., Snider, J., Watson, M., Davies, S., Bernard, P.S., Parker, J.S., Perou, C.M., Ellis, M.J., and Nielsen, T.O. (2009). Ki67 index, HER2 status, and prognosis of patients with luminal B breast cancer. J Natl Cancer Inst *101*, 736-750.

Chen, C.R., Kang, Y., Siegel, P.M., and Massague, J. (2002a). E2F4/5 and p107 as Smad cofactors linking the TGFbeta receptor to c-myc repression. Cell *110*, 19-32.
Chen, D., Riedl, T., Washbrook, E., Pace, P.E., Coombes, R.C., Egly, J.M., and Ali, S. (2000). Activation of estrogen receptor alpha by S118 phosphorylation involves a ligand-dependent interaction with TFIIH and participation of CDK7. Mol Cell *6*, 127-137.
Chen, D., Washbrook, E., Sarwar, N., Bates, G.J., Pace, P.E., Thirunuvakkarasu, V., Taylor, J., Epstein, R.J., Fuller-Pace, F.V., Egly, J.M., Coombes, R.C., and Ali, S. (2002b). Phosphorylation of human estrogen receptor alpha at serine 118 by two distinct signal transduction pathways revealed by phosphorylation-specific antisera. Oncogene *21*, 4921-4931.
Chen, H.H., Wang, Y.C., and Fann, M.J. (2006). Identification and characterization of the CDK12/cyclin L1 complex involved in alternative splicing regulation. Mol Cell Biol *26*, 2736-2745.
Chen, P., Lee, N.V., Hu, W., Xu, M., Ferre, R.A., Lam, H., Bergqvist, S., Solowiej, J., Diehl, W., He, Y.A., Yu, X., Nagata, A., VanArsdale, T., and Murray, B.W. (2016). Spectrum and Degree of CDK Drug Interactions Predicts Clinical Performance. Mol Cancer Ther *15*, 2273-2281.
Chen, R., Wierda, W.G., Chubb, S., Hawtin, R.E., Fox, J.A., Keating, M.J., Gandhi, V., and Plunkett, W. (2009). Mechanism of action of SNS-032, a novel cyclin-dependent kinase inhibitor, in chronic lymphocytic leukemia. Blood *113*, 4637-4645.
Chen, Z., Indjeian, V.B., McManus, M., Wang, L., and Dynlacht, B.D. (2002c). CP110, a cell cycle-dependent CDK substrate, regulates centrosome duplication in human cells. Dev Cell *3*, 339-350.
Cheng, M., Olivier, P., Diehl, J.A., Fero, M., Roussel, M.F., Roberts, J.M., and Sherr, C.J. (1999). The p21(Cip1) and p27(Kip1) CDK 'inhibitors' are essential activators of cyclin D-dependent kinases in murine fibroblasts. EMBO J *18*, 1571-1583.
Chipumuro, E., Marco, E., Christensen, C.L., Kwiatkowski, N., Zhang, T., Hatheway, C.M., Abraham, B.J., Sharma, B., Yeung, C., Altabef, A., Perez-Atayde, A., Wong, K.K., Yuan, G.C., Gray, N.S., Young, R.A., and George, R.E. (2014). CDK7 inhibition suppresses super-enhancer-linked oncogenic transcription in MYCN-driven cancer. Cell *159*, 1126-1139.
Chirackal Manavalan, A.P., Pilarova, K., Kluge, M., Bartholomeeusen, K., Rajecky, M., Oppelt, J., Khirsariya, P., Paruch, K., Krejci, L., Friedel, C.C., and Blazek, D. (2019). CDK12 controls G1/S progression by regulating RNAPII processivity at core DNA replication genes. EMBO Rep *20*, e47592.

Chlebowski, R.T., Kuller, L.H., Prentice, R.L., Stefanick, M.L., Manson, J.E., Gass, M., Aragaki, A.K., Ockene, J.K., Lane, D.S., Sarto, G.E., Rajkovic, A., Schenken, R., Hendrix, S.L., Ravdin, P.M., Rohan, T.E., Yasmeen, S., Anderson, G., and Investigators, W.H.I. (2009). Breast cancer after use of estrogen plus progestin in postmenopausal women. N Engl J Med *360*, 573-587.

Choi, H.J., Jin, S., Cho, H., Won, H.Y., An, H.W., Jeong, G.Y., Park, Y.U., Kim, H.Y., Park, M.K., Son, T., Min, K.W., Jang, K.S., Oh, Y.H., Lee, J.Y., and Kong, G. (2019). CDK12 drives breast tumor initiation and trastuzumab resistance via WNT and IRS1-ErbB-PI3K signaling. EMBO Rep *20*, e48058.

Christensen, C.L., Kwiatkowski, N., Abraham, B.J., Carretero, J., Al-Shahrour, F., Zhang, T., Chipumuro, E., Herter-Sprie, G.S., Akbay, E.A., Altabef, A., Zhang, J., Shimamura, T., Capelletti, M., Reibel, J.B., Cavanaugh, J.D., Gao, P., Liu, Y., Michaelsen, S.R., Poulsen, H.S., Aref, A.R., Barbie, D.A., Bradner, J.E., George, R.E., Gray, N.S., Young, R.A., and Wong, K.K. (2014). Targeting transcriptional addictions in small cell lung cancer with a covalent CDK7 inhibitor. Cancer Cell *26*, 909-922.

Chu, C., Geng, Y., Zhou, Y., and Sicinski, P. (2021). Cyclin E in normal physiology and disease states. Trends Cell Biol *31*, 732-746.

Chytil, A., Waltner-Law, M., West, R., Friedman, D., Aakre, M., Barker, D., and Law, B. (2004). Construction of a cyclin D1-Cdk2 fusion protein to model the biological functions of cyclin D1-Cdk2 complexes. J Biol Chem *279*, 47688-47698.

Cicenas, J., Kalyan, K., Sorokinas, A., Jatulyte, A., Valiunas, D., Kaupinis, A., and Valius, M. (2014). Highlights of the Latest Advances in Research on CDK Inhibitors. Cancers (Basel) *6*, 2224-2242.

Cicenas, J., Kalyan, K., Sorokinas, A., Stankunas, E., Levy, J., Meskinyte, I., Stankevicius, V., Kaupinis, A., and Valius, M. (2015). Roscovitine in cancer and other diseases. Ann Transl Med *3*, 135.

Cidado, J., Boiko, S., Proia, T., Ferguson, D., Criscione, S.W., San Martin, M., Pop-Damkov, P., Su, N., Roamio Franklin, V.N., Sekhar Reddy Chilamakuri, C., D'Santos, C.S., Shao, W., Saeh, J.C., Koch, R., Weinstock, D.M., Zinda, M., Fawell, S.E., and Drew, L. (2020). AZD4573 Is a Highly Selective CDK9 Inhibitor That Suppresses MCL-1 and Induces Apoptosis in Hematologic Cancer Cells. Clin Cancer Res *26*, 922-934.

Clemons, M., and Goss, P. (2001). Estrogen and the risk of breast cancer. N Engl J Med *344*, 276-285.

Collaborative Group on Hormonal Factors in Breast, C. (2012). Menarche, menopause, and breast cancer risk: individual participant meta-analysis, including 118 964 women with breast cancer from 117 epidemiological studies. Lancet Oncol *13*, 1141-1151.
Compe, E., and Egly, J.M. (2012). TFIIH: when transcription met DNA repair. Nat Rev Mol Cell Biol *13*, 343-354.
Condorelli, R., Spring, L., O'Shaughnessy, J., Lacroix, L., Bailleux, C., Scott, V., Dubois, J., Nagy, R.J., Lanman, R.B., Iafrate, A.J., Andre, F., and Bardia, A. (2018). Polyclonal RB1 mutations and acquired resistance to CDK 4/6 inhibitors in patients with metastatic breast cancer. Ann Oncol *29*, 640-645.
Connell, J.W., Lindon, C., Luzio, J.P., and Reid, E. (2009). Spastin couples microtubule severing to membrane traffic in completion of cytokinesis and secretion. Traffic *10*, 42-56.
Corden, J.L., Cadena, D.L., Ahearn, J.M., Jr., and Dahmus, M.E. (1985). A unique structure at the carboxyl terminus of the largest subunit of eukaryotic RNA polymerase II. Proc Natl Acad Sci U S A *82*, 7934-7938.
Cortes, J., Im, S.A., Holgado, E., Perez-Garcia, J.M., Schmid, P., and Chavez-MacGregor, M. (2017). The next era of treatment for hormone receptor-positive, HER2-negative advanced breast cancer: Triplet combination-based endocrine therapies. Cancer Treat Rev *61*, 53-60.
Costa, C., Wang, Y., Ly, A., Hosono, Y., Murchie, E., Walmsley, C.S., Huynh, T., Healy, C., Peterson, R., Yanase, S., Jakubik, C.T., Henderson, L.E., Damon, L.J., Timonina, D., Sanidas, I., Pinto, C.J., Mino-Kenudson, M., Stone, J.R., Dyson, N.J., Ellisen, L.W., Bardia, A., Ebi, H., Benes, C.H., Engelman, J.A., and Juric, D. (2020). PTEN Loss Mediates Clinical Cross-Resistance to CDK4/6 and PI3Kalpha Inhibitors in Breast Cancer. Cancer Discov *10*, 72-85.
Couse, J.F., and Korach, K.S. (1999). Estrogen receptor null mice: what have we learned and where will they lead us? Endocr Rev *20*, 358-417.
Cowley, S.M., Hoare, S., Mosselman, S., and Parker, M.G. (1997). Estrogen receptors alpha and beta form heterodimers on DNA. J Biol Chem *272*, 19858-19862.
Creyghton, M.P., Cheng, A.W., Welstead, G.G., Kooistra, T., Carey, B.W., Steine, E.J., Hanna, J., Lodato, M.A., Frampton, G.M., Sharp, P.A., Boyer, L.A., Young, R.A., and Jaenisch, R. (2010). Histone H3K27ac separates active from poised enhancers and predicts developmental state. Proc Natl Acad Sci U S A *107*, 21931-21936.
Cristofanilli, M., Rugo, H.S., Im, S.-A., Slamon, D.J., Harbeck, N., Bondarenko, I., Masuda, N., Colleoni, M., DeMichele, A., Loi, S., Iwata, H., O'Leary, B., Bananis, E., Liu, Y., Huang, X., Kim, S., Lechuga, M., and Turner, N.C. (2021). Overall survival (OS) with palbociclib (PAL) + fulvestrant (FUL) in women with hormone receptor–positive (HR+), human

epidermal growth factor receptor 2–negative (HER2–) advanced breast cancer (ABC): Updated analyses from PALOMA-3. Journal of Clinical Oncology *39*, 1000-1000.
Cruzalegui, F.H., Cano, E., and Treisman, R. (1999). ERK activation induces phosphorylation of Elk-1 at multiple S/T-P motifs to high stoichiometry. Oncogene *18*, 7948-7957.
Cundell, M.J., Bastos, R.N., Zhang, T., Holder, J., Gruneberg, U., Novak, B., and Barr, F.A. (2013). The BEG (PP2A-B55/ENSA/Greatwall) pathway ensures cytokinesis follows chromosome separation. Mol Cell *52*, 393-405.
Curtis, C., Shah, S.P., Chin, S.F., Turashvili, G., Rueda, O.M., Dunning, M.J., Speed, D., Lynch, A.G., Samarajiwa, S., Yuan, Y., Graf, S., Ha, G., Haffari, G., Bashashati, A., Russell, R., McKinney, S., Group, M., Langerod, A., Green, A., Provenzano, E., Wishart, G., Pinder, S., Watson, P., Markowetz, F., Murphy, L., Ellis, I., Purushotham, A., Borresen-Dale, A.L., Brenton, J.D., Tavare, S., Caldas, C., and Aparicio, S. (2012). The genomic and transcriptomic architecture of 2,000 breast tumours reveals novel subgroups. Nature *486*, 346-352.
Curtis, S.W., Washburn, T., Sewall, C., DiAugustine, R., Lindzey, J., Couse, J.F., and Korach, K.S. (1996). Physiological coupling of growth factor and steroid receptor signaling pathways: estrogen receptor knockout mice lack estrogen-like response to epidermal growth factor. Proc Natl Acad Sci U S A *93*, 12626-12630.
Cuzick, J., Sestak, I., Baum, M., Buzdar, A., Howell, A., Dowsett, M., Forbes, J.F., and investigators, A.L. (2010). Effect of anastrozole and tamoxifen as adjuvant treatment for early-stage breast cancer: 10-year analysis of the ATAC trial. Lancet Oncol *11*, 1135-1141.
Dai, X., Li, T., Bai, Z., Yang, Y., Liu, X., Zhan, J., and Shi, B. (2015). Breast cancer intrinsic subtype classification, clinical use and future trends. Am J Cancer Res *5*, 2929-2943.
Danilov, A.V., Hu, S., Orr, B., Godek, K., Mustachio, L.M., Sekula, D., Liu, X., Kawakami, M., Johnson, F.M., Compton, D.A., Freemantle, S.J., and Dmitrovsky, E. (2016). Dinaciclib Induces Anaphase Catastrophe in Lung Cancer Cells via Inhibition of Cyclin-Dependent Kinases 1 and 2. Mol Cancer Ther *15*, 2758-2766.
Dankort, D., Maslikowski, B., Warner, N., Kanno, N., Kim, H., Wang, Z., Moran, M.F., Oshima, R.G., Cardiff, R.D., and Muller, W.J. (2001). Grb2 and Shc adapter proteins play distinct roles in Neu (ErbB-2)-induced mammary tumorigenesis: implications for human breast cancer. Mol Cell Biol *21*, 1540-1551.
Davies, B.R., Greenwood, H., Dudley, P., Crafter, C., Yu, D.H., Zhang, J., Li, J., Gao, B., Ji, Q., Maynard, J., Ricketts, S.A., Cross, D., Cosulich, S., Chresta, C.C., Page, K., Yates, J., Lane, C., Watson, R., Luke, R., Ogilvie, D., and Pass, M. (2012). Preclinical pharmacology

of AZD5363, an inhibitor of AKT: pharmacodynamics, antitumor activity, and correlation of monotherapy activity with genetic background. Mol Cancer Ther *11*, 873-887.
Davies, C., Pan, H., Godwin, J., Gray, R., Arriagada, R., Raina, V., Abraham, M., Medeiros Alencar, V.H., Badran, A., Bonfill, X., Bradbury, J., Clarke, M., Collins, R., Davis, S.R., Delmestri, A., Forbes, J.F., Haddad, P., Hou, M.F., Inbar, M., Khaled, H., Kielanowska, J., Kwan, W.H., Mathew, B.S., Mittra, I., Muller, B., Nicolucci, A., Peralta, O., Pernas, F., Petruzelka, L., Pienkowski, T., Radhika, R., Rajan, B., Rubach, M.T., Tort, S., Urrutia, G., Valentini, M., Wang, Y., Peto, R., and Adjuvant Tamoxifen: Longer Against Shorter Collaborative, G. (2013). Long-term effects of continuing adjuvant tamoxifen to 10 years versus stopping at 5 years after diagnosis of oestrogen receptor-positive breast cancer: ATLAS, a randomised trial. Lancet *381*, 805-816.
Davies, T.G., Tunnah, P., Meijer, L., Marko, D., Eisenbrand, G., Endicott, J.A., and Noble, M.E. (2001). Inhibitor binding to active and inactive CDK2: the crystal structure of CDK2-cyclin A/indirubin-5-sulphonate. Structure *9*, 389-397.
Day, P.J., Cleasby, A., Tickle, I.J., O'Reilly, M., Coyle, J.E., Holding, F.P., McMenamin, R.L., Yon, J., Chopra, R., Lengauer, C., and Jhoti, H. (2009). Crystal structure of human CDK4 in complex with a D-type cyclin. Proc Natl Acad Sci U S A *106*, 4166-4170.
De Boer, L., Oakes, V., Beamish, H., Giles, N., Stevens, F., Somodevilla-Torres, M., Desouza, C., and Gabrielli, B. (2008). Cyclin A/cdk2 coordinates centrosomal and nuclear mitotic events. Oncogene *27*, 4261-4268.
De Bondt, H.L., Rosenblatt, J., Jancarik, J., Jones, H.D., Morgan, D.O., and Kim, S.H. (1993). Crystal structure of cyclin-dependent kinase 2. Nature *363*, 595-602.
De Bosscher, K., Desmet, S.J., Clarisse, D., Estebanez-Perpina, E., and Brunsveld, L. (2020). Nuclear receptor crosstalk - defining the mechanisms for therapeutic innovation. Nat Rev Endocrinol *16*, 363-377.
de Leeuw, R., Neefjes, J., and Michalides, R. (2011). A role for estrogen receptor phosphorylation in the resistance to tamoxifen. Int J Breast Cancer *2011*, 232435.
Dean, J.L., McClendon, A.K., Hickey, T.E., Butler, L.M., Tilley, W.D., Witkiewicz, A.K., and Knudsen, E.S. (2012). Therapeutic response to CDK4/6 inhibition in breast cancer defined by ex vivo analyses of human tumors. Cell Cycle *11*, 2756-2761.
Dean, J.L., Thangavel, C., McClendon, A.K., Reed, C.A., and Knudsen, E.S. (2010). Therapeutic CDK4/6 inhibition in breast cancer: key mechanisms of response and failure. Oncogene *29*, 4018-4032.
Deng, J., Wang, E.S., Jenkins, R.W., Li, S., Dries, R., Yates, K., Chhabra, S., Huang, W., Liu, H., Aref, A.R., Ivanova, E., Paweletz, C.P., Bowden, M., Zhou, C.W., Herter-Sprie,

G.S., Sorrentino, J.A., Bisi, J.E., Lizotte, P.H., Merlino, A.A., Quinn, M.M., Bufe, L.E., Yang, A., Zhang, Y., Zhang, H., Gao, P., Chen, T., Cavanaugh, M.E., Rode, A.J., Haines, E., Roberts, P.J., Strum, J.C., Richards, W.G., Lorch, J.H., Parangi, S., Gunda, V., Boland, G.M., Bueno, R., Palakurthi, S., Freeman, G.J., Ritz, J., Haining, W.N., Sharpless, N.E., Arthanari, H., Shapiro, G.I., Barbie, D.A., Gray, N.S., and Wong, K.K. (2018). CDK4/6 Inhibition Augments Antitumor Immunity by Enhancing T-cell Activation. Cancer Discov *8*, 216-233.

Desdouets, C., Matesic, G., Molina, C.A., Foulkes, N.S., Sassone-Corsi, P., Brechot, C., and Sobczak-Thepot, J. (1995). Cell cycle regulation of cyclin A gene expression by the cyclic AMP-responsive transcription factors CREB and CREM. Mol Cell Biol *15*, 3301-3309.

Di Lello, P., Jenkins, L.M.M., Jones, T.N., Nguyen, B.D., Hara, T., Yamaguchi, H., Dikeakos, J.D., Appella, E., Legault, P., and Omichinski, J.G. (2006). Structure of the Tfb1/p53 complex: Insights into the interaction between the p62/Tfb1 subunit of TFIIH and the activation domain of p53. Mol Cell *22*, 731-740.

Di Lello, P., Miller Jenkins, L.M., Mas, C., Langlois, C., Malitskaya, E., Fradet-Turcotte, A., Archambault, J., Legault, P., and Omichinski, J.G. (2008). p53 and TFIIEalpha share a common binding site on the Tfb1/p62 subunit of TFIIH. Proc Natl Acad Sci U S A *105*, 106-111.

Dickler, M.N., Tolaney, S.M., Rugo, H.S., Cortes, J., Dieras, V., Patt, D., Wildiers, H., Hudis, C.A., O'Shaughnessy, J., Zamora, E., Yardley, D.A., Frenzel, M., Koustenis, A., and Baselga, J. (2017). MONARCH 1, A Phase II Study of Abemaciclib, a CDK4 and CDK6 Inhibitor, as a Single Agent, in Patients with Refractory HR(+)/HER2(-) Metastatic Breast Cancer. Clin Cancer Res *23*, 5218-5224.

Dickson, M.A., Schwartz, G.K., Keohan, M.L., D'Angelo, S.P., Gounder, M.M., Chi, P., Antonescu, C.R., Landa, J., Qin, L.X., Crago, A.M., Singer, S., Koff, A., and Tap, W.D. (2016). Progression-Free Survival Among Patients With Well-Differentiated or Dedifferentiated Liposarcoma Treated With CDK4 Inhibitor Palbociclib: A Phase 2 Clinical Trial. JAMA Oncol *2*, 937-940.

Dimova, D.K., and Dyson, N.J. (2005). The E2F transcriptional network: old acquaintances with new faces. Oncogene *24*, 2810-2826.

Dohadwala, M., da Cruz e Silva, E.F., Hall, F.L., Williams, R.T., Carbonaro-Hall, D.A., Nairn, A.C., Greengard, P., and Berndt, N. (1994). Phosphorylation and inactivation of protein phosphatase 1 by cyclin-dependent kinases. Proc Natl Acad Sci U S A *91*, 6408-6412.

Dollinger, R., and Gilmour, D.S. (2021). Regulation of Promoter Proximal Pausing of RNA Polymerase II in Metazoans. J Mol Biol *433*, 166897.

Douglas, M.E., Davies, T., Joseph, N., and Mishima, M. (2010). Aurora B and 14-3-3 coordinately regulate clustering of centralspindlin during cytokinesis. Curr Biol *20*, 927-933.
Dowsett, M., Sestak, I., Lopez-Knowles, E., Sidhu, K., Dunbier, A.K., Cowens, J.W., Ferree, S., Storhoff, J., Schaper, C., and Cuzick, J. (2013). Comparison of PAM50 risk of recurrence score with oncotype DX and IHC4 for predicting risk of distant recurrence after endocrine therapy. J Clin Oncol *31*, 2783-2790.
Drapkin, R., Reardon, J.T., Ansari, A., Huang, J.C., Zawel, L., Ahn, K., Sancar, A., and Reinberg, D. (1994). Dual role of TFIIH in DNA excision repair and in transcription by RNA polymerase II. Nature *368*, 769-772.
Driggers, P.H., and Segars, J.H. (2002). Estrogen action and cytoplasmic signaling pathways. Part II: the role of growth factors and phosphorylation in estrogen signaling. Trends Endocrinol Metab *13*, 422-427.
Dutertre, M., and Smith, C.L. (2003). Ligand-independent interactions of p160/steroid receptor coactivators and CREB-binding protein (CBP) with estrogen receptor-alpha: regulation by phosphorylation sites in the A/B region depends on other receptor domains. Mol Endocrinol *17*, 1296-1314.
Dyson, N. (1998). The regulation of E2F by pRB-family proteins. Genes Dev *12*, 2245-2262.
Dziadziunszko, R., Garralda, E., Angelosanto, N., Rzymski, T., Dudziak, R., Brzózka, K., Littlewood, P., Nogai, H., Glasmacher, A.G., and Lugowska, I. (2022). Phase I/II trial of RVU120 (SEL120), a CDK8/CDK19 inhibitor in patients with relapsed/refractory metastatic or advanced solid tumors. Journal of Clinical Oncology *40*, e15091-e15091.
Early Breast Cancer Trialists' Collaborative, G. (2022). Aromatase inhibitors versus tamoxifen in premenopausal women with oestrogen receptor-positive early-stage breast cancer treated with ovarian suppression: a patient-level meta-analysis of 7030 women from four randomised trials. Lancet Oncol *23*, 382-392.
Early Breast Cancer Trialists' Collaborative, G., Davies, C., Godwin, J., Gray, R., Clarke, M., Cutter, D., Darby, S., McGale, P., Pan, H.C., Taylor, C., Wang, Y.C., Dowsett, M., Ingle, J., and Peto, R. (2011). Relevance of breast cancer hormone receptors and other factors to the efficacy of adjuvant tamoxifen: patient-level meta-analysis of randomised trials. Lancet *378*, 771-784.
Eeckhoute, J., Keeton, E.K., Lupien, M., Krum, S.A., Carroll, J.S., and Brown, M. (2007). Positive cross-regulatory loop ties GATA-3 to estrogen receptor alpha expression in breast cancer. Cancer Res *67*, 6477-6483.
English, C.M., Adkins, M.W., Carson, J.J., Churchill, M.E., and Tyler, J.K. (2006). Structural basis for the histone chaperone activity of Asf1. Cell *127*, 495-508.

Erikson, J., Finan, J., Tsujimoto, Y., Nowell, P.C., and Croce, C.M. (1984). The chromosome 14 breakpoint in neoplastic B cells with the t(11;14) translocation involves the immunoglobulin heavy chain locus. Proc Natl Acad Sci U S A *81*, 4144-4148.
Esnault, C., Ghavi-Helm, Y., Brun, S., Soutourina, J., Van Berkum, N., Boschiero, C., Holstege, F., and Werner, M. (2008). Mediator-dependent recruitment of TFIIH modules in preinitiation complex. Mol Cell *31*, 337-346.
Fanning, S.W., and Greene, G.L. (2019). Next-Generation ERalpha Inhibitors for Endocrine-Resistant ER+ Breast Cancer. Endocrinology *160*, 759-769.
Farcas, A.M., Nagarajan, S., Cosulich, S., and Carroll, J.S. (2021). Genome-Wide Estrogen Receptor Activity in Breast Cancer. Endocrinology *162*.
Farkas, S., Szabo, A., Hegyi, A.E., Torok, B., Fazekas, C.L., Ernszt, D., Kovacs, T., and Zelena, D. (2022). Estradiol and Estrogen-like Alternative Therapies in Use: The Importance of the Selective and Non-Classical Actions. Biomedicines *10*.
Feine, O., Hukasova, E., Bruinsma, W., Freire, R., Fainsod, A., Gannon, J., Mahbubani, H.M., Lindqvist, A., and Brandeis, M. (2014). Phosphorylation-mediated stabilization of Bora in mitosis coordinates Plx1/Plk1 and Cdk1 oscillations. Cell Cycle *13*, 1727-1736.
Feng, Y., Manka, D., Wagner, K.U., and Khan, S.A. (2007). Estrogen receptor-alpha expression in the mammary epithelium is required for ductal and alveolar morphogenesis in mice. Proc Natl Acad Sci U S A *104*, 14718-14723.
Feng, Y., Spezia, M., Huang, S., Yuan, C., Zeng, Z., Zhang, L., Ji, X., Liu, W., Huang, B., Luo, W., Liu, B., Lei, Y., Du, S., Vuppalapati, A., Luu, H.H., Haydon, R.C., He, T.C., and Ren, G. (2018). Breast cancer development and progression: Risk factors, cancer stem cells, signaling pathways, genomics, and molecular pathogenesis. Genes Dis *5*, 77-106.
Filardo, E.J., Quinn, J.A., Bland, K.I., and Frackelton, A.R., Jr. (2000). Estrogen-induced activation of Erk-1 and Erk-2 requires the G protein-coupled receptor homolog, GPR30, and occurs via trans-activation of the epidermal growth factor receptor through release of HB-EGF. Mol Endocrinol *14*, 1649-1660.
Finn, R.S., Boer, K., Bondarenko, I., Patel, R., Pinter, T., Schmidt, M., Shparyk, Y.V., Thummala, A., Voitko, N., Bananis, E., McRoy, L., Wilner, K., Huang, X., Kim, S., Slamon, D.J., and Ettl, J. (2020). Overall survival results from the randomized phase 2 study of palbociclib in combination with letrozole versus letrozole alone for first-line treatment of ER+/HER2- advanced breast cancer (PALOMA-1, TRIO-18). Breast Cancer Res Treat *183*, 419-428.
Finn, R.S., Crown, J.P., Lang, I., Boer, K., Bondarenko, I.M., Kulyk, S.O., Ettl, J., Patel, R., Pinter, T., Schmidt, M., Shparyk, Y., Thummala, A.R., Voytko, N.L., Fowst, C., Huang, X.,

Kim, S.T., Randolph, S., and Slamon, D.J. (2015). The cyclin-dependent kinase 4/6 inhibitor palbociclib in combination with letrozole versus letrozole alone as first-line treatment of oestrogen receptor-positive, HER2-negative, advanced breast cancer (PALOMA-1/TRIO-18): a randomised phase 2 study. Lancet Oncol *16*, 25-35.

Finn, R.S., Dering, J., Conklin, D., Kalous, O., Cohen, D.J., Desai, A.J., Ginther, C., Atefi, M., Chen, I., Fowst, C., Los, G., and Slamon, D.J. (2009). PD 0332991, a selective cyclin D kinase 4/6 inhibitor, preferentially inhibits proliferation of luminal estrogen receptor-positive human breast cancer cell lines in vitro. Breast Cancer Res *11*, R77.

Finn, R.S., Martin, M., Rugo, H.S., Jones, S., Im, S.A., Gelmon, K., Harbeck, N., Lipatov, O.N., Walshe, J.M., Moulder, S., Gauthier, E., Lu, D.R., Randolph, S., Dieras, V., and Slamon, D.J. (2016). Palbociclib and Letrozole in Advanced Breast Cancer. N Engl J Med *375*, 1925-1936.

Firestein, R., Bass, A.J., Kim, S.Y., Dunn, I.F., Silver, S.J., Guney, I., Freed, E., Ligon, A.H., Vena, N., Ogino, S., Chheda, M.G., Tamayo, P., Finn, S., Shrestha, Y., Boehm, J.S., Jain, S., Bojarski, E., Mermel, C., Barretina, J., Chan, J.A., Baselga, J., Tabernero, J., Root, D.E., Fuchs, C.S., Loda, M., Shivdasani, R.A., Meyerson, M., and Hahn, W.C. (2008). CDK8 is a colorectal cancer oncogene that regulates beta-catenin activity. Nature *455*, 547-551.

Fishburn, J., Tomko, E., Galburt, E., and Hahn, S. (2015). Double-stranded DNA translocase activity of transcription factor TFIIH and the mechanism of RNA polymerase II open complex formation. Proc Natl Acad Sci U S A *112*, 3961-3966.

Fisher, C.R., Graves, K.H., Parlow, A.F., and Simpson, E.R. (1998). Characterization of mice deficient in aromatase (ArKO) because of targeted disruption of the cyp19 gene. Proc Natl Acad Sci U S A *95*, 6965-6970.

Fisher, R.P. (2005). Secrets of a double agent: CDK7 in cell-cycle control and transcription. J Cell Sci *118*, 5171-5180.

Flaherty, K.T., Lorusso, P.M., Demichele, A., Abramson, V.G., Courtney, R., Randolph, S.S., Shaik, M.N., Wilner, K.D., O'Dwyer, P.J., and Schwartz, G.K. (2012). Phase I, dose-escalation trial of the oral cyclin-dependent kinase 4/6 inhibitor PD 0332991, administered using a 21-day schedule in patients with advanced cancer. Clin Cancer Res *18*, 568-576.

Flanagan, J., Qian, Y., Gough, S., Andreoli, M., Bookbinder, M., Cadelina, G., Bradley, J., Rousseau, E., Willard, R., Pizzano, J., Crews, C., Crew, A., Taylor, I., and Houston, J. (2019). Abstract P5-04-18: ARV-471, an oral estrogen receptor PROTAC degrader for breast cancer. Cancer Research *79*, P5-04-18-P05-04-18.

Flemington, E.K., Speck, S.H., and Kaelin, W.G., Jr. (1993). E2F-1-mediated transactivation is inhibited by complex formation with the retinoblastoma susceptibility gene product. Proc Natl Acad Sci U S A *90*, 6914-6918.

Flores-Rozas, H., Kelman, Z., Dean, F.B., Pan, Z.Q., Harper, J.W., Elledge, S.J., O'Donnell, M., and Hurwitz, J. (1994). Cdk-interacting protein 1 directly binds with proliferating cell nuclear antigen and inhibits DNA replication catalyzed by the DNA polymerase delta holoenzyme. Proc Natl Acad Sci U S A *91*, 8655-8659.

Flynn, J., Jones, J., Johnson, A.J., Andritsos, L., Maddocks, K., Jaglowski, S., Hessler, J., Grever, M.R., Im, E., Zhou, H., Zhu, Y., Zhang, D., Small, K., Bannerji, R., and Byrd, J.C. (2015). Dinaciclib is a novel cyclin-dependent kinase inhibitor with significant clinical activity in relapsed and refractory chronic lymphocytic leukemia. Leukemia *29*, 1524-1529.

Foltman, M., Evrin, C., De Piccoli, G., Jones, R.C., Edmondson, R.D., Katou, Y., Nakato, R., Shirahige, K., and Labib, K. (2013). Eukaryotic replisome components cooperate to process histones during chromosome replication. Cell Rep *3*, 892-904.

Forget, M.A., Turcotte, S., Beauseigle, D., Godin-Ethier, J., Pelletier, S., Martin, J., Tanguay, S., and Lapointe, R. (2007). The Wnt pathway regulator DKK1 is preferentially expressed in hormone-resistant breast tumours and in some common cancer types. Br J Cancer *96*, 646-653.

Foulkes, W.D., Smith, I.E., and Reis-Filho, J.S. (2010). Triple-negative breast cancer. N Engl J Med *363*, 1938-1948.

Fournier, A., Berrino, F., and Clavel-Chapelon, F. (2008). Unequal risks for breast cancer associated with different hormone replacement therapies: results from the E3N cohort study. Breast Cancer Res Treat *107*, 103-111.

Fragkos, M., Ganier, O., Coulombe, P., and Mechali, M. (2015). DNA replication origin activation in space and time. Nat Rev Mol Cell Biol *16*, 360-374.

Franco, J., Balaji, U., Freinkman, E., Witkiewicz, A.K., and Knudsen, E.S. (2016). Metabolic Reprogramming of Pancreatic Cancer Mediated by CDK4/6 Inhibition Elicits Unique Vulnerabilities. Cell Rep *14*, 979-990.

Freeman-Cook, K., Hoffman, R.L., Miller, N., Almaden, J., Chionis, J., Zhang, Q., Eisele, K., Liu, C., Zhang, C., Huser, N., Nguyen, L., Costa-Jones, C., Niessen, S., Carelli, J., Lapek, J., Weinrich, S.L., Wei, P., McMillan, E., Wilson, E., Wang, T.S., McTigue, M., Ferre, R.A., He, Y.A., Ninkovic, S., Behenna, D., Tran, K.T., Sutton, S., Nagata, A., Ornelas, M.A., Kephart, S.E., Zehnder, L.R., Murray, B., Xu, M., Solowiej, J.E., Visswanathan, R., Boras, B., Looper, D., Lee, N., Bienkowska, J.R., Zhu, Z., Kan, Z., Ding, Y., Mu, X.J., Oderup, C.,

Salek-Ardakani, S., White, M.A., VanArsdale, T., and Dann, S.G. (2021a). Expanding control of the tumor cell cycle with a CDK2/4/6 inhibitor. Cancer Cell *39*, 1404-1421 e1411.
Freeman-Cook, K.D., Hoffman, R.L., Behenna, D.C., Boras, B., Carelli, J., Diehl, W., Ferre, R.A., He, Y.A., Hui, A., Huang, B., Huser, N., Jones, R., Kephart, S.E., Lapek, J., McTigue, M., Miller, N., Murray, B.W., Nagata, A., Nguyen, L., Niessen, S., Ninkovic, S., O'Doherty, I., Ornelas, M.A., Solowiej, J., Sutton, S.C., Tran, K., Tseng, E., Visswanathan, R., Xu, M., Zehnder, L., Zhang, Q., Zhang, C., and Dann, S. (2021b). Discovery of PF-06873600, a CDK2/4/6 Inhibitor for the Treatment of Cancer. J Med Chem *64*, 9056-9077.
Fregoso, M., Laine, J.P., Aguilar-Fuentes, J., Mocquet, V., Reynaud, E., Coin, F., Egly, J.M., and Zurita, M. (2007). DNA repair and transcriptional deficiencies caused by mutations in the Drosophila p52 subunit of TFIIH generate developmental defects and chromosome fragility. Mol Cell Biol *27*, 3640-3650.
Fry, D.W., Harvey, P.J., Keller, P.R., Elliott, W.L., Meade, M., Trachet, E., Albassam, M., Zheng, X., Leopold, W.R., Pryer, N.K., and Toogood, P.L. (2004). Specific inhibition of cyclin-dependent kinase 4/6 by PD 0332991 and associated antitumor activity in human tumor xenografts. Mol Cancer Ther *3*, 1427-1438.
Fu, X., Pereira, R., De Angelis, C., Veeraraghavan, J., Nanda, S., Qin, L., Cataldo, M.L., Sethunath, V., Mehravaran, S., Gutierrez, C., Chamness, G.C., Feng, Q., O'Malley, B.W., Selenica, P., Weigelt, B., Reis-Filho, J.S., Cohen, O., Wagle, N., Nardone, A., Jeselsohn, R., Brown, M., Rimawi, M.F., Osborne, C.K., and Schiff, R. (2019). FOXA1 upregulation promotes enhancer and transcriptional reprogramming in endocrine-resistant breast cancer. Proc Natl Acad Sci U S A.
Fullwood, M.J., Liu, M.H., Pan, Y.F., Liu, J., Xu, H., Mohamed, Y.B., Orlov, Y.L., Velkov, S., Ho, A., Mei, P.H., Chew, E.G., Huang, P.Y., Welboren, W.J., Han, Y., Ooi, H.S., Ariyaratne, P.N., Vega, V.B., Luo, Y., Tan, P.Y., Choy, P.Y., Wansa, K.D., Zhao, B., Lim, K.S., Leow, S.C., Yow, J.S., Joseph, R., Li, H., Desai, K.V., Thomsen, J.S., Lee, Y.K., Karuturi, R.K., Herve, T., Bourque, G., Stunnenberg, H.G., Ruan, X., Cacheux-Rataboul, V., Sung, W.K., Liu, E.T., Wei, C.L., Cheung, E., and Ruan, Y. (2009). An oestrogen-receptor-alpha-bound human chromatin interactome. Nature *462*, 58-64.
Funabiki, H., and Murray, A.W. (2000). The Xenopus chromokinesin Xkid is essential for metaphase chromosome alignment and must be degraded to allow anaphase chromosome movement. Cell *102*, 411-424.
Fuqua, S.A., and Cui, Y. (2004). Estrogen and progesterone receptor isoforms: clinical significance in breast cancer. Breast Cancer Res Treat *87 Suppl 1*, S3-10.

Galbraith, M.D., Donner, A.J., and Espinosa, J.M. (2010). CDK8: a positive regulator of transcription. Transcription *1*, 4-12.
Galimberti, F., Thompson, S.L., Liu, X., Li, H., Memoli, V., Green, S.R., DiRenzo, J., Greninger, P., Sharma, S.V., Settleman, J., Compton, D.A., and Dmitrovsky, E. (2010). Targeting the cyclin E-Cdk-2 complex represses lung cancer growth by triggering anaphase catastrophe. Clin Cancer Res *16*, 109-120.
Gandhi, R., Gillespie, P.J., and Hirano, T. (2006). Human Wapl is a cohesin-binding protein that promotes sister-chromatid resolution in mitotic prophase. Curr Biol *16*, 2406-2417.
Gao, T., Han, Y., Yu, L., Ao, S., Li, Z., and Ji, J. (2014). CCNA2 is a prognostic biomarker for ER+ breast cancer and tamoxifen resistance. PLoS One *9*, e91771.
Garcia-Martinez, L., Zhang, Y., Nakata, Y., Chan, H.L., and Morey, L. (2021). Epigenetic mechanisms in breast cancer therapy and resistance. Nat Commun *12*, 1786.
Garrett, S., Barton, W.A., Knights, R., Jin, P., Morgan, D.O., and Fisher, R.P. (2001). Reciprocal activation by cyclin-dependent kinases 2 and 7 is directed by substrate specificity determinants outside the T loop. Mol Cell Biol *21*, 88-99.
Gavet, O., and Pines, J. (2010). Activation of cyclin B1-Cdk1 synchronizes events in the nucleus and the cytoplasm at mitosis. J Cell Biol *189*, 247-259.
Gazdar, A.F., Kurvari, V., Virmani, A., Gollahon, L., Sakaguchi, M., Westerfield, M., Kodagoda, D., Stasny, V., Cunningham, H.T., Wistuba, II, Tomlinson, G., Tonk, V., Ashfaq, R., Leitch, A.M., Minna, J.D., and Shay, J.W. (1998). Characterization of paired tumor and non-tumor cell lines established from patients with breast cancer. Int J Cancer *78*, 766-774.
Gelbert, L.M., Cai, S., Lin, X., Sanchez-Martinez, C., Del Prado, M., Lallena, M.J., Torres, R., Ajamie, R.T., Wishart, G.N., Flack, R.S., Neubauer, B.L., Young, J., Chan, E.M., Iversen, P., Cronier, D., Kreklau, E., and de Dios, A. (2014). Preclinical characterization of the CDK4/6 inhibitor LY2835219: in-vivo cell cycle-dependent/independent anti-tumor activities alone/in combination with gemcitabine. Invest New Drugs *32*, 825-837.
Geley, S., Kramer, E., Gieffers, C., Gannon, J., Peters, J.M., and Hunt, T. (2001). Anaphase-promoting complex/cyclosome-dependent proteolysis of human cyclin A starts at the beginning of mitosis and is not subject to the spindle assembly checkpoint. J Cell Biol *153*, 137-148.
Ghia, P., Scarfo, L., Perez, S., Pathiraja, K., Derosier, M., Small, K., McCrary Sisk, C., and Patton, N. (2017). Efficacy and safety of dinaciclib vs ofatumumab in patients with relapsed/refractory chronic lymphocytic leukemia. Blood *129*, 1876-1878.
Ghosh, M.G., Thompson, D.A., and Weigel, R.J. (2000). PDZK1 and GREB1 are estrogen-regulated genes expressed in hormone-responsive breast cancer. Cancer Res *60*, 6367-6375.

Gibadulinova, A., Pastorek, M., Filipcik, P., Radvak, P., Csaderova, L., Vojtesek, B., and Pastorekova, S. (2016). Cancer-associated S100P protein binds and inactivates p53, permits therapy-induced senescence and supports chemoresistance. Oncotarget *7*, 22508-22522.
Gillett, C., Fantl, V., Smith, R., Fisher, C., Bartek, J., Dickson, C., Barnes, D., and Peters, G. (1994). Amplification and overexpression of cyclin D1 in breast cancer detected by immunohistochemical staining. Cancer Res *54*, 1812-1817.
Girard, F., Strausfeld, U., Fernandez, A., and Lamb, N.J. (1991). Cyclin A is required for the onset of DNA replication in mammalian fibroblasts. Cell *67*, 1169-1179.
Glotzer, M. (2004). Cleavage furrow positioning. J Cell Biol *164*, 347-351.
Glover-Cutter, K., Larochelle, S., Erickson, B., Zhang, C., Shokat, K., Fisher, R.P., and Bentley, D.L. (2009). TFIIH-associated Cdk7 kinase functions in phosphorylation of C-terminal domain Ser7 residues, promoter-proximal pausing, and termination by RNA polymerase II. Mol Cell Biol *29*, 5455-5464.
Goel, S., Bergholz, J.S., and Zhao, J.J. (2022). Targeting CDK4 and CDK6 in cancer. Nat Rev Cancer *22*, 356-372.
Goel, S., DeCristo, M.J., Watt, A.C., BrinJones, H., Sceneay, J., Li, B.B., Khan, N., Ubellacker, J.M., Xie, S., Metzger-Filho, O., Hoog, J., Ellis, M.J., Ma, C.X., Ramm, S., Krop, I.E., Winer, E.P., Roberts, T.M., Kim, H.J., McAllister, S.S., and Zhao, J.J. (2017). CDK4/6 inhibition triggers anti-tumour immunity. Nature *548*, 471-475.
Goetz, M.P., Toi, M., Campone, M., Sohn, J., Paluch-Shimon, S., Huober, J., Park, I.H., Tredan, O., Chen, S.C., Manso, L., Freedman, O.C., Garnica Jaliffe, G., Forrester, T., Frenzel, M., Barriga, S., Smith, I.C., Bourayou, N., and Di Leo, A. (2017). MONARCH 3: Abemaciclib As Initial Therapy for Advanced Breast Cancer. J Clin Oncol *35*, 3638-3646.
Gong, D., Pomerening, J.R., Myers, J.W., Gustavsson, C., Jones, J.T., Hahn, A.T., Meyer, T., and Ferrell, J.E., Jr. (2007). Cyclin A2 regulates nuclear-envelope breakdown and the nuclear accumulation of cyclin B1. Curr Biol *17*, 85-91.
Gonzalez-Angulo, A.M., Chen, H., Karuturi, M.S., Chavez-MacGregor, M., Tsavachidis, S., Meric-Bernstam, F., Do, K.A., Hortobagyi, G.N., Thompson, P.A., Mills, G.B., Bondy, M.L., and Blumenschein, G.R., Jr. (2013). Frequency of mesenchymal-epithelial transition factor gene (MET) and the catalytic subunit of phosphoinositide-3-kinase (PIK3CA) copy number elevation and correlation with outcome in patients with early stage breast cancer. Cancer *119*, 7-15.
Gottlicher, M., Heck, S., and Herrlich, P. (1998). Transcriptional cross-talk, the second mode of steroid hormone receptor action. J Mol Med (Berl) *76*, 480-489.

Gou, X., Anurag, M., Lei, J.T., Kim, B.J., Singh, P., Seker, S., Fandino, D., Han, A., Rehman, S., Hu, J., Korchina, V., Doddapaneni, H., Dobrolecki, L.E., Mitsiades, N., Lewis, M.T., Welm, A.L., Li, S., Lee, A.V., Robinson, D.R., Foulds, C.E., and Ellis, M.J. (2021). Transcriptional Reprogramming Differentiates Active from Inactive ESR1 Fusions in Endocrine Therapy-Refractory Metastatic Breast Cancer. Cancer Res *81*, 6259-6272.
Goutsouliak, K., Veeraraghavan, J., Sethunath, V., De Angelis, C., Osborne, C.K., Rimawi, M.F., and Schiff, R. (2020). Towards personalized treatment for early stage HER2-positive breast cancer. Nat Rev Clin Oncol *17*, 233-250.
Grallert, A., Boke, E., Hagting, A., Hodgson, B., Connolly, Y., Griffiths, J.R., Smith, D.L., Pines, J., and Hagan, I.M. (2015). A PP1-PP2A phosphatase relay controls mitotic progression. Nature *517*, 94-98.
Gray-Bablin, J., Zalvide, J., Fox, M.P., Knickerbocker, C.J., DeCaprio, J.A., and Keyomarsi, K. (1996). Cyclin E, a redundant cyclin in breast cancer. Proc Natl Acad Sci U S A *93*, 15215-15220.
Green, S., Walter, P., Kumar, V., Krust, A., Bornert, J.M., Argos, P., and Chambon, P. (1986). Human oestrogen receptor cDNA: sequence, expression and homology to v-erb-A. Nature *320*, 134-139.
Greene, G.L., Gilna, P., Waterfield, M., Baker, A., Hort, Y., and Shine, J. (1986). Sequence and expression of human estrogen receptor complementary DNA. Science *231*, 1150-1154.
Gronemeyer, H., Gustafsson, J.A., and Laudet, V. (2004). Principles for modulation of the nuclear receptor superfamily. Nat Rev Drug Discov *3*, 950-964.
Grossel, M.J., and Hinds, P.W. (2006). From cell cycle to differentiation: an expanding role for cdk6. Cell Cycle *5*, 266-270.
Grunberg, S., Warfield, L., and Hahn, S. (2012). Architecture of the RNA polymerase II preinitiation complex and mechanism of ATP-dependent promoter opening. Nat Struct Mol Biol *19*, 788-796.
Guan, X., LaPak, K.M., Hennessey, R.C., Yu, C.Y., Shakya, R., Zhang, J., and Burd, C.E. (2017). Stromal Senescence By Prolonged CDK4/6 Inhibition Potentiates Tumor Growth. Mol Cancer Res *15*, 237-249.
Guarducci, C., Bonechi, M., Benelli, M., Biagioni, C., Boccalini, G., Romagnoli, D., Verardo, R., Schiff, R., Osborne, C.K., De Angelis, C., Di Leo, A., Malorni, L., and Migliaccio, I. (2018). Cyclin E1 and Rb modulation as common events at time of resistance to palbociclib in hormone receptor-positive breast cancer. NPJ Breast Cancer *4*, 38.
Hafner, M., Mills, C.E., Subramanian, K., Chen, C., Chung, M., Boswell, S.A., Everley, R.A., Liu, C., Walmsley, C.S., Juric, D., and Sorger, P.K. (2019). Multiomics Profiling

Establishes the Polypharmacology of FDA-Approved CDK4/6 Inhibitors and the Potential for Differential Clinical Activity. Cell Chem Biol *26*, 1067-1080 e1068.
Hahn, S. (2004). Structure and mechanism of the RNA polymerase II transcription machinery. Nat Struct Mol Biol *11*, 394-403.
Hamilton, E.P., Wang, J.S., Pluard, T., Johnston, S., Morikawa, A.A., Dees, C.E., Jones, R.H., Haley, B., Armstrong, A., Cohen, A.L., Munster, P., Wright, G., Kayali, F., Korpal, M., Yu, L., Cantagallo, L., Destenaves, B., Zhang, Z., Gao, L., Pipas, M.J., Sahmouud, T., Gualberto, A., and Juric, D. (2021). Abstract PD8-06: Phase I/II trial of H3B-6545, a novel selective estrogen receptor covalent antagonist (SERCA), in estrogen receptor positive (ER+), human epidermal growth factor receptor 2 negative (HER2-) advanced breast cancer. Cancer Research *81*, PD8-06-PD08-06.
Hammes, S.R., and Levin, E.R. (2007). Extranuclear steroid receptors: nature and actions. Endocr Rev *28*, 726-741.
Hammond, C.M., Stromme, C.B., Huang, H., Patel, D.J., and Groth, A. (2017). Histone chaperone networks shaping chromatin function. Nat Rev Mol Cell Biol *18*, 141-158.
Hanahan, D., and Weinberg, R.A. (2011). Hallmarks of cancer: the next generation. Cell *144*, 646-674.
Hanker, A.B., Sudhan, D.R., and Arteaga, C.L. (2020). Overcoming Endocrine Resistance in Breast Cancer. Cancer Cell *37*, 496-513.
Harbeck, N., Penault-Llorca, F., Cortes, J., Gnant, M., Houssami, N., Poortmans, P., Ruddy, K., Tsang, J., and Cardoso, F. (2019). Breast cancer. Nat Rev Dis Primers *5*, 66.
Harper, J.W., Adami, G.R., Wei, N., Keyomarsi, K., and Elledge, S.J. (1993). The p21 Cdk-interacting protein Cip1 is a potent inhibitor of G1 cyclin-dependent kinases. Cell *75*, 805-816.
Harris, S.L., and Levine, A.J. (2005). The p53 pathway: positive and negative feedback loops. Oncogene *24*, 2899-2908.
Hartmaier, R.J., Trabucco, S.E., Priedigkeit, N., Chung, J.H., Parachoniak, C.A., Vanden Borre, P., Morley, S., Rosenzweig, M., Gay, L.M., Goldberg, M.E., Suh, J., Ali, S.M., Ross, J., Leyland-Jones, B., Young, B., Williams, C., Park, B., Tsai, M., Haley, B., Peguero, J., Callahan, R.D., Sachelarie, I., Cho, J., Atkinson, J.M., Bahreini, A., Nagle, A.M., Puhalla, S.L., Watters, R.J., Erdogan-Yildirim, Z., Cao, L., Oesterreich, S., Mathew, A., Lucas, P.C., Davidson, N.E., Brufsky, A.M., Frampton, G.M., Stephens, P.J., Chmielecki, J., and Lee, A.V. (2018). Recurrent hyperactive ESR1 fusion proteins in endocrine therapy-resistant breast cancer. Ann Oncol *29*, 872-880.

Hashiguchi, T., Bruss, N., Best, S., Lam, V., Danilova, O., Paiva, C.J., Wolf, J., Gilbert, E.W., Okada, C.Y., Kaur, P., Drew, L., Cidado, J., Hurlin, P., and Danilov, A.V. (2019). Cyclin-Dependent Kinase-9 Is a Therapeutic Target in MYC-Expressing Diffuse Large B-Cell Lymphoma. Mol Cancer Ther *18*, 1520-1532.

Haushalter, K.A., and Kadonaga, J.T. (2003). Chromatin assembly by DNA-translocating motors. Nat Rev Mol Cell Biol *4*, 613-620.

Heald, R., and McKeon, F. (1990). Mutations of phosphorylation sites in lamin A that prevent nuclear lamina disassembly in mitosis. Cell *61*, 579-589.

Heldring, N., Pike, A., Andersson, S., Matthews, J., Cheng, G., Hartman, J., Tujague, M., Strom, A., Treuter, E., Warner, M., and Gustafsson, J.A. (2007). Estrogen receptors: how do they signal and what are their targets. Physiol Rev *87*, 905-931.

Helin, K., Harlow, E., and Fattaey, A. (1993). Inhibition of E2F-1 transactivation by direct binding of the retinoblastoma protein. Mol Cell Biol *13*, 6501-6508.

Helin, K., Lees, J.A., Vidal, M., Dyson, N., Harlow, E., and Fattaey, A. (1992). A cDNA encoding a pRB-binding protein with properties of the transcription factor E2F. Cell *70*, 337-350.

Herrera-Abreu, M.T., Palafox, M., Asghar, U., Rivas, M.A., Cutts, R.J., Garcia-Murillas, I., Pearson, A., Guzman, M., Rodriguez, O., Grueso, J., Bellet, M., Cortes, J., Elliott, R., Pancholi, S., Baselga, J., Dowsett, M., Martin, L.A., Turner, N.C., and Serra, V. (2016). Early Adaptation and Acquired Resistance to CDK4/6 Inhibition in Estrogen Receptor-Positive Breast Cancer. Cancer Res *76*, 2301-2313.

Herschkowitz, J.I., He, X., Fan, C., and Perou, C.M. (2008). The functional loss of the retinoblastoma tumour suppressor is a common event in basal-like and luminal B breast carcinomas. Breast Cancer Res *10*, R75.

Herzog, S.K., and Fuqua, S.A.W. (2021). ESR1 mutations and therapeutic resistance in metastatic breast cancer: progress and remaining challenges. Br J Cancer.

Hickey, T.E., Selth, L.A., Chia, K.M., Laven-Law, G., Milioli, H.H., Roden, D., Jindal, S., Hui, M., Finlay-Schultz, J., Ebrahimie, E., Birrell, S.N., Stelloo, S., Iggo, R., Alexandrou, S., Caldon, C.E., Abdel-Fatah, T.M., Ellis, I.O., Zwart, W., Palmieri, C., Sartorius, C.A., Swarbrick, A., Lim, E., Carroll, J.S., and Tilley, W.D. (2021). The androgen receptor is a tumor suppressor in estrogen receptor-positive breast cancer. Nat Med *27*, 310-320.

Hiebert, S.W., Chellappan, S.P., Horowitz, J.M., and Nevins, J.R. (1992). The interaction of RB with E2F coincides with an inhibition of the transcriptional activity of E2F. Genes Dev *6*, 177-185.

Hills, S.A., and Diffley, J.F. (2014). DNA replication and oncogene-induced replicative stress. Curr Biol *24*, R435-444.
Hinohara, K., Wu, H.J., Sebastien, V., McDonald, T.O., Igarashi, K.J., Yamamoto, K.N., Madsen, T., Fassl, A., Egri, S.B., Papanastasiou, M., Ding, L., Peluffo, G., Cohen, O., Kales, S.C., Lal-Nag, M., Rai, G., Maloney, D.J., Jadhav, A., Simeonov, A., Wagle, N., Brown, M., Meissner, A., Sicinski, P., Jaffe, J.D., Jeselsohn, R., Gimelbrant, A.A., Michor, F., and Polyak, K. (2019). KDM5 Histone Demethylase Activity Links Cellular Transcriptomic Heterogeneity to Therapeutic Resistance. Cancer Cell *35*, 330-332.
Hiraga, S.I., Ly, T., Garzon, J., Horejsi, Z., Ohkubo, Y.N., Endo, A., Obuse, C., Boulton, S.J., Lamond, A.I., and Donaldson, A.D. (2017). Human RIF1 and protein phosphatase 1 stimulate DNA replication origin licensing but suppress origin activation. EMBO Rep *18*, 403-419.
Hortobagyi, G.N., Stemmer, S.M., Burris, H.A., Yap, Y.-S., Sonke, G.S., Paluch-Shimon, S., Campone, M., Blackwell, K.L., André, F., Winer, E.P., Janni, W., Verma, S., Conte, P., Arteaga, C.L., Cameron, D.A., Petrakova, K., Hart, L.L., Villanueva, C., Chan, A., Jakobsen, E., Nusch, A., Burdaeva, O., Grischke, E.-M., Alba, E., Wist, E., Marschner, N., Favret, A.M., Yardley, D., Bachelot, T., Tseng, L.-M., Blau, S., Xuan, F., Souami, F., Miller, M., Germa, C., Hirawat, S., and O'Shaughnessy, J. (2016). Ribociclib as First-Line Therapy for HR-Positive, Advanced Breast Cancer. New England Journal of Medicine *375*, 1738-1748.
Hu, S., Danilov, A.V., Godek, K., Orr, B., Tafe, L.J., Rodriguez-Canales, J., Behrens, C., Mino, B., Moran, C.A., Memoli, V.A., Mustachio, L.M., Galimberti, F., Ravi, S., DeCastro, A., Lu, Y., Sekula, D., Andrew, A.S., Wistuba, II, Freemantle, S., Compton, D.A., and Dmitrovsky, E. (2015a). CDK2 Inhibition Causes Anaphase Catastrophe in Lung Cancer through the Centrosomal Protein CP110. Cancer Res *75*, 2029-2038.
Hu, S., Lu, Y., Orr, B., Godek, K., Mustachio, L.M., Kawakami, M., Sekula, D., Compton, D.A., Freemantle, S., and Dmitrovsky, E. (2015b). Specific CP110 Phosphorylation Sites Mediate Anaphase Catastrophe after CDK2 Inhibition: Evidence for Cooperation with USP33 Knockdown. Mol Cancer Ther *14*, 2576-2585.
Hu, S., Marineau, J., Hamman, K., Bradley, M., Savinainen, A., Alnemy, S., Rajagopal, N., Orlando, D., Chuaqui, C., and Olson, E. (2019a). Abstract 4421: SY-5609, an orally available selective CDK7 inhibitor demonstrates broad anti-tumor activity in vivo. Cancer Research *79*, 4421-4421.
Hu, S., Marineau, J.J., Rajagopal, N., Hamman, K.B., Choi, Y.J., Schmidt, D.R., Ke, N., Johannessen, L., Bradley, M.J., Orlando, D.A., Alnemy, S.R., Ren, Y., Ciblat, S., Winter, D.K., Kabro, A., Sprott, K.T., Hodgson, J.G., Fritz, C.C., Carulli, J.P., di Tomaso, E., and

Olson, E.R. (2019b). Discovery and Characterization of SY-1365, a Selective, Covalent Inhibitor of CDK7. Cancer Res *79*, 3479-3491.
Huang, C.H., Lujambio, A., Zuber, J., Tschaharganeh, D.F., Doran, M.G., Evans, M.J., Kitzing, T., Zhu, N., de Stanchina, E., Sawyers, C.L., Armstrong, S.A., Lewis, J.S., Sherr, C.J., and Lowe, S.W. (2014). CDK9-mediated transcription elongation is required for MYC addiction in hepatocellular carcinoma. Genes Dev *28*, 1800-1814.
Hubalek, M.M., Widschwendter, A., Erdel, M., Gschwendtner, A., Fiegl, H.M., Muller, H.M., Goebel, G., Mueller-Holzner, E., Marth, C., Spruck, C.H., Reed, S.I., and Widschwendter, M. (2004). Cyclin E dysregulation and chromosomal instability in endometrial cancer. Oncogene *23*, 4187-4192.
Hui, R., Finney, G.L., Carroll, J.S., Lee, C.S., Musgrove, E.A., and Sutherland, R.L. (2002). Constitutive overexpression of cyclin D1 but not cyclin E confers acute resistance to antiestrogens in T-47D breast cancer cells. Cancer Res *62*, 6916-6923.
Hulsen, T., de Vlieg, J., and Alkema, W. (2008). BioVenn - a web application for the comparison and visualization of biological lists using area-proportional Venn diagrams. BMC Genomics *9*, 488.
Hummer, S., and Mayer, T.U. (2009). Cdk1 negatively regulates midzone localization of the mitotic kinesin Mklp2 and the chromosomal passenger complex. Curr Biol *19*, 607-612.
Hurvitz, S.A., Martin, M., Press, M.F., Chan, D., Fernandez-Abad, M., Petru, E., Rostorfer, R., Guarneri, V., Huang, C.S., Barriga, S., Wijayawardana, S., Brahmachary, M., Ebert, P.J., Hossain, A., Liu, J., Abel, A., Aggarwal, A., Jansen, V.M., and Slamon, D.J. (2020). Potent Cell-Cycle Inhibition and Upregulation of Immune Response with Abemaciclib and Anastrozole in neoMONARCH, Phase II Neoadjuvant Study in HR(+)/HER2(-) Breast Cancer. Clin Cancer Res *26*, 566-580.
Husby, A., Wohlfahrt, J., Oyen, N., and Melbye, M. (2018). Pregnancy duration and breast cancer risk. Nat Commun *9*, 4255.
Hutterer, A., Glotzer, M., and Mishima, M. (2009). Clustering of centralspindlin is essential for its accumulation to the central spindle and the midbody. Curr Biol *19*, 2043-2049.
Hwang, H.C., and Clurman, B.E. (2005). Cyclin E in normal and neoplastic cell cycles. Oncogene *24*, 2776-2786.
Iavarone, A., and Massague, J. (1999). E2F and histone deacetylase mediate transforming growth factor beta repression of cdc25A during keratinocyte cell cycle arrest. Mol Cell Biol *19*, 916-922.
Ignar-Trowbridge, D.M., Nelson, K.G., Bidwell, M.C., Curtis, S.W., Washburn, T.F., McLachlan, J.A., and Korach, K.S. (1992). Coupling of dual signaling pathways: epidermal

growth factor action involves the estrogen receptor. Proc Natl Acad Sci U S A *89*, 4658-4662.
Iida, M., Toyosawa, D., Nakamura, M., Tsuboi, K., Tokuda, E., Niwa, T., Ishida, T., and Hayashi, S.I. (2020). Decreased ER dependency after acquired resistance to CDK4/6 inhibitors. Breast Cancer *27*, 963-972.
Improta-Brears, T., Whorton, A.R., Codazzi, F., York, J.D., Meyer, T., and McDonnell, D.P. (1999). Estrogen-induced activation of mitogen-activated protein kinase requires mobilization of intracellular calcium. Proc Natl Acad Sci U S A *96*, 4686-4691.
Infante, J.R., Shapiro, G., Witteveen, P., Gerecitano, J.F., Ribrag, V., Chugh, R., Issa, I., Chakraborty, A., Matano, A., Zhao, X., Parasuraman, S., and Cassier, P. (2014). A phase I study of the single-agent CDK4/6 inhibitor LEE011 in pts with advanced solid tumors and lymphomas. Journal of Clinical Oncology *32*, 2528-2528.
Ishida, S., Huang, E., Zuzan, H., Spang, R., Leone, G., West, M., and Nevins, J.R. (2001). Role for E2F in control of both DNA replication and mitotic functions as revealed from DNA microarray analysis. Mol Cell Biol *21*, 4684-4699.
Ito, M., Tanaka, T., Toita, A., Uchiyama, N., Kokubo, H., Morishita, N., Klein, M.G., Zou, H., Murakami, M., Kondo, M., Sameshima, T., Araki, S., Endo, S., Kawamoto, T., Morin, G.B., Aparicio, S.A., Nakanishi, A., Maezaki, H., and Imaeda, Y. (2018). Discovery of 3-Benzyl-1-(trans-4-((5-cyanopyridin-2-yl)amino)cyclohexyl)-1-arylurea Derivatives as Novel and Selective Cyclin-Dependent Kinase 12 (CDK12) Inhibitors. J Med Chem *61*, 7710-7728.
Iwamoto, M., Bjorklund, T., Lundberg, C., Kirik, D., and Wandless, T.J. (2010). A general chemical method to regulate protein stability in the mammalian central nervous system. Chem Biol *17*, 981-988.
Jacobs, H.W., Knoblich, J.A., and Lehner, C.F. (1998). Drosophila Cyclin B3 is required for female fertility and is dispensable for mitosis like Cyclin B. Genes Dev *12*, 3741-3751.
James, M.K., Ray, A., Leznova, D., and Blain, S.W. (2008). Differential modification of p27Kip1 controls its cyclin D-cdk4 inhibitory activity. Mol Cell Biol *28*, 498-510.
Jang, M.K., Mochizuki, K., Zhou, M., Jeong, H.S., Brady, J.N., and Ozato, K. (2005). The bromodomain protein Brd4 is a positive regulatory component of P-TEFb and stimulates RNA polymerase II-dependent transcription. Mol Cell *19*, 523-534.
Jawhari, A., Laine, J.P., Dubaele, S., Lamour, V., Poterszman, A., Coin, F., Moras, D., and Egly, J.M. (2002). p52 Mediates XPB function within the transcription/repair factor TFIIH. J Biol Chem *277*, 31761-31767.
Jayasekara, H., MacInnis, R.J., Chamberlain, J.A., Dite, G.S., Leoce, N.M., Dowty, J.G., Bickerstaffe, A., Win, A.K., Milne, R.L., Giles, G.G., Terry, M.B., Eccles, D.M., Southey,

M.C., and Hopper, J.L. (2019). Mortality after breast cancer as a function of time since diagnosis by estrogen receptor status and age at diagnosis. Int J Cancer *145*, 3207-3217.
Jeffrey, P.D., Russo, A.A., Polyak, K., Gibbs, E., Hurwitz, J., Massague, J., and Pavletich, N.P. (1995). Mechanism of CDK activation revealed by the structure of a cyclinA-CDK2 complex. Nature *376*, 313-320.
Jeffrey, P.D., Tong, L., and Pavletich, N.P. (2000). Structural basis of inhibition of CDK-cyclin complexes by INK4 inhibitors. Genes Dev *14*, 3115-3125.
Jeffreys, S.A., Becker, T.M., Khan, S., Soon, P., Neubauer, H., de Souza, P., and Powter, B. (2022). Prognostic and Predictive Value of CCND1/Cyclin D1 Amplification in Breast Cancer With a Focus on Postmenopausal Patients: A Systematic Review and Meta-Analysis. Front Endocrinol (Lausanne) *13*, 895729.
Jensen, E.V., Desombre, E.R., Kawashima, T., Suzuki, T., Kyser, K., and Jungblut, P.W. (1967). Estrogen-binding substances of target tissues. Science *158*, 529-530.
Jeselsohn, R., Buchwalter, G., De Angelis, C., Brown, M., and Schiff, R. (2015). ESR1 mutations-a mechanism for acquired endocrine resistance in breast cancer. Nat Rev Clin Oncol *12*, 573-583.
Jiang, B., Gao, Y., Che, J., Lu, W., Kaltheuner, I.H., Dries, R., Kalocsay, M., Berberich, M.J., Jiang, J., You, I., Kwiatkowski, N., Riching, K.M., Daniels, D.L., Sorger, P.K., Geyer, M., Zhang, T., and Gray, N.S. (2021). Discovery and resistance mechanism of a selective CDK12 degrader. Nat Chem Biol *17*, 675-683.
Jiang, C., and Pugh, B.F. (2009). Nucleosome positioning and gene regulation: advances through genomics. Nat Rev Genet *10*, 161-172.
Jiang, L., Huang, R., Wu, Y., Diao, P., Zhang, W., Li, J., Li, Z., Wang, Y., Cheng, J., and Yang, J. (2019). Overexpression of CDK7 is associated with unfavourable prognosis in oral squamous cell carcinoma. Pathology *51*, 74-80.
Jiang, W., Jimenez, G., Wells, N.J., Hope, T.J., Wahl, G.M., Hunter, T., and Fukunaga, R. (1998). PRC1: a human mitotic spindle-associated CDK substrate protein required for cytokinesis. Mol Cell *2*, 877-885.
Joel, P.B., Smith, J., Sturgill, T.W., Fisher, T.L., Blenis, J., and Lannigan, D.A. (1998). pp90rsk1 regulates estrogen receptor-mediated transcription through phosphorylation of Ser-167. Mol Cell Biol *18*, 1978-1984.
Johannes, J.W., Denz, C.R., Su, N., Wu, A., Impastato, A.C., Mlynarski, S., Varnes, J.G., Prince, D.B., Cidado, J., Gao, N., Haddrick, M., Jones, N.H., Li, S., Li, X., Liu, Y., Nguyen, T.B., O'Connell, N., Rivers, E., Robbins, D.W., Tomlinson, R., Yao, T., Zhu, X., Ferguson,

A.D., Lamb, M.L., Manchester, J.I., and Guichard, S. (2018). Structure-Based Design of Selective Noncovalent CDK12 Inhibitors. ChemMedChem *13*, 231-235.
Johannessen, L.H., Hu, S., Ke, N., D'Ippolito, A., Rajagopal, N., Marineau, J., Savinainen, A., Zamboni, W., and Hodgson, G. (2019). Abstract C091: Preclinical evaluation of PK, PD, and antitumor activity of the oral, non-covalent, potent and highly selective CDK7 inhibitor, SY-5609, provides rationale for clinical development in multiple solid tumor indications. Molecular Cancer Therapeutics *18*, C091-C091.
Johnson, J., Thijssen, B., McDermott, U., Garnett, M., Wessels, L.F., and Bernards, R. (2016). Targeting the RB-E2F pathway in breast cancer. Oncogene *35*, 4829-4835.
Johnston, S., Martin, M., Di Leo, A., Im, S.A., Awada, A., Forrester, T., Frenzel, M., Hardebeck, M.C., Cox, J., Barriga, S., Toi, M., Iwata, H., and Goetz, M.P. (2019). MONARCH 3 final PFS: a randomized study of abemaciclib as initial therapy for advanced breast cancer. NPJ Breast Cancer *5*, 5.
Johnston, S., O'Shaughnessy, J., Martin, M., Huober, J., Toi, M., Sohn, J., Andre, V.A.M., Martin, H.R., Hardebeck, M.C., and Goetz, M.P. (2021). Abemaciclib as initial therapy for advanced breast cancer: MONARCH 3 updated results in prognostic subgroups. NPJ Breast Cancer *7*, 80.
Johnston, S.R.D., Harbeck, N., Hegg, R., Toi, M., Martin, M., Shao, Z.M., Zhang, Q.Y., Martinez Rodriguez, J.L., Campone, M., Hamilton, E., Sohn, J., Guarneri, V., Okada, M., Boyle, F., Neven, P., Cortes, J., Huober, J., Wardley, A., Tolaney, S.M., Cicin, I., Smith, I.C., Frenzel, M., Headley, D., Wei, R., San Antonio, B., Hulstijn, M., Cox, J., O'Shaughnessy, J., Rastogi, P., monarch, E.C.M., and Investigators (2020). Abemaciclib Combined With Endocrine Therapy for the Adjuvant Treatment of HR+, HER2-, Node-Positive, High-Risk, Early Breast Cancer (monarchE). J Clin Oncol *38*, 3987-3998.
Jones, H.E., Gee, J.M., Hutcheson, I.R., Knowlden, J.M., Barrow, D., and Nicholson, R.I. (2006). Growth factor receptor interplay and resistance in cancer. Endocr Relat Cancer *13 Suppl 1*, S45-51.
Jones, R.H., Casbard, A., Carucci, M., Cox, C., Butler, R., Alchami, F., Madden, T.A., Bale, C., Bezecny, P., Joffe, J., Moon, S., Twelves, C., Venkitaraman, R., Waters, S., Foxley, A., and Howell, S.J. (2020). Fulvestrant plus capivasertib versus placebo after relapse or progression on an aromatase inhibitor in metastatic, oestrogen receptor-positive breast cancer (FAKTION): a multicentre, randomised, controlled, phase 2 trial. Lancet Oncol *21*, 345-357.
Jonkers, I., and Lis, J.T. (2015). Getting up to speed with transcription elongation by RNA polymerase II. Nat Rev Mol Cell Biol *16*, 167-177.

Jorda, R., Buckova, Z., Reznickova, E., Bouchal, J., and Krystof, V. (2018). Selective inhibition reveals cyclin-dependent kinase 2 as another kinase that phosphorylates the androgen receptor at serine 81. Biochim Biophys Acta Mol Cell Res *1865*, 354-363.
Joung, J., Konermann, S., Gootenberg, J.S., Abudayyeh, O.O., Platt, R.J., Brigham, M.D., Sanjana, N.E., and Zhang, F. (2017). Genome-scale CRISPR-Cas9 knockout and transcriptional activation screening. Nat Protoc *12*, 828-863.
Juang, Y.L., Huang, J., Peters, J.M., McLaughlin, M.E., Tai, C.Y., and Pellman, D. (1997). APC-mediated proteolysis of Ase1 and the morphogenesis of the mitotic spindle. Science *275*, 1311-1314.
Kainov, D.E., Vitorino, M., Cavarelli, J., Poterszman, A., and Egly, J.M. (2008). Structural basis for group A trichothiodystrophy. Nat Struct Mol Biol *15*, 980-984.
Kalinsky, K., Jacks, L.M., Heguy, A., Patil, S., Drobnjak, M., Bhanot, U.K., Hedvat, C.V., Traina, T.A., Solit, D., Gerald, W., and Moynahan, M.E. (2009). PIK3CA mutation associates with improved outcome in breast cancer. Clin Cancer Res *15*, 5049-5059.
Kanazawa, S., Soucek, L., Evan, G., Okamoto, T., and Peterlin, B.M. (2003). c-Myc recruits P-TEFb for transcription, cellular proliferation and apoptosis. Oncogene *22*, 5707-5711.
Kapoor, A., Goldberg, M.S., Cumberland, L.K., Ratnakumar, K., Segura, M.F., Emanuel, P.O., Menendez, S., Vardabasso, C., Leroy, G., Vidal, C.I., Polsky, D., Osman, I., Garcia, B.A., Hernando, E., and Bernstein, E. (2010). The histone variant macroH2A suppresses melanoma progression through regulation of CDK8. Nature *468*, 1105-1109.
Kato, J., Matsushime, H., Hiebert, S.W., Ewen, M.E., and Sherr, C.J. (1993). Direct binding of cyclin D to the retinoblastoma gene product (pRb) and pRb phosphorylation by the cyclin D-dependent kinase CDK4. Genes Dev *7*, 331-342.
Kato, S., Endoh, H., Masuhiro, Y., Kitamoto, T., Uchiyama, S., Sasaki, H., Masushige, S., Gotoh, Y., Nishida, E., Kawashima, H., Metzger, D., and Chambon, P. (1995). Activation of the estrogen receptor through phosphorylation by mitogen-activated protein kinase. Science *270*, 1491-1494.
Katzenellenbogen, J.A., Mayne, C.G., Katzenellenbogen, B.S., Greene, G.L., and Chandarlapaty, S. (2018). Structural underpinnings of oestrogen receptor mutations in endocrine therapy resistance. Nat Rev Cancer *18*, 377-388.
Kawakami, M., Mustachio, L.M., Liu, X., and Dmitrovsky, E. (2018). Engaging Anaphase Catastrophe Mechanisms to Eradicate Aneuploid Cancers. Mol Cancer Ther *17*, 724-731.
Kelland, L.R. (2000). Flavopiridol, the first cyclin-dependent kinase inhibitor to enter the clinic: current status. Expert Opin Investig Drugs *9*, 2903-2911.

Keller, C., and Krude, T. (2000). Requirement of Cyclin/Cdk2 and protein phosphatase 1 activity for chromatin assembly factor 1-dependent chromatin assembly during DNA synthesis. J Biol Chem *275*, 35512-35521.
Kenny, F.S., Hui, R., Musgrove, E.A., Gee, J.M., Blamey, R.W., Nicholson, R.I., Sutherland, R.L., and Robertson, J.F. (1999). Overexpression of cyclin D1 messenger RNA predicts for poor prognosis in estrogen receptor-positive breast cancer. Clin Cancer Res *5*, 2069-2076.
Kent, L.N., and Leone, G. (2019). The broken cycle: E2F dysfunction in cancer. Nat Rev Cancer *19*, 326-338.
Key, T.J., Verkasalo, P.K., and Banks, E. (2001). Epidemiology of breast cancer. Lancet Oncol *2*, 133-140.
Khan, S.A., Rogers, M.A., Khurana, K.K., Meguid, M.M., and Numann, P.J. (1998). Estrogen receptor expression in benign breast epithelium and breast cancer risk. J Natl Cancer Inst *90*, 37-42.
Kim, K.K., Chamberlin, H.M., Morgan, D.O., and Kim, S.H. (1996). Three-dimensional structure of human cyclin H, a positive regulator of the CDK-activating kinase. Nat Struct Biol *3*, 849-855.
Kim, M.Y., Woo, E.M., Chong, Y.T., Homenko, D.R., and Kraus, W.L. (2006). Acetylation of estrogen receptor alpha by p300 at lysines 266 and 268 enhances the deoxyribonucleic acid binding and transactivation activities of the receptor. Mol Endocrinol *20*, 1479-1493.
Kim, W., Haws, H., Peterson, P., Whatcott, C.J., Weitman, S., Warner, S.L., Bearss, D.J., and Siddiqui-Jain, A. (2017). Abstract 5133: TP-1287, an oral prodrug of the cyclin-dependent kinase-9 inhibitor alvocidib. Cancer Research *77*, 5133-5133.
King, R.W., Deshaies, R.J., Peters, J.M., and Kirschner, M.W. (1996). How proteolysis drives the cell cycle. Science *274*, 1652-1659.
Kingston, B., Cutts, R.J., Bye, H., Beaney, M., Walsh-Crestani, G., Hrebien, S., Swift, C., Kilburn, L.S., Kernaghan, S., Moretti, L., Wilkinson, K., Wardley, A.M., Macpherson, I.R., Baird, R.D., Roylance, R., Reis-Filho, J.S., Hubank, M., Faull, I., Banks, K.C., Lanman, R.B., Garcia-Murillas, I., Bliss, J.M., Ring, A., and Turner, N.C. (2021). Genomic profile of advanced breast cancer in circulating tumour DNA. Nat Commun *12*, 2423.
Klatt, F., Leitner, A., Kim, I.V., Ho-Xuan, H., Schneider, E.V., Langhammer, F., Weinmann, R., Muller, M.R., Huber, R., Meister, G., and Kuhn, C.D. (2020). A precisely positioned MED12 activation helix stimulates CDK8 kinase activity. Proc Natl Acad Sci U S A *117*, 2894-2905.
Knudsen, E.S., and Knudsen, K.E. (2008). Tailoring to RB: tumour suppressor status and therapeutic response. Nat Rev Cancer *8*, 714-724.

Knudsen, E.S., and Witkiewicz, A.K. (2017). The Strange Case of CDK4/6 Inhibitors: Mechanisms, Resistance, and Combination Strategies. Trends Cancer *3*, 39-55.
Knuesel, M.T., Meyer, K.D., Bernecky, C., and Taatjes, D.J. (2009). The human CDK8 subcomplex is a molecular switch that controls Mediator coactivator function. Genes Dev *23*, 439-451.
Kocanova, S., Mazaheri, M., Caze-Subra, S., and Bystricky, K. (2010). Ligands specify estrogen receptor alpha nuclear localization and degradation. BMC Cell Biol *11*, 98.
Koide, A., Zhao, C., Naganuma, M., Abrams, J., Deighton-Collins, S., Skafar, D.F., and Koide, S. (2007). Identification of regions within the F domain of the human estrogen receptor alpha that are important for modulating transactivation and protein-protein interactions. Mol Endocrinol *21*, 829-842.
Kojima, K., Shimanuki, M., Shikami, M., Andreeff, M., and Nakakuma, H. (2009). Cyclin-dependent kinase 1 inhibitor RO-3306 enhances p53-mediated Bax activation and mitochondrial apoptosis in AML. Cancer Sci *100*, 1128-1136.
Konermann, S., Brigham, M.D., Trevino, A.E., Joung, J., Abudayyeh, O.O., Barcena, C., Hsu, P.D., Habib, N., Gootenberg, J.S., Nishimasu, H., Nureki, O., and Zhang, F. (2015). Genome-scale transcriptional activation by an engineered CRISPR-Cas9 complex. Nature *517*, 583-588.
Kouros-Mehr, H., Slorach, E.M., Sternlicht, M.D., and Werb, Z. (2006). GATA-3 maintains the differentiation of the luminal cell fate in the mammary gland. Cell *127*, 1041-1055.
Kowalik, T.F. (2002). Smad about E2F. TGFbeta repressionof c-Myc via a Smad3/E2F/p107 complex. Mol Cell *10*, 7-8.
Kozar, K., Ciemerych, M.A., Rebel, V.I., Shigematsu, H., Zagozdzon, A., Sicinska, E., Geng, Y., Yu, Q., Bhattacharya, S., Bronson, R.T., Akashi, K., and Sicinski, P. (2004). Mouse development and cell proliferation in the absence of D-cyclins. Cell *118*, 477-491.
Krege, J.H., Hodgin, J.B., Couse, J.F., Enmark, E., Warner, M., Mahler, J.F., Sar, M., Korach, K.S., Gustafsson, J.A., and Smithies, O. (1998). Generation and reproductive phenotypes of mice lacking estrogen receptor beta. Proc Natl Acad Sci U S A *95*, 15677-15682.
Krek, W., Xu, G., and Livingston, D.M. (1995). Cyclin A-kinase regulation of E2F-1 DNA binding function underlies suppression of an S phase checkpoint. Cell *83*, 1149-1158.
Krimpenfort, P., Ijpenberg, A., Song, J.Y., van der Valk, M., Nawijn, M., Zevenhoven, J., and Berns, A. (2007). p15Ink4b is a critical tumour suppressor in the absence of p16Ink4a. Nature *448*, 943-946.

Krystof, V., Baumli, S., and Furst, R. (2012). Perspective of cyclin-dependent kinase 9 (CDK9) as a drug target. Curr Pharm Des *18*, 2883-2890.
Kubo, N., Ishii, H., Xiong, X., Bianco, S., Meitinger, F., Hu, R., Hocker, J.D., Conte, M., Gorkin, D., Yu, M., Li, B., Dixon, J.R., Hu, M., Nicodemi, M., Zhao, H., and Ren, B. (2021). Promoter-proximal CTCF binding promotes distal enhancer-dependent gene activation. Nat Struct Mol Biol *28*, 152-161.
Kuehner, J.N., Pearson, E.L., and Moore, C. (2011). Unravelling the means to an end: RNA polymerase II transcription termination. Nat Rev Mol Cell Biol *12*, 283-294.
Kuiper, G.G., Enmark, E., Pelto-Huikko, M., Nilsson, S., and Gustafsson, J.A. (1996). Cloning of a novel receptor expressed in rat prostate and ovary. Proc Natl Acad Sci U S A *93*, 5925-5930.
Kumar, R., and Thompson, E.B. (1999). The structure of the nuclear hormone receptors. Steroids *64*, 310-319.
Kurat, C.F., Yeeles, J.T.P., Patel, H., Early, A., and Diffley, J.F.X. (2017). Chromatin Controls DNA Replication Origin Selection, Lagging-Strand Synthesis, and Replication Fork Rates. Mol Cell *65*, 117-130.
Kwiatkowski, N., Zhang, T., Rahl, P.B., Abraham, B.J., Reddy, J., Ficarro, S.B., Dastur, A., Amzallag, A., Ramaswamy, S., Tesar, B., Jenkins, C.E., Hannett, N.M., McMillin, D., Sanda, T., Sim, T., Kim, N.D., Look, T., Mitsiades, C.S., Weng, A.P., Brown, J.R., Benes, C.H., Marto, J.A., Young, R.A., and Gray, N.S. (2014). Targeting transcription regulation in cancer with a covalent CDK7 inhibitor. Nature *511*, 616-620.
Kwon, Y.G., Lee, S.Y., Choi, Y., Greengard, P., and Nairn, A.C. (1997). Cell cycle-dependent phosphorylation of mammalian protein phosphatase 1 by cdc2 kinase. Proc Natl Acad Sci U S A *94*, 2168-2173.
LaBaer, J., Garrett, M.D., Stevenson, L.F., Slingerland, J.M., Sandhu, C., Chou, H.S., Fattaey, A., and Harlow, E. (1997). New functional activities for the p21 family of CDK inhibitors. Genes Dev *11*, 847-862.
Laganiere, J., Deblois, G., Lefebvre, C., Bataille, A.R., Robert, F., and Giguere, V. (2005). From the Cover: Location analysis of estrogen receptor alpha target promoters reveals that FOXA1 defines a domain of the estrogen response. Proc Natl Acad Sci U S A *102*, 11651-11656.
Lammens, T., Li, J., Leone, G., and De Veylder, L. (2009). Atypical E2Fs: new players in the E2F transcription factor family. Trends Cell Biol *19*, 111-118.

Landis, M.W., Pawlyk, B.S., Li, T., Sicinski, P., and Hinds, P.W. (2006). Cyclin D1-dependent kinase activity in murine development and mammary tumorigenesis. Cancer Cell *9*, 13-22.

Langmead, B., and Salzberg, S.L. (2012). Fast gapped-read alignment with Bowtie 2. Nat Methods *9*, 357-359.

Laoukili, J., Kooistra, M.R., Bras, A., Kauw, J., Kerkhoven, R.M., Morrison, A., Clevers, H., and Medema, R.H. (2005). FoxM1 is required for execution of the mitotic programme and chromosome stability. Nat Cell Biol *7*, 126-136.

Larochelle, S., Amat, R., Glover-Cutter, K., Sanso, M., Zhang, C., Allen, J.J., Shokat, K.M., Bentley, D.L., and Fisher, R.P. (2012). Cyclin-dependent kinase control of the initiation-to-elongation switch of RNA polymerase II. Nat Struct Mol Biol *19*, 1108-1115.

Larochelle, S., Pandur, J., Fisher, R.P., Salz, H.K., and Suter, B. (1998). Cdk7 is essential for mitosis and for in vivo Cdk-activating kinase activity. Genes Dev *12*, 370-381.

Le Romancer, M., Poulard, C., Cohen, P., Sentis, S., Renoir, J.M., and Corbo, L. (2011). Cracking the estrogen receptor's posttranslational code in breast tumors. Endocr Rev *32*, 597-622.

Le Tourneau, C., Faivre, S., Laurence, V., Delbaldo, C., Vera, K., Girre, V., Chiao, J., Armour, S., Frame, S., Green, S.R., Gianella-Borradori, A., Dieras, V., and Raymond, E. (2010). Phase I evaluation of seliciclib (R-roscovitine), a novel oral cyclin-dependent kinase inhibitor, in patients with advanced malignancies. Eur J Cancer *46*, 3243-3250.

Lee, C., Chang, J.H., Lee, H.S., and Cho, Y. (2002). Structural basis for the recognition of the E2F transactivation domain by the retinoblastoma tumor suppressor. Genes Dev *16*, 3199-3212.

Lee, J.O., Russo, A.A., and Pavletich, N.P. (1998). Structure of the retinoblastoma tumour-suppressor pocket domain bound to a peptide from HPV E7. Nature *391*, 859-865.

Lei, T., Zhang, P., Zhang, X., Xiao, X., Zhang, J., Qiu, T., Dai, Q., Zhang, Y., Min, L., Li, Q., Yin, R., Ding, P., Li, N., Qu, Y., Mu, D., Qin, J., Zhu, X., Xiao, Z.X., and Li, Q. (2018). Cyclin K regulates prereplicative complex assembly to promote mammalian cell proliferation. Nat Commun *9*, 1876.

Leng, X., Noble, M., Adams, P.D., Qin, J., and Harper, J.W. (2002). Reversal of growth suppression by p107 via direct phosphorylation by cyclin D1/cyclin-dependent kinase 4. Mol Cell Biol *22*, 2242-2254.

Leonard, J.P., LaCasce, A.S., Smith, M.R., Noy, A., Chirieac, L.R., Rodig, S.J., Yu, J.Q., Vallabhajosula, S., Schoder, H., English, P., Neuberg, D.S., Martin, P., Millenson, M.M., Ely, S.A., Courtney, R., Shaik, N., Wilner, K.D., Randolph, S., Van den Abbeele, A.D.,

Chen-Kiang, S.Y., Yap, J.T., and Shapiro, G.I. (2012). Selective CDK4/6 inhibition with tumor responses by PD0332991 in patients with mantle cell lymphoma. Blood *119*, 4597-4607.

Li, B., Zhao, W.D., Tan, Z.M., Fang, W.G., Zhu, L., and Chen, Y.H. (2006a). Involvement of Rho/ROCK signalling in small cell lung cancer migration through human brain microvascular endothelial cells. FEBS Lett *580*, 4252-4260.

Li, H. (2018). Minimap2: pairwise alignment for nucleotide sequences. Bioinformatics *34*, 3094-3100.

Li, J., Meyer, A.N., and Donoghue, D.J. (1997). Nuclear localization of cyclin B1 mediates its biological activity and is regulated by phosphorylation. Proc Natl Acad Sci U S A *94*, 502-507.

Li, J., Ran, C., Li, E., Gordon, F., Comstock, G., Siddiqui, H., Cleghorn, W., Chen, H.Z., Kornacker, K., Liu, C.G., Pandit, S.K., Khanizadeh, M., Weinstein, M., Leone, G., and de Bruin, A. (2008). Synergistic function of E2F7 and E2F8 is essential for cell survival and embryonic development. Dev Cell *14*, 62-75.

Li, J., Veltri, R.W., Yuan, Z., Christudass, C.S., and Mandecki, W. (2015a). Macrophage inhibitory cytokine 1 biomarker serum immunoassay in combination with PSA is a more specific diagnostic tool for detection of prostate cancer. PLoS One *10*, e0122249.

Li, S., Shen, D., Shao, J., Crowder, R., Liu, W., Prat, A., He, X., Liu, S., Hoog, J., Lu, C., Ding, L., Griffith, O.L., Miller, C., Larson, D., Fulton, R.S., Harrison, M., Mooney, T., McMichael, J.F., Luo, J., Tao, Y., Goncalves, R., Schlosberg, C., Hiken, J.F., Saied, L., Sanchez, C., Giuntoli, T., Bumb, C., Cooper, C., Kitchens, R.T., Lin, A., Phommaly, C., Davies, S.R., Zhang, J., Kavuri, M.S., McEachern, D., Dong, Y.Y., Ma, C., Pluard, T., Naughton, M., Bose, R., Suresh, R., McDowell, R., Michel, L., Aft, R., Gillanders, W., DeSchryver, K., Wilson, R.K., Wang, S., Mills, G.B., Gonzalez-Angulo, A., Edwards, J.R., Maher, C., Perou, C.M., Mardis, E.R., and Ellis, M.J. (2013). Endocrine-therapy-resistant ESR1 variants revealed by genomic characterization of breast-cancer-derived xenografts. Cell Rep *4*, 1116-1130.

Li, Y., Zhang, J., Gao, W., Zhang, L., Pan, Y., Zhang, S., and Wang, Y. (2015b). Insights on Structural Characteristics and Ligand Binding Mechanisms of CDK2. Int J Mol Sci *16*, 9314-9340.

Li, Z., Jiao, X., Wang, C., Ju, X., Lu, Y., Yuan, L., Lisanti, M.P., Katiyar, S., and Pestell, R.G. (2006b). Cyclin D1 induction of cellular migration requires p27(KIP1). Cancer Res *66*, 9986-9994.

Li, Z., McGinn, O., Wu, Y., Bahreini, A., Priedigkeit, N.M., Ding, K., Onkar, S., Lampenfeld, C., Sartorius, C.A., Miller, L., Rosenzweig, M., Cohen, O., Wagle, N., Richer, J.K., Muller, W.J., Buluwela, L., Ali, S., Bruno, T.C., Vignali, D.A.A., Fang, Y., Zhu, L., Tseng, G.C., Gertz, J., Atkinson, J.M., Lee, A.V., and Oesterreich, S. (2022a). ESR1 mutant breast cancers show elevated basal cytokeratins and immune activation. Nat Commun *13*, 2011.

Li, Z., Wu, Y., Yates, M.E., Tasdemir, N., Bahreini, A., Chen, J., Levine, K.M., Priedigkeit, N.M., Nasrazadani, A., Ali, S., Buluwela, L., Arnesen, S., Gertz, J., Richer, J.K., Troness, B., El-Ashry, D., Zhang, Q., Gerratana, L., Zhang, Y., Cristofanilli, M., Montanez, M.A., Sundd, P., Wallace, C.T., Watkins, S.C., Fumagalli, C., Guerini-Rocco, E., Zhu, L., Tseng, G.C., Wagle, N., Carroll, J.S., Jank, P., Denkert, C., Karsten, M.M., Blohmer, J.U., Park, B.H., Lucas, P.C., Atkinson, J.M., Lee, A.V., and Oesterreich, S. (2022b). Hotspot ESR1 Mutations Are Multimodal and Contextual Modulators of Breast Cancer Metastasis. Cancer Res *82*, 1321-1339.

Liang, Y., Besch-Williford, C., Benakanakere, I., Thorpe, P.E., and Hyder, S.M. (2011). Targeting mutant p53 protein and the tumor vasculature: an effective combination therapy for advanced breast tumors. Breast Cancer Res Treat *125*, 407-420.

Liang, Y., Wu, J., Stancel, G.M., and Hyder, S.M. (2005). p53-dependent inhibition of progestin-induced VEGF expression in human breast cancer cells. J Steroid Biochem Mol Biol *93*, 173-182.

Liao, Y., Smyth, G.K., and Shi, W. (2014). featureCounts: an efficient general purpose program for assigning sequence reads to genomic features. Bioinformatics *30*, 923-930.

Likhite, V.S., Stossi, F., Kim, K., Katzenellenbogen, B.S., and Katzenellenbogen, J.A. (2006). Kinase-specific phosphorylation of the estrogen receptor changes receptor interactions with ligand, deoxyribonucleic acid, and coregulators associated with alterations in estrogen and tamoxifen activity. Mol Endocrinol *20*, 3120-3132.

Lin, X., Xiang, H., and Luo, G. (2020). Targeting estrogen receptor alpha for degradation with PROTACs: A promising approach to overcome endocrine resistance. Eur J Med Chem *206*, 112689.

Liu, H., Rankin, S., and Yu, H. (2013). Phosphorylation-enabled binding of SGO1-PP2A to cohesin protects sororin and centromeric cohesion during mitosis. Nat Cell Biol *15*, 40-49.

Liu, M., Xu, S., Wang, Y., Li, Y., Li, Y., Zhang, H., Liu, H., and Chen, J. (2016). PD 0332991, a selective cyclin D kinase 4/6 inhibitor, sensitizes lung cancer cells to treatment with epidermal growth factor receptor tyrosine kinase inhibitors. Oncotarget *7*, 84951-84964.

Liu, P., Cheng, H., Roberts, T.M., and Zhao, J.J. (2009). Targeting the phosphoinositide 3-kinase pathway in cancer. Nat Rev Drug Discov *8*, 627-644.
Liu, P., Kao, T.P., and Huang, H. (2008). CDK1 promotes cell proliferation and survival via phosphorylation and inhibition of FOXO1 transcription factor. Oncogene *27*, 4733-4744.
Liu, S., Xu, Z., Leng, H., Zheng, P., Yang, J., Chen, K., Feng, J., and Li, Q. (2017). RPA binds histone H3-H4 and functions in DNA replication-coupled nucleosome assembly. Science *355*, 415-420.
Liu, Y., Heyman, M., Wang, Y., Falkmer, U., Hising, C., Szekely, L., and Einhorn, S. (1994). Molecular analysis of the retinoblastoma gene in primary ovarian cancer cells. Int J Cancer *58*, 663-667.
Liu, Z., Auboeuf, D., Wong, J., Chen, J.D., Tsai, S.Y., Tsai, M.J., and O'Malley, B.W. (2002). Coactivator/corepressor ratios modulate PR-mediated transcription by the selective receptor modulator RU486. Proc Natl Acad Sci U S A *99*, 7940-7944.
Loeb, K.R., Kostner, H., Firpo, E., Norwood, T., K, D.T., Clurman, B.E., and Roberts, J.M. (2005). A mouse model for cyclin E-dependent genetic instability and tumorigenesis. Cancer Cell *8*, 35-47.
Loi, S., Haibe-Kains, B., Majjaj, S., Lallemand, F., Durbecq, V., Larsimont, D., Gonzalez-Angulo, A.M., Pusztai, L., Symmans, W.F., Bardelli, A., Ellis, P., Tutt, A.N., Gillett, C.E., Hennessy, B.T., Mills, G.B., Phillips, W.A., Piccart, M.J., Speed, T.P., McArthur, G.A., and Sotiriou, C. (2010). PIK3CA mutations associated with gene signature of low mTORC1 signaling and better outcomes in estrogen receptor-positive breast cancer. Proc Natl Acad Sci U S A *107*, 10208-10213.
Loibl, S., Untch, M., Burchardi, N., Huober, J., Sinn, B.V., Blohmer, J.U., Grischke, E.M., Furlanetto, J., Tesch, H., Hanusch, C., Engels, K., Rezai, M., Jackisch, C., Schmitt, W.D., von Minckwitz, G., Thomalla, J., Kummel, S., Rautenberg, B., Fasching, P.A., Weber, K., Rhiem, K., Denkert, C., and Schneeweiss, A. (2019). A randomised phase II study investigating durvalumab in addition to an anthracycline taxane-based neoadjuvant therapy in early triple-negative breast cancer: clinical results and biomarker analysis of GeparNuevo study. Ann Oncol *30*, 1279-1288.
Lolli, G., Lowe, E.D., Brown, N.R., and Johnson, L.N. (2004). The crystal structure of human CDK7 and its protein recognition properties. Structure *12*, 2067-2079.
Louder, R.K., He, Y., Lopez-Blanco, J.R., Fang, J., Chacon, P., and Nogales, E. (2016). Structure of promoter-bound TFIID and model of human pre-initiation complex assembly. Nature *531*, 604-609.

Love, M.I., Huber, W., and Anders, S. (2014). Moderated estimation of fold change and dispersion for RNA-seq data with DESeq2. Genome Biol *15*, 550.
Lowe, S.W., and Sherr, C.J. (2003). Tumor suppression by Ink4a-Arf: progress and puzzles. Curr Opin Genet Dev *13*, 77-83.
Lu, L., Chen, Z., Lin, X., Tian, L., Su, Q., An, P., Li, W., Wu, Y., Du, J., Shan, H., Chiang, C.M., and Wang, H. (2020). Inhibition of BRD4 suppresses the malignancy of breast cancer cells via regulation of Snail. Cell Death Differ *27*, 255-268.
Lucking, U., Scholz, A., Lienau, P., Siemeister, G., Kosemund, D., Bohlmann, R., Briem, H., Terebesi, I., Meyer, K., Prelle, K., Denner, K., Bomer, U., Schafer, M., Eis, K., Valencia, R., Ince, S., von Nussbaum, F., Mumberg, D., Ziegelbauer, K., Klebl, B., Choidas, A., Nussbaumer, P., Baumann, M., Schultz-Fademrecht, C., Ruhter, G., Eickhoff, J., and Brands, M. (2017). Identification of Atuveciclib (BAY 1143572), the First Highly Selective, Clinical PTEFb/CDK9 Inhibitor for the Treatment of Cancer. ChemMedChem *12*, 1776-1793.
Luecking, U.T., Scholz, A., Kosemund, D., Bohlmann, R., Briem, H., Lienau, P., Siemeister, G., Terebesi, I., Meyer, K., Prelle, K., Valencia, R., Ince, S., Nussbaum, F.v., Mumberg, D., Ziegelbauer, K., and Brands, M. (2017). Abstract 984: Identification of potent and highly selective PTEFb inhibitor BAY 1251152 for the treatment of cancer: from p.o. to i.v. application via scaffold hops. Cancer Research *77*, 984-984.
Luger, K., Dechassa, M.L., and Tremethick, D.J. (2012). New insights into nucleosome and chromatin structure: an ordered state or a disordered affair? Nat Rev Mol Cell Biol *13*, 436-447.
Lukas, C., Sorensen, C.S., Kramer, E., Santoni-Rugiu, E., Lindeneg, C., Peters, J.M., Bartek, J., and Lukas, J. (1999). Accumulation of cyclin B1 requires E2F and cyclin-A-dependent rearrangement of the anaphase-promoting complex. Nature *401*, 815-818.
Lundberg, A., Lindstrom, L.S., Li, J., Harrell, J.C., Darai-Ramqvist, E., Sifakis, E.G., Foukakis, T., Perou, C.M., Czene, K., Bergh, J., and Tobin, N.P. (2019). The long-term prognostic and predictive capacity of cyclin D1 gene amplification in 2305 breast tumours. Breast Cancer Res *21*, 34.
Lundgren, S., Kvinnsland, S., and Utaaker, E. (1989). Oral high-dose progestins as treatment for advanced breast cancer. Acta Oncol *28*, 811-816.
Luo, R.X., Postigo, A.A., and Dean, D.C. (1998). Rb interacts with histone deacetylase to repress transcription. Cell *92*, 463-473.
Lyytinen, H.K., Dyba, T., Ylikorkala, O., and Pukkala, E.I. (2010). A case-control study on hormone therapy as a risk factor for breast cancer in Finland: Intrauterine system carries a risk as well. Int J Cancer *126*, 483-489.

Ma, T., Van Tine, B.A., Wei, Y., Garrett, M.D., Nelson, D., Adams, P.D., Wang, J., Qin, J., Chow, L.T., and Harper, J.W. (2000). Cell cycle-regulated phosphorylation of p220(NPAT) by cyclin E/Cdk2 in Cajal bodies promotes histone gene transcription. Genes Dev *14*, 2298-2313.

Macaulay, C., Meier, E., and Forbes, D.J. (1995). Differential mitotic phosphorylation of proteins of the nuclear pore complex. J Biol Chem *270*, 254-262.

Mader, S., Kumar, V., de Verneuil, H., and Chambon, P. (1989). Three amino acids of the oestrogen receptor are essential to its ability to distinguish an oestrogen from a glucocorticoid-responsive element. Nature *338*, 271-274.

Magnaghi-Jaulin, L., Groisman, R., Naguibneva, I., Robin, P., Lorain, S., Le Villain, J.P., Troalen, F., Trouche, D., and Harel-Bellan, A. (1998). Retinoblastoma protein represses transcription by recruiting a histone deacetylase. Nature *391*, 601-605.

Malumbres, M. (2014). Cyclin-dependent kinases. Genome Biol *15*, 122.

Malumbres, M., and Barbacid, M. (2001). To cycle or not to cycle: a critical decision in cancer. Nat Rev Cancer *1*, 222-231.

Malumbres, M., and Barbacid, M. (2007). Cell cycle kinases in cancer. Curr Opin Genet Dev *17*, 60-65.

Malumbres, M., and Barbacid, M. (2009). Cell cycle, CDKs and cancer: a changing paradigm. Nat Rev Cancer *9*, 153-166.

Malumbres, M., Sotillo, R., Santamaria, D., Galan, J., Cerezo, A., Ortega, S., Dubus, P., and Barbacid, M. (2004). Mammalian cells cycle without the D-type cyclin-dependent kinases Cdk4 and Cdk6. Cell *118*, 493-504.

Manavathi, B., Dey, O., Gajulapalli, V.N., Bhatia, R.S., Bugide, S., and Kumar, R. (2013). Derailed estrogen signaling and breast cancer: an authentic couple. Endocr Rev *34*, 1-32.

Mandel, C.R., Bai, Y., and Tong, L. (2008). Protein factors in pre-mRNA 3'-end processing. Cell Mol Life Sci *65*, 1099-1122.

Marineau, J.J., Hamman, K.B., Hu, S., Alnemy, S., Mihalich, J., Kabro, A., Whitmore, K.M., Winter, D.K., Roy, S., Ciblat, S., Ke, N., Savinainen, A., Wilsily, A., Malojcic, G., Zahler, R., Schmidt, D., Bradley, M.J., Waters, N.J., and Chuaqui, C. (2021). Discovery of SY-5609: A Selective, Noncovalent Inhibitor of CDK7. J Med Chem.

Marineau, J.J., Hamman, K.B., Hu, S., Alnemy, S., Mihalich, J., Kabro, A., Whitmore, K.M., Winter, D.K., Roy, S., Ciblat, S., Ke, N., Savinainen, A., Wilsily, A., Malojcic, G., Zahler, R., Schmidt, D., Bradley, M.J., Waters, N.J., and Chuaqui, C. (2022). Discovery of SY-5609: A Selective, Noncovalent Inhibitor of CDK7. J Med Chem *65*, 1458-1480.

Marinoni, J.C., Roy, R., Vermeulen, W., Miniou, P., Lutz, Y., Weeda, G., Seroz, T., Gomez, D.M., Hoeijmakers, J.H., and Egly, J.M. (1997). Cloning and characterization of p52, the fifth subunit of the core of the transcription/DNA repair factor TFIIH. EMBO J *16*, 1093-1102.

Martin, C.A., Cullinane, C., Kirby, L., Abuhammad, S., Lelliott, E.J., Waldeck, K., Young, R.J., Brajanovski, N., Cameron, D.P., Walker, R., Sanij, E., Poortinga, G., Hannan, R.D., Pearson, R.B., Hicks, R.J., McArthur, G.A., and Sheppard, K.E. (2018). Palbociclib synergizes with BRAF and MEK inhibitors in treatment naive melanoma but not after the development of BRAF inhibitor resistance. Int J Cancer *142*, 2139-2152.

Martin, L.A., Ribas, R., Simigdala, N., Schuster, E., Pancholi, S., Tenev, T., Gellert, P., Buluwela, L., Harrod, A., Thornhill, A., Nikitorowicz-Buniak, J., Bhamra, A., Turgeon, M.O., Poulogiannis, G., Gao, Q., Martins, V., Hills, M., Garcia-Murillas, I., Fribbens, C., Patani, N., Li, Z., Sikora, M.J., Turner, N., Zwart, W., Oesterreich, S., Carroll, J., Ali, S., and Dowsett, M. (2017). Discovery of naturally occurring ESR1 mutations in breast cancer cell lines modelling endocrine resistance. Nat Commun *8*, 1865.

Martinez, A.M., Afshar, M., Martin, F., Cavadore, J.C., Labbe, J.C., and Doree, M. (1997). Dual phosphorylation of the T-loop in cdk7: its role in controlling cyclin H binding and CAK activity. EMBO J *16*, 343-354.

Matissek, K.J., Onozato, M.L., Sun, S., Zheng, Z., Schultz, A., Lee, J., Patel, K., Jerevall, P.L., Saladi, S.V., Macleay, A., Tavallai, M., Badovinac-Crnjevic, T., Barrios, C., Bese, N., Chan, A., Chavarri-Guerra, Y., Debiasi, M., Demirdogen, E., Egeli, U., Gokgoz, S., Gomez, H., Liedke, P., Tasdelen, I., Tolunay, S., Werutsky, G., St Louis, J., Horick, N., Finkelstein, D.M., Le, L.P., Bardia, A., Goss, P.E., Sgroi, D.C., Iafrate, A.J., and Ellisen, L.W. (2018). Expressed Gene Fusions as Frequent Drivers of Poor Outcomes in Hormone Receptor-Positive Breast Cancer. Cancer Discov *8*, 336-353.

Matsuo, M., Shimodaira, T., Kasama, T., Hata, Y., Echigo, A., Okabe, M., Arai, K., Makino, Y., Niwa, S., Saya, H., and Kishimoto, T. (2013). Katanin p60 contributes to microtubule instability around the midbody and facilitates cytokinesis in rat cells. PLoS One *8*, e80392.

Matsushime, H., Roussel, M.F., Ashmun, R.A., and Sherr, C.J. (1991). Colony-stimulating factor 1 regulates novel cyclins during the G1 phase of the cell cycle. Cell *65*, 701-713.

Matthews, H.K., Bertoli, C., and de Bruin, R.A.M. (2022). Cell cycle control in cancer. Nat Rev Mol Cell Biol *23*, 74-88.

Mattsson, W. (1983). Current status of high dose progestin treatment in advanced breast cancer. Breast Cancer Res Treat *3*, 231-235.

McCartney, A., Migliaccio, I., Bonechi, M., Biagioni, C., Romagnoli, D., De Luca, F., Galardi, F., Risi, E., De Santo, I., Benelli, M., Malorni, L., and Di Leo, A. (2019). Mechanisms of Resistance to CDK4/6 Inhibitors: Potential Implications and Biomarkers for Clinical Practice. Front Oncol *9*, 666.

McCubrey, J.A., Steelman, L.S., Chappell, W.H., Abrams, S.L., Wong, E.W., Chang, F., Lehmann, B., Terrian, D.M., Milella, M., Tafuri, A., Stivala, F., Libra, M., Basecke, J., Evangelisti, C., Martelli, A.M., and Franklin, R.A. (2007). Roles of the Raf/MEK/ERK pathway in cell growth, malignant transformation and drug resistance. Biochim Biophys Acta *1773*, 1263-1284.

Medema, R.H., Herrera, R.E., Lam, F., and Weinberg, R.A. (1995). Growth suppression by p16ink4 requires functional retinoblastoma protein. Proc Natl Acad Sci U S A *92*, 6289-6293.

Meijer, L., Leclerc, S., and Leost, M. (1999). Properties and potential-applications of chemical inhibitors of cyclin-dependent kinases. Pharmacol Ther *82*, 279-284.

Metzger-Filho, O., Tutt, A., de Azambuja, E., Saini, K.S., Viale, G., Loi, S., Bradbury, I., Bliss, J.M., Azim, H.A., Jr., Ellis, P., Di Leo, A., Baselga, J., Sotiriou, C., and Piccart-Gebhart, M. (2012). Dissecting the heterogeneity of triple-negative breast cancer. J Clin Oncol *30*, 1879-1887.

Meyerson, M., and Harlow, E. (1994). Identification of G1 kinase activity for cdk6, a novel cyclin D partner. Mol Cell Biol *14*, 2077-2086.

Michaloglou, C., Crafter, C., Siersbaek, R., Delpuech, O., Curwen, J.O., Carnevalli, L.S., Staniszewska, A.D., Polanska, U.M., Cheraghchi-Bashi, A., Lawson, M., Chernukhin, I., McEwen, R., Carroll, J.S., and Cosulich, S.C. (2018). Combined Inhibition of mTOR and CDK4/6 Is Required for Optimal Blockade of E2F Function and Long-term Growth Inhibition in Estrogen Receptor-positive Breast Cancer. Mol Cancer Ther *17*, 908-920.

Miki, Y., Suzuki, T., Tazawa, C., Yamaguchi, Y., Kitada, K., Honma, S., Moriya, T., Hirakawa, H., Evans, D.B., Hayashi, S., Ohuchi, N., and Sasano, H. (2007). Aromatase localization in human breast cancer tissues: possible interactions between intratumoral stromal and parenchymal cells. Cancer Res *67*, 3945-3954.

Miller, T.W., Rexer, B.N., Garrett, J.T., and Arteaga, C.L. (2011). Mutations in the phosphatidylinositol 3-kinase pathway: role in tumor progression and therapeutic implications in breast cancer. Breast Cancer Res *13*, 224.

Millevoi, S., Decorsiere, A., Loulergue, C., Iacovoni, J., Bernat, S., Antoniou, M., and Vagner, S. (2009). A physical and functional link between splicing factors promotes pre-mRNA 3' end processing. Nucleic Acids Res *37*, 4672-4683.

Min, A., Kim, J.E., Kim, Y.J., Lim, J.M., Kim, S., Kim, J.W., Lee, K.H., Kim, T.Y., Oh, D.Y., Bang, Y.J., and Im, S.A. (2018). Cyclin E overexpression confers resistance to the CDK4/6 specific inhibitor palbociclib in gastric cancer cells. Cancer Lett *430*, 123-132.
Mishima, M., Kaitna, S., and Glotzer, M. (2002). Central spindle assembly and cytokinesis require a kinesin-like protein/RhoGAP complex with microtubule bundling activity. Dev Cell *2*, 41-54.
Mishima, M., Pavicic, V., Gruneberg, U., Nigg, E.A., and Glotzer, M. (2004). Cell cycle regulation of central spindle assembly. Nature *430*, 908-913.
Mita, M.M., Joy, A.A., Mita, A., Sankhala, K., Jou, Y.M., Zhang, D., Statkevich, P., Zhu, Y., Yao, S.L., Small, K., Bannerji, R., and Shapiro, C.L. (2014). Randomized phase II trial of the cyclin-dependent kinase inhibitor dinaciclib (MK-7965) versus capecitabine in patients with advanced breast cancer. Clin Breast Cancer *14*, 169-176.
Mitra, J., and Enders, G.H. (2004). Cyclin A/Cdk2 complexes regulate activation of Cdk1 and Cdc25 phosphatases in human cells. Oncogene *23*, 3361-3367.
Mittendorf, E.A., Zhang, H., Barrios, C.H., Saji, S., Jung, K.H., Hegg, R., Koehler, A., Sohn, J., Iwata, H., Telli, M.L., Ferrario, C., Punie, K., Penault-Llorca, F., Patel, S., Duc, A.N., Liste-Hermoso, M., Maiya, V., Molinero, L., Chui, S.Y., and Harbeck, N. (2020). Neoadjuvant atezolizumab in combination with sequential nab-paclitaxel and anthracycline-based chemotherapy versus placebo and chemotherapy in patients with early-stage triple-negative breast cancer (IMpassion031): a randomised, double-blind, phase 3 trial. Lancet *396*, 1090-1100.
Miyamoto, H., Shuin, T., Torigoe, S., Iwasaki, Y., and Kubota, Y. (1995). Retinoblastoma gene mutations in primary human bladder cancer. Br J Cancer *71*, 831-835.
Moasser, M.M. (2007). The oncogene HER2: its signaling and transforming functions and its role in human cancer pathogenesis. Oncogene *26*, 6469-6487.
Moberg, K., Starz, M.A., and Lees, J.A. (1996). E2F-4 switches from p130 to p107 and pRB in response to cell cycle reentry. Mol Cell Biol *16*, 1436-1449.
Mohammed, H., Russell, I.A., Stark, R., Rueda, O.M., Hickey, T.E., Tarulli, G.A., Serandour, A.A., Birrell, S.N., Bruna, A., Saadi, A., Menon, S., Hadfield, J., Pugh, M., Raj, G.V., Brown, G.D., D'Santos, C., Robinson, J.L., Silva, G., Launchbury, R., Perou, C.M., Stingl, J., Caldas, C., Tilley, W.D., and Carroll, J.S. (2015). Progesterone receptor modulates ERalpha action in breast cancer. Nature *523*, 313-317.
Montano, M.M., Muller, V., Trobaugh, A., and Katzenellenbogen, B.S. (1995). The carboxy-terminal F domain of the human estrogen receptor: role in the transcriptional activity of the

receptor and the effectiveness of antiestrogens as estrogen antagonists. Mol Endocrinol *9*, 814-825.
Montaudon, E., Nikitorowicz-Buniak, J., Sourd, L., Morisset, L., El Botty, R., Huguet, L., Dahmani, A., Painsec, P., Nemati, F., Vacher, S., Chemlali, W., Masliah-Planchon, J., Chateau-Joubert, S., Rega, C., Leal, M.F., Simigdala, N., Pancholi, S., Ribas, R., Nicolas, A., Meseure, D., Vincent-Salomon, A., Reyes, C., Rapinat, A., Gentien, D., Larcher, T., Bohec, M., Baulande, S., Bernard, V., Decaudin, D., Coussy, F., Le Romancer, M., Dutertre, G., Tariq, Z., Cottu, P., Driouch, K., Bieche, I., Martin, L.A., and Marangoni, E. (2020). PLK1 inhibition exhibits strong anti-tumoral activity in CCND1-driven breast cancer metastases with acquired palbociclib resistance. Nat Commun *11*, 4053.
Morgan, D.O. (1997). Cyclin-dependent kinases: engines, clocks, and microprocessors. Annu Rev Cell Dev Biol *13*, 261-291.
Morgan, L.R. (1985). Megestrol acetate v tamoxifen in advanced breast cancer in postmenopausal patients. Semin Oncol *12*, 43-47.
Mosselman, S., Polman, J., and Dijkema, R. (1996). ER beta: identification and characterization of a novel human estrogen receptor. FEBS Lett *392*, 49-53.
Motokura, T., Bloom, T., Kim, H.G., Juppner, H., Ruderman, J.V., Kronenberg, H.M., and Arnold, A. (1991). A novel cyclin encoded by a bcl1-linked candidate oncogene. Nature *350*, 512-515.
Mousson, F., Lautrette, A., Thuret, J.Y., Agez, M., Courbeyrette, R., Amigues, B., Becker, E., Neumann, J.M., Guerois, R., Mann, C., and Ochsenbein, F. (2005). Structural basis for the interaction of Asf1 with histone H3 and its functional implications. Proc Natl Acad Sci U S A *102*, 5975-5980.
Muniyan, S., Pothuraju, R., Seshacharyulu, P., and Batra, S.K. (2022). Macrophage inhibitory cytokine-1 in cancer: Beyond the cellular phenotype. Cancer Lett *536*, 215664.
Murphy, L.C., Seekallu, S.V., and Watson, P.H. (2011). Clinical significance of estrogen receptor phosphorylation. Endocr Relat Cancer *18*, R1-14.
Murray, B.W., Guo, C., Piraino, J., Westwick, J.K., Zhang, C., Lamerdin, J., Dagostino, E., Knighton, D., Loi, C.M., Zager, M., Kraynov, E., Popoff, I., Christensen, J.G., Martinez, R., Kephart, S.E., Marakovits, J., Karlicek, S., Bergqvist, S., and Smeal, T. (2010). Small-molecule p21-activated kinase inhibitor PF-3758309 is a potent inhibitor of oncogenic signaling and tumor growth. Proc Natl Acad Sci U S A *107*, 9446-9451.
Musgrove, E.A., Caldon, C.E., Barraclough, J., Stone, A., and Sutherland, R.L. (2011). Cyclin D as a therapeutic target in cancer. Nat Rev Cancer *11*, 558-572.

Nag, A., Narsinh, K., and Martinson, H.G. (2007). The poly(A)-dependent transcriptional pause is mediated by CPSF acting on the body of the polymerase. Nat Struct Mol Biol *14*, 662-669.

Nasmyth, K. (2001). Disseminating the genome: joining, resolving, and separating sister chromatids during mitosis and meiosis. Annu Rev Genet *35*, 673-745.

Nayar, U., Cohen, O., Kapstad, C., Cuoco, M.S., Waks, A.G., Wander, S.A., Painter, C., Freeman, S., Persky, N.S., Marini, L., Helvie, K., Oliver, N., Rozenblatt-Rosen, O., Ma, C.X., Regev, A., Winer, E.P., Lin, N.U., and Wagle, N. (2019). Acquired HER2 mutations in ER(+) metastatic breast cancer confer resistance to estrogen receptor-directed therapies. Nat Genet *51*, 207-216.

Nebenfuehr, S., Kollmann, K., and Sexl, V. (2020). The role of CDK6 in cancer. Int J Cancer *147*, 2988-2995.

Neef, R., Gruneberg, U., Kopajtich, R., Li, X., Nigg, E.A., Sillje, H., and Barr, F.A. (2007). Choice of Plk1 docking partners during mitosis and cytokinesis is controlled by the activation state of Cdk1. Nat Cell Biol *9*, 436-444.

Nelson, K.G., Takahashi, T., Bossert, N.L., Walmer, D.K., and McLachlan, J.A. (1991). Epidermal growth factor replaces estrogen in the stimulation of female genital-tract growth and differentiation. Proc Natl Acad Sci U S A *88*, 21-25.

Nelson, L.R., and Bulun, S.E. (2001). Estrogen production and action. J Am Acad Dermatol *45*, S116-124.

Nemunaitis, J.J., Small, K.A., Kirschmeier, P., Zhang, D., Zhu, Y., Jou, Y.M., Statkevich, P., Yao, S.L., and Bannerji, R. (2013). A first-in-human, phase 1, dose-escalation study of dinaciclib, a novel cyclin-dependent kinase inhibitor, administered weekly in subjects with advanced malignancies. J Transl Med *11*, 259.

Nevis, K.R., Cordeiro-Stone, M., and Cook, J.G. (2009). Origin licensing and p53 status regulate Cdk2 activity during G(1). Cell Cycle *8*, 1952-1963.

Nguyen, T.T., Grimm, S.A., Bushel, P.R., Li, J., Li, Y., Bennett, B.D., Lavender, C.A., Ward, J.M., Fargo, D.C., Anderson, C.W., Li, L., Resnick, M.A., and Menendez, D. (2018). Revealing a human p53 universe. Nucleic Acids Res *46*, 8153-8167.

Nguyen, V.T., Barozzi, I., Faronato, M., Lombardo, Y., Steel, J.H., Patel, N., Darbre, P., Castellano, L., Gyorffy, B., Woodley, L., Meira, A., Patten, D.K., Vircillo, V., Periyasamy, M., Ali, S., Frige, G., Minucci, S., Coombes, R.C., and Magnani, L. (2015). Differential epigenetic reprogramming in response to specific endocrine therapies promotes cholesterol biosynthesis and cellular invasion. Nat Commun *6*, 10044.

Ngwenya, S., and Safe, S. (2003). Cell context-dependent differences in the induction of E2F-1 gene expression by 17 beta-estradiol in MCF-7 and ZR-75 cells. Endocrinology *144*, 1675-1685.

Nicholson, R.I., Hutcheson, I.R., Knowlden, J.M., Jones, H.E., Harper, M.E., Jordan, N., Hiscox, S.E., Barrow, D., and Gee, J.M. (2004). Nonendocrine pathways and endocrine resistance: observations with antiestrogens and signal transduction inhibitors in combination. Clin Cancer Res *10*, 346S-354S.

Nielsen, S.J., Schneider, R., Bauer, U.M., Bannister, A.J., Morrison, A., O'Carroll, D., Firestein, R., Cleary, M., Jenuwein, T., Herrera, R.E., and Kouzarides, T. (2001). Rb targets histone H3 methylation and HP1 to promoters. Nature *412*, 561-565.

Nik-Zainal, S., Davies, H., Staaf, J., Ramakrishna, M., Glodzik, D., Zou, X., Martincorena, I., Alexandrov, L.B., Martin, S., Wedge, D.C., Van Loo, P., Ju, Y.S., Smid, M., Brinkman, A.B., Morganella, S., Aure, M.R., Lingjaerde, O.C., Langerod, A., Ringner, M., Ahn, S.M., Boyault, S., Brock, J.E., Broeks, A., Butler, A., Desmedt, C., Dirix, L., Dronov, S., Fatima, A., Foekens, J.A., Gerstung, M., Hooijer, G.K., Jang, S.J., Jones, D.R., Kim, H.Y., King, T.A., Krishnamurthy, S., Lee, H.J., Lee, J.Y., Li, Y., McLaren, S., Menzies, A., Mustonen, V., O'Meara, S., Pauporte, I., Pivot, X., Purdie, C.A., Raine, K., Ramakrishnan, K., Rodriguez-Gonzalez, F.G., Romieu, G., Sieuwerts, A.M., Simpson, P.T., Shepherd, R., Stebbings, L., Stefansson, O.A., Teague, J., Tommasi, S., Treilleux, I., Van den Eynden, G.G., Vermeulen, P., Vincent-Salomon, A., Yates, L., Caldas, C., van't Veer, L., Tutt, A., Knappskog, S., Tan, B.K., Jonkers, J., Borg, A., Ueno, N.T., Sotiriou, C., Viari, A., Futreal, P.A., Campbell, P.J., Span, P.N., Van Laere, S., Lakhani, S.R., Eyfjord, J.E., Thompson, A.M., Birney, E., Stunnenberg, H.G., van de Vijver, M.J., Martens, J.W., Borresen-Dale, A.L., Richardson, A.L., Kong, G., Thomas, G., and Stratton, M.R. (2016). Landscape of somatic mutations in 560 breast cancer whole-genome sequences. Nature *534*, 47-54.

Nishiyama, T., Sykora, M.M., Huis in 't Veld, P.J., Mechtler, K., and Peters, J.M. (2013). Aurora B and Cdk1 mediate Wapl activation and release of acetylated cohesin from chromosomes by phosphorylating Sororin. Proc Natl Acad Sci U S A *110*, 13404-13409.

Nunes Bastos, R., Gandhi, S.R., Baron, R.D., Gruneberg, U., Nigg, E.A., and Barr, F.A. (2013). Aurora B suppresses microtubule dynamics and limits central spindle size by locally activating KIF4A. J Cell Biol *202*, 605-621.

O'Farrell, P.H. (2001). Triggering the all-or-nothing switch into mitosis. Trends Cell Biol *11*, 512-519.

O'Leary, B., Finn, R.S., and Turner, N.C. (2016). Treating cancer with selective CDK4/6 inhibitors. Nat Rev Clin Oncol *13*, 417-430.

O'Shaughnessy, J., Petrakova, K., Sonke, G.S., Conte, P., Arteaga, C.L., Cameron, D.A., Hart, L.L., Villanueva, C., Jakobsen, E., Beck, J.T., Lindquist, D., Souami, F., Mondal, S., Germa, C., and Hortobagyi, G.N. (2018). Ribociclib plus letrozole versus letrozole alone in patients with de novo HR+, HER2- advanced breast cancer in the randomized MONALEESA-2 trial. Breast Cancer Res Treat *168*, 127-134.

Oh, D.S., Troester, M.A., Usary, J., Hu, Z., He, X., Fan, C., Wu, J., Carey, L.A., and Perou, C.M. (2006). Estrogen-regulated genes predict survival in hormone receptor-positive breast cancers. J Clin Oncol *24*, 1656-1664.

Ohtani, N., Zebedee, Z., Huot, T.J., Stinson, J.A., Sugimoto, M., Ohashi, Y., Sharrocks, A.D., Peters, G., and Hara, E. (2001). Opposing effects of Ets and Id proteins on p16INK4a expression during cellular senescence. Nature *409*, 1067-1070.

Olanich, M.E., Sun, W., Hewitt, S.M., Abdullaev, Z., Pack, S.D., and Barr, F.G. (2015). CDK4 Amplification Reduces Sensitivity to CDK4/6 Inhibition in Fusion-Positive Rhabdomyosarcoma. Clin Cancer Res *21*, 4947-4959.

Olayioye, M.A. (2001). Update on HER-2 as a target for cancer therapy: intracellular signaling pathways of ErbB2/HER-2 and family members. Breast Cancer Res *3*, 385-389.

Olson, C.M., Jiang, B., Erb, M.A., Liang, Y., Doctor, Z.M., Zhang, Z., Zhang, T., Kwiatkowski, N., Boukhali, M., Green, J.L., Haas, W., Nomanbhoy, T., Fischer, E.S., Young, R.A., Bradner, J.E., Winter, G.E., and Gray, N.S. (2018). Pharmacological perturbation of CDK9 using selective CDK9 inhibition or degradation. Nat Chem Biol *14*, 163-170.

Olson, C.M., Liang, Y., Leggett, A., Park, W.D., Li, L., Mills, C.E., Elsarrag, S.Z., Ficarro, S.B., Zhang, T., Duster, R., Geyer, M., Sim, T., Marto, J.A., Sorger, P.K., Westover, K.D., Lin, C.Y., Kwiatkowski, N., and Gray, N.S. (2019). Development of a Selective CDK7 Covalent Inhibitor Reveals Predominant Cell-Cycle Phenotype. Cell Chem Biol.

Onitilo, A.A., Engel, J.M., Greenlee, R.T., and Mukesh, B.N. (2009). Breast cancer subtypes based on ER/PR and Her2 expression: comparison of clinicopathologic features and survival. Clin Med Res *7*, 4-13.

Orphanides, G., Lagrange, T., and Reinberg, D. (1996). The general transcription factors of RNA polymerase II. Genes Dev *10*, 2657-2683.

Ortega, S., Malumbres, M., and Barbacid, M. (2002). Cyclin D-dependent kinases, INK4 inhibitors and cancer. Biochim Biophys Acta *1602*, 73-87.

Osada, M., Park, H.L., Park, M.J., Liu, J.W., Wu, G., Trink, B., and Sidransky, D. (2007). A p53-type response element in the GDF15 promoter confers high specificity for p53 activation. Biochem Biophys Res Commun *354*, 913-918.

Osborne, C.K., Yochmowitz, M.G., Knight, W.A., 3rd, and McGuire, W.L. (1980). The value of estrogen and progesterone receptors in the treatment of breast cancer. Cancer *46*, 2884-2888.

Otto, T., and Sicinski, P. (2017). Cell cycle proteins as promising targets in cancer therapy. Nat Rev Cancer *17*, 93-115.

Pan, H., Gray, R., Braybrooke, J., Davies, C., Taylor, C., McGale, P., Peto, R., Pritchard, K.I., Bergh, J., Dowsett, M., Hayes, D.F., and Ebctcg (2017). 20-Year Risks of Breast-Cancer Recurrence after Stopping Endocrine Therapy at 5 Years. N Engl J Med *377*, 1836-1846.

Pancholi, S., Ribas, R., Simigdala, N., Schuster, E., Nikitorowicz-Buniak, J., Ressa, A., Gao, Q., Leal, M.F., Bhamra, A., Thornhill, A., Morisset, L., Montaudon, E., Sourd, L., Fitzpatrick, M., Altelaar, M., Johnston, S.R., Marangoni, E., Dowsett, M., and Martin, L.A. (2020). Tumour kinome re-wiring governs resistance to palbociclib in oestrogen receptor positive breast cancers, highlighting new therapeutic modalities. Oncogene *39*, 4781-4797.

Pandey, K., An, H.J., Kim, S.K., Lee, S.A., Kim, S., Lim, S.M., Kim, G.M., Sohn, J., and Moon, Y.W. (2018). Molecular mechanisms of resistance to CDK4/6 inhibitors in breast cancer: A review. Int J Cancer.

Pandey, K., Park, N., Park, K.S., Hur, J., Cho, Y.B., Kang, M., An, H.J., Kim, S., Hwang, S., and Moon, Y.W. (2020). Combined CDK2 and CDK4/6 Inhibition Overcomes Palbociclib Resistance in Breast Cancer by Enhancing Senescence. Cancers (Basel) *12*.

Papadopoulos, K.P., Sharma, M., Hamilton, E.P., Richardson, D.L., Hodgson, G., Zhou, L., Volkert, A., Jolin, H.A., Madigan, C., Kelly, M., and Roth, D.A. (2020). First-in-human phase I study of SY-5609, an oral, potent, and selective noncovalent CDK7 inhibitor, in adult patients with select advanced solid tumors. Journal of Clinical Oncology *38*, TPS3662-TPS3662.

Park, N.J., Tsao, D.C., and Martinson, H.G. (2004). The two steps of poly(A)-dependent termination, pausing and release, can be uncoupled by truncation of the RNA polymerase II carboxyl-terminal repeat domain. Mol Cell Biol *24*, 4092-4103.

Parry, D., Guzi, T., Shanahan, F., Davis, N., Prabhavalkar, D., Wiswell, D., Seghezzi, W., Paruch, K., Dwyer, M.P., Doll, R., Nomeir, A., Windsor, W., Fischmann, T., Wang, Y., Oft, M., Chen, T., Kirschmeier, P., and Lees, E.M. (2010). Dinaciclib (SCH 727965), a novel and potent cyclin-dependent kinase inhibitor. Mol Cancer Ther *9*, 2344-2353.

Parry, D.H., and O'Farrell, P.H. (2001). The schedule of destruction of three mitotic cyclins can dictate the timing of events during exit from mitosis. Curr Biol *11*, 671-683.

Pascual, J., Gil-Gil, M., Zielinski, C., Hills, M., Ruiz-Borrego, M., Ciruelos, E.M., Garcia-Murillas, I., Muñoz, M., Bermejo, B., Swift, C., Vila, M.M., Torres, A.A., Nissenbaum, B.,

Murillo, L., Liu, Y., Herranz, J., Caballero, R., Guerrero-Zotano, A., Turner, N.C., and Martin, M. (2021). CCNE1 mRNA and cyclin E1 protein expression as predictive biomarkers for efficacy of palbociclib plus fulvestrant versus capecitabine in the phase III PEARL study. Journal of Clinical Oncology *39*, 1014-1014.

Patel, H., Abduljabbar, R., Lai, C.F., Periyasamy, M., Harrod, A., Gemma, C., Steel, J.H., Patel, N., Busonero, C., Jerjees, D., Remenyi, J., Smith, S., Gomm, J.J., Magnani, L., Gyorffy, B., Jones, L.J., Fuller-Pace, F., Shousha, S., Buluwela, L., Rakha, E.A., Ellis, I.O., Coombes, R.C., and Ali, S. (2016). Expression of CDK7, Cyclin H, and MAT1 Is Elevated in Breast Cancer and Is Prognostic in Estrogen Receptor-Positive Breast Cancer. Clin Cancer Res *22*, 5929-5938.

Patel, H., Periyasamy, M., Sava, G.P., Bondke, A., Slafer, B.W., Kroll, S.H.B., Barbazanges, M., Starkey, R., Ottaviani, S., Harrod, A., Aboagye, E.O., Buluwela, L., Fuchter, M.J., Barrett, A.G.M., Coombes, R.C., and Ali, S. (2018). ICEC0942, an Orally Bioavailable Selective Inhibitor of CDK7 for Cancer Treatment. Mol Cancer Ther *17*, 1156-1166.

Patnaik, A., Rosen, L.S., Tolaney, S.M., Tolcher, A.W., Goldman, J.W., Gandhi, L., Papadopoulos, K.P., Beeram, M., Rasco, D.W., Hilton, J.F., Nasir, A., Beckmann, R.P., Schade, A.E., Fulford, A.D., Nguyen, T.S., Martinez, R., Kulanthaivel, P., Li, L.Q., Frenzel, M., Cronier, D.M., Chan, E.M., Flaherty, K.T., Wen, P.Y., and Shapiro, G.I. (2016). Efficacy and Safety of Abemaciclib, an Inhibitor of CDK4 and CDK6, for Patients with Breast Cancer, Non-Small Cell Lung Cancer, and Other Solid Tumors. Cancer Discov *6*, 740-753.

Payton, M., Scully, S., Chung, G., and Coats, S. (2002). Deregulation of cyclin E2 expression and associated kinase activity in primary breast tumors. Oncogene *21*, 8529-8534.

Peake, B.F., Eze, S.M., Yang, L., Castellino, R.C., and Nahta, R. (2017). Growth differentiation factor 15 mediates epithelial mesenchymal transition and invasion of breast cancers through IGF-1R-FoxM1 signaling. Oncotarget *8*, 94393-94406.

Pearson, A., Proszek, P., Pascual, J., Fribbens, C., Shamsher, M.K., Kingston, B., O'Leary, B., Herrera-Abreu, M.T., Cutts, R.J., Garcia-Murillas, I., Bye, H., Walker, B.A., Gonzalez De Castro, D., Yuan, L., Jamal, S., Hubank, M., Lopez-Knowles, E., Schuster, E.F., Dowsett, M., Osin, P., Nerurkar, A., Parton, M., Okines, A.F.C., Johnston, S.R.D., Ring, A., and Turner, N.C. (2020). Inactivating NF1 Mutations Are Enriched in Advanced Breast Cancer and Contribute to Endocrine Therapy Resistance. Clin Cancer Res *26*, 608-622.

Pedram, A., Razandi, M., and Levin, E.R. (2006). Nature of functional estrogen receptors at the plasma membrane. Mol Endocrinol *20*, 1996-2009.

Pek, M., Yatim, S., Chen, Y., Li, J., Gong, M., Jiang, X., Zhang, F., Zheng, J., Wu, X., and Yu, Q. (2017). Oncogenic KRAS-associated gene signature defines co-targeting of CDK4/6 and MEK as a viable therapeutic strategy in colorectal cancer. Oncogene *36*, 4975-4986.
Pernas, S., Tolaney, S.M., Winer, E.P., and Goel, S. (2018). CDK4/6 inhibition in breast cancer: current practice and future directions. Ther Adv Med Oncol *10*, 1758835918786451.
Perou, C.M., Sorlie, T., Eisen, M.B., van de Rijn, M., Jeffrey, S.S., Rees, C.A., Pollack, J.R., Ross, D.T., Johnsen, H., Akslen, L.A., Fluge, O., Pergamenschikov, A., Williams, C., Zhu, S.X., Lonning, P.E., Borresen-Dale, A.L., Brown, P.O., and Botstein, D. (2000). Molecular portraits of human breast tumours. Nature *406*, 747-752.
Peter, M., Nakagawa, J., Doree, M., Labbe, J.C., and Nigg, E.A. (1990). In vitro disassembly of the nuclear lamina and M phase-specific phosphorylation of lamins by cdc2 kinase. Cell *61*, 591-602.
Peterlin, B.M., and Price, D.H. (2006). Controlling the elongation phase of transcription with P-TEFb. Mol Cell *23*, 297-305.
Peters, J.M. (2002). The anaphase-promoting complex: proteolysis in mitosis and beyond. Mol Cell *9*, 931-943.
Pfarr, C.M., Coue, M., Grissom, P.M., Hays, T.S., Porter, M.E., and McIntosh, J.R. (1990). Cytoplasmic dynein is localized to kinetochores during mitosis. Nature *345*, 263-265.
Piccart, M., Hortobagyi, G.N., Campone, M., Pritchard, K.I., Lebrun, F., Ito, Y., Noguchi, S., Perez, A., Rugo, H.S., Deleu, I., Burris, H.A., 3rd, Provencher, L., Neven, P., Gnant, M., Shtivelband, M., Wu, C., Fan, J., Feng, W., Taran, T., and Baselga, J. (2014). Everolimus plus exemestane for hormone-receptor-positive, human epidermal growth factor receptor-2-negative advanced breast cancer: overall survival results from BOLERO-2dagger. Ann Oncol *25*, 2357-2362.
Pichon, M.F., Pallud, C., Brunet, M., and Milgrom, E. (1980). Relationship of presence of progesterone receptors to prognosis in early breast cancer. Cancer Res *40*, 3357-3360.
Pierson-Mullany, L.K., and Lange, C.A. (2004). Phosphorylation of progesterone receptor serine 400 mediates ligand-independent transcriptional activity in response to activation of cyclin-dependent protein kinase 2. Mol Cell Biol *24*, 10542-10557.
Pike, A.C., Brzozowski, A.M., and Hubbard, R.E. (2000). A structural biologist's view of the oestrogen receptor. J Steroid Biochem Mol Biol *74*, 261-268.
Placke, T., Faber, K., Nonami, A., Putwain, S.L., Salih, H.R., Heidel, F.H., Kramer, A., Root, D.E., Barbie, D.A., Krivtsov, A.V., Armstrong, S.A., Hahn, W.C., Huntly, B.J., Sykes, S.M., Milsom, M.D., Scholl, C., and Frohling, S. (2014). Requirement for CDK6 in MLL-rearranged acute myeloid leukemia. Blood *124*, 13-23.

Pohl, C., and Jentsch, S. (2009). Midbody ring disposal by autophagy is a post-abscission event of cytokinesis. Nat Cell Biol *11*, 65-70.
Polager, S., and Ginsberg, D. (2009). p53 and E2f: partners in life and death. Nat Rev Cancer *9*, 738-748.
Pomerantz, J., Schreiber-Agus, N., Liegeois, N.J., Silverman, A., Alland, L., Chin, L., Potes, J., Chen, K., Orlow, I., Lee, H.W., Cordon-Cardo, C., and DePinho, R.A. (1998). The Ink4a tumor suppressor gene product, p19Arf, interacts with MDM2 and neutralizes MDM2's inhibition of p53. Cell *92*, 713-723.
Poon, R.Y., and Hunter, T. (1995). Dephosphorylation of Cdk2 Thr160 by the cyclin-dependent kinase-interacting phosphatase KAP in the absence of cyclin. Science *270*, 90-93.
Portela, A., and Esteller, M. (2010). Epigenetic modifications and human disease. Nat Biotechnol *28*, 1057-1068.
Powell, E., Wang, Y., Shapiro, D.J., and Xu, W. (2010). Differential requirements of Hsp90 and DNA for the formation of estrogen receptor homodimers and heterodimers. J Biol Chem *285*, 16125-16134.
Prossnitz, E.R., and Barton, M. (2011). The G-protein-coupled estrogen receptor GPER in health and disease. Nat Rev Endocrinol *7*, 715-726.
Prossnitz, E.R., and Barton, M. (2014). Estrogen biology: new insights into GPER function and clinical opportunities. Mol Cell Endocrinol *389*, 71-83.
Puntervoll, H.E., Yang, X.R., Vetti, H.H., Bachmann, I.M., Avril, M.F., Benfodda, M., Catricala, C., Dalle, S., Duval-Modeste, A.B., Ghiorzo, P., Grammatico, P., Harland, M., Hayward, N.K., Hu, H.H., Jouary, T., Martin-Denavit, T., Ozola, A., Palmer, J.M., Pastorino, L., Pjanova, D., Soufir, N., Steine, S.J., Stratigos, A.J., Thomas, L., Tinat, J., Tsao, H., Veinalde, R., Tucker, M.A., Bressac-de Paillerets, B., Newton-Bishop, J.A., Goldstein, A.M., Akslen, L.A., and Molven, A. (2013). Melanoma prone families with CDK4 germline mutation: phenotypic profile and associations with MC1R variants. J Med Genet *50*, 264-270.
Puyang, X., Furman, C., Zheng, G.Z., Wu, Z.J., Banka, D., Aithal, K., Agoulnik, S., Bolduc, D.M., Buonamici, S., Caleb, B., Das, S., Eckley, S., Fekkes, P., Hao, M.H., Hart, A., Houtman, R., Irwin, S., Joshi, J.J., Karr, C., Kim, A., Kumar, N., Kumar, P., Kuznetsov, G., Lai, W.G., Larsen, N., Mackenzie, C., Martin, L.A., Melchers, D., Moriarty, A., Nguyen, T.V., Norris, J., O'Shea, M., Pancholi, S., Prajapati, S., Rajagopalan, S., Reynolds, D.J., Rimkunas, V., Rioux, N., Ribas, R., Siu, A., Sivakumar, S., Subramanian, V., Thomas, M., Vaillancourt, F.H., Wang, J., Wardell, S., Wick, M.J., Yao, S., Yu, L., Warmuth, M., Smith, P.G., Zhu, P., and Korpal, M. (2018). Discovery of Selective Estrogen Receptor Covalent

Antagonists for the Treatment of ERalpha(WT) and ERalpha(MUT) Breast Cancer. Cancer Discov *8*, 1176-1193.
Qian, J., Beullens, M., Lesage, B., and Bollen, M. (2013). Aurora B defines its own chromosomal targeting by opposing the recruitment of the phosphatase scaffold Repo-Man. Curr Biol *23*, 1136-1143.
Qiao, R., Weissmann, F., Yamaguchi, M., Brown, N.G., VanderLinden, R., Imre, R., Jarvis, M.A., Brunner, M.R., Davidson, I.F., Litos, G., Haselbach, D., Mechtler, K., Stark, H., Schulman, B.A., and Peters, J.M. (2016). Mechanism of APC/CCDC20 activation by mitotic phosphorylation. Proc Natl Acad Sci U S A *113*, E2570-2578.
Qie, S., and Diehl, J.A. (2016). Cyclin D1, cancer progression, and opportunities in cancer treatment. J Mol Med (Berl) *94*, 1313-1326.
Rahl, P.B., Lin, C.Y., Seila, A.C., Flynn, R.A., McCuine, S., Burge, C.B., Sharp, P.A., and Young, R.A. (2010). c-Myc regulates transcriptional pause release. Cell *141*, 432-445.
Rakha, E.A., El-Sayed, M.E., Green, A.R., Paish, E.C., Powe, D.G., Gee, J., Nicholson, R.I., Lee, A.H., Robertson, J.F., and Ellis, I.O. (2007). Biologic and clinical characteristics of breast cancer with single hormone receptor positive phenotype. J Clin Oncol *25*, 4772-4778.
Raspe, E., Coulonval, K., Pita, J.M., Paternot, S., Rothe, F., Twyffels, L., Brohee, S., Craciun, L., Larsimont, D., Kruys, V., Sandras, F., Salmon, I., Van Laere, S., Piccart, M., Ignatiadis, M., Sotiriou, C., and Roger, P.P. (2017). CDK4 phosphorylation status and a linked gene expression profile predict sensitivity to palbociclib. EMBO Mol Med *9*, 1052-1066.
Raub, T.J., Wishart, G.N., Kulanthaivel, P., Staton, B.A., Ajamie, R.T., Sawada, G.A., Gelbert, L.M., Shannon, H.E., Sanchez-Martinez, C., and De Dios, A. (2015). Brain Exposure of Two Selective Dual CDK4 and CDK6 Inhibitors and the Antitumor Activity of CDK4 and CDK6 Inhibition in Combination with Temozolomide in an Intracranial Glioblastoma Xenograft. Drug Metab Dispos *43*, 1360-1371.
Ray, A., James, M.K., Larochelle, S., Fisher, R.P., and Blain, S.W. (2009). p27Kip1 inhibits cyclin D-cyclin-dependent kinase 4 by two independent modes. Mol Cell Biol *29*, 986-999.
Razavi, P., Chang, M.T., Xu, G., Bandlamudi, C., Ross, D.S., Vasan, N., Cai, Y., Bielski, C.M., Donoghue, M.T.A., Jonsson, P., Penson, A., Shen, R., Pareja, F., Kundra, R., Middha, S., Cheng, M.L., Zehir, A., Kandoth, C., Patel, R., Huberman, K., Smyth, L.M., Jhaveri, K., Modi, S., Traina, T.A., Dang, C., Zhang, W., Weigelt, B., Li, B.T., Ladanyi, M., Hyman, D.M., Schultz, N., Robson, M.E., Hudis, C., Brogi, E., Viale, A., Norton, L., Dickler, M.N., Berger, M.F., Iacobuzio-Donahue, C.A., Chandarlapaty, S., Scaltriti, M., Reis-Filho, J.S.,

Solit, D.B., Taylor, B.S., and Baselga, J. (2018). The Genomic Landscape of Endocrine-Resistant Advanced Breast Cancers. Cancer Cell *34*, 427-438 e426.
Reddy, H.K., Mettus, R.V., Rane, S.G., Grana, X., Litvin, J., and Reddy, E.P. (2005). Cyclin-dependent kinase 4 expression is essential for neu-induced breast tumorigenesis. Cancer Res *65*, 10174-10178.
Ribas, R., Pancholi, S., Guest, S.K., Marangoni, E., Gao, Q., Thuleau, A., Simigdala, N., Polanska, U.M., Campbell, H., Rani, A., Liccardi, G., Johnston, S., Davies, B.R., Dowsett, M., and Martin, L.A. (2015). AKT Antagonist AZD5363 Influences Estrogen Receptor Function in Endocrine-Resistant Breast Cancer and Synergizes with Fulvestrant (ICI182780) In Vivo. Mol Cancer Ther *14*, 2035-2048.
Ribas, R., Pancholi, S., Rani, A., Schuster, E., Guest, S.K., Nikitorowicz-Buniak, J., Simigdala, N., Thornhill, A., Avogadri-Connors, F., Cutler, R.E., Jr., Lalani, A.S., Dowsett, M., Johnston, S.R., and Martin, L.A. (2018). Targeting tumour re-wiring by triple blockade of mTORC1, epidermal growth factor, and oestrogen receptor signalling pathways in endocrine-resistant breast cancer. Breast Cancer Res *20*, 44.
Richters, A., Doyle, S.K., Freeman, D.B., Lee, C., Leifer, B.S., Jagannathan, S., Kabinger, F., Koren, J.V., Struntz, N.B., Urgiles, J., Stagg, R.A., Curtin, B.H., Chatterjee, D., Mathea, S., Mikochik, P.J., Hopkins, T.D., Gao, H., Branch, J.R., Xin, H., Westover, L., Bignan, G.C., Rupnow, B.A., Karlin, K.L., Olson, C.M., Westbrook, T.F., Vacca, J., Wilfong, C.M., Trotter, B.W., Saffran, D.C., Bischofberger, N., Knapp, S., Russo, J.W., Hickson, I., Bischoff, J.R., Gottardis, M.M., Balk, S.P., Lin, C.Y., Pop, M.S., and Koehler, A.N. (2021). Modulating Androgen Receptor-Driven Transcription in Prostate Cancer with Selective CDK9 Inhibitors. Cell Chem Biol *28*, 134-147 e114.
Rimel, J.K., and Taatjes, D.J. (2018). The essential and multifunctional TFIIH complex. Protein Sci *27*, 1018-1037.
Rinaldi, J., Sokol, E.S., Hartmaier, R.J., Trabucco, S.E., Frampton, G.M., Goldberg, M.E., Albacker, L.A., Daemen, A., and Manning, G. (2020). The genomic landscape of metastatic breast cancer: Insights from 11,000 tumors. PLoS One *15*, e0231999.
Robertson, J.F.R., Bondarenko, I.M., Trishkina, E., Dvorkin, M., Panasci, L., Manikhas, A., Shparyk, Y., Cardona-Huerta, S., Cheung, K.L., Philco-Salas, M.J., Ruiz-Borrego, M., Shao, Z., Noguchi, S., Rowbottom, J., Stuart, M., Grinsted, L.M., Fazal, M., and Ellis, M.J. (2016). Fulvestrant 500 mg versus anastrozole 1 mg for hormone receptor-positive advanced breast cancer (FALCON): an international, randomised, double-blind, phase 3 trial. Lancet *388*, 2997-3005.

Robinson, J.L., and Carroll, J.S. (2012). FoxA1 is a key mediator of hormonal response in breast and prostate cancer. Front Endocrinol (Lausanne) *3*, 68.
Roeder, R.G. (1996). The role of general initiation factors in transcription by RNA polymerase II. Trends Biochem Sci *21*, 327-335.
Rogatsky, I., Trowbridge, J.M., and Garabedian, M.J. (1999). Potentiation of human estrogen receptor alpha transcriptional activation through phosphorylation of serines 104 and 106 by the cyclin A-CDK2 complex. J Biol Chem *274*, 22296-22302.
Romagosa, C., Simonetti, S., Lopez-Vicente, L., Mazo, A., Lleonart, M.E., Castellvi, J., and Ramon y Cajal, S. (2011). p16(Ink4a) overexpression in cancer: a tumor suppressor gene associated with senescence and high-grade tumors. Oncogene *30*, 2087-2097.
Rondon-Lagos, M., Verdun Di Cantogno, L., Marchio, C., Rangel, N., Payan-Gomez, C., Gugliotta, P., Botta, C., Bussolati, G., Ramirez-Clavijo, S.R., Pasini, B., and Sapino, A. (2014). Differences and homologies of chromosomal alterations within and between breast cancer cell lines: a clustering analysis. Mol Cytogenet *7*, 8.
Rubin, S.M. (2013). Deciphering the retinoblastoma protein phosphorylation code. Trends Biochem Sci *38*, 12-19.
Rubin, S.M., Gall, A.L., Zheng, N., and Pavletich, N.P. (2005). Structure of the Rb C-terminal domain bound to E2F1-DP1: a mechanism for phosphorylation-induced E2F release. Cell *123*, 1093-1106.
Rugo, H.S., Dieras, V., Gelmon, K.A., Finn, R.S., Slamon, D.J., Martin, M., Neven, P., Shparyk, Y., Mori, A., Lu, D.R., Bhattacharyya, H., Bartlett, C., Iyer, S., Johnston, S., Ettl, J., and Harbeck, N. (2018). Impact of palbociclib plus letrozole on patient-reported health-related quality of life: results from the PALOMA-2 trial. Ann Oncol *29*, 888-894.
Rugo, H.S., Finn, R.S., Dieras, V., Ettl, J., Lipatov, O., Joy, A.A., Harbeck, N., Castrellon, A., Iyer, S., Lu, D.R., Mori, A., Gauthier, E.R., Bartlett, C.H., Gelmon, K.A., and Slamon, D.J. (2019). Palbociclib plus letrozole as first-line therapy in estrogen receptor-positive/human epidermal growth factor receptor 2-negative advanced breast cancer with extended follow-up. Breast Cancer Res Treat *174*, 719-729.
Russo, A.A., Tong, L., Lee, J.O., Jeffrey, P.D., and Pavletich, N.P. (1998). Structural basis for inhibition of the cyclin-dependent kinase Cdk6 by the tumour suppressor p16INK4a. Nature *395*, 237-243.
Rzymski, T., Mikula, M., Wiklik, K., and Brzozka, K. (2015). CDK8 kinase--An emerging target in targeted cancer therapy. Biochim Biophys Acta *1854*, 1617-1629.

Sabile, A., Meyer, A.M., Wirbelauer, C., Hess, D., Kogel, U., Scheffner, M., and Krek, W. (2006). Regulation of p27 degradation and S-phase progression by Ro52 RING finger protein. Mol Cell Biol *26*, 5994-6004.

Safe, S., and Kim, K. (2008). Non-classical genomic estrogen receptor (ER)/specificity protein and ER/activating protein-1 signaling pathways. J Mol Endocrinol *41*, 263-275.

Saini, K.S., Loi, S., de Azambuja, E., Metzger-Filho, O., Saini, M.L., Ignatiadis, M., Dancey, J.E., and Piccart-Gebhart, M.J. (2013). Targeting the PI3K/AKT/mTOR and Raf/MEK/ERK pathways in the treatment of breast cancer. Cancer Treat Rev *39*, 935-946.

Sanchez, C.G., Ma, C.X., Crowder, R.J., Guintoli, T., Phommaly, C., Gao, F., Lin, L., and Ellis, M.J. (2011). Preclinical modeling of combined phosphatidylinositol-3-kinase inhibition with endocrine therapy for estrogen receptor-positive breast cancer. Breast Cancer Res *13*, R21.

Sanchez-Vega, F., Mina, M., Armenia, J., Chatila, W.K., Luna, A., La, K.C., Dimitriadoy, S., Liu, D.L., Kantheti, H.S., Saghafinia, S., Chakravarty, D., Daian, F., Gao, Q., Bailey, M.H., Liang, W.W., Foltz, S.M., Shmulevich, I., Ding, L., Heins, Z., Ochoa, A., Gross, B., Gao, J., Zhang, H., Kundra, R., Kandoth, C., Bahceci, I., Dervishi, L., Dogrusoz, U., Zhou, W., Shen, H., Laird, P.W., Way, G.P., Greene, C.S., Liang, H., Xiao, Y., Wang, C., Iavarone, A., Berger, A.H., Bivona, T.G., Lazar, A.J., Hammer, G.D., Giordano, T., Kwong, L.N., McArthur, G., Huang, C., Tward, A.D., Frederick, M.J., McCormick, F., Meyerson, M., Cancer Genome Atlas Research, N., Van Allen, E.M., Cherniack, A.D., Ciriello, G., Sander, C., and Schultz, N. (2018). Oncogenic Signaling Pathways in The Cancer Genome Atlas. Cell *173*, 321-337 e310.

Santamaria, D., Barriere, C., Cerqueira, A., Hunt, S., Tardy, C., Newton, K., Caceres, J.F., Dubus, P., Malumbres, M., and Barbacid, M. (2007). Cdk1 is sufficient to drive the mammalian cell cycle. Nature *448*, 811-815.

Santarius, T., Shipley, J., Brewer, D., Stratton, M.R., and Cooper, C.S. (2010). A census of amplified and overexpressed human cancer genes. Nat Rev Cancer *10*, 59-64.

Santo, L., Vallet, S., Hideshima, T., Cirstea, D., Ikeda, H., Pozzi, S., Patel, K., Okawa, Y., Gorgun, G., Perrone, G., Calabrese, E., Yule, M., Squires, M., Ladetto, M., Boccadoro, M., Richardson, P.G., Munshi, N.C., Anderson, K.C., and Raje, N. (2010). AT7519, A novel small molecule multi-cyclin-dependent kinase inhibitor, induces apoptosis in multiple myeloma via GSK-3beta activation and RNA polymerase II inhibition. Oncogene *29*, 2325-2336.

Sarafan-Vasseur, N., Lamy, A., Bourguignon, J., Le Pessot, F., Hieter, P., Sesboue, R., Bastard, C., Frebourg, T., and Flaman, J.M. (2002). Overexpression of B-type cyclins alters chromosomal segregation. Oncogene *21*, 2051-2057.
Satyanarayana, A., and Kaldis, P. (2009). Mammalian cell-cycle regulation: several Cdks, numerous cyclins and diverse compensatory mechanisms. Oncogene *28*, 2925-2939.
Sava, G.P., Fan, H., Coombes, R.C., Buluwela, L., and Ali, S. (2020). CDK7 inhibitors as anticancer drugs. Cancer Metastasis Rev *39*, 805-823.
Schmid, P., Cortes, J., Pusztai, L., McArthur, H., Kummel, S., Bergh, J., Denkert, C., Park, Y.H., Hui, R., Harbeck, N., Takahashi, M., Foukakis, T., Fasching, P.A., Cardoso, F., Untch, M., Jia, L., Karantza, V., Zhao, J., Aktan, G., Dent, R., O'Shaughnessy, J., and Investigators, K.-. (2020). Pembrolizumab for Early Triple-Negative Breast Cancer. N Engl J Med *382*, 810-821.
Schmidt, D., Wilson, M.D., Spyrou, C., Brown, G.D., Hadfield, J., and Odom, D.T. (2009). ChIP-seq: using high-throughput sequencing to discover protein-DNA interactions. Methods *48*, 240-248.
Schneider, E., Montenarh, M., and Wagner, P. (1998). Regulation of CAK kinase activity by p53. Oncogene *17*, 2733-2741.
Schoenfelder, S., and Fraser, P. (2019). Long-range enhancer-promoter contacts in gene expression control. Nat Rev Genet *20*, 437-455.
Schulze, A., Zerfass, K., Spitkovsky, D., Middendorp, S., Berges, J., Helin, K., Jansen-Durr, P., and Henglein, B. (1995). Cell cycle regulation of the cyclin A gene promoter is mediated by a variant E2F site. Proc Natl Acad Sci U S A *92*, 11264-11268.
Schwabe, J.W., Chapman, L., Finch, J.T., and Rhodes, D. (1993). The crystal structure of the estrogen receptor DNA-binding domain bound to DNA: how receptors discriminate between their response elements. Cell *75*, 567-578.
Schwartz, G.K., LoRusso, P.M., Dickson, M.A., Randolph, S.S., Shaik, M.N., Wilner, K.D., Courtney, R., and O'Dwyer, P.J. (2011). Phase I study of PD 0332991, a cyclin-dependent kinase inhibitor, administered in 3-week cycles (Schedule 2/1). Br J Cancer *104*, 1862-1868.
Sedlacek, H., Czech, J., Naik, R., Kaur, G., Worland, P., Losiewicz, M., Parker, B., Carlson, B., Smith, A., Senderowicz, A., and Sausville, E. (1996). Flavopiridol (L86 8275; NSC 649890), a new kinase inhibitor for tumor therapy. Int J Oncol *9*, 1143-1168.
Seiler-Tuyns, A., Walker, P., Martinez, E., Merillat, A.M., Givel, F., and Wahli, W. (1986). Identification of estrogen-responsive DNA sequences by transient expression experiments in a human breast cancer cell line. Nucleic Acids Res *14*, 8755-8770.
Serrano, M. (1997). The tumor suppressor protein p16INK4a. Exp Cell Res *237*, 7-13.

Servetto, A., Formisano, L., and Arteaga, C.L. (2021). FGFR signaling and endocrine resistance in breast cancer: Challenges for the clinical development of FGFR inhibitors. Biochim Biophys Acta Rev Cancer *1876*, 188595.

Shang, Y., and Brown, M. (2002). Molecular determinants for the tissue specificity of SERMs. Science *295*, 2465-2468.

Shao, W., and Zeitlinger, J. (2017). Paused RNA polymerase II inhibits new transcriptional initiation. Nat Genet *49*, 1045-1051.

Shapiro, G., Rosen, L.S., Tolcher, A.W., Goldman, J.W., Gandhi, L., Papadopoulos, K.P., Tolaney, S.M., Beeram, M., Rasco, D.W., Kulanthaivel, P., Li, Q., Hu, T., Cronier, D., Chan, E.M., Flaherty, K., Wen, P.Y., and Patnaik, A. (2013). A first-in-human phase I study of the CDK4/6 inhibitor, LY2835219, for patients with advanced cancer. Journal of Clinical Oncology *31*, 2500-2500.

Shaulian, E., and Karin, M. (2002). AP-1 as a regulator of cell life and death. Nat Cell Biol *4*, E131-136.

Shaw, L.E., Sadler, A.J., Pugazhendhi, D., and Darbre, P.D. (2006). Changes in oestrogen receptor-alpha and -beta during progression to acquired resistance to tamoxifen and fulvestrant (Faslodex, ICI 182,780) in MCF7 human breast cancer cells. J Steroid Biochem Mol Biol *99*, 19-32.

Shi, Y., Di Giammartino, D.C., Taylor, D., Sarkeshik, A., Rice, W.J., Yates, J.R., 3rd, Frank, J., and Manley, J.L. (2009). Molecular architecture of the human pre-mRNA 3' processing complex. Mol Cell *33*, 365-376.

Shi, Z., Tian, L., Qiang, T., Li, J., Xing, Y., Ren, X., Liu, C., and Liang, C. (2022). From Structure Modification to Drug Launch: A Systematic Review of the Ongoing Development of Cyclin-Dependent Kinase Inhibitors for Multiple Cancer Therapy. J Med Chem *65*, 6390-6418.

Shiau, A.K., Barstad, D., Loria, P.M., Cheng, L., Kushner, P.J., Agard, D.A., and Greene, G.L. (1998). The structural basis of estrogen receptor/coactivator recognition and the antagonism of this interaction by tamoxifen. Cell *95*, 927-937.

Shreeram, S., Sparks, A., Lane, D.P., and Blow, J.J. (2002). Cell type-specific responses of human cells to inhibition of replication licensing. Oncogene *21*, 6624-6632.

Shu, S., Lin, C.Y., He, H.H., Witwicki, R.M., Tabassum, D.P., Roberts, J.M., Janiszewska, M., Huh, S.J., Liang, Y., Ryan, J., Doherty, E., Mohammed, H., Guo, H., Stover, D.G., Ekram, M.B., Brown, J., D'Santos, C., Krop, I.E., Dillon, D., McKeown, M., Ott, C., Qi, J., Ni, M., Rao, P.K., Duarte, M., Wu, S.Y., Chiang, C.M., Anders, L., Young, R.A., Winer, E., Letai, A., Barry, W.T., Carroll, J.S., Long, H., Brown, M., Liu, X.S., Meyer, C.A., Bradner,

J.E., and Polyak, K. (2016). Response and resistance to BET bromodomain inhibitors in triple-negative breast cancer. Nature *529*, 413-417.
Siersbaek, R., Kumar, S., and Carroll, J.S. (2018). Signaling pathways and steroid receptors modulating estrogen receptor alpha function in breast cancer. Genes Dev *32*, 1141-1154.
Sigrist, S., Jacobs, H., Stratmann, R., and Lehner, C.F. (1995). Exit from mitosis is regulated by Drosophila fizzy and the sequential destruction of cyclins A, B and B3. EMBO J *14*, 4827-4838.
Silva Cascales, H., Burdova, K., Middleton, A., Kuzin, V., Mullers, E., Stoy, H., Baranello, L., Macurek, L., and Lindqvist, A. (2021). Cyclin A2 localises in the cytoplasm at the S/G2 transition to activate PLK1. Life Sci Alliance *4*.
Simigdala, N., Gao, Q., Pancholi, S., Roberg-Larsen, H., Zvelebil, M., Ribas, R., Folkerd, E., Thompson, A., Bhamra, A., Dowsett, M., and Martin, L.A. (2016). Cholesterol biosynthesis pathway as a novel mechanism of resistance to estrogen deprivation in estrogen receptor-positive breast cancer. Breast Cancer Res *18*, 58.
Skourti-Stathaki, K., Proudfoot, N.J., and Gromak, N. (2011). Human senataxin resolves RNA/DNA hybrids formed at transcriptional pause sites to promote Xrn2-dependent termination. Mol Cell *42*, 794-805.
Slamon, D.J., Clark, G.M., Wong, S.G., Levin, W.J., Ullrich, A., and McGuire, W.L. (1987). Human breast cancer: correlation of relapse and survival with amplification of the HER-2/neu oncogene. Science *235*, 177-182.
Slamon, D.J., Hurvitz, S.A., Applebaum, S., Glaspy, J.A., Allison, M.K., DiCarlo, B.A., Courtney, R.D., Kim, S.T., Randolph, S., and Finn, R.S. (2010). Phase I study of PD 0332991, cyclin-D kinase (CDK) 4/6 inhibitor in combination with letrozole for first-line treatment of patients with ER-positive, HER2-negative breast cancer. Journal of Clinical Oncology *28*, 3060-3060.
Slamon, D.J., Neven, P., Chia, S., Fasching, P.A., De Laurentiis, M., Im, S.-A., Petrakova, K., Bianchi, G.V., Esteva, F.J., Martín, M., Nusch, A., Sonke, G.S., De la Cruz-Merino, L., Beck, J.T., Pivot, X., Sondhi, M., Wang, Y., Chakravartty, A., Rodriguez-Lorenc, K., Taran, T., and Jerusalem, G. (2019). Overall Survival with Ribociclib plus Fulvestrant in Advanced Breast Cancer. New England Journal of Medicine *382*, 514-524.
Slamon, D.J., Neven, P., Chia, S., Jerusalem, G., De Laurentiis, M., Im, S., Petrakova, K., Valeria Bianchi, G., Martin, M., Nusch, A., Sonke, G.S., De la Cruz-Merino, L., Beck, J.T., Ji, Y., Wang, C., Deore, U., Chakravartty, A., Zarate, J.P., Taran, T., and Fasching, P.A. (2021). Ribociclib plus fulvestrant for postmenopausal women with hormone receptor-positive, human epidermal growth factor receptor 2-negative advanced breast cancer in the

phase III randomized MONALEESA-3 trial: updated overall survival. Ann Oncol *32*, 1015-1024.

Sledge, G.W., Jr., Toi, M., Neven, P., Sohn, J., Inoue, K., Pivot, X., Burdaeva, O., Okera, M., Masuda, N., Kaufman, P.A., Koh, H., Grischke, E.M., Conte, P., Lu, Y., Barriga, S., Hurt, K., Frenzel, M., Johnston, S., and Llombart-Cussac, A. (2020). The Effect of Abemaciclib Plus Fulvestrant on Overall Survival in Hormone Receptor-Positive, ERBB2-Negative Breast Cancer That Progressed on Endocrine Therapy-MONARCH 2: A Randomized Clinical Trial. JAMA Oncol *6*, 116-124.

Sledge, G.W., Jr., Toi, M., Neven, P., Sohn, J., Inoue, K., Pivot, X., Burdaeva, O., Okera, M., Masuda, N., Kaufman, P.A., Koh, H., Grischke, E.M., Frenzel, M., Lin, Y., Barriga, S., Smith, I.C., Bourayou, N., and Llombart-Cussac, A. (2017). MONARCH 2: Abemaciclib in Combination With Fulvestrant in Women With HR+/HER2- Advanced Breast Cancer Who Had Progressed While Receiving Endocrine Therapy. J Clin Oncol *35*, 2875-2884.

Songyang, Z., Blechner, S., Hoagland, N., Hoekstra, M.F., Piwnica-Worms, H., and Cantley, L.C. (1994). Use of an oriented peptide library to determine the optimal substrates of protein kinases. Curr Biol *4*, 973-982.

Sorlie, T., Perou, C.M., Tibshirani, R., Aas, T., Geisler, S., Johnsen, H., Hastie, T., Eisen, M.B., van de Rijn, M., Jeffrey, S.S., Thorsen, T., Quist, H., Matese, J.C., Brown, P.O., Botstein, D., Lonning, P.E., and Borresen-Dale, A.L. (2001). Gene expression patterns of breast carcinomas distinguish tumor subclasses with clinical implications. Proc Natl Acad Sci U S A *98*, 10869-10874.

Soutourina, J. (2018). Transcription regulation by the Mediator complex. Nat Rev Mol Cell Biol *19*, 262-274.

Spruck, C.H., Won, K.A., and Reed, S.I. (1999). Deregulated cyclin E induces chromosome instability. Nature *401*, 297-300.

Squires, M.S., Feltell, R.E., Wallis, N.G., Lewis, E.J., Smith, D.M., Cross, D.M., Lyons, J.F., and Thompson, N.T. (2009). Biological characterization of AT7519, a small-molecule inhibitor of cyclin-dependent kinases, in human tumor cell lines. Mol Cancer Ther *8*, 324-332.

Stark, R.B., G. (2011). Diffbind: Differential binding analysis of ChIP-Seq peak data.

Stebbing, J., Filipovic, A., Lit, L.C., Blighe, K., Grothey, A., Xu, Y., Miki, Y., Chow, L.W., Coombes, R.C., Sasano, H., Shaw, J.A., and Giamas, G. (2013). LMTK3 is implicated in endocrine resistance via multiple signaling pathways. Oncogene *32*, 3371-3380.

Stebbing, J., Shah, K., Lit, L.C., Gagliano, T., Ditsiou, A., Wang, T., Wendler, F., Simon, T., Szabo, K.S., O'Hanlon, T., Dean, M., Roslani, A.C., Cheah, S.H., Lee, S.C., and Giamas, G. (2018). LMTK3 confers chemo-resistance in breast cancer. Oncogene *37*, 3113-3130.
Steinmetz, E.J., and Brow, D.A. (1996). Repression of gene expression by an exogenous sequence element acting in concert with a heterogeneous nuclear ribonucleoprotein-like protein, Nrd1, and the putative helicase Sen1. Mol Cell Biol *16*, 6993-7003.
Steinmetz, E.J., Conrad, N.K., Brow, D.A., and Corden, J.L. (2001). RNA-binding protein Nrd1 directs poly(A)-independent 3'-end formation of RNA polymerase II transcripts. Nature *413*, 327-331.
Steinmetz, E.J., Warren, C.L., Kuehner, J.N., Panbehi, B., Ansari, A.Z., and Brow, D.A. (2006). Genome-wide distribution of yeast RNA polymerase II and its control by Sen1 helicase. Mol Cell *24*, 735-746.
Stemke-Hale, K., Gonzalez-Angulo, A.M., Lluch, A., Neve, R.M., Kuo, W.L., Davies, M., Carey, M., Hu, Z., Guan, Y., Sahin, A., Symmans, W.F., Pusztai, L., Nolden, L.K., Horlings, H., Berns, K., Hung, M.C., van de Vijver, M.J., Valero, V., Gray, J.W., Bernards, R., Mills, G.B., and Hennessy, B.T. (2008). An integrative genomic and proteomic analysis of PIK3CA, PTEN, and AKT mutations in breast cancer. Cancer Res *68*, 6084-6091.
Stendahl, M., Kronblad, A., Ryden, L., Emdin, S., Bengtsson, N.O., and Landberg, G. (2004). Cyclin D1 overexpression is a negative predictive factor for tamoxifen response in postmenopausal breast cancer patients. Br J Cancer *90*, 1942-1948.
Stephenson, J.J., Nemunaitis, J., Joy, A.A., Martin, J.C., Jou, Y.M., Zhang, D., Statkevich, P., Yao, S.L., Zhu, Y., Zhou, H., Small, K., Bannerji, R., and Edelman, M.J. (2014). Randomized phase 2 study of the cyclin-dependent kinase inhibitor dinaciclib (MK-7965) versus erlotinib in patients with non-small cell lung cancer. Lung Cancer *83*, 219-223.
Stice, J.P., and Knowlton, A.A. (2008). Estrogen, NFkappaB, and the heat shock response. Mol Med *14*, 517-527.
Stoeber, K., Tlsty, T.D., Happerfield, L., Thomas, G.A., Romanov, S., Bobrow, L., Williams, E.D., and Williams, G.H. (2001). DNA replication licensing and human cell proliferation. J Cell Sci *114*, 2027-2041.
Strzalka, W., and Ziemienowicz, A. (2011). Proliferating cell nuclear antigen (PCNA): a key factor in DNA replication and cell cycle regulation. Ann Bot *107*, 1127-1140.
Subramanian, R., Wilson-Kubalek, E.M., Arthur, C.P., Bick, M.J., Campbell, E.A., Darst, S.A., Milligan, R.A., and Kapoor, T.M. (2010). Insights into antiparallel microtubule crosslinking by PRC1, a conserved nonmotor microtubule binding protein. Cell *142*, 433-443.

Sumara, I., Vorlaufer, E., Stukenberg, P.T., Kelm, O., Redemann, N., Nigg, E.A., and Peters, J.M. (2002). The dissociation of cohesin from chromosomes in prophase is regulated by Polo-like kinase. Mol Cell *9*, 515-525.

Sung, H., Ferlay, J., Siegel, R.L., Laversanne, M., Soerjomataram, I., Jemal, A., and Bray, F. (2021). Global Cancer Statistics 2020: GLOBOCAN Estimates of Incidence and Mortality Worldwide for 36 Cancers in 185 Countries. CA Cancer J Clin *71*, 209-249.

Tadesse, S., Yu, M., Kumarasiri, M., Le, B.T., and Wang, S. (2015). Targeting CDK6 in cancer: State of the art and new insights. Cell Cycle *14*, 3220-3230.

Takaki, T., Echalier, A., Brown, N.R., Hunt, T., Endicott, J.A., and Noble, M.E. (2009). The structure of CDK4/cyclin D3 has implications for models of CDK activation. Proc Natl Acad Sci U S A *106*, 4171-4176.

Takaku, M., Grimm, S.A., Shimbo, T., Perera, L., Menafra, R., Stunnenberg, H.G., Archer, T.K., Machida, S., Kurumizaka, H., and Wade, P.A. (2016). GATA3-dependent cellular reprogramming requires activation-domain dependent recruitment of a chromatin remodeler. Genome Biol *17*, 36.

Tan, P.H., Ellis, I., Allison, K., Brogi, E., Fox, S.B., Lakhani, S., Lazar, A.J., Morris, E.A., Sahin, A., Salgado, R., Sapino, A., Sasano, H., Schnitt, S., Sotiriou, C., van Diest, P., White, V.A., Lokuhetty, D., Cree, I.A., and Board, W.H.O.C.o.T.E. (2020). The 2019 World Health Organization classification of tumours of the breast. Histopathology *77*, 181-185.

Tanenbaum, D.M., Wang, Y., Williams, S.P., and Sigler, P.B. (1998). Crystallographic comparison of the estrogen and progesterone receptor's ligand binding domains. Proc Natl Acad Sci U S A *95*, 5998-6003.

Tang, L., Zhu, C., Jin, J., Wang, X., Yu, L., and Guan, X. (2021). Expression of CDK7 correlates with molecular subtypes and predicts clinical outcomes in breast cancer. Transl Cancer Res *10*, 669-680.

Tassan, J.P., Jaquenoud, M., Fry, A.M., Frutiger, S., Hughes, G.J., and Nigg, E.A. (1995). In vitro assembly of a functional human CDK7-cyclin H complex requires MAT1, a novel 36 kDa RING finger protein. EMBO J *14*, 5608-5617.

Taylor, A.H., and Al-Azzawi, F. (2000). Immunolocalisation of oestrogen receptor beta in human tissues. J Mol Endocrinol *24*, 145-155.

Taylor, M., Sosman, J., Gonzalez, R., Carlino, M., Kittaneh, M., Lolkema, M., Miller, W., Marino, A., Zhang, V., Bhansali, S.G., Parasuraman, S., and Postow, M.A. (2014). 1086OPHASE IB/II STUDY OF LEE011 (CDK4/6 INHIBITOR) AND LGX818 (BRAF INHIBITOR) IN BRAF-MUTANT MELANOMA. Japanese Society of Medical Oncology *25*, iv374-iv375.

Teh, J.L.F., and Aplin, A.E. (2019). Arrested Developments: CDK4/6 Inhibitor Resistance and Alterations in the Tumor Immune Microenvironment. Clin Cancer Res *25*, 921-927.
Teo, Z.L., Versaci, S., Dushyanthen, S., Caramia, F., Savas, P., Mintoff, C.P., Zethoven, M., Virassamy, B., Luen, S.J., McArthur, G.A., Phillips, W.A., Darcy, P.K., and Loi, S. (2017). Combined CDK4/6 and PI3Kalpha Inhibition Is Synergistic and Immunogenic in Triple-Negative Breast Cancer. Cancer Res *77*, 6340-6352.
Teyssier, C., Belguise, K., Galtier, F., and Chalbos, D. (2001). Characterization of the physical interaction between estrogen receptor alpha and JUN proteins. J Biol Chem *276*, 36361-36369.
Thomas, R.S., Sarwar, N., Phoenix, F., Coombes, R.C., and Ali, S. (2008). Phosphorylation at serines 104 and 106 by Erk1/2 MAPK is important for estrogen receptor-alpha activity. J Mol Endocrinol *40*, 173-184.
Thomas, Y., Cirillo, L., Panbianco, C., Martino, L., Tavernier, N., Schwager, F., Van Hove, L., Joly, N., Santamaria, A., Pintard, L., and Gotta, M. (2016). Cdk1 Phosphorylates SPAT-1/Bora to Promote Plk1 Activation in C. elegans and Human Cells. Cell Rep *15*, 510-518.
Tien, J.F., Mazloomian, A., Cheng, S.G., Hughes, C.S., Chow, C.C.T., Canapi, L.T., Oloumi, A., Trigo-Gonzalez, G., Bashashati, A., Xu, J., Chang, V.C., Shah, S.P., Aparicio, S., and Morin, G.B. (2017). CDK12 regulates alternative last exon mRNA splicing and promotes breast cancer cell invasion. Nucleic Acids Res *45*, 6698-6716.
Timofeev, O., Cizmecioglu, O., Settele, F., Kempf, T., and Hoffmann, I. (2010). Cdc25 phosphatases are required for timely assembly of CDK1-cyclin B at the G2/M transition. J Biol Chem *285*, 16978-16990.
Tolaney, S.M., Sahebjam, S., Le Rhun, E., Bachelot, T., Kabos, P., Awada, A., Yardley, D., Chan, A., Conte, P., Dieras, V., Lin, N.U., Bear, M., Chapman, S.C., Yang, Z., Chen, Y., and Anders, C.K. (2020a). A Phase II Study of Abemaciclib in Patients with Brain Metastases Secondary to Hormone Receptor-Positive Breast Cancer. Clin Cancer Res *26*, 5310-5319.
Tolaney, S.M., Wardley, A.M., Zambelli, S., Hilton, J.F., Troso-Sandoval, T.A., Ricci, F., Im, S.A., Kim, S.B., Johnston, S.R., Chan, A., Goel, S., Catron, K., Chapman, S.C., Price, G.L., Yang, Z., Gainford, M.C., and Andre, F. (2020b). Abemaciclib plus trastuzumab with or without fulvestrant versus trastuzumab plus standard-of-care chemotherapy in women with hormone receptor-positive, HER2-positive advanced breast cancer (monarcHER): a randomised, open-label, phase 2 trial. Lancet Oncol *21*, 763-775.
Toogood, P.L., Harvey, P.J., Repine, J.T., Sheehan, D.J., VanderWel, S.N., Zhou, H., Keller, P.R., McNamara, D.J., Sherry, D., Zhu, T., Brodfuehrer, J., Choi, C., Barvian, M.R., and Fry,

D.W. (2005). Discovery of a potent and selective inhibitor of cyclin-dependent kinase 4/6. J Med Chem *48*, 2388-2406.
Toy, W., Weir, H., Razavi, P., Lawson, M., Goeppert, A.U., Mazzola, A.M., Smith, A., Wilson, J., Morrow, C., Wong, W.L., De Stanchina, E., Carlson, K.E., Martin, T.S., Uddin, S., Li, Z., Fanning, S., Katzenellenbogen, J.A., Greene, G., Baselga, J., and Chandarlapaty, S. (2017). Activating ESR1 Mutations Differentially Affect the Efficacy of ER Antagonists. Cancer Discov *7*, 277-287.
Toyoshima-Morimoto, F., Taniguchi, E., Shinya, N., Iwamatsu, A., and Nishida, E. (2001). Polo-like kinase 1 phosphorylates cyclin B1 and targets it to the nucleus during prophase. Nature *410*, 215-220.
Traboulsi, T., El Ezzy, M., Gleason, J.L., and Mader, S. (2017). Antiestrogens: structure-activity relationships and use in breast cancer treatment. J Mol Endocrinol *58*, R15-R31.
Tripathy, D., Bardia, A., and Sellers, W.R. (2017). Ribociclib (LEE011): Mechanism of Action and Clinical Impact of This Selective Cyclin-Dependent Kinase 4/6 Inhibitor in Various Solid Tumors. Clin Cancer Res *23*, 3251-3262.
Tripathy, D., Im, S.A., Colleoni, M., Franke, F., Bardia, A., Harbeck, N., Hurvitz, S.A., Chow, L., Sohn, J., Lee, K.S., Campos-Gomez, S., Villanueva Vazquez, R., Jung, K.H., Babu, K.G., Wheatley-Price, P., De Laurentiis, M., Im, Y.H., Kuemmel, S., El-Saghir, N., Liu, M.C., Carlson, G., Hughes, G., Diaz-Padilla, I., Germa, C., Hirawat, S., and Lu, Y.S. (2018). Ribociclib plus endocrine therapy for premenopausal women with hormone-receptor-positive, advanced breast cancer (MONALEESA-7): a randomised phase 3 trial. Lancet Oncol *19*, 904-915.
Trova, M.P., Barnes, K.D., Alicea, L., Benanti, T., Bielaska, M., Bilotta, J., Bliss, B., Duong, T.N., Haydar, S., Herr, R.J., Hui, Y., Johnson, M., Lehman, J.M., Peace, D., Rainka, M., Snider, P., Salamone, S., Tregay, S., Zheng, X., and Friedrich, T.D. (2009). Heterobiaryl purine derivatives as potent antiproliferative agents: inhibitors of cyclin dependent kinases. Part II. Bioorg Med Chem Lett *19*, 6613-6617.
Tsang, F.H., Law, C.T., Tang, T.C., Cheng, C.L., Chin, D.W., Tam, W.V., Wei, L., Wong, C.C., Ng, I.O., and Wong, C.M. (2019). Aberrant Super-Enhancer Landscape in Human Hepatocellular Carcinoma. Hepatology *69*, 2502-2517.
Tsujimoto, Y., Yunis, J., Onorato-Showe, L., Erikson, J., Nowell, P.C., and Croce, C.M. (1984). Molecular cloning of the chromosomal breakpoint of B-cell lymphomas and leukemias with the t(11;14) chromosome translocation. Science *224*, 1403-1406.
Turner, N., Pearson, A., Sharpe, R., Lambros, M., Geyer, F., Lopez-Garcia, M.A., Natrajan, R., Marchio, C., Iorns, E., Mackay, A., Gillett, C., Grigoriadis, A., Tutt, A., Reis-Filho, J.S.,

and Ashworth, A. (2010). FGFR1 amplification drives endocrine therapy resistance and is a therapeutic target in breast cancer. Cancer Res *70*, 2085-2094.
Turner, N.C., Liu, Y., Zhu, Z., Loi, S., Colleoni, M., Loibl, S., DeMichele, A., Harbeck, N., Andre, F., Bayar, M.A., Michiels, S., Zhang, Z., Giorgetti, C., Arnedos, M., Huang Bartlett, C., and Cristofanilli, M. (2019). Cyclin E1 Expression and Palbociclib Efficacy in Previously Treated Hormone Receptor-Positive Metastatic Breast Cancer. J Clin Oncol *37*, 1169-1178.
Turner, N.C., Ro, J., Andre, F., Loi, S., Verma, S., Iwata, H., Harbeck, N., Loibl, S., Huang Bartlett, C., Zhang, K., Giorgetti, C., Randolph, S., Koehler, M., Cristofanilli, M., and Group, P.S. (2015). Palbociclib in Hormone-Receptor-Positive Advanced Breast Cancer. N Engl J Med *373*, 209-219.
Turner, N.C., Slamon, D.J., Ro, J., Bondarenko, I., Im, S.A., Masuda, N., Colleoni, M., DeMichele, A., Loi, S., Verma, S., Iwata, H., Harbeck, N., Loibl, S., Andre, F., Puyana Theall, K., Huang, X., Giorgetti, C., Huang Bartlett, C., and Cristofanilli, M. (2018). Overall Survival with Palbociclib and Fulvestrant in Advanced Breast Cancer. N Engl J Med *379*, 1926-1936.
Tyler, J.K., Adams, C.R., Chen, S.R., Kobayashi, R., Kamakaka, R.T., and Kadonaga, J.T. (1999). The RCAF complex mediates chromatin assembly during DNA replication and repair. Nature *402*, 555-560.
Uehara, R., Tsukada, Y., Kamasaki, T., Poser, I., Yoda, K., Gerlich, D.W., and Goshima, G. (2013). Aurora B and Kif2A control microtubule length for assembly of a functional central spindle during anaphase. J Cell Biol *202*, 623-636.
Uhlmann, F., Wernic, D., Poupart, M.A., Koonin, E.V., and Nasmyth, K. (2000). Cleavage of cohesin by the CD clan protease separin triggers anaphase in yeast. Cell *103*, 375-386.
Vairo, G., Livingston, D.M., and Ginsberg, D. (1995). Functional interaction between E2F-4 and p130: evidence for distinct mechanisms underlying growth suppression by different retinoblastoma protein family members. Genes Dev *9*, 869-881.
Vajdos, F.F., Hoth, L.R., Geoghegan, K.F., Simons, S.P., LeMotte, P.K., Danley, D.E., Ammirati, M.J., and Pandit, J. (2007). The 2.0 A crystal structure of the ERalpha ligand-binding domain complexed with lasofoxifene. Protein Sci *16*, 897-905.
Vale, R.D., Reese, T.S., and Sheetz, M.P. (1985). Identification of a novel force-generating protein, kinesin, involved in microtubule-based motility. Cell *42*, 39-50.
van 't Veer, L.J., Dai, H., van de Vijver, M.J., He, Y.D., Hart, A.A., Mao, M., Peterse, H.L., van der Kooy, K., Marton, M.J., Witteveen, A.T., Schreiber, G.J., Kerkhoven, R.M., Roberts, C., Linsley, P.S., Bernards, R., and Friend, S.H. (2002). Gene expression profiling predicts clinical outcome of breast cancer. Nature *415*, 530-536.

van den Heuvel, S., and Harlow, E. (1993). Distinct roles for cyclin-dependent kinases in cell cycle control. Science *262*, 2050-2054.
van Vugt, M.A., and Medema, R.H. (2005). Getting in and out of mitosis with Polo-like kinase-1. Oncogene *24*, 2844-2859.
VanderWel, S.N., Harvey, P.J., McNamara, D.J., Repine, J.T., Keller, P.R., Quin, J., 3rd, Booth, R.J., Elliott, W.L., Dobrusin, E.M., Fry, D.W., and Toogood, P.L. (2005). Pyrido[2,3-d]pyrimidin-7-ones as specific inhibitors of cyclin-dependent kinase 4. J Med Chem *48*, 2371-2387.
Vassilev, L.T., Tovar, C., Chen, S., Knezevic, D., Zhao, X., Sun, H., Heimbrook, D.C., and Chen, L. (2006). Selective small-molecule inhibitor reveals critical mitotic functions of human CDK1. Proc Natl Acad Sci U S A *103*, 10660-10665.
Vendrell, J.A., Bieche, I., Desmetz, C., Badia, E., Tozlu, S., Nguyen, C., Nicolas, J.C., Lidereau, R., and Cohen, P.A. (2005). Molecular changes associated with the agonist activity of hydroxy-tamoxifen and the hyper-response to estradiol in hydroxy-tamoxifen-resistant breast cancer cell lines. Endocr Relat Cancer *12*, 75-92.
Vesely, J., Havlicek, L., Strnad, M., Blow, J.J., Donella-Deana, A., Pinna, L., Letham, D.S., Kato, J., Detivaud, L., Leclerc, S., and et al. (1994). Inhibition of cyclin-dependent kinases by purine analogues. Eur J Biochem *224*, 771-786.
Wada, T., Takagi, T., Yamaguchi, Y., Watanabe, D., and Handa, H. (1998). Evidence that P-TEFb alleviates the negative effect of DSIF on RNA polymerase II-dependent transcription in vitro. EMBO J *17*, 7395-7403.
Waga, S., Hannon, G.J., Beach, D., and Stillman, B. (1994). The p21 inhibitor of cyclin-dependent kinases controls DNA replication by interaction with PCNA. Nature *369*, 574-578.
Wagner, E., and Glotzer, M. (2016). Local RhoA activation induces cytokinetic furrows independent of spindle position and cell cycle stage. J Cell Biol *213*, 641-649.
Wagner, V., and Gil, J. (2020). Senescence as a therapeutically relevant response to CDK4/6 inhibitors. Oncogene *39*, 5165-5176.
Waks, A.G., and Winer, E.P. (2019). Breast Cancer Treatment: A Review. JAMA *321*, 288-300.
Walker, D.H., and Maller, J.L. (1991). Role for cyclin A in the dependence of mitosis on completion of DNA replication. Nature *354*, 314-317.
Walker, V.R., and Korach, K.S. (2004). Estrogen receptor knockout mice as a model for endocrine research. ILAR J *45*, 455-461.
Wander, S.A., Cohen, O., Gong, X., Johnson, G.N., Buendia-Buendia, J.E., Lloyd, M.R., Kim, D., Luo, F., Mao, P., Helvie, K., Kowalski, K.J., Nayar, U., Waks, A.G., Parsons, S.H.,

Martinez, R., Litchfield, L.M., Ye, X.S., Yu, C., Jansen, V.M., Stille, J.R., Smith, P.S., Oakley, G.J., Chu, Q.S., Batist, G., Hughes, M.E., Kremer, J.D., Garraway, L.A., Winer, E.P., Tolaney, S.M., Lin, N.U., Buchanan, S.G., and Wagle, N. (2020). The Genomic Landscape of Intrinsic and Acquired Resistance to Cyclin-Dependent Kinase 4/6 Inhibitors in Patients with Hormone Receptor-Positive Metastatic Breast Cancer. Cancer Discov *10*, 1174-1193.

Wang, B., Varela-Eirin, M., Brandenburg, S.M., Hernandez-Segura, A., van Vliet, T., Jongbloed, E.M., Wilting, S.M., Ohtani, N., Jager, A., and Demaria, M. (2022). Pharmacological CDK4/6 inhibition reveals a p53-dependent senescent state with restricted toxicity. EMBO J *41*, e108946.

Wang, S., Zang, C., Xiao, T., Fan, J., Mei, S., Qin, Q., Wu, Q., Li, X., Xu, K., He, H.H., Brown, M., Meyer, C.A., and Liu, X.S. (2016). Modeling cis-regulation with a compendium of genome-wide histone H3K27ac profiles. Genome Res *26*, 1417-1429.

Wang, W., Dong, L., Saville, B., and Safe, S. (1999). Transcriptional activation of E2F1 gene expression by 17beta-estradiol in MCF-7 cells is regulated by NF-Y-Sp1/estrogen receptor interactions. Mol Endocrinol *13*, 1373-1387.

Wang, Y., Klijn, J.G., Zhang, Y., Sieuwerts, A.M., Look, M.P., Yang, F., Talantov, D., Timmermans, M., Meijer-van Gelder, M.E., Yu, J., Jatkoe, T., Berns, E.M., Atkins, D., and Foekens, J.A. (2005). Gene-expression profiles to predict distant metastasis of lymph-node-negative primary breast cancer. Lancet *365*, 671-679.

Wang, Y., Zhang, T., Kwiatkowski, N., Abraham, B.J., Lee, T.I., Xie, S., Yuzugullu, H., Von, T., Li, H., Lin, Z., Stover, D.G., Lim, E., Wang, Z.C., Iglehart, J.D., Young, R.A., Gray, N.S., and Zhao, J.J. (2015). CDK7-dependent transcriptional addiction in triple-negative breast cancer. Cell *163*, 174-186.

Ward, G.E., and Kirschner, M.W. (1990). Identification of cell cycle-regulated phosphorylation sites on nuclear lamin C. Cell *61*, 561-577.

Watanabe, N., Broome, M., and Hunter, T. (1995). Regulation of the human WEE1Hu CDK tyrosine 15-kinase during the cell cycle. EMBO J *14*, 1878-1891.

Weber, J.D., Taylor, L.J., Roussel, M.F., Sherr, C.J., and Bar-Sagi, D. (1999). Nucleolar Arf sequesters Mdm2 and activates p53. Nat Cell Biol *1*, 20-26.

Wei, W., Ayad, N.G., Wan, Y., Zhang, G.J., Kirschner, M.W., and Kaelin, W.G., Jr. (2004). Degradation of the SCF component Skp2 in cell-cycle phase G1 by the anaphase-promoting complex. Nature *428*, 194-198.

Weigelt, B., Baehner, F.L., and Reis-Filho, J.S. (2010a). The contribution of gene expression profiling to breast cancer classification, prognostication and prediction: a retrospective of the last decade. J Pathol *220*, 263-280.
Weigelt, B., Geyer, F.C., and Reis-Filho, J.S. (2010b). Histological types of breast cancer: how special are they? Mol Oncol *4*, 192-208.
Wein, L., Savas, P., Van Geelen, C., Caramia, F., Moodie, K., Joshi, S., and Loi, S. (2017). FGFR2 amplification in metastatic hormone-positive breast cancer and response to an mTOR inhibitor. Ann Oncol *28*, 2025-2027.
Weinstein, I.B., and Joe, A.K. (2006). Mechanisms of disease: Oncogene addiction--a rationale for molecular targeting in cancer therapy. Nat Clin Pract Oncol *3*, 448-457.
Welboren, W.J., Sweep, F.C., Span, P.N., and Stunnenberg, H.G. (2009). Genomic actions of estrogen receptor alpha: what are the targets and how are they regulated? Endocr Relat Cancer *16*, 1073-1089.
Wensink, G.E., Elias, S.G., Mullenders, J., Koopman, M., Boj, S.F., Kranenburg, O.W., and Roodhart, J.M.L. (2021). Patient-derived organoids as a predictive biomarker for treatment response in cancer patients. npj Precision Oncology *5*, 30.
Westbrook, T.F., Nguyen, D.X., Thrash, B.R., and McCance, D.J. (2002). E7 abolishes raf-induced arrest via mislocalization of p21(Cip1). Mol Cell Biol *22*, 7041-7052.
Williams, M.M., Spoelstra, N.S., Arnesen, S., O'Neill, K.I., Christenson, J.L., Reese, J., Torkko, K.C., Goodspeed, A., Rosas, E., Hanamura, T., Sams, S.B., Li, Z., Oesterreich, S., Riggins, R.B., Jacobsen, B.M., Elias, A., Gertz, J., and Richer, J.K. (2021). Steroid Hormone Receptor and Infiltrating Immune Cell Status Reveals Therapeutic Vulnerabilities of ESR1-Mutant Breast Cancer. Cancer Res *81*, 732-746.
Wischhusen, J., Melero, I., and Fridman, W.H. (2020). Growth/Differentiation Factor-15 (GDF-15): From Biomarker to Novel Targetable Immune Checkpoint. Front Immunol *11*, 951.
Withers, D.A., Harvey, R.C., Faust, J.B., Melnyk, O., Carey, K., and Meeker, T.C. (1991). Characterization of a candidate bcl-1 gene. Mol Cell Biol *11*, 4846-4853.
Witkiewicz, A.K., Knudsen, K.E., Dicker, A.P., and Knudsen, E.S. (2011). The meaning of p16(ink4a) expression in tumors: functional significance, clinical associations and future developments. Cell Cycle *10*, 2497-2503.
Wong, J.V., Dong, P., Nevins, J.R., Mathey-Prevot, B., and You, L. (2011). Network calisthenics: control of E2F dynamics in cell cycle entry. Cell Cycle *10*, 3086-3094.
Woodbury, E.L., and Morgan, D.O. (2007). Cdk and APC activities limit the spindle-stabilizing function of Fin1 to anaphase. Nat Cell Biol *9*, 106-112.

Woolcott, C.G., SenGupta, S.K., Hanna, W.M., and Aronson, K.J. (2008). Estrogen and progesterone receptor levels in nonneoplastic breast epithelium of breast cancer cases versus benign breast biopsy controls. BMC Cancer *8*, 130.

Wu, G., Xing, M., Mambo, E., Huang, X., Liu, J., Guo, Z., Chatterjee, A., Goldenberg, D., Gollin, S.M., Sukumar, S., Trink, B., and Sidransky, D. (2005). Somatic mutation and gain of copy number of PIK3CA in human breast cancer. Breast Cancer Res *7*, R609-616.

Wu, J.Q., Guo, J.Y., Tang, W., Yang, C.S., Freel, C.D., Chen, C., Nairn, A.C., and Kornbluth, S. (2009). PP1-mediated dephosphorylation of phosphoproteins at mitotic exit is controlled by inhibitor-1 and PP1 phosphorylation. Nat Cell Biol *11*, 644-651.

Wu, Y.M., Cieslik, M., Lonigro, R.J., Vats, P., Reimers, M.A., Cao, X., Ning, Y., Wang, L., Kunju, L.P., de Sarkar, N., Heath, E.I., Chou, J., Feng, F.Y., Nelson, P.S., de Bono, J.S., Zou, W., Montgomery, B., Alva, A., Team, P.S.C.I.P.C.D., Robinson, D.R., and Chinnaiyan, A.M. (2018). Inactivation of CDK12 Delineates a Distinct Immunogenic Class of Advanced Prostate Cancer. Cell *173*, 1770-1782 e1714.

Wyatt, P.G., Woodhead, A.J., Berdini, V., Boulstridge, J.A., Carr, M.G., Cross, D.M., Davis, D.J., Devine, L.A., Early, T.R., Feltell, R.E., Lewis, E.J., McMenamin, R.L., Navarro, E.F., O'Brien, M.A., O'Reilly, M., Reule, M., Saxty, G., Seavers, L.C., Smith, D.M., Squires, M.S., Trewartha, G., Walker, M.T., and Woolford, A.J. (2008). Identification of N-(4-piperidinyl)-4-(2,6-dichlorobenzoylamino)-1H-pyrazole-3-carboxamide (AT7519), a novel cyclin dependent kinase inhibitor using fragment-based X-ray crystallography and structure based drug design. J Med Chem *51*, 4986-4999.

Xiao, B., Spencer, J., Clements, A., Ali-Khan, N., Mittnacht, S., Broceno, C., Burghammer, M., Perrakis, A., Marmorstein, R., and Gamblin, S.J. (2003). Crystal structure of the retinoblastoma tumor suppressor protein bound to E2F and the molecular basis of its regulation. Proc Natl Acad Sci U S A *100*, 2363-2368.

Xiong, Y., Connolly, T., Futcher, B., and Beach, D. (1991). Human D-type cyclin. Cell *65*, 691-699.

Xiong, Y., Hannon, G.J., Zhang, H., Casso, D., Kobayashi, R., and Beach, D. (1993). p21 is a universal inhibitor of cyclin kinases. Nature *366*, 701-704.

Xu, G., Chhangawala, S., Cocco, E., Razavi, P., Cai, Y., Otto, J.E., Ferrando, L., Selenica, P., Ladewig, E., Chan, C., Da Cruz Paula, A., Witkin, M., Cheng, Y., Park, J., Serna-Tamayo, C., Zhao, H., Wu, F., Sallaku, M., Qu, X., Zhao, A., Collings, C.K., D'Avino, A.R., Jhaveri, K., Koche, R., Levine, R.L., Reis-Filho, J.S., Kadoch, C., Scaltriti, M., Leslie, C.S., Baselga, J., and Toska, E. (2020). ARID1A determines luminal identity and therapeutic response in estrogen-receptor-positive breast cancer. Nat Genet *52*, 198-207.

Xu, J., and Li, Q. (2003). Review of the in vivo functions of the p160 steroid receptor coactivator family. Mol Endocrinol *17*, 1681-1692.
Xu, J., Yanagisawa, Y., Tsankov, A.M., Hart, C., Aoki, K., Kommajosyula, N., Steinmann, K.E., Bochicchio, J., Russ, C., Regev, A., Rando, O.J., Nusbaum, C., Niki, H., Milos, P., Weng, Z., and Rhind, N. (2012a). Genome-wide identification and characterization of replication origins by deep sequencing. Genome Biol *13*, R27.
Xu, S., Yu, S., Dong, D., and Lee, L.T.O. (2019). G Protein-Coupled Estrogen Receptor: A Potential Therapeutic Target in Cancer. Front Endocrinol (Lausanne) *10*, 725.
Xu, W.H., Liu, Z.B., Yang, C., Qin, W., and Shao, Z.M. (2012b). Expression of dickkopf-1 and beta-catenin related to the prognosis of breast cancer patients with triple negative phenotype. PLoS One *7*, e37624.
Xu, Y., Zhang, H., Lit, L.C., Grothey, A., Athanasiadou, M., Kiritsi, M., Lombardo, Y., Frampton, A.E., Green, A.R., Ellis, I.O., Ali, S., Lenz, H.J., Thanou, M., Stebbing, J., and Giamas, G. (2014). The kinase LMTK3 promotes invasion in breast cancer through GRB2-mediated induction of integrin beta(1). Sci Signal *7*, ra58.
Yamaguchi, Y., Takagi, T., Wada, T., Yano, K., Furuya, A., Sugimoto, S., Hasegawa, J., and Handa, H. (1999). NELF, a multisubunit complex containing RD, cooperates with DSIF to repress RNA polymerase II elongation. Cell *97*, 41-51.
Yamano, H., Ishii, K., and Yanagida, M. (1994). Phosphorylation of dis2 protein phosphatase at the C-terminal cdc2 consensus and its potential role in cell cycle regulation. EMBO J *13*, 5310-5318.
Yamashita, H., Nishio, M., Kobayashi, S., Ando, Y., Sugiura, H., Zhang, Z., Hamaguchi, M., Mita, K., Fujii, Y., and Iwase, H. (2005). Phosphorylation of estrogen receptor alpha serine 167 is predictive of response to endocrine therapy and increases postrelapse survival in metastatic breast cancer. Breast Cancer Res *7*, R753-764.
Yan, W., Cao, Q.J., Arenas, R.B., Bentley, B., and Shao, R. (2010). GATA3 inhibits breast cancer metastasis through the reversal of epithelial-mesenchymal transition. J Biol Chem *285*, 14042-14051.
Yang, C., Li, Z., Bhatt, T., Dickler, M., Giri, D., Scaltriti, M., Baselga, J., Rosen, N., and Chandarlapaty, S. (2017). Acquired CDK6 amplification promotes breast cancer resistance to CDK4/6 inhibitors and loss of ER signaling and dependence. Oncogene *36*, 2255-2264.
Yang, J., Bardes, E.S., Moore, J.D., Brennan, J., Powers, M.A., and Kornbluth, S. (1998). Control of cyclin B1 localization through regulated binding of the nuclear export factor CRM1. Genes Dev *12*, 2131-2143.

Yang, J., Nie, J., Ma, X., Wei, Y., Peng, Y., and Wei, X. (2019). Targeting PI3K in cancer: mechanisms and advances in clinical trials. Mol Cancer *18*, 26.
Yang, J., Zhang, X., Feng, J., Leng, H., Li, S., Xiao, J., Liu, S., Xu, Z., Xu, J., Li, D., Wang, Z., Wang, J., and Li, Q. (2016). The Histone Chaperone FACT Contributes to DNA Replication-Coupled Nucleosome Assembly. Cell Rep *16*, 3414.
Yang, Z., Yik, J.H., Chen, R., He, N., Jang, M.K., Ozato, K., and Zhou, Q. (2005). Recruitment of P-TEFb for stimulation of transcriptional elongation by the bromodomain protein Brd4. Mol Cell *19*, 535-545.
Yankulov, K.Y., and Bentley, D.L. (1997). Regulation of CDK7 substrate specificity by MAT1 and TFIIH. EMBO J *16*, 1638-1646.
Ye, X., Wei, Y., Nalepa, G., and Harper, J.W. (2003). The cyclin E/Cdk2 substrate p220(NPAT) is required for S-phase entry, histone gene expression, and Cajal body maintenance in human somatic cells. Mol Cell Biol *23*, 8586-8600.
Yokoo, T., Toyoshima, H., Miura, M., Wang, Y., Iida, K.T., Suzuki, H., Sone, H., Shimano, H., Gotoda, T., Nishimori, S., Tanaka, K., and Yamada, N. (2003). p57Kip2 regulates actin dynamics by binding and translocating LIM-kinase 1 to the nucleus. J Biol Chem *278*, 52919-52923.
Yu, G., Wang, L.G., and He, Q.Y. (2015). ChIPseeker: an R/Bioconductor package for ChIP peak annotation, comparison and visualization. Bioinformatics *31*, 2382-2383.
Yu, Q., Geng, Y., and Sicinski, P. (2001). Specific protection against breast cancers by cyclin D1 ablation. Nature *411*, 1017-1021.
Yu, Q., Sicinska, E., Geng, Y., Ahnstrom, M., Zagozdzon, A., Kong, Y., Gardner, H., Kiyokawa, H., Harris, L.N., Stal, O., and Sicinski, P. (2006). Requirement for CDK4 kinase function in breast cancer. Cancer Cell *9*, 23-32.
Yuan, K., Wang, X., Dong, H., Min, W., Hao, H., and Yang, P. (2021). Selective inhibition of CDK4/6: A safe and effective strategy for developing anticancer drugs. Acta Pharm Sin B *11*, 30-54.
Yue, W., Wang, J.P., Conaway, M., Masamura, S., Li, Y., and Santen, R.J. (2002). Activation of the MAPK pathway enhances sensitivity of MCF-7 breast cancer cells to the mitogenic effect of estradiol. Endocrinology *143*, 3221-3229.
Zalmas, L.P., Zhao, X., Graham, A.L., Fisher, R., Reilly, C., Coutts, A.S., and La Thangue, N.B. (2008). DNA-damage response control of E2F7 and E2F8. EMBO Rep *9*, 252-259.
Zeitlinger, J., Stark, A., Kellis, M., Hong, J.W., Nechaev, S., Adelman, K., Levine, M., and Young, R.A. (2007). RNA polymerase stalling at developmental control genes in the Drosophila melanogaster embryo. Nat Genet *39*, 1512-1516.

Zhang, J., Bu, X., Wang, H., Zhu, Y., Geng, Y., Nihira, N.T., Tan, Y., Ci, Y., Wu, F., Dai, X., Guo, J., Huang, Y.H., Fan, C., Ren, S., Sun, Y., Freeman, G.J., Sicinski, P., and Wei, W. (2018). Cyclin D-CDK4 kinase destabilizes PD-L1 via cullin 3-SPOP to control cancer immune surveillance. Nature *553*, 91-95.

Zhang, J., Shi, X., Li, Y., Kim, B.J., Jia, J., Huang, Z., Yang, T., Fu, X., Jung, S.Y., Wang, Y., Zhang, P., Kim, S.T., Pan, X., and Qin, J. (2008). Acetylation of Smc3 by Eco1 is required for S phase sister chromatid cohesion in both human and yeast. Mol Cell *31*, 143-151.

Zhang, M., Zhang, L., Hei, R., Li, X., Cai, H., Wu, X., Zheng, Q., and Cai, C. (2021). CDK inhibitors in cancer therapy, an overview of recent development. Am J Cancer Res *11*, 1913-1935.

Zhang, T., Kwiatkowski, N., Olson, C.M., Dixon-Clarke, S.E., Abraham, B.J., Greifenberg, A.K., Ficarro, S.B., Elkins, J.M., Liang, Y., Hannett, N.M., Manz, T., Hao, M., Bartkowiak, B., Greenleaf, A.L., Marto, J.A., Geyer, M., Bullock, A.N., Young, R.A., and Gray, N.S. (2016). Covalent targeting of remote cysteine residues to develop CDK12 and CDK13 inhibitors. Nat Chem Biol *12*, 876-884.

Zhao, L., and Vogt, P.K. (2008). Class I PI3K in oncogenic cellular transformation. Oncogene *27*, 5486-5496.

Zheng, W., Wang, H., Xue, L., Zhang, Z., and Tong, T. (2004). Regulation of cellular senescence and p16(INK4a) expression by Id1 and E47 proteins in human diploid fibroblast. J Biol Chem *279*, 31524-31532.

Zhou, B.P., Liao, Y., Xia, W., Spohn, B., Lee, M.H., and Hung, M.C. (2001). Cytoplasmic localization of p21Cip1/WAF1 by Akt-induced phosphorylation in HER-2/neu-overexpressing cells. Nat Cell Biol *3*, 245-252.

Zhou, J., Wu, Z., Wong, G., Pectasides, E., Nagaraja, A., Stachler, M., Zhang, H., Chen, T., Zhang, H., Liu, J.B., Xu, X., Sicinska, E., Sanchez-Vega, F., Rustgi, A.K., Diehl, J.A., Wong, K.K., and Bass, A.J. (2017). CDK4/6 or MAPK blockade enhances efficacy of EGFR inhibition in oesophageal squamous cell carcinoma. Nat Commun *8*, 13897.

Zhu, C., and Jiang, W. (2005). Cell cycle-dependent translocation of PRC1 on the spindle by Kif4 is essential for midzone formation and cytokinesis. Proc Natl Acad Sci U S A *102*, 343-348.

Zundelevich, A., Dadiani, M., Kahana-Edwin, S., Itay, A., Sella, T., Gadot, M., Cesarkas, K., Farage-Barhom, S., Saar, E.G., Eyal, E., Kol, N., Pavlovski, A., Balint-Lahat, N., Dick-Necula, D., Barshack, I., Kaufman, B., and Gal-Yam, E.N. (2020). ESR1 mutations are

frequent in newly diagnosed metastatic and loco-regional recurrence of endocrine-treated breast cancer and carry worse prognosis. Breast Cancer Res *22*, 16.
Zuo, L., Weger, J., Yang, Q., Goldstein, A.M., Tucker, M.A., Walker, G.J., Hayward, N., and Dracopoli, N.C. (1996). Germline mutations in the p16INK4a binding domain of CDK4 in familial melanoma. Nat Genet *12*, 97-99.
Zwijsen, R.M., Wientjens, E., Klompmaker, R., van der Sman, J., Bernards, R., and Michalides, R.J. (1997). CDK-independent activation of estrogen receptor by cyclin D1. Cell *88*, 405-415.

Appendix

Appendix I - Summary of common peaks in H3K27ac ChIP-seq comparing Vehicle vs PalboT vs PalboR MCF7 cells

KCNMA1	LINC00882	GSE1	GSN	DBN1	SCUBE3	OPA1-AS1	HAS2-AS1	UPK3A
BTG2	CDH11	UCP3	SLC1A2	TRIM71	YTHDF1	DIRC3	ADAMTS9	COL14A1
EDN1	ZBTB7C	MIR4714	TPCN2	PKMYT1	TMEM191C	SMPD3	TSEN15	ANKRD50
ATXN10	LINC00494	SLC30A3	ANKRD30BL	MIR1247	FOXA2	SNRK	LINC01686	JARID2
WDR89	E2F7	MIR4275	BCAR1	MIR5687	SBNO2	TMED10	KLHDC7B	TMEM164
LMNB2	GSK3B	SESTD1	ARRB1	PGAM1P5	C14orf132	LINC01550	TSC22D3	MRPS27
CD160	KIF5C	SLC4A4	CDCA7	ERF	CLSTN2	SP3	PTPRB	ADAP1
HES1	STMN1	RPL38	CD9	GCNT4	FSCB	DHRS4	SIPA1L2	PRELID3A
EGOT	SLC25A24	KAZN	MIR1208	CACYBP	PKIB	PLEKHD1	TANC1	MAP1B
ABR	TRIM24	SUMO1P1	FXYD4	NRCAM	SMG1P2	MAP4K3-DT	TOM1L2	BACH1
ZNF385B	DEPDC1	ADAM2	PIEZO1	ZFHX3	ABCC11	N4BP1	LITAF	ZMYND11
FRS2	FAM83A	PARD6B	DYNLRB2	EGLN3	PBX1	PRKCH	EGFL7	CDH23
MIR4472-2	EXOC3L4	MIR1287	MRPS30	CUX1	LOC283038	SNTB1	S100G	MTSS1
CETN3	ZDHHC7	LINC01512	EGR3	RAB9BP1	NCOA3	MPRIP	ZNF92	CLRN1-AS1
TMPO-AS1	ENTPD6	AFF3	TSPAN5	LINC00578	ASAP1	TMEM61	STEAP4	C16orf95
MIR101-2	PTGER2	MYB	MCL1	STC2	COL23A1	JDP2	ANO1	SERINC1
TOR3A	FAM184B	XRCC2	ZNF213	GPRC5B	NHLH2	GAPDH	FURIN	PMEPA1
LCMT1	DUPD1	LPP	FOXP4	CACNA2D4	AGO2	LINC00673	PARTICL	LINC00443
PA2G4P4	SH3BP2	GPR107	LINC00111	PPP2R5E	SH3BGRL2	ADAM11	SARM1	PVT1
KIAA1324	PACS1	RHOF	GRB10	ALDH3B1	GALNT2	MIR4295	KYNU	PARD3
PTP4A2	LINC00589	SYNGR3	PLCG2	THSD4	C11orf44	AGTR2	SEPTIN9	CYP24A1
KDM4B	TRAK2	SMAD3	CDYL2	ANKRD55	RUNX1T1	CRYBG1	LINC00689	DNAH5
CENPU	MIR1252	LINC02532	PTPRN2	LHX2	EIF4E1B	INSIG1	GLI3	KAT6B
SPRY2	ZHX2	SLC16A7	INPP4B	MIR4799	NOL11	BEAN1	BHLHA15	DPY19L1
KISS1R	MIR4450	SLCO3A1	DNMBP	RASA3	PCDH15	MLXIP	LAMA5	LINC01004
KLF4	TMC5	KIF18B	LRATD2	TRHDE-AS1	TEX36-AS1	BRDTP1	ADPRHL1	RPS6KB1
HRH2	TXNRD1	CHD6	NBPF10	STUM	DMXL1	SOS1	BMPER	SLC39A6
SVIL	SRGAP1	HMCN1	LINC02111	VAV3	PPM1E	DPPA2P3	CCND3	
TGFB2-AS1	SLC6A8	ZMYND8	FOS	DAAM1	BCL11B	SQOR	BATF	
PAWR	KIAA0895	PDXK	OTOS	S100A9	EGFEM1P	CTNND2	VIPR2	
FAM9B	MTA1	IFFO2	TP53INP1	AHDC1	NR2F2	KLHDC4	SEMA6A	
TMEM189	AGBL1-AS1	FBRSL1	NTN1	RPA4	FGD2	MANBAL	ADGRA2	
NTN4	DDHD1	DHRS13	TFAP2C	SPECC1L	COL9A3	AADAC	DACH2	
KIAA0319L	SH2D4B	ESRRG	VPS28	ARL4A	PRKCZ	POU1F1	KIFC3	
C6orf141	PIK3R1	CDR2	CX3CL1	SNORA11B	IL20	DICER1	CLEC3A	
EHD2	PTPRJ	ZFP36L2	SLC20A1	LRFN5	GATA3	TRPV6	RBCK1	
SLC25A48-AS1	NEURL1B	CD180	SIL1	PIK3R5	FTO	GREB1	TLE1	
LOC653513	PREX1	ANKS1B	MSI2	TENM4	DMXL2	LINC01973	CALML3	
SULF2	IGFBP3	AKAP10	IRF1-AS1	SPIRE2	SFI1	TNFSF10	DENND3	

Appendix II - Summary of common peaks in H3K27ac ChIP-seq comparing Vehicle vs PalboT vs PalboR in MCF7 LTED Y537C cells

CYP11A1

BIRC5

AURKB

SPIDR

MCM10

STMN1

MIR3616

UBE2H

E2F2

PREX1

GINS2

SPC24

E2F8

LINC01973

KIF18B

PCAT6

LINGO1

ARHGAP23

MIR23B

MMP17

HJURP

PVT1

Appendix III – GSEA pathway analysis in MCF7 cells

Pathways UP

NAME	SIZE	ES	NES	FDR q-val	RANK AT MAX
HALLMARK_INTERFERON_ALPHA_RESPONSE	79	-0.72	-2.82	0	2163
HALLMARK_INTERFERON_GAMMA_RESPONSE	136	-0.62	-2.64	0	2163
HALLMARK_TNFA_SIGNALING_VIA_NFKB	140	-0.57	-2.41	0	2917
HALLMARK_INFLAMMATORY_RESPONSE	81	-0.5	-1.98	0	3197
HALLMARK_MYOGENESIS	103	-0.48	-1.98	0	3013
HALLMARK_P53_PATHWAY	167	-0.44	-1.95	0	2214
HALLMARK_HYPOXIA	147	-0.44	-1.92	0.001	3039
HALLMARK_APOPTOSIS	119	-0.44	-1.88	0.001	1429
HALLMARK_IL6_JAK_STAT3_SIGNALING	42	-0.51	-1.76	0.003	2064
HALLMARK_CHOLESTEROL_HOMEOSTASIS	65	-0.46	-1.75	0.003	1978
HALLMARK_ANGIOGENESIS	17	-0.62	-1.74	0.003	2703
HALLMARK_ESTROGEN_RESPONSE_EARLY	190	-0.37	-1.64	0.01	2831
HALLMARK_COAGULATION	55	-0.43	-1.58	0.016	2513
HALLMARK_HEME_METABOLISM	149	-0.36	-1.57	0.018	3489
HALLMARK_UV_RESPONSE_DN	113	-0.37	-1.55	0.021	3461
HALLMARK_COMPLEMENT	112	-0.37	-1.55	0.02	3011
HALLMARK_ALLOGRAFT_REJECTION	79	-0.38	-1.52	0.026	2377
HALLMARK_EPITHELIAL_MESENCHYMAL_TRANSITION	101	-0.35	-1.48	0.034	2512
HALLMARK_BILE_ACID_METABOLISM	63	-0.37	-1.4	0.066	3281
HALLMARK_ADIPOGENESIS	161	-0.31	-1.39	0.067	2646
HALLMARK_KRAS_SIGNALING_DN	70	-0.35	-1.35	0.087	2273
HALLMARK_NOTCH_SIGNALING	27	-0.42	-1.34	0.094	1579
HALLMARK_IL2_STAT5_SIGNALING	121	-0.31	-1.3	0.12	3085
HALLMARK_GLYCOLYSIS	167	-0.29	-1.3	0.119	3128
HALLMARK_PROTEIN_SECRETION	91	-0.32	-1.28	0.131	3271
HALLMARK_HEDGEHOG_SIGNALING	23	-0.42	-1.28	0.127	2383
HALLMARK_REACTIVE_OXYGEN_SPECIES_PATHWAY	45	-0.36	-1.27	0.124	2829
HALLMARK_APICAL_JUNCTION	124	-0.3	-1.26	0.132	2241
HALLMARK_PEROXISOME	83	-0.31	-1.23	0.16	2659
HALLMARK_ANDROGEN_RESPONSE	85	-0.3	-1.19	0.204	2933
HALLMARK_APICAL_SURFACE	25	-0.37	-1.15	0.258	2220
HALLMARK_XENOBIOTIC_METABOLISM	122	-0.27	-1.14	0.268	3048
HALLMARK_FATTY_ACID_METABOLISM	122	-0.27	-1.14	0.26	3233
HALLMARK_UV_RESPONSE_UP	126	-0.26	-1.12	0.282	1878
HALLMARK_WNT_BETA_CATENIN_SIGNALING	32	-0.31	-1.01	0.489	1899
HALLMARK_PI3K_AKT_MTOR_SIGNALING	87	-0.24	-1	0.514	1769
HALLMARK_KRAS_SIGNALING_UP	82	-0.25	-0.99	0.514	3032
HALLMARK_ESTROGEN_RESPONSE_LATE	177	-0.22	-0.98	0.531	3222
HALLMARK_TGF_BETA_SIGNALING	48	-0.25	-0.9	0.693	3213
HALLMARK_UNFOLDED_PROTEIN_RESPONSE	109	-0.19	-0.8	0.875	3093

Pathway DOWN

NAME	SIZE	ES	NES	FDR q-val	RANK AT MAX
HALLMARK_E2F_TARGETS	198	0.78	3.71	0	1571
HALLMARK_G2M_CHECKPOINT	194	0.7	3.25	0	1905
HALLMARK_MYC_TARGETS_V1	200	0.61	2.88	0	3416
HALLMARK_MYC_TARGETS_V2	56	0.59	2.23	0	3221
HALLMARK_MITOTIC_SPINDLE	189	0.47	2.19	0	1984
HALLMARK_SPERMATOGENESIS	63	0.53	2.08	0	2797
HALLMARK_DNA_REPAIR	135	0.41	1.82	0.001	3029
HALLMARK_MTORC1_SIGNALING	186	0.22	1.01	0.486	2523
HALLMARK_OXIDATIVE_PHOSPHORYLATION	191	0.16	0.76	0.932	4061

Appendix IV –– Heatmap cluster gene list in MCF7 cells

Cluster 1

			TvsC		RvsC		RvsT	
	Ensembl	basemean	log2FoldChange	padj	log2FoldChange	padj	log2FoldChange	padj
IFRD1	ENSG00000006652	105.8036298	-1.351320849	0.001738513	0.69708495	0.252282384	2.048405799	6.43103E-08
CD9	ENSG00000010278	345.8862354	0.211150317	0.952918027	0.660173294	0.098679931	0.449022977	0.498457361
NCAPD2	ENSG00000010292	54.43874035	-1.98860024	0.000134593	-0.093737944	0.986380133	1.894862297	0.000648475
GALC	ENSG00000054983	22.2251766	-0.500215668	0.97844888	1.337828311	NA	1.838043979	0.05460643
VMP1	ENSG00000062716	576.2344538	0.253959823	0.825734111	0.666623472	0.014497694	0.412663649	0.349091852
IPO5	ENSG00000065150	89.37930119	-0.497821404	0.749914459	0.454211852	0.700638865	0.952033256	0.099950545
SP100	ENSG00000067066	42.64256161	1.127337562	0.195255838	1.516845117	0.023024487	0.389507555	0.915845123
IFI35	ENSG00000068079	53.14527178	0.654177621	0.702489352	1.622183062	0.002205214	0.968005441	0.209070547
GAL	ENSG00000069482	172.5715625	-1.330309501	5.64451E-05	0.449843432	0.545602394	1.780152933	1.19143E-08
TFRC	ENSG00000072274	238.2150355	-0.821225591	0.035804856	0.389689963	0.65002365	1.210915554	0.000227999
DNAJA1	ENSG00000086061	644.6068837	-0.374868721	0.430757396	0.28378952	0.652672378	0.658658241	0.015743199
FTL	ENSG00000087086	1542.914729	0.188466528	0.917369413	0.515602911	0.063938786	0.327136383	0.498457361
OAS1	ENSG00000089127	65.53618348	0.544172525	0.828190679	1.500196312	0.00664072	0.956023787	0.229503776
BAMBI	ENSG00000095739	341.4346287	0.339427718	0.720809861	1.120693769	1.36617E-05	0.781266051	0.010774084
MKNK2	ENSG00000099875	61.86166869	0.872500443	0.275282852	1.15019262	0.061670266	0.277692177	0.947389359
LGALS1	ENSG00000100097	268.5141444	0.2849656	0.897683406	1.03990892	0.000796295	0.75494332	0.04775255
XBP1	ENSG00000100219	1738.408421	0.458794203	0.149425515	0.527445415	0.064732106	0.068651213	0.992506822
HMOX1	ENSG00000100292	38.90935625	0.083857372	0.999340018	2.228705226	0.000176173	2.144847854	0.000530477
PYGL	ENSG00000100504	38.31250924	0.046278909	0.999340018	1.648494899	0.019611973	1.60221599	0.032251833
HIF1A	ENSG00000100644	65.18277568	0.388912077	0.935878113	1.196967656	0.028905574	0.808055579	0.320084026
ZMYND8	ENSG00000101040	192.6038445	0.21628655	0.953528147	0.745135242	0.051127573	0.528848692	0.349091852
BMP7	ENSG00000101144	111.1022229	-0.294326356	0.941080483	1.080766577	0.008481208	1.375092933	0.000362849
EEF1A2	ENSG00000101210	944.9454357	0.529061314	0.066204669	0.926281726	1.3732E-05	0.397220412	0.319256493
SAMHD1	ENSG00000101347	61.33317698	0.209603881	0.989771744	1.51815275	0.002266938	1.308548869	0.017602327
COTL1	ENSG00000103187	135.2978182	-0.575977082	0.448432651	0.807721917	0.078819968	1.383699	0.000145008
GABPB1	ENSG00000104064	98.10950121	-0.704582858	0.35026354	0.677903582	0.313832923	1.38248644	0.001272331
PYCR3	ENSG00000104524	85.5282037	-0.346756179	0.929375612	0.939660483	0.078525517	0.592904304	0.526385955
ZC3HAV1	ENSG00000105939	105.5973649	0.508537271	0.68607043	1.039141844	0.023024487	0.530604572	0.596867623
DDX58	ENSG00000107201	101.6818988	1.16517078	0.012115703	1.741819798	6.68743E-06	0.576649018	0.521385915
RAD51C	ENSG00000108384	427.8227143	-0.816509681	0.00381655	0.145460866	0.93306971	0.961970547	0.000447914
TUBD1	ENSG00000108423	164.5302366	-0.693764998	0.142670111	0.407196955	0.631300778	1.100961952	0.001719038
TRIM16L	ENSG00000108448	60.28453501	0.138154198	0.992626707	1.300518776	0.016231089	1.162364578	0.05460643
LGALS3BP	ENSG00000108679	780.2579388	0.514474008	0.172045876	1.22005287	2.26112E-07	0.705578862	0.017097606
CTSC	ENSG00000109861	41.08906185	0.565869531	0.930321695	1.757990907	0.022938696	1.192121376	0.279647573
MDK	ENSG00000110492	177.1789267	-0.201544738	0.986113215	0.691169297	0.248331044	0.892714035	0.075828234
OAS3	ENSG00000111331	195.3772703	0.476368449	0.556228212	1.361400485	9.10842E-06	0.885032036	0.019190999
OAS2	ENSG00000111335	84.73254579	0.85802589	0.19367288	1.919747714	1.34867E-06	1.061721824	0.031960549
TPI1	ENSG00000111669	971.8117714	-0.280610193	0.703441491	0.250480539	0.691125631	0.531090733	0.074014944
STC2	ENSG00000113739	80.25415113	0.217574156	0.986113215	1.015715386	0.051742	0.798141229	0.240994551
IFIH1	ENSG00000115267	54.51371793	0.852051969	0.42115595	2.009148136	4.25712E-05	1.157096167	0.073080306
IFIT3	ENSG00000119917	126.6661971	0.479653309	0.737744334	1.762080028	1.34867E-06	1.282426719	0.001375345
IFIT2	ENSG00000119922	77.55377941	0.590729304	0.727641025	2.072639893	2.24983E-06	1.481910589	0.002211885
MASTL	ENSG00000120539	34.40541708	-2.080916387	0.006159584	0.144985795	0.983846687	2.225902182	0.003533997
HSPH1	ENSG00000120694	394.2775557	-0.679324755	0.026062161	-0.065687482	0.977955173	0.613637273	0.078586191
CLU	ENSG00000120885	118.9456841	0.338902463	0.911808323	1.775662596	1.89835E-07	1.436760133	7.32837E-05
OPTN	ENSG00000123240	42.10024863	1.241791127	0.106748958	1.53341588	0.019352525	0.291624754	0.957718488
NMI	ENSG00000123609	55.68328561	1.018982182	0.164122558	1.458610657	0.008356663	0.439628475	0.84769092
ACSL3	ENSG00000123983	82.49588968	0.534272335	0.70931933	0.968393867	0.086519127	0.434121532	0.805891976
TM9SF2	ENSG00000125304	144.8688857	0.489703277	0.66242894	0.902925536	0.050850224	0.413222259	0.75117487
RBCK1	ENSG00000125826	125.9770911	0.298974168	0.939870406	0.880394865	0.061551482	0.581420697	0.439527921
SNRPB2	ENSG00000125870	210.1351273	-0.424604188	0.591613065	0.367846148	0.65002365	0.792450336	0.032574324
IFI6	ENSG00000126709	2767.773261	0.493189768	0.447945084	1.641221568	8.72298E-09	1.1480318	0.000300523
EMG1	ENSG00000126749	104.9533001	-0.582278222	0.553772549	0.703724417	0.254423258	1.286002639	0.002654752
VGF	ENSG00000128564	76.03182876	-0.125742308	0.992626707	0.943769418	0.093628568	1.069511726	0.04775255
SAT1	ENSG00000130066	37.03950419	0.973023081	0.450770051	1.723826954	0.012616434	0.750803873	0.653256529
KLHDC7B	ENSG00000130487	26.8595388	-0.199648443	0.99720327	3.628583891	1.34867E-06	3.828232334	1.84328E-06
GDF15	ENSG00000130513	44.19984336	0.943582982	0.702489352	3.501794011	4.04555E-08	2.55821103	6.51999E-05
HELZ2	ENSG00000130589	63.99345052	0.554723492	0.734929257	1.057628656	0.07729112	0.502905164	0.75398083
CTSL	ENSG00000135047	78.71036029	0.305385196	0.953528147	1.11127565	0.027576661	0.805890453	0.245450971
OASL	ENSG00000135114	70.55520157	0.201530986	0.989771744	1.888013249	6.68743E-06	1.686482263	0.000148778
LAMC1	ENSG00000135862	34.46720782	0.500913376	0.945884939	1.791214166	0.014921233	1.29030079	0.177130852
CTSV	ENSG00000136943	12.78983969	-2.604118795	0.076007002	0.025682142	NA	2.629800936	0.088609338
DSCC1	ENSG00000136982	74.16078568	-0.952617228	0.114386641	0.060000597	0.987496655	1.012617825	0.095588984
DDX60	ENSG00000137628	41.57419528	0.066250823	0.999340018	1.596362931	0.019668557	1.530112107	0.036401666
IFI44L	ENSG00000137959	126.2175529	0.603138731	0.55681213	2.128727396	8.72298E-09	1.525588665	0.000126849
IFI44	ENSG00000137965	155.6890519	-0.07174829	0.99720327	0.963935606	0.013313206	1.035683896	0.007129659
HERC6	ENSG00000138642	34.9217166	0.723733446	0.753662107	1.448003557	0.061670266	0.724270112	0.68529071
PRPSAP2	ENSG00000141127	53.08077413	0.471492021	0.895184676	1.118716302	0.088628749	0.647224281	0.623504618
SECTM1	ENSG00000141574	49.32769813	-0.223074236	0.989771744	0.968293945	0.218472764	1.191368181	0.095401363
MAL2	ENSG00000147676	231.2863342	-0.336031453	0.77152126	0.546258035	0.211044796	0.882289489	0.006141073
STOM	ENSG00000148175	147.2770235	0.249855924	0.951762147	0.755374666	0.098872	0.505518743	0.516155569
FADS1	ENSG00000149485	51.17584379	-1.045802368	0.231411985	0.242485839	0.948178593	1.288288207	0.086357243
CHEK1	ENSG00000149554	23.23985804	-2.227623318	0.02366383	0.255380905	NA	2.483004223	0.008899578
AKR1C2	ENSG00000151632	22.19740501	0.813487765	0.9493549	4.260006403	NA	3.446518638	5.57036E-05
SLC26A2	ENSG00000155850	65.01145786	0.598786982	0.841478688	1.532215928	0.01988457	0.933428946	0.385394803
UBE2L6	ENSG00000156587	143.1780845	0.590611142	0.525765088	1.977280758	2.36923E-08	1.386669616	0.000330979
S100A9	ENSG00000163220	28.26320229	0.357955039	0.989771744	3.102081018	9.10842E-06	2.744125979	0.000166348
S100P	ENSG00000163993	85.32466994	0.914423171	0.321562073	2.267196197	2.24983E-06	1.352773026	0.01982989
MOCS2	ENSG00000164172	191.8029071	-0.29535719	0.896667232	0.436338035	0.544950817	0.731695226	0.086364896
AQP3	ENSG00000165272	32.2742396	-0.410928746	0.98282019	2.090346997	0.002645141	1.679418252	0.032574324
IFI27	ENSG00000165949	2659.990571	0.615883113	0.103624027	1.175706984	8.6289E-06	0.559823871	0.197404938
B2M	ENSG00000166710	1189.552409	0.21691721	0.907931449	1.069538867	1.88699E-06	0.852621657	0.00049045
SLC43A2	ENSG00000167703	49.9978384	0.666644219	0.769098362	1.323920072	0.077010156	0.657275853	0.722233428
CLIC3	ENSG00000169583	63.40334494	1.449462821	0.012436645	1.675856531	0.002051511	0.22639371	0.965537867
ISG20	ENSG00000172183	35.38179821	1.138302384	0.340764719	2.304396547	0.000348251	1.166094162	0.221767239
PARP14	ENSG00000173193	112.2552271	0.753922342	0.263870043	1.159622462	0.012913898	0.40570012	0.817182209
RNF213	ENSG00000173821	60.25833613	0.395360002	0.945884939	1.543171668	0.006395422	1.147811666	0.098066651
UCP2	ENSG00000175567	213.1661131	0.735024907	0.055363899	1.01448662	0.001401852	0.279461713	0.84769092
PARP10	ENSG00000178685	106.1267826	0.806206253	0.134532287	1.289810755	0.000904222	0.483604502	0.635640148
RPP25	ENSG00000178718	104.552669	-0.62137632	0.411086935	0.550157119	0.478192923	1.171533439	0.005025684
GRINA	ENSG00000178719	251.0499871	0.514969361	0.353419116	0.893904867	0.00764096	0.378935506	0.672252436
SEPHS2	ENSG00000179918	122.2523693	-0.283444057	0.950970583	0.648217125	0.313832923	0.931661182	0.06189036
PHLDA2	ENSG00000181649	95.98065614	-0.658500116	0.362384398	0.233816382	0.914734419	0.892316498	0.097478827
UBE2E2	ENSG00000182247	27.11164969	0.970901733	0.720809861	1.877914632	0.051127573	0.907012899	0.686547949
TSKU	ENSG00000182704	328.4994114	0.694771074	0.046322867	0.954024199	0.001075354	0.259253124	0.84769092
CADM1	ENSG00000182985	53.70219615	0.932548804	0.258855019	1.387287849	0.016266822	0.454739045	0.844946682
GPC6	ENSG00000183098	15.92913003	1.497691758	0.918984753	5.660349667	NA	4.162657909	0.000330979
JAG2	ENSG00000184916	14.03400823	-0.841786215	0.940773538	2.164497227	NA	3.006283442	0.009450993
RPS27L	ENSG00000185088	330.0351876	0.374236379	0.64615677	0.791675172	0.011782564	0.417438794	0.498457361
IFIT1	ENSG00000185745	360.2821233	1.066770807	3.81068E-05	1.636469835	7.05825E-12	0.569699027	0.127128788
ISG15	ENSG00000187608	1528.222127	0.451785714	0.196863642	1.050764302	1.20816E-06	0.598978589	0.032574324
PLSCR1	ENSG00000188313	135.2833833	-0.014537693	0.999340018	1.000279947	0.009659388	1.01481764	0.009797932
SPATS2L	ENSG00000196141	260.1795299	0.582603303	0.172045876	0.857739675	0.007414562	0.275136373	0.837600729
CD55	ENSG00000196352	57.43441096	0.367081713	0.952918027	1.491933418	0.006471376	1.124851704	0.094505823
SPTSSB	ENSG00000196542	1210.437386	0.698127162	0.002543748	1.152684687	1.18852E-08	0.454557525	0.171726153
TXNRD1	ENSG00000198431	243.6589899	0.171720094	0.986113215	0.79658623	0.029272745	0.624866136	0.184731497
NRARP	ENSG00000198435	28.11294728	-1.767149533	0.045479272	0.215424071	0.969678908	1.982573604	0.019895413
PSMB8	ENSG00000204264	12.78367128	1.506933033	0.811521007	4.217113005	NA	2.710179972	0.033431802
HSPA1A	ENSG00000204389	268.1375809	-0.558607813	0.24659217	0.505916401	0.313832923	1.064524214	0.00051976
HLA-C	ENSG00000204525	89.25466471	0.680411152	0.468582503	1.810822178	7.08366E-06	1.130411026	0.021533212
HLA-E	ENSG00000204592	127.9235681	0.645373703	0.288009624	1.21699587	0.000918285	0.571622168	0.408315298
SAMD9	ENSG00000205413	33.20708839	1.410590881	0.148994209	2.382168955	0.000348251	0.971578074	0.424934094

HLA-A	ENSG00000206503	149.0248602	0.212166274	0.98282019	1.446398836	2.66034E-05	1.234232562	0.000964328
TRIM16	ENSG00000221926	78.83370189	0.440090009	0.855530499	1.247091655	0.00806514	0.807001646	0.231271349
TAPBP	ENSG00000231925	143.3311231	0.536897929	0.55681213	1.045939089	0.012986962	0.50904116	0.584097458
CYP2T1P	ENSG00000233622	60.21397434	1.540288715	0.010962054	2.928573183	5.93406E-10	1.388284468	0.006901246
HLA-B	ENSG00000234745	64.43219945	0.176977389	0.992117206	1.948690365	2.47136E-05	1.771712975	0.000321111
PSMB9	ENSG00000240065	24.0082719	-0.028960018	0.999340018	1.70442444	NA	1.733384458	0.084694635
NEAT1	ENSG00000245532	56.89490203	0.463113198	0.930325845	1.670788304	0.004112376	1.207675106	0.096850373
H2AJ	ENSG00000246705	328.7923068	-0.477718227	0.348881689	0.373886463	0.572470417	0.85160469	0.006060412
MALAT1	ENSG00000251562	1652.846962	0.45501659	0.18920477	0.804406049	0.000605711	0.349389459	0.491285408
CCL5	ENSG00000271503	50.70433162	0.291278293	0.986113215	1.552524572	0.015267932	1.261246279	0.09720245
CD24	ENSG00000272398	463.7265748	0.602173809	0.071092997	0.928485907	0.000342988	0.326312097	0.669511835

Cluster 2

			TvsC		RvsC		RvsT	
	Ensembl	basemean	log2FoldChange	padj	log2FoldChange	padj	log2FoldChange	padj
SLC25A5	ENSG00000005022	77.18087067	-0.596294873	0.090512355	-0.859021304	0.002205214	-0.262726431	0.833849641
DBF4	ENSG00000006634	259.1534545	-1.148077954	0.00138635	-0.634366362	0.248331044	0.513711592	0.562681095
E2F2	ENSG00000007968	3.76711946	-2.525569631	0.090512355	-0.276695543	NA	2.248874088	0.21799639
ANLN	ENSG00000011426	2.315832037	-2.530286944	0.001248319	-0.618218449	0.794459773	1.912068495	0.06189036
BRCA1	ENSG00000012048	54.79466646	-1.922912641	0.001700199	-0.669681733	0.652672378	1.253230908	0.180215813
TACC3	ENSG00000013810	30.27916175	-2.185242153	1.12014E-05	-0.920529324	0.216880764	1.264712829	0.094862209
DEPDC1	ENSG00000024526	21.24436328	-2.665585079	0.011784299	-0.377716561	NA	2.287868518	0.074430196
HMGB3	ENSG00000029993	4.409755399	-0.959369294	0.013029403	-0.492031952	0.507625213	0.467337342	0.635313248
DEPDC1B	ENSG00000035499	7.412611363	-1.906051396	0.024675025	-1.084969951	NA	0.821081445	0.784942268
SPDL1	ENSG00000040275	58.89872506	-1.237725763	0.068569599	-0.501082513	0.764980933	0.73664325	0.613254014
RFC2	ENSG00000049541	14.09151405	-1.312377428	0.025160049	-0.768162274	0.423446216	0.544215154	0.804339015
MCM10	ENSG00000065328	17.92846839	-3.020307521	1.06485E-06	-0.828344065	0.485938656	2.191963456	0.003551131
ASPM	ENSG00000066279	66.29274027	-2.026128067	7.6669E-05	-1.135206757	0.088628749	0.89092131	0.434234325
PRR11	ENSG00000068489	3.254728594	-1.924210762	1.00525E-05	-0.826826774	0.226640816	1.097383988	0.095401363
NUCKS1	ENSG00000069275	3.743054416	-0.820389282	0.002081132	-0.837169301	0.002060788	-0.016780018	0.997903086
TRIP13	ENSG00000071539	2.715404077	-1.11025006	0.009551231	-0.694535399	0.257047775	0.415714662	0.810422405
SMC1A	ENSG00000072501	130.5448178	-0.999754857	0.043330047	-0.157347929	0.958776926	0.842406928	0.177130852
HMMR	ENSG00000072571	108.0242631	-3.354017916	0.001476119	-0.677872081	0.89612785	2.676145835	0.034874708
TIPIN	ENSG00000075131	16.86775218	-1.435065888	0.072049902	-0.392540563	0.905162116	1.042525325	0.404706707
GTSE1	ENSG00000075218	28.08521072	-3.177886216	0.003342105	-0.615510833	NA	2.562375383	0.060656479
MCM6	ENSG00000076003	27.82466304	-1.458089331	0.00034824	-0.222772887	0.92605483	1.235316445	0.008322784
UNG	ENSG00000076248	6.288439925	-0.949064556	0.042216696	-0.670531424	0.293497847	0.278533132	0.92219177
SPAG5	ENSG00000076382	6.482273483	-3.055510227	0.002081132	-0.532611491	NA	2.522898735	0.036818726
UBE2T	ENSG00000077152	21.02035704	-1.451746801	1.30231E-07	-0.909840498	0.005899366	0.541906303	0.353347052
HSP90AA1	ENSG00000080824	59.87865657	-0.923006009	4.90474E-06	-0.102374402	0.947242354	0.820631608	0.000179689
RBL1	ENSG00000080839	16.9733761	-2.631539807	0.030475378	-0.785806312	NA	1.845733495	0.344456247
NDC80	ENSG00000080986	10.27187105	-3.496996807	0.000162912	-1.263958596	NA	2.233038211	0.098066651
AURKA	ENSG00000087586	3.341349915	-2.343450304	8.96865E-12	-0.539639062	0.480876592	1.803811242	3.07774E-06
KHSRP	ENSG00000088247	8.27465958	-0.498930762	0.448432651	-0.829857321	0.03427865	-0.33092656	0.823112842
TPX2	ENSG00000088325	16.57200384	-1.941018667	2.35436E-08	-0.565844146	0.432926363	1.375174521	0.000938822
BIRC5	ENSG00000089685	112.042042	-2.791712763	1.14557E-20	-0.925954238	0.010373488	1.865758525	2.7285E-08
NUDC	ENSG00000090273	12.93977688	-0.737973892	0.036057912	-0.360102835	0.649873315	0.377871057	0.672252436
KIF4A	ENSG00000090889	132.6774385	-3.15410103	0.001067931	-0.374262282	NA	2.779838748	0.010712317
CDV3	ENSG00000091527	7.602718709	-0.440810265	0.27593834	-0.870405183	0.00055652	-0.429594918	0.356008742
ORC6	ENSG00000091651	222.1557605	-1.765190538	0.001815137	-0.095277367	0.986380133	1.669913171	0.006938207
WDR76	ENSG00000092470	27.84116078	-3.422827734	0.003496727	-1.140970322	NA	2.281857412	0.209070547
PHGDH	ENSG00000092621	77.84605161	-1.003202761	0.041164636	-0.205863478	0.941190519	0.797339283	0.229503776
CLSPN	ENSG00000092853	43.1438532	-3.356184559	0.000754038	-1.348779818	NA	2.007404741	0.225475593
CDC45	ENSG00000093009	2.72729079	-2.481199281	0.000150267	-0.771344517	0.605663858	1.709854765	0.054357942
HNRNPH3	ENSG00000096746	3.517822804	-0.928335686	0.052400063	-0.663335244	0.312215728	0.265000443	0.927845194
CDC7	ENSG00000097046	21.81721793	-2.425307974	0.037917044	-0.568082541	NA	1.857225433	0.264323054
RANBP1	ENSG00000099901	2.291078857	-1.11308977	6.49416E-06	-0.670528302	0.033541129	0.442561468	0.404942048
CENPM	ENSG00000100162	381.437543	-2.007187834	0.001143848	-1.272820987	0.101965993	0.734366847	0.742203415
MCM5	ENSG00000100297	2.480780845	-1.158616836	0.032211018	-0.710794593	0.410149704	0.447822243	0.843045678
POLE2	ENSG00000100479	46.30156674	-2.183765088	0.045479272	-1.442465005	NA	0.741300083	0.896548909
CDKN3	ENSG00000100526	15.44032731	-2.810693657	3.54083E-13	-1.199713648	0.006471376	1.610980009	0.000964328
EIF5	ENSG00000100664	32.99619309	-0.748422669	0.008913685	-0.347555717	0.57577753	0.400866952	0.485952311
MTHFD1	ENSG00000100714	44.40778821	-0.874447881	0.090512355	-0.750708634	0.204829934	0.123739247	0.992751194
PNN	ENSG00000100941	29.94378674	-0.732831208	0.073611442	-0.254343398	0.86396071	0.47848781	0.519809089
GINS1	ENSG00000101003	16.18811793	-1.529328095	0.025357233	-0.479153685	0.831556658	1.05017441	0.337295413
MYBL2	ENSG00000101057	52.10016232	-2.737664421	1.83219E-17	-1.157903697	0.001689592	1.579760724	5.67042E-05
FAM83D	ENSG00000101447	41.35690756	-2.027097152	0.001092489	-0.751679453	0.57577753	1.275417699	0.19019895
PLP2	ENSG00000102007	628.5012134	-0.827796454	0.042466013	-0.737918371	0.103487185	0.089878083	0.994631661
HTATSF1	ENSG00000102241	21.36529725	-0.432659777	0.653935324	-0.746876957	0.094327176	-0.31421718	0.84769092
CCP110	ENSG00000103540	366.0419023	-1.793563534	0.090512355	-1.642405573	0.152114163	0.151157961	0.997903086
MCM4	ENSG00000104738	24.99048056	-1.172224646	0.002196382	-0.418906416	0.677996798	0.753318231	0.205506934
H2AZ2	ENSG00000105968	22.99968649	-0.742399377	0.008313778	-0.603666163	0.068350516	0.138733214	0.959127064
EZH2	ENSG00000106462	59.70293107	-1.227721421	0.00452856	-0.502470226	0.629379542	0.725251195	0.348946148
POLD2	ENSG00000106628	7.163256162	-0.242782915	0.936544549	-0.79429812	0.027879308	-0.551515206	0.312987522
DKK1	ENSG00000107984	117.6898308	-0.861408857	0.08374492	-1.278738272	0.001951059	-0.417329414	0.810587304
GLRX3	ENSG00000108010	10.08687431	-0.453591541	0.644420391	-0.942978131	0.01988457	-0.48938659	0.599678646
SMC3	ENSG00000108055	3.758230488	-0.895847454	0.038198501	-1.495429547	2.85199E-05	-0.599582093	0.460645451
UBE2S	ENSG00000108106	2.706802233	-1.680688135	1.17292E-08	-0.644322842	0.166702886	1.036365294	0.005788766
KPNB1	ENSG00000108424	32.37827978	-0.76179605	0.045479272	-0.48978417	0.416573729	0.27201188	0.871095948
NMU	ENSG00000109255	30.87047985	-3.92826376	0.016891518	-2.125975684	NA	1.802288076	NA
NCAPG	ENSG00000109805	68.69398944	-4.251135442	0.002449867	-1.393450686	NA	2.857684756	0.178239055
CCDC34	ENSG00000109881	15.66693833	-0.980785506	0.090409029	-0.403379085	0.789698588	0.577406421	0.656724509
PTGES3	ENSG00000110958	51.1567067	-0.620414749	0.021480192	-0.210589556	0.811362211	0.409825193	0.336240276
RAD51AP1	ENSG00000111247	68.06518957	-3.720114709	0.006682801	-0.868830627	NA	2.851284082	0.118670678
RFC5	ENSG00000111445	70.44742314	-1.654617612	0.074537275	-0.596388668	NA	1.058228943	0.562128494
NUP107	ENSG00000111581	87.10668028	-1.138319049	0.049604674	-0.548910587	0.671563706	0.589408462	0.690573073
TIMELESS	ENSG00000111602	50.5181958	-1.94004375	8.27449E-05	-0.770122951	0.395573504	1.169920799	0.112930103
CDCA3	ENSG00000111665	21.14885872	-3.871532625	1.95406E-08	-0.613798553	0.688756436	3.257734072	2.37567E-05
FBXO5	ENSG00000112029	9.362708505	-2.124330097	0.0296937	-0.748844792	NA	1.375485305	0.425198222
SRSF3	ENSG00000112081	14.58146901	-0.551920298	0.082701954	-0.42746751	0.290238214	0.124452788	0.964148638
MCM3	ENSG00000112118	12.29366406	-1.237750397	0.016585587	-0.697742303	0.427157724	0.540008094	0.737422944
GMNN	ENSG00000112312	18.33848987	-2.434688486	6.13101E-10	-0.787476567	0.18747223	1.647211919	0.00051993
TTK	ENSG00000112742	22.0183491	-1.64641321	0.080173429	-0.546321312	NA	1.100091898	0.521396353
LMNB1	ENSG00000113368	240.7072095	-1.977469243	2.53344E-05	-0.858359794	0.244685879	1.119109449	0.127104808
SMC4	ENSG00000113810	2.126616733	-1.319566565	0.000107385	-0.722084208	0.134014304	0.597482357	0.401142819
ECT2	ENSG00000114346	46.18696624	-1.021626714	0.027045156	-0.249299524	0.909205766	0.77232719	0.232124185
CENPA	ENSG00000115163	87.48645135	-2.621996609	8.11008E-06	-0.636721841	0.673231519	1.985274768	0.004964665
ODC1	ENSG00000115758	4.81836186	-0.591243121	0.127329429	-0.628777661	0.093127588	-0.03753454	0.997903086
SRSF7	ENSG00000115875	10.27684904	-0.979088397	0.00057518	-0.414228267	0.487396724	0.564860131	0.220206399
CACYBP	ENSG00000116161	21.03997191	-0.875489082	0.000567654	-0.131526529	0.941190519	0.743962553	0.009693363
SFPQ	ENSG00000116560	3.848239974	-0.627134801	0.034535976	-0.337454767	0.565583363	0.289680033	0.736661213
CDC20	ENSG00000117399	14.77178523	-2.006575572	2.43369E-09	-0.747872398	0.136166338	1.258703174	0.002887152
STMN1	ENSG00000117632	54.40263554	-2.203270072	1.4298E-14	-0.876901225	0.017563831	1.326368847	0.000127144
NEK2	ENSG00000117650	10.28504923	-2.108842172	0.082701954	-0.47122868	NA	1.637613492	0.35164367
CENPF	ENSG00000117724	65.21731104	-2.612200452	4.39887E-08	-0.860887549	0.248331044	1.751312903	0.003250765
KIF14	ENSG00000118193	205.7027692	-3.155159902	3.42447E-06	-0.932758539	0.416573729	2.222401363	0.009173217
CASP8AP2	ENSG00000118412	9.644685824	-1.341840693	0.087407694	-0.427578695	0.8832463	0.914261998	0.503440281
CTNNAL1	ENSG00000119326	99.53475459	-1.837692403	0.085020767	-0.890845717	NA	0.946846687	0.757541197
WDR34	ENSG00000119333	19.02336342	-1.078942064	0.012720537	-0.727481504	0.215823079	0.35146056	0.866236253
PHF19	ENSG00000119403	6.688151394	-2.487753202	9.3506E-09	-1.366382564	0.005438542	1.121370638	0.129310484
HELLS	ENSG00000119969	26.57162976	-2.206927561	0.001659497	-1.322336785	0.152114163	0.884590777	0.690380911
CENPL	ENSG00000120334	3.892146708	-2.245168155	0.003704024	-0.861611075	0.615066104	1.383557081	0.290695314
TMPO	ENSG00000120802	32.12010264	-2.009091947	3.62615E-12	-0.950866778	0.00764096	1.05822517	0.005452146
TBX2	ENSG00000121068	21.7698518	-0.46674125	0.801191178	-1.169939261	0.022938696	-0.703198012	0.442738244
NCAPH	ENSG00000121152	51.4235607	-2.370968477	0.001156042	-0.778215041	0.65002365	1.592753436	0.139697038
MND1	ENSG00000121211	138.898441	-2.631567514	0.000256779	-0.653415381	0.733103366	1.978152132	0.030009505
GPSM2	ENSG00000121957	105.8036298	-2.507262051	0.008372847	-0.677520796	NA	1.829741255	0.177267827
CBX3	ENSG00000122565	24.25317781	-0.647322097	0.034535976	-0.508131024	0.175392948	0.139191073	0.958129944
HNRNPA2B1	ENSG00000122566	23.90683228	-0.589489592	0.023256912	-0.34032757	0.458744152	0.249162022	0.763296619
ZWINT	ENSG00000122952	59.93271736	-2.467690531	1.26666E-09	-1.274671083	0.006483478	1.193019448	0.057712845
DDX39A	ENSG00000123136	35.58397681	-1.166162522	0.000433733	-0.995466349	0.006483478	0.170696173	0.965537867

CENPK	ENSG00000123219	7.595957409	-2.659343559	8.94253E-06	-0.695298164	0.628160031	1.964045395	0.007262202
HJURP	ENSG00000123485	105.4905761	-2.81654517	0.002005009	-0.524962397	NA	2.291582774	0.041428745
CKS2	ENSG00000123975	10.46907927	-0.967799473	0.002071348	-0.231218765	0.876147007	0.736580708	0.069815093
H1-3	ENSG00000124575	16.06590748	-3.510462834	2.67666E-07	-1.371501569	0.088507698	2.138961264	0.022081013
DEK	ENSG00000124795	105.9870539	-1.794504691	8.77918E-13	-0.632653172	0.091031819	1.161851519	0.000111045
MT2A	ENSG00000125148	2.086567643	-0.587371862	0.172045876	-1.308020844	2.24983E-06	-0.720648982	0.06189036
DLGAP5	ENSG00000126787	22.33615319	-2.866142314	9.75424E-08	-1.314519657	0.038463636	1.551622656	0.05478983
PKMYT1	ENSG00000127564	138.2168291	-1.988430028	0.066057373	-0.492284338	NA	1.49614569	0.355322584
ECHS1	ENSG00000127884	65.42506598	-0.26983984	0.881153906	-0.977800526	0.001075354	-0.707960685	0.063139488
HAT1	ENSG00000128708	45.95295671	-0.822111391	0.093878438	-0.207499555	0.92605483	0.614611836	0.406842352
KNSTRN	ENSG00000128944	67.70297771	-1.825279161	0.001731635	-0.41748381	0.865840739	1.407795351	0.06030897
DUT	ENSG00000128951	44.63530722	-2.13279916	2.17237E-13	-0.882965251	0.015267932	1.249833909	0.00049045
PIMREG	ENSG00000129195	16.24477999	-3.027952288	0.002081132	-0.896361723	NA	2.131590564	0.129310484
MIS18BP1	ENSG00000129534	37.51423087	-1.127775059	0.024675025	-0.438843737	0.732128362	0.688931322	0.447971314
TOMM40	ENSG00000130204	22.51521027	-0.746763918	0.091092352	-0.471645276	0.525389059	0.275118642	0.890323933
DNMT1	ENSG00000130816	49.8314101	-1.052684106	0.028508574	-0.445456089	0.700638865	0.607228017	0.531378069
GINS2	ENSG00000131153	10.25458451	-2.527198658	1.21007E-10	-1.24396054	0.005899366	1.283238118	0.022136287
TOP2A	ENSG00000131747	12.40673026	-2.966294662	9.74068E-18	-0.958739345	0.034641887	2.007555317	2.42832E-07
SNRPA1	ENSG00000131876	7.81472702	-0.712978176	0.082758765	-0.287031111	0.805180285	0.425947065	0.623367111
RAN	ENSG00000132341	15.20752034	-0.538790599	0.044164875	-0.182024505	0.850268825	0.356766093	0.414939702
H3-3B	ENSG00000132475	6.048264082	-0.551018927	0.03516101	-0.237654999	0.710477151	0.313363928	0.557453657
PCNA	ENSG00000132646	22.44182407	-2.533133897	3.37813E-19	-0.618173789	0.16504809	1.914960108	6.61464E-10
NASP	ENSG00000132780	2.431041702	-1.471967675	1.00525E-05	-0.641119239	0.235644908	0.830848436	0.098066651
RFC3	ENSG00000133119	12.9288349	-1.461013666	0.000738124	-0.976664524	0.075937945	0.484349142	0.782472932
CCNB1	ENSG00000134057	532.6880331	-1.849403679	5.26758E-13	-0.750080869	0.026217765	1.09932281	0.000463532
PSRC1	ENSG00000134222	28.0156919	-2.018469961	1.31066E-05	-0.981266477	0.130334454	1.037203484	0.192995872
TMEM106C	ENSG00000134291	2.379360742	-0.991076781	0.015389183	-0.238045518	0.905162116	0.753031263	0.177130852
LDHA	ENSG00000134333	51.50965878	-0.348587747	0.487457789	-0.548370921	0.063938786	-0.199783174	0.871153193
CDCA8	ENSG00000134690	5.569392849	-2.299022189	0.000225686	-0.760317314	0.590731493	1.538704875	0.075779944
TROAP	ENSG00000135451	2.85555974	-2.559632363	0.001946155	-0.628662711	NA	1.930969653	0.077375645
ESPL1	ENSG00000135476	288.6734378	-1.929285582	0.069054638	-0.07175286	NA	1.857532722	0.112509
DHX9	ENSG00000135829	455.8455501	-0.652254215	0.065625244	-0.272163534	0.761565657	0.38009068	0.613254014
BRIP1	ENSG00000136492	45.50992447	-2.005881687	4.47179E-10	-0.950048397	0.018268918	1.05583329	0.017775707
SMC2	ENSG00000136824	5.326156297	-1.167912363	0.014728146	-0.869654397	0.147706564	0.298257967	0.926472296
ANP32B	ENSG00000136938	1.693086979	-0.580557624	0.069219058	-0.307511657	0.65002365	-0.273045968	0.780241494
HMGA1	ENSG00000137309	53.05763704	-0.804319762	0.023433902	-0.080509906	0.974926632	0.723809856	0.075779944
KIF23	ENSG00000137807	4.312273769	-1.964866901	0.000266212	-0.509090204	0.745692789	1.455776696	0.033421094
KNL1	ENSG00000137812	413.3547336	-2.347179727	0.026062161	-0.901422	NA	1.445757727	0.464738698
KIF11	ENSG00000138160	15.24128531	-2.01370585	0.000284953	-0.766623349	0.485252372	1.247082501	0.142239962
CEP55	ENSG00000138180	22.74949451	-2.843786868	4.33653E-10	-1.146157719	0.042096405	1.697629148	0.003612881
KIF20B	ENSG00000138182	7.809936413	-1.168719856	0.069177223	-0.907387342	0.256284917	0.261332515	0.965537867
BARD1	ENSG00000138376	3.330902737	-1.503553338	0.013168429	-0.674466254	0.614908507	0.829087084	0.516155569
HNRNPD	ENSG00000138668	2.116434985	-0.91556165	0.002081132	-0.492317295	0.313832923	0.423244355	0.551281784
NUP54	ENSG00000138750	46.94586413	-1.253249678	0.056788988	-0.251799349	0.943050285	1.001450329	0.26305915
CENPE	ENSG00000138778	2.679067995	-2.280442944	1.19008E-05	-0.494461864	0.751511968	1.785981081	0.003593318
NEDD1	ENSG00000139350	10.39086634	-1.351355752	0.066204669	-0.790597822	0.546166377	0.56075793	0.845936774
GAS2L3	ENSG00000139354	209.400746	-2.025934156	0.035923668	-1.56291123	NA	0.463022926	0.959127064
FANCI	ENSG00000140525	1385.403734	-1.824805987	0.034535976	-1.131905593	NA	0.692900394	0.850541081
COPS3	ENSG00000141030	1565.737638	-0.877791781	0.055896211	-0.255538811	0.89612785	0.62225297	0.387507314
KIF2C	ENSG00000142945	96.86414675	-3.879872295	0.000376216	-1.237511603	NA	2.642360692	0.084314663
NUF2	ENSG00000143228	29.53345557	-2.535665464	0.000468364	-1.221849497	0.234284931	1.313815968	0.352932106
HDGF	ENSG00000143321	10.40796702	-0.579928068	0.045818673	-0.415490512	0.295607141	0.164437556	0.924137622
ANP32E	ENSG00000143401	13.22453375	-1.907006855	1.60465E-11	-0.776895761	0.040901159	1.130111094	0.001383496
LBR	ENSG00000143815	85.87902071	-1.411339041	0.046221935	-0.385212485	0.89612785	1.026126556	0.347015767
CALM2	ENSG00000143933	3.782800063	-0.690060444	0.051541777	-0.535262538	0.231272275	0.154797906	0.959127064
CDCA7	ENSG00000144354	165.1124224	-1.665474259	0.051657477	-1.003410041	0.473257205	0.662064218	0.84769092
FANCD2	ENSG00000144554	34.13549519	-1.601978199	0.011596658	-1.216307921	0.109770827	0.385670278	0.935922749
LYAR	ENSG00000145220	1.923843708	-0.998517302	0.034535976	-0.510644279	0.599793704	0.487873023	0.701479329
CCNA2	ENSG00000145386	14.69549015	-4.670024122	3.07581E-07	-0.836789101	0.565583363	3.833235021	0.00021047
DDX46	ENSG00000145833	72.60009215	-0.818907814	0.027045156	-0.57760734	0.248707119	0.241363474	0.911519412
C7orf50	ENSG00000146540	2.528033166	-0.468649603	0.500768184	-1.035286099	0.002173432	-0.566636495	0.344456247
CDCA5	ENSG00000146670	58.10603421	-2.352867208	1.31066E-05	-0.44469214	0.816252724	1.908175068	0.002288566
CCT6A	ENSG00000146731	164.0437095	-0.542230392	0.094578349	-0.443553402	0.254423258	0.09867699	0.977221679
NCAPG2	ENSG00000146918	30.77692896	-1.554047505	0.000170454	-0.520227694	0.614908507	1.033819812	0.073080306
RBMX	ENSG00000147274	345.8862354	-0.694071717	0.025745463	-0.236269148	0.816252724	0.457802569	0.35963232
EIF4EBP2	ENSG00000148730	54.43874035	-0.59553005	0.392945988	-0.82497943	0.096694852	-0.229449381	0.945852305
MKI67	ENSG00000148773	4.719363293	-2.900945539	5.26758E-13	-1.60035699	0.000115892	1.300588549	0.03164042
INCENP	ENSG00000149503	27.13661803	-1.857171135	0.042931135	-0.47929863	NA	1.378418505	0.314513107
CENPU	ENSG00000151725	38.89571286	-2.900836881	9.39664E-09	-0.658467384	0.557757317	2.242369498	0.000129333
SPC25	ENSG00000152253	6.818036655	-3.264220337	2.06977E-06	-0.934462681	0.413127227	2.329757657	0.006247569
CENPH	ENSG00000153044	7.282289529	-1.198792618	0.036057912	-0.704391514	0.473257205	0.494401104	0.82360153
SKA1	ENSG00000154839	3.701972181	-3.246610825	0.001762481	-0.803075937	NA	2.443534889	0.075459
ATAD2	ENSG00000156802	16.75666196	-2.087507783	4.52175E-11	-0.511146661	0.473257205	1.576361122	1.2634E-05
CCNB2	ENSG00000157456	3.032401282	-2.061305773	7.77222E-05	-0.599535967	0.672142543	1.461769807	0.02897397
PSMG3	ENSG00000157778	6.759001285	-0.818503786	0.091092352	-0.328936387	0.811317525	0.4895674	0.64075811
TAGLN2	ENSG00000158710	47.56385585	-0.714324849	0.026965251	-0.425446362	0.434134236	0.288878487	0.810587304
LAD1	ENSG00000159166	44.24413428	-0.561505256	0.408861255	-0.944089667	0.022938696	-0.382584412	0.801898489
U2AF1	ENSG00000160201	4.20978599	-0.264684059	0.938093407	-0.892835561	0.021604666	-0.628151502	0.265250964
TONSL	ENSG00000160949	8.44236368	-1.561376446	0.01498244	-0.384785363	0.893496758	1.176591082	0.18657964
SRSF2	ENSG00000161547	7.362677872	-0.7877912	0.059222445	-0.718146531	0.116313563	0.069644669	0.997903086
RACGAP1	ENSG00000161800	37.18028052	-2.016999553	3.44567E-05	-0.3540825	0.879343104	1.662917053	0.002920598
SPC24	ENSG00000161888	3.66453542	-2.02173498	0.001109241	-1.00512418	0.286463625	1.016610799	0.434234325
CCNF	ENSG00000162063	9.994111614	-2.974337104	0.035285943	-1.510516326	NA	1.463820779	0.721452154
USP1	ENSG00000162607	22.77683962	-1.502761464	8.27449E-05	-0.460475307	0.652672378	1.042286157	0.036818726
CIP2A	ENSG00000163507	5.304828645	-1.674757934	0.016529788	-0.522069886	0.811317525	1.152688048	0.289269774
SGO2	ENSG00000163535	25.02403684	-1.900556836	0.004163178	-0.38525862	0.905162116	1.515298215	0.07502716
KIF15	ENSG00000163808	109.3378845	-2.064262724	0.090409029	-1.071694398	NA	0.992568326	0.810587304
RFC4	ENSG00000163918	47.68377542	-2.363681769	0.000959388	-0.65771644	0.726547723	1.705965329	0.076229891
SLBP	ENSG00000163950	68.26159075	-1.133780676	0.011970238	-0.557087449	0.537273178	0.576693227	0.586644703
H2AZ1	ENSG00000164032	348.2172141	-1.287278539	6.6537E-08	-0.683485179	0.02797888	0.60379336	0.109710383
HMGB2	ENSG00000164104	4.349970088	-3.357612655	2.78457E-36	-1.177207059	2.47136E-05	2.180405596	9.32878E-14
MAD2L1	ENSG00000164109	11.280668	-1.73886303	3.046E-06	-0.391652738	0.739019361	1.347210292	0.001947741
ELOVL7	ENSG00000164181	15.86381026	-1.664032365	0.090512355	-0.147790255	NA	1.51624211	0.193341536
PTTG1	ENSG00000164611	31.34398644	-2.846508685	3.17252E-20	-1.224785412	0.000234969	1.621723274	1.2634E-05
RAD21	ENSG00000164754	7.449013595	-1.270583175	3.44884E-05	-0.425026434	0.570582827	0.845556741	0.036401666
PSIP1	ENSG00000164985	27.15910592	-0.972227874	0.088383262	-0.314527484	0.8832463	0.657745391	0.510996558
ZNF367	ENSG00000165244	41.7790957	-2.605504956	0.009641129	-1.796925682	NA	0.808579275	0.887369965
MELK	ENSG00000165304	28.78364324	-1.481932929	0.040895229	-0.460653049	0.862840791	1.02127988	0.385985209
SKA3	ENSG00000165480	17.11677933	-2.166442488	0.001405524	-0.869650585	0.525989245	1.296791902	0.252115897
LRR1	ENSG00000165501	8.619447947	-2.172077803	0.026062161	-0.720023527	NA	1.452054276	0.369795181
DDX21	ENSG00000165732	5.403255206	-0.452441415	0.350794135	-0.693024319	0.031622357	-0.240582904	0.864696416
E2F7	ENSG00000165891	29.21169962	-2.996834754	0.03516101	-1.530703716	NA	1.466131037	0.730937282
NOLC1	ENSG00000166197	45.68898655	-0.30377237	0.854116124	-0.709307261	0.07729112	-0.405534891	0.645150326
WEE1	ENSG00000166483	40.53632701	-1.602818421	0.082701954	-0.486017918	0.891160199	1.116800502	0.469252658
MCM7	ENSG00000166508	16.77219356	-1.845859079	3.54083E-13	-0.774042666	0.01988457	1.071816413	0.000530477
PCLAF	ENSG00000166803	29.43695742	-2.78365711	0.00034824	-1.423001895	0.180598855	1.360655215	0.390575937
SNRPD1	ENSG00000167088	26.84278517	-0.608874588	0.098637078	-0.402385395	0.496498818	0.206489193	0.914965181
CDT1	ENSG00000167513	10.96862102	-2.177956454	1.03529E-08	-0.632330937	0.389184212	1.545625517	0.000638083
TK1	ENSG00000167900	8.36106	-2.440724163	7.66835E-18	-1.06194261	0.000976092	1.378781553	7.17018E-05
PBK	ENSG00000168078	167.8247928	-3.168163374	7.13376E-10	-0.647798397	0.551482328	2.520364976	1.56723E-05
H1-4	ENSG00000168298	12.1777577	-2.413447069	0.000234083	-1.834356197	0.011439346	0.579090872	0.890790671
DTYMK	ENSG00000168393	23.32124123	-1.542484691	2.7881E-07	-0.878375076	0.019352525	0.664109615	0.231271349
FEN1	ENSG00000168496	15.79085417	-1.544341868	0.000836321	-0.286290508	0.905162116	1.25805136	0.022638826
BUB1	ENSG00000169679	8.764387274	-2.268672618	0.000284953	-1.064396784	0.254423258	1.204275834	0.289269774
CENPX	ENSG00000169689	168.7022288	-0.470426659	0.250839601	-0.576326471	0.093300672	-0.105899813	0.973851732
CDK1	ENSG00000170312	18.22671399	-2.657313228	1.36075E-16	-0.658622568	0.198554449	1.99869066	1.88429E-08
SHCBP1	ENSG00000171241	585.8240032	-2.349365922	0.000234083	-0.60193104	0.726547723	1.747434882	0.03164042
ESCO2	ENSG00000171320	9.478557408	-3.040718077	5.49014E-05	-1.145539475	0.299529893	1.895178602	0.086364896
RRM2	ENSG00000171848	49.59485056	-3.709796449	1.96299E-06	-0.805373833	0.745692789	2.904422616	0.001028391
CKS1B	ENSG00000173207	17.81651492	-0.971555539	0.001014576	-0.271761621	0.785767889	0.699793917	0.074014944
EXO1	ENSG00000174371	8.44432008	-2.950783324	0.021480192	-0.79370167	NA	2.157081654	0.251331796
ZWILCH	ENSG00000174442	31.14061379	-1.481909267	0.092962037	-0.648906493	0.745692789	0.833002774	0.699573229
UBE2C	ENSG00000175063	14.87533139	-2.646697549	1.18095E-21	-0.752066504	0.038463636	1.894631045	5.46665E-10
CKAP5	ENSG00000175216	21.35435991	-1.118511099	0.025511273	-0.445115059	0.726547723	0.673396039	0.466658302

RMI1	ENSG00000178966	20.68045034	-1.946119041	0.013728679	-0.708239043	0.710477151	1.237879999	0.359332258	
SELENOW	ENSG00000178980	19.61257558	-0.09974263	0.990352478	-0.681196568	0.038463636	-0.581453938	0.140153104	
AURKB	ENSG00000178999	41.42694058	-3.793271388	4.72927E-09	-0.290707472	0.923097327	3.502563917	3.45053E-07	
DHTKD1	ENSG00000181192	73.6348663	-1.073889128	0.007169658	-0.098639307	0.974328399	0.975249821	0.03164042	
KPNA2	ENSG00000182481	3.871268669	-1.205070606	3.19052E-08	-0.378384511	0.421790829	0.826686095	0.001443683	
SKA2	ENSG00000182628	51.41641592	-0.7952907	0.018572648	-0.318389902	0.710477151	0.476900798	0.432038759	
PSMG1	ENSG00000183527	53.71403882	-0.983778995	0.0296937	-0.637330645	0.343498308	0.34644835	0.866236253	
ASCL2	ENSG00000183734	10.71638704	-0.213622938	0.988689368	-1.294955208	0.038632042	-1.08133227	0.164932315	
IQGAP3	ENSG00000183856	45.37500616	-4.935318627	0.001868521	-1.217341039	NA	3.717977588	0.074430196	
CDCA2	ENSG00000184661	118.1391876	-2.000130596	0.034535976	-0.80194374	NA	1.198186856	0.531378069	
H1-10	ENSG00000184897	241.2419077	-1.810418421	9.22584E-06	-0.827108061	0.173725333	0.98331036	0.127104808	
SUMO3	ENSG00000184900	50.37580737	-0.140507094	0.986113215	-0.705127336	0.078525517	-0.564620242	0.284054915	
SIVA1	ENSG00000184990	9.21922641	-0.992845938	0.000551791	-0.824459683	0.010373488	0.168386255	0.954834302	
ERCC6L	ENSG00000186871	38.06334554	-2.823181325	0.072049902	-0.964818562	NA	1.858362763	0.524881227	
PTMA	ENSG00000187514	47.85299047	-0.548751548	0.097676929	-0.444364398	0.270289904	0.10438715	0.969693208	
H2AX	ENSG00000188486	28.75026485	-1.92832467	5.52418E-10	-0.686951374	0.150363406	1.241373296	0.001081985	
FAM111B	ENSG00000189057	102.0379552	-3.835919107	4.05979E-05	-0.523520984	NA	3.312398123	0.001512699	
H1-0	ENSG00000189060	3.751269631	-1.798301586	2.21201E-07	-0.648148779	0.273364593	1.150152807	0.010079492	
HMGB1	ENSG00000189403	128.570778	-1.24781367	1.84394E-10	-0.741721721	0.001431316	0.506091949	0.104870171	
TUBB	ENSG00000196230	41.88406013	-0.866790999	0.001874291	-0.497418822	0.245649439	0.369372177	0.611240789	
H4C3	ENSG00000197061	6.750138209	-2.794963248	7.62088E-16	-1.556419647	1.66652E-05	1.238543601	0.011217631	
HNRNPAB	ENSG00000197451	33.67366579	-0.871068569	0.065625244	-0.415792603	0.691125631	0.455275966	0.696543673	
MCMBP	ENSG00000197771	16.35788543	-1.284670338	0.00646136	-0.9044949	0.13405021	0.380175438	0.879988798	
TFDP1	ENSG00000198176	8.737472479	-1.222192092	0.001372607	-0.553260512	0.465047215	0.66893158	0.340554912	
WDHD1	ENSG00000198554	42.99952433	-1.626702338	0.028821149	-0.847839965	0.539351971	0.778862373	0.720431942	
ARHGAP11A	ENSG00000198826	110.3821771	-2.029217605	0.02173673	-0.755817653	NA	1.273399952	0.424133003	
HMGN2	ENSG00000198830	8.002227139	-1.014555291	3.4222E-06	-0.648255449	0.016266822	0.366299842	0.469252658	
CENPW	ENSG00000203760	23.05795262	-1.435188929	0.01808875	-0.507187469	0.751511968	0.928001146	0.367087698	
C4orf46	ENSG00000205208	43.48831334	-1.813769908	0.052646794	-0.40242952	NA	1.411340388	0.285668278	
HMGN1	ENSG00000205581	31.94598928	-0.262754944	0.810198631	-0.835423347	0.000796295	-0.572668403	0.078419974	
MXD3	ENSG00000213347	5.324368789	-2.340159067	0.036057912	-1.009279435	NA	1.330879632	0.599678646	
SBDSP1	ENSG00000225648	2.58693977	-1.272836249	0.048681888	-0.941371498	0.254423258	0.33146475	0.946383262	
DHFR	ENSG00000228716	4.11914531	-2.004694763	1.33989E-07	-0.536650818	0.565583363	1.468043945	0.001081985	
KIFC1	ENSG00000237649	1.876672271	-2.593250712	0.001014576	-0.942263769	0.565583363	1.650986943	0.176092483	
H2BC9	ENSG00000275713	27.92108491	-2.411063877	0.029161499	-1.888062456	NA	0.52300142	0.964148638	
U2AF1L5	ENSG00000275895	34.46926228	-0.497232549	0.661340753	-1.090843116	0.013574966	-0.593610567	0.498457361	
MIR1244-2	ENSG00000283498	41.27218903	-0.866426229	0.016529788	-0.56852428	0.26970932	0.29790195	0.84769092	

Cluster 3

			TvsC		RvsC		RvsT	
cluster3	Ensembl	basemean	log2FoldChange	padj	log2FoldChange	padj	log2FoldChange	padj
TNFRSF12A	ENSG00000006327	205.7027692	0.463730949	0.494682164	0.685936374	0.094327176	0.222205425	0.914965181
TRAPPC6A	ENSG00000007255	67.70297771	1.16745997	0.037917044	0.150156028	0.971078877	-1.017303941	0.133471348
MVP	ENSG00000013364	9.478557408	3.130943063	0.069219058	2.709505186	NA	-0.421437877	NA
GPRC5A	ENSG00000013588	73.6348663	1.263717773	0.024837153	1.097393847	0.090182298	-0.166323926	0.983160871
GRN	ENSG00000030582	253.6960046	0.808803348	0.010705042	0.608838599	0.130334454	-0.199964749	0.921215048
TMSB10	ENSG00000034510	307.0707487	0.748729235	0.053774818	0.354193282	0.691125631	-0.394539554	0.670777828
LTBP1	ENSG00000049323	82.42913237	1.089750008	0.046171171	0.539398159	0.674004631	-0.550351849	0.681038134
BCAS1	ENSG00000064787	46.01257183	1.67013146	0.003587973	1.142025788	0.156351682	-0.528105672	0.810587304
GSTZ1	ENSG00000100577	98.33606796	0.876896179	0.09570676	-0.052785109	0.987496655	-0.929681288	0.086516643
CST3	ENSG00000101439	214.7169655	0.874631534	0.017388868	0.849399878	0.025811007	-0.025231657	0.997903086
PCSK1N	ENSG00000102109	160.1384932	0.891306949	0.01720803	0.65556058	0.182308225	-0.235746369	0.914965181
QPRT	ENSG00000103485	98.07653609	0.98947342	0.109381317	1.074885835	0.066501356	0.085412415	0.997903086
LACTB	ENSG00000103642	33.66219751	1.629599262	0.028508574	1.28321507	0.173725333	-0.346384192	0.953809975
ZKSCAN1	ENSG00000106261	93.58187131	1.040368989	0.026243313	0.454039448	0.700638865	-0.586329542	0.521396353
STN1	ENSG00000107960	23.59967865	1.915993526	0.044164875	1.280628894	NA	-0.635364631	0.866236253
CCND1	ENSG00000110092	267.3313649	0.553772152	0.201964817	0.638991231	0.095995231	0.085219078	0.993391921
RAB5B	ENSG00000111540	54.48515569	1.169885825	0.051041375	0.43911192	0.831556658	-0.730773905	0.486200512
STAT1	ENSG00000115415	337.0352391	0.988713139	0.000154832	1.151172738	5.20981E-06	0.162459599	0.941091746
IGFBP5	ENSG00000115461	114.4781771	1.258791296	0.000726589	0.429644111	0.691125631	-0.829147185	0.098203551
KIAA1324	ENSG00000116299	142.7096288	1.231737294	0.00029739	0.306846327	0.841051986	-0.924890967	0.024849403
KDM5B	ENSG00000117139	60.72164899	1.192323691	0.048824053	0.751733763	0.478662111	-0.440589928	0.84769092
PIK3R3	ENSG00000117461	34.68524402	1.485443932	0.051657477	1.08238341	0.313832923	-0.403060522	0.924137622
CTSD	ENSG00000117984	705.3604371	0.785681009	0.007537351	0.209534564	0.878868327	-0.576146445	0.134320916
PPL	ENSG00000118898	18.86388291	2.131008606	0.033826952	1.45632095	NA	-0.674687656	0.866236253
YPEL5	ENSG00000119801	36.27063368	1.983309096	0.002081132	1.317908969	0.15359694	-0.665400127	0.739622214
MXD4	ENSG00000123933	114.392845	1.738902985	8.67613E-07	1.710615462	2.69041E-06	-0.028287523	0.997903086
CDKN1A	ENSG00000124762	73.01170227	0.871372797	0.222510994	1.11232377	0.051742	0.240950973	0.957718488
IVD	ENSG00000128928	128.0481017	0.963284674	0.023433902	0.351629949	0.792233617	-0.611654726	0.380164924
SH3BGRL	ENSG00000131171	142.9236075	1.103794431	0.002071348	0.703504112	0.173725333	-0.400290318	0.725138356
TBC1D5	ENSG00000131374	77.89302632	1.038924371	0.059222445	0.536844095	0.668045094	-0.502080276	0.736661213
MCCC2	ENSG00000131844	210.2047984	0.675250751	0.092962037	0.690870169	0.087074541	0.015619419	0.997903086
LGALS3	ENSG00000131981	305.4722388	0.802018155	0.009910065	0.62535278	0.100505952	-0.176665375	0.936646234
KDM6B	ENSG00000132510	28.82041263	1.348963311	0.199539704	1.547839619	0.094688226	0.198876308	0.992506822
PARP9	ENSG00000138496	116.9303987	0.913527509	0.066204669	1.255415195	0.002060788	0.341887686	0.850541081
CCNG2	ENSG00000138764	44.94234089	1.525346859	0.012720537	1.249914355	0.091795128	-0.275432504	0.959127064
MBNL2	ENSG00000139793	16.78168608	2.043427825	0.090512355	1.382069113	NA	-0.661358712	0.893351539
ETFA	ENSG00000140374	488.7826388	0.678558414	0.014637395	0.536427356	0.110622055	-0.142131058	0.954635233
MAP1LC3B	ENSG00000140941	122.3161607	0.767654047	0.130719805	0.909687937	0.039816027	0.14203389	0.977221679
IFITM3	ENSG00000142089	1908.714118	0.373851915	0.340764719	0.492752284	0.091074488	0.118900369	0.957718488
LMTK3	ENSG00000142235	102.0193455	0.956170333	0.052495372	0.992571679	0.041671425	0.036401346	0.997903086
RPL13A	ENSG00000142541	789.6177137	0.54104305	0.191723769	-0.085284626	0.971078877	-0.626327676	0.098066651
SELENBP1	ENSG00000143416	71.44374553	1.374583577	0.00379282	0.968667603	0.131075127	-0.405915974	0.846522775
ATP8B2	ENSG00000143515	12.38664394	2.511633603	0.065625244	1.966272552	NA	-0.545361051	0.949280788
EXOC6B	ENSG00000144036	8.508394896	3.114284999	0.061807392	0.979745847	NA	-2.134539152	NA
PNRC1	ENSG00000146278	72.35037361	1.420054074	0.00904566	1.307570329	0.025811007	-0.112483745	0.997434865
MSRB2	ENSG00000148450	181.6511274	0.594478608	0.234355083	0.771920626	0.05084903	0.177442018	0.957718488
TM7SF2	ENSG00000149809	92.67780957	1.093021323	0.026764365	0.784629034	0.248331044	-0.308392289	0.911519412
PRSS23	ENSG00000150687	757.3812448	0.777482763	0.001058073	0.550266595	0.068939498	-0.227216169	0.832500522
HSPB8	ENSG00000152137	716.8096277	0.732626928	0.005613225	0.111704566	0.949295465	-0.620922362	0.045660251
BTG2	ENSG00000159388	30.29264032	1.517152564	0.090512355	1.509087997	0.098554675	-0.008064567	0.999189976
ARHGAP35	ENSG00000160007	94.53993752	0.93721322	0.058084286	0.229999403	0.930194851	-0.707213817	0.312987522
S100A11	ENSG00000163191	1710.797085	0.8115245	0.000134593	0.314071287	0.517264159	-0.497453213	0.095401363
SHISA5	ENSG00000164054	154.0996443	0.771561857	0.092150567	0.733649843	0.130334454	-0.037912013	0.997903086
TP53INP1	ENSG00000164938	17.95294539	1.974839213	0.093388908	1.433027508	NA	-0.541811705	0.928691176
SPINT1	ENSG00000166145	56.16666776	1.108932173	0.085020767	0.783016778	0.423446216	-0.325915395	0.924137622
TUBA1A	ENSG00000167552	171.0476346	1.163467365	0.006467383	0.229560652	0.930194851	-0.933906712	0.075585726
TMC4	ENSG00000167608	24.2936649	2.006652823	0.014728146	1.149604379	NA	-0.857048444	0.67476946
MFSD3	ENSG00000167700	128.7436161	1.166683088	0.001653379	0.89817779	0.046776967	-0.268505298	0.90296802
PFKFB3	ENSG00000170525	46.71510655	1.691451569	0.012020091	1.032997106	0.351959088	-0.658454463	0.745840841
MAGED1	ENSG00000179222	117.1435951	1.045962942	0.022832637	0.797080001	0.173725333	-0.248882941	0.935922749
LDOC1	ENSG00000182195	164.6789381	0.915003186	0.010395625	0.280071758	0.848115879	-0.634931428	0.217664783
ANXA2	ENSG00000182718	952.1799219	0.639595233	0.012912765	0.144863481	0.91030536	-0.494731752	0.136992025
ABAT	ENSG00000183044	94.32159843	1.992409947	7.55411E-08	1.647323474	4.43784E-05	-0.345086473	0.852473767
TSPYL2	ENSG00000184205	23.97539828	1.944037273	0.040154712	1.81586435	NA	-0.128172923	0.997903086
TACSTD2	ENSG00000184292	277.3303337	0.977392321	0.001101912	0.598738223	0.168156649	-0.378654097	0.654181014
SEPTIN9	ENSG00000184640	211.3478181	0.665488678	0.09570676	0.448978511	0.486418104	-0.216510167	0.914965181
LRP10	ENSG00000197324	140.0084402	1.185007825	0.001008794	0.882933873	0.046776967	-0.302073952	0.866236253
GSTK1	ENSG00000197448	159.7725595	0.766170117	0.09778166	0.209234389	0.920056596	-0.556935728	0.428637203
PSAP	ENSG00000197746	688.7839439	0.504529107	0.116188405	0.642360995	0.016816886	0.137831888	0.949280788
S100A10	ENSG00000197747	863.1214922	0.817907394	0.001014576	0.04952617	0.986380133	-0.768381225	0.003768435
TRIM26	ENSG00000234127	52.33407213	0.808446088	0.448432651	1.166221295	0.087074541	0.357775206	0.914965181
LINC00886	ENSG00000240875	27.0615762	1.842371696	0.020106125	1.056941349	0.487179999	-0.785430346	0.699902247
H2AC19	ENSG00000272196	30.73645042	1.499586328	0.090512355	1.210940752	0.276525317	-0.288645576	0.966304618

Cluster 4

			TvsC		RvsC		RvsT	
	Ensembl	basemean	log2FoldChange	padj	log2FoldChange	padj	log2FoldChange	padj
CROT	ENSG00000005469	68.06518957	0.273298208	0.98282019	68.06518957	-1.357025209	-1.630323417	0.001536609
SPATA20	ENSG00000006282	65.21731104	1.096223312	0.06112803	65.21731104	0.186926712	-0.9092966	0.226098717
ADIPOR2	ENSG00000006831	105.9870539	0.779191977	0.147349283	105.9870539	-0.358550238	-1.137742215	0.009797932
FAM214A	ENSG00000047346	81.3807682	0.982613723	0.059038925	81.3807682	0.060675325	-0.921938398	0.11925607
CCN5	ENSG00000064205	141.4483087	0.308768573	0.940773538	141.4483087	-0.859000227	-1.1677688	0.017493258
SLC9A3R2	ENSG00000065054	133.7795052	0.291466951	0.938652827	133.7795052	-0.715712906	-1.007179856	0.024414956
SEMA3C	ENSG00000075223	156.6078004	0.413964352	0.711824584	156.6078004	-0.576782846	-0.990747199	0.011684781
TUBA3D	ENSG00000075886	45.69215207	-0.062445028	0.999340018	45.69215207	-2.694226396	-2.631781368	3.66817E-05
LXN	ENSG00000079257	107.3481142	1.254864087	0.000920741	107.3481142	-0.395271882	-1.650135969	1.2634E-05
PGR	ENSG00000082175	91.89717842	0.697499519	0.405039669	91.89717842	-0.726566368	-1.424065887	0.003516848
ITGB5	ENSG00000082781	148.428728	0.176091582	0.986113215	148.428728	-0.784919459	-0.961011041	0.016924894
TTC39A	ENSG00000085831	175.5517469	0.395713516	0.721245863	175.5517469	-0.485487644	-0.88120116	0.030585625

RPLP0	ENSG00000089157	5323.050585	0.148333993	0.952918027	5323.050585	-0.437600188	-0.585934181	0.013298695
TSPAN15	ENSG00000099282	118.3534912	0.706883336	0.231411985	118.3534912	-0.574191788	-1.281075124	0.002035612
KCNK6	ENSG00000099337	170.7964944	0.613702959	0.232517136	170.7964944	-0.179769488	-0.793472447	0.071964631
RPL3	ENSG00000100316	2228.713989	0.492059001	0.067074664	2228.713989	-0.193164587	-0.685223588	0.002274842
BLVRA	ENSG00000106605	162.8883253	0.417538547	0.700627569	162.8883253	-0.435486173	-0.85302472	0.04775255
EIF3A	ENSG00000107581	316.7925999	0.124312106	0.988689368	316.7925999	-0.564966846	-0.689278952	0.063498589
DNAJC12	ENSG00000108176	34.96731987	0.210831017	0.990352478	34.96731987	-2.234202976	-2.445033993	0.000892469
UGDH	ENSG00000109814	303.1196279	1.188160196	3.65644E-06	303.1196279	-0.037329409	-1.225489606	5.25522E-06
CREBL2	ENSG00000111269	29.16379891	-0.010656262	0.999660578	29.16379891	-1.623061141	-1.612404879	0.113075738
ERGIC1	ENSG00000113719	142.1680775	0.619113428	0.370649548	142.1680775	-0.271655135	-0.890768563	0.078419974
EEF1B2	ENSG00000114942	1238.545311	0.014653036	0.999340018	1238.545311	-0.498924401	-0.513577438	0.095401363
ST3GAL5	ENSG00000115525	11.08426906	0.696591268	0.951762147	11.08426906	-2.436508093	-3.133099361	0.063139488
RPL22	ENSG00000116251	66.92205399	0.428354146	0.881153906	66.92205399	-0.64029218	-1.068646326	0.098066651
PREX1	ENSG00000124126	766.8204731	0.897508548	6.64259E-05	766.8204731	-0.395801673	-1.29331022	1.2866E-09
BCAS4	ENSG00000124243	616.6602701	-0.081737564	0.992626707	616.6602701	-1.008426533	-0.926688968	0.000463532
SPDEF	ENSG00000124664	239.7630299	0.340026734	0.748550266	239.7630299	-0.377503065	-0.717529799	0.06189036
ID1	ENSG00000125968	134.6261527	0.337647375	0.869000254	134.6261527	-0.992314113	-1.329961487	0.000362849
PODXL	ENSG00000128567	57.4382781	-0.012953566	0.999340018	57.4382781	-1.145711273	-1.132757707	0.099950545
PPT1	ENSG00000131238	391.7640878	0.287051421	0.792360652	391.7640878	-0.357797153	-0.644848574	0.05460643
RTL8C	ENSG00000134590	70.26982869	0.818570865	0.218180638	70.26982869	-0.382656736	-1.201227601	0.025090066
SOX3	ENSG00000134595	33.06025563	1.001112129	0.359038005	33.06025563	-0.441695414	-1.442807542	0.091755408
PKIB	ENSG00000135549	643.1529114	0.117759527	0.986113215	643.1529114	-0.586717267	-0.704476795	0.014537264
MYOF	ENSG00000138119	176.4971874	0.688327632	0.184790706	176.4971874	-0.242015162	-0.930342794	0.03164042
EXOC6	ENSG00000138190	27.55399166	-0.207069455	0.992626707	27.55399166	-1.638983108	-1.431913653	0.197580367
RPS24	ENSG00000138326	3784.07503	0.126281756	0.988689368	3784.07503	-0.647050609	-0.773332365	0.022460684
BCAS3	ENSG00000141376	1408.683248	-0.186640062	0.917369413	1408.683248	-1.01908017	-0.832440108	0.000145008
SLC39A6	ENSG00000141424	571.6236905	0.358323979	0.675841282	571.6236905	-1.070049926	-1.428373905	3.11142E-08
IGFBP4	ENSG00000141753	147.4970221	0.074066087	0.996663201	147.4970221	-0.794028186	-0.868094273	0.047716508
PFKL	ENSG00000141959	113.9855895	0.0571264	0.997370812	113.9855895	-0.872820343	-0.929946743	0.075585726
CELSR2	ENSG00000143126	93.12455446	0.513226457	0.665727701	93.12455446	-0.429088124	-0.94231458	0.086378556
RPS27A	ENSG00000143947	2357.335129	0.093573672	0.989771744	2357.335129	-0.673384617	-0.766958289	0.002170659
ADD3	ENSG00000148700	52.80405143	0.480694415	0.893236452	52.80405143	-2.999635851	-3.480330266	4.61682E-08
RGS10	ENSG00000148908	55.32702125	0.308747896	0.978598912	55.32702125	-0.95086359	-1.259611486	0.06189036
PDCD4	ENSG00000150593	74.95469378	0.611213599	0.537995487	74.95469378	-0.718007599	-1.329221197	0.007129659
GFRA1	ENSG00000151892	86.14433705	0.162222017	0.989873189	86.14433705	-1.000343208	-1.162565225	0.030133456
PDLIM3	ENSG00000154553	50.70987503	0.780548498	0.448432651	50.70987503	-0.820135594	-1.600684092	0.007642038
EEF1A1	ENSG00000156508	6422.138793	0.321775379	0.530375646	6422.138793	-0.172983943	-0.494759322	0.098066651
HK1	ENSG00000156515	120.856146	0.189297724	0.986113215	120.856146	-0.69354616	-0.882843884	0.075459
TMEM164	ENSG00000157600	98.83934862	1.50940273	0.000332948	98.83934862	-1.071679349	-2.581082079	6.92139E-10
CSRP1	ENSG00000159176	236.8152117	0.479020828	0.359038005	236.8152117	-0.364567056	-0.843587884	0.010712317
TFF1	ENSG00000160182	6853.101566	0.84619638	0.000920741	6853.101566	-0.864535945	-1.710732325	3.69443E-15
PDXK	ENSG00000160209	183.3050502	0.159720741	0.986113215	183.3050502	-0.673225935	-0.832946676	0.030403747
GATD3A	ENSG00000160221	38.02294986	0.470426718	0.919206734	38.02294986	-0.869950057	-1.340376775	0.098066651
LSS	ENSG00000160285	60.57345408	0.416115015	0.899304239	60.57345408	-0.89617287	-1.312287885	0.023201126
DMKN	ENSG00000161249	63.5744048	0.720204403	0.465529146	63.5744048	-0.437287045	-1.157491448	0.073080306
IL20	ENSG00000162891	135.0788033	0.884915557	0.028821149	135.0788033	-0.058203232	-0.943118789	0.023201126
SMIM14	ENSG00000163683	194.8396978	0.991260935	0.003267158	194.8396978	-0.166556274	-1.157817209	0.000530477
NPY1R	ENSG00000164128	70.41518604	0.613323197	0.666016802	70.41518604	-0.86142169	-1.474744887	0.008371494
RHOBTB3	ENSG00000164292	172.5270068	0.139429005	0.989638871	172.5270068	-1.761009962	-1.900438967	3.93285E-09
GPER1	ENSG00000164850	22.14477434	0.529232406	0.940773538	22.14477434	-2.346837553	-2.876069959	0.002870849
PRDX3	ENSG00000165672	303.9366253	-0.149986938	0.986113215	303.9366253	-0.686176076	-0.536189138	0.254111343
EEF2	ENSG00000167658	1303.350137	0.493281727	0.136209563	1303.350137	-0.171827126	-0.665108853	0.014684245
DEGS2	ENSG00000168350	58.45810206	0.075750646	0.99720327	58.45810206	-1.169096263	-1.244846909	0.046375334
RAB31	ENSG00000168461	24.16718976	0.853819202	0.731278953	24.16718976	-1.649298049	-2.503117252	0.007129659
CCDC110	ENSG00000168491	13.70900977	1.634022627	0.265077015	13.70900977	-1.231966197	-2.865988823	0.024849403
AFAP1L2	ENSG00000169129	15.39106892	0.672503929	0.939870406	15.39106892	-1.618837955	-2.291341884	0.095264624
KRT19	ENSG00000171345	3128.806421	0.665061884	0.001815137	3128.806421	-0.086299602	-0.751361486	0.000362849
DSCAM	ENSG00000171587	29.29144377	1.231067366	0.181838402	29.29144377	-0.7320851	-1.963152466	0.010771456
RPS7	ENSG00000171863	1880.962848	0.07793615	0.992626707	1880.962848	-0.485779739	-0.563715889	0.091331824
MUCL1	ENSG00000172551	43.62367135	0.96142762	0.28306218	43.62367135	-0.945457974	-1.906885593	0.002394972
RHOD	ENSG00000173156	138.0051077	0.466687625	0.668918971	138.0051077	-0.959365662	-1.426053288	0.000190724
SYT12	ENSG00000173227	89.54351545	0.345909672	0.917369413	89.54351545	-0.736990857	-1.082900529	0.037753041
GOLGB1	ENSG00000173230	130.823525	0.893016273	0.055896211	130.823525	0.087512133	-0.80550414	0.142398563
PDZK1	ENSG00000174827	257.6922458	0.960835328	0.001995284	257.6922458	-2.384810156	-3.345645484	9.11515E-31
TOM1L2	ENSG00000175662	23.99208039	1.630841729	0.116188405	23.99208039	-0.316494002	-1.947335731	0.057712845
DOK7	ENSG00000175920	44.46877331	-0.190623567	0.990352478	44.46877331	-1.561767418	-1.371143851	0.073173385
MRFAP1	ENSG00000179010	1212.973126	0.043560794	0.99720327	1212.973126	-0.55527169	-0.598832484	0.02471491
NRIP1	ENSG00000180530	25.96145063	0.768805321	0.83719673	25.96145063	-1.306817661	-2.075622982	0.045660251
TTC3	ENSG00000182670	99.72540011	0.13448529	0.990352478	99.72540011	-0.831083597	-0.965568888	0.07502716
IMMP2L	ENSG00000184903	96.37526725	1.006056639	0.064594088	96.37526725	-0.052447064	-1.058503703	0.06130771
MUC1	ENSG00000185499	33.34242247	1.067504349	0.30572817	33.34242247	-0.916768142	-1.984272492	0.007878076
S100A16	ENSG00000188643	436.1545561	0.481233781	0.32276361	436.1545561	-1.247548553	-1.728782334	1.50318E-11
APOD	ENSG00000189058	16.46607619	0.243669965	0.992626707	16.46607619	-1.994755658	-2.238425624	0.098142174
S100A14	ENSG00000189334	655.3190737	0.684028471	0.011384227	655.3190737	-0.560786117	-1.244814587	3.11142E-08
GREB1	ENSG00000196208	441.1162448	0.611449279	0.063506752	441.1162448	-0.141675571	-0.75312485	0.011478681
ANXA6	ENSG00000197043	123.0567821	0.728621321	0.148994209	123.0567821	-0.263416497	-0.992037817	0.021241663
RPS4X	ENSG00000198034	2712.705926	0.397500458	0.243243529	2712.705926	-0.163193777	-0.560694234	0.03164042
MT1F	ENSG00000198417	44.44981118	0.142121378	0.993512638	44.44981118	-1.61533668	-1.757458058	0.013670618
ND1	ENSG00000198888	975.3612336	0.146872127	0.977921721	975.3612336	-0.393735485	-0.540607612	0.076598847
APRT	ENSG00000198931	735.7016651	0.376005287	0.389704877	735.7016651	-0.148497012	-0.524502299	0.096495758
RACK1	ENSG00000204628	4081.860231	0.347140359	0.447043888	4081.860231	-0.183993087	-0.531133445	0.065779789
TMSB4X	ENSG00000205542	2418.457074	0.391855771	0.2875453	2418.457074	-0.276791678	-0.668647449	0.006141073
RPL21P28	ENSG00000220749	781.7432939	0.13166847	0.986113215	781.7432939	-0.471750665	-0.603419135	0.048166149
DSCAM-AS1	ENSG00000235123	1640.313401	0.137046196	0.98282019	1640.313401	-0.625332938	-0.762379135	0.000811548
TMEM150C	ENSG00000249242	75.06950436	0.814466779	0.41092321	75.06950436	-0.765884879	-1.580351658	0.007129659
LINC02762	ENSG00000250303	47.40681132	0.545562366	0.811521007	47.40681132	-1.555247749	-2.101810115	0.000362849
TXNIP	ENSG00000265972	220.2276264	0.573135108	0.193279694	220.2276264	-0.189301563	-0.762436672	0.038613303

Appendix V – GSEA pathway analysis in LTED Y537C cells

Pathways UP

NAME	SIZE	ES	NES	FDR q-val	RANK AT MAX
HALLMARK_ESTROGEN_RESPONSE_EARLY	36	0.54	2.55	0	227
HALLMARK_P53_PATHWAY	15	0.49	1.79	0.011	166
HALLMARK_ESTROGEN_RESPONSE_LATE	31	0.27	1.25	0.249	83
HALLMARK_EPITHELIAL_MESENCHYMAL_TRANSITION	18	0.27	1.04	0.47	360
HALLMARK_APOPTOSIS	17	0.21	0.8	0.776	190

Pathways DOWN

NAME	SIZE	ES	NES	FDR q-val	RANK AT MAX
HALLMARK_E2F_TARGETS	102	-0.67	-3.01	0	234
HALLMARK_G2M_CHECKPOINT	79	-0.62	-2.65	0	176
HALLMARK_MYC_TARGETS_V1	35	-0.57	-2.11	0	274
HALLMARK_MITOTIC_SPINDLE	37	-0.47	-1.8	0.006	173
HALLMARK_MTORC1_SIGNALING	27	-0.36	-1.3	0.19	217
HALLMARK_DNA_REPAIR	17	-0.39	-1.22	0.234	258
HALLMARK_GLYCOLYSIS	15	-0.37	-1.11	0.313	165

Appendix VI – Heatmap cluster gene list in MCF7 LTED Y537C cells

Cluster 1

			PalboT Veh		PalboR vs Veh		PalboR vs PalboT	
	ensembl	baseMean	log2FoldChange	padj	log2FoldChange	padj	log2FoldChange	padj
DBF4	ENSG00000006634	76.99956635	-1.212810331	0.014868417	-0.985709604	0.076928319	-0.227100727	0.999167959
NCAPD2	ENSG00000010292	52.88460088	-1.824670783	0.000776189	-0.970878034	0.212686282	-0.853792749	0.581782444
ANLN	ENSG00000011426	26.40191746	-2.888929272	0.000428421	-1.241432718	0.304467852	-1.647496554	0.257468311
BRCA1	ENSG00000012048	36.53060338	-2.942409115	1.83453E-05	-1.067341882	0.315246153	-1.875067233	0.043775041
TACC3	ENSG00000013810	45.08781559	-2.519514503	3.36269E-05	-0.942197984	0.355500416	-1.577316519	0.062660818
DEPDC1	ENSG00000024526	19.23769219	-2.656368636	0.007318513	-1.343496665	0.339877062	-1.312871971	0.704168095
HMGB3	ENSG00000029993	178.3624983	-0.892934918	0.028032729	-0.036719293	0.985634381	-0.856215625	0.045207778
CENPQ	ENSG00000031691	20.25215683	-1.942876726	0.066813317	-0.636179744	0.810602881	-1.306696982	0.557009385
DEPDC1B	ENSG00000035499	20.78482557	-2.319185076	0.021975059	-1.302918901	0.367439066	-1.016266175	0.910936128
SPDL1	ENSG00000040275	37.88638419	-1.692866884	0.020786264	-0.778722896	0.579777357	-0.914143988	0.680107134
RFC2	ENSG00000049541	52.40147608	-1.626612243	0.0030934	-0.950441276	0.21412154	-0.676170967	0.825168332
NOP58	ENSG00000055044	186.919856	-0.68037972	0.213299698	0.188612538	0.911316095	-0.868992257	0.043693452
MCM10	ENSG00000065328	39.64839096	-5.093138633	9.76855E-09	-1.271508764	0.107797748	-3.821629869	0.000180108
ASPM	ENSG00000066279	67.06292537	-2.024723992	3.43767E-05	-1.005622316	0.13652032	-1.019101676	0.257468311
PRR11	ENSG00000068489	78.09283755	-2.102257577	1.822E-06	-0.379551671	0.802658022	-1.722705906	0.000435621
TRIP13	ENSG00000071539	79.24553342	-1.417817101	0.002279685	-0.367289943	0.810602881	-1.050527158	0.07960488
HMMR	ENSG00000072571	33.99754267	-4.098578152	9.63352E-08	-1.669318392	0.026994931	-2.429259759	0.019326138
GTSE1	ENSG00000075218	24.88469002	-3.378357734	0.00010657	-1.370514406	0.236878317	-2.007843328	0.1386194
WDR62	ENSG00000075702	12.20928388	-3.014961501	0.02061184	-2.377066634	0.070391959	-0.637894867	0.999167959
MCM6	ENSG00000076003	134.0393738	-1.624449604	1.84249E-05	-0.321088356	0.817392771	-1.303361247	0.002709284
UNG	ENSG00000076248	123.1189987	-1.251382987	0.001869018	-0.900779674	0.06806623	-0.350603313	0.999167959
UBE2T	ENSG00000077152	138.4291513	-2.258497571	3.4186E-12	-1.719033352	2.86032E-07	-0.539464219	0.73186275
HSP90AA1	ENSG00000080824	4190.506627	-0.743839929	0.001595912	-0.347008522	0.445474669	-0.396831407	0.444708768
RBL1	ENSG00000080839	11.69374559	-3.302881138	0.01789566	-1.482862172	0.429759042	-1.820018966	0.659291895
NDC80	ENSG00000080986	23.50705292	-3.748606685	0.000154146	-1.149182418	0.469021135	-2.599424267	0.048084171
ORC1	ENSG00000085840	14.47782415	-3.427655902	0.00797623	-1.593868622	0.363795151	-1.83378728	0.614289794
AURKA	ENSG00000087586	94.24061367	-2.800090105	6.96857E-13	-1.129031523	0.013959947	-1.671058582	0.00044457
TPX2	ENSG00000088325	115.21963	-2.394264568	6.7324E-11	-1.23331613	0.003594111	-1.160948438	0.026484827
BIRC5	ENSG00000089685	194.3730719	-3.203914343	3.87819E-26	-1.169619002	0.000287017	-2.034295341	9.27638E-10
AARS1	ENSG00000090861	230.3096788	-0.734279313	0.089268814	-0.238076655	0.851613391	-0.496202658	0.582020906
KIF4A	ENSG00000090889	17.30866247	-3.8127128	0.000746191	-1.117678117	0.525716988	-2.695034684	0.077553765
ORC6	ENSG00000091651	38.32002366	-1.693390118	0.019565408	-0.156548176	0.966415674	-1.536841943	0.054335641
G2E3	ENSG00000092140	35.68088706	-1.604784804	0.026882042	-1.017389885	0.303173894	-0.587394919	0.999167959
WDR76	ENSG00000092470	13.36082194	-4.398476087	0.001527095	-1.992380482	0.116529768	-2.406095606	0.447959203
PHGDH	ENSG00000092621	89.36598128	-1.592009695	0.000550445	-0.59733928	0.546451061	-0.994670415	0.152491731
CLSPN	ENSG00000092853	9.828425838	-6.971744902	0.001159515	-1.695201547	0.408283992	-5.276543355	0.05839427
CDC45	ENSG00000093009	44.54495049	-4.144557544	7.10176E-11	-2.124644365	0.000104309	-2.019913179	0.031518421
CDC6	ENSG00000094804	33.0732128	-1.670635666	0.033559985	-0.499385396	0.822819788	-1.17125027	0.375723158
CBX5	ENSG00000094916	130.8134856	-1.006464717	0.023980737	-0.632746395	0.332043638	-0.373718322	0.999167959
TMEM38B	ENSG00000095209	59.95682496	-1.00121527	0.217102621	-1.152394701	0.088633463	0.151179431	0.999167959
RANBP1	ENSG00000099901	340.7915559	-1.107013616	5.88806E-05	-1.009283044	0.000522276	-0.097730571	0.999167959
CENPM	ENSG00000100162	35.34053268	-2.953021216	7.80016E-06	-1.254359109	0.133959715	-1.698662107	0.079280225
MCM5	ENSG00000100297	61.61600867	-1.899784982	0.000188458	-0.649035406	0.553680456	-1.250749575	0.073048057
TRMU	ENSG00000100416	36.49603327	-1.465029314	0.067815435	-0.747677619	0.602815336	-0.717351695	0.908082018
POLE2	ENSG00000100479	24.56160208	-1.682236919	0.086597375	-0.974649933	0.50745935	-0.707586986	0.999167959
CDKN3	ENSG00000100526	112.2769722	-3.453362812	4.37348E-20	-1.775528134	8.49646E-07	-1.677834679	0.00046305
GINS1	ENSG00000101003	27.32505414	-2.028254234	0.015464349	-1.21240637	0.291176417	-0.815847864	0.949354063
MYBL2	ENSG00000101057	162.6519456	-2.824306865	1.27701E-18	-1.357606949	7.54678E-05	-1.466699916	0.000219616
PSMA7	ENSG00000101182	1230.006153	-0.61630173	0.034436898	-0.409651247	0.332043638	-0.206650483	0.999167959
CDC25B	ENSG00000101224	127.7269279	-1.012950567	0.027226781	-0.215172462	0.904812603	-0.797778105	0.182839357
E2F1	ENSG00000101412	28.83589987	-3.292904076	2.04005E-05	-0.849245527	0.557167289	-2.44365855	0.010077324
FAM83D	ENSG00000101447	27.3479965	-2.141177771	0.02061184	-1.30541133	0.304870373	-0.83576644	0.975084121
PLP2	ENSG00000102007	163.9008396	-0.789806215	0.089495064	-0.634527544	0.242996771	-0.155278671	0.999167959
UBL4A	ENSG00000102178	147.5315966	-0.81956547	0.119189352	0.204685759	0.907053512	-1.024251229	0.019228124
MCM4	ENSG00000104738	147.3089707	-1.369394271	5.71437E-05	-1.444490411	2.475E-05	0.07509614	0.999167959
H2AZ2	ENSG00000105968	508.0003482	-1.040639937	5.16869E-05	-0.85356247	0.002878587	-0.187077467	0.999167959
RPA3	ENSG00000106399	134.4036729	-1.271329528	0.00101261	-0.586706639	0.404883168	-0.684622889	0.38459401
EZH2	ENSG00000106462	66.33509955	-1.437075468	0.006833336	-0.875579836	0.236624109	-0.561495632	0.915191704
RHEB	ENSG00000106615	202.1474287	-0.786853389	0.059873327	-0.501740261	0.423844107	-0.285113128	0.999167959
UBE2S	ENSG00000108106	137.014244	-1.902429259	7.5667E-09	-1.115684399	0.003442942	-0.786744861	0.182839357
RAD51C	ENSG00000108384	413.5229115	-0.928606323	0.00100342	-0.512818628	0.240214096	-0.415787695	0.634965933
TUBD1	ENSG00000108423	150.9667545	-0.818094643	0.089268814	-0.030078537	0.987500219	-0.788016106	0.119466828
NEIL3	ENSG00000109674	10.00437975	-3.624989078	0.018456583	-2.712327789	0.063657214	-0.912661289	0.999167959
NSD2	ENSG00000109685	66.69492757	-1.161410883	0.064964237	-0.301489788	0.888020444	-0.859921095	0.399233065
NCAPG	ENSG00000109805	12.59053164	-3.071971454	0.042788612	-0.448939631	0.929779275	-2.623031823	0.157907671
RAD51AP1	ENSG00000111247	19.53989402	-3.465143499	0.000515281	-1.132338854	0.464702365	-2.332804644	0.097019961
RFC5	ENSG00000111445	25.71247142	-1.71073286	0.079142727	-0.469069788	0.871699742	-1.241663072	0.472899791
TIMELESS	ENSG00000111602	74.41027704	-1.80929397	3.71515E-05	-0.757087145	0.294387096	-1.052206824	0.106201715
CDCA3	ENSG00000111665	35.16738009	-4.63732681	2.84403E-09	-2.262734921	0.000165126	-2.374591889	0.038624161
FBXO5	ENSG00000112029	29.16460732	-2.978744182	5.84235E-05	-1.285323515	0.189333976	-1.693420667	0.158348144
MCM3	ENSG00000112118	102.8519766	-1.619920045	2.76265E-05	-0.866022031	0.094053684	-0.753898014	0.350794177
GMNN	ENSG00000112312	79.69519767	-2.949381047	4.28955E-12	-1.395686473	0.002513823	-1.553694574	0.006748169
TTK	ENSG00000112742	23.39589977	-2.632913363	0.004093238	-0.705802023	0.780555687	-1.927119341	0.121793058
LMNB1	ENSG00000113368	53.68093657	-2.186467781	7.12066E-05	-0.59471938	0.670012103	-1.591748442	0.020478268
SMC4	ENSG00000113810	85.58565035	-1.35248965	0.032789575	-0.162955649	0.960055022	-1.189534001	0.101738766
ECT2	ENSG00000114346	100.3849475	-1.417918311	0.000328111	-1.286991333	0.001914926	-0.130926979	0.999167959
CENPA	ENSG00000115163	33.02996843	-4.054610557	1.35845E-07	-1.781046526	0.0159678	-2.273564031	0.037394796
SRSF7	ENSG00000115875	301.8438484	-1.180648289	2.8117E-05	-0.593949875	0.157329723	-0.586698414	0.248231308
CACYBP	ENSG00000116161	298.4726158	-0.896546148	0.004826786	-0.568232313	0.205104626	-0.328313834	0.937942642
CDC20	ENSG00000117399	80.36581074	-3.715407943	5.57397E-16	-1.843728181	2.03509E-05	-1.871679762	0.001942694
STMN1	ENSG00000117632	251.951969	-2.247254374	1.59562E-17	-1.446518036	2.0375E-07	-0.800736338	0.053965963
NEK2	ENSG00000117650	18.16165541	-2.748966149	0.007204146	-0.964100573	0.632467797	-1.784865576	0.312867898
CENPF	ENSG00000117724	72.08158715	-3.062214236	3.74133E-11	-0.989885471	0.101279603	-2.072328764	0.000139291
KIF14	ENSG00000118193	26.65719799	-3.697182363	9.80138E-06	-1.656647637	0.06623458	-2.040534726	0.119684679
DCLRE1B	ENSG00000118655	72.44107988	-1.198235363	0.035306272	-0.932854308	0.1618976	-0.265381055	0.999167959
CTNNAL1	ENSG00000119326	27.69494259	-2.999073712	5.16869E-05	-1.712392377	0.036887772	-1.286681336	0.550364896
WDR34	ENSG00000119333	57.69502949	-0.847932331	0.335038473	-1.147560692	0.065531856	0.299628361	0.999167959
PHF19	ENSG00000119403	66.81063844	-2.23252755	1.14517E-06	-1.091540915	0.063271781	-1.140986635	0.112775917
HELLS	ENSG00000119969	40.97217957	-1.390283213	0.074928593	-0.752924658	0.57688359	-0.637358555	0.960178229
MASTL	ENSG00000120539	29.83363875	-2.682157697	0.000553799	-0.872054665	0.593484666	-1.810103032	0.094816664
TMPO	ENSG00000120802	184.1877657	-1.580586458	3.11964E-07	-0.920999907	0.015515666	-0.659586551	0.283316474
NCAPH	ENSG00000121152	37.24304752	-2.822639779	1.25698E-05	-0.78919118	0.530036286	-2.033448599	0.011025091
MND1	ENSG00000121211	31.94265238	-3.973743151	1.02723E-06	-1.036234133	0.369195165	-2.937509018	0.002394874
HNRNPA2B1	ENSG00000122566	1399.842343	-0.792936874	0.001490667	-0.56542846	0.073929467	-0.227508414	0.999167959
ZWINT	ENSG00000122952	114.0271116	-2.591871136	5.45054E-13	-0.919466824	0.051290577	-1.672404313	7.07987E-05
CIT	ENSG00000122966	13.79670124	-2.362640156	0.088569974	-0.604006273	0.875294001	-1.758633883	0.463837655
PRDX4	ENSG00000123131	235.5391043	-0.667807814	0.136137847	-0.885809699	0.013411613	0.218001885	0.999167959
DDX39A	ENSG00000123136	134.4264721	-1.625401	4.51594E-06	-1.321714593	0.00045493	-0.303686407	0.999167959
CENPK	ENSG00000123219	30.16584005	-3.07998483	4.02377E-05	-1.120839965	0.321314958	-1.959144865	0.061169042
HJURP	ENSG00000123485	23.01848792	-3.008814522	0.000862515	-0.586338391	0.828930161	-2.422476131	0.025572444
CKS2	ENSG00000123975	129.5243791	-1.157633391	0.003598391	-1.068707933	0.011566372	-0.088925458	0.999167959
H1-3	ENSG00000124575	22.29834082	-4.141940103	0.000438597	-1.035088813	0.660772152	-3.10685129	0.036959628
DEK	ENSG00000124795	320.2588904	-1.126836582	6.10819E-05	-0.780816515	0.022891141	-0.346020067	0.901482384
SNRPB	ENSG00000125835	194.1793905	-0.951159573	0.034988698	-0.710226511	0.210666163	-0.240933063	0.999167959
DLGAP5	ENSG00000126787	47.99096966	-4.40094047	1.47232E-11	-2.150368072	7.84482E-05	-2.250572398	0.013570142
YEATS4	ENSG00000127337	116.6942099	-1.159207033	0.004863447	-0.982887131	0.03136697	-0.176319902	0.999167959
PKMYT1	ENSG00000127564	17.44102261	-2.449713216	0.018660919	-1.107664169	0.510078758	-1.342049047	0.661160644
RIBC2	ENSG00000128408	7.820200934	-3.584520469	0.07422196	-1.805252645	NA	-1.779267824	0.9287985
KNSTRN	ENSG00000128944	34.52417001	-3.226748885	1.26857E-06	-1.264053359	0.115274316	-1.962695526	0.031119383
DUT	ENSG00000128951	139.5391685	-2.513752264	3.30959E-13	-1.513990688	4.13554E-05	-0.999761576	0.068344015
E2F8	ENSG00000129173	7.318195998	-6.747731757	0.004093238	-2.766087629	NA	-3.981644127	0.444708768
PIMREG	ENSG00000129195	12.59743412	-4.922207288	0.002922591	-2.008975195	0.140914371	-2.913232094	0.378603138
MIS18BP1	ENSG00000129534	106.1925711	-1.045576945	0.028493743	-0.723206896	0.24647954	-0.322370049	0.999167959
SGO1	ENSG00000129810	9.697919969	-3.187657545	0.057580993	-2.473296253	0.140281231	-0.714361291	0.999167959
TOMM40	ENSG00000130204	131.1788702	-0.892599824	0.056551871	-0.648374431	0.28120239	-0.244225393	0.999167959
LSM4	ENSG00000130520	560.8735338	-0.770995115	0.014597543	-0.413955018	0.448007896	-0.357040097	0.812959694
DNMT1	ENSG00000130816	118.2290732	-1.323041138	0.000444819	-0.867944508	0.06806623	-0.45509663	0.897126282
GINS2	ENSG00000131153	122.0859268	-3.56190607	3.56663E-20	-1.433007164	0.000257042	-2.128898907	1.83841E-06
TOP2A	ENSG00000131747	151.8894872	-3.062505094	3.344E-20	-1.372990078	7.61424E-05	-1.689515016	1.81773E-05
SNRPA1	ENSG00000131876	254.1589445	-1.036768573	0.001041262	-0.726334217	0.06806623	-0.310434356	0.995838092
RAN	ENSG00000132341	1703.909292	-0.606353873	0.034988698	-0.440308011	0.242330514	-0.166045862	0.999167959
H3-3B	ENSG00000132475	1340.784984	-0.70958848	0.007132938	-0.248244375	0.750164845	-0.461344105	0.288784038
PCNA	ENSG00000132646	161.0079262	-3.14516932	2.02561E-22	-1.516806782	3.54221E-06	-1.628362538	2.88669E-05
NASP	ENSG00000132780	135.253969	-1.328735538	0.000546475	-0.728364414	0.197817123	-0.600371125	0.582020906
RFC3	ENSG00000133119	122.0818768	-1.310276145	0.000597033	-0.421164398	0.669609076	-0.889111746	0.087304397
CCNB1	ENSG00000134057	139.8574071	-2.532234367	2.55776E-11	-1.470307456	0.000480277	-1.062016911	0.077113068
PSRC1	ENSG00000134222	41.37853745	-2.693226327	1.50369E-05	-1.264953361	0.112591479	-1.428272967	0.165214277
TMEM106C	ENSG00000134291	230.0722746	-0.830168662	0.048895784	0.211652569	0.888020444	-1.041821231	0.00469874
YWHAQ	ENSG00000134308	405.3944265	-0.775887069	0.025900311	-0.785952408	0.023425227	0.010065339	0.999167959
CDCA8	ENSG00000134690	41.6092339	-1.990429229	0.001135309	-0.59067459	0.708752509	-1.399754639	0.090816111
TROAP	ENSG00000135451	24.01357185	-4.364120222	9.43401E-06	-1.340447582	0.198446398	-3.02367264	0.015663265

ESPL1	ENSG00000135476	20.39972093	-3.513295404	0.000369179	-1.02109142	0.55174474	-2.492203985	0.056647648
BRIP1	ENSG00000136492	86.7150775	-2.244012484	4.05584E-08	-1.080689181	0.035017451	-1.163323304	0.051078116
TRA2B	ENSG00000136527	208.6232518	-0.798784681	0.050719328	-0.096280712	0.961272269	-0.702503968	0.137165369
SMC2	ENSG00000136824	64.71497506	-0.777182066	0.422701585	-1.076667966	0.088105707	0.299485901	0.999167959
DSCC1	ENSG00000136982	68.59105331	-2.049814785	8.34642E-06	-0.633155062	0.498260937	-1.416659723	0.013570142
NRM	ENSG00000137404	13.66454871	-4.378291239	0.001553346	-1.752375326	0.202923187	-2.625915913	0.300549269
GGH	ENSG00000137563	60.26154413	-1.716773911	0.000896237	-0.320396295	0.875915846	-1.396377616	0.021683264
KIF23	ENSG00000137807	57.01354847	-2.634583545	1.42028E-07	-0.971806382	0.169421662	-1.662777163	0.010290757
KIF11	ENSG00000138160	58.94361585	-2.207997009	1.22937E-05	-1.34260512	0.023251045	-0.865391889	0.569535115
CEP55	ENSG00000138180	58.88383582	-3.193921369	2.2029E-10	-1.289776808	0.023251045	-1.904144561	0.003173226
KIF20B	ENSG00000138182	84.66606778	-1.13879454	0.034000526	-0.803847052	0.242330514	-0.334947488	0.999167959
BARD1	ENSG00000138376	57.38465102	-1.186221168	0.055572812	-1.518444192	0.00445215	0.332223025	0.999167959
HNRNPD	ENSG00000138668	340.3383144	-0.798362507	0.014137509	-0.497757532	0.302328792	-0.300604975	0.961476482
CENPE	ENSG00000138778	36.72703622	-3.234373185	1.16498E-06	-0.992266145	0.321314958	-2.242107039	0.006773657
GAS2L3	ENSG00000139354	22.97575874	-2.146376817	0.043901731	-0.781779622	0.760541861	-1.364597196	0.568864248
BRCA2	ENSG00000139618	38.77250711	-1.570246096	0.059939317	-0.184555536	0.961272269	-1.385690056	0.156987143
DIAPH3	ENSG00000139734	20.28415021	-3.171790627	0.000805978	-1.238288588	0.381821319	-1.933502039	0.218649956
FANCI	ENSG00000140525	18.37594263	-3.35123374	0.000918283	-1.051995857	0.539687053	-2.299237882	0.106201715
PLK4	ENSG00000142731	27.65464592	-2.871188087	0.000174732	-0.919213729	0.506189614	-1.951974358	0.059065199
KIF2C	ENSG00000142945	25.95360327	-3.471886101	4.31223E-05	-0.999433331	0.471721056	-2.47245277	0.021683264
NUF2	ENSG00000143228	31.18552924	-3.331500084	4.9612E-06	-1.470479166	0.079013877	-1.861020918	0.091668022
ANP32E	ENSG00000143401	161.4196515	-1.521426502	3.71312E-06	-1.001331606	0.010097059	-0.520094896	0.670537986
DTL	ENSG00000143476	16.78405278	-4.225196451	0.000411172	-1.547715689	0.236439095	-2.677480762	0.139517974
TPM3	ENSG00000143549	499.0543805	-0.631556447	0.074050664	-0.422984655	0.410816	-0.208571792	0.999167959
ILF2	ENSG00000143621	330.7247682	-0.675965631	0.074928593	-0.522341258	0.261571148	-0.153624372	0.999167959
LBR	ENSG00000143815	72.66439624	-1.43085353	0.004779629	-0.291098552	0.887963357	-1.139754977	0.067444429
CDCA7	ENSG00000144354	23.09766862	-3.500834655	2.45132E-05	-2.483642381	0.001619666	-1.017192274	0.949354063
FANCD2	ENSG00000144554	31.22109493	-1.843938822	0.025466853	-0.836377028	0.598077652	-1.007561793	0.691238165
CCNA2	ENSG00000145386	33.06021386	-4.882628993	5.48553E-08	-1.524051645	0.039601522	-3.358577347	0.002226361
MMS22L	ENSG00000146263	16.0298123	-2.165503774	0.092836461	-0.993578109	0.670382891	-1.171925665	0.889135838
MTFR2	ENSG00000146410	11.4895501	-2.614071131	0.098148481	-1.07926939	0.715879571	-1.534801741	0.80391431
CDCA5	ENSG00000146670	50.18950055	-3.203634788	3.5098E-07	-0.623566641	0.703428277	-2.580068148	0.000249958
NCAPG2	ENSG00000146918	89.48352025	-2.029194535	5.34072E-07	-1.254162849	0.007241804	-0.775031686	0.454638454
MKI67	ENSG00000148773	76.1170523	-3.779757326	2.65615E-14	-1.486905466	0.003411117	-2.29285186	0.000130344
CHEK1	ENSG00000149554	28.58278193	-2.310571098	0.002039216	-1.006627629	0.421220278	-1.303943469	0.402714821
DSN1	ENSG00000149636	39.17871027	-2.215420006	0.000336024	-0.955222098	0.334766153	-1.260197908	0.238618045
HIRIP3	ENSG00000149929	40.66277073	-2.403285105	0.000281902	-0.089584048	0.980879952	-2.313701056	0.000873132
TEX30	ENSG00000151287	36.56564838	-1.951193227	0.007297629	-0.930391466	0.448007896	-1.02080176	0.616480702
CENPU	ENSG00000151725	55.23184435	-3.235504624	2.60799E-09	-1.331151371	0.035143367	-1.904353253	0.007888732
SPC25	ENSG00000152253	28.29101679	-4.363188637	1.02723E-06	-1.504680731	0.082638065	-2.858507906	0.013429286
HNRNPDL	ENSG00000152795	294.8893563	-0.739917232	0.038493456	-0.696452859	0.062378114	-0.043464372	0.999167959
CENPH	ENSG00000153044	45.84155849	-1.924727703	0.000737728	-1.266180138	0.06674571	-0.658547564	0.921857556
NRGN	ENSG00000154146	20.90572528	-2.853728806	0.001322133	-1.473242233	0.188548171	-1.380486573	0.59033491
BUB3	ENSG00000154473	152.9780262	-0.606927077	0.394324983	-0.924923976	0.038767485	0.317996899	0.999167959
SKA1	ENSG00000154839	16.31144837	-3.699944	0.001111214	-2.131321178	0.06977867	-1.568622822	0.766647944
ATAD2	ENSG00000156802	183.93134011	-1.900515064	1.12138E-10	-0.771291652	0.060866872	-1.129223411	0.002223382
BUB1B	ENSG00000156970	12.02110563	-3.246392396	0.042797924	-0.269709814	0.965477941	-2.976682582	0.094816664
CCNB2	ENSG00000157456	62.97741599	-2.107066042	2.83349E-05	-1.219123613	0.05226296	-0.887942429	0.51119369
PSMG3	ENSG00000157778	75.83593286	-1.055436714	0.068812803	-0.473586888	0.702689458	-0.581849826	0.795752099
NAE1	ENSG00000159593	193.4365467	-0.608227762	0.244092487	-0.747042908	0.070742011	0.138815146	0.999167959
TONSL	ENSG00000160949	36.15607219	-1.568355934	0.03814335	-0.921961778	0.416936789	-0.646394156	0.974853293
RECQL4	ENSG00000160957	49.13887343	-1.456709616	0.017583609	-0.875519944	0.318336381	-0.581189672	0.954878756
RACGAP1	ENSG00000161800	64.7441066	-2.285826595	3.47122E-06	-0.973295513	0.170141853	-1.312531082	0.062660818
SPC24	ENSG00000161888	34.4315352	-2.577812253	0.000258479	-1.224673828	0.215184352	-1.353138425	0.33815477
USP1	ENSG00000162607	94.39756036	-1.48734055	0.002350204	-0.874971794	0.212862805	-0.612368756	0.812959694
CIP2A	ENSG00000163507	30.3198814	-2.026095962	0.005033695	-1.121552247	0.267409397	-0.904543715	0.788319931
SGO2	ENSG00000163535	30.33230368	-2.369059951	0.0013228	-0.939642812	0.469587838	-1.429417139	0.259040002
GMPS	ENSG00000163655	99.12135319	-1.142460875	0.029186262	-0.973655119	0.089059987	-0.168805756	0.999167959
RFC4	ENSG00000163918	43.52130232	-2.034421785	0.002121028	-0.742181673	0.609126816	-1.292240111	0.223441738
SLBP	ENSG00000163950	103.7181155	-1.168047562	0.010260359	-0.639694294	0.385847993	-0.528353269	0.812959694
H2AZ1	ENSG00000164032	361.162984	-1.704211621	2.99728E-12	-0.900741532	0.002148769	-0.80347009	0.017917261
HMGB2	ENSG00000164104	376.6329679	-3.527833705	1.2707E-42	-1.750677033	4.77342E-12	-1.777156672	9.27638E-10
MAD2L1	ENSG00000164109	112.6695386	-1.695387463	9.43401E-06	-1.058613697	0.022417928	-0.636773766	0.591042942
PTTG1	ENSG00000164611	100.8895325	-3.375744534	6.80467E-16	-2.187140878	9.21024E-08	-1.188603657	0.096227836
RAD21	ENSG00000164754	209.7429112	-1.262806459	4.92509E-05	-0.643822597	0.161956636	-0.618983862	0.302512944
ZNF367	ENSG00000165244	13.48171186	-2.594399207	0.061730389	-0.855180923	0.792596268	-1.739218284	0.557009385
MELK	ENSG00000165304	25.89540589	-3.408615401	2.6103E-05	-1.240264554	0.239885887	-2.168350847	0.053336411
SKA3	ENSG00000165480	42.71671211	-2.76239144	8.39846E-06	-1.013403176	0.294387096	-1.748988265	0.035870402
DDIAS	ENSG00000165490	31.89775437	-1.562654189	0.080311277	-0.150371602	0.968636316	-1.412282587	0.165793591
HPRT1	ENSG00000165704	190.631035	-0.813766904	0.050719328	-0.899708136	0.020417501	0.085941232	0.999167959
E2F7	ENSG00000165891	9.300076104	-6.962164188	0.001406196	-1.974122344	0.309632853	-4.988041844	0.097061223
PACSIN3	ENSG00000165912	34.56293956	-1.218626526	0.260617011	0.410433047	0.87180915	-1.629059572	0.037822115
CCT2	ENSG00000166226	569.0549994	-0.606600951	0.089268814	-0.516131236	0.188548171	-0.084469715	0.999167959
WEE1	ENSG00000166483	33.09503835	-1.752069986	0.018456583	-0.75862979	0.602497907	-0.993440196	0.596196596
MCM7	ENSG00000166508	264.1201587	-2.081295666	8.75952E-13	-1.188634163	0.000334754	-0.892661503	0.037822115
PCLAF	ENSG00000166803	30.42153816	-2.752808115	0.000120928	-1.368022727	0.129177936	-1.384785388	0.357989388
CDT1	ENSG00000167513	98.66230154	-2.160771412	2.52538E-08	-0.842441171	0.132052917	-1.318330241	0.008684194
TK1	ENSG00000167900	218.3621277	-3.300875322	1.88935E-26	-1.199742476	0.000338644	-2.101132847	5.78018E-10
PBK	ENSG00000168078	48.79946293	-3.544693678	3.41705E-10	-1.919099451	0.000387817	-1.625594227	0.068067492
DTYMK	ENSG00000168393	113.6850636	-2.114840494	1.98131E-09	-1.448235629	0.00011497	-0.666604865	0.530419745
FEN1	ENSG00000168496	57.21504079	-1.808911778	0.000497585	-1.151595085	0.072412309	-0.657316693	0.866856936
BUB1	ENSG00000169679	36.50931751	-3.202335107	1.18389E-06	-1.519753064	0.040960707	-1.682582043	0.101738766
HNRNPF	ENSG00000169813	565.4856484	-0.470626685	0.356256391	-0.680191456	0.044412621	0.209564772	0.999167959
HNRNPA3	ENSG00000170144	373.7305445	-0.641168098	0.089495064	0.12335408	0.938158496	-0.764522178	0.021673011
CDK1	ENSG00000170312	165.8937918	-3.137653996	6.55409E-19	-1.232324811	0.002295075	-1.905329186	2.55712E-06
CDCA4	ENSG00000170779	16.90269843	-2.830129543	0.012900313	-0.483174318	0.900017404	-2.346955225	0.087579394
SHCBP1	ENSG00000171241	17.08918113	-4.330531797	0.001229443	-0.507574145	0.888284538	-3.822957652	0.01271735
RRM2	ENSG00000171848	71.36019407	-4.368778672	8.97882E-15	-0.771421891	0.304467852	-3.597356781	1.75746E-09
CKS1B	ENSG00000173207	217.9797632	-1.667341912	1.12499E-08	-0.606011302	0.211852723	-1.061330609	0.003287186
CBX2	ENSG00000173894	54.39193797	-1.250660802	0.089268814	-0.064129473	0.984287455	-1.186531329	0.132955959
EXO1	ENSG00000174371	21.12240166	-3.819832448	0.000103269	-1.131311127	0.426420048	-2.688521321	0.036683575
UBE2C	ENSG00000175063	151.2728391	-3.660748512	5.52462E-26	-1.466669603	1.41267E-05	-2.194078908	1.77369E-08
RMI2	ENSG00000175643	54.87630287	-1.906508509	0.000379368	-1.198288831	0.0704595	-0.708219678	0.818200975
SFN	ENSG00000175793	124.2139324	-0.94830052	0.038493456	-0.325934031	0.802658022	-0.622366489	0.488651405
LMNB2	ENSG00000176619	44.56006434	-2.092636619	0.000189203	-1.093117577	0.142986931	-0.999519043	0.4555897713
POLE	ENSG00000177084	26.00572897	-1.901086582	0.031610352	-0.345395753	0.915395718	-1.555690829	0.161289532
BEND3	ENSG00000178409	11.0884267	-2.687141318	0.09435968	-1.610870894	0.434324757	-1.076270424	0.999167959
AURKB	ENSG00000178999	22.33548203	-4.028755208	4.29922E-05	-1.484727822	0.186248804	-2.544027386	0.068522727
RTKN2	ENSG00000182010	25.96314987	-1.757072032	0.056551871	-0.766782202	0.673636182	-0.99028983	0.755612163
KPNA2	ENSG00000182481	407.9091275	-2.04427972	1.67512E-16	-1.325699593	8.24412E-07	-0.718580127	0.070364308
SKA2	ENSG00000182628	372.5580854	-0.747757172	0.026657292	0.056954817	0.972659436	-0.804711989	0.014611375
TRAIP	ENSG00000183763	9.604778726	-3.175248043	0.07409292	-0.965791061	0.799622058	-2.209456982	0.535835485
IQGAP3	ENSG00000183856	10.16937765	-4.087865768	0.049516037	-0.364743059	0.957074456	-3.723122709	0.112769546
KNTC1	ENSG00000184445	17.88797119	-2.440574283	0.029111008	-0.967788397	0.659505752	-1.472785885	0.582020906
CDCA2	ENSG00000184661	14.84768187	-2.251137938	0.074490036	-1.39805166	0.404883168	-0.853086278	0.999167959
H1-10	ENSG00000184897	77.87644175	-1.840783718	0.000533825	-0.659151511	0.587078205	-1.181632207	0.126433592
SIVA1	ENSG00000184990	472.8074953	-0.887902808	0.003074756	-0.844928074	0.007877086	-0.042974733	0.999167959
UBALD2	ENSG00000185262	65.16439597	-1.208462892	0.049028354	-0.650634663	0.534422988	-0.557828229	0.917762673
KIF18B	ENSG00000186185	11.03926684	-5.475111501	0.023284565	-0.964287298	0.763711596	-4.510824203	0.137165369
ERCC6L	ENSG00000186871	12.88592364	-4.711635829	0.009477083	-1.089068659	0.734012773	-3.62256717	0.133370837
RPS19BP1	ENSG00000187051	135.6899937	-0.894299401	0.047294649	-0.465985831	0.580201171	-0.42831357	0.897126282
TUBB4B	ENSG00000188229	57.5880111	-1.491067457	0.010121378	-1.252025882	0.050211193	-0.239041575	0.999167959
H2AX	ENSG00000188486	159.3947178	-1.417329486	3.65069E-05	-0.978258876	0.016397548	-0.43907061	0.889135838
FAM111B	ENSG00000189057	15.21719166	-4.959061056	0.001704935	-1.076338408	0.602244183	-3.882722648	0.051078116
H1-0	ENSG00000189060	115.487889	-1.564484649	5.31473E-05	-0.42480247	0.698650159	-1.139682178	0.016817854
HMGB1	ENSG00000189403	2621.238225	-1.326178124	2.3653E-09	-0.413755256	0.369850133	-0.912422868	0.000439346
TUBB	ENSG00000196230	521.6881032	-1.24964218	2.13123E-06	-0.733627316	0.03136697	-0.516014864	0.378497373
PPP1R26	ENSG00000196422	13.06952655	-1.807536792	0.28467794	-2.718689275	0.03136697	0.911152483	0.999167959
FAM72A	ENSG00000196550	10.84702517	-4.642749814	0.008745832	-1.817939466	0.289232675	-2.824810348	0.447959203
XRCC2	ENSG00000196584	26.53219183	-2.458100098	0.003399481	-0.55841754	0.831762623	-1.899682558	0.074786065
H4C3	ENSG00000197061	133.2347751	-2.622959538	0.003598391	-1.361863567	0.381628929	-1.261095971	0.654059639
BLM	ENSG00000197299	11.61159032	-2.45432627	0.098347856	-1.1884548	0.622970159	-1.26587147	0.920772592
MCMBP	ENSG00000197771	95.55146946	-1.008616226	0.057580993	-0.765202795	0.236392543	-0.243413431	0.999167959
GRK6	ENSG00000198055	49.26349971	-1.222034998	0.095328798	-0.27484661	0.915395718	-0.947188388	0.40741566
WDHD1	ENSG00000198554	49.71565252	-2.044918987	0.00020955	-0.393636127	0.840953301	-1.65128286	0.010944505
ARHGAP11A	ENSG00000198826	14.55753449	-2.395928353	0.059873327	-0.970111092	0.695193067	-1.425817261	0.705458127
HMGN2	ENSG00000198830	1679.611146	-0.659542931	0.012728019	-0.543514746	0.074669816	-0.116028185	0.999167959
CENPW	ENSG00000203760	40.08804455	-1.764646948	0.013613792	-0.583969987	0.759239794	-1.180676962	0.325601577
MZT1	ENSG00000204899	102.7445276	-1.043521896	0.034583708	-0.711901065	0.28814927	-0.331620831	0.999167959
MXD3	ENSG00000213347	13.06135914	-4.389696818	0.002382071	-2.228533476	0.094063916	-2.161163343	0.631295112
FAM72D	ENSG00000215784	10.94097875	-3.277072843	0.02326874	-1.84744502	0.265133008	-1.429627823	0.932368884
DHFR	ENSG00000228716	88.50138864	-3.264553028	9.67083E-16	-1.833387814	3.57945E-06	-1.431165214	0.014421716
KIFC1	ENSG00000237649	26.72261361	-3.409527427	3.27815E-05	-1.092575072	0.381047496	-2.316952355	0.031518421
H2AJ	ENSG00000246705	329.1826861	-0.609618629	0.211939085	0.098160776	0.960665079	-0.707779406	0.093922789
MIR924HG	ENSG00000267374	9.764157609	-3.834142639	0.026882042	-1.47317499	0.531110701	-2.360967648	0.561180904
U2AF1L5	ENSG00000275895	101.5487896	-0.749453612	0.242258486	-0.881361031	0.090202432	0.131907419	0.999167959
UHRF1	ENSG00000276043	13.99623197	-3.134340123	0.018456583	-1.621311146	0.363795151	-1.513028976	0.82056797

Cluster 2

			TvsC		RvsC		RvsT	
	ensembl	baseMean	log2FoldChange	padj	log2FoldChange	padj	log2FoldChange	padj
CYP26B1	ENSG00000003137	13.6978726	2.14737154	0.15152527	-3.1772357	0.21454938	5.32460723	0.0017265
SLC7A2	ENSG00000003989	46.223458	1.47867713	0.01956541	-1.4400218	0.08328981	2.91869893	8.1387E-08
ADIPOR2	ENSG00000006831	144.925681	0.7112625	0.20118287	-0.7117395	0.21412154	1.42300199	6.6503E-05
PLEKHO1	ENSG00000023902	22.0629789	-1.6299828	0.11943264	-1.680398	0.08276078	0.05041521	0.99916796
GAB2	ENSG00000033327	32.0173578	-1.7213728	0.13534218	-2.3682987	0.01108551	0.64692594	0.99916796
FOXC1	ENSG00000054598	9.42615624	0.18799252	0.9918095	-3.9642084	0.06405917	4.15220092	0.04808417
PKP2	ENSG00000057294	36.3299489	0.01931114	0.99826494	-1.4145799	0.09405368	1.43389101	0.09769972
MPPED2	ENSG00000066382	12.4250362	0.35481132	0.98719604	-4.2792382	0.02325105	4.63404952	0.01109645
ISOC1	ENSG00000066583	63.0657969	-0.7073225	0.50631178	-1.1819736	0.04094395	0.47465114	0.99197842
GAL	ENSG00000069482	26.2941121	-1.4209938	0.17909286	-1.9120321	0.02289114	0.49103835	0.99916796
ARHGAP10	ENSG00000071205	19.8587312	0.56887753	0.95055897	-2.4276106	0.04935332	2.99648817	0.00504838
FERMT2	ENSG00000073712	51.5581182	-0.1693999	0.99009685	-1.2235529	0.07035802	1.05415301	0.21072568
TIPIN	ENSG00000075131	28.0306119	-1.3149188	0.21919183	-1.5256074	0.08810571	0.21068864	0.99916796
MBNL3	ENSG00000076770	17.8265157	0.31387506	0.98635944	-3.2113666	0.00787709	3.52524163	0.00219399
PGR	ENSG00000082175	25.6952459	1.01448382	0.54712586	-0.9900121	0.58584187	2.00449589	0.017549
ITGB5	ENSG00000082781	109.561175	0.00705635	0.99915118	-1.0664095	0.03136697	1.0734658	0.03207643
FAT1	ENSG00000083857	29.8172505	0.75662558	0.76517221	-1.180547	0.35501337	1.93717257	0.01524045
NRCAM	ENSG00000091129	38.3666579	0.95317794	0.42719524	-2.006883	0.0103917	2.96006096	2.5571E-06
CDV3	ENSG00000091527	443.135798	-0.5965031	0.15119896	-0.9549993	0.00132659	0.35849614	0.84391307
LGALS1	ENSG00000100097	226.540728	0.38405381	0.7268427	-0.6183789	0.21948913	1.00243275	0.00469874
ITPK1	ENSG00000100605	137.311873	0.6942835	0.22409394	-0.2969751	0.83768458	0.9912586	0.01841622
MTHFD1	ENSG00000100714	101.797014	-0.9703103	0.07737353	-1.0015873	0.05876814	0.03127697	0.99916796
BMP7	ENSG00000101144	201.911238	-0.2119467	0.95511564	-1.0256189	0.00549068	0.81367218	0.06581915
SGCG	ENSG00000102683	50.8849721	-0.4701377	0.90164217	-1.3798073	0.04248603	0.90966965	0.50231785
RUNDC3B	ENSG00000105784	10.7605635	-0.0337535	0.99826494	-2.9084461	0.07241231	2.87469258	0.0902667
CAV2	ENSG00000105971	17.2233597	0.77735673	0.8984458	-1.6858237	0.32988421	2.4631804	0.03795542
CAV1	ENSG00000105974	32.556478	0.88267543	0.57146488	-3.7677218	7.6142E-05	4.65039722	9.8303E-08
BLVRA	ENSG00000106605	105.272283	-0.2907279	0.94207241	-0.8956036	0.08276078	0.60487566	0.58767989
SPIN1	ENSG00000106723	70.7570834	0.05441641	0.99572019	-1.1601799	0.0686344	1.21459628	0.05275485
PLGRKT	ENSG00000107020	78.5383264	0.34767961	0.93001315	-0.9368652	0.15389916	1.28454483	0.01357014
PDLIM1	ENSG00000107438	91.9048424	-0.0073636	0.99915118	-1.2819672	0.00776066	1.2746036	0.00910533
SMC3	ENSG00000108055	135.220718	-0.8604117	0.07342183	-0.9109261	0.04488584	0.05051434	0.99916796
SLC9A3R1	ENSG00000109062	260.895563	0.61750402	0.27662571	-0.4563222	0.55926761	1.07382626	0.00320445
COL12A1	ENSG00000111799	22.494316	1.78657649	0.05993932	-1.9568291	0.15508934	3.74340563	1.4946E-05
CAP2	ENSG00000112186	56.9096432	0.66562323	0.66931527	-0.6960208	0.59858277	1.36164401	0.03566467
IFT57	ENSG00000114446	51.6243816	0.18701969	0.9872657	-1.1438894	0.10952393	1.33090913	0.03841544
EFEMP1	ENSG00000115380	71.5071219	0.06052953	0.9955656	-2.0274549	3.6452E-05	2.08798444	1.4946E-05
IGFBP2	ENSG00000115457	74.4930237	-0.165368	0.98862616	-1.2875631	0.01985014	1.12219512	0.07203319
ID2	ENSG00000115738	181.547535	0.38565903	0.74634456	-0.3833969	0.66779246	0.76905595	0.07638144
EPHA4	ENSG00000116106	10.8334378	0.08719352	0.99826494	-4.2278352	0.03775685	4.31502875	0.03476058
C1orf21	ENSG00000116667	15.1911412	0.02860555	0.99826494	-3.395311	0.01028125	3.42391656	0.01034502
PTPA	ENSG00000119383	220.600793	-0.2364761	0.94296487	-1.1265571	0.00062231	0.89008099	0.02047827
RAB14	ENSG00000119396	132.831376	-0.2513032	0.96318994	-1.0410858	0.06222247	0.78978257	0.36072058
OGFRL1	ENSG00000119900	33.6372573	-0.3694224	0.96239083	-1.6751427	0.0346208	1.30572024	0.22739104
TBX4	ENSG00000121075	7.46764833	0.91119618	0.93748704	-5.6877219	NA	6.59891808	0.00723292
NUP85	ENSG00000125450	101.696987	-0.751837	0.29041843	-0.9089704	0.09781307	0.1571334	0.99916796
EMG1	ENSG00000126749	66.8037735	-0.6055428	0.68540785	-1.170046	0.06025777	0.56450323	0.90808202
SGCE	ENSG00000127990	19.5938121	-0.9096616	0.73890762	-1.775837	0.09672732	0.8663221	0.96054818
PALLD	ENSG00000129116	27.575448	0.85081411	0.69660763	-0.8205823	0.68443382	1.67139638	0.06806749
PHF20L1	ENSG00000129292	61.6936248	-0.1567668	0.99046362	-1.3507058	0.03136697	1.19393899	0.09392279
ASS1	ENSG00000130707	258.7787	0.25314004	0.91378209	-1.3559076	4.8466E-06	1.60823765	7.2351E-09
TBC1D5	ENSG00000131374	83.7770317	0.39870693	0.88488774	-0.6346924	0.49615719	1.03339932	0.07458678
TUBG1	ENSG00000131462	69.7670912	-1.0758143	0.08949506	-1.031649	0.09886801	-0.0441653	0.99916796
NUP210	ENSG00000132182	99.5780773	-0.8725748	0.13900219	-0.9765034	0.06140065	0.10392863	0.99916796
ELP2	ENSG00000134759	218.94636	0.56256791	0.30630703	-0.4500017	0.50997208	1.01256957	0.00270928
RNFT2	ENSG00000135119	9.8376335	-2.5036077	0.13205995	-2.579956	0.08851527	0.07634837	0.99916796
PKIB	ENSG00000135549	140.91167	0.02559735	0.99826494	-3.2361274	5.8666E-15	3.26172473	1.902E-15
KCTD3	ENSG00000136636	109.260835	0.13436206	0.99009685	-0.8270623	0.14298693	0.96142436	0.06040653
CDK9	ENSG00000136807	33.1260773	-0.1038312	0.99224706	-1.4264777	0.09988051	1.32264654	0.18965867
ATP6V1G1	ENSG00000136888	427.736673	0.28795984	0.81567279	-0.4814607	0.29670415	0.76942058	0.01461137
DPM2	ENSG00000136908	76.4077044	-0.3492791	0.92450062	-1.0433611	0.0690079	0.69408191	0.57764721
NCBP1	ENSG00000136937	49.1284694	-0.5088484	0.85799218	-1.2079252	0.09406392	0.69907678	0.81809203
ANP32B	ENSG00000136938	823.409799	-0.7384125	0.02924181	-0.8870012	0.00397052	0.14858874	0.99916796
RPL35	ENSG00000136942	480.752839	0.57588684	0.40050062	-0.3090815	0.80361432	0.88496839	0.04091026
MYC	ENSG00000136997	273.625559	0.58294493	0.22257304	-0.1796882	0.90206625	0.76263318	0.04107414
PCDH10	ENSG00000138650	8.61720938	0.38066189	0.99034815	-3.7553848	NA	4.13604666	0.07168257
PPA2	ENSG00000138777	198.79929	-0.221585	0.95208484	-0.7749604	0.06486897	0.55337541	0.45892691
COMMD4	ENSG00000140365	154.473199	-0.7847904	0.09686895	-0.715835	0.14350039	-0.0689553	0.99916796
BCAS3	ENSG00000141376	1594.8371	-0.1857039	0.94614772	-0.5732364	0.09435098	0.38753244	0.62086516
SLC39A6	ENSG00000141424	1305.93356	0.4127752	0.40255637	-0.5130345	0.15389916	0.92580971	0.00024586
IGFBP4	ENSG00000141753	238.425136	0.6019575	0.21406672	-0.5741017	0.25966212	1.17605918	0.00013929
ITGB3BP	ENSG00000142856	32.9240999	-1.6802243	0.0204423	-1.6532297	0.02233284	-0.0269946	0.99916796
HMCN1	ENSG00000143341	12.3033148	-0.2587734	0.99046362	-3.9838722	0.01341161	3.72509882	0.03030085
SLC4A10	ENSG00000144290	20.6563062	0.43936547	0.97068972	-1.7722294	0.21255078	2.21159486	0.06034413
RPL32	ENSG00000144713	3710.41367	0.62323287	0.21919183	-0.4025571	0.6174896	1.02579001	0.00350004
AOPEP	ENSG00000148120	125.485086	0.26029884	0.94614772	-1.2874726	0.00151487	1.54777146	3.0398E-05
POLE3	ENSG00000148229	100.61975	-0.6223132	0.45968825	-0.985758	0.04488584	0.36344487	0.99916796
SURF4	ENSG00000148248	167.616806	0.19007528	0.9679126	-0.7813493	0.1089423	0.97142461	0.02167301
SURF1	ENSG00000148290	119.240939	0.34731191	0.87163572	-0.804273	0.13205292	1.15158486	0.00580528
SURF6	ENSG00000148296	78.212425	0.27380743	0.96318994	-1.0224672	0.13777734	1.29627459	0.02547928
RPL7A	ENSG00000148303	3323.09612	0.391075	0.36714186	-0.8965	6.321E-05	1.28757504	2.1473E-10
GFRA1	ENSG00000151892	283.744	0.6572669	0.16535652	-1.3931124	1.3361E-05	2.05037929	4.5232E-13
BAG3	ENSG00000151929	117.700338	0.30996541	0.91596763	-1.0274118	0.02726978	1.33737726	0.00075816
PLOD2	ENSG00000152952	28.7710104	0.05538084	0.99782947	-2.2247077	0.00631438	2.27675058	0.00478385
RPUSD3	ENSG00000156990	104.187883	0.29749601	0.94614772	-0.7972274	0.24210963	1.0947338	0.03668646
SEC13	ENSG00000157020	179.438639	-0.4709663	0.5946833	-0.9069785	0.02587108	0.43601214	0.8266833
ATP5MC1	ENSG00000159199	349.531399	0.04634634	0.99385117	-0.7088546	0.06485898	0.75520096	0.0426651
CIART	ENSG00000159208	17.7911955	-0.7529858	0.87163572	-2.280146	0.03299156	1.52716017	0.45892691
THEM4	ENSG00000159445	23.2942446	0.55277235	0.94614772	-1.4750314	0.30487037	2.0278037	0.0557966
TFF1	ENSG00000160182	2408.20031	1.02457986	0.0005638	-0.5034075	0.3449969	1.52798739	1.3902E-08
VPS28	ENSG00000160948	264.782063	0.47322625	0.46946384	-0.4030775	0.5810523	0.87630376	0.01125738
RPL8	ENSG00000161016	6792.52051	0.10384777	0.98126742	-0.5384762	0.0637899	0.64232395	0.0148938
RHOBTB3	ENSG00000164292	247.050229	0.5502949	0.35920762	-0.9566208	0.01028125	1.50691567	5.3358E-07
TNFRSF11B	ENSG00000164761	6.74098154	-0.1387294	0.99572019	-6.1393268	NA	6.00059742	0.0242721
CFL2	ENSG00000165410	67.2732997	-0.1510423	0.99046362	-1.2440655	0.04008556	1.09302325	0.11562555
RET	ENSG00000165731	34.7268332	0.55363652	0.89000217	-0.9280337	0.4885533	1.48167026	0.0755664
HDGFL3	ENSG00000166503	133.757997	-0.2160824	0.96324136	-0.8774406	0.07222301	0.66135821	0.40854658
FILIP1L	ENSG00000168386	8.50739663	0.49566613	0.98162257	-3.6680808	NA	4.16374697	0.06331644
AFAP1L2	ENSG00000169129	14.6892068	0.96060199	0.80664178	-4.1588728	0.02708748	5.11947474	0.00217873
UBE2V2	ENSG00000169139	224.502967	-0.6497897	0.21919183	-1.1584682	0.00082202	0.5086785	0.6302309
C15orf40	ENSG00000169609	65.2991847	0.495381	0.81567279	-0.7453711	0.42975904	1.24075206	0.03207643
CENPX	ENSG00000169689	403.097503	-0.5089165	0.3019779	-0.6365715	0.0865939	0.12765501	0.99916796
ALCAM	ENSG00000170017	141.938137	1.02587536	0.02267511	-0.2105477	0.91539572	1.23642301	0.00270928
LSM3	ENSG00000170860	309.38007	-0.305203	0.90633627	-0.8128316	0.08366151	0.50762852	0.69403812
TMEM43	ENSG00000170876	47.5962256	0.52242301	0.84764743	-0.7339545	0.56711473	1.25637748	0.07711307
PKIA	ENSG00000171033	42.2971808	-0.3587604	0.95511564	-2.6730381	1.239E-05	2.31427767	0.00039615
JAGN1	ENSG00000171135	109.346995	-0.0859935	0.99143407	-0.9432981	0.09742573	0.85730469	0.21072568
TADA3	ENSG00000171148	165.575427	-0.1353821	0.98719604	-0.8920027	0.04386944	0.75662062	0.15834814
CXXC5	ENSG00000171604	80.5689899	0.3151553	0.94614772	-0.7809618	0.31326153	1.09611715	0.05292628
BCL2	ENSG00000171791	50.1711831	0.63986506	0.71552206	-1.0269322	0.25016443	1.66679729	0.00578924
RPL15	ENSG00000174748	3418.23008	0.25963765	0.7758874	-0.3672703	0.39448311	0.62690799	0.0216730
PDZK1	ENSG00000174827	15.4711706	2.13491146	0.08001514	-1.7410169	0.46631529	3.87592832	0.00054772
CYC1	ENSG00000179091	845.508202	-0.2677902	0.8104116	-0.9674153	7.1109E-05	0.69962511	0.01658973
MAF1	ENSG00000179632	174.387965	0.06360485	0.9918095	-0.8274288	0.06452385	0.89103361	0.03761538
PUF60	ENSG00000179950	426.953682	-0.2768417	0.87259471	-0.7689207	0.03136697	0.492079	0.4886886
DHTKD1	ENSG00000181192	68.8729831	-1.071174	0.07726039	-1.2067451	0.02793598	0.1355711	0.99916796
LDOC1	ENSG00000182195	287.555746	0.37798116	0.71332645	-0.5446105	0.31050646	0.92259165	0.00086556
CRIP2	ENSG00000182809	470.799513	-0.1188761	0.98162257	-0.761129	0.01509941	0.64225292	0.07537042
CADM1	ENSG00000182985	17.1277652	0.94904938	0.77273838	-1.8172857	0.24233051	2.7663351	0.01061702
PSMG1	ENSG00000183527	72.0923293	-0.9579231	0.12912576	-1.0610667	0.06086687	0.10314365	0.99916796
SOCS3	ENSG00000184557	31.379425	1.46212118	0.12208211	-0.4591938	0.89003884	1.92131497	0.01357014
LUZP2	ENSG00000187398	16.6292708	-0.4747604	0.96520344	-5.117553	0.00168603	4.64279257	0.00886556
THSD4	ENSG00000187720	31.0529286	1.50103335	0.10676681	-0.6173331	0.82220881	2.11836642	0.0053909
C9orf152	ENSG00000188959	23.3662645	-0.5937302	0.93312265	-2.2911136	0.01874403	1.69738344	0.21695855
GREB1	ENSG00000196208	125.388449	0.94455095	0.03662609	-1.2433269	0.00442325	2.18787782	2.1473E-10
CD47	ENSG00000196776	364.852298	0.4283827	0.52372175	-1.0485732	0.00036688	1.47695586	1.3902E-08
ANXA6	ENSG00000197043	89.2127603	0.71537205	0.35413024	-2.5054346	2.8856E-08	3.22080665	6.958E-15
S100A10	ENSG00000197747	1175.02324	0.7773628	0.00283678	-1.501744	1.2999E-11	2.27910684	2.8911E-28
GPAA1	ENSG00000197858	309.497506	-0.1950027	0.95382929	-0.9071934	0.00442325	0.71219077	0.06337537
RPL12	ENSG00000197958	3160.39766	0.59692937	0.0953288	-0.1130333	0.94274862	0.70996268	0.02678767
TFDP1	ENSG00000198176	70.4051663	-0.6555562	0.58637999	-1.1091509	0.06967482	0.45359472	0.99916796
TMSB4X	ENSG00000205542	2091.39465	0.26273694	0.79001993	-0.3630844	0.42975904	0.62582137	0.03071204
SMIM30	ENSG00000214194	104.804183	0.60230653	0.52912871	-0.5798479	0.52103899	1.18215447	0.0108655
FGD5-AS1	ENSG00000225733	240.166451	-0.3022921	0.84764743	-1.2021832	7.8448E-05	0.89989115	0.01301409
PRKDC	ENSG00000253729	62.1770384	0.2773577	0.9679126	-0.9419677	0.29247928	1.21932537	0.08530223
BRK1	ENSG00000254999	520.964691	0.53242528	0.25917644	-0.290034	0.75571736	0.82245926	0.01246779
CD24	ENSG00000272398	315.773765	0.69289257	0.13115835	-2.4573933	4.1913E-16	3.15028589	2.8911E-28

Cluster 3

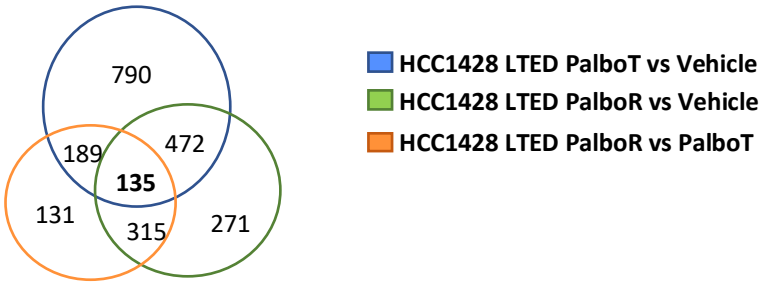
			TvsC		RvsC		RvsT	
	ensembl	baseMean	log2FoldChange	padj	log2FoldChange	padj	log2FoldChange	padj
GRN	ENSG00000030582	393.545924	0.71269497	0.09834786	0.5168401	0.38079345	0.19585487	0.99916796
SPATA7	ENSG00000042317	13.5593243	2.60585646	0.08698126	2.19748425	0.21268628	0.40837221	0.99916796
EIF4B	ENSG00000063046	195.005814	1.19254964	0.0003305	0.74850835	0.09886801	0.44404129	0.72696498
EPS15	ENSG00000085832	142.524579	0.88445516	0.07823809	0.36135801	0.787463	0.52309715	0.69622513
NRP1	ENSG00000099250	37.0106645	1.63513453	0.05987333	0.58127182	0.82441185	1.05386272	0.49713762
ZC3H7B	ENSG00000100403	54.1943963	1.13613835	0.20118287	1.35609055	0.06140065	-0.2199522	0.99916796
MAGED2	ENSG00000102316	222.597515	0.76201953	0.09145285	0.45330507	0.55716729	0.30871446	0.99916796
EIF3E	ENSG00000104408	1099.17092	0.63717044	0.03426511	0.17675788	0.8683783	0.46041256	0.32923623
ZKSCAN1	ENSG00000106261	123.793281	1.029542	0.02924181	0.93441791	0.06730425	0.0951241	0.99916796
RPL28	ENSG00000108107	2581.75682	0.63158829	0.08031128	0.48474782	0.2929345	0.14684046	0.99916796
INPP4B	ENSG00000109452	139.59607	0.89438801	0.05110012	0.29785813	0.83782654	0.59652989	0.46690257
RAB5B	ENSG00000111540	127.977966	0.94074926	0.07052419	0.49327455	0.63270515	0.44747471	0.90359062
STC2	ENSG00000113739	318.955687	1.38140327	1.7674E-07	0.07837798	0.96728224	1.30302529	1.3229E-06
MXD4	ENSG00000123933	139.920276	1.10891412	0.01373295	1.03041512	0.03136697	0.078499	0.99916796
MYO1B	ENSG00000128641	182.992898	0.87828177	0.05352682	0.82859291	0.07692832	0.04968886	0.99916796
RARA	ENSG00000131759	59.505321	1.17952654	0.06681332	0.14486363	0.96547794	1.03466291	0.14289565
GSTM3	ENSG00000134202	62.0657311	1.04738332	0.28156035	1.24588981	0.09886801	-0.1985065	0.99916796
CCNG2	ENSG00000138764	87.2346729	1.17392028	0.02092886	1.21675974	0.01551567	-0.0428395	0.99916796
ANXA3	ENSG00000138772	10.3776985	2.38242706	0.15152527	-1.96035973	0.60792838	4.3430244	0.00679277
PTPRF	ENSG00000142949	269.481645	0.79238882	0.03849346	0.65083489	0.14350039	0.14165393	0.99916796
TACC1	ENSG00000147526	187.9572	0.86285142	0.0591731	0.84437487	0.06730425	0.01847655	0.99916796
ANKRD1	ENSG00000148677	135.004363	1.47183656	0.00089217	1.5054913	0.00081438	-0.0336547	0.99916796
PRSS23	ENSG00000150687	121.327242	1.08063451	0.01272802	0.65534445	0.33753668	0.42529006	0.90148238
FREM2	ENSG00000150893	102.680115	1.15188452	0.01195313	0.51695749	0.6174896	0.63492703	0.50989102
CRIM1	ENSG00000150938	66.9894215	1.61077811	0.00145453	1.1744569	0.06835997	0.43632121	0.99916796
SFXN2	ENSG00000156398	60.6470877	1.36277764	0.01956541	0.18585384	0.95703814	1.1769238	0.06266082
TFF3	ENSG00000160180	147.792542	1.14169491	0.01459754	0.81671565	0.18348396	0.32497925	0.99916796
RPL29	ENSG00000162244	1389.0008	0.6161544	0.07619292	0.31133582	0.66077215	0.30481858	0.90808202
S100A11	ENSG00000163191	1550.36936	0.65381457	0.01866092	0.4612648	0.21412154	0.19254977	0.99916796
NPY1R	ENSG00000164128	78.330265	1.33617591	0.0170885	1.3606445	0.01509941	-0.0244686	0.99916796
CITED2	ENSG00000164442	193.129552	1.2951341	5.4399E-05	0.92009166	0.0204175	0.37504244	0.89712628
MOAP1	ENSG00000165943	111.746939	0.91121745	0.08659737	0.62878212	0.4108 16	0.28243533	0.99916796
TUBA1A	ENSG00000167552	132.617087	0.76791377	0.30644484	0.99234474	0.06967482	-0.224431	0.99916796
EEF2	ENSG00000167658	1757.62793	0.81446251	0.00171301	0.55068976	0.11001501	0.26377275	0.96147648
NPNT	ENSG00000168743	213.453446	0.97920239	0.01052931	0.40409654	0.6644821	0.57510585	0.44470877
CLIC3	ENSG00000169583	165.828162	1.56760181	4.3777E-06	1.2065805	0.00197544	0.36102131	0.96054818
KRT86	ENSG00000170442	15.3024426	2.18252086	0.24967677	2.85182757	0.0427577	-0.6693067	0.99916796
KRT19	ENSG00000171345	2763.24646	0.76409881	0.00921545	0.3842434	0.48409289	0.37985541	0.68407384
SEZ6L2	ENSG00000174938	135.486822	0.90578954	0.0953288	1.03493762	0.03136697	-0.1291481	0.99916796
RPL35A	ENSG00000182899	3646.76687	0.67485456	0.16799018	0.88147682	0.02289114	-0.2066223	0.99916796
ABAT	ENSG00000183044	85.0643973	1.79330449	9.136E-05	0.83476328	0.32131496	0.95854121	0.14199278
ACTG1	ENSG00000184009	2373.13188	0.57575491	0.09763186	0.51410644	0.17195697	0.06164848	0.99916796
TACSTD2	ENSG00000184292	355.016055	0.91049026	0.00409324	0.83434481	0.01561582	0.07614544	0.99916796
COMMD6	ENSG00000188243	214.964936	0.88673126	0.07231948	0.31836161	0.82281979	0.56836965	0.59033491
S100A6	ENSG00000197956	1213.45496	0.85542768	0.05095333	0.80166612	0.07966469	0.05376156	0.99916796
H2AC18	ENSG00000203812	58.3454829	1.97759925	0.00039331	1.387656	0.05447255	0.58994325	0.8983129
DSCAM-AS1	ENSG00000235123	765.180665	0.64857255	0.03574807	0.38050388	0.45806835	0.26806867	0.95866722
C4orf48	ENSG00000243449	153.900267	0.97359645	0.05655187	0.5645392	0.52103899	0.40905725	0.96092231
TXNIP	ENSG00000265972	199.149781	0.7931225	0.05620111	0.25774894	0.84290115	0.53537357	0.47289979
SNHG8	ENSG00000269893	225.659389	1.2378742	5.2709E-05	0.68504433	0.12896106	0.55282987	0.37572316
H2AC19	ENSG00000272196	55.7709238	1.478117	0.04292623	1.3166886	0.0953743	0.1614284	0.99916796

Cluster 4

			TvsC		RvsC		RvsT	
	ensembl	baseMean	log2FoldChange	padj	log2FoldChange	padj	log2FoldChange	padj
TNFRSF12A	ENSG00000006327	191.930465	0.25410054	0.9351783	0.84671133	0.03136697	-0.5926108	0.33108385
SCIN	ENSG00000006747	128.552059	0.48182954	0.72736775	1.38229755	0.00045493	-0.900468	0.06891555
CYB561	ENSG00000008283	394.49431	-0.0297372	0.99605943	0.63092938	0.10041707	-0.6606666	0.08842529
CD9	ENSG00000010278	695.604018	0.22731228	0.90010323	0.65092071	0.03551947	-0.4236084	0.47289979
IDS	ENSG00000010404	62.4309428	-0.1168256	0.99122235	1.20399286	0.04362089	-1.3208184	0.01865712
HEBP1	ENSG00000013583	326.832187	0.21378652	0.9465809	1.61186872	5.7412E-10	-1.3980822	1.0425E-07
GPRC5A	ENSG00000013588	20.5162779	1.74505139	0.25497883	2.59221841	0.01179314	-0.847167	0.90940696
CYBA	ENSG00000051523	399.135976	0.46598016	0.51286421	0.81584362	0.02289114	-0.3498635	0.90101819
ZNF275	ENSG00000063587	14.134925	0.94463757	0.90832822	2.52908051	0.06086687	-1.5844429	0.4479592
EYA2	ENSG00000064655	16.7488203	-0.9624357	0.84839213	1.23259949	0.48943371	-2.1950352	0.06907915
BCAS1	ENSG00000064787	78.5995884	0.72524968	0.58710631	1.82389401	0.00031113	-1.0986443	0.0902667
FAM107B	ENSG00000065809	55.6300341	1.11727904	0.21167422	1.27959367	0.08451747	-0.1623146	0.99916796
ARFGEF1	ENSG00000066777	44.3605984	-0.215544	0.98879101	1.31045337	0.07523904	-1.5259973	0.02417827
MTFR1	ENSG00000066855	110.100637	0.11933307	0.99046362	0.85337985	0.09742573	-0.7340468	0.25839266
TRAM1	ENSG00000067167	214.13092	-0.0995262	0.99046362	0.77707225	0.06140065	-0.8765985	0.02286118
ATP6AP1	ENSG00000071553	206.662716	0.43857421	0.78962175	1.08043404	0.0159678	-0.6418598	0.46690257
FAM50A	ENSG00000071859	135.107165	-0.2390672	0.95511564	0.62798667	0.31304884	-0.8679539	0.06869271
CYBRD1	ENSG00000071967	22.0948884	-0.7136673	0.91968631	1.6227054	0.14045187	-2.3363727	0.01308276
ACADVL	ENSG00000072778	83.9433788	0.57530391	0.66649101	0.98655592	0.08725786	-0.411252	0.99583809
PANX2	ENSG00000073150	17.5681105	-0.6145552	0.95511564	1.44591147	0.31304884	-2.0604666	0.06968757
TNRC6C	ENSG00000078687	37.4506882	0.5237334	0.94606876	1.57155793	0.08144806	-1.0478245	0.54094984
FAM234B	ENSG00000084444	58.277439	0.17764875	0.99009685	1.13314158	0.07762682	-0.9554928	0.22344174
FTL	ENSG00000087086	1364.4929	0.14842142	0.96231303	0.56453964	0.07222301	-0.4161182	0.44470877
LTBP4	ENSG00000090006	22.3815583	1.56520827	0.23465549	1.8428916	0.08154979	-0.2776833	0.99916796
YPEL3	ENSG00000090238	222.475109	0.47901955	0.56332404	0.80769926	0.05021193	-0.3286797	0.97139121
SCD	ENSG00000099194	1656.93527	0.57897812	0.08031128	1.4940631	5.5144E-12	-0.915085	0.00026724
ERMP1	ENSG00000099219	53.04701	0.74804135	0.60980993	1.48289427	0.01556629	-0.7348529	0.63496593
ZMYND8	ENSG00000101040	169.32632	0.48615512	0.64512434	1.27680587	0.00045493	-0.7906507	0.10318382
MID1	ENSG00000101871	20.9644605	1.3653502	0.44510201	1.99010075	0.06140065	-0.6247506	0.99916796
NAA10	ENSG00000102030	52.0226562	-0.3712251	0.95511564	0.99587922	0.25134766	-1.3671044	0.04950117
FMR1	ENSG00000102081	122.025349	0.22636793	0.96397328	0.95555587	0.04488584	-0.7291879	0.25746662
COTL1	ENSG00000103187	80.1308595	0.31326633	0.95511564	1.20056759	0.02898067	-0.8873013	0.22344174
QPRT	ENSG00000103485	161.777543	0.64651106	0.46757117	1.63894566	2.4545E-05	-0.9924346	0.03982408
AP3B2	ENSG00000103723	9.06961055	4.22100112	0.18584773	4.71295292	0.08451747	-0.4919518	0.99916796
LAPTM4B	ENSG00000104341	687.613589	-0.0414938	0.99421697	0.77686927	0.00962886	-0.8183631	0.00571652
TRPS1	ENSG00000104447	119.590175	0.3953657	0.86037728	1.19160047	0.00826503	-0.7962348	0.2015774
ECH1	ENSG00000104823	63.7926055	-0.4210265	0.91596763	0.72855223	0.44441205	-1.1495788	0.07696244
SLC1A5	ENSG00000105281	157.436972	-0.4898223	0.63831353	0.47374299	0.57061409	-0.9635653	0.02642004
DKK1	ENSG00000107984	626.983281	-0.0943926	0.98879101	0.78533447	0.00649017	-0.879727	0.00137696
RASD1	ENSG00000108551	8.50992756	-1.3271052	0.92896127	2.51234085	NA	-3.8394461	0.0409066
PMP22	ENSG00000109099	306.144909	-0.1641706	0.97068972	0.92573566	0.00780279	-1.0899063	0.00071277
UGDH	ENSG00000109814	272.553274	0.57405745	0.24921755	0.99972528	0.00151298	-0.4256678	0.66001103
CCND1	ENSG00000110092	259.099393	0.56216752	0.33283363	1.37918108	3.005E-06	-0.8170136	0.02546388
UPK2	ENSG00000110375	89.4296823	0.8928898	0.19791273	1.36683141	0.00414183	-0.4739416	0.90808202
KRT18	ENSG00000111057	1594.91384	0.54711289	0.12288541	1.3339817	2.795E-09	-0.7868688	0.00426238
VDR	ENSG00000111424	24.3993324	1.30525706	0.49947185	2.59133065	0.00288789	-1.2860736	0.3263161
BCL6	ENSG00000113916	113.48956	-0.1264735	0.99046362	0.97066184	0.08971304	-1.0971353	0.04107414
HES1	ENSG00000114315	76.7512667	0.19895715	0.98162257	0.9997212	0.09406392	-0.8007641	0.34293218
TANC1	ENSG00000115183	27.3509292	0.66424063	0.89619149	1.85839381	0.02793598	-1.1941532	0.34287609
PDE1A	ENSG00000115252	9.5149391	-0.2403875	0.99494981	3.36669583	0.05674764	-3.6070834	0.03364945
REEP6	ENSG00000115255	57.5023655	0.66963097	0.70284436	1.42619186	0.02011335	-0.7565609	0.58767989
DLX2	ENSG00000115844	13.0346754	-0.0712751	0.99826494	2.92000241	0.0233902	-2.9912775	0.01549816
RND3	ENSG00000115963	25.5539739	-0.7769609	0.85046541	1.35244619	0.21412154	-2.1294071	0.01308276
SUMO1	ENSG00000116030	368.627784	0.25273099	0.90832822	0.93561051	0.00287859	-0.6628795	0.07711307
FBXO2	ENSG00000116661	18.1631014	0.64332478	0.95258761	2.06002178	0.07523904	-1.416697	0.43866352
IFI27L2	ENSG00000119632	61.1844053	1.29233315	0.08031128	2.07620571	0.00011439	-0.7838726	0.54240256
MSX2	ENSG00000120149	68.5568681	0.0532583	0.99594398	1.13778731	0.05674764	-1.084529	0.07711307
EGR1	ENSG00000120738	54.4291993	0.58483573	0.82330065	1.84273533	0.00073314	-1.2578996	0.04573487
CHST3	ENSG00000122863	17.3856838	0.22215029	0.99175278	3.077326616	0.00735458	-2.8551759	0.01012351
HOXC11	ENSG00000123388	61.5000166	-0.4882637	0.86693389	0.9767189	0.16209698	-1.4649826	0.0085383
PREX1	ENSG00000124126	2366.55583	0.91234001	0.0002801	1.0306151	3.1989E-05	-0.1182751	0.99916796
PMEPA1	ENSG00000124225	35.6095335	1.6386943	0.05916607	2.14841572	0.00253027	-0.5097214	0.99916796
BST2	ENSG00000130303	21.4094026	-0.193967	0.99175278	2.79976748	0.00182623	-2.9937345	0.00052702
GDF15	ENSG00000130513	19.9203792	-0.2915446	0.99046362	2.86363159	0.00250589	-3.1551762	0.00054772
PGPEP1	ENSG00000130517	27.0660676	1.28515365	0.33614533	1.59669497	0.09672732	-0.3115413	0.99916796
SH3BGRL	ENSG00000131171	154.602211	0.87240658	0.09932473	1.11459933	0.01095217	-0.2421928	0.99916796
BTG1	ENSG00000133639	70.130954	0.74629576	0.54121214	1.98974849	1.9436E-05	-1.2434527	0.01827178
SLC38A2	ENSG00000134294	895.374649	0.6800144	0.01899666	1.12160348	1.7251E-06	-0.4415891	0.37860314
GOLM1	ENSG00000135052	56.0987748	0.11211324	0.99143407	1.40772614	0.01984407	-1.2956129	0.0373948
SYTL2	ENSG00000137501	166.364564	0.83185834	0.10506996	1.78273549	1.0971E-07	-0.9508772	0.02118655
FAM117B	ENSG00000138439	15.718041	2.19753406	0.18314023	2.56298006	0.06199157	-0.365446	0.99916796
ABI2	ENSG00000138443	47.0922567	0.21206148	0.98862616	1.53831612	0.01706684	-1.3262546	0.05433564
PPP3CA	ENSG00000138814	523.79092	0.53790808	0.18584773	0.82007721	0.00431144	-0.2821691	0.94850765
CLSTN3	ENSG00000139182	16.3748009	1.28010581	0.71900207	2.39581598	0.06835997	-1.1157102	0.83065528
DHX38	ENSG00000140829	60.4411682	0.43322981	0.91624978	1.36323429	0.02289114	-0.9300045	0.2777845
MAP1LC3B	ENSG00000140941	160.826724	0.59094252	0.39031592	0.82808945	0.06450662	-0.2371469	0.99916796
FKBP10	ENSG00000141756	99.86087	0.66027903	0.49113018	1.25384586	0.0068969	-0.5935668	0.6302309
IFITM3	ENSG00000142089	587.698508	0.44502083	0.44008578	0.67808659	0.04959417	-0.2330658	0.99916796

APP	ENSG00000142192	120.263506	0.39922568	0.83896715	0.93826246	0.05511695	-0.5390368	0.67053799
LMTK3	ENSG00000142235	89.184005	1.42010463	0.00409324	2.25272058	6.5522E-08	-0.832616	0.18283936
TUFT1	ENSG00000143367	42.9920383	0.87915214	0.55901914	1.36878392	0.07523904	-0.4896318	0.99916796
MCL1	ENSG00000143384	176.293494	0.44739332	0.65630399	0.83763346	0.04711173	-0.3902401	0.89281627
RIT1	ENSG00000143622	40.6676146	1.15510989	0.23016845	1.38461465	0.07074201	-0.2295048	0.99916796
SCCPDH	ENSG00000143653	162.36355	-0.2379011	0.9533381	0.67603196	0.17250814	-0.913933	0.0239667
CDC42BPA	ENSG00000143776	65.2157879	0.56767381	0.76989908	1.30593329	0.02090126	-0.7382595	0.5245579
UBXN4	ENSG00000144224	173.190261	0.28589325	0.92450062	0.9696473	0.01592918	-0.6837541	0.21864996
DLX1	ENSG00000144355	60.877146	-0.2454047	0.9765341	1.11312341	0.07250753	-1.3585281	0.01461137
ACKR3	ENSG00000144476	128.308512	-0.5909575	0.57604526	0.96346123	0.05568327	-1.5544188	0.00010436
LPP	ENSG00000145012	78.7592662	1.00546872	0.18314023	1.33872121	0.01984407	-0.3332525	0.99916796
KLHL8	ENSG00000145332	38.9911767	-0.8515449	0.63831353	0.84398569	0.48818828	-1.6955306	0.01892265
CAMK2D	ENSG00000145349	65.6875722	-0.0009371	0.99986776	1.87981152	7.8448E-05	-1.8807486	5.9565E-05
PNRC1	ENSG00000146278	107.037844	1.1254416	0.01845658	1.17199727	0.0128333	-0.0465557	0.99916796
CETN2	ENSG00000147400	74.2065045	0.53753759	0.77117485	1.25446769	0.01914253	-0.7169301	0.50026019
RPL10	ENSG00000147403	649.152982	0.36058821	0.65371235	0.86751846	0.00305445	-0.5069303	0.31372638
RPL7	ENSG00000147604	260.506856	0.45456813	0.61325359	0.91742286	0.01592918	-0.4628547	0.67853881
MTDH	ENSG00000147649	439.718126	-0.1823111	0.95511564	0.53744431	0.2011888	-0.7197554	0.03563592
POLR2K	ENSG00000147669	315.979761	-0.2913818	0.90452341	0.51678498	0.42296675	-0.8081668	0.0632387
TM7SF2	ENSG00000149809	234.308874	0.76930377	0.08930548	0.99696308	0.00776066	-0.2276593	0.99916796
HNMT	ENSG00000150540	20.3116537	0.28623733	0.99046362	2.33047863	0.01509941	-2.0442413	0.0332138
RILPL2	ENSG00000150977	50.1101897	1.00198813	0.31473939	1.55185166	0.01364574	-0.5498635	0.93798236
TMEM45B	ENSG00000151715	47.3365044	0.99797445	0.33852413	1.31300571	0.06972973	-0.3150313	0.99916796
MGAT5	ENSG00000152127	32.9076269	0.98528996	0.65856908	1.66231782	0.08905999	-0.6770279	0.99583809
HSPB8	ENSG00000152137	653.677819	0.75620229	0.01859489	1.77458162	5.8714E-14	-1.0183793	0.00016381
ELOC	ENSG00000154582	280.436997	-0.2433518	0.93362917	0.48206777	0.41268635	-0.7254196	0.07637224
NDUFAF6	ENSG00000156170	83.5621214	-0.6131626	0.66655157	0.73548358	0.37278432	-1.3486462	0.01029076
UQCRB	ENSG00000156467	299.2299	0.15980349	0.98162257	0.80014781	0.08366151	-0.6403443	0.34287609
TSC22D3	ENSG00000157514	141.577493	0.9170064	0.14014112	2.63119295	1.46E-13	-1.7141865	1.7907E-06
G6PD	ENSG00000160211	180.492563	0.1863293	0.96773692	0.94072471	0.0142847	-0.7543954	0.09189761
ELF3	ENSG00000163435	20.2385856	0.41841809	0.97996174	2.05533474	0.05607015	-1.6369167	0.18640781
PTPN13	ENSG00000163629	70.8568788	0.90200093	0.3593464	2.22617656	2.7102E-06	-1.3241756	0.01308276
S100P	ENSG00000163993	46.8918721	0.57753446	0.9506526	4.10727504	2.2885E-10	-3.5297406	3.9887E-10
TP53INP1	ENSG00000164938	101.755994	1.99772024	2.4513E-05	3.34541147	7.803E-16	-1.3476912	0.00096356
CLEC3A	ENSG00000166509	22.4881538	2.35502476	0.16535652	4.02096937	0.00028702	-1.6659446	0.16986818
MIDN	ENSG00000167470	73.0955457	0.70024057	0.56476616	1.16414917	0.05412218	-0.4639086	0.97338657
SLC43A2	ENSG00000167703	47.0724268	1.22744223	0.21042572	1.77517065	0.01028125	-0.5477284	0.99583809
KRT80	ENSG00000167767	152.294031	0.9087793	0.06213589	1.21254985	0.00251382	-0.3037705	0.99916796
IGFBP6	ENSG00000167779	13.5174776	-0.4742349	0.98551742	2.30920561	0.08451747	-2.7834405	0.02724623
GSTM4	ENSG00000168765	103.938848	0.71366556	0.39798233	1.63881538	5.334E-05	-0.9251498	0.07693282
TMEM150A	ENSG00000168890	29.9216207	1.53077904	0.23038623	1.84774304	0.06967482	-0.316964	0.99916796
FASN	ENSG00000169710	408.562963	0.4112074	0.60727995	1.17509895	4.5256E-05	-0.7638915	0.0326643
RAC3	ENSG00000169750	63.1070425	-0.4903864	0.84511563	0.6263563	0.55368046	-1.1167427	0.0735082
KRT8	ENSG00000170421	6756.88429	0.61680115	0.06103233	1.11055491	5.6135E-06	-0.4937538	0.28103135
NUDT9	ENSG00000170502	62.8624973	0.17831112	0.99009685	1.12281178	0.09988051	-0.9445007	0.28878404
ZNF217	ENSG00000171940	263.52053	0.77214333	0.07321697	1.2343385	0.0001189	-0.4621942	0.65405964
SNCG	ENSG00000173267	108.670547	-0.839159	0.64512434	3.94899343	3.8409E-21	-4.7881524	8.1813E-27
NUDT4	ENSG00000173598	124.436595	0.14084834	0.99009685	1.35239559	0.00058824	-1.2115473	0.00327772
JUP	ENSG00000173801	317.845371	0.436743	0.55901914	0.72502772	0.05672971	-0.2882847	0.99825005
NET1	ENSG00000173848	103.900698	-0.3706317	0.91596763	0.6372614	0.46448088	-1.0078931	0.0873044
CTSF	ENSG00000174080	22.8950581	1.42672718	0.32487868	1.81755797	0.078342	-0.3908308	0.99916796
MARCKSL1	ENSG00000175130	315.760153	0.85966698	0.04526865	0.93730827	0.02090126	-0.0776413	0.99916796
PLEKHF2	ENSG00000175895	157.71853	-0.1221128	0.99009685	1.10189819	0.00397914	-1.224011	0.00076929
NUPR1	ENSG00000176046	220.870037	-0.1261226	0.99009685	2.38891357	1.0214E-14	-2.5150361	9.5611E-17
PNPLA2	ENSG00000177666	19.4132483	1.35871598	0.50546235	1.94920212	0.08905999	-0.5904861	0.99916796
CALML5	ENSG00000178372	14.4409017	0.61411601	0.96702942	2.72952652	0.0242438	-2.1154105	0.09166802
CALR	ENSG00000179218	161.593243	0.38382387	0.88219504	1.01083047	0.04747567	-0.6270066	0.56757505
TSPYL5	ENSG00000180543	138.192013	0.4418106	0.73506452	0.95246946	0.02793598	-0.5106589	0.66001103
ARSJ	ENSG00000180801	27.6791083	-1.3487566	0.49947185	2.05079724	0.01028125	-3.3995539	1.2513E-05
SSR4	ENSG00000180879	417.739919	0.18908337	0.95511564	0.87246608	0.00410205	-0.6833827	0.05664765
LIMK2	ENSG00000182541	19.4413127	0.6671549	0.94614772	2.05313347	0.07523904	-1.3859786	0.46338025
MACC1	ENSG00000183742	14.0232133	2.38712926	0.24489248	2.8992587	0.07173196	-0.5121294	0.99916796
B3GALT5	ENSG00000183778	30.5973301	0.31665773	0.99009685	3.29305635	6.0873E-05	-2.9763986	0.00013929
TSPYL2	ENSG00000184205	24.7156929	1.57750193	0.19602156	1.90453405	0.05226296	-0.3270321	0.99916796
NCMAP	ENSG00000184454	20.4728812	0.17030605	0.9918095	2.33970865	0.02241793	-2.1694026	0.03358052
METTL7A	ENSG00000185432	53.6981151	-0.0023489	0.99986776	1.15927203	0.09224711	-1.161621	0.09798055
ZFP36L1	ENSG00000185650	182.171562	0.21000721	0.96318994	1.36288728	5.334E-05	-1.1528801	0.00117543
BCAP31	ENSG00000185825	393.304574	0.05674521	0.9918095	0.72118581	0.06967482	-0.6644406	0.13706109
UBE2H	ENSG00000186591	124.566679	0.7735606	0.22228055	1.00102846	0.0396699	-0.2274679	0.99916796
C17orf58	ENSG00000186665	149.473521	0.27292924	0.94614772	0.84950905	0.08276078	-0.5765798	0.55700939
MITF	ENSG00000187098	59.2805053	0.15189891	0.99046362	2.2968359	6.1771E-06	-2.144937	1.4946E-05
BCAM	ENSG00000187244	162.038517	0.58721101	0.47881568	1.08077355	0.00992022	-0.4935625	0.72807524
APOD	ENSG00000189058	15.3339401	1.89280175	0.54023462	3.88853614	0.00273846	-1.9957344	0.1043483
S100A14	ENSG00000189334	308.215054	0.73050243	0.05966495	0.99957908	0.00161116	-0.2690766	0.99916796
AKR1C3	ENSG00000196139	36.7965844	0.70927106	0.99046362	7.51064675	5.6085E-05	-6.8013757	2.716E-07
SPTSSB	ENSG00000196542	2143.2524	0.34876502	0.57654479	0.65626073	0.02498347	-0.3074957	0.84701477
FLNA	ENSG00000196924	232.874469	0.30356222	0.89616462	0.97669304	0.00889441	-0.6731308	0.18640781
C6orf141	ENSG00000197261	36.6363677	-0.8698859	0.72763583	1.60051597	0.04502648	-2.4704018	0.00032322
PSAP	ENSG00000197746	651.087155	0.36368537	0.59339865	0.58038914	0.09406392	-0.2167038	0.99916796
PAPSS2	ENSG00000198682	23.9954252	0.81910155	0.83067045	1.97954899	0.01135305	-1.1604474	0.46690257
SELENOM	ENSG00000198832	17.1896676	1.5197153	0.45713276	2.27084056	0.05412218	-0.7511253	0.99916796
ND3	ENSG00000198840	2037.87075	0.2868168	0.82333875	1.0440427	0.00011747	-0.7572259	0.02048322
ND4	ENSG00000198886	4478.72338	-0.2865503	0.85028276	0.53891594	0.24299677	-0.8254662	0.01545208
L1CAM	ENSG00000198910	27.3300511	0.82568686	0.78962175	1.70282738	0.06237811	-0.8771405	0.75916008
GDI1	ENSG00000203879	112.837269	-0.3164354	0.93362917	0.6011881	0.43056387	-0.9176235	0.08530223
TRIQK	ENSG00000205133	107.095512	0.34807491	0.9189798	1.00344128	0.06086687	-0.6553664	0.52657605
PDE7A	ENSG00000205268	34.644086	-0.7926977	0.78399918	1.25581628	0.18830897	-2.048514	0.00578086
CLDN9	ENSG00000213937	75.3043249	1.05907153	0.15050435	2.20318599	1.3343E-06	-1.1441145	0.03563592
UBE2QL1	ENSG00000215218	16.3284124	-1.3965975	0.70284436	2.00850697	0.08905999	-3.4051045	0.00219399
FOXD3-AS1	ENSG00000230798	18.8304838	1.25622821	0.58493901	1.95835118	0.08905999	-0.702123	0.99916796
LNCAROD	ENSG00000231131	15.6897492	1.27443244	0.96482631	6.24388625	0.00371973	-4.9694538	0.00027571
NEAT1	ENSG00000245532	43.0537598	-0.0402882	0.99826494	1.758681	0.02090126	-1.7989692	0.01566327
TMEM150C	ENSG00000249242	212.246738	0.25906546	0.9351173	1.18266825	0.0003445	-0.9236028	0.01345875
MALAT1	ENSG00000251562	1888.39801	0.71951074	0.7895626	1.8200304	0.01377335	-1.1005197	0.44940254

Appendix VII – GSEA pathway analysis of DEGs in HCC1428 LTED cells



Pathways UP

NAME	SIZE	ES	NES	FDR q-val	RANK AT MAX
HALLMARK_E2F_TARGETS	120	0.8	3.22	0	409
HALLMARK_G2M_CHECKPOINT	109	0.8	3.22	0	286
HALLMARK_MITOTIC_SPINDLE	61	0.68	2.47	0	229
HALLMARK_SPERMATOGENESIS	20	0.78	2.33	0	272
HALLMARK_MYC_TARGETS_V1	82	0.55	2.18	0	779
HALLMARK_DNA_REPAIR	30	0.55	1.81	0.005	282
HALLMARK_UV_RESPONSE_UP	34	0.48	1.6	0.042	743
HALLMARK_GLYCOLYSIS	44	0.4	1.4	0.178	170
HALLMARK_MTORC1_SIGNALING	78	0.35	1.34	0.231	559
HALLMARK_PI3K_AKT_MTOR_SIGNALING	16	0.44	1.25	0.337	340
HALLMARK_UNFOLDED_PROTEIN_RESPONSE	28	0.34	1.09	0.618	536
HALLMARK_ESTROGEN_RESPONSE_LATE	96	0.24	0.96	0.846	493
HALLMARK_APOPTOSIS	49	0.26	0.94	0.823	340
HALLMARK_APICAL_JUNCTION	38	0.25	0.85	0.946	1072
HALLMARK_ALLOGRAFT_REJECTION	21	0.25	0.76	1	971
HALLMARK_KRAS_SIGNALING_UP	16	0.27	0.75	0.967	718
HALLMARK_FATTY_ACID_METABOLISM	40	0.2	0.71	0.951	970
HALLMARK_PEROXISOME	28	0.16	0.53	1	1005
HALLMARK_XENOBIOTIC_METABOLISM	43	0.14	0.5	0.985	1109

Pathways DOWN

	SIZE	ES	NES	FDR q-val	RANK AT MAX
HALLMARK_HEME_METABOLISM	42	-0.27	-1.36	1	332
HALLMARK_COAGULATION	20	-0.33	-1.36	0.936	418
HALLMARK_IL2_STAT5_SIGNALING	34	-0.25	-1.2	1	621
HALLMARK_MYOGENESIS	38	-0.22	-1.09	1	357
HALLMARK_BILE_ACID_METABOLISM	19	-0.27	-1.08	1	310
HALLMARK_TGF_BETA_SIGNALING	15	-0.3	-1.08	1	1356
HALLMARK_INTERFERON_GAMMA_RESPONSE	30	-0.23	-1.06	1	614
HALLMARK_OXIDATIVE_PHOSPHORYLATION	56	-0.2	-1.04	1	1752
HALLMARK_HYPOXIA	51	-0.19	-1.03	0.983	418
HALLMARK_UV_RESPONSE_DN	30	-0.21	-0.99	1	144
HALLMARK_PROTEIN_SECRETION	21	-0.24	-0.98	0.978	618
HALLMARK_P53_PATHWAY	65	-0.14	-0.82	1	464
HALLMARK_TNFA_SIGNALING_VIA_NFKB	46	-0.16	-0.81	1	434
HALLMARK_ESTROGEN_RESPONSE_EARLY	107	-0.13	-0.78	1	1943
HALLMARK_EPITHELIAL_MESENCHYMAL_TRANSITION	41	-0.15	-0.75	1	295
HALLMARK_KRAS_SIGNALING_DN	19	-0.18	-0.72	1	260
HALLMARK_CHOLESTEROL_HOMEOSTASIS	29	-0.15	-0.67	1	127
HALLMARK_INTERFERON_ALPHA_RESPONSE	15	-0.18	-0.65	1	139
HALLMARK_INFLAMMATORY_RESPONSE	19	-0.15	-0.6	1	1931
HALLMARK_ANDROGEN_RESPONSE	44	-0.12	-0.57	1	302
HALLMARK_ADIPOGENESIS	44	-0.11	-0.55	1	453
HALLMARK_COMPLEMENT	31	-0.08	-0.36	1	701

Appendix VIII – Heatmap cluster gene list in HCC1428 LTED cells

Cluster 1

			TvsC		RvsC		RvsT	
	ensembl	baseMean	log2FoldChange	padj	log2FoldChange	padj	log2FoldChange	padj
MCUB	ENSG00000005059	31.4886878	1.11488265	0.18361066	0.57945456	0.60620078	-0.5354281	0.69609974
CRLF1	ENSG00000006016	15.7550431	2.80183946	0.00425974	2.41753664	0.01591386	-0.3843028	0.8835844
RALA	ENSG00000006451	163.888521	0.545436	0.18945288	0.34049666	0.48440508	-0.2049393	0.80047664
GGCT	ENSG00000006625	165.61828	0.95412739	0.00447629	0.77135145	0.02786845	-0.1827759	0.85503697
E2F2	ENSG00000007968	17.3974147	2.92519102	0.01067925	3.15364752	0.00275971	0.22845651	0.93911055
MGST1	ENSG00000008394	1346.21433	0.49169662	0.02539684	-0.6833627	0.00028158	-1.1750594	4.78E-12
MAPK8IP2	ENSG00000008735	14.7575074	2.65636982	0.00780344	0.06007912	0.9834822	-2.5962907	0.01055637
BRCA1	ENSG00000012048	30.9575616	2.37441883	0.00032045	2.18130322	0.00105429	-0.1931156	0.92441713
TACC3	ENSG00000013810	30.1771456	3.81903874	9.6168E-06	3.87129272	3.98E-06	0.05225398	0.97983413
DERA	ENSG00000023697	41.1453433	1.22158225	0.07840877	1.6943091	0.00188764	0.47272685	0.68663269
ABCC2	ENSG00000023839	40.4780305	0.83894545	0.2874844	-0.2809722	0.82942882	-1.1199176	0.08919425
GCLM	ENSG00000023909	118.027291	0.71037208	0.08867057	0.08759812	0.9226402	-0.622774	0.16586088
NCAPH2	ENSG00000025770	41.433654	2.19685875	3.8029E-05	1.16413923	0.09258545	-1.0327195	0.1278104
HMGB3	ENSG00000029993	213.048335	1.0556824	0.00044327	1.07598065	0.0002128	0.02029826	0.98488071
DEPDC1B	ENSG00000035499	15.1563101	4.10110158	0.00157483	3.87771692	0.00242965	-0.2233847	0.93818914
SPDL1	ENSG00000040275	20.1265463	1.68032687	0.07283567	1.51768359	0.09530548	-0.1626433	0.94925399
RTN4R	ENSG00000040608	7.5957565	1.93251119	0.31269616	0.80604029	0.77099005	-1.1264709	0.65771821
HSPA5	ENSG00000044574	445.769821	0.36196771	0.33067369	0.09941944	0.86505924	-0.2625483	0.57438673
EPN3	ENSG00000049283	117.602398	0.75886847	0.05810353	0.2142361	0.77189549	-0.5446324	0.27110881
RFC2	ENSG00000049541	65.6954314	1.82876285	0.00013056	1.54120844	0.00191303	-0.2875544	0.83214737
MSMO1	ENSG00000052802	79.4191762	0.91665217	0.05069246	-0.3180554	0.70498213	-1.2347076	0.0033522
ENTPD2	ENSG00000054179	48.5916013	0.62608187	0.45417001	-0.5090382	0.54933066	-1.1351201	0.04653992
SYNE2	ENSG00000054654	27.6877078	1.2822692	0.1468149	0.95021281	0.32113185	-0.3320564	0.87433261
NDC1	ENSG00000058804	49.724994	1.00471053	0.16277804	0.84166154	0.24115279	-0.163049	0.93004621
CNN2	ENSG00000064666	5.05775417	2.61297832	0.3051879	2.49513588	0.26731769	-0.1178424	0.98034096
IPO5	ENSG00000065150	78.5851147	0.97863915	0.04425731	0.32421506	0.70050576	-0.6544241	0.29630012
ME1	ENSG00000065833	69.4647864	0.82420377	0.13337035	0.25056451	0.79172002	-0.5736393	0.41398635
ASPM	ENSG00000066279	49.4657417	4.37997075	3.2225E-10	4.16045341	2.1205E-09	-0.2195173	0.89471532
ISOC1	ENSG00000066583	184.419421	0.75062047	0.0329851	0.15433649	0.83726952	-0.596284	0.14070959
FECH	ENSG00000066926	42.8996454	1.24237013	0.04876677	0.91347526	0.18888518	-0.3288949	0.82363894
IDI1	ENSG00000067064	168.596079	0.7236177	0.0286875	0.08814628	0.90874716	-0.6354714	0.07395893
KLF6	ENSG00000067082	114.711903	1.18934095	0.00204173	0.53247319	0.34107016	-0.6568678	0.21115035
PRR11	ENSG00000068489	87.9539504	2.96958689	6.2813E-15	2.51698996	1.4392E-10	-0.4525969	0.49021798
VPS35	ENSG00000069329	265.664873	0.41088949	0.33616864	-0.0060507	0.99323688	-0.4169402	0.31799885
UFD1	ENSG00000070010	37.0658901	1.50864136	0.03123027	0.83295357	0.37020949	-0.6756878	0.55760316
SLC44A1	ENSG00000070214	196.998166	0.67843651	0.0427922	0.21194739	0.71834078	-0.4664891	0.27573564
TRIP13	ENSG00000071539	50.6834054	3.18566828	2.3199E-09	2.55272318	4.9044E-06	-0.6329451	0.44808798
SMC1A	ENSG00000072501	204.968132	0.46365638	0.27872385	0.06183299	0.93514299	-0.4018234	0.39287458
HSD17B10	ENSG00000072506	384.346596	0.56858652	0.02842255	0.29655033	0.38949569	-0.2720362	0.53299209
HMMR	ENSG00000072571	25.0014561	2.93747676	0.00063438	2.7456373	0.00136985	-0.1918395	0.94074844
ACADVL	ENSG00000072778	84.6823756	0.6692354	0.25762485	0.22515305	0.80864322	-0.4440823	0.57224856
PANX2	ENSG00000073150	39.7586787	1.69823982	0.00184773	-0.1533041	0.92112593	-1.8515439	0.00070016
SDHA	ENSG00000073578	134.602823	0.94775444	0.0116135	0.37430552	0.52719617	-0.5734489	0.25796839
HACD3	ENSG00000074696	353.425217	0.03227308	0.97896393	-0.8680528	0.00038154	-0.9003259	0.00031894
ENO1	ENSG00000074800	1028.73758	0.34914882	0.25004669	0.12002682	0.79191648	-0.229122	0.57655721
GTSE1	ENSG00000075218	21.5117742	3.30204816	0.00011502	2.73509422	0.00236099	-0.5669539	0.72886435
SLC25A3	ENSG00000075415	1083.80582	0.46502226	0.0589326	0.05495906	0.91887353	-0.4100632	0.12099643
SPAG5	ENSG00000076382	15.6483233	2.77688479	0.01956669	3.02094583	0.00509556	0.24406105	0.93479291
TPD52	ENSG00000076554	191.456843	0.89764511	0.00458759	0.09515904	0.90546411	-0.8024861	0.01628359
RAP1GAP	ENSG00000076864	29.2473894	0.95253836	0.30196368	-1.3472744	0.10597726	-2.2998128	0.00061236
UBE2T	ENSG00000077152	168.793327	2.64223835	7.1049E-21	2.33870391	3.6844E-16	-0.3035344	0.61835269
FBLN1	ENSG00000077942	61.5579848	0.55556449	0.51746335	-0.5362467	0.48819814	-1.0918112	0.04784697
TULP3	ENSG00000078246	54.9971592	0.86265229	0.16402514	0.3200839	0.74204654	-0.5425684	0.53177569
VDAC3	ENSG00000078668	215.130094	0.69460904	0.02443573	0.42668978	0.25545758	-0.2679193	0.65179607
FDFT1	ENSG00000079459	290.095853	0.58719729	0.0744384	-0.189919	0.73368207	-0.7771163	0.00629637
HSPB11	ENSG00000081870	427.081228	1.3353129	7.6038E-10	0.67580076	0.00883739	-0.6595121	0.01230574
RNF13	ENSG00000082996	60.3761226	0.36432469	0.73391348	-0.8924046	0.11128098	-1.2567293	0.01157707
DIS3	ENSG00000083520	49.1659958	0.77228576	0.27523243	-0.5187146	0.5418325	-1.2910004	0.0158394
AKR1B1	ENSG00000085662	110.836634	1.28145977	0.00072284	-1.0353333	0.02284248	-2.3167931	1.1191E-10
DDHD2	ENSG00000085788	33.8718536	0.90095852	0.32290591	0.303871	0.82962892	-0.5970875	0.61710721
ORC1	ENSG00000085840	12.401086	2.24952974	0.13284913	2.44508521	0.05481128	0.19555547	0.95332
AURKA	ENSG00000087586	199.601089	2.0727336	2.0753E-15	1.97723232	5.1915E-14	-0.0955013	0.92414061
PIR	ENSG00000087842	90.88109	0.73926923	0.14900027	0.21850905	0.80845245	-0.5207602	0.42716767
RFX2	ENSG00000087903	6.74673332	2.45632103	0.33502385	2.77290484	0.16301098	0.31658381	0.94760837
TPX2	ENSG00000088325	86.2062973	1.97126957	2.0677E-06	1.71307621	5.4913E-05	-0.2581934	0.83214737
ANKRD10	ENSG00000088448	29.3394903	1.83494516	0.00390459	0.20162616	0.90546411	-1.633319	0.01389108
BLVRB	ENSG00000090013	542.686504	1.03352624	3.1995E-07	0.50727396	0.0425929	-0.5262523	0.03933552
AARS1	ENSG00000090861	161.388631	0.57912127	0.25573353	-0.0642431	0.94676789	-0.6433644	0.16444509
WDR76	ENSG00000092470	22.7747632	4.60620674	0.00015048	4.73870141	5.4084E-05	0.13249467	0.95807242
PHGDH	ENSG00000092621	145.60255	1.38650783	9.2073E-06	0.87610678	0.0142393	-0.510401	0.31001751
CDC6	ENSG00000094804	27.6047472	3.26729774	2.8811E-05	3.03279455	0.00010947	-0.2345032	0.91149121
CBX5	ENSG00000094916	94.2467705	0.78578432	0.20524265	0.36609541	0.66387518	-0.4196889	0.66423432
MAP3K1	ENSG00000095015	31.7677871	1.15561954	0.14157082	-0.0597607	0.9713729	-1.2153802	0.11129737
BAMBI	ENSG00000095739	41.2394864	1.25647016	0.03385224	0.88332865	0.19166857	-0.3731415	0.77040135
TMEM14A	ENSG00000096092	135.472305	0.30774297	0.65521477	-0.5376079	0.19285401	-0.8453509	0.01459007
PSMD8	ENSG00000099341	733.612795	0.73430773	0.00014473	0.5403909	0.00941812	-0.1939168	0.65894697
TIMM13	ENSG00000099800	171.619077	0.48407258	0.29258589	0.24614004	0.6693553	-0.2379325	0.74974582
RANBP1	ENSG00000099901	202.375217	1.58695571	1.0134E-10	1.16580987	7.7702E-06	-0.4211458	0.30754831
SLC25A1	ENSG00000100075	297.098534	0.65749025	0.01114358	0.02349703	0.97112443	-0.6339932	0.01668719
LGALS1	ENSG00000100097	1008.7352	1.22556833	2.1028E-10	-0.2743113	0.42734518	-1.4998796	1.5018E-15
TRIOBP	ENSG00000100106	74.0043211	1.27425729	0.0021931	0.36242015	0.64819949	-0.9118371	0.05828278
SNU13	ENSG00000100138	338.338788	0.70566089	0.00781781	0.09523231	0.8810728	-0.6104286	0.03150502
POLR2F	ENSG00000100142	162.103169	0.92735162	0.00923332	0.4113032	0.42867615	-0.5160484	0.31198229
CENPM	ENSG00000100162	35.7743867	2.91758674	2.243E-06	2.48204857	9.7647E-05	-0.4355382	0.74539466
SEPTIN3	ENSG00000100167	21.0556383	3.93031174	1.0977E-05	2.18586912	0.05177271	-1.7444426	0.04257617
TOMM22	ENSG00000100216	210.211508	0.8364255	0.01459257	0.56316787	0.15174269	-0.2732576	0.70849037
FBXO7	ENSG00000100225	78.568101	1.10171049	0.01349621	0.28920125	0.74228891	-0.8125092	0.12152114
CYB5R3	ENSG00000100243	550.178379	0.90072354	4.0141E-06	0.12288931	0.80096643	-0.7778342	0.00013979
LMF2	ENSG00000100258	37.0263769	1.41955266	0.0182355	0.13518223	0.93146911	-1.2843704	0.04219657
PACSIN2	ENSG00000100266	65.2229164	0.87423003	0.12509483	-0.9325476	0.10444633	-1.8067776	5.1205E-05
HMOX1	ENSG00000100292	40.5075178	1.91060563	0.00016249	0.38194193	0.74497951	-1.5286637	0.00444458
MCM5	ENSG00000100297	56.7581531	2.98278397	9.7303E-10	2.67889098	6.344E-08	-0.303893	0.80289893
TTLL12	ENSG00000100304	41.203356	1.22156414	0.09238505	0.83329142	0.31435067	-0.3882727	0.79674417
SYNGR1	ENSG00000100321	94.9609219	0.76696345	0.11999701	-0.1121227	0.91260429	-0.8790861	0.05352719
FOXRED2	ENSG00000100350	56.092411	0.75475815	0.33331949	0.7198639	0.29276584	-0.0348942	0.98463257
IFT27	ENSG00000100360	46.6174861	0.99833616	0.16340197	-0.0980403	0.94867615	-1.0963765	0.10807087
PVALB	ENSG00000100362	43.493533	2.51956509	4.0619E-07	-5.3237285	0.00490848	-7.8432936	5.3036E-06
ST13	ENSG00000100380	317.916397	0.64641801	0.01346018	-0.0375455	0.95369193	-0.6839635	0.00766865
RBX1	ENSG00000100387	232.484393	0.88249478	0.01586552	-0.1084033	0.90303258	-0.9908981	0.00473614
PHF5A	ENSG00000100410	66.0449295	1.09532972	0.0213048	0.56840825	0.38307008	-0.5269215	0.48585119
TRIM9	ENSG00000100505	20.0301078	1.47299764	0.20287351	0.16608971	0.9435865	-1.3069079	0.29577425
GINS1	ENSG00000101003	31.5883905	2.1244543	0.00387858	2.26135971	0.00105332	0.13690541	0.95014208
PSMA7	ENSG00000101182	1502.32068	0.70544202	0.00010869	0.64655502	0.0003781	-0.058887	0.93172202
EEF1A2	ENSG00000101210	757.239068	0.33096821	0.29258589	-0.0262082	0.9647021	-0.3571764	0.22006529
TRIB3	ENSG00000101255	57.8258535	0.80427062	0.22480589	-0.0893189	0.94590262	-0.8935895	0.14653367
TTI1	ENSG00000101407	18.0320921	1.67266058	0.14358269	0.83078738	0.60101514	-0.8418732	0.62538879
E2F1	ENSG00000101412	46.9074078	3.22333108	6.8229E-07	3.64847892	3.3775E-09	0.42514784	0.73876325
TBL1X	ENSG00000101849	99.3715014	0.92512825	0.02656752	0.59776994	0.22876378	-0.3273583	0.69594025
PRPS2	ENSG00000101911	101.201093	0.8051958	0.07752262	0.37922148	0.55673574	-0.4259743	0.546088
PLP2	ENSG00000102007	277.714829	1.43747016	2.5848E-09	0.48901873	0.16582422	-0.9484514	0.00032677
RBBP7	ENSG00000102054	292.74403	0.78703446	0.00168048	0.63354372	0.01554806	-0.1534907	0.83179003

NDFIP2	ENSG00000102471	71.1028496	0.97499654	0.04220317	-0.1481986	0.8921634	-1.1231952	0.01343788
MAPK3	ENSG00000102882	207.701185	0.46230592	0.26959229	-0.042988	0.95430531	-0.505294	0.19041899
CYB5B	ENSG00000103018	127.542858	0.85177092	0.01904477	0.2421877	0.72220784	-0.6095832	0.16474426
PSMD7	ENSG00000103035	18.7871804	1.61017794	0.11472356	0.92329701	0.47865352	-0.6868809	0.68835324
IKBKB	ENSG00000104365	25.3499662	1.29746697	0.1572248	-0.0376339	0.98480087	-1.3351009	0.14259409
SQLE	ENSG00000104549	474.576331	0.5724907	0.03230251	-0.5830684	0.02389792	-1.1555591	6.1983E-08
GSR	ENSG00000104687	72.4042856	0.83325946	0.14600609	-0.1502454	0.89496737	-0.9835048	0.05922088
MCM4	ENSG00000104738	202.30432	1.17125489	2.3795E-05	1.00545748	0.00039212	-0.1657974	0.85462739
NFKBIB	ENSG00000104825	23.6625233	1.4440932	0.14654856	0.43093961	0.81211853	-1.0131536	0.41373679
ANKRD27	ENSG00000105186	49.8877111	1.06643791	0.08874056	0.72729888	0.30944772	-0.339139	0.79674417
GPI	ENSG00000105220	183.473576	0.74506638	0.07587517	0.59057593	0.17101201	-0.1544904	0.89471532
RPL18A	ENSG00000105640	347.664648	0.68883436	0.07748984	0.34627841	0.50666491	-0.3425559	0.59426269
AVL9	ENSG00000105778	27.1799808	1.00695633	0.30199411	0.86126566	0.35317917	-0.1456907	0.94773579
GARS1	ENSG00000106105	134.327135	0.52145794	0.29059704	-0.0285473	0.97560058	-0.5500052	0.24075617
IMPDH1	ENSG00000106348	170.280992	0.82103751	0.01051317	0.18973603	0.774678	-0.6313015	0.08556047
RPA3	ENSG00000106399	216.911549	0.98703725	0.00070406	0.69208672	0.03244929	-0.2949505	0.63053303
EZH2	ENSG00000106462	49.9240134	2.19621859	1.3734E-05	2.25263742	4.3702E-06	0.05641883	0.97330497
TSPAN13	ENSG00000106537	593.667158	0.34845168	0.29305008	-0.3956859	0.14382769	-0.7441376	0.00056341
RHEB	ENSG00000106615	208.184792	1.18201514	8.0017E-06	1.10948968	2.5999E-05	-0.0725255	0.9439606
TGFBR1	ENSG00000106799	25.2712191	1.05801833	0.26347275	-0.3710264	0.81773779	-1.4290447	0.07333424
SETX	ENSG00000107290	46.3054327	0.89569422	0.24486128	0.19133082	0.88773672	-0.7043634	0.434079
MICU1	ENSG00000107745	87.3888879	0.57975292	0.31483553	-0.3780941	0.57558375	-0.957847	0.02434218
GIT1	ENSG00000108262	32.1329427	1.04281125	0.26955103	1.03414419	0.20443138	-0.0086671	0.99605451
TRIM37	ENSG00000108395	43.8144131	0.83791873	0.27127403	-0.2494709	0.84887879	-1.0873897	0.09212291
CBX1	ENSG00000108468	217.268192	0.46415296	0.25661369	0.04782983	0.95056328	-0.4163231	0.34139653
PFN1	ENSG00000108518	176.856476	0.55935859	0.32131062	0.29790911	0.66145771	-0.2614495	0.78422227
VAT1	ENSG00000108828	236.873662	0.48686912	0.16154366	-0.3209567	0.43511171	-0.8078259	0.00266606
YWHAE	ENSG00000108953	854.261352	0.51118143	0.04977115	0.4406476	0.0878763	-0.0705338	0.92839393
TMEM97	ENSG00000109084	51.8278645	1.53334516	0.00695111	1.4910892	0.00657372	-0.042256	0.98187312
CDR2L	ENSG00000109089	83.9007046	0.80704158	0.08798851	0.28429845	0.71505328	-0.5227431	0.40970949
NMU	ENSG00000109255	13.3952083	2.0904835	0.0780741	0.63529818	0.77934029	-1.4551853	0.29084566
MTCH2	ENSG00000109919	342.055604	0.38204407	0.33004782	0.43389826	0.15869088	0.05185419	0.95152692
FOXM1	ENSG00000111206	19.7506586	2.58581942	0.01547288	2.4836314	0.01582293	-0.102188	0.97281114
ENO2	ENSG00000111674	49.4375671	0.93166246	0.16777762	-0.1645383	0.90375316	-1.0962007	0.07609381
GCNT2	ENSG00000111846	5.69643294	2.15354859	0.31269616	0.15196654	0.97096412	-2.001582	0.36805864
FBXO5	ENSG00000112029	12.4590622	3.09084959	0.01437577	2.28755163	0.10642517	-0.803298	0.70509428
PPARD	ENSG00000112033	19.9646322	1.48288809	0.17190724	0.64816198	0.68471263	-0.8347261	0.5944276
SRSF3	ENSG00000112081	342.184816	0.66479458	0.01299986	0.75350383	0.00188764	0.08870924	0.91720208
MRPL18	ENSG00000112110	112.380074	0.80461478	0.04208865	0.38919625	0.48440508	-0.4154185	0.50265743
MCM3	ENSG00000112118	97.1940048	1.67801538	1.6919E-06	1.45889403	4.852E-05	-0.2191213	0.83597683
CRYBG1	ENSG00000112297	59.1058628	0.90380139	0.13725186	0.0175104	0.98929026	-0.886291	0.14696157
GMNN	ENSG00000112312	50.1862053	2.1450846	2.797E-05	2.17154296	1.3566E-05	0.02645836	0.98766681
CCND3	ENSG00000112576	84.3129091	0.76683564	0.12552881	0.40544762	0.53815365	-0.361388	0.66997186
TTK	ENSG00000112742	13.5385145	1.7194196	0.17017391	1.40143247	0.27547551	-0.3179871	0.91221707
TENT4A	ENSG00000112941	28.3491637	1.26901578	0.17782765	1.79592748	0.00985092	0.52691171	0.72586256
GHR	ENSG00000112964	25.4866436	1.6360033	0.03487677	0.89585104	0.38852893	-0.7401523	0.54815875
KIF20A	ENSG00000112984	7.09874026	2.31075898	0.28999311	2.43790304	0.17364223	0.12714406	0.97491022
NNT	ENSG00000112992	17.7744012	2.24096513	0.03117259	1.56407084	0.19098339	-0.6768943	0.73876325
HSPA9	ENSG00000113013	321.691359	0.39891186	0.30511927	0.1298032	0.82939049	-0.2691087	0.6034188
MRPS27	ENSG00000113048	40.0736294	0.82746908	0.30032929	0.03279464	0.98255687	-0.7946744	0.33168486
HMGCR	ENSG00000113161	79.4842331	0.91959206	0.06247724	-0.0664539	0.95299671	-0.9860459	0.03830515
TARS1	ENSG00000113407	111.109218	0.55096655	0.29789541	0.35027079	0.5549776	-0.2006958	0.85246966
NUP155	ENSG00000113569	66.9520981	1.17654169	0.05840507	1.01685997	0.09989177	-0.1596817	0.92917419
TTC33	ENSG00000113638	13.3936172	1.3865494	0.33004782	0.54432611	0.79257095	-0.8422233	0.65894697
MACROH2A1	ENSG00000113648	159.211184	0.53314843	0.31398615	0.13328052	0.87649542	-0.3998679	0.53934471
HGD	ENSG00000113924	85.9901044	1.10969824	0.00742231	-0.9413758	0.05466435	-2.051074	4.9696E-08
ECT2	ENSG00000114346	142.984321	1.72403524	1.3518E-06	0.89451632	0.04317102	-0.8295189	0.06851702
C3orf14	ENSG00000114405	198.021983	0.6118578	0.09789384	-0.7492387	0.02295246	-1.3610965	8.3995E-07
IQCG	ENSG00000114473	24.236172	0.4224597	0.8257516	-1.639458	0.05037276	-2.0619177	0.0088074
HEMK1	ENSG00000114735	11.3551534	1.49205906	0.31922851	0.51616182	0.8283046	-0.9758972	0.612042
DHCR24	ENSG00000116133	390.161377	0.02629041	0.98218478	-0.6811739	0.00531907	-0.7074644	0.00513948
LRRC42	ENSG00000116212	56.6430568	1.14220519	0.02538347	0.84429736	0.13334823	-0.2979078	0.80097497
CAPZA1	ENSG00000116489	287.586117	0.49649143	0.32114437	0.50315307	0.23214339	0.00666163	0.99605451
C1orf21	ENSG00000116667	136.267608	0.85549576	0.00981891	-1.8075994	2.2266E-08	-2.6630952	1.1892E-18
AKR1A1	ENSG00000117448	248.683548	0.645578	0.03143639	-0.8084944	0.00387307	-1.4540724	1.7927E-09
PRDX1	ENSG00000117450	117.98273	0.65293653	0.15622359	-0.3707167	0.53994837	-1.0236533	0.00544104
CNN3	ENSG00000117519	63.0204335	2.3132629	6.6855E-08	1.62766394	0.00054189	-0.685599	0.29240617
STMN1	ENSG00000117632	384.016188	2.28347731	2.8979E-27	2.06793347	3.0147E-22	-0.2155438	0.69185728
NEK2	ENSG00000117650	42.2340663	3.83906849	6.1367E-08	3.74760303	9.3992E-08	-0.0914655	0.9610645
KIF14	ENSG00000118193	15.3753361	3.29057233	0.00729503	3.30523431	0.00454097	0.01466198	0.99605451
MFSD1	ENSG00000118855	108.623708	0.32134452	0.69134587	-0.6669146	0.12910591	-0.9882591	0.00963022
C1orf198	ENSG00000119280	96.0315278	0.63827699	0.33502385	0.22652599	0.81910717	-0.411751	0.6475712
CNTRL	ENSG00000119397	15.9926111	1.79692069	0.10062284	0.64441503	0.7269322	-1.1525057	0.40625712
HSDL2	ENSG00000119471	58.3976411	1.32753833	0.00851342	0.95897343	0.08921588	-0.3685649	0.73973172
CUTC	ENSG00000119929	64.855143	0.73922137	0.23783223	-0.0430129	0.97101953	-0.7822343	0.19028115
HELLS	ENSG00000119969	39.9132783	2.10657451	0.00011678	1.42157183	0.02329991	-0.6850027	0.45081665
CYSTM1	ENSG00000120306	58.9852779	0.24252896	0.85973314	-1.0615903	0.0399036	-1.3041192	0.00829447
CCDC77	ENSG00000120647	15.5765093	2.15961339	0.05511133	2.20787447	0.03097272	0.04826108	0.98712112
WASHC3	ENSG00000120860	56.5437901	0.7245295	0.30580098	0.24335101	0.82664243	-0.4811785	0.60945771
NCAPH	ENSG00000121152	21.7705758	3.07637594	0.00149333	3.12774187	0.00077147	0.05136593	0.98463257
GPSM2	ENSG00000121957	14.3646598	2.11621784	0.06052537	1.77701214	0.12147483	-0.3392057	0.906361
SHLD2	ENSG00000122376	51.0584712	0.80333224	0.23055734	0.18336984	0.87828637	-0.6199624	0.43793967
PRXL2A	ENSG00000122378	332.682777	0.55632638	0.076062	-0.1492607	0.79914716	-0.7055871	0.01041217
HNRNPA2B1	ENSG00000122566	1135.60507	0.74111157	7.7974E-05	0.57516734	0.00359487	-0.1659442	0.72883745
ZWINT	ENSG00000122952	164.153541	2.77730643	7.6826E-20	2.62168796	1.2829E-17	-0.1556185	0.88308723
RASSF8	ENSG00000123094	5.13470781	2.81252329	0.22319999	2.33174609	0.30799455	-0.4807772	0.91542334
DDX39A	ENSG00000123136	112.361417	1.04157617	0.00727446	0.93739588	0.0151005	-0.1041803	0.936752
PKN1	ENSG00000123143	40.1498503	1.09469952	0.1553349	0.57622048	0.57043189	-0.518479	0.68663269
CKS2	ENSG00000123975	90.3521766	1.44022534	0.00013797	1.09721902	0.00724043	-0.3430663	0.68835324
PREX1	ENSG00000124126	160.744872	0.51064713	0.31190026	-0.3299424	0.56809129	-0.8405895	0.02150932
PLCG1	ENSG00000124181	13.8564927	1.63178346	0.27945693	1.35731382	0.35412581	-0.2744696	0.93275838
PEPD	ENSG00000124299	180.655178	0.52833075	0.17799682	0.46479322	0.21688455	-0.0635375	0.95014208
LYPD3	ENSG00000124466	30.0625936	0.11813476	0.96192858	-2.2158648	0.00198508	-2.3339996	0.00137052
H1-3	ENSG00000124575	17.0820104	3.35547649	0.00052412	2.25358379	0.04599682	-1.1018927	0.39425311
CDKN1A	ENSG00000124762	16.2327371	3.29150436	0.0009073	2.55755071	0.01675132	-0.7339536	0.6772657
GLO1	ENSG00000124767	354.801501	0.59613577	0.05515106	-0.6147643	0.03755491	-1.2109	5.465E-07
DEK	ENSG00000124795	181.968649	1.38112744	1.0033E-05	1.31301455	2.3059E-05	-0.0681129	0.95154246
TMTC4	ENSG00000125247	19.4223512	0.86082979	0.54308717	-1.6821237	0.10796216	-2.5429535	0.00425819
RAP2A	ENSG00000125249	47.1022501	1.10939714	0.04571266	-0.0234918	0.98653522	-1.1328889	0.04067102
TM9SF2	ENSG00000125304	240.660454	0.88474939	0.00297327	-0.7801288	0.01515824	-1.6648782	2.322E-10
CLPP	ENSG00000125656	65.0932675	0.82164709	0.16954027	0.14055903	0.9044233	-0.6810881	0.31875383
DSTN	ENSG00000125868	2290.6994	0.84772997	3.9345E-07	-0.1225885	0.75245839	-0.9703184	2.4088E-09
CEP250	ENSG00000126001	7.09664382	2.68273298	0.11902159	1.56943579	0.4760177	-1.1132972	0.65894697
TUBGCP3	ENSG00000126216	25.9301082	1.53632343	0.04897377	0.36107013	0.82748467	-1.1752533	0.18986324
MCF2L	ENSG00000126217	36.6328771	0.83853239	0.33094865	-0.4806347	0.6683558	-1.3191671	0.04835596
PCID2	ENSG00000126226	36.6542911	1.21744613	0.08301806	0.12394971	0.93829767	-1.0934964	0.14307295
CAPNS1	ENSG00000126247	804.08542	0.37113222	0.22505142	-0.149793	0.7302945	-0.5209253	0.03135657
COX6B1	ENSG00000126267	1455.44449	0.62357224	0.02390726	0.29083339	0.44810528	-0.3327388	0.43277389
FAM78A	ENSG00000126882	5.79086982	5.74680403	0.02026027	5.63338769	0.01623001	-0.1134163	0.98168024
PKMYT1	ENSG00000127564	16.5335033	3.30297532	0.00336273	3.30644212	0.00221174	0.0034668	0.99825809
PAICS	ENSG00000128050	219.421191	0.7455269	0.02638157	0.29352129	0.57558375	-0.4520056	0.33036028
ADM2	ENSG00000128165	5.95855293	2.51810542	0.23520262	-1.3760667	0.72376054	-3.8941722	0.07502229
DGCR6L	ENSG00000128185	116.516116	0.56617414	0.23670667	-0.0483902	0.95764113	-0.6145643	0.16885
SDF2L1	ENSG00000128228	119.079132	0.55365187	0.3407496	0.63041408	0.1655961	0.07676221	0.95066459
YWHAH	ENSG00000128245	34.4909564	1.65341085	0.00535292	0.44172521	0.71368064	-1.2116856	0.07090675
ATF4	ENSG00000128272	155.842213	1.402917	3.6389E-06	0.22644347	0.75160251	-1.1764735	0.00020937
CDC42EP1	ENSG00000128283	21.7422536	1.44806486	0.11862796	0.46959856	0.76899952	-0.9784663	0.40499241
TPST2	ENSG00000128294	30.8668754	1.2645824	0.11121496	0.29390563	0.88725664	-1.0351868	0.24488176
MPST	ENSG00000128309	52.1884452	0.79612241	0.20638634	-0.539101	0.48921902	-1.3352234	0.00694241
APOBEC3A	ENSG00000128383	5.11128028	2.46304496	0.28710631	-0.4874426	0.91712411	-2.9504876	0.19041899
KNSTRN	ENSG00000128944	37.4487922	2.41416163	8.1715E-05	2.2024647	0.0003738	-0.2116969	0.91149121
PIMREG	ENSG00000129195	25.3442784	3.68931688	1.2295E-05	3.04037163	0.00057521	-0.6489452	0.6210995
CDKN2D	ENSG00000129355	51.8685143	1.40842252	0.00780222	0.22339061	0.8630347	-1.1850319	0.03734265
CDC16	ENSG00000130177	55.2653715	0.89339663	0.14600609	-0.0873074	0.94800049	-0.9807041	0.09130529
GTPBP3	ENSG00000130299	60.4356062	0.74847256	0.23791906	0.56578585	0.38677412	-0.1826867	0.90100125
MRPL34	ENSG00000130312	206.938721	0.67520211	0.06509427	0.4485221	0.28724307	-0.22668	0.7707366
CEP85	ENSG00000130695	20.55468	1.30361433	0.21223612	1.32643794	0.14410709	0.02282361	0.99303418
ATP6V1E1	ENSG00000131100	132.365757	0.65818063	0.09411333	-0.214061	0.75468504	-0.8722416	0.01050384
COX4I1	ENSG00000131143	1998.07382	0.36314504	0.22505142	0.12071372	0.79269464	-0.2424313	0.54495954
DIAPH1	ENSG00000131504	73.5048469	0.6820052	0.31469636	0.55022295	0.40282468	-0.1317823	0.931418
UBE2D2	ENSG00000131508	208.582265	0.44647103	0.3318301	0.50924532	0.15860092	0.06277429	0.95038361
ANO1	ENSG00000131620	97.2754581	0.2444185	0.81711412	-0.9609189	0.01701945	-1.2053374	0.00168292
TOP2A	ENSG00000131747	117.40584	3.33673901	1.2236E-16	3.20993559	1.8487E-15	-0.1268034	0.92590018
LGALS3	ENSG00000131981	154.202201	1.48355055	4.4313E-08	0.51834826	0.20353443	-0.9652023	0.00120546
ITGB4	ENSG00000132470	21.4978956	1.4815458	0.12364864	0.90883939	0.43757185	-0.5727064	0.73876325
WBP2	ENSG00000132471	316.966488	0.17705383	0.78696776	-0.46667	0.10799222	-0.6437238	0.01466959
PCNA	ENSG00000132646	81.6192328	2.36096891	7.7909E-09	2.22080341	5.7372E-08	-0.1401655	0.92174256
PPP1R3D	ENSG00000132825	259.339093	1.32083803	2.9127E-08	-0.6098426	0.06044989	-1.9306806	1.3713E-16
SLC39A11	ENSG00000133195	211.418043	0.44851007	0.3393052	0.41941396	0.31053253	-0.0290961	0.97755473
FOPNL	ENSG00000133393	86.433976	0.57588827	0.33204396	0.48600343	0.38497581	-0.0898848	0.94773579
TMEM254	ENSG00000133678	96.8469138	0.52899525	0.34370397	-0.5827117	0.23684839	-1.111707	0.00283306
LRRCC1	ENSG00000133739	112.442456	0.9474027	0.00815839	0.21276796	0.77945065	-0.7346347	0.06963427
CCNB1	ENSG00000134057	189.220114	2.67542869	4.9712E-20	2.5302785	7.1051E-18	-0.1451502	0.89150006
PSRC1	ENSG00000134222	28.6125776	1.95822426	0.00491946	1.72422727	0.01474554	-0.233997	0.91037122
TIMM17A	ENSG00000134375	343.593313	0.51849742	0.11862796	0.27027941	0.52990856	-0.248218	0.65774267
YARS1	ENSG00000134684	64.2138183	0.90954944	0.09307344	0.44685458	0.55277353	-0.4626949	0.58858191
CDCA8	ENSG00000134690	29.0398403	2.77395279	0.00017666	2.49831838	0.00089573	-0.2756344	0.90085678
TPGS2	ENSG00000134779	124.338809	0.55862505	0.29591346	-0.0347317	0.97101953	-0.5933567	0.2411174
ARGLU1	ENSG00000134884	118.723089	1.10472189	0.00204979	0.22547799	0.77580933	-0.8792439	0.02591594

BIVM	ENSG00000134897	15.3064653	1.58205737	0.17788402	0.54255795	0.78262718	-1.0394994	0.49222432
CARS2	ENSG00000134905	43.724519	1.58851724	0.00527566	0.74108155	0.37318345	-0.8474357	0.28291672
MTO1	ENSG00000135297	7.07273753	2.35336587	0.27285194	1.43726416	0.5761602	-0.9161017	0.77629897
B4GALNT1	ENSG00000135454	9.96353207	2.25998854	0.10916793	1.50207479	0.36664079	-0.7579137	0.76045009
MPHOSPH6	ENSG00000135698	179.42494	0.64205435	0.08370559	0.06732045	0.93442132	-0.5747339	0.14628299
CKAP2	ENSG00000136108	194.586093	0.83140171	0.01108037	0.8474515	0.00611018	0.01604979	0.98766681
TBC1D4	ENSG00000136111	12.93703	1.39050998	0.29006723	-0.3950966	0.86634367	-1.7856066	0.12299827
GPNMB	ENSG00000136235	8.24333138	2.00555422	0.22347983	0.60797134	0.83475221	-1.3975829	0.47528648
CALCOCO2	ENSG00000136436	331.412494	0.09543363	0.91350543	-0.545314	0.04611534	-0.6407477	0.01761343
NDUFB5	ENSG00000136521	410.396975	0.35714739	0.32624138	-0.0151653	0.98094654	-0.3723127	0.28560639
NIPSNAP3A	ENSG00000136783	103.515657	0.57657629	0.30004615	-0.1409942	0.87945188	-0.7175705	0.13179723
TXN	ENSG00000136810	1207.21344	0.99782335	2.5433E-07	0.58290693	0.00818738	-0.4149164	0.13880723
CDK5RAP2	ENSG00000136861	56.2290354	0.66830414	0.34039355	0.26714836	0.78578928	-0.4011558	0.68663269
DPM2	ENSG00000136908	143.282643	1.10609379	0.00128918	0.50295297	0.3057822	-0.6031408	0.1962965
PSMB7	ENSG00000136930	390.381083	0.7940076	0.0045078	0.45085237	0.19600609	-0.3431552	0.4716901
CTSV	ENSG00000136943	9.31047383	5.23527203	0.02113608	4.40410232	0.0582538	-0.8311697	0.73876325
ARHGEF39	ENSG00000137135	5.9440828	2.90034432	0.26818953	3.04131994	0.16071107	0.1409756	0.97417445
PPIL1	ENSG00000137168	45.1006055	0.9666566	0.26931085	0.65363261	0.49186168	-0.313024	0.86580127
NRM	ENSG00000137404	27.109438	2.33680071	0.00269904	2.11583603	0.00680007	-0.2209647	0.9245108
SLTM	ENSG00000137776	125.845464	0.5314176	0.29939237	0.26090018	0.69157094	-0.2705174	0.73876325
KIF23	ENSG00000137807	64.3758543	2.50326334	2.0251E-08	2.27127585	4.8878E-07	-0.2319875	0.8676758
KIF11	ENSG00000138160	45.0497344	3.45886649	4.0919E-08	3.54787947	8.7826E-09	0.08901298	0.95911967
KIF20B	ENSG00000138182	64.4952229	1.66737417	0.00021619	1.19000136	0.01785148	-0.4773728	0.58719021
DNA2	ENSG00000138346	13.3502364	1.7316632	0.22949964	1.89699457	0.10970776	0.16533137	0.95807242
BARD1	ENSG00000138376	84.2938132	1.1288275	0.0103154	1.08703305	0.01050925	-0.0417944	0.97577483
MNS1	ENSG00000138587	14.8755703	3.04044458	0.00519296	2.83885086	0.00818738	-0.2015937	0.9449136
HNRNPD	ENSG00000138668	241.018244	0.56926878	0.13542509	0.60892247	0.06367802	0.03965369	0.96908684
CENPE	ENSG00000138778	55.4587924	2.27808006	7.7742E-07	1.98935358	2.5501E-05	-0.2887265	0.81191656
HADH	ENSG00000138796	127.960668	0.8445108	0.04702232	0.29165498	0.68315093	-0.5528558	0.32390427
RNF185	ENSG00000138942	18.7610662	1.81772598	0.10190495	0.75635601	0.65968178	-1.06137	0.48266875
AMIGO2	ENSG00000139211	64.2064953	2.30013329	4.4763E-08	-2.2443277	0.00074961	-4.544461	2.8072E-16
NEDD1	ENSG00000139350	58.7902531	0.76236622	0.25762485	0.75244552	0.19860127	-0.0099207	0.99595651
GAS2L3	ENSG00000139354	38.7724132	3.48661767	3.1995E-07	2.75950226	0.00012306	-0.7271154	0.50583577
BRCA2	ENSG00000139618	7.8064355	2.89054084	0.16173508	2.74080642	0.15033076	-0.1497344	0.97266203
RBM26	ENSG00000139746	48.9433083	0.62564717	0.50325148	-0.9316881	0.17763423	-1.5573353	0.00550193
RAB20	ENSG00000139832	31.8899161	1.94016304	0.00140393	-0.1291532	0.9435865	-2.0693162	0.00076016
GRTP1	ENSG00000139835	34.5391533	1.14814618	0.09906691	0.38375178	0.74538703	-0.7643944	0.39709545
CUL4A	ENSG00000139842	68.1416921	1.11512181	0.01956669	-0.2763275	0.78321424	-1.3914493	0.00192512
EFCAB11	ENSG00000140025	11.1301984	1.50318622	0.33067369	0.50382108	0.83733819	-0.9993651	0.61056699
CPNE2	ENSG00000140848	30.785348	2.09608653	0.00180484	0.69346957	0.56645159	-1.402617	0.06728675
IMPA2	ENSG00000141401	78.2040233	1.37136003	0.00061168	0.62070254	0.2843334	-0.7506575	0.15204885
NFIC	ENSG00000141905	127.862972	0.7779683	0.071117	0.64082758	0.14143668	-0.1371407	0.91133444
SOD1	ENSG00000142168	1339.28333	0.69722859	0.0010913	0.1748575	0.6683558	-0.5223711	0.03135657
APP	ENSG00000142192	301.837811	0.46551156	0.26123087	-0.2615017	0.60670017	-0.7270132	0.01824082
PGD	ENSG00000142657	163.176999	0.63867643	0.1845484	0.17144725	0.83974705	-0.4672292	0.44026741
PLK4	ENSG00000142731	19.0357991	1.88535276	0.07715719	2.07643759	0.02429661	0.19108483	0.94616617
ITGB3BP	ENSG00000142856	34.6408454	1.20789525	0.12233845	0.613895	0.56161972	-0.5940003	0.63269275
NUF2	ENSG00000143228	80.4297693	3.14592682	1.1277E-13	3.14283888	9.0873E-14	-0.0030879	0.99743623
DTL	ENSG00000143476	28.0893346	5.02434874	6.215E-06	4.84730378	9.7947E-06	-0.177045	0.93331726
EIF2D	ENSG00000143486	77.8926858	0.6280041	0.31244612	-0.1271282	0.9044233	-0.7551323	0.16333847
SMYD2	ENSG00000143499	60.2081413	0.74924754	0.31405651	0.88549177	0.12330371	0.13624423	0.93656725
TPM3	ENSG00000143549	1059.14931	0.31707766	0.29258589	0.19692516	0.55730366	-0.1201525	0.84172585
DEGS1	ENSG00000143753	294.304119	0.25421545	0.65261052	-0.4206506	0.2143645	-0.6748661	0.0169401
CNIH4	ENSG00000143771	307.774155	0.76415376	0.00207836	-0.0796156	0.90303258	-0.8437694	0.00051467
WNT9A	ENSG00000143816	15.2493728	1.17657089	0.38506029	-1.1758076	0.42735301	-2.3523785	0.02259372
EML4	ENSG00000143924	39.1249616	0.8967919	0.27998595	0.53778639	0.57947856	-0.3590055	0.80761407
FANCD2	ENSG00000144554	22.7803381	2.0710113	0.00830978	1.59486826	0.06127124	-0.476143	0.78684768
PHLDB2	ENSG00000144824	31.5587648	1.47273623	0.02732349	0.14940209	0.93072212	-1.3233341	0.06100196
RABL3	ENSG00000144840	93.3077889	1.13198208	0.00210531	-0.1203379	0.90362302	-1.25232	0.00059005
STXBP5L	ENSG00000145087	60.6166214	0.76000873	0.24485836	-0.1906245	0.86917136	-0.9506332	0.09130529
ENOPH1	ENSG00000145293	90.4572175	0.63053582	0.29258589	0.05446829	0.96084294	-0.5760675	0.36706947
SKP2	ENSG00000145604	52.9274571	1.29137053	0.01610548	1.054079	0.06067407	-0.2372915	0.8796271
SLC30A5	ENSG00000145740	31.2050421	1.29983238	0.07573653	0.67098742	0.50339326	-0.628845	0.58667363
BTF3	ENSG00000145741	884.652569	0.43981	0.0785122	0.12018036	0.78834426	-0.3196296	0.30345186
PRIM2	ENSG00000146143	20.5676611	1.52184814	0.14770515	1.32858434	0.19430855	-0.1932638	0.94350212
MMS22L	ENSG00000146263	15.2257865	1.64469242	0.17424856	0.86719175	0.59515574	-0.7775007	0.68232797
ARMT1	ENSG00000146476	1193.15381	0.13809553	0.8257516	-0.6083239	0.00338569	-0.7464194	0.00021168
NIPSNAP2	ENSG00000146729	83.6913703	0.67709423	0.2472713	0.35721622	0.63068963	-0.319878	0.73975286
NOM1	ENSG00000146909	19.2380306	1.71156666	0.07848738	1.08377666	0.36235941	-0.62779	0.72175628
CCNB3	ENSG00000147082	5.98123341	6.00684947	0.01324801	5.33450048	0.02801735	-0.672349	0.8835844
EBP	ENSG00000147155	170.837984	1.13665723	0.00016434	0.61350488	0.1085301	-0.5231523	0.23856531
MAL2	ENSG00000147676	484.855564	0.37055645	0.28352313	0.17536549	0.69425725	-0.195191	0.72219958
CEP78	ENSG00000148019	34.8279758	1.11866387	0.18267821	0.82430388	0.36335004	-0.29436	0.88308723
NR6A1	ENSG00000148200	10.0664319	1.65933683	0.32054229	-0.1925039	0.95109975	-1.8518407	0.24601786
ALAD	ENSG00000148218	76.2365792	0.76562162	0.145142	0.4758746	0.44482748	-0.289747	0.77502695
SLC25A25	ENSG00000148339	6.2946236	2.72756654	0.28509256	3.17704723	0.10812664	0.44948069	0.92441713
SH3GLB2	ENSG00000148341	114.036997	0.72091334	0.15064042	0.71593299	0.11081096	-0.0049803	0.99605451
PAXX	ENSG00000148362	233.982298	0.66836065	0.02801475	0.60899618	0.0410037	-0.0593645	0.95014208
EIF4EBP2	ENSG00000148730	457.970919	0.48617461	0.2672216	0.24237639	0.65994356	-0.2437982	0.73222071
FADS1	ENSG00000149485	14.5775167	2.06586363	0.12552881	1.87185421	0.1451371	-0.1940094	0.95066459
DSN1	ENSG00000149636	31.4840387	1.60796892	0.02198054	1.27004227	0.09099625	-0.3379266	0.85502977
TMCO3	ENSG00000150403	105.168766	0.96322334	0.01526487	-0.9393696	0.02852087	-1.902593	3.6129E-08
CCT5	ENSG00000150753	72.0268164	0.77423349	0.28446567	0.41549319	0.64256522	-0.3587403	0.7670282
SEC24D	ENSG00000150961	82.4478375	0.78246093	0.12442051	-0.1914953	0.8474186	-0.9739562	0.03106108
SLC7A11	ENSG00000151012	7.02467032	1.60637982	0.43057294	-3.3030791	0.24384798	-4.9094589	0.04024416
CACNA2D4	ENSG00000151062	5.1212241	2.54794559	0.28366613	0.16456626	0.97216927	-2.3833793	0.3262559
TEX30	ENSG00000151287	61.3860254	1.73300322	6.7562E-05	0.68772409	0.30434316	-1.0452791	0.04003206
NADK2	ENSG00000152620	60.3273963	0.77564695	0.26063638	-0.1323595	0.91637227	-0.9080064	0.1405485
HNRNPDL	ENSG00000152795	239.177347	0.55995226	0.09841011	0.54419508	0.07987742	-0.0157572	0.98766681
PLOD2	ENSG00000152952	37.5149794	1.81449783	0.00290526	1.83314513	0.00172712	0.0186473	0.99268948
CWC27	ENSG00000153015	38.7186208	0.99815379	0.23154962	0.66550458	0.47530907	-0.3326492	0.84986935
CENPH	ENSG00000153044	29.9768148	2.50585619	0.00010869	2.10274522	0.00190563	-0.403111	0.79325718
FAM49B	ENSG00000153310	294.954086	0.64779241	0.03144715	0.11408648	0.8630828	-0.5337059	0.11443277
ING1	ENSG00000153487	20.3808959	1.55441828	0.11999701	0.62097068	0.69324633	-0.9334476	0.49129666
CMIP	ENSG00000153815	36.6883444	1.16747243	0.15278693	0.49365099	0.68315093	-0.6738214	0.56950446
CEBPG	ENSG00000153879	96.7577032	0.70054397	0.17586652	0.71793678	0.11382168	0.01739281	0.98932401
ELOC	ENSG00000154582	684.5646	0.32926983	0.34350779	0.06696136	0.9044233	-0.2623085	0.51946158
MRPL39	ENSG00000154719	96.5913827	0.67879118	0.16157449	0.3454634	0.59505828	-0.3333278	0.68021822
ADAMTS1	ENSG00000154734	178.3067	2.54319215	1.1532E-21	0.91773715	0.00702786	-1.625455	1.1617E-09
SKA1	ENSG00000154839	10.5950481	2.64989614	0.11175047	3.22359006	0.01622031	0.57369392	0.8491931
SLC25A28	ENSG00000155287	34.9023609	0.90831313	0.33004782	0.95095331	0.21699954	0.04264018	0.98396978
ADK	ENSG00000156110	194.243071	1.06606915	0.00015076	0.81839074	0.0065993	-0.2476784	0.71839174
NDUFAF6	ENSG00000156170	158.119141	0.5002322	0.2595128	-0.1736557	0.80281701	-0.6738879	0.06243132
BACH1	ENSG00000156273	197.903362	0.85241651	0.00815839	-0.0320089	0.97096412	-0.8844254	0.00559144
TIAM1	ENSG00000156299	12.4898668	1.55062598	0.30142662	-0.4957784	0.8523205	-2.0464044	0.12193644
BUB1B	ENSG00000156970	13.3129615	2.48954369	0.02837289	2.08721365	0.07615717	-0.40233	0.88934778
SEC13	ENSG00000157020	157.240396	0.5721846	0.16954027	-0.1654943	0.82570306	-0.7376789	0.03926868
LRP8	ENSG00000157193	17.9722502	1.31689411	0.3053004	0.45407801	0.82500379	-0.8628161	0.60658414
VPS26C	ENSG00000157538	48.0081519	1.22481868	0.02765467	0.72511277	0.3051808	-0.4997059	0.61252271
CDC25C	ENSG00000158402	15.6548879	3.2275095	0.00805594	3.02045254	0.01129041	-0.207057	0.94773579
MIS18A	ENSG00000159055	72.9900758	1.12230245	0.01907626	1.27041498	0.00314026	0.14811253	0.91811898
DONSON	ENSG00000159147	12.8741209	1.81645254	0.17185323	1.90101704	0.10032393	0.08456449	0.97755473
LAD1	ENSG00000159166	109.803508	0.7016225	0.14358269	0.20213058	0.81412736	-0.4994919	0.41030646
ATP5MC1	ENSG00000159199	441.13475	0.82431613	0.00026734	0.00990512	0.98800454	-0.814411	0.00038899
CHAF1B	ENSG00000159259	20.0011102	1.56531567	0.15825389	1.01780863	0.43204981	-0.547507	0.79564228
PSMB4	ENSG00000159377	672.899701	0.40878191	0.29270035	0.25650312	0.55277353	-0.1522788	0.8479132
KALRN	ENSG00000160145	11.7502128	1.59816716	0.26107904	0.44333521	0.85782026	-1.1548319	0.5010799
WDR4	ENSG00000160191	19.8974765	1.51538884	0.18662389	1.21257937	0.30408101	-0.3028095	0.91149121
CBS	ENSG00000160200	14.9660132	2.28898841	0.01241968	-0.1856751	0.9435865	-2.4746635	0.00770692
PDXK	ENSG00000160209	158.301769	1.03330212	0.00042607	0.52699539	0.17250242	-0.5063067	0.23098945
CSTB	ENSG00000160213	499.424074	0.78809004	0.0008767	-0.0389578	0.95114974	-0.8270478	0.00043006
LSS	ENSG00000160285	64.4665451	0.89903183	0.0774555	-0.4546432	0.5476837	-1.353675	0.00192512
C21orf58	ENSG00000160298	16.8015112	2.25735619	0.02254098	1.85588787	0.07375926	-0.4014683	0.87542764
PRMT2	ENSG00000160310	124.977121	0.55335017	0.28295346	-0.0861436	0.92655844	-0.6394938	0.16242373
C9orf116	ENSG00000160345	15.2920359	1.67027156	0.17601177	1.06276938	0.4681399	-0.6075022	0.79191624
ZNF385A	ENSG00000161642	80.673214	0.26069928	0.83137788	-0.9816439	0.040579	-1.2423432	0.00607217
MPP3	ENSG00000161647	33.5840383	0.9641434	0.29939237	0.82960126	0.34519931	-0.1345421	0.95014208
SPC24	ENSG00000161888	14.689889	4.11371303	0.00180856	4.04141939	0.00158252	-0.0722936	0.97976498
SNRNP25	ENSG00000161981	170.385931	0.79411048	0.01391117	0.81333765	0.00746782	0.01922717	0.98489125
USP1	ENSG00000162607	70.9759625	0.83353373	0.11987595	0.64327096	0.25209772	-0.1902628	0.89187243
LRRC58	ENSG00000163428	136.191442	0.67708894	0.26818953	-0.0560511	0.96084294	-0.7331401	0.19379048
FSTL1	ENSG00000163430	14.2672262	1.8956253	0.07476472	-2.5248397	0.1255738	-4.420465	0.00063711
CIP2A	ENSG00000163507	26.2245983	2.7552869	0.0003344	1.59714612	0.10216607	-1.1581408	0.24194277
LIPH	ENSG00000163898	39.729772	0.45296817	0.7310237	-1.7889664	0.00485159	-2.2419345	0.0002015
TKT	ENSG00000163931	403.069222	0.9595819	0.00063868	0.44965191	0.2414862	-0.50993	0.19218241
S100P	ENSG00000163993	18.9017114	1.51545411	0.12843028	-1.832488	0.12601508	-3.3479421	0.00030534
H2AZ1	ENSG00000164032	316.994214	1.72150899	9.3898E-13	1.44293928	4.899E-09	-0.2785697	0.62079034
HMGB2	ENSG00000164104	121.228164	2.89939265	1.1421E-17	2.91904536	5.0497E-18	0.01965271	0.9869593
MAD2L1	ENSG00000164109	96.8208212	2.60600633	3.9224E-12	2.62618239	1.743E-12	0.02017606	0.98766681
ANXA5	ENSG00000164111	290.901851	0.38741478	0.35276274	-0.2579275	0.57125416	-0.6453422	0.02804283
ICE1	ENSG00000164151	23.8921834	1.09803073	0.31398615	0.74380935	0.52985451	-0.3542214	0.87434773
CMBL	ENSG00000164237	375.436625	0.50046616	0.10353729	-0.2853338	0.46444652	-0.7858	0.00137147
NDUFS4	ENSG00000164258	158.510693	0.57928096	0.16402514	0.09421637	0.90700167	-0.4850646	0.30773196
PTTG1	ENSG00000164611	244.690892	3.06918459	7.4451E-34	2.68064997	1.3368E-25	-0.3885346	0.34955637
TMUB1	ENSG00000164897	61.7282251	0.80988653	0.17372107	0.61896145	0.32387212	-0.1909251	0.89556348
MID1IP1	ENSG00000165175	182.53391	0.71104293	0.04516417	0.27946259	0.61767306	-0.4315803	0.38589414
VDAC2	ENSG00000165637	703.805213	0.55683322	0.02026027	0.07603837	0.88879569	-0.4807949	0.06427766
GHITM	ENSG00000165678	474.634363	0.3740538	0.24899369	-0.020519	0.97269488	-0.3945728	0.19538744
ZMYND19	ENSG00000165724	98.6602375	1.14887092	0.00208582	1.18546776	0.00090905	0.03659685	0.97622389

GPT2	ENSG00000166123	33.0595418	1.05132478	0.22764412	0.55659624	0.62294227	-0.4947285	0.73067985
CENPN	ENSG00000166451	8.42979809	3.21071906	0.07182079	3.12091551	0.05877252	-0.0898036	0.98171223
CIAO2B	ENSG00000166595	287.245901	0.49482894	0.16139306	0.10185843	0.87783913	-0.3929705	0.34955637
PLK1	ENSG00000166851	10.3704326	4.82180917	0.04527447	4.91198511	0.02545755	0.09017594	0.98034096
RCCD1	ENSG00000166965	21.6377609	1.11155906	0.29721281	0.44117105	0.77739227	-0.670388	0.64939128
NUDT21	ENSG00000167005	250.462719	0.58841947	0.07980569	0.19524223	0.72618994	-0.3931772	0.37732075
MVD	ENSG00000167508	45.0774945	0.90660872	0.17619083	-0.6779767	0.39997576	-1.5845854	0.00293306
RPL13	ENSG00000167526	2295.12734	0.34840675	0.27384539	-0.0694807	0.89723096	-0.4178875	0.12466605
CHAF1A	ENSG00000167670	25.8945731	1.8368642	0.01459257	1.88921849	0.00742867	0.05235429	0.98085199
GGT6	ENSG00000167741	37.2050178	1.22547001	0.0546783	0.18172548	0.9017678	-1.0437445	0.13422322
CDK2AP2	ENSG00000167797	105.700949	0.5543313	0.3393052	0.50002209	0.34038014	-0.0543092	0.96568248
MRPL58	ENSG00000167862	175.152913	0.46852349	0.32712945	0.27797896	0.61527647	-0.1905445	0.83025809
PBK	ENSG00000168078	23.7365412	4.20112925	7.4429E-05	4.14720679	6.6003E-05	-0.0539225	0.98280854
TTC39C	ENSG00000168234	26.6659901	1.22238368	0.17916307	1.15971695	0.16594078	-0.0626667	0.97755473
H1-4	ENSG00000168298	19.3634927	1.12837781	0.33004782	0.64758312	0.64218584	-0.4807947	0.80308511
RFWD3	ENSG00000168411	48.1033899	1.09233661	0.09238505	1.32234825	0.01342577	0.23001164	0.89118103
RAB31	ENSG00000168461	11.9899058	1.52837745	0.28999311	-0.2314723	0.93402761	-1.7598497	0.19041899
DNAJC21	ENSG00000168724	139.566438	0.62198049	0.13533341	-0.1685609	0.82784731	-0.7905414	0.02839283
UQCRFS1	ENSG00000169021	488.005965	0.61327248	0.00950156	0.51796868	0.03084743	-0.0953038	0.90100125
UPF3A	ENSG00000169062	92.0556503	0.75105476	0.09276299	-0.5142128	0.35338877	-1.2652675	0.00053426
HINT1	ENSG00000169567	756.488528	1.19850159	1.191E-08	0.60864484	0.01490647	-0.5898567	0.02536946
CENPX	ENSG00000169689	660.048121	0.3293057	0.29721281	-0.215479	0.53728933	-0.5447847	0.01584847
FASN	ENSG00000169710	913.878375	0.15937114	0.76102965	-1.1340391	1.3611E-10	-1.2934102	1.2719E-13
TM4SF1	ENSG00000169908	118.101738	0.19505431	0.84652754	-1.1856461	0.00055499	-1.3807004	4.1353E-05
ARL6IP1	ENSG00000170540	161.443317	1.22822945	2.83E-05	0.6306758	0.09479805	-0.5975536	0.13217057
TSEN34	ENSG00000170892	181.744803	0.58035861	0.1446208	0.52315087	0.16365021	-0.0572077	0.95641767
FAM241B	ENSG00000171224	79.7954876	1.15816176	0.00847771	0.78633491	0.12147483	-0.3718268	0.68176621
SHCBP1	ENSG00000171241	54.9165284	2.7554557	4.0294E-08	2.7363167	3.1986E-08	-0.019139	0.99038345
TBCA	ENSG00000171530	343.822891	0.7332114	0.02703096	0.36636556	0.41468749	-0.3668458	0.49087591
ENC1	ENSG00000171617	24.7893927	1.3479569	0.11472356	0.8454948	0.41224762	-0.5024621	0.74752754
MTBP	ENSG00000172167	18.3523523	1.46503633	0.15324671	0.84906625	0.51360989	-0.6191301	0.72586256
CKS1B	ENSG00000173207	187.719433	1.84885242	1.3628E-11	1.91456188	1.2648E-12	0.06570947	0.95014208
VANGL1	ENSG00000173218	37.3953805	1.3598033	0.08290811	1.66696027	0.00990874	0.30715697	0.87343359
SNCG	ENSG00000173267	107.794399	0.66553682	0.14294929	-3.6563485	2.0319E-14	-4.3218853	2.2383E-20
NAA20	ENSG00000173418	327.509364	0.49195178	0.11902159	-0.1278884	0.82813811	-0.6198401	0.02346178
ZWILCH	ENSG00000174442	22.4382597	1.63416796	0.07587517	1.58128111	0.06538707	-0.0528869	0.98280854
IGDCC3	ENSG00000174498	9.29283092	2.34225317	0.11988019	1.24067116	0.54511243	-1.101582	0.612042
UBE2C	ENSG00000175063	178.72008	3.58584262	9.2322E-28	3.58265243	5.6808E-28	-0.0031902	0.99679384
CKAP5	ENSG00000175216	242.395696	0.55160735	0.18713457	0.57947731	0.10834269	0.02786995	0.9797031
MRPL48	ENSG00000175581	59.7842339	0.77824034	0.21288721	0.39528386	0.63401333	-0.3829565	0.70664866
RMI2	ENSG00000175643	48.9280026	1.57102426	0.0027219	1.29309958	0.01830636	-0.2779247	0.8529326
AURKAIP1	ENSG00000175756	350.231075	0.41049795	0.29270035	0.135968	0.82208119	-0.2745299	0.59754291
SFN	ENSG00000175793	7.68503518	2.19261913	0.22505142	-0.4539467	0.90412613	-2.6465659	0.12844213
NUPR1	ENSG00000176046	45.4107078	1.93504878	4.8155E-05	-1.3251645	0.06325611	-3.2602133	3.1352E-10
GPX2	ENSG00000176153	12.0846812	0.77776418	0.73166849	-1.9499406	0.21202413	-2.7277047	0.04597182
ACBD7	ENSG00000176244	9.79291603	1.45411399	0.39914634	-2.0129893	0.28149249	-3.4671033	0.01532423
PRR15	ENSG00000176532	120.985949	0.51946337	0.32119918	-2.5269425	7.2387E-12	-3.0464059	1.8747E-17
MYO1D	ENSG00000176658	33.1962707	0.93848314	0.2529714	-0.3037412	0.82954393	-1.2422244	0.07383835
METRNL	ENSG00000176845	128.591697	0.75798537	0.042979	0.28817783	0.63526971	-0.4698075	0.36243042
POLE	ENSG00000177084	34.2281909	0.92653909	0.3031926	1.02662751	0.15566096	0.10008842	0.95911967
AP3S1	ENSG00000177879	381.734887	0.51498421	0.28663633	0.09903432	0.90394952	-0.4159499	0.45483688
COX5A	ENSG00000178741	330.451462	0.50207401	0.13522667	0.04541774	0.94867615	-0.4566563	0.19531859
RMI1	ENSG00000178966	21.8240853	1.55714791	0.12059131	1.41946581	0.1360965	-0.1376821	0.95591153
EIF3K	ENSG00000178982	243.329983	0.44155194	0.2696924	0.11655587	0.86058371	-0.3249961	0.51291267
GPC5	ENSG00000179399	45.7464734	2.81008877	4.6401E-10	-2.2178082	0.00904636	-5.027897	4.2572E-14
FJX1	ENSG00000179431	20.5850623	1.68905131	0.10448317	0.46740977	0.81773779	-1.2216415	0.32460894
PCED1B	ENSG00000179715	11.878903	2.29536405	0.04547752	-1.1873935	0.59446585	-3.4827575	0.00406619
RCC1	ENSG00000180198	45.3001289	1.14650771	0.10815315	1.11386175	0.08951678	-0.032646	0.98667112
PPA1	ENSG00000180817	949.760558	0.54559078	0.11862796	0.40270665	0.27562873	-0.1428841	0.87293541
NQO1	ENSG00000181019	2554.79934	1.2230605	1.9454E-15	-0.7588858	6.1393E-06	-1.9819463	2.4126E-40
DHTKD1	ENSG00000181192	126.124946	1.58156291	5.5161E-07	1.15408829	0.00071867	-0.4274746	0.46220655
RTKN2	ENSG00000182010	24.3800047	2.66376542	0.00058382	2.71317813	0.00028252	0.04941271	0.98280854
IDH2	ENSG00000182054	240.144215	0.28508284	0.59907575	-0.6469447	0.02663305	-0.9320275	0.00041741
FAM89A	ENSG00000182118	13.0409705	2.19901165	0.06402764	1.3960597	0.33621151	-0.8029519	0.69483546
MRPL41	ENSG00000182154	327.570238	0.42683807	0.28333745	-0.0658954	0.92577438	-0.4927334	0.15995573
CEP97	ENSG00000182504	15.0998539	1.4619994	0.29059704	1.22672407	0.35648538	-0.2352753	0.94053638
SKA2	ENSG00000182628	342.861589	1.03216578	5.1643E-06	0.35521636	0.31398973	-0.6769494	0.00889847
NA	ENSG00000183022	10.9234563	1.96109178	0.20135369	1.92814254	0.15900938	-0.0329492	0.99284764
GAS6	ENSG00000183087	17.2573243	1.6308623	0.1845484	1.11077137	0.42385913	-0.5200909	0.83886499
SMDT1	ENSG00000183172	216.499945	0.59459697	0.12442051	-1.0012162	0.00108413	-1.5958132	6.3285E-09
SF3A3	ENSG00000183431	82.4214962	0.61684206	0.33145585	0.6193601	0.25103106	0.00251804	0.99825809
PSMG1	ENSG00000183527	85.291427	1.11037703	0.00582296	0.97337936	0.01671122	-0.1369977	0.91450227
ZNRF3	ENSG00000183579	14.6907922	1.46957752	0.22601346	0.25466414	0.91260429	-1.2149134	0.37401773
HMCES	ENSG00000183624	94.8960532	0.73914306	0.1355694	0.60694083	0.22220013	-0.1322022	0.91916333
IQGAP3	ENSG00000183856	28.2427444	2.92117294	7.4053E-05	2.29766778	0.0036738	-0.6235052	0.63706824
UQCR10	ENSG00000184076	552.898533	0.53918658	0.10302178	-0.3589734	0.34652941	-0.89816	0.00049032
NIPSNAP1	ENSG00000184117	70.5005134	0.3751001	0.70255147	-0.7954756	0.13862672	-1.1705757	0.01215494
KNTC1	ENSG00000184445	23.9542701	1.5997558	0.07563575	1.1479301	0.25256029	-0.4518257	0.81638214
XPOT	ENSG00000184575	150.639706	0.6637384	0.11005221	0.42661237	0.37724733	-0.237126	0.77938123
H1-10	ENSG00000184897	176.006692	0.53249953	0.31369388	0.23997375	0.72818743	-0.2925258	0.71839174
SUMO3	ENSG00000184900	330.9903	0.49578406	0.11903547	0.61465636	0.01686564	0.1188723	0.88627625
NDUFA6	ENSG00000184983	238.941142	1.21132575	2.4739E-06	0.37612812	0.37500424	-0.8351976	0.00356149
UBALD2	ENSG00000185262	103.985937	0.9872025	0.013209	-0.0755576	0.94268284	-1.0627601	0.00663066
GAS2L1	ENSG00000185340	52.9594403	0.85010739	0.1717771	0.2757868	0.79131149	-0.5743206	0.4814335
MRPL40	ENSG00000185608	61.6428552	0.7684418	0.22065304	-0.0693054	0.95415902	-0.8377472	0.15514493
UBE2L3	ENSG00000185651	160.287917	0.5291085	0.19534881	-0.021824	0.97836194	-0.5509325	0.16444509
DRG1	ENSG00000185721	99.4212344	0.92049642	0.02638157	0.59559746	0.22597642	-0.324899	0.69681311
MORF4L1	ENSG00000185787	445.715057	0.47812613	0.14834547	0.16917935	0.74251675	-0.3089468	0.49772547
DNAH14	ENSG00000185842	19.2268428	1.18779941	0.30196368	0.82421607	0.50810345	-0.3635833	0.87788333
LAMP1	ENSG00000185896	238.494358	0.61229838	0.145142	0.08498027	0.91923746	-0.5273181	0.25521048
RASA3	ENSG00000185989	6.13078162	2.81498577	0.20135369	2.22461097	0.33099853	-0.5903748	0.89238219
INSIG1	ENSG00000186480	130.636299	1.05414675	0.00158639	-0.1306263	0.88140997	-1.184773	0.00030523
BCR	ENSG00000186716	27.0057047	1.27201891	0.12442051	0.98870388	0.25704706	-0.283315	0.89195972
PPARA	ENSG00000186951	7.80856801	2.68268018	0.08346498	1.15253084	0.63846815	-1.5301493	0.42798079
RPS19BP1	ENSG00000187051	140.004475	0.53197738	0.28663633	0.20573411	0.77354745	-0.3262433	0.6419236
IFT140	ENSG00000187535	10.1371482	1.65300928	0.28643986	-0.2531597	0.93442132	-1.9061689	0.19156427
EXD3	ENSG00000187609	25.3888593	1.69060631	0.02937183	-0.0803135	0.96985809	-1.7709198	0.0221215
WNT7B	ENSG00000188064	51.5667103	0.97662817	0.10670185	0.87584826	0.13139226	-0.1007799	0.95014208
COMMD6	ENSG00000188243	177.3921	0.97412569	0.01024779	-0.4479212	0.42597676	-1.4220468	2.8385E-05
HES4	ENSG00000188290	127.415609	0.79352482	0.07961868	0.08739798	0.93146911	-0.7061268	0.14438854
FAM72B	ENSG00000188610	13.187472	3.94258442	0.00399927	3.50785833	0.01111329	-0.4347261	0.87700964
S100A16	ENSG00000188643	547.607746	0.49007301	0.09813055	-3.0439521	1.0265E-41	-3.5340251	1.6852E-56
SMIM15	ENSG00000188725	41.6596639	0.84466018	0.29589188	0.50447758	0.59515574	-0.3401826	0.81489046
C9orf152	ENSG00000188959	42.3488286	0.38379174	0.78768801	-1.9142638	0.00177596	-2.2980555	0.00010232
S100A14	ENSG00000189334	107.275629	0.7971321	0.04977115	-2.9448463	3.2296E-12	-3.7419784	4.0199E-20
TUBB	ENSG00000196230	400.418612	1.8290139	3.6467E-19	1.77977062	3.7649E-18	-0.0492433	0.95066459
XRCC6	ENSG00000196419	269.746773	0.80780626	0.01547288	0.41218553	0.36003903	-0.3956207	0.46027385
FAM72A	ENSG00000196550	11.6046612	1.9295063	0.14189911	1.46057088	0.29930755	-0.4689354	0.87433261
PLXNB2	ENSG00000196576	82.8457047	0.88329147	0.0589326	0.24357456	0.78176764	-0.6397169	0.26396225
XRCC2	ENSG00000196584	15.6929342	2.43455139	0.04344317	2.91437413	0.00450532	0.47982274	0.84946995
CD47	ENSG00000196776	1226.20679	0.90134063	6.9988E-08	0.66764269	0.00015174	-0.2336979	0.48918419
TLE1	ENSG00000196781	53.4388351	0.67906118	0.33996873	-0.584417	0.42866893	-1.2634782	0.01233407
H4C3	ENSG00000197061	99.638084	2.19403616	3.3519E-10	1.15708486	0.00579471	-1.0369513	0.00920438
UAP1L1	ENSG00000197355	26.4515188	1.25189557	0.1406966	-0.4147107	0.79072299	-1.6666063	0.02744584
SSPO	ENSG00000197558	6.32750501	2.74552332	0.33226503	2.88511044	0.2143645	0.13958712	0.97577483
ATAD3A	ENSG00000197785	41.593723	0.8109849	0.31874682	0.55189163	0.52980472	-0.2590933	0.87788333
ADH5	ENSG00000197894	206.019133	0.52899904	0.14048668	0.23725782	0.64084797	-0.2917412	0.59435775
TEAD4	ENSG00000197905	79.0434905	0.69640756	0.22343417	0.05735892	0.95881101	-0.6390486	0.29142629
S100A6	ENSG00000197956	24.3491143	2.49215427	0.00032883	-0.4496352	0.8186795	-2.9417895	4.8243E-05
TFDP1	ENSG00000198176	125.00331	1.74577333	4.3968E-08	0.8528346	0.0326182	-0.8929387	0.01820344
PIM3	ENSG00000198355	66.6132115	1.36020733	0.00587349	0.90727484	0.11300023	-0.4529325	0.64428882
TXNRD1	ENSG00000198431	319.843911	0.99903058	0.00024872	0.30405745	0.52018218	-0.6949731	0.02815806
CHAMP1	ENSG00000198824	34.2811603	1.39953747	0.03696926	0.02711309	0.98732455	-1.3724244	0.04434325
HMGN2	ENSG00000198830	1215.78769	0.8047855	6.5631E-06	0.84047076	1.1411E-06	0.03568527	0.95807242
SREBF2	ENSG00000198911	87.8306354	1.19330561	0.00236294	-0.0409175	0.97096412	-1.2342231	0.00173206
CENPW	ENSG00000203760	33.7128986	2.56081165	5.3676E-05	2.39788179	0.00015657	-0.1629299	0.93612313
SOX18	ENSG00000203883	8.91175225	2.41151302	0.14507384	2.45290377	0.09418658	0.04139075	0.99038345
MZT1	ENSG00000204899	130.160282	1.70833039	1.3244E-08	0.49838476	0.32193083	-1.2099456	0.00015896
SMN1	ENSG00000205571	85.9748295	0.98829899	0.02765467	0.82378121	0.07451582	-0.1645178	0.90100125
ITSN1	ENSG00000205726	52.6182257	0.89748442	0.1451955	0.6449726	0.33919869	-0.2525118	0.86251002
DIO1	ENSG00000211452	195.649967	0.74662168	0.01171378	-0.9386657	0.00122532	-1.6852874	2.3184E-11
MXD3	ENSG00000213347	19.871101	4.13665248	3.38E-05	2.48506647	0.04146629	-1.651586	0.071277
NA	ENSG00000213442	2388.44621	0.56466265	0.0161613	0.28377874	0.36808411	-0.2808839	0.45726674
CENPBD1P1	ENSG00000213753	13.2277659	1.59491663	0.29416163	1.25737181	0.4104992	-0.3375448	0.91450227
NUDT19	ENSG00000213965	115.595462	0.65163622	0.2842908	0.73244968	0.13081311	0.08081346	0.95308027
NAXD	ENSG00000213995	42.6138064	1.11507836	0.09238505	-0.751962	0.38528381	-1.8670403	0.00082501
NEURL1B	ENSG00000214357	13.5694452	3.74457822	0.00243738	3.19181465	0.01223356	-0.5527636	0.81716581
FAM72D	ENSG00000215784	8.6982083	3.44150487	0.10029729	3.95106563	0.02370895	0.50956076	0.88934778
FNIP1	ENSG00000217128	49.9979627	0.80720283	0.2300135	0.12474494	0.92192673	-0.6824579	0.36848477
SBDSP1	ENSG00000225648	61.2626248	1.31656991	0.01051851	1.26519131	0.01099911	-0.0513786	0.97417445
FGD5-AS1	ENSG00000225733	192.287723	0.20996743	0.77936927	-0.5011927	0.16028732	-0.7111601	0.02571289
NA	ENSG00000225976	16.0621596	2.14905765	0.02796786	1.27173583	0.31226331	-0.8773218	0.57996094
TMEM191A	ENSG00000226287	35.2457301	0.8998813	0.31490279	0.16213134	0.91686547	-0.73775	0.46849381
NA	ENSG00000228519	10.2773203	2.35878659	0.11711803	1.56366106	0.37376101	-0.7951255	0.7670282
DHFR	ENSG00000228716	135.587287	3.14098388	6.6312E-22	2.97482207	1.3341E-19	-0.1661618	0.87168105
NA	ENSG00000229028	7.27879433	2.59708813	0.15116431	0.65553919	0.85445419	-1.9415489	0.34139653
NA	ENSG00000229932	8.38212805	2.03522502	0.2545654	1.56252592	0.39297174	-0.4726991	0.89761891
NA	ENSG00000230330	87.8302964	0.84372011	0.06022184	0.67064706	0.15149684	-0.173073	0.89118103
HSBP1	ENSG00000230989	724.124621	0.38723111	0.2595128	-0.1815629	0.68647763	-0.568794	0.02930843

NA	ENSG00000231434	25.7580482	1.45058723	0.16139306	1.15726378	0.27863665	-0.2933235	0.90915148
NA	ENSG00000231991	41.6355302	0.92804227	0.20448159	0.57433472	0.50860293	-0.3537076	0.79652678
NA	ENSG00000231993	5.60440819	2.67530011	0.25762485	2.09893895	0.38181081	-0.5763612	0.89766704
NA	ENSG00000232187	49.320784	0.85838503	0.17699108	-0.3853757	0.69240462	-1.2437608	0.0189492
SNHG7	ENSG00000233016	47.1470892	0.93637615	0.15324671	0.22876904	0.85396862	-0.7076071	0.37444577
C5orf58	ENSG00000234511	55.9408939	0.77037827	0.26959229	-0.1072976	0.93402761	-0.8776758	0.16444509
NA	ENSG00000234619	89.8943057	0.69570743	0.17239447	0.28416011	0.70972785	-0.4115473	0.57996094
OLMALINC	ENSG00000235823	41.8083044	0.60989533	0.51161397	-1.5594893	0.01033342	-2.1693846	8.5184E-05
NA	ENSG00000237350	16.4809848	1.28662383	0.29258589	0.2384847	0.9132252	-1.0481391	0.44777006
PI4KA	ENSG00000241973	55.9329512	0.9223245	0.09997856	-0.1017666	0.93442132	-1.0240911	0.05406602
HAUS5	ENSG00000249115	43.0009008	1.12984196	0.10207223	0.83595766	0.26441846	-0.2938843	0.86221301
NA	ENSG00000249353	102.40028	0.62954303	0.26818953	0.4356966	0.47307074	-0.1938464	0.87675675
LSM14A	ENSG00000257103	452.125021	0.61640552	0.01018912	0.436162	0.10197222	-0.1802435	0.74095209
TMEM179	ENSG00000258986	16.3413627	1.43012329	0.31051818	2.19482989	0.01828435	0.7647066	0.6555099
NA	ENSG00000261061	15.8278592	3.37804675	0.00435376	3.45823315	0.0020958	0.0801864	0.97807953
NA	ENSG00000261087	13.7947185	1.36684739	0.28336416	-0.9329634	0.58614455	-2.2998108	0.02819638
ZNF850	ENSG00000267041	13.3319404	1.5263833	0.32054229	1.8257177	0.11731374	0.2993344	0.92222697
MIR924HG	ENSG00000267374	6.19042607	5.86300209	0.02048693	5.35142736	0.03131014	-0.5115747	0.91916333
CD24	ENSG00000272398	695.990044	0.92838858	6.6952E-06	-0.8935345	2.765E-05	-1.8219231	7.878E-22
NA	ENSG00000272779	37.2303232	1.02287636	0.15324671	0.00789974	0.9949846	-1.0149766	0.15845046
LHX1	ENSG00000273706	21.634625	1.20827476	0.28010253	0.80410341	0.51573802	-0.4041714	0.85736176
CBSL	ENSG00000274276	8.76113898	2.0852765	0.26123087	0.13895258	0.97096412	-1.9463239	0.31052476
PCCA-DT	ENSG00000274605	28.0492736	0.88566249	0.36592494	-0.5831212	0.62932298	-1.4687837	0.04719941
LOC102723996	ENSG00000277117	13.930429	1.69154956	0.15672161	-0.2697274	0.91712411	-1.961277	0.08585893
NA	ENSG00000280088	10.3718724	2.33426686	0.11219659	-0.0350707	0.99232686	-2.3693375	0.10749645
NA	ENSG00000280206	5.61479006	4.07140674	0.18011345	4.01264023	0.13912981	-0.0587665	0.99038345

Cluster 2

	ensembl	baseMean	TvsC log2FoldChange	padj	RvsC log2FoldChange	padj	RvsT log2FoldChange	padj
NIPAL3	ENSG00000001461	105.311171	-0.378212	0.62668178	-1.1514976	0.00192325	-0.7732856	0.11363354
CD99	ENSG00000002586	577.89543	-0.2560078	0.59170535	-0.5435466	0.03098796	-0.2875388	0.51050664
LIG3	ENSG00000005156	33.0060281	-0.1888975	0.93272593	-1.4835491	0.02759344	-1.2946516	0.10471417
IBTK	ENSG00000005700	56.3125564	-0.4481822	0.68940547	-1.5050879	0.00301689	-1.0569057	0.10807087
ST3GAL1	ENSG00000008513	161.872333	-0.0580512	0.96334195	-1.7535324	3.4575E-10	-1.6954812	2.8454E-09
SEC62	ENSG00000008952	266.283055	0.0741469	0.94766509	-0.679259	0.01478065	-0.7534059	0.00744261
ALOX5	ENSG00000012779	17.7235429	-0.8986537	0.52593337	-2.0006894	0.0241021	-1.1020357	0.47388661
CALCOCO1	ENSG00000012822	27.5045428	-0.7108268	0.55746484	-1.5796996	0.02612868	-0.8688728	0.47780434
RWDD2A	ENSG00000013392	8.29697651	-1.0789436	0.66781747	-3.7568403	0.03337231	-2.6778968	0.28934052
PHF20	ENSG00000025293	210.213305	-0.8207232	0.00351951	-1.0132008	8.9515E-05	-0.1924776	0.8079946
CD44	ENSG00000026508	161.794488	-0.293744	0.67017607	-0.8126277	0.01129041	-0.5188837	0.26188394
RABEP1	ENSG00000029725	134.768916	-0.4170758	0.48369374	-1.0287449	0.00183477	-0.6116692	0.195282
GABARAPL2	ENSG00000034713	599.919258	-0.0633891	0.94332213	-0.5291598	0.0170729	-0.4657706	0.06791821
SH3YL1	ENSG00000035115	53.6470066	-0.2736299	0.86780526	-1.4654596	0.00779947	-1.1918297	0.06963521
CDH1	ENSG00000039068	524.443282	0.34011184	0.45133101	-0.4718829	0.13054695	-0.8119948	0.00163362
RAB27B	ENSG00000041353	18.0139746	0.53280693	0.7943959	-2.4817944	0.01524293	-3.0146013	0.00208625
RETSAT	ENSG00000042445	63.1050226	-0.551712	0.4828875	-1.1791036	0.01107128	-0.6273915	0.425821
ATP6V1H	ENSG00000047249	194.749311	-0.1584186	0.86758062	-0.658202	0.04586466	-0.4997834	0.25340806
PPP1R3F	ENSG00000049769	27.3864052	0.55811144	0.72704207	-1.5173916	0.0796168	-2.075503	0.00769556
HERPUD1	ENSG00000051108	240.741451	-0.0544577	0.96354514	-1.6774595	3.9469E-11	-1.6230018	3.4484E-10
AKR7A2	ENSG00000053371	275.818708	-0.1711621	0.82214362	-0.8883188	0.00033055	-0.7171567	0.01051733
HHAT	ENSG00000054392	20.8859202	-0.5691908	0.75665249	-1.8423711	0.03259618	-1.2731803	0.31089586
ATP9A	ENSG00000054793	53.2806421	-0.5567352	0.51843511	-1.620467	0.00070655	-1.0637318	0.09130529
F7	ENSG00000057593	8.45980382	0.92206063	0.71694816	-3.1479033	0.11255838	-4.0699639	0.02656282
SLC12A2	ENSG00000064651	78.7315301	-0.3414678	0.73391348	-1.3444847	0.00156554	-1.0030169	0.05406602
BCAS1	ENSG00000064787	380.022558	-0.4876313	0.14319551	-3.8206222	1.409E-49	-3.3329909	4.8555E-37
REEP1	ENSG00000068615	84.7746401	-0.5621342	0.39818127	-1.7146824	1.1106E-05	-1.1525482	0.01547055
ERLEC1	ENSG00000068912	118.884401	-0.5198046	0.32849374	-0.7398982	0.05333973	-0.2200936	0.8317003
PPP2R5B	ENSG00000068971	3.76883647	-1.9068194	NA	-5.4634334	0.03001727	-3.556614	0.37444966
NUCB2	ENSG00000070081	362.936679	-0.3346026	0.47605109	-0.7459774	0.00436973	-0.4113748	0.31201585
NDST1	ENSG00000070614	89.5649252	-0.5469952	0.38506029	-1.1143892	0.00490861	-0.567394	0.39924564
CYBRD1	ENSG00000071967	73.5615336	0.27873375	0.84727392	-1.3510938	0.00990874	-1.6298275	0.00130654
SREBF1	ENSG00000072310	192.662413	-0.2302858	0.77434914	-2.0479174	3.217E-13	-1.8176317	3.9364E-10
ATP2A3	ENSG00000074370	26.9558036	-1.4500333	0.07840877	-2.0298847	0.00481675	-0.5798514	0.76775103
SEMA3C	ENSG00000075223	156.043965	-0.5473137	0.31842342	-2.0421613	4.8871E-10	-1.4948477	4.0543E-05
DGKD	ENSG00000077044	56.0093397	-0.3353783	0.76919589	-2.2326625	1.3191E-06	-1.8972842	0.00015888
CAPZB	ENSG00000077549	490.467907	-0.1867135	0.7310237	-0.5538356	0.01776646	-0.3671221	0.26714273
NEBL	ENSG00000078114	193.758653	-0.0887668	0.94914686	-1.1121962	0.00057901	-1.0234294	0.00322227
RIMS1	ENSG00000079841	28.3787791	-0.0987667	0.96910399	-3.2083618	4.5336E-05	-3.1095951	0.00015457
MAGI3	ENSG00000081026	72.6047732	0.2836622	0.822831	-0.8474543	0.11382168	-1.1311165	0.02144845
BZW1	ENSG00000082153	140.336259	-0.3329439	0.64176089	-1.1240425	0.00057358	-0.7910986	0.05089477
BCKDHB	ENSG00000083123	24.1379956	0.08784574	0.97925186	-2.103982	0.01413706	-2.1918277	0.01378175
SMAP2	ENSG00000084070	101.298162	0.19128148	0.8616132	-0.9924561	0.00779947	-1.1837376	0.00109477
CPNE3	ENSG00000085719	769.596742	-0.2578781	0.69765928	-0.8784792	0.00136464	-0.6206011	0.06791821
ATG16L1	ENSG00000085978	78.6154364	-0.8219108	0.08500838	-1.5070637	7.1389E-05	-0.6851529	0.2785846
CHMP5	ENSG00000086065	219.221042	-0.0113805	0.99483103	-0.6454355	0.03789574	-0.634055	0.06279154
CEACAM6	ENSG00000086548	16.0618509	-1.3061324	0.28806771	-7.0973694	0.00013287	-5.7912371	0.00589094
DTX2	ENSG00000091073	47.7874997	-0.4929985	0.65721985	-1.5238244	0.00481675	-1.0308259	0.1582747
ESR1	ENSG00000091831	1104.59397	-0.2173528	0.6775377	-3.0586894	3.5689E-55	-2.8413367	2.6156E-47
SLC7A8	ENSG00000092068	579.929804	-0.7073044	0.00484283	-1.1928201	2.5793E-08	-0.4855157	0.13187438
DSP	ENSG00000096696	36.5724703	-1.5303835	0.00837276	-3.454677	4.0552E-08	-1.9242935	0.01977934
SCD	ENSG00000099194	4140.89372	0.11848014	0.87293553	-2.6748683	8.1573E-49	-2.7933484	4.5799E-53
WASHC2A	ENSG00000099290	108.015983	-0.3079528	0.72704207	-1.2298442	0.00083357	-0.9218914	0.03699158
DDX17	ENSG00000100201	104.877717	0.39816923	0.66807301	-0.7519188	0.15498522	-1.150088	0.01105948
XBP1	ENSG00000100219	1251.13389	-0.1612814	0.7619592	-1.951176	3.7174E-30	-1.7898946	4.3612E-25
TSPO	ENSG00000100300	410.49112	0.28022404	0.57135919	-0.6755596	0.0087152	-0.9557836	5.7318E-05
PDGFB	ENSG00000100311	53.9345646	-0.1158963	0.95126426	-1.2551948	0.01446509	-1.1392985	0.04941052
RPL3	ENSG00000100316	1978.74775	0.28692642	0.46145653	-0.4394542	0.07987742	-0.7263806	0.0006895
SPTLC2	ENSG00000100596	79.0693313	-0.4083803	0.63820549	-1.1128049	0.00941812	-0.7044246	0.25923879
PXMP4	ENSG00000101417	194.689708	-0.2414657	0.80037329	-1.6262282	2.0754E-07	-1.3847624	3.7984E-05
STS	ENSG00000101846	108.527671	-0.5622683	0.26959229	-1.913124	5.9421E-09	-1.3509642	0.00031102
MAGED2	ENSG00000102316	207.89942	-0.4479197	0.29258589	-1.3509259	1.5619E-07	-0.9030063	0.00279944
TSC22D1	ENSG00000102804	244.308848	-0.1742669	0.82389446	-1.2013668	8.3896E-07	-1.0270999	8.9975E-05
FAH	ENSG00000103876	206.788849	-0.1472242	0.87126514	-0.6681504	0.02775731	-0.5209262	0.17621517
ZDHHC2	ENSG00000104219	14.5845756	-1.4678865	0.22657388	-1.8223116	0.07156288	-0.3544252	0.91402661
EMC2	ENSG00000104412	311.187028	-0.1640234	0.84078268	-0.5917067	0.04468058	-0.4276833	0.29200079
NDRG1	ENSG00000104419	175.053305	-0.2631282	0.72704207	-1.0494366	0.00063026	-0.7863084	0.03157269
TRPS1	ENSG00000104447	294.990128	-0.2664585	0.68763162	-0.6746156	0.0279629	-0.4081571	0.39372259
GSDME	ENSG00000105928	27.6194127	-0.1737651	0.94916686	-2.387539	0.0019993	-2.2137739	0.0082565
ATP6V0A4	ENSG00000105929	9.85706391	-0.7988112	0.75694968	-2.8564968	0.04388993	-2.0576856	0.31001751
HIBADH	ENSG00000106049	89.3770565	-0.347676	0.7090889	-0.8782348	0.04715864	-0.5305588	0.4564597
AGR2	ENSG00000106541	42.6337138	0.19625749	0.92348796	-2.3852197	0.00013855	-2.5814772	4.0146E-05
CORO2A	ENSG00000106789	17.3667397	-0.6118926	0.77434914	-2.6207936	0.01163916	-2.0089009	0.13169702
GATA3	ENSG00000107485	1480.74756	-0.219331	0.54869656	-0.7115524	3.9691E-05	-0.4922215	0.01691848
ZMIZ1	ENSG00000108175	157.952776	-0.2495841	0.78187745	-1.0021068	0.0032869	-0.7525227	0.07159605
SYNGR2	ENSG00000108639	876.457286	-0.4189597	0.14457517	-1.144959	1.5232E-09	-0.7259992	0.00090543
ABCC3	ENSG00000108846	11.585756	1.2056849	0.43356513	-2.9066565	0.05832045	-4.1117314	0.00246036
PMP22	ENSG00000109099	16.4165331	-0.9835582	0.49737278	-2.7888575	0.0147692	-1.2952993	0.40572127
LAMTOR3	ENSG00000109270	142.152906	-0.3243558	0.62336212	-0.8385312	0.01051399	-0.5141754	0.29240617
UGDH	ENSG00000109814	26.6164418	-0.3103369	0.87737913	-1.7129006	0.0166191	-1.4025637	0.10972503
TRIM3	ENSG00000110171	32.8800359	-0.0967454	0.96890536	-1.4923316	0.02759344	-1.3955862	0.06708655
SLC1A2	ENSG00000110436	42.4663	-0.3849726	0.78578133	-1.7118595	0.00261679	-1.3268869	0.05419806
SERINC1	ENSG00000111897	107.794415	-0.2117685	0.84652754	-0.8252767	0.04251916	-0.6135082	0.26396225
SASH1	ENSG00000111961	28.0720798	-1.0065397	0.3518217	-1.6332898	0.0324196	-0.6267502	0.72420775
PERP	ENSG00000112378	146.054357	0.43131637	0.4188	-1.6069286	1.972E-07	-2.038245	6.7896E-12
ARFGEF3	ENSG00000112379	39.732343	-0.5053388	0.69739576	-1.6324443	0.00686765	-1.1271055	0.16444509
ERGIC1	ENSG00000113719	344.015099	-0.0488417	0.96325814	-1.705343	6.886E-15	-1.6565013	7.5033E-14
KAT2B	ENSG00000114166	18.2976363	-0.9413555	0.49413768	-2.2189805	0.01212705	-1.2776249	0.38022778
C3orf52	ENSG00000114529	22.6200677	0.61689074	0.70518074	-1.3904776	0.15033076	-2.0073684	0.01691848
ABCC5	ENSG00000114770	414.956127	-0.3751412	0.37273058	-1.0616057	7.2863E-06	-0.6864645	0.0169946
KLHL24	ENSG00000114796	33.3628146	-0.8335838	0.3792848	-1.5165454	0.01760457	-0.6829617	0.59426761
FOXP1	ENSG00000114861	28.320499	-0.709602	0.58467271	-1.881995	0.00892494	-1.172393	0.27652649
REEP6	ENSG00000115255	234.384207	-0.3128884	0.58008802	-0.6686394	0.02663305	-0.3557509	0.49264228
ST3GAL5	ENSG00000115525	13.0903654	-0.4176608	0.88522508	-2.3345756	0.04211609	-1.9169148	0.18458948
ID2	ENSG00000115738	138.830429	0.09388867	0.94956873	-1.4169566	6.4366E-05	-1.5108453	2.4908E-05
SLC1A4	ENSG00000115902	196.474448	-0.2690732	0.68265549	-1.5182013	9.3074E-09	-1.2491281	1.1505E-05
COX7A2L	ENSG00000115944	392.939488	-0.4300061	0.22190943	-0.4886359	0.09095231	-0.0586298	0.94925399
SCP2	ENSG00000116171	252.726422	-0.1478013	0.85521131	-0.7040292	0.00936411	-0.5562279	0.09155897
KIAA1324	ENSG00000116299	83.5318422	-1.0512978	0.01920736	-3.183175	1.1898E-13	-2.1318772	1.0635E-05
CRYZ	ENSG00000116791	45.9718025	-0.2545951	0.87852918	-1.4922299	0.00756998	-1.2376348	0.06125849
HMGCL	ENSG00000117305	48.9668663	0.16578064	0.92874478	-1.2045579	0.03244929	-1.3703385	0.01481853
CD46	ENSG00000117335	512.386488	-0.4269541	0.41429866	-0.8313277	0.00767665	-0.4043736	0.45465603
KLF7	ENSG00000118263	19.8798864	-0.7712642	0.63133745	-3.3176502	0.000624	-2.5463861	0.02795577
ALDH6A1	ENSG00000119711	54.2068393	-0.4305798	0.67033208	-1.7764471	0.00012443	-1.3458673	0.01321144
SLC17A5	ENSG00000119899	34.2209703	-0.6170629	0.58334593	-1.5095935	0.01544077	-0.8925306	0.37203226
SERP1	ENSG00000120742	720.753739	-0.1502518	0.78686534	-0.4731262	0.03133903	-0.3228744	0.29978786
LYPLA1	ENSG00000120992	427.977895	-0.2251488	0.72154197	-0.7740013	0.00281052	-0.5488525	0.09322539
CSTA	ENSG00000121552	19.884252	0.84580532	0.6034083	-2.1053584	0.04736647	-2.9511637	0.0019218
COPA	ENSG00000122218	188.193748	-0.2473882	0.73322041	-0.7300104	0.02147952	-0.4826222	0.29084566
DCAF10	ENSG00000122741	118.2883	-0.5648877	0.26818953	-1.2324319	0.0002422	-0.6675442	0.17441159
KIAA1549	ENSG00000122778	13.7946399	0.74875224	0.71031716	-1.6401656	0.22436549	-2.3889178	0.03810089
WWP1	ENSG00000123124	94.9849522	-0.4467635	0.51646283	-1.1859945	0.00156554	-0.739231	0.15406616
MXD4	ENSG00000123933	114.306601	-0.5140835	0.33004782	-1.0938408	0.00118321	-0.5797573	0.26921828
FAM210B	ENSG00000124098	437.838256	-0.4065067	0.2986901	-1.0445958	9.2165E-06	-0.6380891	0.03106108
NCOA3	ENSG00000124151	35.2632918	-0.5965342	0.6867131	-1.4828312	0.04437819	-0.886297	0.46027385
ATP8A1	ENSG00000124406	4.28515132	-0.9312942	NA	-5.1942402	0.04317102	-4.262946	0.19242241
SPDEF	ENSG00000124664	501.293447	-0.6385077	0.0116135	-1.8583578	1.1315E-19	-1.2198501	3.6153E-08
AHNAK	ENSG00000124942	562.834857	-0.3966028	0.17868984	-0.977173	5.6523E-07	-0.5805702	0.01636302
GOT2	ENSG00000125166	132.71467	0.09549518	0.94369489	-0.9483636	0.00490861	-1.0438588	0.00205262
SOX9	ENSG00000125398	17.0537627	-0.7889968	0.63007768	-3.6577077	0.00105033	-2.8687109	0.03022519
ALKBH7	ENSG00000125652	79.2303742	-0.0689892	0.96803715	-0.9174924	0.04387148	-0.8485031	0.10375459
OTOR	ENSG00000125879	27.8408386	0.98632172	0.33067369	-0.3761968	0.81716331	-1.3625185	0.10571763
DYNLRB1	ENSG00000125971	245.197062	-0.2389969	0.71365324	-0.645821	0.02879902	-0.4068241	0.36434088
SIX1	ENSG00000126778	26.567972	-1.1501604	0.22190943	-2.0909406	0.00421232	-0.9407802	0.50657944

MACF1	ENSG00000127603	59.5820773	-0.6545203	0.49884651	-2.6322894	1.0417E-06	-1.9777691	0.00122423
MYO1B	ENSG00000128641	73.7405168	-0.7296693	0.23185674	-1.3992982	0.00116448	-0.6696289	0.3641539
FOXA1	ENSG00000129514	423.832618	-0.3652183	0.49906356	-1.4486292	2.9422E-08	-1.0834109	0.00018642
REEP5	ENSG00000129625	1425.48751	0.26534815	0.41988147	-1.1086359	2.3351E-11	-1.3739841	2.3698E-17
SYT5	ENSG00000129990	78.9819826	-0.5929365	0.34490208	-1.0422331	0.01358921	-0.4492966	0.59774063
OSBPL2	ENSG00000130703	136.011079	-0.2934713	0.70927832	-0.8933598	0.01006895	-0.5998885	0.20919369
PPT1	ENSG00000131238	540.707804	-0.4482738	0.16554496	-1.4821858	1.743E-12	-1.0339119	7.6475E-06
ACLY	ENSG00000131473	226.6871	0.19071319	0.82160517	-0.5490726	0.11192407	-0.7397858	0.01979763
NDFIP1	ENSG00000131507	225.515026	0.05995118	0.95888715	-0.6826126	0.01891009	-0.7425638	0.01233227
MCC2	ENSG00000131844	364.130326	-0.5964527	0.04090542	-1.0153614	1.2997E-05	-0.4189287	0.28291672
ARFIP2	ENSG00000132254	82.7438451	-0.723722	0.19477941	-1.1404379	0.00672336	-0.4167159	0.65535715
ALDH3B2	ENSG00000132746	109.493939	-0.3714929	0.61917915	-1.0111291	0.00620075	-0.6396361	0.22348277
MRPS36	ENSG00000134056	150.717433	0.39531655	0.55370469	-0.431309	0.41674084	-0.8266255	0.03763106
BHLHE40	ENSG00000134107	113.109603	-0.7300529	0.12233845	-2.7562774	2.6901E-14	-2.0262245	2.427E-07
HMGCS2	ENSG00000134240	12.4922263	-3.2414044	0.0059534	-7.0920082	0.00020597	-3.8506038	0.1962965
EMP1	ENSG00000134531	16.6866941	-1.4662654	0.18288099	-7.3310684	6.994E-05	-5.864803	0.00511585
CYP2J2	ENSG00000134716	26.8664404	-0.7468303	0.53294594	-1.6492416	0.02204037	-0.9024112	0.46703533
ARHGAP32	ENSG00000134909	82.785703	-0.5136103	0.48807333	-1.249969	0.00284624	-0.7363587	0.23417048
HILPDA	ENSG00000135245	108.777609	0.27580593	0.81801279	-0.7777382	0.1260158	-1.0535442	0.02316249
CD164	ENSG00000135535	257.344677	-0.5812043	0.10284104	-1.2154403	2.9038E-06	-0.634236	0.07396306
MDM2	ENSG00000135679	59.3929756	-0.6762398	0.36884037	-1.1928141	0.01696675	-0.5165743	0.61081292
NIBAN1	ENSG00000135842	36.1256338	0.56508333	0.65985823	-1.262636	0.094335	-1.8277193	0.00554419
GCC2	ENSG00000135968	74.9360897	-0.7840985	0.18566896	-1.0038372	0.03518745	-0.2197387	0.88918513
FLNB	ENSG00000136068	127.951371	-0.3113722	0.71694816	-1.4018691	5.4837E-05	-1.0904969	0.00598307
ITM2B	ENSG00000136156	341.912563	-0.6077022	0.02488851	-0.9029912	7.4295E-05	-0.295289	0.53761591
ATP6V1G1	ENSG00000136888	1213.22472	-0.1030911	0.889753	-1.0845431	1.3034E-08	-0.981452	7.659E-07
RPS6	ENSG00000137154	3169.41619	0.02405071	0.98099172	-0.4581546	0.03620019	-0.4822053	0.03579907
TFAP2A	ENSG00000137203	118.459311	-0.0061894	1	-1.189366	0.00124655	-1.1831766	0.00205262
IER3	ENSG00000137331	34.1853252	-0.2102015	0.92651853	-4.038162	1.4656E-06	-3.8279604	1.221E-05
RNF144B	ENSG00000137393	28.8028934	0.11120905	0.96496233	-2.0144983	0.00437725	-2.1257073	0.00323665
BCAR3	ENSG00000137936	63.0425491	-0.5867648	0.46966363	-1.5320522	0.00101021	-0.9452875	0.14375289
ARHGAP29	ENSG00000137962	114.278779	-0.4215197	0.53560696	-1.0207941	0.0058746	-0.5992744	0.28597918
NA	ENSG00000137970	3402.16286	-0.091042	0.88135364	-0.5638335	0.00146308	-0.4727915	0.01763032
COX17	ENSG00000138495	376.333249	0.38540217	0.49499989	-0.5674848	0.13686124	-0.952887	0.00270201
BMPR1B	ENSG00000138696	29.1866541	0.8806239	0.36890802	-2.7888835	0.00088875	-3.6695074	2.7574E-06
CCNG2	ENSG00000138764	61.7576447	-0.5114413	0.53560696	-2.1574145	1.3056E-06	-1.6459731	0.00114152
NA	ENSG00000139239	183.84044	0.16307945	0.88135364	-0.9333298	0.00660565	-1.0964092	0.00114368
ETFA	ENSG00000140374	276.485408	0.30257795	0.58287002	-1.127063	1.3566E-05	-1.429641	9.979E-09
ABHD2	ENSG00000140526	160.598309	-1.5982293	2.3457E-07	-2.4977491	8.4122E-16	-0.8995198	0.04531083
ZFHX3	ENSG00000140836	43.1979244	-0.5307297	0.61291163	-1.2427082	0.02746058	-0.7119785	0.44614542
PCTP	ENSG00000141179	74.0957427	-0.6559369	0.26452402	-1.3167464	0.00105429	-0.6608095	0.31540646
TOB1	ENSG00000141232	1907.2145	-0.1966646	0.72424845	-1.3446876	4.6435E-12	-1.1480229	1.381E-08
RAB40B	ENSG00000141542	61.5042313	-0.6127753	0.41178695	-1.2817238	0.00557197	-0.6689485	0.38808582
ERBB2	ENSG00000141736	33.1361324	-0.5111122	0.70854504	-1.3477973	0.04406529	-0.8366851	0.43164788
RPL13A	ENSG00000142541	356.398794	-0.5788082	0.17839767	-0.7145442	0.03876521	-0.135736	0.90191288
KIAA0319L	ENSG00000142687	98.9439354	-0.5392835	0.3366727	-1.0984818	0.00244886	-0.5591983	0.35269555
PRKACB	ENSG00000142875	31.2605801	0.03399195	0.99070167	-2.3313817	0.00066166	-2.3653737	0.00079824
PTPRF	ENSG00000142949	336.632232	-0.1626233	0.85096308	-0.8394734	0.00275289	-0.67685	0.03810089
IGSF3	ENSG00000143061	97.6089182	-0.6130217	0.27945693	-1.8446245	4.0482E-07	-1.2316028	0.0045645
CREG1	ENSG00000143162	312.422564	0.01316532	0.9923498	-0.9302443	0.00023273	-0.9434097	0.00030139
SDHC	ENSG00000143252	256.225992	-0.1017326	0.92370987	-0.748563	0.00910147	-0.6468304	0.04998439
SELENBP1	ENSG00000143416	132.844235	-0.3758665	0.60816091	-1.3414632	9.097E-05	-0.9655966	0.01810231
CREB3L4	ENSG00000143578	31.6198241	-1.0561268	0.2986901	-2.1531882	0.00298926	-1.0970615	0.37654266
ITPKB	ENSG00000143772	33.734181	-0.3214199	0.84537521	-1.436948	0.02098	-1.1155281	0.16109143
MBOAT2	ENSG00000143797	136.127795	-1.094957	0.00148223	-3.0912323	1.4739E-19	-1.9962753	1.1771E-07
SLC20A1	ENSG00000144136	93.5719422	-0.5443003	0.40929233	-1.1366582	0.00496421	-0.5923579	0.38065701
ACKR3	ENSG00000144476	257.384829	-0.36567	0.455859	-1.6837956	1.4639E-11	-1.3181256	8.0564E-07
USP53	ENSG00000145390	80.0815851	-0.9214442	0.06206927	-1.4201405	0.00049948	-0.4986963	0.56792518
IQGAP2	ENSG00000145703	17.8824742	-0.0021724	1	-2.1475437	0.04383488	-2.1453713	0.06353171
YIPF5	ENSG00000145817	107.535464	0.16038147	0.89325195	-0.9034577	0.01914012	-1.0638392	0.0050141
SLC16A2	ENSG00000147100	43.2682801	-0.970126	0.15992502	-2.9625575	2.5256E-07	-1.9924315	0.00380562
NFIB	ENSG00000147862	113.039071	-0.534596	0.3782421	-1.4021726	0.00010577	-0.8675766	0.06791821
GSN	ENSG00000148180	132.402036	-0.6206376	0.15324671	-1.1545591	0.00028628	-0.5339215	0.31540646
MINDY3	ENSG00000148481	38.985472	-0.8650833	0.31831206	-0.7994968	0.30300764	0.06558645	0.97417445
LRMDA	ENSG00000148655	44.6356095	0.43483733	0.77334529	-0.9941702	0.20351527	-1.4290075	0.03722841
GLUD1	ENSG00000148672	79.8395566	-0.0798667	0.96446264	-1.2490676	0.00538793	-1.1692009	0.01675528
ZNF827	ENSG00000151612	27.1480691	-0.6645643	0.58595588	-1.6013033	0.02024834	-0.936739	0.40499241
GPD1L	ENSG00000152642	58.4558091	0.11583572	0.95305616	-1.0923957	0.0512163	-1.2082314	0.03424218
TEKT5	ENSG00000153060	7.81732955	-0.9743402	0.70536491	-3.2125231	0.04238275	-2.2381829	0.33367583
MSI2	ENSG00000153944	212.607488	-0.4593903	0.31772607	-1.2993218	2.1068E-06	-0.8399315	0.01122935
DBI	ENSG00000155368	1708.55988	-0.513965	0.06875007	-1.6814765	9.2299E-18	-1.1675115	2.4134E-08
RMND1	ENSG00000155906	400.855315	0.31307537	0.4317329	-1.7152339	1.9111E-16	-2.0283092	3.0322E-23
KCNMA1	ENSG00000156113	391.079839	-0.4433352	0.1468149	-2.8873134	1.0176E-39	-2.4439782	1.048E-27
C8orf37	ENSG00000156172	33.542245	-0.3694067	0.82769903	-1.6390538	0.01163916	-1.2696471	0.12225954
ZFAND3	ENSG00000156639	89.4640687	0.00244319	1	-1.0357378	0.0115119	-1.037681	0.01685543
DHRS1	ENSG00000157379	22.9309506	0.19026764	0.9468563	-1.6790207	0.04604422	-1.8692884	0.02781151
APPL1	ENSG00000157500	33.557158	-0.8466947	0.3366727	-1.157745	0.07950079	-0.3110504	0.87569467
TMEM268	ENSG00000157693	75.9121329	0.09920954	0.95607849	-1.322985	0.00358162	-1.4221945	0.00200452
NBL1	ENSG00000158747	423.553371	-0.051624	0.96003994	-0.8241072	0.00033345	-0.7724831	0.00153222
HK2	ENSG00000159399	25.8184039	-0.7589614	0.54715534	-1.7988968	0.01490647	-1.0399355	0.38748353
ALDH4A1	ENSG00000159423	90.2808844	-0.1332117	0.9309227	-2.2270372	1.7775E-08	-2.0938255	2.9874E-07
ARHGAP35	ENSG00000160007	157.068309	-0.4184044	0.4123733	-0.9904385	0.00088211	-0.572024	0.17814361
ABCG1	ENSG00000160179	125.531729	0.11690836	0.9309227	-0.9718168	0.00910147	-1.0887251	0.00356149
FGFR4	ENSG00000160867	165.465285	-0.2152255	0.80538879	-2.7121022	7.4641E-19	-2.4968767	9.9502E-16
VPS28	ENSG00000160948	58.0907314	-0.3965304	0.71995996	-1.0618451	0.0425929	-0.6653147	0.41753652
SQSTM1	ENSG00000161011	40.3622009	0.57993592	0.58538901	-0.994089	0.16760809	-1.5740249	0.00841721
ZG16B	ENSG00000162078	46.3342275	-0.1528893	0.9468563	-1.5790785	0.00662424	-1.4261892	0.02786752
SHANK2	ENSG00000162105	39.6563161	-0.0508374	0.98391477	-1.6067668	0.00521937	-1.5559294	0.0112742
AK4	ENSG00000162433	147.497314	-0.1819304	0.85418719	-1.1564642	0.00020597	-0.9745337	0.00498342
TM2D1	ENSG00000162604	79.9562011	-0.4910604	0.48269717	-0.8808208	0.04149735	-0.3897605	0.65774267
ZNF281	ENSG00000162702	27.0122202	0.36934198	0.85676093	-1.3076087	0.01927887	-1.6769507	0.04307221
COQ8A	ENSG00000163050	25.7207884	-0.5034955	0.7697417	-1.7787501	0.02111163	-1.2752545	0.22854665
SLC16A14	ENSG00000163053	76.899209	-0.9306168	0.04977115	-1.2269804	0.0028182	-0.2963636	0.80112179
NOSTRIN	ENSG00000163072	10.47167	-1.3525966	0.47544777	-6.6038879	0.00101021	-5.2512912	0.02607009
NA	ENSG00000163364	31.8863349	-0.951339	0.32255007	-1.4011225	0.04807903	-0.4497835	0.80668701
SMIM14	ENSG00000163683	121.295151	0.39048113	0.66453398	-1.1676423	0.00630497	-1.5581235	9.8346E-05
IL17RE	ENSG00000163701	27.7914034	-0.0427258	0.98933793	-2.0099357	0.00751829	-1.9672099	0.01416712
PRRT3	ENSG00000163704	23.412761	-0.7968999	0.50571188	-1.6332597	0.02917848	-0.8363598	0.54617888
SGMS2	ENSG00000164023	44.0270437	-1.059131	0.12953133	-2.7521043	1.5399E-06	-1.6929732	0.01982217
PGRMC2	ENSG00000164040	226.456001	-0.3028157	0.62844485	-1.0719751	0.00013107	-0.7691594	0.02144845
SPRY1	ENSG00000164056	3.92118691	-1.4257636	NA	-5.5072133	0.02763462	-4.0814497	0.23652667
C4orf3	ENSG00000164096	313.414021	-0.5396808	0.13188516	-0.800327	0.0036405	-0.2606462	0.68232797
ZNF704	ENSG00000164684	87.1168097	0.36084503	0.67017607	-0.6959679	0.15254967	-1.0568129	0.0111092
CTSB	ENSG00000164733	282.388381	-0.0867535	0.94409565	-0.7859564	0.00904636	-0.6992029	0.03914517
TP53INP1	ENSG00000164938	103.336315	-1.4219105	0.00029196	-2.6565845	3.5445E-12	-1.234674	0.01459007
PDP1	ENSG00000164951	62.704821	0.03757977	0.98809915	-1.3478511	0.01648423	-1.3854309	0.01874971
METTL27	ENSG00000165171	28.245222	-0.4467671	0.78968222	-1.8789435	0.00807123	-1.4321765	0.11058242
COMTD1	ENSG00000165644	134.085958	-0.060165	0.96496233	-1.318841	2.4926E-05	-1.258676	0.00012354
CLMN	ENSG00000165959	72.8422431	-0.4146479	0.65488382	-1.681921	7.4238E-05	-1.2672731	0.01050384
ZFYVE19	ENSG00000166140	33.1448897	0.41209652	0.822831	-1.1209703	0.19292647	-1.5330668	0.04822545
AP1G1	ENSG00000166747	223.910308	0.05938817	0.95983494	-0.717804	0.01291334	-0.7771922	0.00829447
PEX11A	ENSG00000166821	40.0391384	-0.7453106	0.38073018	-1.2913517	0.02473116	-0.5460411	0.65418849
MS4A7	ENSG00000166927	7.36100152	-1.1769156	0.64749784	-6.1882587	0.00350284	-5.011343	0.04719941
GOLGA2	ENSG00000167110	181.457349	0.38979885	0.50061731	-0.5818858	0.14208999	-0.9716847	0.00309142
CERCAM	ENSG00000167123	28.3490304	-0.2048049	0.92992206	-2.0261712	0.00416685	-1.8213664	0.02035597
CDC42EP5	ENSG00000167617	41.7097767	-0.0882371	0.96893546	-1.2422211	0.04601859	-1.153984	0.10588529
HID1	ENSG00000167861	216.978994	-0.2434352	0.73589591	-1.6551839	6.5581E-10	-1.4117487	5.8626E-07
ABCA3	ENSG00000167972	54.5014655	-0.5243086	0.58595588	-1.0929951	0.04429096	-0.5686866	0.56713917
FTH1	ENSG00000167996	130.903466	0.65594583	0.18842909	-0.4808082	0.39222109	-1.136754	0.0026717
LMBRD1	ENSG00000168216	37.9798234	-0.4527126	0.72704207	-1.3043281	0.03368842	-0.8516154	0.36130993
CX3CR1	ENSG00000168329	8.01143422	0.55129585	0.90674082	-5.7483902	0.01344386	-6.2996861	0.00735023
ADAM9	ENSG00000168615	81.4229071	0.34406731	0.74907651	-0.8618856	0.10169823	-1.205953	0.01041217
LRATD2	ENSG00000168672	141.517091	-0.0221246	0.98962603	-1.2357326	0.00018403	-1.216508	0.00043006
TMEM208	ENSG00000168701	113.974991	0.17242466	0.87852918	-0.6774396	0.1097138	-0.8498643	0.0356752
RNF181	ENSG00000168894	547.502032	-0.4225186	0.28835895	-0.7015969	0.00896607	-0.2790783	0.61081292
VAMP5	ENSG00000168899	47.2796153	-1.6759364	0.00370363	-1.9606422	0.00039832	-0.2847058	0.89482985
SLC25A6	ENSG00000169100	1030.91426	-0.0267877	0.97821663	-0.5186037	0.01216663	-0.4918159	0.02909055
APEX2	ENSG00000169188	206.849252	0.35740658	0.5955902	-0.5703757	0.17790489	-0.9277822	0.00859287
EFNA1	ENSG00000169242	84.2299205	-0.5727735	0.34668456	-0.8545942	0.04693683	-0.2818207	0.79493462
SLC33A1	ENSG00000169359	41.1261988	-0.3932101	0.76547909	-1.5026162	0.00724043	-1.109406	0.12330252
MYRIP	ENSG00000170011	5.24962315	-0.0854219	0.98962603	-5.5457663	0.01845546	-5.4603444	0.03152211
GPRC5C	ENSG00000170412	77.996305	-0.524773	0.46492032	-1.1933205	0.00481364	-0.6685475	0.31540646
SDR16C5	ENSG00000170786	67.4175209	-0.9433962	0.06318385	-1.5817722	0.00015736	-0.638376	0.4179621
CHCHD7	ENSG00000170791	185.729998	-0.2578918	0.7151038	-0.7381278	0.01932458	-0.4802359	0.29455809
FEZ2	ENSG00000171055	59.1587599	-0.6132501	0.4154505	-1.1428867	0.01686564	-0.5296366	0.56713917
CANT1	ENSG00000171302	183.958806	-0.4693562	0.31239006	-0.7720214	0.01468101	-0.3026652	0.65275548
BPTF	ENSG00000171634	195.0227	-0.2707175	0.69473992	-0.7862534	0.01075853	-0.5155359	0.23405019
EPHX4	ENSG00000172031	29.4243019	0.41360311	0.81131827	-1.4535115	0.05720655	-1.8671146	0.00864518
ZNF24	ENSG00000172262	86.3004621	-0.496503	0.48700663	-1.4579465	0.00018964	-0.9614435	0.05457766
WASHC2C	ENSG00000172661	52.6057874	-0.5389642	0.59907575	-1.4494251	0.00677049	-0.9104609	0.24075617
GOLGB1	ENSG00000173230	223.437007	-0.3297519	0.62031695	-1.0282618	0.00085966	-0.69851	0.07344579
SPATA3	ENSG00000173699	5.29179813	-2.4682829	0.29789541	-5.719912	0.01309345	-3.2516291	0.42506855
TOMM20	ENSG00000173726	523.403444	0.32070653	0.43215979	-0.5319612	0.04346973	-0.8526677	0.00020384
GPR160	ENSG00000173890	236.44482	-0.3762466	0.39685393	-1.1671092	2.0121E-06	-0.7908627	0.00660682
CTSF	ENSG00000174080	95.8538229	-0.4431007	0.55222846	-1.4254524	0.000173	-0.9823517	0.03642549
RPL15	ENSG00000174748	1453.79351	-0.0836367	0.91217952	-0.4747828	0.03754833	-0.3911461	0.16308323
PLEKHF2	ENSG00000175895	310.98812	0.00736451	0.99918077	-1.9345438	2.1018E-14	-1.9419083	2.3322E-14
ARL4D	ENSG00000175906	96.8746199	0.40580393	0.59374102	-1.2164132	0.00193427	-1.6222172	9.813E-06
BNIP3	ENSG00000176171	395.268234	-0.2017429	0.73796934	-0.6435169	0.01082167	-0.4417739	0.19280084
ERBB4	ENSG00000178568	39.3826357	-1.1507508	0.1179402	-5.3681723	3.4864E-07	-4.2174215	0.00030755
TAF7	ENSG00000178913	196.093209	-0.3454375	0.53250379	-0.6897089	0.02890738	-0.3442713	0.54815875
MAGED1	ENSG00000179222	90.9228972	-0.3038185	0.75510365	-1.4747886	8.8048E-05	-1.1709702	0.00618357
LDLRAD3	ENSG00000179241	134.470838	0.00971814	0.99918077	-0.9902497	0.00660565	-0.9999678	0.0088074
PITPNB	ENSG00000180957	62.2294835	0.40807485	0.77334529	-1.1150077	0.09212323	-1.5230825	0.01105948
FRAT2	ENSG00000181274	59.3424848	-0.4411009	0.64176089	-1.2089811	0.01033342	-0.7678801	0.26460839
CREB3L2	ENSG00000182158	44.4796677	-0.1054649	0.96373859	-1.2508039	0.04871318	-1.145339	0.11970655
TTC3	ENSG00000182670	258.395069	-0.0454394	0.97191751	-1.4142398	1.0321E-07	-1.3688004	5.4207E-07
ARHGEF37	ENSG00000183111	40.058532	0.09654359	0.9669083	-2.8581479	1.1921E-05	-2.9546915	8.7104E-06

CCDC125	ENSG00000183323	53.1167586	-0.576577	0.48103639	-1.5099253	0.00124703	-0.9333483	0.15236984
TMEM50A	ENSG00000183726	173.650514	-0.2801627	0.69226533	-0.7666458	0.01760158	-0.4864831	0.31001751
GPR39	ENSG00000183840	9.74580456	-1.269363	0.50061731	-3.5836836	0.01446509	-2.3143206	0.29205734
SRARP	ENSG00000183888	5.45025708	-0.9852938	0.78760801	-5.6150806	0.01474554	-4.6297868	0.1013687
TACSTD2	ENSG00000184292	224.813262	-0.3890981	0.41988147	-0.8718041	0.00189351	-0.4827061	0.25521048
FAM174B	ENSG00000185442	67.6589349	-0.2310538	0.87281228	-1.1498145	0.01757538	-0.9187607	0.12679236
PBX1	ENSG00000185630	726.814632	-0.0060957	0.99918077	-1.6127567	6.0939E-15	-1.606661	1.1279E-14
SEPTIN10	ENSG00000186522	84.7195117	-0.7630814	0.15659732	-1.820643	3.8185E-06	-1.0575616	0.04062463
C17orf58	ENSG00000186665	289.472825	-1.0420159	2.0708E-05	-1.7211028	7.2301E-14	-0.6790869	0.03236891
BCAM	ENSG00000187244	203.914707	-0.6576587	0.05703325	-0.9201868	0.00133731	-0.2627282	0.714847
ZC3H6	ENSG00000188177	23.1156367	-0.3002206	0.90127288	-2.1469495	0.00910147	-1.8467289	0.05406602
NANOS1	ENSG00000188613	55.1819431	0.37926159	0.73902365	-0.9475263	0.1085301	-1.3267879	0.01157707
RPL14	ENSG00000188846	604.623718	0.11744018	0.86898752	-0.5148096	0.02947543	-0.6322497	0.00586788
HACD4	ENSG00000188921	40.3729108	0.04697236	0.98568861	-1.5085459	0.01544077	-1.5555183	0.01696858
H1-0	ENSG00000189060	180.725297	0.22103639	0.77334529	-0.5742325	0.1027598	-0.7952689	0.01228086
LITAF	ENSG00000189067	573.348542	-0.2691961	0.51968559	-1.0692749	7.3295E-08	-0.8000788	0.00029695
CLDN4	ENSG00000189143	400.904585	0.18694481	0.74907651	-0.6492654	0.00619365	-0.8362102	0.00021029
CD55	ENSG00000196352	357.921469	-0.1588548	0.82612806	-1.3839094	1.4162E-10	-1.2250545	4.8645E-08
SPTSSB	ENSG00000196542	300.056809	0.21213037	0.76154567	-0.6945645	0.01581748	-0.9066949	0.00083316
MYO6	ENSG00000196586	161.693978	-0.8857117	0.01914409	-1.3941009	1.4212E-05	-0.5083893	0.39888981
GM2A	ENSG00000196743	78.768985	-0.3654546	0.69259771	-0.9867873	0.0236582	-0.6213327	0.35041707
HCAR1	ENSG00000196917	56.8291897	-1.0914342	0.05931827	-2.2481937	4.2582E-06	-1.1567596	0.10257586
SERPINA1	ENSG00000197249	12.1332902	-2.6336885	0.02589352	-4.0003654	0.00296436	-1.3666769	0.68663269
GATA3-AS1	ENSG00000197308	37.0873005	-1.1458859	0.11992693	-4.7223854	4.744E-07	-3.5764994	0.00073542
LRP10	ENSG00000197324	228.919334	-0.8580905	0.00182608	-1.7665506	5.783E-13	-0.9084602	0.00266606
SLC2A10	ENSG00000197496	44.7902952	-0.2053951	0.90651478	-1.348697	0.01358921	-1.143302	0.07571072
FAM114A1	ENSG00000197712	17.9456131	-0.4577521	0.84356402	-2.3417597	0.01243087	-1.8840077	0.10366463
MB	ENSG00000198125	157.300618	0.00254104	1	-1.9585079	1.6385E-09	-1.9610489	2.7349E-09
SOWAHC	ENSG00000198142	94.5950254	-0.4784624	0.51923035	-1.29586	0.00133866	-0.8173976	0.13972421
WWP2	ENSG00000198373	63.6301771	-0.1035757	0.96003994	-1.218273	0.02329991	-1.1146973	0.06744096
CTNND1	ENSG00000198561	166.889137	-0.2637914	0.76257553	-0.7900317	0.03218559	-0.5262403	0.3262559
LRBA	ENSG00000198589	59.1054354	-0.6375721	0.45352597	-1.1129385	0.03943644	-0.4753665	0.67757704
CYTB	ENSG00000198727	2826.44923	0.1515204	0.8523749	-0.7055659	0.00777186	-0.8570863	0.00088719
SGMS1	ENSG00000198964	76.2926459	-0.3551419	0.69739576	-0.9687416	0.02402029	-0.6135998	0.34714162
H2AC18	ENSG00000203812	162.822846	-0.6254927	0.15825389	-0.7709222	0.03259618	-0.1454294	0.90100125
C2orf72	ENSG00000204128	99.1026826	-1.1904328	0.00103645	-3.1506628	4.2118E-16	-1.9602301	9.8011E-06
NEU1	ENSG00000204386	86.6054701	-0.2077904	0.87126514	-1.0590908	0.01280722	-0.8513005	0.10202853
DDR1	ENSG00000204580	226.938697	-0.2162446	0.76144485	-0.7620399	0.0073456	-0.5457953	0.13891273
RACK1	ENSG00000204628	1560.93264	0.25906909	0.42180452	-0.3723706	0.09042554	-0.6314397	0.00063098
ST8SIA6-AS1	ENSG00000204832	195.508809	-0.0178749	0.99067864	-0.7566245	0.01966206	-0.7387496	0.03575615
TRIQK	ENSG00000205133	111.629094	0.15761639	0.90669903	-1.1180749	0.00481364	-1.2756913	0.00114368
ZBTB10	ENSG00000205189	63.3700945	-0.6930684	0.26556454	-1.249244	0.00408798	-0.5561755	0.4996208
JPT2	ENSG00000206053	305.593287	0.09580447	0.92196405	-0.6591534	0.01587253	-0.7549578	0.00564206
GPX3	ENSG00000211445	56.6968672	0.30867636	0.8213239	-1.4141652	0.00646156	-1.7228415	0.00056027
NA	ENSG00000211459	1706.06643	-0.6052429	0.05225612	-1.1010477	3.7115E-06	-0.4958048	0.16186116
NA	ENSG00000212802	1623.82989	0.13375592	0.84230704	-0.398755	0.12863943	-0.5325109	0.02893885
EMP2	ENSG00000213853	436.378807	0.22973727	0.77146371	-0.4921964	0.20269373	-0.7219337	0.03375226
MYCBP	ENSG00000214114	63.9685366	-0.8333833	0.29059704	-0.9793508	0.11731374	-0.1459675	0.94191161
LOC100130449	ENSG00000218416	21.6755913	-0.3561783	0.86898752	-1.7782234	0.02777698	-1.422045	0.16432608
NA	ENSG00000223361	79.3262943	-0.183599	0.90651478	-1.1008693	0.02159626	-0.9170303	0.11342424
ZNF844	ENSG00000223547	14.8413121	-0.947283	0.6536786	-3.8934065	0.00489083	-2.9461235	0.08914974
NA	ENSG00000225438	17.266872	-1.6333491	0.10297613	-4.9626461	0.00046198	-3.329297	0.06974108
ARHGAP29-AS1	ENSG00000226835	13.2803152	-1.1023867	0.49737278	-3.3299634	0.0061709	-2.2275768	0.19106547
SPINK8	ENSG00000229453	11.9751286	-0.2948774	0.93272593	-4.0409241	0.01114298	-3.7460467	0.03403119
NA	ENSG00000232022	28.0794409	-0.0414053	0.98931314	-3.6348482	2.3631E-05	-3.5934429	5.3781E-05
NA	ENSG00000232573	376.827628	0.19275673	0.82767858	-0.5421558	0.13069959	-0.7349126	0.0261437
NA	ENSG00000233823	19.9940514	-0.5236148	0.81131827	-2.5292911	0.00683273	-2.0056764	0.07871305
CKMT1B	ENSG00000237289	70.572094	-0.1584814	0.91900657	-1.0129487	0.03259618	-0.8544673	0.13962915
LINC00888	ENSG00000240024	11.9778228	-1.0335544	0.55541914	-2.4264996	0.02931537	-1.3929453	0.46179135
DRAIC	ENSG00000245750	12.4152921	-1.0628908	0.55903622	-6.593543	0.00071201	-5.5306522	0.01215494
NA	ENSG00000247627	44.0209444	0.55985178	0.69595649	-1.0066798	0.24890885	-1.5665315	0.03135657
TRIL	ENSG00000255690	54.740811	-0.5640232	0.51746335	-1.0815036	0.04118763	-0.5174804	0.61572974
NA	ENSG00000259457	5.23365435	-2.1059275	0.39550684	-5.7282581	0.01249729	-3.6223307	0.31540646
LOC102724163	ENSG00000260228	14.2168101	-0.6313151	0.80252133	-2.8231058	0.0139633	-2.1917906	0.1338773
NA	ENSG00000261104	6.5633243	-0.7874629	0.86563801	-5.546026	0.02147952	-4.7585631	0.10003622
NA	ENSG00000265246	17.0379767	-1.115203	0.39750545	-3.1453769	0.00171363	-2.030174	0.14464232
TXNIP	ENSG00000265972	197.620712	-0.8303487	0.01051851	-1.4016229	4.6293E-07	-0.5712742	0.1962965
NA	ENSG00000272894	26.9202071	-0.9133571	0.3870859	-1.7630957	0.0145522	-0.8497386	0.53901562
NA	ENSG00000273143	4.76530738	-0.2680162	NA	-5.2494881	0.033441	-4.9814719	0.07211612
LOC102724770	ENSG00000278817	44.2478654	0.52372338	0.60705006	-1.0561787	0.09448772	-1.579902	0.00366242

Cluster 3

	ensembl	baseMean	TvsC log2FoldChange	padj	RvsC log2FoldChange	padj	RvsT log2FoldChange	padj
TSPAN6	ENSG00000000003	45.7107081	-1.0111295	0.12848038	-0.5039939	0.54886617	0.50713558	0.65894697
NFYA	ENSG00000001167	23.7091007	-1.131855	0.26176556	-0.2807185	0.85816958	0.85113657	0.50315902
KLHL13	ENSG00000003096	7.05193839	-5.6666347	0.01835368	0.7144041	0.78321424	6.38103876	0.0045645
RBM6	ENSG00000004534	57.85487	-0.8246884	0.30643104	-0.3296972	0.75964611	0.49499123	0.68000787
KMT2E	ENSG00000005483	70.538188	-0.7287651	0.20306942	-0.3436958	0.64618429	0.38506928	0.68663269
RHBDD2	ENSG00000005486	61.2704971	-1.023609	0.07509377	-0.3666518	0.6699458	0.65695726	0.41834052
LAMP2	ENSG00000005893	526.76934	-0.6354283	0.01572512	0.11465424	0.83974729	0.75008256	0.00211021
TMEM132A	ENSG00000006118	32.2499033	-0.8379563	0.39634996	-1.4786956	0.02612868	-0.6407394	0.64653001
KDM7A	ENSG00000006459	17.6825727	-1.5229826	0.20025929	-0.0547727	0.97920816	1.46820989	0.22916139
CD9	ENSG00000010278	957.70049	-0.5015807	0.03135889	-0.1541204	0.70163173	0.34746031	0.24256556
IDS	ENSG00000010404	34.5936542	-1.4192888	0.05220476	-0.3069868	0.82087601	1.11230203	0.20180166
CD4	ENSG00000010610	5.3372528	-4.7005577	0.08174176	-5.9725422	0.0083875	-1.2719844	0.89659908
GPRC5A	ENSG00000013588	70.8075399	-0.8446166	0.12509483	0.2547324	0.7643172	1.09934898	0.01696093
CDC58C	ENSG00000015133	18.1630636	-1.6819004	0.1628737	-0.2924326	0.88580864	1.38946777	0.3262559
CXorf56	ENSG00000018610	84.1279481	-0.7555548	0.27753524	0.16018227	0.88527677	0.91573703	0.12025763
NLRP2	ENSG00000022556	71.5317473	-0.6329472	0.33004782	-0.1183476	0.90851415	0.51459953	0.50121006
SLC39A9	ENSG00000029364	70.4317435	-0.8891722	0.16347045	-0.6665655	0.31441487	0.22260666	0.89471532
GRN	ENSG00000030582	300.260125	-0.8629004	0.00036798	-0.5345339	0.05349046	0.32836653	0.4668342
FUT8	ENSG00000033170	45.5693742	-1.7958236	0.00039916	-1.2756246	0.01524293	0.52019909	0.68138542
RNF19A	ENSG00000034677	69.6185228	-0.6603154	0.28093192	-1.218052	0.00407021	-0.5577366	0.47475653
CTPS2	ENSG00000047230	62.8098224	-0.7659637	0.33067369	-0.4911607	0.55999408	0.27480297	0.8692304
RRM2B	ENSG00000048392	77.0113377	-0.6567388	0.30245589	-0.4972197	0.43050476	0.15951913	0.91420595
RSF1	ENSG00000048649	104.180573	-0.6419674	0.22657388	-0.6467103	0.16257128	-0.0047429	0.99625918
HEBP2	ENSG00000051620	164.577085	-0.5091728	0.26291139	-0.4357716	0.30719321	0.07340115	0.94925399
CYFIP2	ENSG00000055163	14.5277718	-2.2700797	0.12208006	-0.9309497	0.62391573	1.33912995	0.55404852
PRDM6	ENSG00000061455	32.4823318	-1.4825455	0.03722983	-1.3772487	0.04406529	0.10529687	0.96374605
OAT	ENSG00000065154	197.65965	-0.6027107	0.15084194	-0.3735807	0.43775802	0.22912995	0.79191624
GRIPAP1	ENSG00000068400	66.4543356	-0.6973239	0.28999311	-0.7660819	0.1563169	-0.068758	0.96532772
LAPTM4A	ENSG00000068697	703.886995	-0.5474056	0.01961055	-0.3602407	0.17766523	0.18716487	0.71326947
WIPI1	ENSG00000070540	27.4124203	-2.1244514	0.00173533	-1.2745868	0.07884648	0.84986466	0.53313378
SEL1L	ENSG00000071537	99.4610552	-0.7449529	0.16327954	-0.1847683	0.84308591	0.56018455	0.40499241
ATP6AP1	ENSG00000071553	243.43282	-0.9574627	0.00115436	-0.1797898	0.77189549	0.77767295	0.01696093
PTPN18	ENSG00000072135	78.5734673	-0.8331924	0.09333796	-0.2141977	0.80615317	0.61899469	0.32027349
MPP5	ENSG00000072415	26.9864431	-1.1321666	0.20593357	-1.173053	0.13541187	-0.0408864	0.98764222
SIDT1	ENSG00000072858	93.0096625	-0.7769247	0.17369621	-1.1424865	0.00949321	-0.3655618	0.73538913
SCARB1	ENSG00000073060	60.5803506	-0.9899569	0.11756216	-0.6660313	0.33520929	0.32392562	0.82549001
CA12	ENSG00000074410	760.53363	-0.4801764	0.07512036	0.08274712	0.87868457	0.56292349	0.02010071
EIF4G3	ENSG00000075151	54.791074	-1.0015007	0.14294929	0.03796692	0.97765908	1.03949758	0.11377453
ZNF638	ENSG00000075292	94.8288051	-0.879619	0.06039321	-0.3653789	0.58429576	0.51424006	0.46427218
ACTN2	ENSG00000077522	10.3639771	-2.8065667	0.06794451	0.47748806	0.82514793	3.28405474	0.0167481
P2RY10	ENSG00000078589	9.98399867	-6.8296613	0.00076214	-2.9227153	0.02295246	3.906946	0.19965987
ITM2A	ENSG00000078596	13.6081973	-5.7007709	0.00589534	-1.40795	0.24142288	4.29282084	0.07983776
ITCH	ENSG00000078747	28.9199502	-1.0349046	0.26818953	-0.3997475	0.74820008	0.63515703	0.6457953
PGM1	ENSG00000079739	19.7178138	-1.2338252	0.30306492	-0.5550916	0.7066945	0.67873357	0.72883745
MID2	ENSG00000080561	13.9369314	-3.2998478	0.01019338	-1.360242	0.27332778	1.93960585	0.32420038
AACS	ENSG00000081760	53.029487	-0.7336771	0.34290924	-0.8150291	0.19303275	-0.081352	0.96349811
OXCT1	ENSG00000083720	12.4708756	-1.9786504	0.13606475	-0.4944232	0.80508525	1.48422721	0.38216174
ZNF586	ENSG00000083828	8.3140788	-2.1420399	0.27530167	-0.2865969	0.92089877	1.85544297	0.39943411
SSH1	ENSG00000084112	23.4075696	-1.4870725	0.16437605	0.3487315	0.83726952	1.83580404	0.04464771
KIF3C	ENSG00000084731	10.6877731	-1.574095	0.29671579	-2.2149099	0.07013807	-0.6408149	0.86321658
ATRX	ENSG00000085224	137.520462	-1.1117224	0.00858243	-0.43258	0.49049509	0.67914236	0.24475495
MGST2	ENSG00000085871	64.9437671	-0.7867373	0.2416063	-0.6767431	0.28466549	0.1099941	0.95014208
B4GALT1	ENSG00000086062	71.6935581	-0.693415	0.29173815	-0.0263761	0.98192765	0.66703892	0.31908698
FTL	ENSG00000087086	855.31667	-0.3433749	0.23185674	-0.4600295	0.03274912	-0.1166546	0.85429529
GNAS	ENSG00000087460	4945.31781	-0.3397388	0.15359761	-0.1935078	0.50339955	0.14623095	0.73856784
TFAP2C	ENSG00000087510	392.857203	-1.4873977	1.2E-10	-0.1953551	0.69850654	1.2920426	5.9915E-08
DYNLL1	ENSG00000088986	355.795507	-0.6388248	0.04471356	0.06074279	0.93256885	0.69956759	0.019709
RPL6	ENSG00000089009	681.65792	-0.5034144	0.11756216	-0.2695281	0.50590846	0.23388625	0.68000787
RPLP0	ENSG00000089157	4159.40229	-0.3168845	0.25004669	-0.1913401	0.54106614	0.12554446	0.80893148
ERP29	ENSG00000089248	241.124009	-0.4664689	0.20749683	-0.4167755	0.22994302	0.04969339	0.95807242
IGBP1	ENSG00000089289	28.6512937	-1.1262415	0.2000065	-1.2150006	0.11033941	-0.0887591	0.97105871
DDX24	ENSG00000089737	151.24711	-0.5624738	0.20135369	0.1434527	0.84635635	0.70592653	0.05884269
PITPNM2	ENSG00000090975	19.4961185	-2.7174812	0.00458759	-0.3026035	0.86743387	2.41487769	0.01874971
DLD	ENSG00000091140	137.851873	-0.5076914	0.3051879	-0.1909247	0.78232732	0.31676674	0.65535715
ZFHX4	ENSG00000091656	7.37291057	-2.7709926	0.23537215	0.18818905	0.95547408	2.95918162	0.17108805
TMEM101	ENSG00000091947	9.58148334	-5.6128526	0.00858243	-2.2994106	0.05576193	3.313442	0.29530535
SIRT1	ENSG00000096717	36.815085	-0.9390718	0.27320255	-0.7394479	0.37465863	0.19962386	0.92441713
IFT74	ENSG00000096872	27.7059352	-1.0165527	0.28509256	-1.0900303	0.17127928	-0.0734776	0.9747879
MARCHF2	ENSG00000099785	35.7072351	-1.0644692	0.2000065	-0.4202439	0.71357405	0.64422527	0.60941622
MKNK2	ENSG00000099875	93.2094596	-0.7881789	0.08475268	-0.6894125	0.12021752	0.09876644	0.9449136
KHNYN	ENSG00000100441	7.43686533	-3.7442017	0.06509427	-1.0622727	0.61326818	2.68192903	0.31628124
DAAM1	ENSG00000100592	100.438651	-0.6030171	0.31190026	0.45944814	0.40356064	1.06246521	0.00774138
DHRS7	ENSG00000100612	27.9443581	-1.5153129	0.06686343	-0.6899808	0.51573802	0.82533213	0.54420796
HIF1A	ENSG00000100644	33.9229596	-1.4375721	0.05496637	0.39741262	0.72480594	1.83498471	0.00460795
DICER1	ENSG00000100697	61.1451675	-0.7419247	0.26063638	-0.1518218	0.88716032	0.59010291	0.45317159
TRIP11	ENSG00000100815	74.1586491	-0.8082487	0.17056077	-0.1579459	0.8810728	0.65030279	0.35705356
ARHGAP5	ENSG00000100852	29.8981491	-1.3479056	0.14358269	-0.7441179	0.49327431	0.60378768	0.72957039
PTK6	ENSG00000101213	113.340269	-0.6741635	0.14294929	-1.0226083	0.00407021	-0.3484447	0.67046089
PSMD10	ENSG00000101843	176.391979	-0.8645326	0.01324801	-0.1507909	0.84160834	0.71374176	0.06791821
NKAP	ENSG00000101882	44.7853475	-0.9779022	0.160529	-0.2216671	0.85635929	0.75623512	0.38216174
ALG13	ENSG00000101901	80.0074865	-1.1742346	0.00540159	0.027855	0.97822331	1.20208959	0.00429795

XIAP	ENSG00000101966	65.8579992	-1.2253781	0.01280057	-0.5958115	0.35296022	0.62956658	0.43388978
MAGT1	ENSG00000102158	99.6172911	-0.8356344	0.07961868	0.27307187	0.70765974	1.10870629	0.00586788
PBDC1	ENSG00000102390	41.7000729	-1.0932631	0.12212159	0.05460965	0.96993073	1.14787276	0.0895534
GLA	ENSG00000102393	168.811867	-3.4603104	6.841E-27	-1.4100186	1.7943E-06	2.05029189	1.0476E-08
ARMCX3	ENSG00000102401	104.922392	-2.9387905	8.3082E-17	-1.1759566	0.00065905	1.76283398	1.4731E-05
BEX4	ENSG00000102409	14.7838752	-1.9922739	0.15992502	-0.6901908	0.72553964	1.3020831	0.52305616
LONP2	ENSG00000102910	96.1624396	-0.8086138	0.0801809	-0.3552198	0.5767545	0.45339399	0.53702357
NME3	ENSG00000103024	138.635664	-0.8392043	0.02842255	-0.2514127	0.70040642	0.58779162	0.23362771
HCFC1R1	ENSG00000103145	91.5092881	-1.0125096	0.01376738	-0.600638	0.21674719	0.4118716	0.6135163
METRN	ENSG00000103260	457.955177	-0.6337324	0.01484528	-0.1467552	0.77290735	0.48697713	0.11102139
CRYM	ENSG00000103316	6.19200317	-2.6951674	0.26818953	-1.7004217	0.45055772	0.99474568	0.86083162
NIPAL2	ENSG00000104361	30.0224595	-1.0865063	0.26818953	-0.3124005	0.83411644	0.77410579	0.54533303
NUCB1	ENSG00000104805	88.719513	-0.6761602	0.25130605	-0.2335549	0.78578928	0.44260528	0.58793732
PRKD2	ENSG00000105287	22.5005496	-1.2866618	0.1915608	-0.3911239	0.79152017	0.89553786	0.50605018
RABAC1	ENSG00000105404	6.79204966	-2.1582555	0.25806488	-2.050001	0.22575356	0.10825447	0.98435169
CNFN	ENSG00000105427	28.8842401	-1.3915277	0.10325329	-1.016324	0.25209772	0.37520363	0.87196209
CLEC11A	ENSG00000105472	60.519947	-1.0910127	0.02937183	-0.5692398	0.36791777	0.52177291	0.55872978
ZNF175	ENSG00000105497	11.8643244	-2.3477349	0.05152067	-1.8109573	0.12354908	0.53677765	0.89111814
LENG1	ENSG00000105617	11.4376377	-2.2163969	0.1587394	-0.9548307	0.62283997	1.2615622	0.62066092
PON3	ENSG00000105852	28.705112	-2.0108274	0.00519296	-0.2510191	0.8657144	1.75980828	0.02410098
PON2	ENSG00000105854	52.0863579	-1.5248928	0.00269904	-0.1183224	0.92089877	1.40657041	0.00829447
TSPAN12	ENSG00000106025	29.0445923	-2.3725469	0.00083468	-2.1937322	0.00171629	0.17881477	0.95014208
ZKSCAN1	ENSG00000106261	109.144305	-0.5659064	0.32742516	-0.6244222	0.18050182	-0.0585159	0.96501499
ZNHIT1	ENSG00000106400	128.133284	-0.6382278	0.15672161	-0.3263997	0.56945449	0.31182811	0.69248896
AMBP	ENSG00000106927	11.313336	-1.4831897	0.369621	-3.0385503	0.02463976	-1.5553606	0.54485982
MPDZ	ENSG00000107186	27.7740776	-2.2035379	0.00473105	-2.0749837	0.00655261	0.1285542	0.9657657
ANKRD26	ENSG00000107890	63.8605056	-1.2301677	0.00847771	-0.5020102	0.44192748	0.72815746	0.28409528
TASOR2	ENSG00000108021	95.1179309	-0.6135062	0.26063638	0.29691018	0.6497479	0.91041634	0.02472596
SHOC2	ENSG00000108061	150.199404	-1.7957276	7.6096E-10	-0.5481997	0.1588933	1.24752785	0.000144
FBXL20	ENSG00000108306	13.8638927	-1.4606296	0.27530167	-0.1539357	0.94375488	1.30669385	0.37203226
DDX5	ENSG00000108654	574.718165	-0.3014124	0.40739877	0.28607371	0.34519931	0.58748608	0.00913181
LGALS3BP	ENSG00000108679	28.320676	-1.0957144	0.26826293	-1.1056504	0.19621216	-0.009936	0.99605451
KRT32	ENSG00000108759	46.8897865	-1.6012195	0.00117675	-3.6348449	3.4575E-10	-2.0336254	0.00559144
SLC9A3R1	ENSG00000109062	812.072003	-0.6355661	0.02229115	0.40412702	0.20430797	1.03969317	6.122E-06
SUPT6H	ENSG00000109111	46.5738907	-1.0426679	0.20664912	-0.9762647	0.1957037	0.06640324	0.97554119
TRIM2	ENSG00000109654	61.2583513	-0.7251339	0.34756784	0.40589106	0.62932298	1.13102499	0.03819641
SH3D19	ENSG00000109686	14.1472266	-1.4589602	0.28357673	-0.8602588	0.5551927	0.59870134	0.82854915
MFSD10	ENSG00000109736	56.8408247	-0.7474273	0.2696924	-1.065994	0.03449253	-0.3185667	0.81343405
SIAE	ENSG00000110013	8.22900135	-2.4365318	0.20135369	-0.7655679	0.74475025	1.67096388	0.53735269
CCND1	ENSG00000110092	211.216242	-1.2805268	3.5699E-06	0.19928366	0.72736035	1.4798105	2.6737E-08
UBE4A	ENSG00000110344	21.246996	-1.212862	0.29270035	-1.3229688	0.17034511	-0.1101068	0.96980657
DDX6	ENSG00000110367	148.349572	-0.8259954	0.04746308	-0.6551189	0.12639227	0.17087647	0.89238219
MDK	ENSG00000110492	72.3818661	-1.0421505	0.03971867	0.3394825	0.65708842	1.381633	0.00153222
GTF2H1	ENSG00000110768	47.7092251	-0.7818488	0.31483553	0.10930752	0.93222983	0.89115632	0.19504498
PRDM4	ENSG00000110851	25.4406002	-1.0268778	0.33067369	-1.2240923	0.14627308	-0.1972144	0.94191161
BCL7A	ENSG00000110987	58.5751009	-0.95724	0.08451466	-0.426944	0.56945449	0.53029602	0.54913507
ARPC3	ENSG00000111229	207.763234	-0.7566001	0.04547752	-0.240255	0.70229687	0.51634504	0.29968392
MGP	ENSG00000111341	912.538022	-1.7499915	4.6603E-14	-3.6124323	8.3166E-54	-1.8624408	1.3454E-13
RAB5B	ENSG00000111540	152.583887	-0.5976627	0.25750716	-0.6988988	0.09756306	-0.1012362	0.94132028
ENPP5	ENSG00000112796	17.9356009	-1.9468331	0.0383867	-2.0558581	0.02007251	-0.109025	0.97417445
C5orf15	ENSG00000113583	95.8046515	-0.6953514	0.16445719	-0.5331241	0.30223051	0.16222724	0.90198482
STC2	ENSG00000113739	247.070665	-2.3656176	4.7508E-23	-0.3354609	0.37307763	2.03015671	1.0424E-16
HES1	ENSG00000114315	148.668475	-0.6586046	0.10940566	0.29593763	0.58422976	0.95454225	0.00376125
PLCH1	ENSG00000114805	23.6260592	-1.160705	0.32353304	-2.1921778	0.00963878	-1.0314728	0.52599814
EEF1B2	ENSG00000114942	545.279879	-0.4161221	0.25004669	-0.1495498	0.77723028	0.2665723	0.59435775
RTKN	ENSG00000114993	62.2875475	-0.7797366	0.29666658	0.1976263	0.86258702	0.97736289	0.11363354
ACTR1B	ENSG00000115073	87.4031071	-0.6475651	0.24735562	-0.358507	0.58618343	0.28905812	0.77763043
SLC35F5	ENSG00000115084	78.8459192	-0.7887707	0.12848038	-0.8462019	0.06304413	-0.0574311	0.96954174
ACTR3	ENSG00000115091	245.229422	-0.6727079	0.04695506	-0.5004364	0.16393771	0.17227146	0.85303578
PPM1G	ENSG00000115241	295.846343	-0.4476626	0.24073231	0.3857869	0.26321542	0.8334495	0.00129644
CLIP4	ENSG00000115295	13.0251095	-1.8570433	0.22724983	0.47589228	0.82012349	2.33293559	0.06541866
STAT1	ENSG00000115415	78.1123575	-0.6796604	0.28446567	-0.1454177	0.88638329	0.53424265	0.48171984
IGFBP5	ENSG00000115461	1495.74308	-3.1762105	2.4833E-75	-1.371853	3.4294E-15	1.8043576	2.0174E-23
GGCX	ENSG00000115486	121.805525	-0.6531651	0.15324671	-0.1981168	0.78798677	0.45504836	0.45483688
COQ10B	ENSG00000115520	81.4206079	-0.7622476	0.14475347	-0.2392331	0.77189549	0.52301448	0.45723299
SF3B1	ENSG00000115524	273.049907	-0.45711	0.28380334	-0.4796743	0.17622083	-0.0225642	0.98280854
SLC9A2	ENSG00000115616	53.6088399	-0.9416296	0.1468249	-1.2241571	0.02111163	-0.2825276	0.8683482
MLPH	ENSG00000115648	326.102751	-0.4238322	0.24811793	-0.4884618	0.09874864	-0.0646297	0.94653184
UXS1	ENSG00000115652	61.0769208	-0.7702879	0.2696924	-0.2186947	0.83974705	0.55159314	0.54420796
SDC1	ENSG00000115884	197.5871	-1.268769	1.4519E-05	-1.0038948	0.0008738	0.26487422	0.74097668
ORC4	ENSG00000115947	61.1369699	-0.8892229	0.12442051	0.06422203	0.95365225	0.95344494	0.07983776
PCYOX1	ENSG00000116005	150.77642	-0.7254571	0.09885972	-0.5973516	0.17083002	0.12810552	0.91916333
EPAS1	ENSG00000116016	23.9747465	-1.4207706	0.14475347	0.05384595	0.97736923	1.47461653	0.11622186
SUMO1	ENSG00000116030	469.428803	-0.3824118	0.28356195	-0.0286085	0.96519035	0.35380335	0.34254319
SPR	ENSG00000116096	105.084948	-0.8381621	0.04072558	-0.4140992	0.43780528	0.42406289	0.54264774
BCL9	ENSG00000116128	21.6864193	-1.4843208	0.11545546	-0.3289827	0.83732494	1.15533809	0.31643124
KDM5B	ENSG00000117139	44.5587029	-0.9019603	0.22831966	-1.0788545	0.07702702	-0.1768942	0.92837088
ECE1	ENSG00000117298	87.5373503	-1.5092095	2.3428E-05	-1.4435577	4.6455E-05	0.06565179	0.96367294
IRF6	ENSG00000117595	159.316824	-0.6101401	0.15084194	-0.6056905	0.11192407	0.00444961	0.99605451
MESD	ENSG00000117899	112.550982	-0.5243279	0.33067369	-0.3542254	0.53058985	0.17010255	0.88792189
MUC5B	ENSG00000117983	4.78958953	-2.7576947	NA	-5.6902518	0.01768714	-2.9325571	0.53878241
MREG	ENSG00000118242	89.2950263	-1.0452275	0.02539684	-0.1273121	0.90281412	0.91791534	0.06963427
VAMP8	ENSG00000118640	892.461516	-0.5911907	0.02539684	-0.4556443	0.10197222	0.13554643	0.85737085
KLF9	ENSG00000119138	8.64083873	-3.6684178	0.0212429	-1.1914651	0.4830412	2.47695269	0.25266573
NEK9	ENSG00000119638	32.7666149	-1.1083541	0.19299847	-0.2204776	0.87868457	0.88787647	0.3881788
ACOT2	ENSG00000119673	85.1781066	-0.855017	0.06642092	-0.1582186	0.86264585	0.69679838	0.19379048
MLH3	ENSG00000119684	13.2010633	-1.7677743	0.25749746	-0.1619504	0.95037344	1.60582394	0.33503018
SUPT7L	ENSG00000119760	33.9132938	-0.9416354	0.29258589	-0.1941956	0.88879569	0.74743978	0.4859345
YPEL5	ENSG00000119801	136.695801	-0.9699698	0.00408176	-0.3634636	0.47293778	0.60650618	0.18089693
FAM98A	ENSG00000119812	57.9888483	-0.6782817	0.33004782	-0.6427783	0.2932956	0.03550336	0.98334842
YIPF4	ENSG00000119820	117.603677	-0.7403411	0.01367214	-0.4336211	0.42511123	0.30151996	0.74095209
OGFRL1	ENSG00000119900	27.8698136	-1.0057739	0.29496786	-1.1273742	0.15419923	-0.1216003	0.95911967
PDZD11	ENSG00000120509	98.5836251	-0.766376	0.10228949	0.17949067	0.82939049	0.9458667	0.01984353
KIAA1217	ENSG00000120549	130.709012	-0.5499627	0.25699245	-0.5935988	0.13979397	-0.0436361	0.97176739
CLU	ENSG00000120885	570.849272	-1.1131879	1.7368E-07	-0.517612	0.04611534	0.59557588	0.02704329
ABCC11	ENSG00000121270	60.1550888	-4.6472206	2.3727E-16	-6.0697967	1.8218E-12	-1.4225761	0.50043691
ZMYM2	ENSG00000121741	28.0721739	-1.0194606	0.32570589	-0.5702384	0.62932298	0.44922224	0.81441544
TNFSF10	ENSG00000121858	8.61905773	-1.8962247	0.28380334	-2.2578748	0.13054695	-0.3616501	0.94285895
MTERF4	ENSG00000122085	12.3591667	-1.6129966	0.25762485	-0.3965157	0.85396862	1.21648095	0.49913447
MED13L	ENSG00000123066	49.8403567	-0.9557267	0.18093323	0.10381929	0.93698191	1.05954598	0.10854807
SSPN	ENSG00000123096	5.39341859	-3.0667787	0.18176911	-2.4350137	0.24626765	0.63176494	0.92441713
SMUG1	ENSG00000123415	69.4200971	-1.4253859	0.00323075	-0.2910196	0.75468504	1.13436632	0.03926868
FAM199X	ENSG00000123575	35.8017753	-1.1130045	0.15535124	-0.6291188	0.49409796	0.48388567	0.74832782
CHPF	ENSG00000123989	43.9446974	-1.140327	0.08110417	-0.3084747	0.77739227	0.83185232	0.31993207
DNPEP	ENSG00000123992	126.859936	-0.7329488	0.0614274	-0.3560482	0.49172885	0.37690062	0.56569421
PARD6B	ENSG00000124171	126.170159	-0.5914081	0.266217	-0.3312321	0.59515574	0.26017605	0.79012457
PMEPA1	ENSG00000124225	141.230821	-1.2921641	2.3064E-05	-1.1880806	9.5907E-05	0.10408359	0.93462218
BCAS4	ENSG00000124243	54.2101805	-0.8641407	0.15533927	-0.848333	0.12501027	0.01580769	0.99304392
IQSEC2	ENSG00000124313	45.0389952	-0.8374414	0.29140527	-0.7118095	0.33725314	0.12563188	0.95014208
XG	ENSG00000124343	129.356521	-1.1419977	0.00035873	-1.2426027	6.2246E-05	-0.1006049	0.93911055
NDP	ENSG00000124479	26.2882528	-4.1081564	0.00010869	0.46622346	0.71319615	4.57437985	8.7486E-06
RAB17	ENSG00000124839	47.5008981	-1.0400912	0.13794281	-0.4936755	0.58501069	0.54641566	0.63982429
NDUFA1	ENSG00000125356	465.899551	-0.5654572	0.21639346	-0.0979718	0.9044233	0.46748537	0.37444966
BMP4	ENSG00000125378	97.9857568	-1.0901328	0.0038544	-2.470584	1.0029E-11	-1.3804512	0.0020082
MBOAT7	ENSG00000125505	176.245755	-0.6685258	0.10213468	-0.1188453	0.88066045	0.54968053	0.24075617
PPDPF	ENSG00000125534	4343.75615	-0.3540803	0.19208528	-0.2703173	0.33190694	0.08376295	0.90100125
CHCHD5	ENSG00000125611	31.9088813	-2.4792357	0.00068377	0.50807601	0.62294227	2.98731173	1.221E-05
THOC2	ENSG00000125676	73.9870538	-1.1312173	0.01629668	-0.6041646	0.30408101	0.52705277	0.5350028
MMP24OS	ENSG00000126005	41.2636216	-1.2863057	0.04199418	-0.8830417	0.19664402	0.40326405	0.79493462
KDM5C	ENSG00000126012	110.706838	-0.6169218	0.1845484	-0.5877453	0.16649118	0.02917651	0.98248708
HNRNPH2	ENSG00000126945	54.0118156	-2.0986083	2.5155E-05	-0.1838145	0.87037606	1.9147938	0.00023941
ARMCX1	ENSG00000126947	60.1934876	-1.8447086	5.8092E-05	0.0023785	0.99835048	1.84708706	6.7207E-05
HIVEP3	ENSG00000127124	29.1690326	-1.5228701	0.04540679	-0.719315	0.45583085	0.80355512	0.53244427
CCNT1	ENSG00000129315	36.2959767	-1.0872442	0.29258589	-0.6182314	0.5984789	0.46901276	0.80668701
MAP7D3	ENSG00000129680	7.68900212	-2.5480706	0.37804276	1.53325433	0.38419927	4.0813249	0.03373933
SH3BP4	ENSG00000130147	59.5568951	-0.9725096	0.15823448	-1.0878942	0.06558579	-0.1153846	0.95066459
NECTIN2	ENSG00000130202	71.4299326	-0.832067	0.12225837	-0.4039896	0.56169299	0.42807738	0.63687594
CHMP2A	ENSG00000130724	294.985832	-0.4830518	0.1628737	9.9904E-05	0.99998465	0.48315168	0.16109143
ARHGEF9	ENSG00000131089	16.6816444	-2.0355796	0.0373884	-1.0717648	0.3407518	0.96381481	0.59766485
TRAF3	ENSG00000131323	25.9967927	-1.2302444	0.24292734	-0.5114597	0.71040301	0.71878474	0.65615233
KCNC3	ENSG00000131398	27.7366463	-1.2325471	0.16481624	0.24460395	0.86910317	1.4771511	0.05711443
IL13RA1	ENSG00000131724	43.880342	-1.8924388	0.0003044	-0.4814324	0.5615099	1.41100644	0.02148563
RARA	ENSG00000131759	51.0278577	-0.903357	0.29258589	0.16090457	0.90697493	1.06426159	0.15047314
FMO5	ENSG00000131781	7.35731834	-3.6227721	0.03437354	-4.0748701	0.02295246	-0.452098	0.95014208
PRKAB2	ENSG00000131791	49.7651307	-1.3496399	0.00807126	-1.3961287	0.00425165	-0.0464888	0.98034096
THAP1	ENSG00000131931	33.3619926	-0.9102456	0.31190026	-0.4172058	0.71040301	0.49303981	0.7343206
TRIM5	ENSG00000132256	21.2204945	-1.2005473	0.25951209	-0.4764231	0.73090605	0.72412425	0.65105638
PCED1A	ENSG00000132635	7.17629174	-2.5467895	0.25363983	-0.3423022	0.91686547	2.20448731	0.37823597
TCEAL4	ENSG00000133142	435.167956	-1.1659489	9.648E-05	-0.3412659	0.49595014	0.82472199	0.0169946
THUMPD3	ENSG00000134077	16.3527936	-1.710033	0.11618128	-0.6390003	0.66266951	1.07103269	0.50744075
KIDINS220	ENSG00000134313	53.137958	-1.021369	0.07528244	-0.9959216	0.06187415	0.02544739	0.98836215
RERG	ENSG00000134533	73.1124421	-1.7526746	4.8488E-05	-0.0111887	0.99232686	1.74148589	6.7738E-05
RTL8C	ENSG00000134590	70.0874625	-1.343028	0.00209813	-0.7525441	0.14268074	0.59048391	0.44916063
TAOK3	ENSG00000135090	89.0108082	-0.9270592	0.08773329	0.35736285	0.64106431	1.28442203	0.00406619
TRAFD1	ENSG00000135148	56.0782221	-0.8252025	0.23617672	-0.4686946	0.5615962	0.3565079	0.78853959
PHF21A	ENSG00000135365	44.8259883	-1.3563456	0.02000931	-0.7261107	0.30591009	0.63023495	0.55425557
EHF	ENSG00000135373	64.325438	-4.089954	9.2951E-12	-1.4846397	0.00579471	2.60531425	0.00017066
ELF5	ENSG00000135374	208.47914	-2.1338768	3.5034E-16	-0.6210222	0.03550833	1.5128546	8.6732E-08
ACVR1B	ENSG00000135503	50.4194433	-1.0366568	0.15622359	-0.1858514	0.88715481	0.85080537	0.31913593
SEMA4F	ENSG00000135622	9.90892502	-1.7975246	0.2325896	-1.0612898	0.51049587	0.73623488	0.80872055
RAB11FIP5	ENSG00000135631	20.3979423	-1.3290429	0.25032427	-0.2980413	0.87037606	1.03100164	0.46410408
GNS	ENSG00000135677	151.912129	-0.4897257	0.31945404	-0.4531328	0.30289243	0.03659293	0.97417445
TMEM127	ENSG00000135956	152.211613	-1.1741604	0.00031902	-0.908809	0.00764897	0.26535135	0.76845099
C2orf49	ENSG00000135974	67.8679303	-0.8955381	0.09924415	-0.577128	0.34519931	0.31841017	0.7925113
ISCU	ENSG00000136003	184.217405	-0.5432286	0.16139306	-0.5170084	0.14600959	0.02632019	0.98034096
CKAP4	ENSG00000136026	44.7502861	-1.0804731	0.09885972	0.05397416	0.96866166	1.13444721	0.07008832
IREB2	ENSG00000136381	40.0381807	-0.8024398	0.34039355	-0.6452272	0.41951479	0.15721262	0.9390791
CBWD2	ENSG00000136682	105.590816	-0.5588162	0.31957879	0.10351298	0.90747351	0.66232919	0.17025998

IL1RN	ENSG00000136689	8.05728933	-4.2692472	0.10739039	0.10656635	0.97101953	4.37581352	0.08737308
CCDC115	ENSG00000136710	85.8269074	-0.7964117	0.09867378	-0.3915993	0.53077096	0.40481238	0.62037629
KIF12	ENSG00000136883	60.4058847	-0.8296747	0.15825389	-1.3248357	0.00395704	-0.4951611	0.62067667
YAP1	ENSG00000137693	35.8970363	-1.1410504	0.189635	-0.2226719	0.88160106	0.91837845	0.38022778
HADHB	ENSG00000138029	143.924839	-0.6636113	0.10128263	-0.2408439	0.69548403	0.42276734	0.45978463
RAB1A	ENSG00000138069	354.128428	-0.4134631	0.2435983	-0.1583186	0.75245839	0.25514449	0.6158609
PREPL	ENSG00000138078	42.9418908	-1.1019842	0.07666929	-1.0825744	0.06062352	0.01940978	0.99256964
CIR1	ENSG00000138433	82.987053	-0.6584133	0.24735562	-0.7923003	0.08081658	-0.1338871	0.92502368
ITGAV	ENSG00000138448	43.6670028	-0.8243264	0.2696924	-0.9361834	0.12611201	-0.111857	0.95133572
SLC40A1	ENSG00000138449	220.077987	-1.4285064	1.24E-05	0.41728278	0.41488297	1.84028913	1.9525E-09
USP8	ENSG00000138592	78.1215446	-0.6431127	0.31487409	-0.3448008	0.64819949	0.29831196	0.7925113
SDSL	ENSG00000139410	17.6122217	-1.5812494	0.21043584	0.0805601	0.97096412	1.66180948	0.16586088
CERS5	ENSG00000139624	27.2672777	-1.4301184	0.10302178	-0.2991207	0.84693297	1.13099775	0.28711372
GALNT6	ENSG00000139629	241.711709	-0.4100155	0.3031926	-0.650343	0.01827037	-0.2403276	0.6967435
RB1	ENSG00000139687	21.9722317	-2.8295753	0.00207752	0.21811551	0.89779645	3.04769085	0.0006362
SETD1B	ENSG00000139718	45.155076	-1.0719993	0.08485043	-0.7084199	0.30350498	0.36357942	0.79734628
ARMH4	ENSG00000139971	6.87372314	-3.3343607	0.145142	0.0677621	0.98328428	3.40212282	0.12679236
NAA30	ENSG00000139977	84.3746427	-0.6964709	0.19699773	-0.3260263	0.64665449	0.37044464	0.67961022
WDR89	ENSG00000140006	10.6787253	-1.7008651	0.27998595	-0.413077	0.85816103	1.28778806	0.51624319
ARRDC4	ENSG00000140450	19.0888575	-1.4631608	0.16139306	-0.8854325	0.44433467	0.57772835	0.79493462
PML	ENSG00000140464	13.1253943	-1.4320872	0.30385386	-0.5827981	0.73851933	0.84928907	0.6920323
MFGE8	ENSG00000140545	11.1366378	-1.8178052	0.25004669	-1.2658907	0.42091189	0.55191445	0.88934778
ABCC12	ENSG00000140798	4.3004841	-6.082986	NA	-5.926162	0.01299338	0	1
NPEPPS	ENSG00000141279	197.539242	-0.5080114	0.17420011	-0.6657285	0.02450834	-0.1577171	0.86418864
CACNG8	ENSG00000142408	5.82757506	-2.3519434	0.29721281	-2.1985814	0.27078784	0.15336203	0.97983413
CYP4B1	ENSG00000142973	102.530074	-0.7285912	0.10899063	-2.1930911	1.027E-09	-1.3903198	0.00060576
ACP1	ENSG00000143727	311.57586	-0.3966979	0.3111922	-0.2551066	0.54777283	0.14159126	0.86418864
PSEN2	ENSG00000143801	24.2860619	-1.3237643	0.1587698	-0.80076	0.44629009	0.52300433	0.7925113
PDIA6	ENSG00000143870	39.6560189	-0.8386325	0.33004782	-0.6623996	0.42198868	0.17623291	0.93047906
RHOB	ENSG00000143878	972.707502	-0.5972901	0.00407059	-0.8295891	5.9157E-06	-0.232299	0.56365381
RPS27A	ENSG00000143947	2125.29507	-0.3706269	0.32665469	-0.2436349	0.54484377	0.12699191	0.87305328
DUSP11	ENSG00000144048	47.2827182	-1.0658643	0.09238505	0.29547753	0.76497256	1.36134179	0.0112742
THNSL2	ENSG00000144115	47.6151723	-1.2452358	0.02788641	-0.5267874	0.50109785	0.71844848	0.40951496
LIPT1	ENSG00000144182	5.93055366	-3.1222141	0.19939655	-0.3731811	0.9075707	2.74903304	0.3134638
ABCA12	ENSG00000144452	193.247791	-1.2046351	3.3389E-05	-0.9530568	0.00150076	0.25157828	0.75531463
AGTR1	ENSG00000144891	46.2900984	-8.393031	1.5104E-06	-0.7757299	0.26254576	7.61730107	2.3692E-05
MUC4	ENSG00000145113	8.80945681	-3.1035629	0.04977115	-1.284489	0.45760376	1.81907396	0.4626732
CXCL14	ENSG00000145824	162.046874	-5.9475391	7.6852E-31	-2.4014035	6.1581E-18	3.54613555	3.2677E-10
RNF44	ENSG00000146083	52.5568509	-0.7422773	0.30839843	-0.6285662	0.35722321	0.1137111	0.94978923
PNRC1	ENSG00000146278	47.7285538	-0.8902491	0.22348187	-1.5512714	0.00387307	-0.6610223	0.53299209
TMEM181	ENSG00000146433	19.9449484	-1.1550738	0.29939237	-0.7771082	0.50018129	0.37796562	0.88339628
SLC12A9	ENSG00000146828	26.8109814	-1.0261214	0.34032858	-0.1203992	0.94400468	0.90581224	0.44496357
SHROOM2	ENSG00000146950	20.4018961	-2.0207895	0.02120757	-0.3804003	0.81028762	1.6403892	0.10784185
MSN	ENSG00000147065	19.2508735	-1.9785851	0.06432987	0.11196236	0.95505715	2.0905475	0.04090658
TAF1	ENSG00000147133	26.8636401	-1.7003183	0.08949925	0.35996781	0.82580964	2.06028611	0.01802827
SNX12	ENSG00000147164	58.0159549	-1.1338633	0.02703096	0.00761026	0.99369191	1.14147359	0.02571289
PRPS1	ENSG00000147224	46.5002242	-0.8247459	0.27096427	-0.3615711	0.70953316	0.46317473	0.69474177
RPL10	ENSG00000147403	470.902016	-0.525162	0.2672216	-0.0006772	0.99958705	0.52448481	0.25710808
C9orf72	ENSG00000147894	10.3263643	-1.6903506	0.26663629	-0.9706491	0.5516493	0.7197015	0.80796301
AOPEP	ENSG00000148120	143.241074	-0.8525409	0.04511381	-0.8731582	0.02563834	-0.0206173	0.98766681
RGS10	ENSG00000148908	105.49392	-0.6658486	0.1644439	-0.0690005	0.94099807	0.59684808	0.25512701
HSD17B12	ENSG00000149084	15.1964399	-1.3695674	0.32665469	-0.6022293	0.72009516	0.76733817	0.73223139
TNKS1BP1	ENSG00000149115	131.847083	-0.8728497	0.05225612	-0.7418351	0.09756306	0.13101462	0.9245108
LAMTOR1	ENSG00000149357	318.10779	-0.4467594	0.17839767	-0.1879983	0.68675876	0.25876109	0.61081292
ST14	ENSG00000149418	88.0677139	-0.6400681	0.29294303	0.20190886	0.82412837	0.84197695	0.08304409
SIDT2	ENSG00000149577	35.2070566	-0.971093	0.29789541	-0.8188965	0.34983868	0.15219649	0.94773579
TMEM25	ENSG00000149582	56.1759623	-1.1336012	0.03130082	-1.1024548	0.02786845	0.03114641	0.98634429
TM7SF2	ENSG00000149809	68.2582424	-1.0407904	0.02842255	-1.5840153	0.00013567	-0.5432249	0.54252995
HNMT	ENSG00000150540	15.8345178	-1.4348955	0.27945693	-0.1223617	0.95357376	1.31253377	0.3553269
PDCD4	ENSG00000150593	397.675743	-2.8077541	1.1031E-33	-0.1891423	0.71000785	2.6186118	4.407E-29
UBC	ENSG00000150991	1257.68685	-0.339214	0.31490279	-0.0329032	0.95357376	0.30631079	0.39492557
ITPR1	ENSG00000150995	48.3313856	-1.3479502	0.00997407	-2.1674577	8.8094E-06	-0.8195075	0.37732075
TMEM263	ENSG00000151135	175.300906	-0.6700602	0.08485043	-0.5934051	0.11330589	0.07665512	0.94867623
BTBD11	ENSG00000151136	23.9117003	-1.875576	0.01289674	-6.2921129	0.00051739	-4.4165369	0.05101164
THRSP	ENSG00000151365	11.3000342	-2.1824395	0.1374827	-0.8630641	0.6327898	1.3193754	0.56315036
DST	ENSG00000151914	78.5994454	-0.9150494	0.04702232	-0.8518767	0.05350833	0.06317272	0.96501499
BCL2L11	ENSG00000153094	21.5810309	-1.2592354	0.28806771	0.34670587	0.83475221	1.60594126	0.09322539
TMEM87B	ENSG00000153214	91.8765376	-0.7788891	0.15868117	-0.8321513	0.08417509	-0.0532622	0.97285336
LURAP1L	ENSG00000153714	41.2452447	-1.0729292	0.13542509	-1.0665675	0.10197222	0.00636172	0.99655127
TRIP12	ENSG00000153827	87.1926121	-0.7369665	0.16816206	0.14212024	0.88060466	0.87908678	0.06249623
PROM2	ENSG00000155066	59.6767862	-1.1542089	0.03117259	-0.9488541	0.07987742	0.20535482	0.906361
TTC39B	ENSG00000155158	12.3319027	-1.4278624	0.3320282	-1.1734324	0.38949569	0.25442999	0.94639707
DEPTOR	ENSG00000155792	22.669575	-1.2830472	0.20093879	-0.1136186	0.95056328	1.16942857	0.28229004
RRAGA	ENSG00000155876	113.780601	-0.5822111	0.24811793	0.02263503	0.97991838	0.60484613	0.20829616
PXYLP1	ENSG00000155893	13.1784272	-1.7570068	0.1468149	-0.9260232	0.50666491	0.83098353	0.71761201
RAB39B	ENSG00000155961	6.28372283	-3.325135	0.13941982	-0.3532005	0.90700167	2.9719345	0.22299544
MAGEA8	ENSG00000156009	103.210451	-1.0758126	0.0077461	-0.355016	0.57947818	0.72079664	0.16586088
ELMSAN1	ENSG00000156030	58.90278	-1.3113127	0.01108037	0.037532	0.97587687	1.34884474	0.0082565
PHF6	ENSG00000156531	34.6877517	-0.9389571	0.29270035	-0.0156631	0.99216427	0.92329401	0.30347086
KAT6B	ENSG00000156650	105.591788	-1.3265847	0.0001549	-1.5732575	3.5538E-06	-0.2466728	0.83579422
UTP14A	ENSG00000156697	80.3703839	-0.7083325	0.20507948	-0.1921059	0.83475221	0.51622661	0.47304214
FBRS	ENSG00000156860	91.9097702	-0.8540984	0.0550036	-0.7617608	0.07840526	0.09233763	0.94925399
TSC22D3	ENSG00000157514	181.258325	-1.085619	8.415E-05	-1.9051293	5.1755E-13	-0.8195103	0.02193392
UBN2	ENSG00000157741	36.1687546	-0.9928502	0.25146819	-1.2177878	0.07884648	-0.2249376	0.91916333
DUSP2	ENSG00000158050	29.1260679	-1.1614893	0.19336864	-0.0804508	0.96192974	1.08103841	0.25414607
CUL4B	ENSG00000158290	127.7901	-0.87769	0.01800094	0.09006891	0.91474386	0.96775888	0.0063
H2BC5	ENSG00000158373	68.8433681	-1.4537606	0.00289696	-0.1512321	0.8921634	1.30252852	0.01184119
H4C8	ENSG00000158406	90.8364812	-1.2580782	0.00092101	-1.0011454	0.01049352	0.25693278	0.8276536
EIF5B	ENSG00000158417	320.239644	-0.5013793	0.24163951	-0.0391473	0.96084294	0.46223196	0.30345186
CNOT11	ENSG00000158435	77.5549428	-0.7581872	0.16139306	-0.4312857	0.50668553	0.32690151	0.75178314
EMSY	ENSG00000158636	42.9861328	-0.8840499	0.31541666	-0.6353858	0.47581814	0.24866414	0.90133995
PAGE5	ENSG00000158639	163.132169	-3.5999374	5.0635E-23	0.30578476	0.57011666	3.90572221	1.7269E-27
SIM2	ENSG00000159263	7.90305755	-3.316244	0.0589326	-1.7843169	0.28223486	1.5319271	0.6555099
PIP	ENSG00000159763	15.8470881	-4.5454977	0.00026063	-2.2888054	0.01344386	2.25669236	0.26416616
TFF3	ENSG00000160180	944.229455	-0.7163776	0.01053511	-0.6300037	0.02329991	0.08637395	0.92610943
TFF1	ENSG00000160182	1926.29154	-1.0640416	3.5025E-09	-0.3732652	0.13113463	0.69077636	0.00065192
AZGP1	ENSG00000160862	10.5368805	-2.7967169	0.02732349	-6.8616553	0.00044628	-4.0649384	0.15596926
GRIN2C	ENSG00000161509	6.42652022	-2.2626416	0.28779081	-2.1641556	0.24754669	0.09848602	0.98632965
COA7	ENSG00000162377	34.3138634	-1.4150913	0.06396992	-0.552875	0.61181941	0.8622163	0.44545753
AKR7A3	ENSG00000162482	156.445407	-2.0797264	6.2813E-15	-3.4943082	1.9474E-29	-1.4145818	0.00031077
C1orf115	ENSG00000162817	18.9940665	-1.2936483	0.24735562	-2.3045499	0.00858064	-1.0109015	0.5728859
SLC66A3	ENSG00000162976	189.285657	-0.6709798	0.04540679	-0.9713767	0.00052644	-0.3003969	0.6419236
INHBB	ENSG00000163083	163.42181	-0.7938596	0.02163086	-1.2906015	1.0398E-05	-0.4967419	0.34528897
DCAF16	ENSG00000163257	19.3857188	-1.5688622	0.08983573	-1.5179395	0.07718943	0.05092271	0.98642238
PPM1K	ENSG00000163644	33.7283164	-2.0288079	0.00387858	0.22824506	0.87725063	2.25705291	0.00077441
TIPARP	ENSG00000163659	20.0078358	-1.6535302	0.14358269	0.19001348	0.92546944	1.8435437	0.07266955
TMEM158	ENSG00000163762	94.2231816	-1.0994538	0.00830978	-2.5444254	3.2963E-11	-1.4449717	0.0020416
SLC4A1AP	ENSG00000163798	72.5301529	-0.6775199	0.27998595	-0.2374698	0.79072299	0.44005004	0.6158609
WDR43	ENSG00000163811	74.9686151	-0.6383464	0.33067369	0.27551303	0.73247913	0.9138594	0.06393824
HEYL	ENSG00000163909	9.4685626	-1.9505557	0.27945693	-0.0190126	0.99338213	1.93154314	0.28238861
IFT122	ENSG00000163913	123.231512	-1.0259717	0.00637658	-1.3044946	0.00014334	-0.2785229	0.7835707
TMEM144	ENSG00000164124	29.1106335	-1.0861326	0.25699245	0.15943922	0.91789725	1.24557183	0.1399955
OTUD4	ENSG00000164164	35.7835554	-0.8582396	0.33105672	-0.2622734	0.83917364	0.59596621	0.61428176
DYNLT3	ENSG00000165169	56.3309959	-1.255536	0.02477863	0.50617186	0.48455895	1.76170784	0.00021168
CLDN3	ENSG00000165215	208.036599	-1.638958	4.942E-11	-0.4169177	0.24966238	1.22204028	6.6832E-06
BRWD3	ENSG00000165288	12.8935449	-1.7646349	0.22505142	-0.1480767	0.95109975	1.61655824	0.29964139
TC2N	ENSG00000165929	52.0585966	-0.7479631	0.29939237	-0.7520805	0.22668695	-0.0041173	0.99741771
MOAP1	ENSG00000165943	124.930635	-0.8625553	0.05875724	-0.9944754	0.01280722	-0.1319201	0.92502368
PTER	ENSG00000165983	27.9286606	-1.4092776	0.09624959	-0.8093319	0.40741632	0.59994566	0.72457395
TAF1D	ENSG00000166012	40.6257283	-0.8496143	0.33923245	-0.4957281	0.61909699	0.35388616	0.83734498
AMOTL1	ENSG00000166025	129.424581	-1.9309256	6.5129E-11	-1.8009368	1.0449E-09	0.12998884	0.92174256
ALKBH3	ENSG00000166199	45.7639514	-1.0041209	0.13725186	-0.4993235	0.55683299	0.50479741	0.66550194
ARIH1	ENSG00000166233	34.557529	-0.9122676	0.30080916	-0.6145089	0.50666491	0.29775874	0.88308723
WDR72	ENSG00000166415	52.461002	-1.2261067	0.02120126	-0.3259187	0.72182435	0.90018805	0.17234535
TMEM41B	ENSG00000166471	73.9056783	-0.7998793	0.14382655	-0.3846412	0.58843825	0.41523812	0.65105638
STAT6	ENSG00000166888	33.5742908	-1.6458162	0.01108037	-0.0735861	0.96048448	1.57223008	0.01842205
TSC22D4	ENSG00000166925	102.813199	-0.6405736	0.21758968	-0.1550876	0.86000042	0.485486	0.4526757
CCNDBP1	ENSG00000166946	37.3478265	-0.9211461	0.27984935	-0.4303217	0.68507219	0.49082439	0.72596691
TMC4	ENSG00000167608	42.4373526	-1.3589944	0.01411052	-1.2230756	0.02466675	0.13591881	0.94760837
GHDC	ENSG00000167925	16.5703546	-1.8874704	0.05847544	-1.1730784	0.27702494	0.714392	0.74352054
PCMTD1	ENSG00000168300	226.715652	-1.1082764	7.4053E-05	-1.1744475	1.4962E-05	-0.0661986	0.95066459
DEGS2	ENSG00000168350	267.646032	-1.2183646	2.1678E-06	-0.1096893	0.87037606	1.10867523	3.1316E-05
SCNN1B	ENSG00000168447	23.7456353	-1.2342922	0.19734519	-2.2116541	0.00425169	-0.9773618	0.52495058
C2orf68	ENSG00000168887	70.4811503	-0.6573388	0.31490279	-0.2244516	0.81537885	0.43288718	0.63189997
TMEM150A	ENSG00000168890	46.432764	-1.4203924	0.00752105	-1.3551669	0.00872422	0.06522549	0.97389284
AR	ENSG00000169083	127.538542	-1.9269922	6.7272E-10	-0.6937236	0.06818997	1.23326857	0.00065028
CCDC126	ENSG00000169193	35.8994604	-1.1806754	0.10124138	-0.930516	0.19860127	0.25015942	0.906361
GP2	ENSG00000169347	6.61295111	-2.1891452	0.33249531	-1.9421657	0.33520929	0.24697955	0.96421716
SYAP1	ENSG00000169895	609.956292	-0.5841055	0.01046204	-0.7128519	0.00018964	-0.1671264	0.76677947
MAP3K2	ENSG00000169967	57.5282766	-0.8515555	0.33447946	-0.1677622	0.90431802	0.68379278	0.51243333
TMED10	ENSG00000170348	284.546607	-0.9238177	0.00120107	-0.1090202	0.8751515	0.81479748	0.00709808
KIAA0232	ENSG00000170871	48.8951631	-0.9051166	0.19699773	-0.6283311	0.39945401	0.27678552	0.87196209
NDUFA3	ENSG00000170906	276.169791	-0.5166519	0.27998595	-0.1339603	0.86178341	0.38269157	0.52083446
TANC2	ENSG00000170921	20.4381516	-1.2967229	0.21380536	-0.8691434	0.4270035	0.42757955	0.86580127
SCAND1	ENSG00000171222	327.901668	-1.1397775	4.9602E-07	-0.7695561	0.00147705	0.37022141	0.38099954
KRT19	ENSG00000171345	8044.32301	-0.7973696	1.5501E-05	-0.7552214	3.3912E-05	0.04214821	0.95133572
KRT15	ENSG00000171346	33.9672387	-1.3481711	0.09220704	-1.8817395	0.00565021	-0.5336239	0.77221466
KRT13	ENSG00000171401	27.1424857	-3.518365	6.6952E-06	-2.6910548	0.00014293	0.82731017	0.72272376
ZNF581	ENSG00000171425	37.6205719	-1.1050053	0.11988019	-0.5024277	0.59260356	0.60257758	0.60343458
ZNF217	ENSG00000171940	192.115477	-1.1092118	9.4051E-05	-1.1617208	2.6688E-05	-0.052509	0.96134569
TCEAL1	ENSG00000172465	34.5792387	-1.4502861	0.03889268	-0.1746945	0.90349334	1.27559158	0.0968117
TMEM134	ENSG00000172663	89.3640578	-1.0813214	0.01209351	-0.9351655	0.02956725	0.14615593	0.92162815
SP3	ENSG00000172845	122.553937	-0.7109223	0.10661805	-0.1664977	0.83494621	0.54442462	0.31348818
FKBP2	ENSG00000173486	212.473909	-0.5507057	0.12692409	-0.4137892	0.27260953	0.13691653	0.88934778
AGFG1	ENSG00000173744	53.4949919	-0.7018088	0.45224433	0.53278605	0.90028801	1.23459487	0.03615512
ZHX3	ENSG00000174306	12.3073623	-1.7777331	0.18987797	-1.4021522	0.2895966	0.37558092	0.91941425
ATP2A2	ENSG00000174437	163.210231	-0.4926892	0.27523243	0.22820677	0.68358063	0.720896	0.03298267
CNTNAP2	ENSG00000174469	17.0365024	-2.8214079	0.00928958	-2.2705144	0.02772091	0.5508935	0.89066016

SEZ6L2	ENSG00000174938	71.0014615	-0.7204854	0.23104557	-0.6396268	0.25310012	0.08085863	0.95807242
PACS1	ENSG00000175115	44.1478929	-1.1655372	0.0687513	-0.6191311	0.42932744	0.54640614	0.63982429
YPEL2	ENSG00000175155	9.47769815	-1.9423794	0.20284791	-3.7323859	0.01082167	-1.7900065	0.5293447
SCUBE2	ENSG00000175356	120.811175	-2.8417021	2.1149E-15	0.27221766	0.66998777	3.11391979	1.1892E-18
PPP2R2D	ENSG00000175470	52.2768787	-0.7582266	0.29246252	0.14899935	0.89506262	0.90722595	0.14070959
UCP2	ENSG00000175567	391.926771	-1.0648112	1.175E-06	-1.0268014	2.1634E-06	0.03800976	0.96538342
MTLN	ENSG00000175701	131.636557	-0.762649	0.06061018	-0.4294574	0.38689412	0.33319155	0.66238979
MLXIP	ENSG00000175727	81.0030952	-1.2325236	0.003951	-0.2813701	0.72334057	0.95115353	0.05662305
ZNF613	ENSG00000176024	9.2337592	-1.9208765	0.25126831	-0.8161388	0.68270015	1.1047377	0.68000787
DNAJC30	ENSG00000176410	13.7179753	-1.6103333	0.23947982	-0.2509401	0.90816922	1.35939315	0.38748353
PNMA1	ENSG00000176903	72.2916169	-0.9532981	0.06917926	-0.1591366	0.87769054	0.79416152	0.18089693
ZDHHC22	ENSG00000177108	37.0749981	-1.5526	0.03173158	0.54719688	0.57558375	2.09979691	0.00069882
ULK1	ENSG00000177169	59.1649268	-0.9182752	0.14621355	-0.2960864	0.76057575	0.62218882	0.4691269
ACOT4	ENSG00000177465	67.1788346	-0.9688671	0.06148834	-0.1056339	0.92214442	0.86323316	0.12349663
ZBTB33	ENSG00000177485	47.0233506	-1.1223558	0.11472356	-0.1951624	0.88235269	0.92719335	0.25779248
POLR2L	ENSG00000177700	700.63123	-0.4498605	0.34039355	0.28375465	0.57558375	0.73361514	0.02603899
COX14	ENSG00000178449	84.3845895	-0.9796319	0.08196595	-0.2217672	0.83274918	0.75786474	0.26416616
NA	ENSG00000178464	100.086078	-0.8096611	0.09561657	-0.2460753	0.75657158	0.56358581	0.38022778
SLC25A20	ENSG00000178537	18.8703935	-1.4509466	0.16816206	-1.5569959	0.09530548	-0.1060492	0.97285336
ZNF664	ENSG00000179195	211.484219	-0.8071092	0.01263451	-0.5039059	0.17994669	0.30320333	0.64750848
CITED4	ENSG00000179862	77.3630209	-0.7258974	0.22072573	0.23628112	0.78414324	0.96217851	0.04442567
ABCA13	ENSG00000179869	14.7469721	-2.0238113	0.07587517	-1.0168044	0.44541831	1.00700691	0.62067667
OAZ2	ENSG00000180304	104.89574	-0.6319351	0.22025768	-0.4423021	0.41674084	0.18963307	0.87707677
ZNF609	ENSG00000180357	32.4855537	-1.3559561	0.11522083	-0.3814895	0.78289633	0.97446656	0.38332596
H2AC6	ENSG00000180573	138.935296	-0.5461345	0.20593357	-0.8495995	0.00807067	-0.303465	0.67684408
H2BC4	ENSG00000180596	34.8382726	-1.3162516	0.09238505	-0.7395024	0.42269127	0.5767492	0.7025717
SSR4	ENSG00000180879	541.396272	-0.5028495	0.07303099	0.23219564	0.53989333	0.73504511	0.0013097
D2HGDH	ENSG00000180902	45.6024813	-0.8176379	0.28336416	-0.8248408	0.20769114	-0.007203	0.99605451
TCEAL8	ENSG00000180964	49.1459565	-0.8290282	0.26128436	-0.078746	0.95109975	0.7502822	0.34492043
PJA1	ENSG00000181191	16.6401894	-1.3598608	0.31364173	-0.1405481	0.94851731	1.2193127	0.40683096
RNF135	ENSG00000181481	35.9900963	-1.0307552	0.18432443	-0.272919	0.83065668	0.7578362	0.45162911
YIPF6	ENSG00000181704	112.887746	-0.624199	0.21379488	0.3346776	0.5636816	0.95887663	0.01050384
C16orf72	ENSG00000182831	64.9320853	-0.9122419	0.11999697	-0.5709732	0.38998169	0.3412687	0.78457814
CADM1	ENSG00000182985	32.5538554	-1.0475008	0.2986901	-1.2257317	0.13012388	-0.1782309	0.94616617
CALN1	ENSG00000183166	5.49058148	-6.2715266	0.01080569	-4.6895945	0.06777561	1.58193218	0.868138
EP400	ENSG00000183495	24.864883	-1.0608602	0.27753524	-0.7524424	0.44482748	0.30841774	0.89471532
COA5	ENSG00000183513	80.0915239	-0.6256487	0.29270035	-0.4272845	0.49327431	0.19836417	0.88365775
NDUFB1	ENSG00000183648	297.263732	-0.550824	0.32665469	-0.473865	0.35998185	0.07695899	0.95066459
ZNF703	ENSG00000183779	145.523465	-1.994713	2.6189E-12	-0.6996238	0.03667886	1.29508925	6.4618E-05
FAM3B	ENSG00000183844	27.1766947	-2.2294774	0.00191984	-1.2172591	0.12240956	1.01221831	0.43415231
ACOT1	ENSG00000184227	46.2217772	-0.9574695	0.18916218	-0.70415	0.35296022	0.25331951	0.89438578
NCMAP	ENSG00000184454	12.4250369	-2.8480017	0.02849242	-0.3339332	0.88500456	2.5140685	0.07533879
H2BC21	ENSG00000184678	144.055921	-1.2033882	0.00017363	-0.4696556	0.2990986	0.73373269	0.07647126
ARMCX2	ENSG00000184867	91.2581954	-2.4462602	6.7272E-10	-0.8281935	0.07876633	1.61806674	0.00037597
RBM43	ENSG00000184898	9.47398787	-2.3309698	0.12958965	-0.6733194	0.74475025	1.65765036	0.42400794
SIGIRR	ENSG00000185187	27.9988279	-1.1671293	0.24292734	0.14570726	0.93187171	1.31283652	0.14275187
TNFAIP2	ENSG00000185215	10.5758073	-2.1342703	0.14358269	-0.4880016	0.82664243	1.64626864	0.36893325
SP140L	ENSG00000185404	31.9070019	-1.3010734	0.09265901	-0.5173992	0.63130841	0.78367415	0.50528507
ZBTB3	ENSG00000185670	9.90108627	-1.586057	0.33004782	-1.3357075	0.37020949	0.25034953	0.95014208
BCAP31	ENSG00000185825	681.85542	-0.3145238	0.33067369	-0.0530065	0.92087795	0.26151723	0.47475653
LINC00839	ENSG00000185904	16.9075458	-2.0102019	0.04208865	-2.316913	0.01242377	-0.3064893	0.93047906
ZBTB6	ENSG00000186130	24.6559894	-1.0886683	0.32508665	0.13283463	0.94006741	1.22150289	0.21656388
NAP1L2	ENSG00000186462	13.9052806	-2.3270148	0.07933502	-0.1431333	0.95109975	2.18388148	0.11463493
SMIM29	ENSG00000186577	101.962458	-0.7857098	0.08110417	-1.9456137	2.9321E-08	-1.1599039	0.00756346
HEXIM1	ENSG00000186834	21.9524609	-1.1337876	0.29919378	-0.9234542	0.37318345	0.21033342	0.94053638
ENTPD5	ENSG00000187097	16.9319559	-1.5603015	0.14944954	-1.9879871	0.03079647	-0.4276856	0.89238219
TAF9B	ENSG00000187325	54.8665723	-0.8310279	0.19646523	-0.3348426	0.70879251	0.49618522	0.61418166
H1-2	ENSG00000187837	371.347315	-0.8646723	0.00997407	-0.5964358	0.10837024	0.26823649	0.72883745
C6orf132	ENSG00000188112	84.7901342	-0.7846285	0.11412056	-0.6327027	0.20277458	0.15192579	0.91259955
AGRN	ENSG00000188157	45.2226465	-0.9593153	0.14754448	-1.0317489	0.07598456	-0.0724336	0.9695841
NBR1	ENSG00000188554	92.0530709	-0.7254743	0.14600609	-0.8390596	0.04648975	-0.1135852	0.93818914
ZDHHC9	ENSG00000188706	99.4280146	-0.7548733	0.14600609	-0.4034387	0.52980472	0.35143458	0.70665224
SYCP2	ENSG00000196074	386.85366	-0.5919186	0.06402764	-0.1866927	0.72390469	0.40522593	0.33248824
HLA-DRB1	ENSG00000196126	7.71624973	-2.2230769	0.31563831	0.40364834	0.88580864	2.62672522	0.16314302
ACADSB	ENSG00000196177	30.8091577	-1.2131693	0.15378417	-1.4376718	0.04690506	-0.2245024	0.92672475
ASB13	ENSG00000196372	93.1381426	-0.8029671	0.06554076	-0.7957242	0.04891244	0.00724288	0.99605451
ARMCX4	ENSG00000196440	5.0783451	-4.99169	0.09810853	-0.0163146	0.99648336	4.97537537	0.0951528
TCEAL3	ENSG00000196507	101.952152	-1.5962712	3.6106E-05	-1.9866423	1.4044E-07	-0.3903711	0.72069155
COL27A1	ENSG00000196739	7.9216051	-2.3203529	0.17916307	-1.9831927	0.22023293	0.33716013	0.94773579
MAML3	ENSG00000196782	14.6610934	-1.6563233	0.14000077	-1.7032319	0.09169467	-0.0469086	0.98879888
KIAA1211L	ENSG00000196872	37.5687422	-0.942603	0.24929431	0.22668533	0.85816103	1.16928831	0.08508871
SLC39A10	ENSG00000196950	29.6308859	-1.0484621	0.29929102	0.0954117	0.95333489	1.14387383	0.21739748
CXorf40B	ENSG00000197021	91.7632283	-0.7494654	0.13753188	0.09936297	0.91710116	0.84882839	0.06394869
CH17-340M24.3	ENSG00000197180	38.3033455	-1.066098	0.17650108	-0.5232583	0.6011855	0.54283971	0.69123044
C6orf141	ENSG00000197261	9.99823784	-2.415281	0.2045438	1.01784526	0.5551927	3.43312627	0.01809605
ZNF720	ENSG00000197302	27.4080739	-1.159563	0.18989371	-0.5675063	0.608116	0.59205671	0.70231128
ZNF786	ENSG00000197362	9.72423602	-1.9572812	0.29300907	-0.5624127	0.82663222	1.39486854	0.57505875
CXorf40A	ENSG00000197620	32.1348107	-1.1582631	0.17788402	0.2636895	0.85058145	1.42195263	0.05387177
MPZL1	ENSG00000197965	116.147233	-0.5799361	0.28253418	-0.2514153	0.72182435	0.32852083	0.69227017
RPS4X	ENSG00000198034	3011.44698	-0.5085187	0.00517559	-0.253704	0.29247296	0.2548147	0.37203226
SLC29A3	ENSG00000198246	56.7861776	-1.5543302	0.00888492	-0.0676158	0.96277338	1.48671443	0.01459007
HELZ	ENSG00000198265	82.7894639	-0.7034705	0.23185674	-0.5729529	0.3178904	0.13051762	0.93047906
STK39	ENSG00000198648	161.044214	-1.4425558	5.0376E-06	-1.4954085	1.461E-06	-0.0528527	0.96823437
ABCA4	ENSG00000198691	10.6721093	-1.9038833	0.22847079	-0.2461445	0.92192673	1.65773885	0.35232701
CDC42BPB	ENSG00000198752	39.8648085	-0.8511348	0.2986901	-0.2693617	0.82580964	0.58177315	0.60214436
PRMT6	ENSG00000198890	35.2945485	-0.9625326	0.2672216	-0.301905	0.81764563	0.66062763	0.57224856
SHISA4	ENSG00000198892	21.4079807	-1.3160277	0.19710351	-0.495671	0.72349582	0.82035669	0.59036645
CIPC	ENSG00000198894	16.9669029	-1.2125837	0.34363041	-0.6447953	0.65708842	0.56778845	0.80047664
RPL39	ENSG00000198918	119.139492	-0.6637131	0.32035886	-0.1905719	0.8531263	0.47314111	0.5817645
ARMCX6	ENSG00000198960	88.2652192	-2.1249347	7.7531E-10	-1.528431	9.3368E-06	0.59650369	0.40284962
PCMTD2	ENSG00000203880	140.700455	-0.6007327	0.15430218	-0.7504455	0.02867131	-0.1497128	0.89471532
RTL8A	ENSG00000203950	97.9110158	-0.8051905	0.07528244	-0.1266652	0.88710885	0.67852533	0.1805816
NA	ENSG00000204072	27.9019804	-1.9061272	0.00956092	-1.0154125	0.23637764	0.89071464	0.50304628
MACO1	ENSG00000204178	42.2570628	-0.836657	0.31340637	-1.0351227	0.11081096	-0.1984657	0.92174256
BMPR2	ENSG00000204217	69.2212071	-1.4105332	0.00179028	-0.2928672	0.73090605	1.11766601	0.02909055
TRIM27	ENSG00000204713	103.748934	-0.6543148	0.15533927	-0.8727942	0.01785148	-0.2184793	0.84587155
TECPR1	ENSG00000205356	15.3436593	-1.5889923	0.17782765	-0.3334222	0.86289107	1.25557001	0.38644414
NA	ENSG00000207422	135.72828	-4.5965001	4.2672E-20	0.4825667	0.27260953	5.07906681	7.0196E-25
RTL8B	ENSG00000212747	27.9928683	-1.0354205	0.31487409	0.27184015	0.85653791	1.30726069	0.12128364
NA	ENSG00000213280	91.7785111	-0.7904057	0.1446208	-0.7349559	0.14208999	0.05544979	0.97105871
PPP1CB	ENSG00000213639	323.247687	-0.4831001	0.20593357	-0.0221642	0.97666012	0.4609359	0.24075617
FIS1	ENSG00000214253	104.961831	-0.5402097	0.34350779	0.00852415	0.99306973	0.54873385	0.3235999
STARD10	ENSG00000214530	1201.88731	-0.3939211	0.11573011	-0.0406751	0.93689006	0.35324596	0.18206512
ZSWIM8	ENSG00000214655	7.69216592	-1.9789554	0.31340637	-1.0428416	0.61884846	0.93611381	0.79533463
GAGE4	ENSG00000215269	18.4105516	-4.6657264	0.00015222	-2.5210607	0.00473859	2.14466576	0.31540646
NA	ENSG00000223749	13.0944339	-2.6086278	0.05405026	-0.472809	0.82954393	2.1358188	0.17315093
NA	ENSG00000223808	168.930321	-1.3147241	9.2073E-06	-0.0563349	0.94463946	1.25838918	3.2914E-05
NA	ENSG00000224631	1082.12084	-0.4396138	0.15324671	-0.2937826	0.3883494	0.14583119	0.83161875
GAGE2E	ENSG00000224659	85.1043545	-0.7316058	0.19088935	-0.059137	0.95444364	0.67246879	0.26091326
NA	ENSG00000225770	54.0579037	-0.8874547	0.24500244	-0.3326664	0.75468504	0.55478831	0.61428176
FTCDNL1	ENSG00000226124	27.1865592	-1.1184999	0.2300135	-0.9407293	0.28869542	0.17777058	0.94448359
TMEM185B	ENSG00000226479	43.5395347	-1.0276594	0.17497849	0.22260029	0.86178341	1.25025968	0.05634909
LINC01918	ENSG00000226508	35.8445781	-3.0284466	7.6666E-07	-1.8584582	0.00114098	1.16998833	0.29127526
NA	ENSG00000226976	371.176468	-0.4788057	0.3329121	-0.254444	0.66342198	0.22436167	0.7925113
OST4	ENSG00000228474	23.6302062	-1.2274185	0.33180908	0.04309153	0.98308128	1.18350323	0.36181627
NA	ENSG00000229014	26.5668702	-1.1480313	0.24843481	-0.767691	0.46005802	0.38034029	0.86844435
NA	ENSG00000229119	471.612665	-0.564306	0.17916307	-0.2001097	0.75413429	0.36419634	0.53761591
NA	ENSG00000231767	95.5695558	-1.0188028	0.04992715	-0.7543906	0.16975591	0.26441217	0.85303958
NA	ENSG00000231940	89.9457743	-0.9453397	0.05041378	-0.4098236	0.54429087	0.53551611	0.47075401
LOC101928380	ENSG00000231963	3.85311559	-5.5995027	NA	-5.4426787	0.03643365	0	1
TMEM238	ENSG00000233493	161.290593	-0.518658	0.31957879	0.14650881	0.85396862	0.66516678	0.11739738
NA	ENSG00000233913	781.800229	-0.6491015	0.00102146	-0.1595123	0.66950589	0.48958921	0.02992504
PAGE2	ENSG00000234068	348.638726	-11.326579	2.271E-12	0.15942871	0.82580964	11.4860073	8.5601E-13
HLA-B	ENSG00000234745	30.1871128	-1.1751208	0.20593357	-0.8569744	0.36990497	0.31814645	0.89471532
LOC105373958	ENSG00000234949	27.2590175	-1.3280055	0.11862796	-0.5737155	0.61175614	0.75428995	0.57896788
C19orf81	ENSG00000235034	39.9609533	-0.9254776	0.31244612	-0.1704897	0.90627909	0.7549879	0.47991162
NA	ENSG00000235174	964.072386	-0.9729039	0.07915207	-0.1580119	0.88725664	0.81489205	0.18473726
NA	ENSG00000235552	1591.69018	-0.409554	0.0917754	-0.2397784	0.41225313	0.16977565	0.71315732
GAGE2C	ENSG00000236362	18.1471774	-4.2401697	0.000108	-2.8918271	0.00108097	1.34834263	0.61523477
ZNF737	ENSG00000237440	6.86697111	-2.2754781	0.27523243	-1.6048508	0.414497	0.67062728	0.89659908
SHISA9	ENSG00000237515	10.8028953	-1.7565211	0.2696924	-1.9317845	0.15944659	-0.1752634	0.96846322
FAM200B	ENSG00000237765	24.2812162	-1.0772438	0.30032929	-0.0612605	0.97101953	1.01598321	0.35218734
NA	ENSG00000238178	12.5784325	-2.6801215	0.03117259	-0.6178966	0.7269322	2.06222491	0.17441159
SMKR1	ENSG00000240204	17.3349817	-1.488939	0.24406176	-0.6516422	0.68315093	0.83729684	0.68232797
NA	ENSG00000242375	8.29583762	-1.783594	0.33331949	-0.6775555	0.76497256	1.10603853	0.68854669
NA	ENSG00000243829	9.09440919	-1.6712612	0.33502385	-0.9390989	0.61939256	0.73216226	0.82548086
NA	ENSG00000244398	1306.81265	-0.9117292	0.00067298	-0.0937211	0.88957628	0.81800807	0.00356149
NA	ENSG00000244468	1934.36798	-1.1624906	4.9033E-08	-2.5235893	1.8953E-37	-1.3610987	1.7674E-10
H2AJ	ENSG00000246705	720.811349	-0.869506	9.072E-05	-0.4585654	0.0963788	0.41465067	0.20910982
NA	ENSG00000253170	14.8051194	-7.3985998	0.00010869	-7.2417757	0.00010577	0	1
LINC01606	ENSG00000253301	9.03176523	-1.6519828	0.33616864	-1.2003659	0.4681399	0.45161686	0.91149121
NA	ENSG00000253395	14.5095658	-1.5962918	0.22657388	-0.4931578	0.79152017	1.10313399	0.54368309
BRK1	ENSG00000254999	552.396396	-0.3832899	0.19699773	-0.2194266	0.53838548	0.16386336	0.7670282
SNHG9	ENSG00000255198	64.2003952	-1.39175	0.02589352	-0.7494097	0.33392009	0.64234028	0.56792518
EID1	ENSG00000255302	164.173748	-0.7123187	0.04471356	0.24705552	0.64951276	0.95937425	0.00158993
ZNF350	ENSG00000256683	36.2927402	-1.1608101	0.11802888	-1.1730897	0.08094164	-0.0122796	0.99605451
MIR200CHG	ENSG00000257084	10.4705702	-2.0581929	0.14164692	-2.7861654	0.03071932	-0.7279724	0.86418864
NORAD	ENSG00000260032	299.32635	-0.6604539	0.06190607	-0.4901529	0.1918599	0.17030097	0.85737085
NA	ENSG00000260401	32.7464518	-0.9833581	0.28999311	-0.8548838	0.31870811	0.12847431	0.95467848
NA	ENSG00000261538	10.3755346	-3.8279659	0.01330831	-6.7360132	0.00082851	-2.9080473	0.49402927
NA	ENSG00000263266	913.414679	-0.4815338	0.12417396	-0.2350551	0.57011666	0.24647868	0.62962208
SRSF8	ENSG00000263465	77.7012486	-0.8707493	0.07587517	-0.4566483	0.45493453	0.41410104	0.63682236
SNHG25	ENSG00000266402	25.9456733	-1.2730767	0.15992502	-0.8874376	0.35586635	0.38563916	0.86736333
NBPF12	ENSG00000268043	53.365327	-1.7552151	0.00024077	-1.6851098	0.00037766	0.07010524	0.97176739
TMEM185A	ENSG00000269556	30.5031337	-1.4371977	0.071117	-1.3222476	0.07987742	0.11495007	0.96221695
SLC25A53	ENSG00000269743	12.3668787	-1.4568777	0.34363041	-1.0011663	0.51137662	0.45571139	0.89556348
H4C14	ENSG00000270882	64.639819	-0.7886574	0.19208528	0.27201882	0.75232656	1.06067622	0.03016683
H2AC19	ENSG00000272196	165.935929	-0.513902	0.27984935	-0.6345347	0.08416124	-0.1206327	0.91450227

NA	ENSG00000273015	29.5212338	-0.9834921	0.3161415	-1.1014208	0.17021434	-0.1179287	0.96026088
H2BC8	ENSG00000273802	77.3183286	-1.1183623	0.01359907	-0.3919065	0.57351351	0.72645585	0.23804036
PPP4R3B	ENSG00000275052	81.9031608	-0.7253492	0.20759954	-0.4386339	0.50698973	0.28671535	0.80097497
NA	ENSG00000276900	16.3749445	-4.2160509	0.0001805	-1.3448198	0.18013743	2.87123111	0.0391088
H3C10	ENSG00000278828	27.7043104	-1.6207446	0.03722983	-0.6067102	0.57588562	1.01403441	0.37444577
NA	ENSG00000279864	5.03949771	-4.9016572	NA	0.60112143	0.85693316	5.50277864	0.02849703
NA	ENSG00000280614	546.640509	-1.4417702	1.1157E-08	-1.3889591	2.7644E-08	0.05281108	0.95911967
NA	ENSG00000280800	541.599221	-1.3982399	3.7E-08	-1.2317092	1.3683E-06	0.16653072	0.85737085
NA	ENSG00000281181	354.405538	-1.5269917	1.3309E-10	-1.4623278	6.6199E-10	0.06466391	0.95014208
NA	ENSG00000281383	47.09006	-1.6493658	0.0015168	-1.7031346	0.00077926	-0.0537688	0.97924732
NA	ENSG00000283041	298.344526	-0.6633436	0.04845459	-0.5211179	0.13282809	0.14222569	0.88703955
NA	ENSG00000283342	21.5211808	-2.0332735	0.01618305	-1.5068389	0.07876633	0.52643468	0.83317008
LINC02780	ENSG00000284668	7.01248148	-3.2890491	0.1468149	0.00575904	0.99844549	3.29480817	0.14203954
NA	ENSG00000285822	6.56506949	-3.1462979	0.17619083	0.26890504	0.93241743	3.41520298	0.11424352

Cluster 4

	ensembl	baseMean	TvsC log2FoldChange	padj	RvsC log2FoldChange	padj	RvsT log2FoldChange	padj
AOC1	ENSG00000002726	14.7218475	-3.459225	0.31818308	4.83601098	1.0398E-05	8.29523593	9.0138E-06
CYP26B1	ENSG00000003137	4.22548925	0	NA	6.57135902	0.0061709	6.57625762	0.00913181
TFPI	ENSG00000003436	6.14174474	-0.0350114	1	3.8265142	0.01737033	3.86152561	0.02492979
FKBP4	ENSG00000004478	123.94521	0.83875186	0.11005221	1.47561864	8.8048E-05	0.63686678	0.27683104
SLC25A5	ENSG00000005022	303.167181	0.19843653	0.8394187	1.4329113	1.3477E-07	1.23447477	1.6183E-05
PRKAR2B	ENSG00000005249	63.1766595	-0.8922423	0.15468432	0.69732689	0.21484279	1.58956924	0.00037597
CROT	ENSG00000005469	48.6230413	-0.2483329	0.89689383	1.52848827	0.00228659	1.77682115	0.00046375
YBX2	ENSG00000006047	16.3308161	1.54138812	0.25944338	2.715489	0.00171606	1.17410088	0.31993207
CX3CL1	ENSG00000006210	13.3551799	0.30938787	0.95888715	4.31585687	6.8022E-05	4.006469	0.00017418
TNFRSF12A	ENSG00000006327	107.304173	0.17262228	0.89108484	0.95274656	0.00894659	0.78012428	0.0654987
DBF4	ENSG00000006634	43.5423083	1.15576229	0.0626833	1.19745373	0.03227668	0.04169143	0.98094919
IFRD1	ENSG00000006652	48.2243156	0.85614638	0.23185674	1.44744593	0.00254628	0.59129955	0.46880331
SCIN	ENSG00000006747	6.79514596	-0.9659608	0.91626226	4.76836426	0.0066045	5.73432504	0.01187589
CCDC124	ENSG00000007080	165.184121	0.83847295	0.00755718	0.99005219	0.00037981	0.16057924	0.8617399
NCAPD2	ENSG00000010292	63.9039534	0.92102406	0.16240849	1.90735495	1.0398E-05	0.98633089	0.06836994
PLAUR	ENSG00000011422	9.91194656	-2.1874051	0.27059838	1.05858083	0.51286505	3.24598592	0.02292808
ANLN	ENSG00000011426	44.373674	2.45623064	2.4287E-05	2.86085678	1.4914E-07	0.40462614	0.74539466
ELOVL5	ENSG00000012660	168.133525	0.14143281	0.90091853	1.2488584	9.1467E-06	1.10742559	0.00019838
POLA2	ENSG00000014138	11.5262635	2.0911662	0.24680442	3.11944066	0.01136897	1.02827446	0.59351661
RNH1	ENSG00000023191	89.8430794	-0.5299456	0.41988147	0.40542679	0.48951822	0.93537242	0.02619524
STRAP	ENSG00000023734	219.514011	0.16298522	0.85096308	0.85473716	0.00124655	0.69175194	0.02061901
DEPDC1	ENSG00000024526	12.1679316	2.69115415	0.05437427	2.83267004	0.02358386	0.14151589	0.96374605
RAI14	ENSG00000039560	26.8152428	1.82049903	0.06396992	3.3884973	1.4039E-06	1.5679983	0.03926868
ZIC2	ENSG00000043355	6.8126076	3.12325985	0.21559027	4.12349466	0.02764947	1.00023481	0.73876325
ADRB1	ENSG00000043591	4.79653601	0.0191779	NA	5.24900267	0.03010078	5.22982477	0.04284945
OFD1	ENSG00000046651	90.1427032	-0.2694575	0.84030073	1.15788311	0.00488504	1.42734064	0.00044627
GPM6B	ENSG00000046653	6.08850074	0.00532135	1	4.4667952	0.01554806	4.46147384	0.02281102
WWC3	ENSG00000047644	113.339128	-0.1998801	0.87737913	1.76208827	2.9511E-08	1.96196836	1.0806E-09
USP28	ENSG00000048028	25.8181183	-0.8588297	0.47540839	0.62846466	0.53261467	1.4872944	0.04859807
MAPK9	ENSG00000050748	131.249524	0.29173399	0.72704207	0.84780874	0.01477129	0.55607475	0.24216871
POLQ	ENSG00000051341	8.20807967	3.99318979	0.15209255	4.54970596	0.04704086	0.55651618	0.87788333
CYBA	ENSG00000051523	80.0320161	-1.6147101	0.01391117	3.07760519	1.4019E-16	4.69231528	3.2968E-24
FOXC1	ENSG00000054598	3.2407552	-3.4166695	NA	2.22450864	0.42504676	5.64117817	0.04650241
IL17RB	ENSG00000056736	12.1608688	-0.7682783	0.82659334	2.2759535	0.03437999	3.04423185	0.0069163
TRAF3IP2	ENSG00000056972	37.2059348	0.53936484	0.69151274	1.55285409	0.00531907	1.01348925	0.14969946
ATP11B	ENSG00000058063	7.23282868	-0.0340839	1	4.66199998	0.00680269	4.69608384	0.00997827
WNK1	ENSG00000060237	445.265712	0.38400372	0.37132932	0.66865821	0.01316229	0.28465449	0.58184529
ISOC2	ENSG00000063241	139.208322	0.18248701	0.87293553	0.87505986	0.0120464	0.69257285	0.09770869
CASP8	ENSG00000064012	41.2833103	-0.9671023	0.23947982	0.69393172	0.35188603	1.661034	0.0033522
INTS13	ENSG00000064102	34.843393	0.10530883	0.96803715	1.28963307	0.03557463	1.18432424	0.08540317
SUGP2	ENSG00000064607	56.9980552	0.83348155	0.18267821	0.71573956	0.24182069	-0.117742	0.94322045
MCM10	ENSG00000065328	33.7406579	2.49910147	0.00317619	3.52697131	1.0772E-06	1.02786984	0.27874874
KARS1	ENSG00000065427	217.7409	0.48575454	0.26063638	0.70376278	0.02142135	0.21800824	0.76677947
FAM107B	ENSG00000065809	40.5940764	0.85495709	0.39750545	2.5496696	3.6917E-07	1.6947125	0.0013097
SLC9A7	ENSG00000065923	35.8459859	-0.5818363	0.67301174	0.99748311	0.13927887	1.57931946	0.01041217
YBX1	ENSG00000065978	1315.0864	-0.1271228	0.82767858	0.67768276	0.00013567	0.80480554	4.3723E-06
MPPED2	ENSG00000066382	8.31153584	-1.4533927	0.87587059	6.07583196	0.00350099	7.52922462	0.00025793
FGFR2	ENSG00000066468	17.0790854	0.84476863	0.66417964	1.83886938	0.0457787	0.99410075	0.48209244
ATP11A	ENSG00000068650	12.0076903	1.98822514	0.18793682	2.38929247	0.04648975	0.40106732	0.90153216
MAST4	ENSG00000069020	32.6798524	0.63759896	0.64696966	1.96106049	0.00061109	1.32346152	0.04442567
SDK2	ENSG00000069188	3.73189424	-3.4180364	NA	2.69312371	0.24694273	6.11116008	0.01874971
NUCKS1	ENSG00000069275	1170.25064	0.55461606	0.02680389	0.67868644	0.00180175	0.12407038	0.86251002
GAL	ENSG00000069482	13.2100799	-1.0153025	0.90521693	5.62035776	7.4238E-05	6.63566024	0.00064327
PFN2	ENSG00000070087	31.975765	-0.1225023	0.96334195	1.30734476	0.03601966	1.42984703	0.02786904
TCOF1	ENSG00000070814	44.7935701	0.65625354	0.49906356	1.52357222	0.0022009	0.86731869	0.1924224
EPHA8	ENSG00000070886	8.69455467	-1.4398586	0.8765924	6.11672835	0.00295569	7.55658692	0.00020587
MAP4K4	ENSG00000071054	90.3361751	-0.3118141	0.77334529	1.00520466	0.0107498	1.31701877	0.00060264
MGAT4A	ENSG00000071073	162.887591	-0.5455299	0.46146547	1.454945	6.3657E-05	2.00047485	1.6589E-08
LMCD1	ENSG00000071282	66.2519458	0.20551846	0.89102893	1.01440311	0.02444584	0.80888465	0.1405485
TCF3	ENSG00000071564	104.141596	0.45530992	0.52441077	0.87435409	0.02816251	0.41904418	0.55059913
DAZAP1	ENSG00000071626	152.974782	0.82780036	0.02539684	1.1546116	0.00017146	0.32681124	0.62067667
HLTF	ENSG00000071794	90.8249247	0.59858457	0.33004782	0.67411795	0.16461192	0.07553338	0.95519804
FAM3A	ENSG00000071889	37.6686859	-0.8554294	0.38070373	0.52915668	0.57351351	1.3845819	0.0359151
ACTN1	ENSG00000072110	86.7561966	0.30199493	0.77799374	1.63479861	1.1703E-06	1.33280369	0.00017648
ACTB	ENSG00000075624	3271.51694	0.43149238	0.0427922	0.60110672	0.00057901	0.16961433	0.68256483
WDR62	ENSG00000075702	31.8818573	3.41620364	0.0546783	3.61846088	0.02245315	0.20225724	0.96740542
MCM6	ENSG00000076003	111.447091	1.64223922	5.0167E-06	2.17916462	3.9756E-11	0.5369254	0.31799885
SLC25A43	ENSG00000077713	85.6400616	0.36116192	0.7737783	1.30240988	0.00454097	0.94124796	0.09324931
TNS1	ENSG00000079308	30.9494878	-0.6978618	0.63133745	1.17621052	0.10626197	1.87407229	0.00539321
OPHN1	ENSG00000079482	11.7316232	-2.6910127	0.15868117	1.4589621	0.27029117	4.14997478	0.00352707
HSP90AA1	ENSG00000080824	2451.43301	0.42230341	0.04012212	0.68759739	2.5822E-05	0.26529398	0.35144926
NDC80	ENSG00000080986	15.4220897	3.86297169	0.00386341	3.99827777	0.00156554	0.13530608	0.9610645
STK17B	ENSG00000081320	15.8585087	1.54707795	0.17839767	1.46208715	0.16743781	-0.0849908	0.97468421
PGR	ENSG00000082175	7.09679774	0	1	7.32181667	0.00036824	7.32671467	0.00059523
ITGB5	ENSG00000082781	162.424226	-0.2390548	0.76831582	0.90340161	0.00168527	1.14245642	4.9807E-05
TNPO1	ENSG00000083312	129.655749	0.18556167	0.889753	0.93994682	0.01891009	0.75438515	0.11985756
STARD7	ENSG00000084090	264.989015	-0.2127686	0.7691854	0.4912249	0.13012388	0.70399349	0.01698405
NKAIN1	ENSG00000084628	45.2160722	1.0404996	0.15468432	1.22061037	0.04149735	0.18011077	0.92174256
MAPRE3	ENSG00000084764	129.377106	-0.2437088	0.81604182	1.35168391	7.3812E-06	1.59539266	1.2279E-07
TTC39A	ENSG00000085831	246.250595	-0.4330549	0.32966531	1.23668593	1.2129E-07	1.66974079	4.9672E-13
EPDR1	ENSG00000086289	62.1762766	0.8382587	0.23670667	2.41505625	1.576E-09	1.57679755	0.00015413
SEPHS1	ENSG00000086475	190.723893	0.14208845	0.88240255	0.66912292	0.02577362	0.52703446	0.15500507
SULT2B1	ENSG00000088002	32.2013563	0.93236375	0.3407496	1.69916308	0.00446883	0.76679933	0.4155594
FUS	ENSG00000089280	151.561113	0.38553115	0.5774665	0.92750213	0.0061709	0.54197098	0.26510835
BIRC5	ENSG00000089685	299.725312	2.97950495	7.4451E-34	3.29227072	2.0193E-42	0.31276577	0.47492913
MLF2	ENSG00000089693	296.054304	0.44747574	0.25023561	0.38853278	0.28723341	-0.058943	0.95014208
KIF4A	ENSG00000090889	32.5582908	2.15194179	0.00522218	2.9195973	9.5574E-06	0.76765071	0.46179135
CMTM6	ENSG00000091317	68.7868377	-0.3479386	0.75510365	0.66129997	0.21756089	1.00923857	0.03492402
MAP3K20	ENSG00000091436	73.6962883	0.55326913	0.46959984	0.92047776	0.0463275	0.36720863	0.69594025
CDV3	ENSG00000091527	625.669724	0.27122859	0.51273705	0.85508969	1.6827E-05	0.5838611	0.01215494
ORC6	ENSG00000091651	86.3536525	2.77904918	4.7497E-11	2.94440733	1.1174E-12	0.16535815	0.90495794
CLSPN	ENSG00000092853	10.7163472	2.38691718	0.09846021	2.74425252	0.02295246	0.35733535	0.91149121
CDC45	ENSG00000093009	16.0060214	4.58368416	0.00246801	4.67817144	0.00121864	0.09448728	0.97285336
MSH2	ENSG00000095002	77.9759492	0.3878061	0.68578015	1.17220233	0.00283164	0.78439623	0.11113099
EPB41L4B	ENSG00000095203	36.8991673	0.95637089	0.22657388	0.97503168	0.15289248	0.01866078	0.99256964
TMEM38B	ENSG00000095209	48.1615615	1.90521927	0.00052218	2.10795215	2.8212E-05	0.20244263	0.90520171
FKBP5	ENSG00000096060	27.4390421	1.09765096	0.2696924	1.69152578	0.01164561	0.59387482	0.64673696
SRPK1	ENSG00000096063	58.1009857	0.50750388	0.64689406	1.08153532	0.04621934	0.57403144	0.52495058
ACOT7	ENSG00000097021	64.1591558	1.28227512	0.0065967	1.5651568	0.00018388	0.28288169	0.7994437
SYDE2	ENSG00000097096	17.1083926	1.05501599	0.52573107	1.86372097	0.047303	0.80870499	0.62177404
KCNK6	ENSG00000099337	132.643182	-0.8386767	0.04117204	0.78389707	0.02788576	1.62257382	1.766E-07
HNRNPM	ENSG00000099783	161.685069	0.47948208	0.33226503	0.57590133	0.12763041	0.09641926	0.93047906
RASSF7	ENSG00000099849	47.4535015	-0.6732659	0.47605109	0.82479394	0.16780116	1.49805984	0.00384625
SNRPD3	ENSG00000100028	301.50327	0.74665876	0.00362969	0.72658605	0.00353246	-0.0200727	0.98208854
MYH9	ENSG00000100345	195.172899	0.54774992	0.17839767	0.35000952	0.45415196	-0.1977404	0.81017969
POLE2	ENSG00000100479	23.7677683	1.84004657	0.0363099	2.40386061	0.00096052	0.56381404	0.70331151
PYGL	ENSG00000100504	116.145608	-0.7846704	0.07871309	0.54191612	0.23047002	1.32658648	0.00010232
CDKN3	ENSG00000100526	169.761308	2.90528056	1.1532E-21	3.40297418	1.4377E-30	0.49769362	0.20892389
PSMA3	ENSG00000100567	386.270632	0.24467773	0.62587441	0.61316679	0.00963878	0.36848905	0.28751945
RIN3	ENSG00000100599	3.7624691	-4.2251469	NA	1.66008029	0.52787929	5.88522724	0.02369734
CHGA	ENSG00000100604	6.76608109	-2.3473413	0.62650063	2.91254352	0.05092871	5.25988479	0.02447412
ITPK1	ENSG00000100605	139.972304	-0.1605386	0.88731859	1.36555663	9.5174E-07	1.52609525	5.3379E-08
PPM1A	ENSG00000100614	123.276321	-0.4604497	0.47605109	1.11823681	0.00039212	1.57868655	2.6841E-07
ERH	ENSG00000100632	229.191483	-0.1983412	0.82596593	0.49005612	0.1886727	0.6883973	0.0438152
VRK1	ENSG00000100749	49.2365615	0.39793195	0.78578133	1.15111542	0.04448475	0.75318347	0.3546615
YY1	ENSG00000100811	318.672057	-0.0037139	1	0.60928675	0.01586989	0.61300068	0.02222851
DHRS2	ENSG00000100867	103.3036	-0.4536132	0.57984612	1.42021388	2.9221E-05	1.87382708	3.169E-08
MYBL2	ENSG00000101057	190.855193	1.72522036	4.2643E-08	2.26274222	1.9008E-14	0.53752186	0.25848485
CDC25B	ENSG00000101224	22.1254621	2.15618147	0.01391117	2.26862129	0.00531907	0.11243982	0.96184081
MYL9	ENSG00000101335	22.0599572	-1.0967063	0.49312673	1.78017373	0.02247977	2.87687999	0.00028237
CST3	ENSG00000101439	335.342587	-0.4592531	0.22132487	0.35236413	0.33816238	0.81161727	0.00208625
FAM83D	ENSG00000101447	26.1372437	2.53432494	0.00404796	3.34370034	1.1547E-05	0.8093754	0.46264383
RBBP8	ENSG00000101773	30.4721929	1.45397868	0.12552881	3.40942699	1.3034E-08	1.95544831	0.00061766
PGRMC1	ENSG00000101856	234.243362	-0.445101	0.43797222	0.91869297	0.00356966	1.36379402	4.0329E-06
ATP11C	ENSG00000101974	19.7973304	-0.6218071	0.78621972	1.76232248	0.02295246	2.38412957	0.00259179
FMR1	ENSG00000102081	84.4756037	-0.2666243	0.8257516	0.66598077	0.16531254	0.93260505	0.03685917
PGK1	ENSG00000102144	798.041089	-0.4739806	0.05115504	0.21290025	0.528075	0.68688082	0.00069068
CDK16	ENSG00000102225	292.492857	0.3639148	0.42850421	0.63562068	0.02311487	0.27170589	0.61710721
HTATSF1	ENSG00000102241	129.067577	-0.367977	0.60041774	0.47780156	0.28859544	0.8457786	0.02148563
VGLL1	ENSG00000102243	31.6293706	-0.9711554	0.34631295	1.04431206	0.12910591	2.01546745	0.00106355
TIMP1	ENSG00000102265	106.278759	-3.28875	1.9837E-15	0.82359026	0.01898116	4.11234029	6.8185E-25
CMC2	ENSG00000103121	41.3545351	1.24182693	0.06760567	1.11705079	0.09151021	-0.1247761	0.94925399
NME4	ENSG00000103202	138.39596	-0.1983236	0.86283993	0.63607082	0.12870854	0.83439439	0.03639589
SLC7A5	ENSG00000103257	134.955507	1.22384699	0.00016517	1.76286766	1.0904E-09	0.53902067	0.22916139
PYCARD	ENSG00000103490	7.91564623	-2.3703833	0.43392613	2.11265653	0.13718694	4.48303983	0.01186934

SGK3	ENSG00000104205	41.87306	0.68811297	0.54409971	2.17876892	1.5774E-05	1.49065595	0.00688537
CPQ	ENSG00000104324	19.920684	-1.6795651	0.18097615	1.62922107	0.04130488	3.30878619	6.8893E-05
POP1	ENSG00000104356	50.198656	0.21903208	0.90172088	1.20669313	0.01648423	0.98766105	0.09465912
TUBB4A	ENSG00000104833	3.3528782	4.41440221	NA	5.26997559	0.04448475	0.85557338	0.87433261
ASF1B	ENSG00000105011	8.73937925	2.35996971	0.21378655	2.68013935	0.08081658	0.32016964	0.93221629
CCNE1	ENSG00000105173	23.0068131	1.65450219	0.08186846	1.56190304	0.08081658	-0.0925991	0.97105871
PDCD5	ENSG00000105185	380.149779	0.75044414	0.00692202	0.73508944	0.0058074	-0.0153547	0.98766681
FBL	ENSG00000105202	164.079962	0.98326127	0.00157824	1.0479761	0.00037101	0.06471484	0.95066459
HNRNPUL1	ENSG00000105323	305.062967	0.09061507	0.92404639	0.71438226	0.00307573	0.62376719	0.01944786
TGFB1	ENSG00000105329	6.7568823	0.60324034	0.9270987	3.47558612	0.02567155	2.87234578	0.08240461
LIG1	ENSG00000105486	16.1558456	1.6227358	0.21709025	2.3843336	0.01008878	0.76159781	0.65367261
ISYNA1	ENSG00000105655	92.7653925	0.97465689	0.03052428	1.33648886	0.00034533	0.36183198	0.65926206
LSR	ENSG00000105699	200.927064	0.41975136	0.34756784	0.65711126	0.02663305	0.2373599	0.71473493
H2AZ2	ENSG00000105968	549.543207	0.60227557	0.01078289	0.72634122	0.0005538	0.12406565	0.85737085
CAV2	ENSG00000105971	12.1531508	0.48531548	0.8960218	2.37251379	0.02429661	1.88719831	0.11692618
HSPB1	ENSG00000106211	4171.9041	0.30274099	0.33226503	0.3220785	0.20515621	0.0193375	0.97781208
NUDT1	ENSG00000106268	87.1395808	0.86704362	0.08211743	1.16980387	0.0032869	0.30276024	0.75192881
C1GALT1	ENSG00000106392	13.8744214	1.49933375	0.30004615	1.90595502	0.07451582	0.40662127	0.88827225
CHCHD3	ENSG00000106554	134.88689	0.81682203	0.02666313	0.97274227	0.00258133	0.15592024	0.88471107
POLD2	ENSG00000106628	289.660034	0.38657082	0.34656089	0.66332485	0.01148049	0.27675403	0.58193437
PTGR1	ENSG00000106853	44.2714482	-0.3341374	0.84290387	1.12067117	0.04601859	1.45480859	0.00804945
PDLIM1	ENSG00000107438	261.427486	0.39739913	0.31429041	0.44930394	0.15053352	0.05190482	0.95285457
SFXN3	ENSG00000107819	40.6286132	0.46264839	0.76213137	1.50879504	0.0088447	1.04614666	0.14728457
GTPBP4	ENSG00000107937	214.498166	-0.1678583	0.84356402	0.46711901	0.16308641	0.63497729	0.04249219
DKK1	ENSG00000107984	224.154875	0.99016529	0.78968222	9.26980991	1.8535E-24	8.27964461	6.9853E-37
GLRX3	ENSG00000108010	172.147464	0.38416261	0.48269717	0.78979417	0.00871247	0.40563156	0.40284962
SMC3	ENSG00000108055	166.411187	0.56765708	0.15659732	0.88936889	0.00230947	0.3217118	0.57642784
UBE2S	ENSG00000108106	276.064652	2.41996826	6.47E-23	2.67018829	1.9528E-28	0.25022003	0.66250785
LGI1	ENSG00000108231	34.0371272	0.32690172	0.95541438	6.08349937	2.7729E-11	5.75659764	9.12E-12
RAPGEFL1	ENSG00000108352	18.72126	-0.5518814	0.87325479	3.20089008	5.8485E-05	3.75277152	1.4819E-05
RGS9	ENSG00000108370	29.4443173	1.88059509	0.0228285	2.74465537	3.8378E-05	0.86406028	0.37823597
RAD51C	ENSG00000108384	88.1055264	0.74842589	0.1845484	1.19875771	0.00276003	0.45033182	0.54845441
KPNB1	ENSG00000108424	220.179615	0.44791352	0.29721281	0.64608665	0.03184608	0.19817312	0.78968226
PSMD11	ENSG00000108671	125.107195	0.7587432	0.06009087	0.66366108	0.10159751	-0.0950821	0.93911055
HSD17B1	ENSG00000108786	18.928989	-1.0701958	0.51530841	1.34768266	0.1496023	2.41787846	0.00540465
MPP2	ENSG00000108852	31.067207	0.66667131	0.7232324	3.19135439	2.513E-07	2.52468308	3.7007E-05
MMD	ENSG00000108960	87.4524045	0.67234987	0.20593357	0.72499276	0.10742182	0.05264289	0.96846322
AREG	ENSG00000109321	8.60197122	-2.3886304	0.62188565	3.62814151	0.00897804	6.01677191	0.00675852
INPP4B	ENSG00000109452	20.2870231	-0.5943509	0.79528972	1.87467356	0.01111329	2.46902442	0.00108346
NSD2	ENSG00000109685	41.8909476	1.92157833	0.00123368	2.24110644	3.9692E-05	0.31952811	0.82959656
CRYAB	ENSG00000109846	34.092903	-1.0325281	0.39342185	2.14511988	8.7678E-05	3.17764797	8.4173E-08
CTSC	ENSG00000109861	23.780338	-0.621438	0.76083171	1.74980205	0.01416832	2.37114589	0.00107574
CCDC34	ENSG00000109881	97.3712223	0.88332557	0.1250028	2.68835589	4.0511E-14	1.80503032	4.4004E-07
HSPA8	ENSG00000109971	1623.20285	0.34245065	0.39439644	0.7475049	0.00116448	0.40505424	0.23268058
CHORDC1	ENSG00000110172	58.4041612	-0.0580766	0.98099172	1.09701744	0.0262481	1.15509405	0.02576601
ARHGEF17	ENSG00000110237	43.1684723	0.34242107	0.84469554	1.3550387	0.01757538	1.01261763	0.1504201
CD81	ENSG00000110651	163.154789	-0.671813	0.10464109	0.54521099	0.16028732	1.21702396	6.6904E-05
HPS5	ENSG00000110756	31.3191575	-0.6240656	0.69259771	1.35786368	0.04238275	1.98192924	0.00209916
PTGES3	ENSG00000110958	522.854895	0.1653289	0.81359184	0.70695701	0.00234445	0.54162811	0.04916987
LIN7A	ENSG00000111052	12.7064281	4.12443341	0.0152351	5.06367686	0.00062145	0.94124345	0.60544885
KRT18	ENSG00000111057	1683.59738	-0.0140496	0.99087564	0.58663009	0.02158118	0.60067966	0.02592921
SLC6A12	ENSG00000111181	8.70577773	2.43070043	0.12628754	2.0841749	0.18430461	-0.3465255	0.92441713
MAGOHB	ENSG00000111196	83.368188	0.73898235	0.22072573	1.20901332	0.00356331	0.47003098	0.54418184
RAD51AP1	ENSG00000111247	30.3641469	3.22384316	4.0045E-05	3.55727554	1.7679E-06	0.33343239	0.86054526
OAS3	ENSG00000111331	23.6867297	0.58513728	0.80240824	2.33331124	0.0019538	1.74817396	0.03783306
NUP107	ENSG00000111581	63.5787695	0.90922862	0.14358269	1.41021027	0.00178879	0.50098165	0.55563456
TIMELESS	ENSG00000111602	34.9843844	0.83872525	0.48770147	2.13649254	0.00031275	1.29776728	0.06413679
CDCA3	ENSG00000111665	46.7418187	2.45085967	2.4657E-05	3.22961031	8.648E-10	0.77875064	0.26416616
TPI1	ENSG00000111669	756.677039	0.02153176	0.98477896	0.70402161	0.00121864	0.68248984	0.00288173
COL12A1	ENSG00000111799	120.281183	-0.7544688	0.1915608	2.13948264	1.8529E-11	2.89395144	1.2583E-18
MAN1A1	ENSG00000111885	5.68620484	0	1	7.00392393	0.00128957	7.00882203	0.00197126
HDDC2	ENSG00000111906	85.6283259	0.10234772	0.95154251	1.12651258	0.0038353	1.02416486	0.0153659
FANCE	ENSG00000112039	9.12292981	3.59793695	0.02539684	3.35241367	0.0313534	-0.2455233	0.94773579
PHACTR1	ENSG00000112137	47.822412	-0.9185648	0.39315812	2.52801356	6.4583E-08	3.44657834	9.9805E-12
BMP5	ENSG00000112175	2.84624715	0	NA	6.00213795	NA	6.00703777	0.04834216
RBM24	ENSG00000112183	21.9641326	-2.5389635	0.01865884	1.54462304	0.04528032	4.08358657	2.7296E-06
CAP2	ENSG00000112186	44.0275683	-0.7697885	0.39818127	0.72803899	0.28639529	1.49782744	0.00650643
HMGCS1	ENSG00000112972	53.9754862	0.90916696	0.18713457	0.77716308	0.24896335	-0.1320039	0.94191161
LMNB1	ENSG00000113368	43.2420303	2.38559305	2.8183E-05	2.59299745	1.8229E-06	0.2074044	0.906361
BRIX1	ENSG00000113460	57.5394126	1.28624286	0.01080569	1.23791907	0.01120069	-0.0483238	0.9747879
PPWD1	ENSG00000113593	25.8704649	1.04037462	0.29155042	0.75059374	0.46841816	-0.2897809	0.89251345
SMC4	ENSG00000113810	141.749175	1.33149784	3.939E-05	1.43545748	3.8286E-06	0.10395963	0.92837088
RBP2	ENSG00000114113	4.80514429	2.06156675	NA	5.04509135	0.04577811	2.9835246	0.18670901
RBP1	ENSG00000114115	13.6784925	-2.8215414	0.21559027	2.5707234	0.007996	5.39226478	0.00030755
BCHE	ENSG00000114200	7.12609015	-2.4452728	0.66781747	4.76356899	0.00489083	7.20884178	0.00061656
GNAI2	ENSG00000114353	185.092891	-0.0583475	0.96390188	0.74161129	0.01342577	0.79995874	0.00944329
IFT57	ENSG00000114446	283.055218	1.00367216	0.00017114	2.24536758	1.0942E-23	1.24169542	8.622E-08
GNB4	ENSG00000114450	145.4095	0.83049206	0.02783507	1.21167964	8.7668E-05	0.38118758	0.53227802
ARHGEF26	ENSG00000114790	78.6751347	-0.1893508	0.90778477	1.0477383	0.02056988	1.23708908	0.0063247
NCL	ENSG00000115053	904.894164	-0.2945727	0.4425208	0.41132663	0.10889802	0.70589938	0.00108346
CENPA	ENSG00000115163	43.8288043	2.61841439	2.4986E-05	3.18985187	2.6939E-08	0.57143748	0.54418184
EFEMP1	ENSG00000115380	197.419845	0.67772208	0.06190607	1.5692917	6.7238E-10	0.89156961	0.0020416
IGFBP2	ENSG00000115457	1388.72659	-0.6533349	0.00190495	0.3995869	0.10141697	1.05292177	8.9679E-09
HPCAL1	ENSG00000115756	207.033092	-0.0510055	0.97177335	0.9237272	0.00279678	0.97473275	0.00208625
SRSF7	ENSG00000115875	211.009394	0.32145353	0.55350141	0.62780161	0.03468284	0.30634808	0.56568028
TRAK2	ENSG00000115993	36.7573805	0.64630259	0.58538901	1.44130722	0.01358854	0.79500462	0.36130993
CACYBP	ENSG00000116161	345.453166	0.94658493	0.00166217	0.87586578	0.00327386	-0.0707192	0.94806059
UCHL5	ENSG00000116750	73.469326	0.76299273	0.26818953	1.43310125	0.00101076	0.67010852	0.31662858
LGALS8	ENSG00000116977	30.1010135	-0.1887432	0.94739613	1.25370119	0.07095063	1.44244442	0.04251143
SIPA1L2	ENSG00000116991	7.73337056	2.40866775	0.23822146	2.88911208	0.06786882	0.48044433	0.90100125
SDHB	ENSG00000117118	323.602345	0.3293144	0.44391311	0.65222868	0.00838003	0.32291424	0.43415231
MFAP2	ENSG00000117122	13.6479542	5.09511516	0.03122609	8.03435331	1.2529E-05	2.93923815	0.00245059
ID3	ENSG00000117318	11.042687	0.69055435	0.84587541	2.82324435	0.0090519	2.13269	0.07008832
CDC20	ENSG00000117399	133.707247	2.73109269	1.8286E-16	3.10565049	9.7283E-22	0.37455779	0.52819601
F3	ENSG00000117525	8.70262209	1.7466784	0.49985936	3.69986678	0.00565021	1.95318838	0.18389021
CENPF	ENSG00000117724	86.7294697	2.70628714	4.1816E-11	2.4973363	1.4472E-09	-0.2089508	0.87541786
ESYT2	ENSG00000117868	103.011343	0.56896841	0.34364718	0.87180469	0.0294464	0.30283628	0.73223139
CTSD	ENSG00000117984	91.0705378	-0.7064027	0.17839767	0.7756956	0.05295001	1.48209827	2.4908E-05
TGIF2	ENSG00000118707	23.7650734	-0.9440852	0.52794365	1.60706537	0.02772091	2.55114892	0.0004334
CTNNAL1	ENSG00000119326	23.9471643	2.27169795	0.00362719	2.51243819	0.0004949	0.24074024	0.91259955
WDR34	ENSG00000119333	84.0730716	1.31426936	0.00095209	1.40146336	0.00020488	0.08719401	0.94968363
SET	ENSG00000119335	1418.43116	0.67589393	0.00085177	0.99076453	2.8825E-08	0.3148706	0.31540646
TRIM32	ENSG00000119401	44.8042958	-0.0418484	0.98809915	1.49382636	0.00509556	1.53567473	0.0057823
PHF19	ENSG00000119403	53.9954814	2.30710911	5.6607E-06	2.88038153	8.648E-10	0.57327242	0.4692677
BSPRY	ENSG00000119411	109.06658	0.89236381	0.01979205	0.68931348	0.094335	-0.2030503	0.8471728
IFIT2	ENSG00000119922	17.1572317	-0.7805769	0.74915762	2.29965282	0.00368715	3.08022976	0.00028237
PPP1R3C	ENSG00000119938	11.367219	-2.3192576	0.14449494	0.79028903	0.638268	3.10954663	0.01459007
MTHFD1L	ENSG00000120254	10.4592642	1.95759644	0.30274149	3.10415435	0.01176439	1.1465579	0.52917575
CENPL	ENSG00000120334	19.7299555	2.51249881	0.01299986	3.05806178	0.00053559	0.54556297	0.76677947
NUDCD1	ENSG00000120526	125.477736	0.39297568	0.56380504	0.7428482	0.04715864	0.34987251	0.612042
MASTL	ENSG00000120539	32.3282584	1.04736022	0.27530167	1.7243444	0.00607796	0.67698418	0.53878241
TMPO	ENSG00000120802	247.414649	1.32958317	1.1515E-06	1.86443947	1.1559E-13	0.5348563	0.15227294
NFYB	ENSG00000120837	73.7752335	0.47433661	0.55370469	0.87981304	0.04891244	0.40547643	0.62067667
MND1	ENSG00000121211	14.6703857	4.75432289	0.03814186	6.10254029	0.00144949	1.3482174	0.26826399
KIF18A	ENSG00000121621	10.6043491	2.0028071	0.29394303	2.83117064	0.03098796	0.82836353	0.73037
ADGRB2	ENSG00000121753	6.35852044	0.97572238	0.84030073	3.27703283	0.03686765	2.30131045	0.19242241
KHDRBS1	ENSG00000121774	256.933897	0.34840327	0.50055476	0.62901519	0.03754833	0.28061192	0.62777923
CBX3	ENSG00000122565	593.19716	0.44976688	0.12953133	0.31495465	0.33182654	-0.1348122	0.84953926
WIPF3	ENSG00000122574	8.50067121	2.22149526	0.19699773	2.20230216	0.14939608	-0.0191931	0.99605451
ACADS	ENSG00000122971	16.1713456	-0.9323842	0.58927553	0.95776682	0.39330897	1.89015099	0.04597182
CDKN2C	ENSG00000123080	14.8200958	1.46226238	0.29589188	1.40713211	0.25310012	-0.0551303	0.98488071
NECAB1	ENSG00000123119	44.97564	0	1	9.98586248	1.576E-09	9.99076335	2.7349E-09
CENPK	ENSG00000123219	32.5079685	3.49077411	6.442E-07	3.1353811	9.8189E-06	-0.355393	0.83418054
CDK2	ENSG00000123374	38.7656698	1.27938355	0.09415528	1.44197972	0.02663031	0.16259617	0.93911055
STIL	ENSG00000123473	24.2114769	3.22866869	0.00028064	2.89408744	0.00141147	-0.3345812	0.87675675
HJURP	ENSG00000123485	37.5198581	2.77891574	4.6638E-05	3.00073049	4.0279E-06	0.22181475	0.90795096
RAP2C	ENSG00000123728	108.67954	0.2735142	0.77592215	0.88078274	0.01590255	0.60726854	0.20765695
PFKFB2	ENSG00000123836	16.5551259	1.34955186	0.31483553	1.40467836	0.20792239	0.0551265	0.98488071
RAB38	ENSG00000123892	11.1574778	0.30005592	0.95154251	3.0683688	0.00335433	2.76831289	0.01050384
AGO2	ENSG00000123908	94.9006869	0.02608722	0.98931314	0.96890062	0.00888055	0.9428134	0.0169946
CSE1L	ENSG00000124207	150.022435	0.44060358	0.47544777	0.77950523	0.03170111	0.33890164	0.62693109
MAGEA10	ENSG00000124260	24.0689006	-0.9368559	0.49710964	1.14781517	0.15778169	2.08467104	0.00474028
POF1B	ENSG00000124429	42.2085248	-1.1101236	0.19280035	1.21367613	0.04411142	2.32379976	3.1316E-05
MT2A	ENSG00000125148	1254.39736	1.24107941	1.2464E-06	1.02626275	8.9414E-05	-0.2148167	0.76677947
RBM42	ENSG00000126254	240.375616	0.58465437	0.06190607	0.50616348	0.10248414	-0.0784909	0.93257802
FRMD8	ENSG00000126391	102.841942	0.09331022	0.9535375	1.12520167	0.00144113	1.03189145	0.0063247
BCL2L12	ENSG00000126453	69.755045	1.37760534	0.00234612	2.07517428	6.4027E-08	0.69756894	0.20262586
PRMT1	ENSG00000126457	102.944447	0.16280273	0.90091853	0.95669747	0.00917496	0.79389475	0.06191654
IFI6	ENSG00000126709	28.214341	-0.3335331	0.90778853	2.21603385	0.00124655	2.54513698	0.00031102
KTN1	ENSG00000126777	469.036131	-0.4068994	0.20638634	0.35857831	0.22436549	0.76547773	0.0006362
DLGAP5	ENSG00000126787	42.0099013	2.18263807	0.00023212	2.64566455	1.1767E-06	0.46302648	0.68854669
AIF1L	ENSG00000126878	86.9456334	0.59697228	0.34039355	1.10967751	0.00398463	0.51270523	0.4200631
CTAG2	ENSG00000126890	414.893471	0.66120979	0.01324801	0.86178034	0.00019027	0.20057055	0.73591667
SLC10A3	ENSG00000126903	55.5766664	0.92627987	0.1644439	2.169517	2.3506E-07	1.24323713	0.00766865
TIMM8A	ENSG00000126953	32.099835	-1.2594044	0.15064042	0.54172447	0.60633817	1.80112885	0.00846549
FGFRL1	ENSG00000127418	33.0062705	0.32040487	0.89108484	2.13961583	0.00039116	1.81921096	0.0047094
AUNIP	ENSG00000127423	12.6262189	0.45909744	0.90376257	2.24110251	0.03227668	1.78200507	0.13872976
HP1BP3	ENSG00000127483	125.591213	0.39030995	0.5774665	1.45212681	9.426E-07	1.06181686	0.00101064
EPS15L1	ENSG00000127527	62.8173613	0.2793554	0.84356402	1.02621306	0.03137769	0.74685766	0.22854665
NA	ENSG00000127589	49.3326172	1.16473675	0.07576121	1.49332171	0.00509484	0.32858496	0.81371626
KDM4B	ENSG00000127663	60.1125175	-0.4889702	0.61142978	1.15450937	0.00704422	1.64347954	7.8059E-05
GNAI1	ENSG00000127955	28.1379793	0.48320755	0.82767858	2.57150277	3.5697E-05	2.08829522	0.00118639
SGCE	ENSG00000127990	8.30268666	-0.9904042	0.91166912	5.05023385	0.00183402	6.04063809	0.00498683
A4GALT	ENSG00000128274	24.9103406	-1.4483013	0.86898752	7.65305318	1.1357E-05	9.10135452	2.0305E-07
HAT1	ENSG00000128708	101.625825	0.37715785	0.65833503	0.83174905	0.04403087	0.4545912	0.50265743
DUT	ENSG00000128951	155.539425	1.43548215	2.9359E-05	1.7374825	5.9723E-08	0.30200034	0.71030461
E2F8	ENSG00000129173	7.51201083	1.60645284	0.59422062	3.24701593	0.03001727	1.64056309	0.39287458
MIS18BP1	ENSG00000129534	34.761918	1.36467479	0.09238505	1.78712699	0.00560428	0.4224522	0.78800015

FGF13	ENSG00000129682	20.5182751	0.97777638	0.91003718	7.37836072	3.403E-05	6.40058434	1.9144E-06
TOMM40	ENSG00000130204	167.835542	0.72768295	0.0356298	1.04543184	0.00020597	0.31774889	0.58631889
BST2	ENSG00000130303	140.252801	-2.6239316	7.4208E-12	1.14452012	0.00071201	3.76845171	1.142E-25
PXDN	ENSG00000130508	29.6094433	0.03569012	0.99143097	1.53808698	0.01946295	1.50239686	0.03424218
LSM4	ENSG00000130520	1016.65752	0.77956423	0.00106685	0.67932088	0.00480367	-0.1002434	0.9036899
JUND	ENSG00000130522	436.072862	0.71827839	0.02991855	0.63397299	0.05239061	-0.0843054	0.93785297
OLFM1	ENSG00000130558	105.833004	1.01896575	0.01859231	1.88640468	1.838E-08	0.86743893	0.03615512
COL5A1	ENSG00000130635	3.08794486	-2.4468648	NA	3.55956459	NA	6.00642942	0.03212692
GATA5	ENSG00000130700	29.2658647	0.74720727	0.60388687	2.61282029	7.0477E-06	1.86561302	0.00200761
ASS1	ENSG00000130707	348.770792	1.10240039	5.7753E-06	1.98260694	3.2477E-20	0.88020655	0.0002847
EXOSC2	ENSG00000130713	44.4165684	1.26175325	0.04153545	1.14430947	0.05856247	-0.1174438	0.94925399
TRIM28	ENSG00000130726	355.269976	0.2185901	0.76344217	0.94722303	0.00022407	0.72863293	0.01261419
DNMT1	ENSG00000130816	83.3396366	1.60859582	0.00013567	2.06889909	6.8457E-08	0.46030327	0.54485982
DKC1	ENSG00000130826	237.933336	0.19414547	0.83724001	0.81686305	0.00742885	0.62271757	0.09301869
GINS2	ENSG00000131153	158.240429	2.2597771	5.6679E-12	2.5263766	2.7267E-15	0.26659951	0.75059532
TUBG1	ENSG00000131462	97.3674979	1.48099188	0.00039916	1.46395931	0.00034607	-0.0170326	0.99038345
SNRPA1	ENSG00000131876	173.087267	0.54940366	0.17619083	0.54475986	0.13282809	-0.0046438	0.99605451
ABHD12B	ENSG00000131969	16.7180801	-1.1187521	0.69002595	3.42275036	3.1865E-05	4.54150247	5.2245E-06
HSD17B7	ENSG00000132196	37.5033891	0.81250497	0.39750545	1.27963441	0.03495756	0.46712944	0.70665224
ILKAP	ENSG00000132323	42.8019423	0.34870969	0.83596646	1.26270316	0.02391636	0.91399347	0.1962965
RAMP1	ENSG00000132329	31.6153502	-1.5797378	0.66649149	5.40628806	1.166E-11	6.98602589	3.0072E-08
RAN	ENSG00000132341	1008.30301	0.18179896	0.69163499	0.64387654	0.0004513	0.46207758	0.03520645
FIGNL1	ENSG00000132436	16.4896549	1.68648757	0.14358269	1.8626629	0.05493262	0.17617533	0.9496524
H3-3B	ENSG00000132475	1241.71997	0.29268638	0.37568313	0.46717672	0.02956725	0.17449034	0.71007296
EIF5A	ENSG00000132507	465.739403	0.55022675	0.2487825	0.93360505	0.00363606	0.3833783	0.52830663
MATN2	ENSG00000132561	31.9127132	0.96838369	0.37787678	2.74767267	7.8659E-07	1.77928898	0.00193359
MTSS2	ENSG00000132613	32.1584647	0.96983598	0.31051818	0.80225487	0.38268187	-0.1675811	0.94021761
NASP	ENSG00000132780	89.3794366	1.17809314	0.01459257	1.50488456	0.0003158	0.32679142	0.75805341
RBM38	ENSG00000132819	71.9902093	-0.3769353	0.75665249	0.90065879	0.08048379	1.27759404	0.00786158
NA	ENSG00000132967	178.924158	1.04338925	0.00300757	1.24053497	0.00010409	0.19714573	0.84953926
RFC3	ENSG00000133119	44.0811436	1.44237059	0.01371041	1.81743893	0.0003398	0.37506834	0.76230724
STARD13	ENSG00000133121	14.3211452	0.03642975	0.99755275	2.64279232	0.00489809	2.60636258	0.00822545
C1QTNF6	ENSG00000133466	14.5620903	-0.111893	0.98477896	3.14622201	0.00178879	3.25811503	0.00200761
C12orf29	ENSG00000133641	58.011754	0.69520285	0.36241244	1.09933914	0.0262481	0.40413629	0.69427978
MICAL2	ENSG00000133816	15.3868986	-0.7337185	0.7844887	1.86637925	0.05103513	2.60009771	0.00709808
MBD2	ENSG00000134046	55.6993624	0.51883349	0.59511588	1.20057442	0.01154189	0.68174094	0.3262559
YWHAQ	ENSG00000134308	510.449334	0.31860059	0.4012325	0.56827276	0.01416723	0.24967217	0.56792518
LDHA	ENSG00000134333	695.423862	0.18529907	0.76154567	0.80437879	0.00020894	0.61907972	0.01238373
IL6ST	ENSG00000134352	25.1104875	1.14813293	0.29140527	1.44815054	0.07423758	0.30001761	0.89492305
RBM17	ENSG00000134453	196.523717	0.57395585	0.15229601	1.05404474	0.00014334	0.4800889	0.25923879
SOX3	ENSG00000134595	8.30397553	-2.5679961	0.5497996	3.36448682	0.00817494	5.93248288	0.00599784
STK26	ENSG00000134602	56.2096375	0.30297431	0.84356402	1.69778344	0.00010423	1.39480913	0.00295773
C5AR2	ENSG00000134830	20.7918446	-1.6730527	0.2703813	2.5994404	0.0001774	4.27249309	5.1484E-07
CEMIP2	ENSG00000135048	10.4122181	-0.6345788	0.87440812	2.47456791	0.02147952	3.10914667	0.00713783
CCNJL	ENSG00000135083	5.55710159	1.39990539	0.74016609	3.5351393	0.04180204	2.13523391	0.29084566
OASL	ENSG00000135114	6.51047874	-4.5966503	0.10228949	1.99180754	0.22367434	6.58845784	0.00266654
BICDL1	ENSG00000135127	26.035919	1.032015 34	0.3625932	1.59789727	0.02954459	0.56588193	0.70331151
CAPRIN1	ENSG00000135387	442.907084	-0.2913029	0.55405497	0.28916015	0.4529506	0.58046304	0.0451712
TROAP	ENSG00000135451	37.3594334	3.82045351	1.1599E-06	4.24952339	1.393E-08	0.42906988	0.73883818
ESPL1	ENSG00000135476	19.7825481	1.73182716	0.11005221	2.53831097	0.00170847	0.80648381	0.55691265
HNRNPA1	ENSG00000135486	543.190027	0.41884035	0.1553349	0.87996982	8.8094E-06	0.46112947	0.07992587
PKIB	ENSG00000135549	45.4344499	-0.3578515	0.8257516	1.35882744	0.00680007	1.71667899	0.00060576
GLUL	ENSG00000135821	578.516512	0.52271744	0.07560391	1.21142047	3.8824E-09	0.68870302	0.00474797
DHX9	ENSG00000135829	227.072342	0.37352487	0.42325175	0.63222392	0.02824896	0.25869905	0.65528043
BRIP1	ENSG00000136492	8.65319864	2.86458788	0.13063482	3.30519831	0.03337231	0.44061043	0.90100125
TRA2B	ENSG00000136527	191.07906	0.43664408	0.42642583	0.70622084	0.04134633	0.26957676	0.71723319
GATA4	ENSG00000136574	25.6093153	0.75341757	0.68738929	3.12385957	1.6517E-06	2.370442	0.00023102
BIN1	ENSG00000136717	11.1267536	-1.4514465	0.87325479	6.47623621	0.00092767	7.92768266	4.6547E-05
HS6ST1	ENSG00000136720	30.1312589	-0.7436623	0.5774665	0.82013019	0.34413224	1.56379248	0.02909055
ODF2	ENSG00000136811	36.4021779	1.04070387	0.29059704	1.47583585	0.03184608	0.43513198	0.78898264
SMC2	ENSG00000136824	95.9917768	1.3699321	0.00062021	1.79422907	5.764E-07	0.42429697	0.5598439
ST6GALNAC4	ENSG00000136840	25.9951959	-0.0193194	0.99918077	1.61989286	0.01542967	1.63921227	0.02064756
ANP32B	ENSG00000136938	571.504778	0.85215052	0.00348858	0.80396321	0.00481364	-0.0481873	0.9610645
LMX1B	ENSG00000136944	34.3209512	-0.0128722	0.99993814	1.30876852	0.02797055	1.32164068	0.03819641
DSCC1	ENSG00000136982	86.9551537	3.73821941	5.449E-15	4.17236489	5.0913E-19	0.43414548	0.54636518
PIM1	ENSG00000137193	8.48949749	2.54268396	0.09843576	1.93928472	0.2411323	-0.6033992	0.85303958
TUBB2A	ENSG00000137267	21.4913679	1.43306386	0.17790682	1.45480956	0.12101614	0.93980669	0.09380669
MDC1	ENSG00000137337	20.3140333	2.0024958	0.03147711	2.46453929	0.00192926	0.46204348	0.80388812
GGH	ENSG00000137563	213.949668	1.05701306	0.00024498	1.30871803	8.2993E-07	0.25170496	0.70664866
THBS1	ENSG00000137801	5.54161266	0.62972984	0.94321858	4.35730214	0.02177194	3.7275723	0.04653992
IFI44	ENSG00000137965	3.79048776	-2.4463346	NA	3.83818655	0.09169467	6.28452114	0.01304963
SLC5A6	ENSG00000138074	124.382215	-0.0717281	0.96143363	0.89553717	0.00822924	0.96726528	0.00545529
ARL3	ENSG00000138175	182.265196	0.62306716	0.08524351	0.781067	0.00871247	0.15799984	0.86418864
CEP55	ENSG00000138180	105.997333	3.38336808	1.5372E-16	3.45689318	1.8896E-17	0.07352511	0.9551239
PLCE1	ENSG00000138193	13.4486035	2.70883521	0.02276004	2.82126779	0.01006895	0.11243258	0.97048088
PCDH10	ENSG00000138650	6.64540415	0	1	7.22808527	0.00053868	7.23298328	0.00082525
SEPTIN11	ENSG00000138758	184.30312	0.16554023	0.86709047	0.6521983	0.04923122	0.48665807	0.26735716
GSTCD	ENSG00000138780	44.1623381	1.88614383	0.00235608	3.19664965	3.0571E-10	1.31050581	0.0118611
B4GALNT3	ENSG00000139044	24.632032	1.17379113	0.38512562	2.81053794	8.9772E-05	1.63674681	0.04062463
PHLDA1	ENSG00000139289	12.806932	-1.4358489	0.50410376	1.96018698	0.06818997	3.3960359	0.00216215
SNRPF	ENSG00000139343	318.379327	0.52482005	0.2542401	0.84964323	0.00672336	0.32482318	0.60761836
TDG	ENSG00000139372	108.013398	-0.4943713	0.465461	0.4215343	0.45618861	0.91590561	0.02820017
FAM222A	ENSG00000139438	12.2853841	3.44224532	0.06912649	4.62606102	0.00204179	1.1838157	0.43345321
DIAPH3	ENSG00000139734	15.8071124	2.24877578	0.09415528	3.21394004	0.00168241	0.96516426	0.54913507
RAB15	ENSG00000139998	28.9072592	-0.6887353	0.63184893	0.89403036	0.28758309	1.5827657	0.02839283
JDP2	ENSG00000140044	35.7730058	0.53511533	0.69338409	1.30806912	0.02956747	0.77295379	0.38432084
TPM1	ENSG00000140416	49.4929676	0.28352252	0.87482397	1.87773288	7.9814E-05	1.59421036	0.00158993
PIF1	ENSG00000140451	10.1024201	6.20050267	0.00362655	6.48949594	0.00120868	0.28899327	0.93612313
FURIN	ENSG00000140564	42.2466108	-0.7131708	0.45133101	0.60233361	0.42511123	1.31550445	0.0227737
EIF4A3	ENSG00000141543	178.206862	0.75653837	0.01670363	0.91671074	0.00103463	0.16017237	0.85736176
IGFBP4	ENSG00000141753	119.73452	-0.1090273	0.94720476	2.26849842	1.08E-15	2.37752575	8.0487E-17
SAE1	ENSG00000142230	146.05134	0.43369196	0.42652549	0.86294476	0.00595684	0.42925281	0.39720144
EFHD2	ENSG00000142634	128.257117	-0.4667809	0.51530841	0.60870714	0.19529776	1.07548808	0.00598307
KIF2C	ENSG00000142945	24.2715386	2.96145429	0.00042904	2.96554734	0.00029069	0.00409305	0.99825809
LMO4	ENSG00000143013	60.1340839	0.75664051	0.42061151	2.83472249	1.033E-10	2.07808197	2.2284E-06
MGST3	ENSG00000143198	251.753674	0.55923738	0.1915608	0.51519217	0.19415152	-0.0440452	0.96846322
CRABP2	ENSG00000143320	1269.17768	0.11147302	0.86701776	0.54182953	0.00886172	0.43035651	0.08207591
HDGF	ENSG00000143321	628.057395	0.7889708	0.00020424	0.9657651	9.426E-07	0.1767943	0.73950473
ANP32E	ENSG00000143401	110.655754	0.95018562	0.03482677	1.95139161	4.2112E-09	1.0017405	0.00942572
S100A8	ENSG00000143546	52.431756	0.44215161	0.87737913	5.16313574	5.0497E-18	4.72098413	6.984E-18
CALM2	ENSG00000143933	530.022303	0.49552927	0.11218929	0.94348226	1.8523E-05	0.447953	0.15946406
TPRKB	ENSG00000144034	120.473252	-0.2255032	0.85973314	1.00944826	0.01046613	1.23495143	0.00147615
PKP4	ENSG00000144283	165.791882	0.25097579	0.7702191	0.73618266	0.03259618	0.48520687	0.32309878
ZNF385B	ENSG00000144331	28.2119865	0	1	9.30118287	4.662E-08	9.30608795	7.8231E-08
CDCA7	ENSG00000144354	52.4485137	4.04962906	1.191E-08	4.67881906	5.8557E-12	0.62919001	0.4564597
GULP1	ENSG00000144366	65.8602291	-2.643148	0.28806771	5.3773072	1.3611E-10	8.02045523	2.9811E-09
FAM171B	ENSG00000144369	8.16785649	-0.7329216	0.89973191	3.24608374	0.01479304	3.97900536	0.00993961
HSPD1	ENSG00000144381	932.516218	0.3569418	0.21378655	0.61834808	0.00170847	0.26140628	0.45973622
BOC	ENSG00000144857	12.0291268	1.44406398	0.49929989	2.96749125	0.00800043	1.52342728	0.28109603
LPP	ENSG00000145012	31.7016856	1.24107231	0.17839767	0.95169997	0.32512242	-0.2893723	0.89695759
CCNA2	ENSG00000145386	26.9875821	2.91517629	0.00021619	3.06275353	5.2004E-05	0.14757724	0.94773579
NDUFS6	ENSG00000145494	327.951753	0.73256827	0.01258968	0.50808987	0.12364783	-0.2244784	0.73270586
PLK2	ENSG00000145632	118.135729	1.72286309	1.0211E-06	1.58531032	7.2455E-06	-0.1375528	0.91294421
PIK3R1	ENSG00000145675	57.1371176	-0.0520937	0.98310271	1.68055703	8.7174E-05	1.7326507	8.2968E-05
SSBP2	ENSG00000145687	38.2385346	1.44625914	0.0124351	1.13101734	0.07721486	-0.3152418	0.84014113
SLC25A48	ENSG00000145832	9.17508345	-2.0120716	0.56560738	2.7622572	0.02697358	4.77432875	0.00513948
DCDC2	ENSG00000146038	43.989541	0.54268901	0.66281441	1.48443355	0.00588337	0.94176455	0.17895999
TPBG	ENSG00000146242	47.5558093	-0.7161687	0.42954423	0.72681887	0.26928672	1.44298758	0.00694241
CDCA5	ENSG00000146670	75.9372216	2.65415581	5.848E-10	3.0705111	8.753E-14	0.41635529	0.58719021
CCT6A	ENSG00000146731	449.950122	0.05075303	0.95888715	0.55409927	0.01717137	0.50334624	0.05455727
NCAPG2	ENSG00000146918	41.8796089	2.19377982	9.0175E-05	2.44708755	3.7584E-06	0.25330773	0.87675675
NONO	ENSG00000147140	558.33031	-0.4593671	0.09238505	0.51937811	0.02130226	0.97874517	4.9482E-07
RBMX	ENSG00000147274	217.299172	0.29738448	0.61038655	0.66882505	0.02153215	0.37140057	0.42318963
TACC1	ENSG00000147526	93.6558186	0.99084159	0.04540679	2.02401538	1.7893E-08	1.03317379	0.01380698
TRIM55	ENSG00000147573	7.57478706	-5.2561148	0.03075316	1.54794708	0.32258202	6.80406191	0.00120798
SYBU	ENSG00000147642	6.01403141	-2.3086011	0.64923346	3.07764212	0.05088546	5.38624322	0.02389372
FAM83A	ENSG00000147689	9.21267642	0.3102524	0.96196531	3.7850515	0.00318318	3.4747991	0.00713783
PLIN2	ENSG00000147872	26.8087381	1.40515545	0.14319551	2.08828859	0.00285755	0.68313314	0.59426269
CDKN2A	ENSG00000147889	77.531749	0.80599069	0.1468149	1.16691318	0.00506224	0.36092248	0.69258543
SIGMAR1	ENSG00000147955	149.474456	0.15670435	0.8835275	0.99796926	0.00077824	0.84126491	0.00997827
UGCG	ENSG00000148154	121.569408	0.65763744	0.31244612	0.89484566	0.05486771	0.23720822	0.8544103
STOM	ENSG00000148175	127.722496	1.86873325	9.9442E-09	1.95451765	8.4878E-10	0.0857844	0.94616617
ASTN2	ENSG00000148219	15.770618	0.15708815	0.96957806	2.10900655	0.02056988	1.95191841	0.05025715
POLE3	ENSG00000148229	107.164674	0.50706307	0.45417001	0.89277221	0.0264559	0.38570914	0.61487843
PTGES	ENSG00000148344	178.425587	-0.7366329	0.15825389	3.38208165	3.6073E-38	4.1187145	1.0446E-47
MSRB2	ENSG00000148450	136.347848	-0.3473947	0.60805652	0.41557911	0.36162472	0.76297386	0.03570067
RPP30	ENSG00000148688	58.4909874	0.85482481	0.16037921	1.16205665	0.01243087	0.30723183	0.79012457
FRA10AC1	ENSG00000148690	148.846849	-0.105226	0.94873921	2.35845475	4.7672E-16	2.4636808	3.6059E-17
ADD3	ENSG00000148700	21.5189927	-1.659692	0.16154366	1.55012439	0.0466089	3.2098144	6.0313E-05
MKI67	ENSG00000148773	119.005415	4.08657951	1.7816E-21	4.01845443	8.1599E-21	-0.0681251	0.95591153
GSTO1	ENSG00000148834	215.503119	0.57226976	0.09897832	0.5086419	0.12819134	-0.0636279	0.94925399
IMMP1L	ENSG00000148950	62.791825	0.63057379	0.41988147	1.10481311	0.0184426	0.47423932	0.58220963
SSRP1	ENSG00000149136	68.5544	0.78315699	0.21046459	0.79215664	0.14631698	0.00899965	0.99605451
ENDOD1	ENSG00000149218	128.219627	-0.9445054	0.03696926	1.81154019	2.0222E-09	2.7560456	1.1892E-18
AASDHPPT	ENSG00000149313	26.9856554	-0.8058611	0.53701631	0.74702617	0.42866893	1.55288725	0.04024416
INCENP	ENSG00000149503	29.5412754	2.15156229	0.00296775	2.18364556	0.00166428	0.03208327	0.98766681
EI24	ENSG00000149547	177.1522	0.06451311	0.96017437	0.65667122	0.03907393	0.59215811	0.10616272
CHEK1	ENSG00000149554	28.0029615	1.62360767	0.07171825	2.31564198	0.00092699	0.69203431	0.58220963
CABLES2	ENSG00000149679	63.1528739	0.5961465	0.49737278	1.25682596	0.00770924	0.66067945	0.36233036
HIRIP3	ENSG00000149929	36.95302	1.33880539	0.05390621	1.60274458	0.00653943	0.2639392	0.88308723
LYPD6B	ENSG00000150556	27.4403027	1.26128891	0.18916218	1.01559453	0.29907284	-0.2456944	0.91515732
CRIM1	ENSG00000150938	31.0480735	2.41260713	0.0103154	4.61583612	1.547E-10	2.20322899	0.00012297
ABCB9	ENSG00000150967	23.1855946	-0.5172338	0.81484182	1.32784856	0.09448772	1.84508235	0.0169946
GPR158	ENSG00000151025	26.187255	-0.9795299	0.4154505	0.8838046	0.3190993	1.86333449	0.00998109
C12orf45	ENSG00000151131	33.7016773	0.49408801	0.74294777	1.41253081	0.01958644	0.9184428	0.25834535
NCAPD3	ENSG00000151503	20.1807667	1.76071086	0.09577269	2.10167159	0.01566361	0.34096073	0.8922633
CENPU	ENSG00000151725	11.780268	2.53893016	0.07871309	3.0216871	0.01169515	0.48275694	0.86700599
CCL28	ENSG00000151882	39.2727533	-0.4741476	0.83537121	3.42066608	4.1155E-11	3.89481366	2.2167E-12

BAG3	ENSG00000151929	555.202498	-0.294774	0.48253492	0.36940251	0.2037459	0.66417648	0.00488552
PTPN14	ENSG00000152104	41.3818412	0.94971927	0.18793682	0.90199397	0.17127928	-0.0477253	0.97921349
HSPB8	ENSG00000152137	610.334966	-0.393545	0.2774575	2.90272938	2.2733E-60	3.29627442	1.1513E-74
HAUS1	ENSG00000152240	25.4502843	1.15679696	0.30385386	1.90935594	0.00883739	0.75255899	0.55772758
SPC25	ENSG00000152253	62.9674992	3.07102414	6.7163E-09	3.89527716	5.1612E-15	0.82425302	0.12337822
TCF7L1	ENSG00000152284	26.5450205	-0.5032103	0.79491513	1.39620222	0.04437586	1.89941253	0.00540442
MBNL1	ENSG00000152601	58.0931644	0.80027406	0.26818953	0.69080101	0.30944772	-0.1094731	0.94978923
GJA1	ENSG00000152661	83.8734128	2.42478837	0.62668178	10.879256	1.6428E-11	8.45446767	3.8223E-13
DAB2	ENSG00000153071	34.2188351	-1.1974992	0.27196661	2.38804673	5.5962E-06	3.58554592	1.0771E-09
RBMS1	ENSG00000153250	28.3346166	0.41503583	0.84912825	2.16153541	0.00056723	1.74649958	0.00933126
CFDP1	ENSG00000153774	46.9221001	0.81695543	0.28346949	0.78870214	0.23684839	-0.0282533	0.98766681
ANKRD29	ENSG00000154065	5.96087423	4.76203239	0.09151453	6.64163564	0.00201581	1.87960325	0.38065701
ANKH	ENSG00000154122	6.97073563	1.97199553	0.49413768	3.39955407	0.03647033	1.42755854	0.5136961
NRGN	ENSG00000154146	19.556019	0.75490934	0.73362134	1.98995247	0.03129712	1.23504314	0.32700006
ANGPT1	ENSG00000154188	5.12344714	2.34183759	0.49737278	3.926817 56	0.04898745	1.58497997	0.54418184
PITPNC1	ENSG00000154217	24.9273021	0.65809983	0.7310237	2.64344615	8.0568E-05	1.98534632	0.00483452
C4orf19	ENSG00000154274	5.08693729	-0.9834789	0.92102023	4.21805199	0.03943644	5.2015309	0.04628182
PGM5	ENSG00000154330	8.34955071	1.4443997	0.87587059	7.50920519	0.00014334	6.06480549	0.00474028
CCSAP	ENSG00000154429	15.2665039	1.22423857	0.45558734	1.97663951	0.04572537	0.75240094	0.68000787
BUB3	ENSG00000154473	197.908173	0.75296535	0.01599318	0.8377693	0.00324911	0.08480395	0.93267801
BTG3	ENSG00000154640	4.22991437	5.08427434	NA	5.44382951	0.03168914	0.35955516	0.94925399
KLF10	ENSG00000155090	75.4957837	-0.7948682	0.160529	0.82488387	0.06219489	1.61975207	2.6984E-05
OTUD6B	ENSG00000155100	125.200911	-0.2673943	0.7619592	0.55845161	0.17348852	0.82584593	0.02576601
TMEM237	ENSG00000155755	29.8634763	1.09437162	0.26063638	1.47741586	0.03527203	0.38304424	0.82740428
SLC26A2	ENSG00000155850	13.3206165	-0.3194312	0.95126426	3.33236399	0.00111911	3.65179521	0.00077441
VBP1	ENSG00000155959	282.744871	0.61419553	0.84469554	0.64025313	0.02512121	0.4760576	0.195282
MMP16	ENSG00000156103	48.0472917	2.08597634	0.00070311	3.64661529	1.0335E-12	1.56063895	0.00114912
CCT8	ENSG00000156261	353.295837	0.4687642	0.18119691	0.64648437	0.01511909	0.17772017	0.79493462
TBC1D31	ENSG00000156787	30.4394163	1.56635295	0.02788641	1.58481859	0.01701643	0.01846564	0.99304392
ATAD2	ENSG00000156802	225.519806	2.10665877	5.5275E-17	2.24752369	1.4552E-19	0.14086492	0.87434773
PAXIP1	ENSG00000157212	40.1563942	0.17560633	0.94002616	1.15793897	0.04839725	0.98233263	0.15849584
SUSD3	ENSG00000157303	21.7401275	1.63093441	0.28380334	4.2732057	2.004E-07	2.64227129	0.00017418
CCNB2	ENSG00000157456	100.188695	2.67498691	8.0212E-13	2.9342555	9.3533E-16	0.25926859	0.77629897
TMEM164	ENSG00000157600	55.5956613	-0.3933726	0.78007286	2.08233947	4.3725E-07	2.47761205	5.0156E-09
PSMG3	ENSG00000157778	89.633281	0.50820064	0.51317488	1.10707584	0.00711498	0.5988752	0.33435175
FMNL2	ENSG00000157827	5.25753089	-1.9701755	0.73391348	3.14702298	0.06843643	5.11719852	0.03967477
PPP1R9A	ENSG00000158528	3.63337572	-3.7572781	NA	2.08938362	0.40317829	5.84666169	0.0266635
TAGLN2	ENSG00000158710	724.2305	0.76718619	0.00010464	0.87175611	3.0188E-06	0.10456993	0.87845757
GART	ENSG00000159131	80.7042303	0.64113427	0.28446567	0.7958121	0.07937038	0.15467783	0.90763381
IGF2BP1	ENSG00000159217	7.46006507	1.77258492	0.66029709	4.66272156	0.0522057	2.89013664	0.04441968
PTMS	ENSG00000159335	594.386877	0.31837942	0.37530256	0.93038574	1.3035E-06	0.61200633	0.00627744
ATP13A2	ENSG00000159363	43.4801452	0.29980747	0.86563801	1.58861203	0.00170847	1.28880456	0.02150932
NR2F6	ENSG00000160113	171.165157	0.52967486	0.21435954	0.49956687	0.19701279	-0.030108	0.97755473
TMPRSS3	ENSG00000160183	40.5101662	1.24287558	0.04977115	1.04901895	0.10352806	-0.1938566	0.91259955
U2AF1	ENSG00000160201	147.486836	0.75763154	0.02765467	0.66966307	0.05046751	-0.0879685	0.936752
RRP1	ENSG00000160214	23.0841258	1.15236233	0.2595128	1.14486405	0.19510784	-0.0074983	0.99647695
SRSF2	ENSG00000161547	166.098229	0.45234596	0.43023317	0.79313571	0.02239714	0.34078976	0.60970469
PLCD3	ENSG00000161714	74.0847886	-0.6141094	0.48823916	2.45213599	2.1957E-12	3.06624541	8.0487E-17
RACGAP1	ENSG00000161800	93.6436847	1.90547572	2.1152E-06	2.71422289	8.9341E-14	0.80874716	0.06791821
PLIP3	ENSG00000162407	3.16163998	-2.4019308	NA	3.31713798	NA	5.7190688	0.04441968
CAMK2N1	ENSG00000162545	69.156506	1.00455583	0.12442051	2.34843054	2.937E-08	1.34387471	0.00406619
WNT4	ENSG00000162552	26.6954849	-0.8354987	0.55746484	0.89061697	0.34983868	1.72611567	0.02820017
FAM102B	ENSG00000162636	49.1367939	1.36614589	0.016163	2.00473414	1.7575E-05	0.63858825	0.41919235
IER5	ENSG00000162783	16.3067523	1.76206326	0.12442051	1.96329708	0.0425929	0.20123382	0.9439606
NA	ENSG00000162840	58.8585234	1.11443113	0.0375786	1.13900604	0.0211739	0.02457491	0.98766681
KIF26B	ENSG00000162849	3.21066015	0	NA	6.07540131	0.02198089	6.08030691	0.03199234
MAPKAPK2	ENSG00000162889	147.1964	0.21573963	0.83944553	2.0521986	5.6848E-14	1.83645897	2.4268E-11
IL20	ENSG00000162891	124.29897	-0.4710776	0.53100263	2.73409601	3.005E-22	3.20517358	8.5498E-28
FCMR	ENSG00000162894	53.6144107	0.00871442	1	1.91557151	3.0936E-05	1.90685709	5.7642E-05
REL	ENSG00000162924	30.9536946	0.34916479	0.86252138	1.3649731	0.03538844	1.01580832	0.21517538
CCDC74A	ENSG00000163040	16.4394077	1.06509025	0.51746335	2.07798423	0.01827709	1.01289397	0.44566902
PDLIM5	ENSG00000163110	62.5654406	1.05453483	0.06396992	1.43246134	0.00175417	0.37792651	0.72586256
SGO2	ENSG00000163535	40.0698003	1.5500101	0.01120503	1.76665506	0.00136985	0.21664496	0.90100125
TOPBP1	ENSG00000163781	51.1168966	0.97493588	0.12059131	1.12484619	0.03138932	0.14991031	0.92610943
RFC4	ENSG00000163918	54.0878365	1.34095839	0.00814406	1.43911919	0.00218933	0.0981608	0.95014208
CDC25A	ENSG00000164045	9.36081356	5.94841786	0.00854442	6.77626708	0.00088875	0.82784922	0.76677947
POC1A	ENSG00000164087	18.2194741	1.64250316	0.11988319	1.76174782	0.05333973	0.11924466	0.96211266
GASK1B	ENSG00000164125	55.4578754	-1.7871896	0.00199256	1.38118194	0.00327386	3.16837153	3.1663E-11
NPY1R	ENSG00000164128	32.8441583	-3.3399528	0.01174466	2.75140557	3.1101E-07	6.09135838	5.9772E-09
ITGA2	ENSG00000164171	40.2962027	0.95938925	0.29457884	2.07295354	0.00012297	1.11356429	0.10223667
MOCS2	ENSG00000164172	165.740362	0.77954918	0.02408232	1.82983859	5.9971E-13	1.05028941	0.00014015
RHOBTB3	ENSG00000164292	306.352153	1.11028473	1.1485E-05	2.28405652	1.5923E-25	1.17377179	2.9077E-07
GPX8	ENSG00000164294	16.7972769	-1.8211496	0.19229325	1.44401468	0.13446195	3.26516423	0.00062124
SEPTIN8	ENSG00000164402	136.68094	0.75322728	0.04445826	0.93883435	0.00308285	0.18560707	0.84787788
KCNK5	ENSG00000164626	49.5713657	-0.6019826	0.59125811	0.97589637	0.1075328	1.57787901	0.00379948
FNDC1	ENSG00000164694	6.25673948	3.92073963	0.18793682	4.90611033	0.03323043	0.9853707	0.73804012
DLC1	ENSG00000164741	10.8028204	0.34369137	0.95126426	3.56675139	0.00227545	3.22306002	0.00702226
RAD21	ENSG00000164754	229.752087	0.92695135	0.00116925	0.9906076	0.00024779	0.06365625	0.95014208
MED30	ENSG00000164758	96.6716049	0.7155909	0.1544515	0.96639625	0.01235547	0.25080535	0.79674417
OSGIN2	ENSG00000164823	258.618205	0.72475269	0.02830553	0.6912767	0.02835319	-0.033476	0.97417445
GEM	ENSG00000164949	8.3697552	1.22288874	0.71318306	3.34165798	0.01231475	2.11876924	0.1578966
PSIP1	ENSG00000164985	16.0282682	1.27208553	0.39300545	1.92608515	0.04500135	0.65399962	0.73270586
PCDH19	ENSG00000165194	15.2082877	-1.4420135	0.87281228	6.9661481	0.00016331	8.40816155	5.4206E-06
STRBP	ENSG00000165209	79.6248424	-0.033239	0.987022	0.83900514	0.04621934	0.87224411	0.05171612
ZNF367	ENSG00000165244	33.3971551	2.91244662	8.7669E-05	3.86578673	6.9498E-09	0.95334011	0.20446763
MELK	ENSG00000165304	41.5465643	5.24949871	7.7742E-07	5.67590588	2.7304E-08	0.42640716	0.72349115
SPTSSA	ENSG00000165389	692.132155	0.64114115	0.0036549	1.30604696	3.4831E-13	0.66490582	0.00157416
CFL2	ENSG00000165410	45.7668163	1.96698722	0.00061122	2.48726159	1.5085E-06	0.52027436	0.62067667
SKA3	ENSG00000165480	15.077105	3.21147617	0.00501885	3.20010362	0.00356331	-0.0113725	0.99605451
DDIAS	ENSG00000165490	13.6731105	1.15573257	0.6293394	2.7641397	0.01111329	1.60840713	0.24075617
HPRT1	ENSG00000165704	91.784787	-0.6122182	0.33067269	0.69036877	0.12846896	1.30258698	0.00067911
RET	ENSG00000165731	31.167853	-1.4705675	0.11992693	1.73090579	0.00277204	3.20147325	2.6841E-07
E2F7	ENSG00000165891	10.9543725	2.36041102	0.16751667	3.02882915	0.0218149	0.66841814	0.80967496
PSMC3	ENSG00000165916	339.237281	0.63928872	0.01499159	0.75010584	0.00143461	0.11081713	0.89251345
CKB	ENSG00000166165	305.34153	0.72564839	0.00643242	1.36018694	2.398E-10	0.63453854	0.01696858
WEE1	ENSG00000166483	65.4686277	1.01848126	0.05879311	1.71647308	2.0551E-05	0.69799181	0.23869813
MCM7	ENSG00000166508	102.185839	2.17712748	1.4652E-07	2.98501645	6.0939E-15	0.80788896	0.09932022
BLCAP	ENSG00000166619	88.7154319	0.21893138	0.8640001	1.34461578	0.00014857	1.1256844	0.00335475
BEX3	ENSG00000166681	160.635301	-1.0509402	0.00084036	0.50631343	0.17681588	1.55725362	2.3261E-08
B2M	ENSG00000166710	353.160163	0.95410454	2.9359E-05	1.340332	1.1277E-10	0.38622746	0.26416616
SAAL1	ENSG00000166788	15.4576521	1.47246472	0.36071614	2.79446122	0.00304993	1.3219965	0.29240617
PCLAF	ENSG00000166803	30.1841929	3.79682785	1.4369E-05	4.2995402	1.9225E-07	0.50271235	0.72349115
TMEM170A	ENSG00000166822	37.9933698	1.02030292	0.19646523	1.1550781	0.07634882	0.13477518	0.94715243
NEMP1	ENSG00000166881	37.4766196	1.08053843	0.15825389	1.3842553	0.0208415	0.30371687	0.85555398
PBX3	ENSG00000167081	13.939245	2.06812184	0.10796584	2.98484497	0.00197677	0.91672314	0.55639737
RRM1	ENSG00000167325	41.9823847	0.51568998	0.68738929	1.49121845	0.00476142	0.97552847	0.1440565
TPM4	ENSG00000167460	53.4508779	0.8857488	0.2259964	1.2733837	0.01542967	0.38763488	0.74352054
GPX4	ENSG00000167468	613.173667	-0.4912863	0.08110417	0.92281422	3.9053E-06	1.41410049	1.3116E-13
GATAD2A	ENSG00000167491	183.474201	0.26274187	0.70536491	1.12583275	1.0398E-05	0.86309089	0.00211021
CDT1	ENSG00000167513	38.1060853	3.42969906	1.2832E-06	3.68206266	6.4359E-08	0.2523636	0.89249921
TUBA1A	ENSG00000167552	110.418216	-0.414405	0.59899086	0.86180634	0.02563834	1.27621137	0.00039953
YIF1B	ENSG00000167645	147.391672	0.56888505	0.21028157	0.95213044	0.00239411	0.38324539	0.50438628
C19orf48	ENSG00000167747	104.308635	0.77112329	0.12442051	1.33578356	0.00018284	0.56466027	0.31993207
TK1	ENSG00000167900	369.50265	2.628602	6.195E-30	2.84035173	1.4243E-35	0.21174973	0.72711184
EC1	ENSG00000167969	152.024303	0.41850742	0.46302588	0.94150684	0.00214549	0.52299942	0.23417048
RPSA	ENSG00000168028	470.098738	0.35097438	0.33204396	0.29209066	0.39054432	-0.0588837	0.9449136
LTBP3	ENSG00000168056	153.441787	-0.4856427	0.33852236	0.7031564	0.03259618	1.1887991	5.7375E-05
SCARA3	ENSG00000168077	23.8897964	1.70044406	0.04715492	1.9733741	0.00764897	0.27293005	0.90154657
DTYMK	ENSG00000168393	174.630576	1.53054156	6.8229E-07	1.69197745	1.0527E-08	0.16143589	0.88012206
HR	ENSG00000168453	15.2598994	1.31341796	0.45133101	2.91746956	0.00127259	1.60405159	0.12861864
FEN1	ENSG00000168496	54.5147561	1.4984705	0.00378224	1.65145497	0.00057521	0.15298447	0.92441713
ING2	ENSG00000168556	18.8656173	2.28422326	0.06917926	3.95109706	1.2519E-05	1.6668738	0.05104095
AHCYL1	ENSG00000168710	231.223398	0.72117498	0.01450968	0.64757582	0.02682156	-0.0735992	0.94191161
NPNT	ENSG00000168743	385.043039	0.12529768	0.91161702	1.61167074	5.4246E-10	1.48637306	2.4493E-08
FAM178B	ENSG00000168754	40.2463419	1.00941771	0.32024727	3.25330118	2.952E-10	2.24388347	5.4009E-06
HNRNPH1	ENSG00000169045	324.381291	0.61907575	0.04199418	0.97801962	4.6404E-05	0.35894387	0.39943411
GSG1L	ENSG00000169181	5.01443454	-0.9911993	NA	4.26914343	0.02881822	5.26034273	0.03669121
NR0B1	ENSG00000169297	41.1075992	6.38455386	0.00092706	9.72217329	5.099E-09	3.33761943	2.1027E-11
SDC2	ENSG00000169439	102.344307	-0.5475455	0.93526772	6.24275422	3.9684E-06	6.79029973	1.5603E-06
CKAP2L	ENSG00000169607	22.7793998	2.33427821	0.01079728	2.95394656	0.0001819	0.61966835	0.67614126
BUB1	ENSG00000169679	43.3975019	2.71160622	2.701E-05	3.47397817	3.7364E-09	0.76237194	0.33498148
MT1E	ENSG00000169715	548.282832	1.20389318	1.4661E-05	1.16051241	2.2241E-05	-0.0433808	0.96716641
RAC3	ENSG00000169750	28.0134055	1.08148786	0.29258589	1.65908027	0.01613268	0.57759241	0.67757704
ROBO1	ENSG00000169855	10.8492669	-0.0081878	1	6.45410052	0.00096052	6.46228834	0.00132094
UBE2E3	ENSG00000170035	42.4972626	0.43008166	0.76400225	1.32153713	0.01637666	0.89145547	0.21523021
HNRNPA3	ENSG00000170144	355.730874	0.49504766	0.10915402	1.05258667	7.2855E-07	0.557539	0.03826583
CDK1	ENSG00000170312	438.246722	3.52320872	2.1791E-45	3.99528161	2.0042E-59	0.4720729	0.15946406
KRT8	ENSG00000170421	7218.49958	-0.3631635	0.14600609	0.29911128	0.22326438	0.66227478	0.0002771
PAQR4	ENSG00000170515	109.98448	0.59366061	0.47154347	1.21408005	0.00783044	0.62041944	0.39735985
PFKFB3	ENSG00000170525	36.1222916	-0.7036122	0.55037249	1.15390322	0.05966045	1.85751543	0.00122146
CDCA4	ENSG00000170779	16.6934738	1.58640715	0.15229601	1.8410761	0.0425929	0.25466895	0.92222697
TRIAP1	ENSG00000170855	72.8658408	-0.5029532	0.58595588	0.61646539	0.30457906	1.1194186	0.02238758
PRKCE	ENSG00000171132	10.0634865	-0.8508161	0.83845987	2.7082596	0.01623001	3.55907567	0.00467201
ESCO2	ENSG00000171320	11.5974073	1.77401098	0.31483553	2.76694961	0.01622031	0.99293863	0.60658414
SPSB1	ENSG00000171621	20.952111	1.37133376	0.20030029	1.13478424	0.2885943	-0.2365495	0.92573822
ATF7IP	ENSG00000171681	39.915769	0.90226186	0.37743999	1.5812167	0.01150859	0.67895484	0.54111774
RGS19	ENSG00000171700	52.5493622	0.33958414	0.82213362	1.1215751	0.0426366	0.77199096	0.30831337
BCL2	ENSG00000171791	16.1030503	-1.1137158	0.50438526	1.16537321	0.26441846	2.27908898	0.01443936
RHNO1	ENSG00000171792	69.4581358	1.1349487	0.04498171	1.67878442	0.00018119	0.54383572	0.51820433
RRM2	ENSG00000171848	93.9853657	4.56135826	3.5503E-16	4.96946101	1.7026E-19	0.40810275	0.58667183
SYNPO	ENSG00000171992	34.651367	0.78763047	0.47108051	1.99482684	0.00025076	1.20719637	0.06450039
SMN1	ENSG00000172062	85.5693211	0.78650998	0.15837856	0.91165057	0.04742907	0.12514959	0.93047906
CYCS	ENSG00000172115	650.640841	0.64200177	0.00235608	0.7787672	4.9745E-05	0.13676543	0.81181999
CALB2	ENSG00000172137	12.7847511	0.99758607	0.86291292	5.56590798	0.00010577	4.56832191	0.00010501
FRMD3	ENSG00000172159	5.4411097	0.51927386	0.95425485	4.17576144	0.03672317	3.65648757	0.07333424
ID4	ENSG00000172201	3.17696995	-1.4648676	NA	4.64984309	NA	6.1147107	0.03220775
COPRS	ENSG00000172301	83.7453797	0.63619537	0.29018962	0.75141164	0.10787488	0.11521627	0.93356396
GNB2	ENSG00000172354	219.931416	-0.0360987	0.98218478	0.7523057	0.02007251	0.78840436	0.01958189

COPS9	ENSG00000172428	496.691635	-0.469334	0.35388995	0.72297659	0.0291073	1.19231061	4.9078E-05
ZNF738	ENSG00000172687	23.8036263	1.15254845	0.27878861	1.42945747	0.07430618	0.27690902	0.90100125
EGFL7	ENSG00000172889	91.1683577	-0.3203474	0.72704207	0.62592779	0.16077642	0.94627514	0.01816033
RHOD	ENSG00000173156	149.868381	0.07287991	0.96077167	1.48327976	2.5404E-07	1.41039985	1.8988E-06
SYT12	ENSG00000173227	48.3838874	-0.600157	0.58538901	1.41221675	0.0036738	2.01237379	2.7568E-05
PPP1R14B	ENSG00000173457	357.103742	0.30563357	0.49985936	0.62540768	0.01288236	0.31977411	0.44516034
NUDT4	ENSG00000173598	308.412419	-0.1750877	0.84030073	0.66528319	0.02227293	0.84037086	0.00284811
HEG1	ENSG00000173706	8.98942919	1.30769738	0.79528972	4.83531104	0.0021985	3.52761366	0.00749949
EXO1	ENSG00000174371	17.3605824	6.99855565	0.00026017	7.40259873	5.3042E-05	0.40404308	0.86736333
AKIRIN1	ENSG00000174574	93.3730319	-0.528977	0.41467233	0.83624669	0.51585349	0.91522369	0.02944019
FAM241A	ENSG00000174749	116.186147	0.58435891	0.31469636	0.6500262	0.16124233	0.06566729	0.95911967
PDZK1	ENSG00000174827	285.443805	-2.503831	5.6288E-05	5.18034259	1.0308E-77	7.68417363	1.4589E-54
MARCKSL1	ENSG00000175130	188.041911	-0.9466071	0.00316491	0.9284272	0.00100544	1.87503431	6.9321E-13
NRIP3	ENSG00000175352	49.2434818	-1.9655434	0.00041975	0.81043461	0.17101201	2.77597797	2.4134E-08
DOK7	ENSG00000175920	4.7821555	-1.4365107	NA	5.2871053	0.03001727	6.72361604	0.0047094
TUBB6	ENSG00000176014	41.6855236	1.07659005	0.12442051	1.44327536	0.00800043	0.3666853	0.78053909
SPHK1	ENSG00000176170	20.1039747	0.66885099	0.72704207	1.91681109	0.01267801	1.2479601	0.19496469
HSD11B2	ENSG00000176387	11.0461482	1.09276568	0.71075762	3.35171001	0.00275971	2.25894433	0.05248209
RNPEP	ENSG00000176393	78.81461	0.43207337	0.62550458	1.0808773	0.00850528	0.64880393	0.26091326
LMNB2	ENSG00000176619	63.6754531	1.27865972	0.01320887	1.71131038	9.7614E-05	0.43265065	0.64772226
BOK	ENSG00000176720	21.6810301	-1.2160925	0.2986901	0.73467915	0.49606159	1.95077167	0.01590181
FAM89B	ENSG00000176973	19.8717732	-1.2527182	0.32665469	0.92388289	0.37975779	2.17660105	0.00920438
EPS8L2	ENSG00000177106	21.2177991	-1.0641016	0.46190853	1.10341995	0.23982356	2.16752154	0.00821992
RPS6KA3	ENSG00000177189	16.8693696	1.9747321	0.15378417	2.90691748	0.00421232	0.93218538	0.61244602
IRX3	ENSG00000177508	469.509142	0.54350979	0.04655839	0.5353325	0.03467804	-0.0081773	0.99268948
NAALADL2	ENSG00000177694	6.23902879	1.21952553	0.78696937	3.40130434	0.04140177	2.18177882	0.23574188
DDX10	ENSG00000178105	48.0120334	-0.4606495	0.72704207	1.03181922	0.07403963	1.4924687	0.00581013
POGLUT3	ENSG00000178202	4.73655812	-4.4485521	NA	1.60407426	0.47242138	6.05262633	0.01175642
BEND3	ENSG00000178409	6.59349322	3.39614964	0.13304271	3.71145191	0.05238637	0.31530227	0.94285895
CA8	ENSG00000178538	51.2081462	3.45826519	0.0001723	6.16330651	3.4294E-15	2.70504132	2.6812E-10
SNX18	ENSG00000178996	61.4795157	0.74616086	0.25661369	0.97670177	0.04468058	0.23054091	0.86805906
AURKB	ENSG00000178999	30.452089	4.25704563	3.7742E-06	4.23946139	2.5287E-06	-0.0175842	0.99380669
FAM133A	ENSG00000179083	7.82657933	-0.3825677	0.95543715	3.40191215	0.01138692	3.78447988	0.01008304
EGR3	ENSG00000179388	7.226184 11	-4.5971297	0.09088909	2.46852134	0.0751074	7.0660831	0.00077441
TSPYL5	ENSG00000180543	461.319299	-0.7890638	0.00091634	0.95854891	3.8286E-06	1.74761274	7.6669E-19
TMEM64	ENSG00000180694	426.593581	0.3658017	0.53380138	2.98499779	1.8378E-36	2.61919609	1.5617E-28
SHISA2	ENSG00000180730	10.0799697	7.06104376	0.00058382	6.48031857	0.00158512	-0.5807252	0.85742523
CUEDC1	ENSG00000180891	39.8935264	0.33903013	0.85072228	1.93449137	0.00013567	1.59546124	0.00320569
AEN	ENSG00000181026	20.6259998	1.81846533	0.06217996	2.02048718	0.01701643	0.20202185	0.93950915
NPM1	ENSG00000181163	872.030824	0.44267795	0.06141662	0.40430257	0.07430618	-0.0383754	0.95591153
MEX3D	ENSG00000181588	63.5706562	0.80732554	0.27872385	1.0789594	0.04606363	0.27163386	0.85626155
PHLDA2	ENSG00000181649	59.4421585	2.2132013	2.0239E-05	2.93700958	4.8871E-10	0.72380945	0.31052476
SIAH2	ENSG00000181788	69.9387949	0.47144251	0.6433648	1.84386449	3.5333E-06	1.37242198	0.0013698
CLDN7	ENSG00000181885	22.391065	1.26565881	0.22686371	1.53000497	0.06127547	0.26434617	0.9108649
LDOC1	ENSG00000182195	203.183881	-0.9846792	0.00204689	1.5547682	2.447E-10	2.53944739	3.2968E-24
SHMT2	ENSG00000182199	45.8175414	0.8710277	0.26347275	1.10412505	0.05877252	0.23309735	0.89238097
BACE2	ENSG00000182240	34.5080018	1.36125096	0.11902159	2.84858236	7.6406E-07	1.4873314	0.01715077
NXPH4	ENSG00000182379	82.9250967	0.30621592	0.77962346	0.92154679	0.03084743	0.61533087	0.29975599
KPNA2	ENSG00000182481	471.498686	1.84956257	1.3163E-20	2.28377469	3.1702E-32	0.43421211	0.1278104
GLRX5	ENSG00000182512	385.892199	0.36695169	0.36890802	0.72489483	0.00309993	0.35794311	0.36893325
TSKU	ENSG00000182704	153.910937	0.38455348	0.55222846	1.00556392	0.00144949	0.62101044	0.13592742
ANXA2	ENSG00000182718	1283.39228	0.71627009	0.00013737	0.47677257	0.02295246	-0.2394975	0.5109862
PCP4	ENSG00000183036	6.27771715	3.00307557	0.50259248	7.00130651	0.00078128	3.99823094	0.01880268
ABAT	ENSG00000183044	134.049539	-0.5097898	0.35292515	0.66383126	0.0751074	1.17362104	0.00028714
CAMK1D	ENSG00000183049	12.4310895	1.94540504	0.15468432	2.24580214	0.04523175	0.3003971	0.92174256
RUVBL2	ENSG00000183207	198.020403	0.34977475	0.57241337	0.90182105	0.00247019	0.55204631	0.16886888
SMG1P5	ENSG00000183604	16.8002674	0.87009726	0.66453398	1.97831381	0.03119504	1.10821655	0.40366515
LHFPL6	ENSG00000183722	16.1620477	1.67047755	0.23947982	2.80495622	0.00272448	1.13447867	0.41819616
KMT5A	ENSG00000183955	106.56167	-0.0697329	0.96578365	1.04492255	0.00282051	1.11465541	0.00190228
PTP4A2	ENSG00000184007	654.737855	0.11122877	0.88731859	1.00727956	5.0206E-07	0.89605079	2.185E-05
ACTG1	ENSG00000184009	2363.3429	0.2253801	0.55144301	0.65069299	0.00034873	0.42531289	0.06394869
CTAG1B	ENSG00000184033	5.49109508	0.98356738	0.91574013	5.32941515	0.01942651	4.34584777	0.02804283
TBX1	ENSG00000184058	10.2145561	1.80749787	0.26959229	1.85615742	0.17733065	0.04865956	0.98869004
NR2C2AP	ENSG00000184162	23.1050753	1.45109206	0.14122783	1.24052269	0.19920389	-0.2105694	0.93356396
PGP	ENSG00000184207	127.216621	0.50671832	0.37078729	1.23318653	7.97E-05	0.72646821	0.06353171
IRAK1	ENSG00000184216	107.501537	-0.063836	0.96869234	1.23524591	0.00014147	1.29908187	9.3396E-05
CMSS1	ENSG00000184220	64.9397335	0.10106812	0.95839173	1.01670181	0.02387867	0.91563369	0.07102153
KCNK12	ENSG00000184261	47.5613896	1.12943938	0.13619067	3.03438904	5.9348E-11	1.90494966	2.6809E-05
PKP3	ENSG00000184363	60.9277642	-0.7114596	0.31563831	0.69231829	0.20346294	1.40377787	0.00165055
CSF1	ENSG00000184371	7.21087999	-1.7930916	0.65498126	2.78140116	0.04293481	4.5744928	0.01018901
STING1	ENSG00000184584	21.1638161	0.16272295	0.96117859	1.65178648	0.0326182	1.48906353	0.08666453
SIVA1	ENSG00000184990	281.806463	0.5802937	0.11005221	0.79156881	0.00544113	0.21127512	0.76881055
BRI3BP	ENSG00000184992	106.062146	0.58598335	0.34125251	0.61038997	0.22998588	0.02440662	0.98581749
ROBO2	ENSG00000185008	11.6670493	0	1	8.04209898	1.7552E-05	8.04699729	3.0678E-05
SLC24A3	ENSG00000185052	8.25208229	-2.0128964	0.5774665	2.88260873	0.02317524	4.89550515	0.00444904
TCEAL9	ENSG00000185222	28.8884018	-0.6119588	0.72197294	1.82042535	0.00281668	2.43238418	9.7425E-05
TNFAIP8L1	ENSG00000185361	15.6957139	1.46289444	0.33067369	2.62034447	0.00417535	1.15745002	0.36233036
PARPBP	ENSG00000185480	17.5080597	1.62871157	0.14157082	1.9553002	0.02786845	0.32658863	0.89589207
MUC1	ENSG00000185499	34.1040084	1.4392141	0.05693613	2.22900556	0.00011816	0.78979146	0.39709545
PSMD13	ENSG00000185627	84.2989473	-0.1478572	0.9239809	0.76852225	0.09212323	0.91637941	0.04441968
ZFP36L1	ENSG00000185650	110.169589	-0.8009143	0.07950972	0.65230809	0.11748734	1.4532224	1.9775E-05
MYBL1	ENSG00000185697	40.2596159	2.17801978	0.00192481	3.86234687	1.3867E-11	1.68432709	0.0011941
KCNQ5	ENSG00000185760	4.16278766	0	NA	6.55182435	0.00642049	6.5567269	0.00942572
KIF18B	ENSG00000186185	22.1662697	2.9227736	0.00133809	3.19477104	0.000173	0.27199744	0.90763381
PPP1CC	ENSG00000186298	211.144628	0.04091782	0.97618371	0.69399122	0.02208712	0.65307339	0.05164132
TSPYL4	ENSG00000187189	52.1358289	-0.7958632	0.29789541	0.81535962	0.14471436	1.61122278	0.00073128
FAM9C	ENSG00000187268	45.6462655	3.0269996	2.8183E-05	4.42045611	6.6182E-12	1.3934565	0.02118994
PTMA	ENSG00000187514	872.65809	0.15065579	0.84587541	0.77566783	0.00143461	0.62501204	0.02469576
HSPA14	ENSG00000187522	45.4230597	0.15108764	0.95154251	1.54180465	0.00779947	1.39071702	0.02827633
ISG15	ENSG00000187608	26.0870598	-0.6593228	0.69473992	1.66716128	0.00915113	2.32648405	0.00032619
NA	ENSG00000187653	135.420294	0.2629232	0.77334309	1.78582347	1.361E-10	1.52289867	8.622E-08
TPRG1	ENSG00000188001	5.95859295	1.00041521	0.91335236	5.49042191	0.01450152	4.4900067	0.01928131
PRKAR1B	ENSG00000188191	17.7752797	0.94049954	0.61902661	2.72261495	0.00060974	1.7821154	0.03819641
TUBB4B	ENSG00000188229	81.4172701	1.8573066	7.3233E-05	1.79434935	0.0001031	-0.0629572	0.9695841
H2AX	ENSG00000188486	131.733554	1.51075468	0.00012676	2.53654222	1.1001E-13	1.02578754	0.00942572
HBA2	ENSG00000188536	19.0713835	-1.1895141	0.44366507	1.6848133	0.03151165	2.87432741	0.00038905
NA	ENSG00000188985	22.089615	3.38063386	0.0005283	3.8196748	2.5949E-05	0.43904094	0.82167875
FAM111B	ENSG00000189057	42.3263976	3.33922828	6.2924E-06	4.01267792	5.8248E-09	0.67344964	0.53313378
JPT1	ENSG00000189159	408.46192	0.85831786	0.00231194	1.37093585	1.1144E-08	0.51261798	0.15204885
HMGB1	ENSG00000189403	988.474074	0.84663004	1.9151E-05	1.11788904	9.0847E-10	0.27125899	0.46276244
GREB1	ENSG00000196208	154.98777	-1.870549	0.02114445	5.04707582	2.4535E-47	6.91762483	7.3068E-38
RYR1	ENSG00000196218	12.7183319	-0.0674212	0.99028823	2.4997489	0.01478065	2.56717005	0.01810613
PPIA	ENSG00000196262	3588.3163	0.45215096	0.02744729	0.39111776	0.05486771	-0.0610332	0.92441713
WDR5	ENSG00000196363	68.7419215	0.60010452	0.42077806	0.94405333	0.04611534	0.34394881	0.73497288
RABL6	ENSG00000196642	157.229299	0.60824794	0.12848038	0.53526234	0.16433439	-0.0729856	0.94773579
H2BU1	ENSG00000196890	21.2559548	0.71334955	0.69259771	1.84314769	0.01587253	1.12979814	0.26921828
FLNA	ENSG00000196924	117.069662	0.185275	0.91009921	2.36218416	4.7296E-11	2.17690916	2.2264E-09
LAGE3	ENSG00000196976	62.9774966	-0.1463201	0.94321858	1.64776676	5.2692E-05	1.79408685	1.6425E-05
SRC	ENSG00000197122	54.9049127	0.41440197	0.79735449	2.84652612	2.3939E-10	2.43212415	5.3617E-08
PELI1	ENSG00000197329	16.8809826	-0.3925187	0.91606529	2.88420008	0.00030249	3.27671883	0.00012575
ZNF655	ENSG00000197343	7.37080678	-3.2608404	0.3840262	2.33357105	0.16594078	5.59441148	0.0196468
VEPH1	ENSG00000197415	23.5176673	-0.1679229	0.95888715	1.79879063	0.01105019	1.96671351	0.00735023
STMN3	ENSG00000197457	203.781906	0.46703521	0.31340637	1.60219852	8.6429E-11	1.13516332	1.5893E-05
PDGFA	ENSG00000197461	23.4913156	0.59590618	0.78561563	2.47907729	0.00048418	1.8831711	0.01380698
MCMBP	ENSG00000197771	110.853178	0.74236619	0.09817228	1.21105467	0.00025076	0.46868852	0.4104414
ELOVL2	ENSG00000197977	17.8739817	0	1	8.6493384	1.1019E-06	8.6542405	1.8848E-06
ZNF273	ENSG00000198039	14.3252838	1.25634322	0.50379334	2.72913348	0.00451273	1.47279026	0.20727166
TMEM229B	ENSG00000198133	30.455046	-1.004424	0.39818127	1.32247026	0.05836346	2.32689425	0.00039953
HMGN5	ENSG00000198157	16.9172234	-2.1703982	0.10617967	1.28362871	0.22932832	3.45402691	0.00060576
ASPH	ENSG00000198363	58.7172228	2.04451915	1.37E-05	2.52237671	6.7526E-09	0.47785756	0.58117933
WDHD1	ENSG00000198554	51.4331229	1.11369882	0.0917754	1.35882668	0.01223356	0.24512786	0.88365775
NA	ENSG00000198618	1644.78828	0.40056407	0.15378417	0.40531046	0.10242501	0.00474639	0.99595651
MAGEA1	ENSG00000198681	74.6539993	0.0746048	0.96898626	0.99417077	0.0262481	0.92155597	0.0654987
INPP5F	ENSG00000198825	34.7505339	0.87664363	0.34656089	1.46268538	0.01310103	0.58604175	0.58667363
ARHGAP11A	ENSG00000198826	13.5107969	2.4464266	0.07283567	3.10415517	0.00491214	0.65772857	0.76677947
PNMA5	ENSG00000198883	164.254565	-0.0665852	0.96128686	1.25330029	5.2651E-06	1.31988552	2.3808E-06
LINC00632	ENSG00000203930	7.70674691	1.44540395	0.87659724	7.41669193	0.00022194	5.97128798	0.0065069
LSM2	ENSG00000204392	115.629687	1.02349848	0.00749658	0.93835285	0.0128976	-0.0851456	0.94773579
MICB	ENSG00000204516	24.7985694	0.42477226	0.84652754	1.56517501	0.0343839	1.14040275	0.22578582
SPDYC	ENSG00000204710	53.6541206	-0.725623	0.36028749	0.42523766	0.60451222	1.15086067	0.03639589
AARD	ENSG00000205002	9.84040115	-1.0931827	0.70114475	1.67285344	0.19285401	2.76603613	0.02912333
C4orf46	ENSG00000205208	16.8888999	0.48314995	0.86656019	2.17216691	0.01015716	1.68901696	0.07749055
LGR4	ENSG00000205213	43.6017589	0.15493798	0.94914686	2.3849995	1.995E-07	2.23006152	1.7614E-06
INSYN1	ENSG00000205363	8.89938806	0	1	7.62843894	9.5075E-05	7.63334029	0.00015888
TMSB4X	ENSG00000205542	1797.53334	0.13994008	0.8166992	1.58398757	1.4628E-21	1.44404748	7.3969E-18
HMGN1	ENSG00000205581	619.876495	0.42422426	0.13959689	0.4086488	0.11592275	-0.0155755	0.98463331
RNPS1	ENSG00000205937	215.478962	0.3021255	0.60758331	0.62300396	0.04100023	0.32087845	0.54418184
HACD2	ENSG00000206527	92.3911608	0.28384181	0.78760801	0.86347297	0.03467804	0.57963117	0.3121471
SLC48A1	ENSG00000211584	81.2237736	-0.2100118	0.89222806	0.82871075	0.10495837	1.03872255	0.03770399
SLC35F6	ENSG00000213699	78.5366039	-0.6199013	0.38364773	0.36447136	0.62749245	0.9843727	0.04531083
NA	ENSG00000214391	36.8610188	1.49950468	0.03385224	2.08316468	0.00030072	0.58365999	0.60463762
NA	ENSG00000214653	35.0525659	0.81086785	0.47544777	1.54303087	0.01481931	0.73216302	0.47789021
NA	ENSG00000214975	62.2349736	0.68676799	0.34369851	1.0587781	0.02757434	0.37201011	0.72069155
NA	ENSG00000215859	17.3642531	0.76072229	0.88189341	5.51116482	1.7255E-06	4.75044252	1.6521E-06
CEBPD	ENSG00000221869	28.8484252	-0.1474866	0.96049998	1.86928531	0.00243046	2.01677193	0.00152234
UBA52	ENSG00000221983	2161.64758	0.51551891	0.16083991	0.51429149	0.11511569	-0.0012274	0.99825809
NA	ENSG00000224126	36.4004962	2.05612963	0.00216443	2.53813248	1.084E-05	0.48200285	0.70087667
NA	ENSG00000224411	68.3117232	0.79382472	0.17413096	0.97326341	0.03649366	0.1794387	0.89926198
SMIM13	ENSG00000224531	38.4870949	0.24006824	0.90674082	1.1891295	0.04903825	0.94906126	0.20165334
NA	ENSG00000224578	29.7419487	1.23984642	0.15837856	1.67928409	0.01207547	0.43943768	0.7794239
NA	ENSG00000226964	52.317074	0.84392495	0.27753524	1.22121969	0.02407948	0.37729474	0.76045009
NA	ENSG00000228232	120.307331	0.5651649	0.24476641	0.62155255	0.11808064	0.05638765	0.96071317
NA	ENSG00000229358	11.5984719	0.68159292	0.83028986	2.4381769	0.01740272	1.75658398	0.14438854
LOC101928336	ENSG00000230392	8.8540607	-2.8855027	0.22505142	1.3144182	0.40579087	4.19992088	0.01715077
GPX1	ENSG00000233276	169.554993	-0.4632631	0.36413738	0.79944319	0.00871247	1.26270626	7.8688E-06
CYP2T1P	ENSG00000233622	34.5273386	-2.0385311	0.07231003	3.02254707	2.2545E-08	5.06107815	1.2099E-11
NA	ENSG00000233966	48.248653	2.46594994	3.6924E-05	3.05812433	2.7644E-08	0.59217439	0.54913507
NA	ENSG00000234261	11.6065541	0.29884651	0.94814032	2.25103735	0.03088633	1.95219083	0.0948715

LINC01287	ENSG00000234722	65.9997147	-2.1645684	4.8155E-05	1.58030886	4.3223E-05	3.74487727	2.5035E-16
DSCAM-AS1	ENSG00000235123	237.28928	1.70317139	1.1241E-08	4.14619488	4.5871E-58	2.44302349	4.4822E-27
C12orf75	ENSG00000235162	69.8756597	1.28941575	0.00425974	1.54562569	0.00014147	0.25620994	0.82770698
LINC01695	ENSG00000236532	54.168796	-0.0546374	0.98310271	2.01467948	1.0772E-06	2.06931684	9.1298E-07
RNF223	ENSG00000237330	19.8570447	0.38284407	0.89518028	2.01266592	0.0120464	1.62982185	0.07266955
KIFC1	ENSG00000237649	30.725343	4.90914716	1.8878E-05	5.35065106	9.9186E-07	0.44150389	0.7925113
PAGE2B	ENSG00000238269	7.20886047	-5.3709947	0.02732349	0.99405692	0.64026512	6.36505161	0.00382806
C1orf226	ENSG00000239887	14.6063112	-1.0725427	0.6433648	1.95120197	0.05103513	3.02374465	0.00282527
PEG10	ENSG00000242265	80.246897	-0.013467	1	7.3667412	6.9294E-19	7.38020825	9.5634E-19
NA	ENSG00000244300	6.68651957	-3.3392707	0.3255255	1.70724865	0.31184869	5.04651934	0.03475822
LINC02762	ENSG00000250303	12.8397482	-1.6518204	0.51110823	2.72713753	0.00681322	4.37895792	0.00030755
NA	ENSG00000253125	3.16292367	-1.4343033	NA	4.44999591	NA	5.88429926	0.03417232
NA	ENSG00000254251	97.6624183	0	1	11.105019	4.8806E-12	11.1099219	7.6852E-12
NA	ENSG00000254285	266.716767	-0.2867324	0.60483488	0.39065199	0.26549793	0.67738436	0.01824107
CYP2B7P	ENSG00000256612	15.6512547	-1.317277	0.77334529	4.6023575	3.8286E-06	5.91963448	2.4979E-05
NA	ENSG00000259781	81.2058608	1.26081417	0.01108037	1.30153974	0.00521937	0.04072558	0.9797031
KDM7A-DT	ENSG00000260231	19.5983501	-1.633681	0.17839767	0.75209861	0.57219985	2.38577961	0.01038091
WFDC21P	ENSG00000261040	61.019179	0	1	10.42207	1.9784E-10	10.4269748	3.2677E-10
VPS9D1-AS1	ENSG00000261373	6.55741794	-1.9793327	0.59174506	2.04862456	0.21079521	4.02795724	0.03882173
NA	ENSG00000264589	3.45913354	-3.4477928	NA	2.45173801	0.31012163	5.89953078	0.02516923
SRGAP2	ENSG00000266028	27.861173	1.04227426	0.34370397	1.53048512	0.03923716	0.48821086	0.76677947
CTAG1A	ENSG00000268651	5.440008	1.02889806	0.87555727	4.24852388	0.02429661	3.21962582	0.07806179
CT45A1	ENSG00000268940	8.08237868	-1.5940918	0.70999086	3.01839789	0.0184426	4.61248973	0.00694241
NA	ENSG00000268942	18.2920328	1.6609297	0.14358269	1.80281248	0.06214314	0.14188278	0.95807242
NA	ENSG00000270619	4.61006323	-4.0104903	NA	2.19865292	0.34519931	6.20914325	0.01459007
PAXIP1-AS1	ENSG00000273344	64.1209641	-0.286349	0.83845987	1.31919207	0.00119057	1.60554112	8.3779E-05
GAGE13	ENSG00000274274	21.773076	-2.3718178	0.01369911	0.9738271	0.28724307	3.34564494	4.5774E-05
U2AF1L5	ENSG00000275895	93.5949521	0.86511235	0.03991326	0.81773526	0.04245661	-0.0473771	0.9695841
UHRF1	ENSG00000276043	13.17123	3.42295687	0.0209214	4.13374031	0.00129503	0.71078343	0.72741131
MARCKS	ENSG00000277443	62.5612461	0.11983935	0.94990867	1.54945228	0.00014944	1.42961293	0.00085223
MIR1244-2	ENSG00000283498	388.012007	0.26023812	0.77419334	1.01456687	0.00201903	0.75432875	0.05634909